

**Development of sustainable reaction systems for the  
palladium-catalyzed methoxy- and hydroxycarbonylation of  
alkenes: Boon and bane of multiphase systems**

vorgelegt von

M.Sc.

Marcel Schmidt

aus Weißenfels

Fakultät II - Mathematik und Naturwissenschaften

der Technischen Universität Berlin

zur Erlangung des akademischen Grades

Doktor der Ingenieurwissenschaften

- Dr.-Ing. -

genehmigte Dissertation

Promotionsausschuss:

Vorsitzender: Prof. Dr. Thomas Friedrich, TU Berlin

Gutachter: Prof. Dr. Reinhard Schomäcker, TU Berlin

Gutachter: Prof. Dr. Dieter Vogt, TU Dortmund

Tag der wissenschaftlichen Aussprache: 28.05.2019

**Berlin 2019**



## **Eidesstattliche Erklärung**

Hiermit erkläre ich an Eidesstatt, dass ich die vorliegende Arbeit "Development of sustainable reaction systems for the palladium-catalyzed methoxy- and hydroxycarbonylation of alkenes: Boon and bane of multiphase systems" selbstständig und eigenhändig sowie ohne unerlaubte Hilfe und ausschließlich unter Verwendung der aufgeführten Quellen und Hilfsmittel angefertigt habe. Die Darstellung meiner Eigenanteile in den aufgeführten Publikationen ist zutreffend.

Ort, Datum

Marcel Schmidt



## Erklärung zur Dissertation

Ich erkläre hiermit, dass ich bisher an keiner anderen Hochschule oder Fakultät meine Promotionsabsicht beantragt habe.

Die vorliegende kumulative Dissertation wurde bereits in Form von wissenschaftlichen Publikationen veröffentlicht. Es handelt sich hierbei um folgende Publikationen, die anhand des Publikationsdatums chronologisch aufgelistet sind. Für alle in dieser Arbeit vorkommenden Publikationen liegen die entsprechenden Genehmigungen der Verlage (Reprint permissions) zur Zweitpublikation vor.

**PAPER 1:** Superior catalyst recycling in surfactant based multiphase systems - Quo vadis catalyst complex?

Tobias Pogrzeba, David Müller, Markus Illner, **Marcel Schmidt**, Yasemin Kasaka, Ariane Weber, Günter Wozny, Reinhard Schomäcker, Michael Schwarze

Chemical Engineering and Processing: Process Intensification, 2016, 99, 155-166

Eigenanteil: Vierter Autor. Der Einfluss verschiedener Parameter wie Temperatur, Hydrophobizität des Tensids etc. auf die Verteilung eines homogenen Katalysatorkomplexes in Mikroemulsionssystemen wurde gezeigt. Weiterhin wurden diese Informationen verwendet um einen Entwurf für ein entsprechendes Trennverfahren im industriellen Maßstab zu erarbeiten. Das gesamte Publikationsteam hat die Konzeption des Forschungsansatzes und die Versuchsplanung diskutiert. Ich habe mit Unterstützung der studentischen Hilfskraft Ariane Weber die experimentellen Untersuchungen zur Katalysatorverteilung und deren Auswertung und Interpretation übernommen. Außerdem wurde der entsprechende Teil im Manuskript von mir verfasst. David Müller und Markus Illner, die wissenschaftliche Mitarbeiter in der Arbeitsgruppe von Prof. Repke sind, haben mit Unterstützung des übrigen Publikationsteams ein entsprechendes Prozesskonzept für Reaktionen im Mikroemulsionssystem entworfen und verfasst.

**PAPER 2:** Verteilungsgleichgewichte von Liganden in mizellaren Lösungsmittelsystemen

Marcel Schmidt, Tobias Pogrzeba, Dmitrij Stehl, René Sachse, Michael Schwarze, Regine von Klitzing, Reinhard Schomäcker

Chemie Ingenieur Technik, 2016, 88, 119-127

Eigenanteil: Erstautor. Mizellare Medien als Reaktionssystem für die homogene Katalyse sind eine vielversprechende Alternative zu konventionellen Lösungsmittelsystemen. Dieser Beitrag untersucht die Verteilung von Liganden bzw. des Katalysatorkomplexes in wässrig-mizellaren Medien und in einzelnen Phasen eines tensid-basierten Mehrphasensystems. Die Konzeption des Forschungsansatzes stammt von Michael Schwarze. Ich war hauptverantwortlich für die Datenanalyse und -interpretation und das Schreiben des Manuskriptes. Die Datenerhebung war Teil der Bachelorarbeit von René Sachse. Ergänzende Untersuchungen wurde von mir zur Vervollständigung der Daten durchgeführt. Der wissenschaftliche Mitarbeiter Tobias Pogrzeba unterstützte bei der Interpretation der Daten. Die Oberflächenspannung wurde von Dmitrij Stehl (wissenschaftlicher Mitarbeiter der Arbeitsgruppe von Prof. von Klitzing) gemessen.

**PAPER 3:** Hydroformylation in microemulsions: Proof of concept in a miniplant

Markus Illner and David Müller, Erik Esche, Tobias Pogrzeba, **Marcel Schmidt**, Reinhard Schomäcker, Günter Wozny, Jens-Uwe Repke

Industrial & Engineering Chemistry Research, 2016, 55, 8616-8626

Eigenanteil: Vierter Autor. Die Laborergebnisse der Hydroformylierung von 1-Dodecen wurden in einer kontinuierlich-betriebenen Miniplant verifiziert. In diesem Beitrag wurde der Aufbau und Betrieb dieser Anlage, sowie die entsprechenden Ergebnisse, insbesondere zur Phasentrennung in dem speziell dafür entwickelten Dekanter, erläutert. Ich lieferte einen erheblichen Beitrag bei der Versuchsplanung, Analytik und durchgehenden Betrieb (200 Betriebsstunden) der Miniplant. Hauptverantwortlich für den Betrieb der Anlage waren Markus Illner, David Müller und Erik Esche, welche allesamt wissenschaftliche Mitarbeiter der Arbeitsgruppe von Prof. Repke sind.

**PAPER 4:** Catalytic reactions in aqueous surfactant-free multiphase emulsions

Tobias Pogrzeba, **Marcel Schmidt**, Lena Hohl, Ariane Weber, Georg Buchner, Joschka Schulz, Michael Schwarze, Matthias Kraume, Reinhard Schomäcker

Industrial & Engineering Chemistry Research, 2016, 55, 12765-12775

Eigenanteil: Zweiter Autor. Am Beispiel der Hydroformylierung von 1-Dodecen und der Suzuki Kupplung wurde ein tensidfreies Reaktionssystem mit einem kurzkettigen Amphiphil als Lösungsvermittler vorgestellt. Hauptaugenmerk lag hierbei auf der Möglichkeit durch entsprechende Wahl der Versuchsbedingungen den Katalysatorkomplex quantitativ zu recyceln. Die Datenerhebung erfolgte größtenteils im Rahmen der Bachelorarbeit von Ariane Weber (Hydroformylierung) und der Masterarbeit von Georg Buchner (Suzuki Kupplung). Ich habe Tobias Pogrzeba bei der Versuchsplanung, Dateninterpretation und bei ergänzenden Untersuchungen unterstützt. Lena Hohl (wissenschaftliche Mitarbeiterin der Arbeitsgruppe von Prof. Kraume) und der Student Joschka Schulz haben die Phasenvolumina bestimmt.

**PAPER 5:** Microemulsion systems as switchable reaction media for the catalytic upgrading of long-chain alkenes

Tobias Pogrzeba, Markus Illner, **Marcel Schmidt**, Jens-Uwe Repke, Reinhard Schomäcker

Chemie Ingenieur Technik, 2017, 89, 459-463

Eigenanteil: Dritter Autor. In dieser Arbeit wurde die Anwendbarkeit von Mikroemulsionssystemen für die Hydroformylierung von 1-Dodecen gezeigt. Dabei wurde insbesondere auf die Übertragung der Laborergebnisse auf den kontinuierlichen Betrieb der Miniplant eingegangen. Ich habe den wissenschaftlichen Mitarbeiter Tobias Pogrzeba bei der Versuchsplanung und Dateninterpretation unterstützt. Weiterhin war ich aktiver Bestandteil des Teams beim Betrieb der Miniplant, welcher von Markus Illner (wissenschaftlicher Mitarbeiter der Arbeitsgruppe von Prof. Repke) geleitet wurde.

**PAPER 6:** Improving the catalytic activity in the rhodium-mediated hydroformylation of styrene by a Bis(N-heterocyclic silyene) ligand

**Marcel Schmidt**, Burgert Blom, Tibor Szilvási, Reinhard Schomäcker, Matthias Driess

European Journal of Inorganic Chemistry, 2017, 9, 1284-1291

Eigenanteil: Erstautor. Zur Steigerung der Aktivität von homogen-katalysierten Reaktionen spielen neuartige Liganden eine entscheidende Rolle. In dieser Arbeit wurden neuartige N-heterozyklische Silyene als Liganden am Beispiel der rhodium-katalysierten Hydroformylierung von Styrol untersucht. Reinhard Schomäcker und Matthias Driess lieferten das Konzept der Forschungsarbeit. Ich habe die Versuche mit Unterstützung von Burgert Blom (Post-doc der Arbeitsgruppe von Prof. Driess) geplant, durchgeführt und ausgewertet, wobei Burgert Blom vorwiegend den analytischen Teil durchgeführt hat. Tibor Szilvási hat die DFT Berechnungen ausgeführt. Ich war für das Schreiben des Manuskriptes zuständig.

**PAPER 7:** Palladium-catalyzed methoxycarbonylation of 1-dodecene in biphasic systems - Optimization of catalyst recycling

**Marcel Schmidt**, Tobias Pogrzeba, Lena Hohl, Ariane Weber, André Kielholz, Matthias Kraume, Reinhard Schomäcker

Molecular Catalysis, 2017, 439, 1-8

Eigenanteil: Erstautor. In dieser Veröffentlichung wurde die Verwendung eines Zweiphasensystems hinsichtlich der quantitativen Abtrennung des Katalysators für die Methoxycarbonylierung von 1-Dodecen demonstriert. Besonderes Augenmerk lag auf dem Zusammenhang zwischen Reaktionsperformance und Güte des Katalysatorrecyclings. Ich war hauptverantwortlich für die Konzeption des Forschungsansatzes, der Planung der Untersuchungen sowie für das Schreiben des Manuskriptes. Ein Großteil der experimentellen Untersuchungen wurden im Zuge der Bachelorarbeit von André Kielholz durchgeführt, die von mir betreut wurde. Ergänzende experimentelle Untersuchungen wurden von mir durchgeführt. Tobias Pogrzeba (wissenschaftlicher Mitarbeiter) und Ariane Weber (studentische Hilfskraft) unterstützen bei der Interpretation der Daten. Lena Hohl (wissenschaftliche Mitarbeiterin der Arbeitsgruppe von Prof. Kraume) führte die Untersuchungen zur Grenzflächenspannung und Tröpfchengröße durch.

**PAPER 8:** Understanding the role of nonionic surfactants during the catalysis in microemulsion systems on the example of rhodium-catalyzed hydroformylation

Tobias Pogrzeba, **Marcel Schmidt**, Natasa Milojevic, Carolina Urban, Markus Illner, Jens-Uwe Repke, Reinhard Schomäcker

Industrial & Engineering Chemistry Research, 2017, 56, 9934-9941

Eigenanteil: Zweiter Autor. In dieser Arbeit wurde der Einfluss nichtionischer Tenside auf die Hydroformylierung von 1-Dodecen untersucht. Durch systematische Variation der Temperatur, Tensidkonzentration und der Hydrophobizität des Tensids konnte der Einfluss des Phasenverhaltens des Mikroemulsionssystems auf die Reaktionsergebnisse diskutiert werden. Die Datenerhebung erfolgte größtenteils im Rahmen der Bachelorarbeit von Natasa Milojevic und Carolina Urban, die beide von Tobias Pogrzeba betreut wurden. Ergänzende experimentelle Untersuchungen wurden von Tobias Pogrzeba durchgeführt. Ich habe Tobias Pogrzeba bei der Versuchsplanung und Dateninterpretation unterstützt.

**PAPER 9:** Alkaline hydrolysis of methyl decanoate in surfactant based systems

Marcel Schmidt, Johannes Deckwerth, Reinhard Schomäcker, Michael Schwarze

The Journal of Organic Chemistry, 2018, 83, 14, 7398-7406

Eigenanteil: Erstautor. Die basische Verseifung von langkettigen Estern ist durch die geringe Löslichkeit des Substrates in wässrigen Medien gehemmt. In dieser Veröffentlichung wurden systematisch eine Reihe von ionischen und nichtionischen Tensiden zur Modifizierung des Reaktionssystems getestet um die basische Verseifung von Methyldecanoat in wässrigen Medien zu ermöglichen. Es stellte sich heraus, dass das resultierende Produkt der Verseifung, die Decansäure, selbst grenzflächenaktiv ist und somit autokatalytisch die Verseifung beschleunigt. Für die Konzeption des Forschungsansatzes und die Versuchsplanung war ich verantwortlich. Ein Großteil der veröffentlichten Daten wurden von Johannes Deckwerth im Rahmen seiner Bachelorarbeit erbracht, die von mir betreut wurde, wobei ergänzende Untersuchungen von mir durchgeführt wurden. Für das Schreiben des Manuskriptes war ich ebenfalls zuständig, wobei Michael Schwarze die Einleitung dieser Veröffentlichung verfasst hat.

**PAPER 10:** Palladium-catalyzed methoxycarbonylation of 1-dodecene in a two-phase system: The path toward a continuous process

Markus Illner and **Marcel Schmidt**, Tobias Pogrzeba, Carolina Urban, Erik Esche, Reinhard Schomäcker, Jens-Uwe Repke

Industrial & Engineering Chemistry Research, 2018, 57, 8884-8894

Eigenanteil: Geteilte Erstautorenschaft mit Markus Illner. In diesem Beitrag werden Laborergebnisse und deren Übertragung in eine kontinuierlich-betriebene Miniplant für die palladium-katalysierte Methoxycarbonylierung präsentiert. Die Erreichung eines stabilen Betriebspunktes, der sich durch eine hohe Ausbeute mit stabiler Phasentrennung auszeichnet, war hierbei der Schwerpunkt. Für die Konzeption des Forschungsansatzes und die Versuchsplanung waren Markus Illner (wissenschaftlicher Mitarbeiter der Arbeitsgruppe von Prof. Repke) und ich zuständig. Die Labordaten wurden von mir mit Unterstützung von der studentischen Hilfskraft Carolina Urban erhoben, wobei deren Interpretation mit dem gesamten Publikationsteam diskutiert wurden. Weiterhin habe ich beim Betrieb des Prozesses in der Miniplant maßgeblich mitgearbeitet und auch diese Ergebnisse vorwiegend mit Markus Illner ausgewertet und interpretiert. Für das Schreiben des Manuskriptes waren in gleichen Anteilen Markus Illner und ich verantwortlich.

**PAPER 11:** Palladium-catalyzed hydroxycarbonylation of 1-dodecene in microemulsion systems: Does reaction performance care about phase behavior?

Marcel Schmidt, Carolina Urban, Svenja Schmidt, Reinhard Schomäcker

ACS Omega, 2018, 3, 13355-13364

Eigenanteil: Erstautor. In diesem Beitrag wurde die Hydrocarboxylierung von 1-Dodecen im Mikroemulsionssystem untersucht. Schwerpunkt lag auf der Erörterung des Zusammenhangs zwischen Phasenverhalten und Reaktionsleistung um die Rolle des Tensids zu verdeutlichen. Ich war für den methodischen Schwerpunkt des Forschungsansatzes, die detaillierte Versuchsplanung, die Datenauswertung und -interpretation sowie das Schreiben des Manuskriptes zuständig. Ein Teil der Daten (ca. 30%) wurden von Svenja Schmidt im Rahmen ihrer Bachelorarbeit erhoben, die von mir betreut wurde. Ein Großteil der experimentellen Untersuchungen wurden von mir mit Unterstützung von Carolina Urban (studentische Hilfskraft) durchgeführt.

Im Anhang dieser Dissertation sind die jeweiligen Exemplare der hier aufgeführten Publikationen beigelegt.

Ort, Datum

Marcel Schmidt



## Abstract

Catalysis plays a major role in chemistry. In particular, homogeneous catalysis opens the door to a sustainable synthesis of many products, offering mild reaction conditions, excellent activity as well as selectivity. However, the recycling of the expensive catalyst complexes is a major drawback, hampering the implementation of homogeneous catalysis for industrial application. Hence, alternative approaches for the recycling of homogeneous catalysts in its active form are in the focus of current research, combining the advantages of both, homogeneous and heterogeneous catalysis. In this thesis, the applicability of multiphase systems for the palladium-catalyzed methoxy- and hydroxycarbonylation of different substrates is investigated, enabling a consecutive catalyst recycling and product separation via temperature-induced phase separation. Special attention is given to the selection of the solvents/additives to ensure catalyst stability, quantitative catalyst recycling, product separation and overall good reaction performance. The immobilization of the palladium-based catalyst in the polar phase is guaranteed by the use of the watersoluble ligand SulfoXantPhos and methane sulfonic acid as co-catalyst in a ratio of 1:4:40, facilitating the long term catalyst stability.

For the methoxycarbonylation of 1-dodecene in multiphase systems, the path toward a continuous process is reported, including solvent selection, parameter studies and the proof of concept in a miniplant. A simple biphasic system can be used composed of water/methanol as polar phase and octane/1-dodecene as nonpolar phase, leading to a good reaction performance and fast phase separation at room temperature (Pd leaching < 1 ppm). Parameter studies reveal catalyst stability up to 80 °C, achieving a yield of 92% to the corresponding ester after a reaction time of 20 h. Moreover, the transfer of the lab scale results into a continuously operated miniplant (reaction volume scale up factor: 19) is shown, operating continuously over 100 h with stable phase separation (Pd leaching < 25 ppb) and under steady state conditions (yield to the ester = 83.5%).

In contrast, the palladium-catalyzed hydroxycarbonylation of 1-dodecene is not feasible in a simple biphasic system without additives, since the solubility of the substrate is too low in the catalyst phase. Herein, the complex role of surfactants as additives and the interaction between the phase behavior and reaction performance is investigated. The investigations reveal that not the phase behavior of the microemulsion system but mainly the size of the oil–water interface and the local concentrations at this interface control the reaction performance of the hydroxycarbonylation in these systems.



## Zusammenfassung

Katalyse spielt in der Chemie eine große Rolle. Insbesondere die homogene Katalyse ebnet den Weg zu einer nachhaltigen Synthese vieler Produkte, da milde Reaktionsbedingungen, hervorragende Aktivitäten sowie Selektivitäten realisiert werden können. Jedoch ist das Recycling des meist teuren Katalysatorkomplexes ein entscheidender Nachteil, der die industrielle Umsetzung der homogenen Katalyse erschwert. Daher stehen alternative Ansätze für das Recycling von homogenen Katalysatoren im Fokus der aktuellen Forschung. In dieser Arbeit wird die Anwendbarkeit von Mehrphasensystemen für die Palladium-katalysierte Methoxy- und Hydroxycarbonylierung verschiedener Substrate untersucht, was eine anschließende Katalysatorrückführung und Produktabtrennung durch Phasentrennung ermöglicht. Besonderes Augenmerk wird dabei auf die Auswahl der Lösungsmittel/Additive gelegt, um Katalysatorstabilität, quantitatives Katalysatorrecycling, Produktabtrennung und eine gute Reaktionsleistung zu gewährleisten. Die Immobilisierung des Palladium-basierten Katalysators in der polaren Phase wird durch die Verwendung des wasserlöslichen Liganden SulfoXantPhos ermöglicht. Um die Langzeitstabilität des Katalysators zu gewährleisten, wird Methansulfonsäure als Kokatalysator eingesetzt, wobei ein Pd:Ligand:Kokatalysator Verhältnis von 1:4:40 verwendet wird.

Für die Methoxycarbonylierung von 1-Dodecen im Mehrphasensystem wird der Weg vom Labor zu einem kontinuierlichen Prozess im Pilotanlagenmaßstab beschrieben, einschließlich Lösungsmittelauswahl, Parameterstudien und Konzeptnachweis in der Pilotanlage. Es kann ein einfaches Zweiphasensystem verwendet werden, welches aus Wasser/Methanol als polare Phase und Oktan/1-Dodecen als unpolare Phase besteht, was zu einer guten Reaktionsleistung und schnellen Phasentrennung bei Raumtemperatur führt (Pd-Verlust < 1 ppm). Die Parameterstudien zeigen, dass die Katalysatorstabilität bis 80 °C gegeben ist, wobei eine Ausbeute zum entsprechenden Ester von 92% nach 20 h Reaktionszeit erzielt wird. Darüber hinaus wird die Übertragung der Laborergebnisse in eine kontinuierlich-betriebene Pilotanlage (Reaktionsvolumen-Skalierungsfaktor: 19) gezeigt, welche über 100 Stunden kontinuierlich mit stabiler Phasentrennung (Pd-Verlust < 25 ppb) und unter stationären Bedingungen (Ausbeute des Esters = 83,5%) betrieben wurde.

Im Gegensatz dazu ist die Palladium-katalysierte Hydroxycarbonylierung von 1-Dodecen in einem einfachen Zweiphasensystem ohne Additive nicht möglich, da die Löslichkeit des Substrats in der Katalysatorphase zu gering ist. Hierbei wird die komplexe Rolle von Tensiden als Additiv und die Wechselwirkung zwischen Phasenverhalten und Reaktionsverhalten untersucht. Die Untersuchungen zeigen, dass nicht das Phasenverhalten des Mikroemulsionssystems, sondern hauptsächlich die Größe der Öl-Wasser-Grenzfläche und die lokalen Konzentrationen der Substrate und des Katalysatorkomplexes an dieser Grenzfläche die Reaktionsleistung der Hydroxycarbonylierung steuern.



## List of Publications

### Contributing publications

Here, all publications are listed in chronological order which contribute to this cumulative thesis.

**PAPER 1:** Superior catalyst recycling in surfactant based multiphase systems - Quo vadis catalyst complex?

T. Pogrzeba, D. Müller, M. Illner, **M. Schmidt**, Y. Kasaka, A. Weber, G. Wozny, R. Schomäcker, M. Schwarze: *Chem. Eng. Process.*, **2016**, 99, 155-166.

DOI: [10.1016/j.cep.2015.09.003](https://doi.org/10.1016/j.cep.2015.09.003)

**PAPER 2:** Verteilungsgleichgewichte von Liganden in mizellaren Lösungsmittelsystemen

**M. Schmidt**, T. Pogrzeba, D. Stehl, R. Sachse, M. Schwarze, R. von Klitzing, R. Schomäcker: *Chem. Ing. Tech.*, **2016**, 88, 119-127.

DOI: [10.1002/cite.201500125](https://doi.org/10.1002/cite.201500125)

**PAPER 3:** Hydroformylation in microemulsions: Proof of concept in a miniplant

M. Illner and D. Müller, E. Esche, T. Pogrzeba, **M. Schmidt**, R. Schomäcker, G. Wozny, J.-U. Repke: *Ind. Eng. Chem. Res.*, **2016**, 55, 8616-8626.

DOI: [10.1021/acs.iecr.6b00547](https://doi.org/10.1021/acs.iecr.6b00547)

**PAPER 4:** Catalytic reactions in aqueous surfactant-free multiphase emulsions

T. Pogrzeba, **M. Schmidt**, L. Hohl, A. Weber, G. Buchner, J. Schulz, M. Schwarze, M. Kraume, R. Schomäcker: *Ind. Eng. Chem. Res.*, **2016**, 55, 12765-12775.

DOI: [10.1021/acs.iecr.6b03384](https://doi.org/10.1021/acs.iecr.6b03384)

**PAPER 5:** Microemulsion systems as switchable reaction media for the catalytic upgrading of long-chain alkenes

T. Pogrzeba, M. Illner, **M. Schmidt**, J.-U. Repke, R. Schomäcker: *Chem. Ing. Tech.*, **2017**, 89, 459-463.

DOI: [10.1002/cite.201600140](https://doi.org/10.1002/cite.201600140)

**PAPER 6:** Improving the catalytic activity in the rhodium-mediated hydroformylation of styrene by a Bis(N-heterocyclic silyene) ligand

**M. Schmidt**, B. Blom, T. Szilvási, R. Schomäcker, M. Driess: Eur. J. Inorg. Chem., **2017**, 9, 1284-1291.

DOI: [10.1002/ejic.201700148](https://doi.org/10.1002/ejic.201700148)

**PAPER 7:** Palladium-catalyzed methoxycarbonylation of 1-dodecene in biphasic systems - Optimization of catalyst recycling

**M. Schmidt**, T. Pogrzeba, L. Hohl, A. Weber, A. Kielholz, M. Kraume, R. Schomäcker: Mol. Catal., **2017**, 439, 1-8.

DOI: [10.1016/j.mcat.2017.06.014](https://doi.org/10.1016/j.mcat.2017.06.014)

**PAPER 8:** Understanding the role of nonionic surfactants during the catalysis in microemulsion systems on the example of rhodium-catalyzed hydroformylation

T. Pogrzeba, **M. Schmidt**, N. Milojevic, C. Urban, M. Illner, J.-U. Repke, R. Schomäcker: Ind. Eng. Chem. Res., **2017**, 56, 9934-9941.

DOI: [10.1021/acs.iecr.7b02242](https://doi.org/10.1021/acs.iecr.7b02242)

**PAPER 9:** Alkaline hydrolysis of methyl decanoate in surfactant based systems

**M. Schmidt**, J. Deckwerth, R. Schomäcker, M. Schwarze: J. Org. Chem., **2018**, 83, 14, 7398-7406.

DOI: [10.1021/acs.joc.8b00247](https://doi.org/10.1021/acs.joc.8b00247)

**PAPER 10:** Palladium-catalyzed methoxycarbonylation of 1-dodecene in a two-phase system: The path toward a continuous process

M. Illner and **M. Schmidt**, T. Pogrzeba, C. Urban, E. Esche, R. Schomäcker, J.-U. Repke: Ind. Eng. Chem. Res., **2018**, 57, 8884-8894.

DOI: [10.1021/acs.iecr.8b01537](https://doi.org/10.1021/acs.iecr.8b01537)

**PAPER 11:** Palladium-catalyzed hydroxycarbonylation of 1-dodecene in microemulsion systems: Does reaction performance care about phase behavior?

**M. Schmidt**, C. Urban, S. Schmidt, R. Schomäcker: ACS Omega, **2018**, 3, 13355-13364.

DOI: [10.1021/acsomega.8b01708](https://doi.org/10.1021/acsomega.8b01708)

**Non-contributing publications**

In the following, all publications are listed which were published during the time as scientific assistant at the chair of technical chemistry, TU Berlin, but do not contribute to this thesis.

**PAPER 12:** A novel process concept for the three step Boscalid<sup>®</sup> synthesis

I. Volovych, M. Neumann, **M. Schmidt**, G. Buchner, J.-Y. Yang, J. Wölk, T. Sottmann, R. Strey, R. Schomäcker, M. Schwarze: RSC Adv., **2016**, 6, 58279-58287.

DOI: [10.1039/C6RA10484C](https://doi.org/10.1039/C6RA10484C)

**PAPER 13:** Characteristics of stable pickering emulsions under process conditions

D. Stehl, L. Hohl, **M. Schmidt**, J. Hübner, M. Lehmann, M. Kraume, R. Schomäcker, R. von Klitzing: Chem. Ing. Tech., **2016**, 88, 1806-1814.

DOI: [10.1002/cite.201600065](https://doi.org/10.1002/cite.201600065)

**PAPER 14:** Hydrogenation of itaconic acid in micellar solutions: Catalyst recycling with cloud point extraction?

**M. Schmidt**, S. Schreiber, L. Franz, H. Langhoff, A. Farhang, M. Horstmann, H.-J. Drexler, D. Heller, M. Schwarze: Ind. Eng. Chem. Res., **2019**, 58, 2445-2453.

DOI: [10.1021/acs.iecr.8b03313](https://doi.org/10.1021/acs.iecr.8b03313)



---

## Table of Contents

<b>Eidesstattliche Erklärung</b> .....	<b>I</b>
<b>Erklärung zur Dissertation</b> .....	<b>III</b>
<b>Abstract</b> .....	<b>XI</b>
<b>Zusammenfassung</b> .....	<b>XIII</b>
<b>List of Publications</b> .....	<b>XV</b>
Contributing publications .....	XV
Non-contributing publications .....	XVII
<b>Table of Contents</b> .....	<b>XIX</b>
<b>Symbols and Abbreviations</b> .....	<b>XXI</b>
<b>List of Figures</b> .....	<b>XXIII</b>
<b>List of Tables</b> .....	<b>XXV</b>
<b>1. Introduction</b> .....	<b>1</b>
1.1 Motivation.....	1
1.2 Outline of this Work .....	2
<b>2. Theoretical Background</b> .....	<b>4</b>
2.1 Reppe Carbonylation.....	4
2.1.1 "Carboxy" vs. "Hydride" Mechanism .....	5
2.1.2 Mechanism of Methoxycarbonylation.....	6
2.1.3 Deactivation pathways of homogeneous palladium catalysts .....	8
2.1.4 Kinetic studies .....	9
2.1.5 Industrial application .....	11
2.2 Green Chemistry .....	12
2.3 Multiphase Systems.....	13
2.3.1 Aqueous biphasic systems .....	15
2.3.2 Surfactant-based multiphase systems.....	16
2.3.3 Miscellaneous multiphase systems.....	18
<b>3. Experimental Part</b> .....	<b>21</b>
3.1 Chemicals .....	21

3.2	Determination of CMC .....	21
3.3	Investigation on the phase behavior .....	21
3.4	Preformation of the Catalyst for Carbonylation Reactions.....	22
3.5	Setup for Carbonylation Reactions .....	22
3.6	Experimental Procedure for Carbonylation Reactions .....	23
3.7	Determination of Catalyst Leaching and Product Distribution .....	24
3.8	General procedure of the Alkaline Hydrolysis.....	24
<b>4.</b>	<b>Results and Discussion.....</b>	<b>26</b>
4.1	Green Chemistry and InPROMPT .....	26
4.1.1	Status Quo - Hydroformylation in Microemulsion Systems .....	27
4.1.2	Silylene Ligands as Alternatives .....	28
4.2	Methoxycarbonylation in Microemulsion Systems .....	30
4.2.1	Impact of Methanol on the Phase Behavior .....	31
4.2.2	Impact of Methanol on the Reaction Performance .....	32
4.3	Methoxycarbonylation in Biphasic Systems.....	33
4.3.1	Solvent Selection .....	34
4.3.2	Parameter studies.....	38
4.3.3	Proof of concept in a miniplant.....	40
4.4	Hydroxycarbonylation in Microemulsion Systems.....	42
4.4.1	Catalyst Behavior in Microemulsion Systems.....	42
4.4.2	Nonionic Surfactants as Phase Transfer Agent.....	44
4.4.3	Ionic Surfactants as Phase Transfer Agent.....	47
4.5	Alkaline Hydrolysis of long chain esters.....	50
4.5.1	Alkaline Hydrolysis in Water .....	50
4.5.2	Alkaline Hydrolysis in Surfactant-Based Systems.....	51
<b>5.</b>	<b>Conclusion.....</b>	<b>54</b>
	<b>References .....</b>	<b>56</b>
	<b>Acknowledgement.....</b>	<b>63</b>
	<b>Appendix .....</b>	<b>64</b>

## Symbols and Abbreviations

Table I. List of abbreviations.

Abbreviation	Description
CMC	Critical micelle concentration
CTAB	Hexadecyltrimethylammonium bromide
DecMIM	1-Methyl-3-decylimidazolium bromide
DeTAB	Decyltrimethylammonium bromide
DFT	Density functional theory
DodecMIM	1-Methyl-3-dodecylimidazolium bromide
DTAB	Dodecyltrimethylammonium bromide
d <sup>l</sup> bpx	1,2-bis(di- <i>tert</i> -butylphosphinomethyl)benzene
FID	Flame ionization detector
ICP-OES	Inductively coupled plasma optical emission spectrometry
MMA	Methyl methacrylate
MSA	Methane sulfonic acid
NHSi	N-heterocyclic silylene
NMR	Nuclear magnetic resonance
<i>p</i> -TSA	<i>para</i> -Toluenesulfonic acid
OMIM	1-Methyl-3-octylimidazolium bromide
RDS	Rate-determining step
scCO <sub>2</sub>	Supercritical carbon dioxide
SDS	Sodium dodecyl sulfate
SX	SulfoXantPhos
TFA	Trifluoroacetic acid
TMS	Thermomorphic multicomponent system
TOF	Turn over frequency
TPP	Triphenylphosphine
TPPTS	3,3',3''-Phosphanetriyltris(benzenesulfonic acid) trisodium salt
TTAB	Tetradecyltrimethylammonium bromide



---

## List of Figures

<b>Figure 1.</b> Outline of this work. ....	2
<b>Figure 2.</b> Reppe Carbonylation of alkenes with different nucleophiles.....	4
<b>Figure 3.</b> Proposed "hydride" and "carboxy" mechanism for the methoxycarbonylation of ethene.....	5
<b>Figure 4.</b> Proposed "hydride" mechanism for the methoxycarbonylation of an olefin (green background) including the formation of active palladium-hydride species (yellow background) and possible catalyst deactivation pathways (red background), L = CO, MeOH, solvent, coordinating anion of the acid or anion of palladium precursor, ligand.	7
<b>Figure 5.</b> The Twelve Principles of Green Chemistry. ....	12
<b>Figure 6.</b> Gibbs phase prism for a microemulsion system consisting of oil, water and a nonionic surfactant (left picture), cut of the phase prism at $\alpha=0.5$ (right picture).....	17
<b>Figure 7.</b> Experimental setup for methoxy- and hydroxycarbonylation reaction. ....	22
<b>Figure 8.</b> Schematic process concept for the hydroformylation of long-chain alkenes in microemulsion systems.....	26
<b>Figure 9.</b> Miniplant operation results for the hydroformylation of 1-dodecene. ....	28
<b>Figure 10.</b> Schematic comparison between the hydroformylation and methoxycarbonylation reaction. ....	30
<b>Figure 11.</b> Phase boundaries for the microemulsion system consisting of water, 1-dodecene and Marlipal 24/70 with different amounts of MeOH. ....	31
<b>Figure 12.</b> Yield of tridecanoic acid, dodecane and methyl tridecanoate for the methoxycarbonylation in microemulsion systems. ....	33
<b>Figure 13.</b> Reaction mixture after phase separation at room temperature (separation time of 10 min).....	36
<b>Figure 14.</b> Mini-plant operation results for the methoxycarbonylation of 1-dodecene...	41
<b>Figure 15.</b> Schematic pictures of the oil-in-water microemulsion, triphasic system and water-in-oil microemulsion for the palladium-catalyzed hydroxycarbonylation of 1-dodecene. ....	44
<b>Figure 16.</b> Phase diagram of a mixture of 1-dodecene, dodecane, water, and Marlipal (24/50). ....	45
<b>Figure 17.</b> Effect of the surfactant concentration on the hydroxycarbonylation of 1-dodecene. ....	46
<b>Figure 18.</b> Reaction sequence for the synthesis of carboxylic acids from olefins. ....	50
<b>Figure 19.</b> Effect of the temperature on the conversion plot of the alkaline hydrolysis of methyl decanoate in water.....	51



## List of Tables

<b>Table 1.</b> Conversion, l:b ratio and TOF of the hydroformylation with [HRh(CO)(PPh <sub>3</sub> )L <sub>2</sub> ] complexes containing bidentate ligands L <sub>2</sub> at different temperatures.....	29
<b>Table 2.</b> Methoxycarbonylation of 1-dodecene: Modification of the polar phase.....	35
<b>Table 3.</b> Methoxycarbonylation in biphasic systems: Substrate scope.....	37
<b>Table 4.</b> Methoxycarbonylation of 1-dodecene: Variation of the temperature.....	39
<b>Table 5.</b> Hydroxycarbonylation of 1-dodecene: Ionic surfactants as phase transfer agents.....	47
<b>Table 6.</b> Hydroxycarbonylation of 1-dodecene: Ionic liquids as phase transfer agents..	48
<b>Table 7.</b> Hydroxycarbonylation of 1-dodecene: Variation of OMIM concentration.....	49
<b>Table 8.</b> CMC values and initial reaction rates for the alkaline hydrolysis in surfactant-based systems.....	52



# 1. Introduction

## 1.1 Motivation

The world changes. Futuristic cars creep without a sound along the street, wind parks emboss the natural scenery, biobased foodstuffs capture the racks in supermarkets, photovoltaic systems cover the roofs of many houses, different colored waste container awaits you in the backyard of buildings, green labels mark the packing of consumer products and many more. All these facts can be connected to the term sustainability. Circumstances have changed and as a result, the thinking of humans changed. 200 years ago, the term sustainability had no relevance in society because human action is subliminally based on sustainability. With the beginning of the Industrial Revolution at the end of the 18th century, the structural change from agriculture to industry is strongly associated with a huge growth of population and the increase in living standard. Thus, fossil resources have been made accessible to meet the needs of the growing society like energy demand and the craving for new products. However, the consumption of fossil resources is limited, which was not considered for a long time. Nowadays, the global annual oil production is still increasing but it is a question of time that the oil peak will come in near future and new solutions have to be established. Not only in this field but also in a lot of different areas like transportation, living, food, materials and many more, the global society faces new challenges because of the changed way of life. In all these areas, the term sustainability is on everyone's lips. A major role can be attributed to the natural and engineering sciences to meet the new requirements. Especially in chemistry, the way of thinking has changed. Formerly, the product itself with a certain functionality and its synthesis as much cheap as possible was in the focus. Nowadays, the term sustainability hovers above all. This means that not only economical but also ecological and social aspects have to be considered. Pioneering work was done by Paul Anastas and John Warner who established a guideline for a green and sustainable chemistry, opening out into the Twelve Principles of Green Chemistry.<sup>1</sup>

In this doctoral thesis, chemistry and engineering have been done, following the requirements of Green Chemistry. For sure, in the context of all global challenges, this work is only a drop in the bucket but it is a step in the right direction, gaining visibility and sensitizing the society for the future challenges. Herein, alternative reaction media for organic transformations, especially for the palladium-catalyzed methoxy- and hydroxycarbonylation reaction, have been investigated in the context of Green Chemistry, avoiding toxic solvents and using aqueous multiphase systems as the desired reaction medium. This

approach facilitates the recycling of the expensive catalyst in its active form and the separation of the product from the reaction mixture via simple phase separation. Moreover, the applicability of multiphase systems with subsequent catalyst recycling has been studied in a continuously operated miniplant. This methodology represents a green and sustainable approach for organic transformations on large scale with respect to economic, ecological, and even human demand.

## 1.2 Outline of this Work

This doctoral thesis is a cumulative work, based on eleven peer-reviewed papers in different international journals. Additional to the data from the papers, unpublished results are presented to illustrate the topical context of the published results. Mainly, this work is divided into three topics, which are depicted in Figure 1.

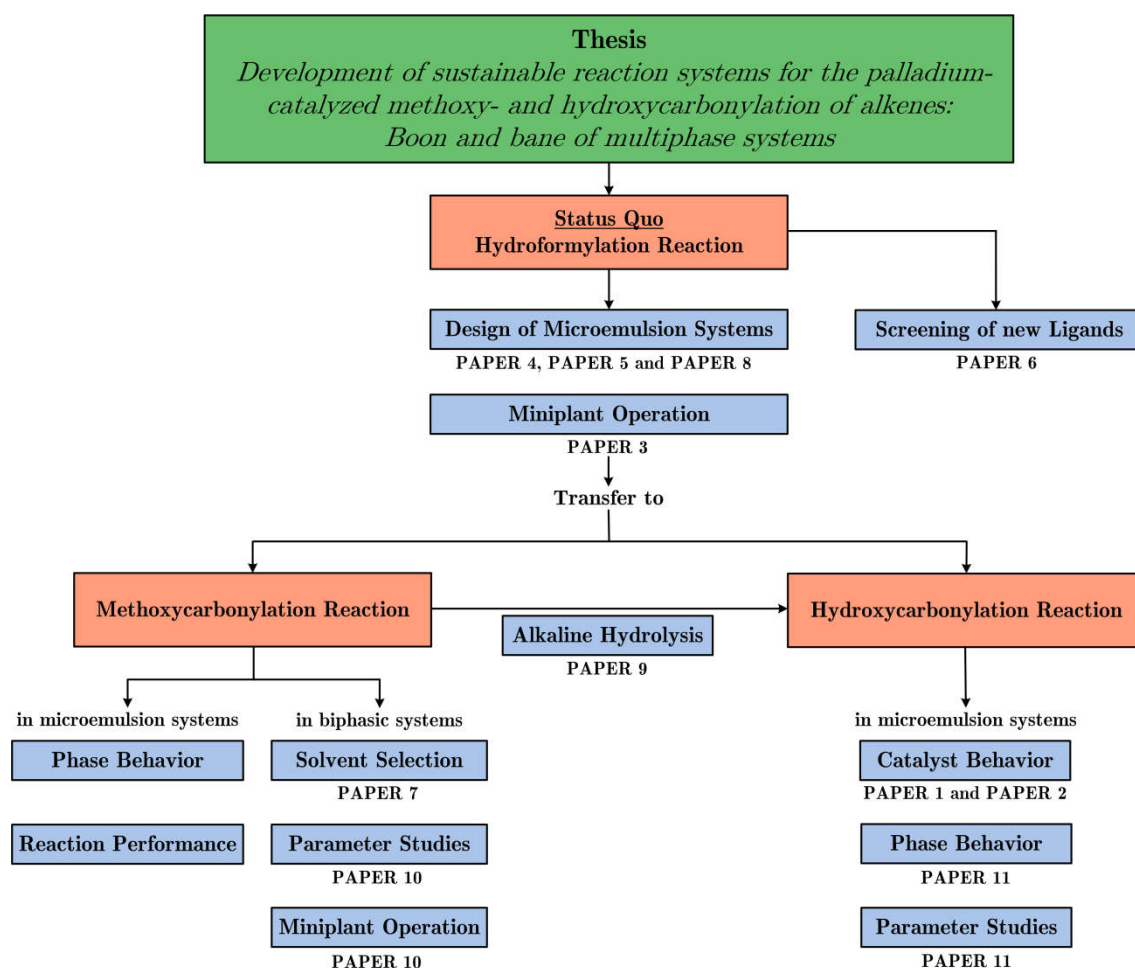


**Figure 1.** Outline of this work.

First, the status quo for the hydroformylation of 1-dodecene in microemulsion systems is presented, which was mainly a result of the doctoral thesis of former members from our group.<sup>2,3</sup> Additionally, new ligands for the hydroformylation

reaction that are based on silicon were tested, giving a significant boost in the catalytic activity. Second, the methoxycarbonylation of different alkenes in biphasic systems is investigated, including solvent selection, parameter studies, and the proof of concept in a continuously operated miniplant. Moreover, the methoxycarbonylation of 1-dodecene in microemulsion systems is presented, investigating the phase behavior and the reaction performance. Third, the hydroxycarbonylation of 1-dodecene in surfactant-based systems is studied, containing the catalyst behavior in microemulsion systems, the phase behavior of these systems, and parameter studies such as surfactant concentration.

## 2. Theoretical Background

### 2.1 Reppe Carbonylation<sup>4-6</sup>

Since the discovery in the 1930s, the Reppe carbonylation is one of the most important reactions functionalizing low-value feedstocks.<sup>7-12</sup> Initially, Walter Reppe reported the successful transformation of ethylene with carbon monoxide and water to acrylic acid, using nickel as catalyst. The principles of this reaction can be easily extended to a broad range of substrates, particularly alkenes and alkynes, which offers access to a wide spectrum of bulk and fine chemicals as well as intermediates for organic synthesis. Furthermore, a lot of different functional groups are tolerated during the reaction sequence, increasing the spectrum of possible products and thus, the attention of chemists.

In general, the Reppe carbonylation is a very atom economic transformation combining three different reactants: an unsaturated carbon chain, a source for the carbonyl unit and a nucleophile. Herein, the carbonylation of alkenes is in the focus (see Figure 2), but alkynes and conjugated dienes, especially butadiene<sup>13</sup>, can be used as well. Mostly, pure carbon monoxide is used as the carbonyl source. However, due to the difficult handling of gaseous carbon monoxide and its toxic properties, alternative carbonyl sources has been investigated like formic acid and its derivatives, metal carbonyl complexes or even aldehydes.<sup>14</sup>



**Figure 2.** Reppe Carbonylation of alkenes with different nucleophiles.

Depending on the applied nucleophile, different functional groups can be incorporated into the final product. If water or an alcohol is used as the nucleophile, the corresponding carboxylic acid or ester is formed, which is known as hydroxycarbonylation or alkoxy carbonylation, respectively. Moreover, carboxylic acids, amines or thiols can also be used as the nucleophile, producing the corresponding derivatives of the carboxylic acid. The reaction itself is catalyzed by several transition metals like Fe, Ru, Co, Rh, Ir, Pd and Pt. However, palladium as the catalyst precursor outperforms clearly the others in its catalytic activity and selectivity and thus, it is in focus of current research. To obtain high activity and selectivity, the presence and interaction of the

catalytic system consisting of the metal precursor, ligands and acidic co-catalysts is crucial, which is still intensively investigated.<sup>15-18</sup>

### 2.1.1 "Carboxy" vs. "Hydride" Mechanism

In order to control the activity and selectivity of any reaction sequence, a profound knowledge about a detailed mechanism of the reaction is indispensable. Initially, two different mechanisms for the methoxycarbonylation of olefins were proposed, which are schematically depicted in Figure 3.<sup>15,19,20</sup>

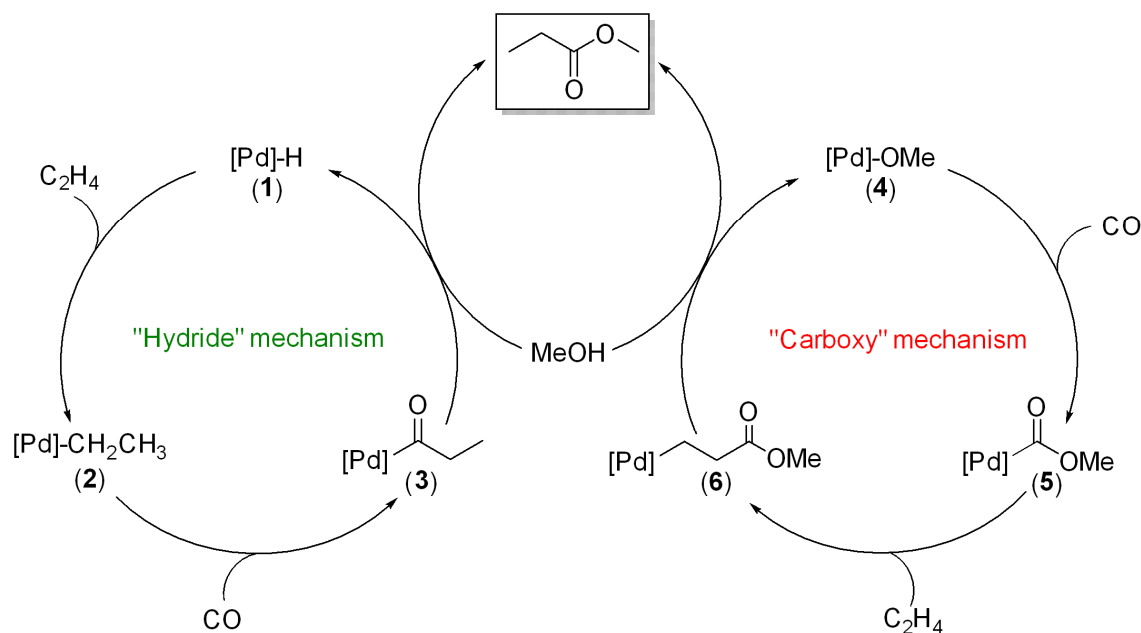


**Figure 3.** Proposed "hydride" and "carboxy" mechanism for the methoxycarbonylation of ethene.

On the one hand, the "carboxy" mechanism is based on the assumption of the formation of a palladium-methoxycarbonyl complex (5) from the CO insertion into the active palladium-methoxy species (4). The nucleophilic attack of methanol into the palladium-carbonyl species is also conceivable to obtain complex (5). Subsequently, an olefin insertion (6) and methanolysis step leads to the corresponding ester and reactivated methoxy species (4). In contrast, the "hydride" mechanism proposes a palladium-hydride (1) as the active catalyst species. The formation of the palladium-alkyl complex (2) by olefin insertion follows a CO insertion, forming the palladium-acyl species (3). The last step of the catalytic cycle is the nucleophilic attack of methanol, resulting in the corresponding ester and regenerating the active palladium-hydride complex (1). Based on theoretical and experimental studies with ethylene as the substrate, the "hydride" mechanism was found to dominate the methoxycarbonylation reaction.<sup>19,21-23</sup> The "hydride" mechanism was also confirmed for other substrates like styrene, methyl oleate and octene.<sup>24-26</sup> Nevertheless, dependent on the

reaction conditions and applied catalytic system, the "carboxy" mechanism cannot be excluded or both cycles could operate simultaneously.<sup>27</sup>

It is worth mentioning that two different products can be obtained using ethylene as substrate: Firstly, the methoxycarbonylation leads to the formation of the low boiling liquid methyl propanoate. Secondly, an alternating copolymerization of ethene and carbon monoxide can occur forming polyketones, which is a widely used thermoplast with an extra high resilience. Hereby, the chemoselectivity of the reaction is determined mainly by the choice of an appropriate phosphine ligand. Electron-donating and bulky diphosphines with a wide bite-angle favors the formation of the ester over the copolymerisation.<sup>28</sup>

### 2.1.2 Mechanism of Methoxycarbonylation

In the following, the "hydride" mechanism for the methoxycarbonylation of olefins is considered in more detail. Hereby, the formation of the active palladium-hydride complex, possible deactivation pathways of the catalyst system as well as the equilibria between the different intermediates in the catalytic cycle are in focus, which is illustrated in Figure 4. Particularly, bidentate phosphines are promising ligands for the methoxycarbonylation, leading to a good catalytic performance and selectivity, whereby 1,2-bis(di-*tert*-butylphosphinomethyl)benzene (*d*<sup>t</sup>bpx) as ligand outperforms the other diphosphines with its superior linear to branched selectivity.<sup>16</sup> Hence, the illustrated catalytic cycle is established for diphosphines. Moreover, acids with non-coordinating anions such as para-toluenesulfonic acid (*p*-TSA), methane sulfonic acid (MSA) or trifluoroacetic acid (TFA) act as co-catalyst and are necessary to perform the methoxycarbonylation reaction. Exemplarily, MSA is described in the proposed catalytic cycle.

Initially, the formation of the active palladium-hydride species is crucial for the methoxycarbonylation reaction, which was investigated in several studies. Starting from a palladium(II)-precursor, mostly the acetate or halide salt of palladium, the addition of a diphosphine and an acidic co-catalyst leads to the formation of cationic palladium complex (**7**), stabilized by the cis-coordinated diphosphine and coordinated acid. After addition of methanol, which coordinates to palladium complex (**7**), formaldehyde is eliminated via a  $\beta$ -hydride elimination.<sup>15,23</sup> As a result, the palladium-hydride complex (**8**) is formed, in which the solvent methanol is at the free coordination site. Depending on the reaction medium and conditions, the coordinated methanol could dissociate, giving the palladium complex (**9**). In contrast, palladium(0)-precursor are also suitable precursors to form the active palladium-hydride complex. Hereby, traces of oxygen or additional oxidizing agents could oxidize the zerovalent palladium precursor to palladium(II) in the presence of acid.<sup>23</sup>

Moreover, an oxidative addition of protonated phosphine ligand into zerovalent palladium species could form the active palladium-hydride complex (**9**).<sup>26</sup>

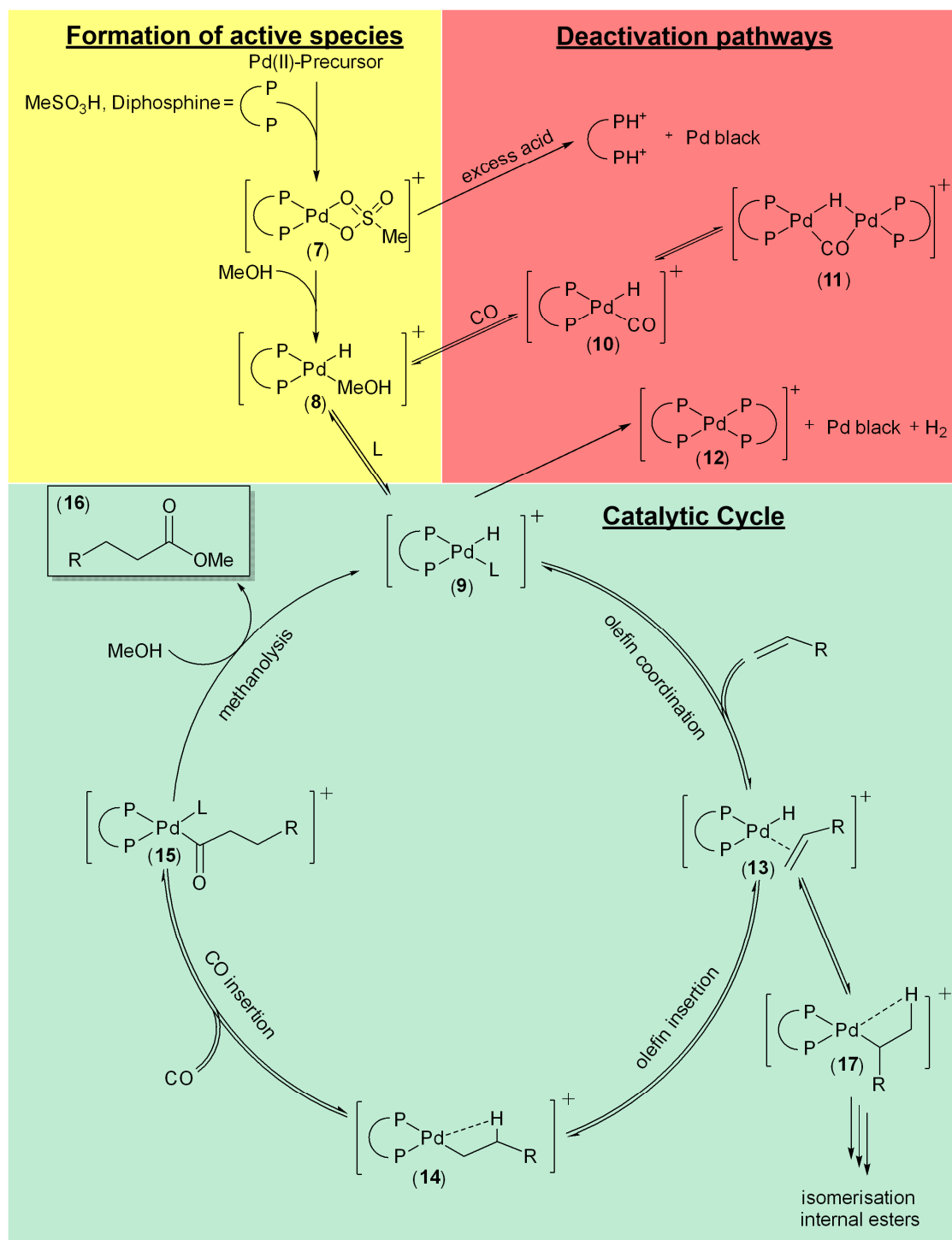


**Figure 4.** Proposed "hydride" mechanism for the methoxycarbonylation of an olefin (green background), including the formation of active palladium-hydride species (yellow background) and possible catalyst deactivation pathways (red background), L = CO, MeOH, solvent, coordinating anion of the acid or anion of the palladium precursor, ligand.

Indeed, the formation of the active catalyst complex is a difficult issue. However, different pathways occur presumably in parallel, depending on the

applied precursor, acid, ligand, solvents, reactants and conditions like temperature and pressure.

After formation of the active palladium-hydride complex (**9**), the first step of the catalytic cycle is the coordination of the olefin, giving the  $\pi$ -complex (**13**). This complex is a reactive intermediate and could not be observed via spectroscopic methods. After that, the insertion of the olefin into the palladium-hydride bond takes place, forming either the linear palladium-alkyl complex (**14**) or the branched one (**17**). Both complexes are stabilized by weak  $\beta$ -agostic interaction. It was shown that a series of  $\beta$ -hydride elimination and olefin insertion steps lead to the formation of internal olefins.<sup>24</sup> Furthermore, based on the branched palladium-alkyl complex (**17**), internal esters can be formed. Thus, the linear to branched regioselectivity of the methoxycarbonylation is determined by the olefin insertion step. Addition of CO to complex (**14**) gives the palladium-acyl complex (**15**) via a insertion of CO into the palladium-alkyl bond. Notably, the CO insertion step is reversible, which was observed by NMR measurements and confirmed by DFT calculations.<sup>24</sup> Moreover, depending on the partial pressure of CO, the corresponding palladium-acyl-carbonyl complex can be formed, inhibiting the subsequent methanolysis step. Finally, the methanolysis of the palladium-acyl complex (**15**) regenerates the active palladium-hydride complex (**9**) and the corresponding linear alkyl ester (**16**) as the final product is eliminated.

It is worth to mention that the proposed catalytic cycle is also valid for the hydroxycarbonylation of olefins, although the formation of the active palladium-hydride species is not initiated by a  $\beta$ -hydride elimination of the coordinated methanol. However, the palladium-hydride could be formed via a kind of water-gas shift reaction. The palladium complex could coordinate CO and water, giving a palladium-COOH complex. The subsequent elimination of carbon dioxide leads to the active palladium-hydride complex.<sup>26,29</sup>

### 2.1.3 Deactivation pathways of homogeneous palladium catalysts

Since deactivation of the active catalyst complex in homogeneous catalysis is unavoidable, particularly in palladium chemistry, a deeper look into this topic was taken. An overall review concerning the stability of homogeneous metal catalysts was published by Robert Crabtree.<sup>30</sup> In Figure 4, just a few possible deactivation pathways for the palladium-catalyzed methoxycarbonylation are shown, leading to a lower amount of the active palladium-hydride species and thus, to an overall lower reaction performance. On the one hand, it was shown that based on complex (**8**) and after pressurizing with CO, the corresponding palladium-hydridocarbonyl complex (**10**) is formed. The hydridocarbonyl complex undergoes dimerization, giving the palladium dimer (**11**), in which CO

and the hydride act as bridging ligand.<sup>29,31,32</sup> However, these species are in equilibrium to each other, which is affected by the local concentrations and conditions. Thus, the dimer is a kind of reservoir for the formation of the active palladium-hydride species (**9**). Moreover, Claver and coworkers observed that the amount and type of acid can be crucial for the stability of the catalyst system.<sup>15</sup> Depending on the basicity of the ligand and strength of the applied acid, the diphosphine can be protonated. Hence, a decoordination of the diphosphine leads to destabilization of the homogeneous palladium complex and thus, palladium black is formed in the reaction mixture. Another possible deactivation pathway is the irreversible bimolecular reaction of palladium-hydride species (**9**), which was investigated by Mecking and coworkers.<sup>33</sup> The products are the fully coordinated palladium complex (**12**), palladium black and hydrogen, which could hydrogenate the olefin. Furthermore, this side reaction is also possible between the palladium-alkyl complex (**14**) and palladium-hydride species (**9**), forming the corresponding alkane and palladium black.

#### 2.1.4 Kinetic studies

For the design and optimization of chemical reactors as well as the improvement of the reaction performance, a kinetic analysis of the reaction is essential. An empirical model based on a formal kinetic approach, in which a simple power law is used, is the easiest way to describe the reaction rate of chemical transformations. However, catalytic reactions undergo a series of elementary steps, forming very reactive intermediates in the catalytic cycle, which make the description of the kinetics via a power law not reliable. Furthermore, preformation steps of the catalyst, catalyst deactivation processes, interactions of different reactants and catalytic as well as non-catalytic side reactions are involved in many metal-catalyzed reactions, which make the use of a formal kinetic approach only useful in a limited and narrow concentration range.<sup>34</sup> In addition, mass transfer, especially for liquid-gaseous reactions such as the methoxycarbonylation, has to be considered to get a real picture of the kinetics. Hence, kinetic studies have to be performed under reactions conditions, in which the reaction is not limited by mass transfer. A general approach to study the kinetics of a chemical transformation is based on a mechanistic approach. On the basis of the reaction mechanism, a mathematical model is developed, describing the kinetic on a molecular level. All intermediates of the reaction mechanism are involved, in which the different reaction steps in the catalytic cycle are assumed to be reversible and not rate-determining.<sup>35</sup> Not only the description of one-site catalytic cycles is possible with this general approach, but also the kinetic analysis of coupled cycles, competing cycles, connected cycles as well as pre-equilibria for instance the formation of the active catalyst complex. Semi-empirical approaches include rate-determining steps (RDS), irreversible

steps and/or the concept of the most abundant species in the catalytic cycle in order to reduce the complexity of the mathematical description.

The kinetic analysis of the methoxycarbonylation reaction was investigated in literature for different substrates and catalytic systems. Morris and co-workers studied the methoxycarbonylation of ethylene, using a catalytic system containing a palladium source, the ligand d<sup>t</sup>bpx and MSA in a ratio Pd:ligand:MSA = 1:5:450.<sup>36</sup> Assuming an irreversible methanolysis step and steady-state conditions for all catalytic intermediates, a kinetic model is proposed, in which the methanolysis step is rate-determining with first order concerning MeOH, a fractional order for CO and zero order relating to ethylene. Furthermore, Cavinato and co-workers investigated the methoxycarbonylation of cyclohexene with a catalytic system containing palladium acetate, triphenylphosphine (TPP) and p-TSA, showing also the methanolysis as RDS.<sup>37</sup> In contrast to the methoxycarbonylation of ethylene, a linear dependency concerning cyclohexene was found. Rodionova and co-workers studied the same catalytic system for the methoxycarbonylation of cyclohexene, investigating additionally the impact of TPP and p-TSA concentration on the reaction rate.<sup>38</sup> Similar results were obtained compared to the investigations of Cavinato and co-workers. However, a complex dependency of TPP and p-TSA concentration was implemented in their kinetic model, suggesting ligand exchange and decomposition processes of the active catalyst complex. Moreover, the methoxycarbonylation of the long chain olefin 1-hexene has been studied by Baricelli and co-workers.<sup>39</sup> It was found that the methanolysis step is rate-determining. Hereby, a rate law was derived as shown in equation 1. The parameters a, b and c are constants, including the product of different rate constants and equilibrium constants.

$$r = \frac{a[Pd][olefin][CO][MeOH]}{1 + b[olefin] + c[olefin][CO]} \quad (\text{Eq. 1})$$

Recently, the rate law for the methoxycarbonylation of 1-decene was derived using a semi-empirical approach for the catalytic system Pd/d<sup>t</sup>bpx.<sup>40</sup> Not only the methoxycarbonylation to the linear ester but also reaction network to the branched ester and the isomerization of 1-decene was considered. In agreement with the investigations of Baricelli and co-workers, an inhibiting effect of the substrate 1-decene was observed as seen in equation 2. Furthermore, it was found that the isomerization of 1-decene is inhibited by an increased partial pressure of CO (see equation 3). The coefficients d, e, and f are temperature-dependent, describing the product of different equilibrium constants. The coefficients  $k_{\text{methoxy}}$  and  $k_{\text{isom}}$  are the corresponding rate constants for the methoxycarbonylation and isomerization, respectively.

$$r_{methoxy.} = \frac{k_{methoxy.}[Pd][olefin][CO][MeOH]}{1 + e[olefin]} \quad (\text{Eq. 2})$$

$$r_{isom.} = \frac{k_{isom.}[Pd] \left( [1 - decene] - \frac{[iso - decenes]}{d} \right)}{1 + e[olefin] + f[CO]} \quad (\text{Eq. 3})$$

In summary, it is mentionable that the mathematical description of the reaction rate depends on the applied catalytic system and the substrate. However, the methanolysis step seems to be the rate-determining step in the catalytic cycle of the methoxycarbonylation as showed for different substrates and ligands.

### 2.1.5 Industrial application

The production of methyl methacrylate (MMA) represents the most prominent example for an industrial application of the methoxycarbonylation reaction, commercialized by Lucite International with the Alpha process in 2008. MMA is the building block for the production of the polymeric poly-methyl methacrylate (pMMA), which is mainly used as a substitute of glasses. Since pMMA does not interact with the human body, it is also applicable for artificial lenses, bone cement, and dentures.<sup>41</sup> The application of MMA with other monomers offers access to many other polymers with unique properties, which are used in specialized end products. The worldwide demand for MMA is steadily increasing and reached 3 million tons per year in 2007.<sup>42</sup> Besides the Alpha process, there are some traditional synthetic routes still existing. For instance, the ACH process was developed in the late 1930s, using acetone and the extremely toxic hydrogen cyanide and sulphuric acid, which is still the most widely used process for MMA production. In contrast, the Alpha process is a green and sustainable alternative, involving a two-step process and starting with easily available feedstocks. In a first step, ethylene is catalytically converted with methanol and carbon monoxide to methyl propionate. Hereby, a catalytic system comprising a palladium source, the diphosphine d'bpx, and MSA is used, offering a high activity and selectivity. Since the boiling point of the produced methyl propionate is low, the product can be easily separated via distillation and the catalytic system can be recycled. In a second condensation step, methyl propionate is heterogeneously converted with formaldehyde to the corresponding MMA. Lucite International has built a plant with an annual capacity of 120.000 tons MMA in Singapore and has advanced plans for a second plant producing MMA.<sup>41</sup>

Inspired by this process, other feedstocks have a high industrial potential for the Reppe carbonylation in the future. Recently, Walther published an article focussing on renewable feedstocks based on plant oils.<sup>43</sup> Diesters can be obtained after the functionalization with the methoxycarbonylation reaction, which are

platform chemicals for the corresponding diacids, diols or diamines. With these intermediates, polymers like polyamides, polyurethanes or polyesters can be produced with established procedures based on renewables. Furthermore, the hydroxycarbonylation of styrene derivatives offers easy access to arylpropionic acids like Ibuprofen, Naproxen or Ketoprofen, which are pharmaceutical active ingredients in anti-inflammatory drugs.<sup>44,45</sup>

## 2.2 Green Chemistry

For decades, the final chemical product and its function were paramount in classical chemistry. But classical chemistry has changed due to the pioneering work of Paul T. Anastas and John C. Warner at the end of the 1990s. They introduced the term Green Chemistry, which is defined as the "design of chemical products and processes to reduce or eliminate the use and generation of hazardous substances".<sup>1</sup> The concept of Green Chemistry has the goal to achieve sustainability in the field of chemistry and its following sectors. To reach the goal, the Twelve Principles of Green Chemistry were introduced as a guideline for chemists, including rules for designing sustainable chemicals and processes (see Figure 5).

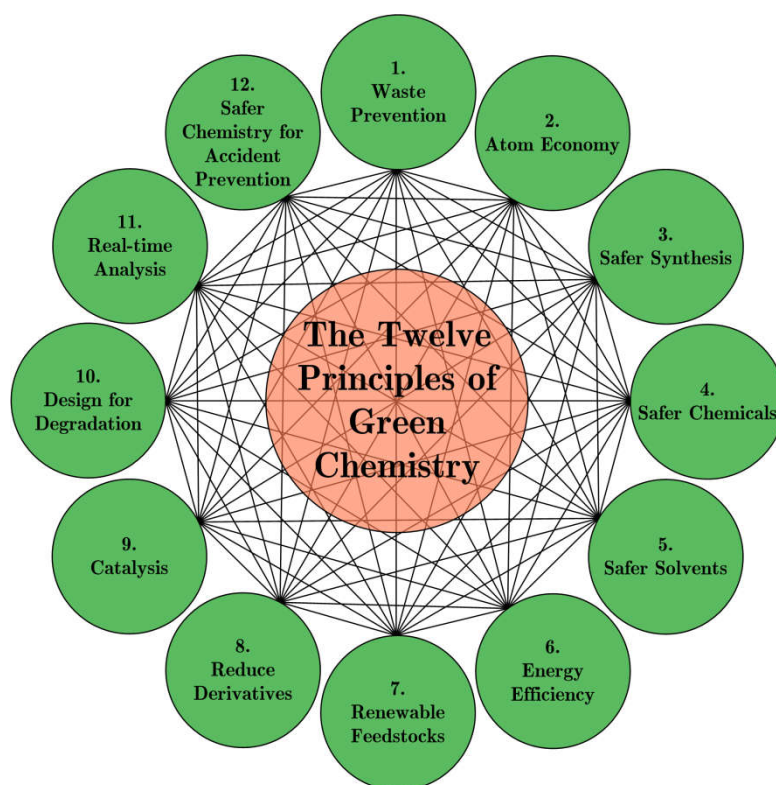


**Figure 5.** The Twelve Principles of Green Chemistry.

Rule number 1 is waste prevention. Especially in organic synthesis, plenty of toxic solvents are used, which have to be cleaned after their use. To quantify the efficiency of waste prevention in chemical processes, Sheldon and co-workers

introduced the E-Factor (Environmental Impact Factor), which is defined as the mass of waste (reagents, solvents, additives, and required fuels or energy) produced during the whole process related to the mass of the final product.<sup>46</sup> In fine chemistry, the E-factor reaches often values above 50, meaning that for the synthesis of 1 kg of the desired product 50 kg of waste is produced. Designing synthetic routes with a high atom economy is directly linked to waste prevention, which represents the second of the Twelve Principles. An easy methodology to achieve a high atom economy is the use of catalysis instead of stoichiometric reactions (Principle 9). Furthermore, catalysis can help to improve the selectivity, preventing undesired side products and increase the atom economy. A point, which is considered with much effort in research, is the use of safer solvents for chemical synthesis (Principle 5). In fact, solventless systems are the best solution, what reaches its limits in many chemical transformations. Instead, greener solvents like water or supercritical fluids are tested as an alternative to organic solvents. Since the safer solvents must be isolated after the use from the desired product, the separation process got into the focus of green chemists. Connected to that, the process should be designed for energy efficiency, operating chemical reaction and separation processes at mild pressures and temperatures (Principle 6). Furthermore, chemicals should be developed, minimizing the risk to the environment and human, while maintaining the function of the final product (Principle 4). Not only the final product itself but also the route to it should be designed in a less hazardous way with less impact for human health and environment (Principle 3). As a result, processes are safer and accidents can be prevented (Principle 12). Besides that, chemicals and processes should be designed considering the use of renewable feedstocks, reduction of derivatization, design for biodegradation and online monitoring for pollution prevention.

In summary, the Twelve Principles are a guideline to meet the requirements of Green Chemistry. It is not wise to consider each point independently. In contrast, all principles are interconnected, constituting the framework of Green Chemistry. These principles of Green Chemistry, realized in part or even completely, can lead not only to ecological advantages and social acceptance of chemistry but also to processes which are economically beneficial.

### **2.3 Multiphase Systems**

As mentioned, the search for an alternative, environmentally friendly reaction media for organic reactions is of high interest in the current research, meeting the requirements of green and sustainable chemistry. Particularly, multiphase systems for metal-catalyzed organic transformations combine advantages such as the substitution of conventional organic solvents, having often toxic properties, and the possibility of recycling the catalytic system, which prevents

waste. Besides the application of multiphase systems for efficient catalyst recycling, several other techniques are reviewed such as immobilization of the catalysts on solid supports or organic nanofiltration.<sup>47,48</sup> In the case of multiphase systems, the reaction system consists ideally of two phases, one product containing phase, which has preferably no additional organic solvent, and a second phase containing the catalytic system, which can be recycled via a liquid/liquid phase separation several times. In order to reach a high separation efficiency, the homogeneous catalyst is functionalized with specific groups/ligands to immobilize quantitatively the catalyst into the catalyst containing phase. Despite the high potential of multiphase systems for homogeneously catalyzed reactions, the use of these systems is boon and bane at the same moment. On the one hand, the recycling and reuse of the often expensive catalytic system in its active form is the main benefit using multiphase systems, which is important for ecological and economic reasons. Furthermore, energy-demanding separation processes such as distillation can be substituted through a non-energy intensive liquid/liquid phase separation. As well, conventional solvents, which have often toxic properties, can be avoided by the use of multiphase systems, particularly if water is applied as the catalyst or product containing phase. On the other hand, the use of multiphase systems in lab and industrial processes bear some drawbacks and difficulties. The catalytic performance is mainly determined by the solubility of the substrate in the catalyst containing phase. The lower the solubility of the substrate, the lower is the reaction rate. Moreover, since two phases exist, the catalytic activity can be limited by mass transfer of the substrate into the catalyst phase, lowering the catalytic performance. Hence, the determination of the kinetics is more complex in multiphase systems compared to ordinary organic solvents. Not only the microkinetics of the reaction has to be investigated, but also the rate for mass transport is important to obtain the macrokinetic picture, describing the catalytic performance. Another point to consider in multiphase systems is the catalyst stability, which can be problematic, especially if water is applied as the solvent. Moreover, the compatibility of the applied multiphase system with the substrates, products and reaction itself has to be considered to avoid side reactions and maintain product stability. These points hinder the fast process development of organic reactions in multiphase systems, which have to be solved in future to establish these systems in industrial processes.

In the following, some multiphase systems are presented and examples for catalytic transformations in these systems with subsequent catalyst recycling, particularly for the Reppe carbonylation, are given. Since surfactant based systems are the main element of this thesis, the focus has been set on these systems.

### 2.3.1 Aqueous biphasic systems

The easiest approach to perform organic reactions in multiphase systems is the application of aqueous biphasic systems, in which the homogeneous catalyst is modified with water-soluble ligands to immobilize it into the aqueous phase. The Ruhrchemie/Rhone Poulenc (RCH/RP) process represents a milestone of aqueous biphasic systems on industrial scale, developed in the 1980s. Propylene is converted with synthesis gas (a mixture of CO and H<sub>2</sub>) to butanal, using a rhodium catalyst, which is immobilized with the water-soluble ligand 3,3',3''-Phosphanetriyltris(benzenesulfonic acid) trisodium salt (TPPTS) in the aqueous phase. The product forms the upper phase and can be continuously separated via facile liquid/liquid phase separation, whereas the catalyst can be recycled back to the reactor. The leaching of the rhodium catalyst is lower than 1 ppb.<sup>49</sup>

Inspired by this process, the transfer of this concept to the methoxy- and hydroxycarbonylation was studied in academia. The first attempts to perform the hydroxycarbonylation of alkenes in aqueous biphasic systems were independently reported in 1997 by the groups of Mortreux<sup>50</sup> and Sheldon<sup>51</sup>. In both groups, TPPTS has been used as the ligand to immobilize the homogeneous palladium catalyst in the aqueous phase, testing several substrates like propylene, styrene and its derivatives. However, recycling experiments were not reported and the product was extracted with an organic solvent, subsequently. In contrast, Chaudhari and co-workers have investigated the hydroxycarbonylation of different vinyl aromatics with palladium as the catalyst, modified with pyridine carboxylate and TPPTS.<sup>52</sup> The biphasic mixture was composed of water as the catalyst phase and toluene as the organic phase. With that, subsequent recycling experiments were performed via liquid/liquid phase separation and the palladium loss was lower than 0.1 ppm. Besides propylene and styrene derivatives as substrates for the hydroxycarbonylation, several other alkenes, especially linear  $\alpha$ -olefins, have been also investigated. Sheldon and co-workers have studied the hydroxycarbonylation of 1-octene in aqueous biphasic systems, leading to a very low catalytic activity, caused by the low solubility of 1-octene in the aqueous catalyst phase.<sup>53</sup> With the introduction of the bidentate water-soluble SulfoXantPhos (SX) ligand by van Leeuwen and co-workers 1998, leading to an increased regioselectivity for linear  $\alpha$ -olefins and enhanced stability of the catalyst complex, the application of biphasic palladium-catalyzed hydroxycarbonylation have got much more attention.<sup>54</sup> Claver and co-workers have investigated the hydroxycarbonylation of styrene with novel sulfonated diphosphines and found that the catalyst can be recycled several times.<sup>55</sup>

However, the use of an aqueous biphasic system, in which the catalyst system is immobilized in the aqueous phase, is limited to substrates being slightly soluble

in the catalyst phase. To overcome limitations by the solubility of the substrate and mass transfer, plenty of innovative multiphase systems have been developed. Some of them are presented in the following sections. Furthermore, aqueous biphasic systems are not suitable for the hydroesterification of alkenes due to the formation of the corresponding acid as a side product. Hence, some studies with organic/organic biphasic systems are available. Monflier and co-workers have investigated the hydroesterification of several linear  $\alpha$ -olefins under polyol/organic phase biphasic conditions.<sup>56</sup> For this purpose, the ligand TPP, functionalized with dimethylamino groups, was used to immobilize the catalytic system in the polyol phase. The polyol, mainly ethylene glycol, acts as both, the reactant and the phase for catalyst immobilization. Even biobased polyols like isosorbide can be transformed into the corresponding diester under biphasic conditions.<sup>57</sup>

### 2.3.2 Surfactant-based multiphase systems

A promising tool to overcome problems caused by ordinary biphasic systems, especially mass transfer limitations, is the use of surface active agents (surfactants), whereby the selection of an appropriate surfactant is crucial for the catalytic activity and separation behavior. For instance, the charge, costs, physiochemical properties such as the critical micelle concentration (CMC) and the environmental impact have to take into account for the selection of a suitable surfactant for homogeneously catalyzed organic reactions in water. A whole zoo of different surfactants is available, making the selection of the surfactant rather difficult. In principle, surfactants can be classified by their charge into cationic, anionic, zwitterionic and nonionic ones, whereby classical representatives are cetyltrimethylammonium bromide (CTAB), sodium dodecyl sulfate (SDS) or Triton X-100.

In general, there are two different possibilities to perform organic reactions in surfactant-based media. On the one hand, an aqueous micellar solution is formed by adding a surfactant to water, if the surfactant concentration is above the CMC. Micelles are aggregates of surfactants, acting as nanoreactors due to the different hydrophobicity in the core of the micelles. The size and shape of the formed micelles are influenced by the type and concentration of the applied surfactant. Thus, small amounts of the organic substrate can be solubilized into the nanoreactors. Due to the enhanced solubility of the organic substrate in the aqueous phase, the organic transformation proceeds with much faster reaction rates. A subsequent separation of the dissolved catalyst complex and the organic product can be realized with micellar enhanced ultrafiltration (MEUF) or cloud point extraction (CPE). However, only small amounts of the organic substrate can be applied to obtain a macroscopic homogeneous reaction system, which makes this approach not applicable to the production of large-scale chemicals.

The second approach is based on adding larger amounts of oil to an aqueous micellar solution, leading to the formation of microemulsion systems. The basics of these systems were elaborately described in **PAPER 11**. Microemulsions are mixtures of two immiscible liquids, predominantly water and oil, with an amphiphile as the emulsifier. The phase behavior can be easily described by the Gibbs phase prism in which the base of this prism represents the ternary system of oil, water, and the amphiphile (Figure 6, left). The composition of the ternary system is characterized by the surfactant concentration  $\gamma$ , denoted as the mass fraction of the amphiphile to the total mass of the microemulsion system (Equation 4), and the oil mass fraction  $\alpha$  in the water-oil mixture (Equation 5).

$$\gamma = \frac{m_{\text{amphiphile}}}{m_{\text{amphiphile}} + m_{\text{water}} + m_{\text{oil}}} \quad (\text{Eq. 4})$$

$$\alpha = \frac{m_{\text{oil}}}{m_{\text{water}} + m_{\text{oil}}} \quad (\text{Eq. 5})$$

The Gibbs phase prism can be reduced to Kahlweit's fish diagram which is created by cutting the Gibbs phase prism at a fixed oil mass fraction  $\alpha$ , exemplarily illustrated in Figure 6 (right).

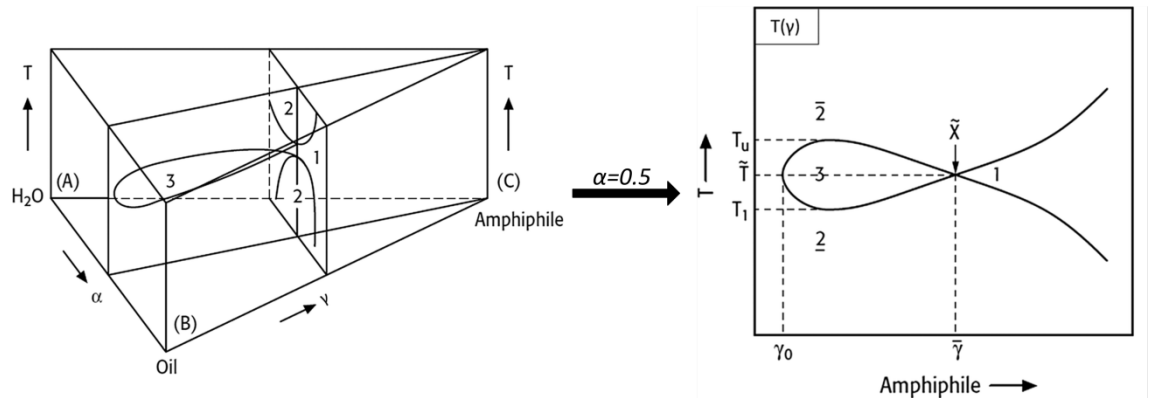


**Figure 6.** Gibbs phase prism for a microemulsion system consisting of oil, water, and a nonionic surfactant (left picture), cut of the phase prism at  $\alpha=0.5$  (right picture), taken from **PAPER 11**.

The phase boundaries resemble the shape of the fish where the body of the fish represents the three-phase region of the microemulsion system. In the fish-diagram,  $\gamma_0$  marks the minimal concentration of surfactant which is needed to form a microemulsion system. The solubility of the nonionic surfactant changes with the temperature causing the transition of the system between different phase states. At low temperatures the nonionic surfactant is more hydrophilic and thus mainly soluble in the water phase, forming an oil-in-water microemulsion with an excess oil phase ( $\underline{2}\Phi$ ). In contrast, increasing the temperature leads to a water-in-oil microemulsion with an excess water phase ( $\bar{2}\Phi$ ) caused by the higher solubility of the surfactant in the corresponding oil phase. In between, the mixture forms a three-phase region in which the middle

phase is the surfactant-rich microemulsion phase. At high surfactant concentrations, the microemulsion system reaches a macroscopic one phase state. The minimal surfactant concentration, at which a one phase microemulsion is obtained, is denoted with  $\tilde{\gamma}$  with the associated temperature  $\tilde{T}$ . Since the different phases can be converted into each other by changing the temperature, the reaction system can be adapted for different requirements. Obviously, the recycling of the catalyst complex or other additives and the separation of the product can be easily induced by a temperature-controlled liquid/liquid phase separation.

To the best of our knowledge, surfactant based multiphase systems are not applied so far in the hydroxy- or methoxycarbonylation reaction. However, several other organic reactions are performed in these systems such as C-C coupling reactions<sup>58-60</sup>, hydrolyses<sup>61</sup> or hydrogenations<sup>62,63</sup>. Furthermore, the application of surfactant based systems for organic transformations is reviewed in literature.<sup>64-66</sup> Even the synthesis of pharmaceutical active ingredients (API) can benefit from the application of micellar systems in an ecological and economic perspective, showed recently by Novartis Pharma AG.<sup>67</sup>

### 2.3.3 Miscellaneous multiphase systems

Besides the addition of surfactants as phase transfer agents, there are several further possibilities to overcome the limits of ordinary biphasic systems. In particular, switchable solvents, which change the physical properties by an external stimulus like temperature or pressure, are in focus of current research.

This includes for instance cyclodextrin modified aqueous biphasic systems, which is intensively investigated by the group of Monflier and collaborators.<sup>68,69</sup> Cyclodextrins are biobased compounds from sugar molecules, which are linked together forming a ring. Due to the ring formation, the core of the cyclodextrins acts as a lipophilic carrier, whereby the external surface facilitates the water solubility. Dependent on the number of sugar molecules, the size of the ring can be varied to adapt it to the size of the molecule, which should be transferred to the aqueous phase such as the substrate. Hence, the reaction performance is enhanced by hampering mass transfer limitations and the possibility to recycle the catalyst is given. Interestingly, a thermocontrolled approach is possible in which the cyclodextrins act as the carrier of the catalyst.<sup>70</sup> At high temperatures, the carrier releases the ligand-modified organometallic catalyst and thus, the reaction takes place in the organic phase. Afterward, the temperature is decreased, leading to an encapsulation of the catalyst in the core of the cyclodextrin. Hence, the catalyst can be immobilized in the aqueous phase and recycled for a next catalytic run. The applicability of cyclodextrin-based biphasic reaction media has been studied for the hydroxycarbonylation of 1-

decene.<sup>71</sup> The reaction performance is mainly influenced by the solubility of the cyclodextrin in both, the aqueous and organic phase. Hence, chemical modifications of cyclodextrins by substituting the hydroxyl groups with other functional moieties was shown to be effective for improving the catalytic activity. Furthermore, the regioselectivity toward the terminal acid can be significantly increased by shielding the internal double bond through the encapsulated substrate. Recycling experiments have been successfully done, whereby the palladium leaching was less than 1 ppm. However, the leaching of the applied ligand TPPTS was rather high with 10 ppm.

Moreover, thermomorphic multicomponent systems (TMS), which were introduced in catalysis by Behr and co-workers, are promising concerning the recycling of homogeneously dissolved catalyst systems.<sup>72</sup> The TMS benefits from the miscibility gap between a polar and nonpolar organic solvent, which is controlled by temperature. Heating of the solvent mixture leads to a homogeneous reaction media, in which the reaction can take place without any mass transfer limitations. After the reaction, the mixture is cooled and a phase separation of the TMS occurs, in which the catalyst and product are located in different phases. Thus, the catalyst phase can be recycled for a next run. Hereby, the selection of appropriate solvents for TMS is crucial in order to adjust the separation in a certain temperature window and to obtain low leaching of the catalyst into the product phase. Behr and co-workers have studied the methoxycarbonylation of methyl oleate in a TMS composed of methanol and decane.<sup>73</sup> The selection of methanol as the polar phase is beneficial since methanol acts also as the substrate in this reaction. The proof of concept for catalyst recycling was shown in three consecutive recycling runs. However, the leaching of palladium and phosphorous into the product phase was 3 ppm and 2 ppm, respectively, which is too high for an industrial application. Afterward, the methoxycarbonylation of methyl 10-undecanoate has been investigated, in which eight recycling runs could be performed, due to the addition of co-catalyst after each recycling procedure.<sup>74</sup>

In the last years, the use of supercritical carbon dioxide (scCO<sub>2</sub>) as reaction media opened a wide field for homogeneous catalysis.<sup>75</sup> Besides reaching high activities and selectivities for gas-liquid reactions, for instance, hydrogenation<sup>76</sup> and hydroformylation reactions<sup>77</sup>, the use of scCO<sub>2</sub> offers the advantage to recycle the homogeneous catalyst. Due to the creativity of researchers, several methods are available for the recycling of the catalyst from scCO<sub>2</sub> based reaction media, including for instance lowering the pressure for catalyst precipitation or using biphasic reaction media with scCO<sub>2</sub> as one phase. The Reppe carbonylation has also been investigated in scCO<sub>2</sub>. Estorach and co-workers have studied the methoxycarbonylation of linear alpha olefins in scCO<sub>2</sub>, using fluorinated ligands.<sup>78</sup> As a result, the catalyst complex shows an enhanced

solubility in the supercritical fluid and thus, better reaction rates could be obtained. Furthermore, the methoxycarbonylation of norbornene in  $\text{scCO}_2$  has been described by the group of Li.<sup>79</sup> However, both groups did not show any recycling experiments, which can be expected for the Reppe carbonylation in  $\text{scCO}_2$  based reaction media in near future.

### 3. Experimental Part

#### 3.1 Chemicals

The applied chemicals, the supplier and the purity are listed in the appendix (Table A1-A4). All chemicals were used as received without further purification steps.

#### 3.2 Determination of CMC

The bubble pressure tensiometer BP50 of the company *Krüß* was used to determine the critical micelle concentration (CMC) of the applied surfactants. For this purpose, aqueous solutions with different concentrations of the corresponding surfactants were prepared and measured. The dynamic surface tension of the solution was measured, starting at the surface age of 30 ms and ending at 16 s. After each measurement, the capillary was flushed with air for 5 s. Three values were measured at each surface age and the average was calculated. At a surface age of 14 s, when the surface tension remains constant, the surface tension value was taken and plotted versus the concentration of the surfactant to determine the CMC. All reported values were measured at 25 °C and are indicated as moles of surfactant per volume.

#### 3.3 Investigation on the phase behavior

The investigations on the phase behavior were performed in 10 mL Schlenk tubes. In case of nonionic surfactants as phase transfer agents, the co-solvent dodecane (2.25 g), 1-dodecene (0.75 g), the surfactant, sodium sulfate ( $\text{Na}_2\text{SO}_4$ ) and the co-catalyst methanesulfonic acid (MSA) were weighted into the Schlenk tube and flushed with Argon. A stock solution of the precursor  $\text{Pd}_2(\text{allyl})_2\text{Cl}_2$  and the ligand SulfoXantPhos (SX) was prepared in water with standard Schlenk technique and stirred overnight. The catalyst solution (3.0 g) was added to the Schlenk tube under Argon counterflow, simulating the initial reaction mixtures and the tubes were closed with a septum. Afterward, the Schlenk tubes were placed in a water bath and the phase behavior of the microemulsion systems was investigated in a temperature range between 50 °C and 90 °C in 1 °C steps. For that, the temperature of the water bath was adjusted as desired, then the tubes were shaken and the phase separation was observed visually after 10 minutes. In the same manner, the phase behavior was investigated for the ionic surfactants using the co-solvent octane (2.25 g), 1-dodecene (0.75 g), the ionic surfactant, and the co-catalyst methanesulfonic acid (MSA). A stock solution of the precursor  $\text{Pd}(\text{OAc})_2$  and the ligand

SulfoXantPhos (SX) was prepared in water with standard Schlenk technique, which was added through a septum into the Schlenk tube.

### 3.4 Preformation of the Catalyst for Carbonylation Reactions

The catalyst precursor  $\text{Pd}(\text{OAc})_2$  or  $\text{Pd}_2(\text{allyl})_2\text{Cl}_2$  and the ligand SX were evacuated and flushed with argon three times in a Schlenk tube. The degassed polar phase (methanol and/or water) was added through a septum and the reaction mixture was stirred overnight. A homogenous green solution indicates the formation of the catalyst complex.

### 3.5 Setup for Carbonylation Reactions

All experiments were carried out in a 100 mL stainless steel autoclave built by Halmosi GmbH. An overview of the reactor setup is given in Figure 7.

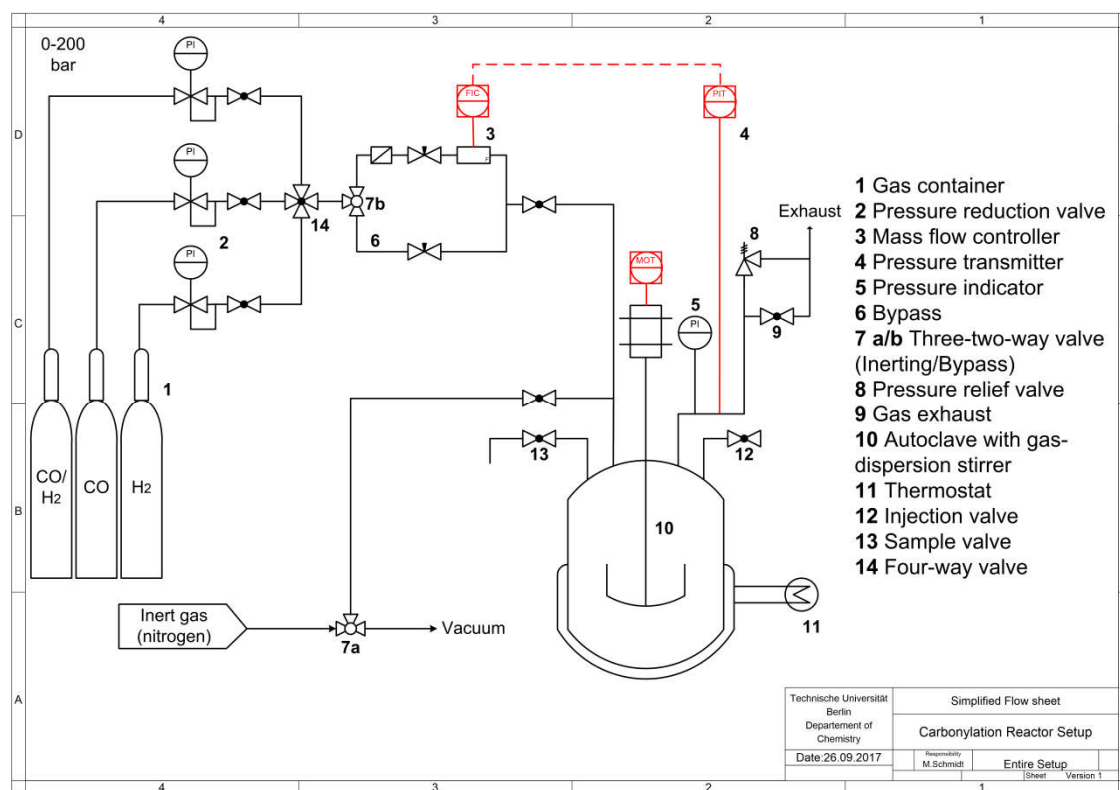


**Figure 7.** Experimental setup for methoxy- and hydroxycarbonylation reaction.

The autoclave (10) is equipped with a gas dispersion stirrer, a PTFE baffle to ensure the dispersion of the reaction mixture, and a PTFE inlay to avoid the formation of palladium black at the inner surface of the reactor wall. To maintain isobaric reaction conditions a pressure transmitter (4) is connected to a mass flow controller (3) to the reactor. For a fast initial pressurization of the reactor with carbon monoxide, a bypass was installed (6), which can be controlled with a pressure indicator (5) connected directly to the reactor.

Additionally, the autoclave has connections for sampling (**13**), inertization (**7a**) and the injection of reactants (**12**) under nitrogen counterflow. A process control system monitors all process- and the corresponding set-values like pressure, temperature, gas flow and stirring speed and records the data. A pressure relief valve (**8**) is used to limit the pressure to 60 bar. After finishing the reaction, the toxic gas can be exhausted (**9**) to the ventilation of the fume hood. For safety reasons, the gas containers (**1**) are located in a gas cylinder cabinet, equipped with a gas alarm device, in which the gas charge can be disconnected with a pneumatic valve.

### 3.6 Experimental Procedure for Carbonylation Reactions

In a typical experiment, the co-solvent, the substrate, the surfactant, nonane as internal standard (300 mg) and MSA as co-catalyst were weighted into the PTFE inlay and introduced to the reactor. After evacuation and flushing the reactor with nitrogen three times, the catalyst solution was injected with a syringe under nitrogen counterflow. Under stirring at 200 rpm, the reactor was heated up to the desired reaction temperature and pressurized with carbon monoxide. After reaching the process values, the stirrer speed was increased to 1200 rpm, marking the start of the reaction. Samples were taken at fixed time intervals, diluted with acetone and centrifuged in order to precipitate the ligand from the solution. GC analysis was performed on a Shimadzu GC2010 Plus with a FID (flame ionization detector) packed with a Restek RTX5-MS column (30 m × 0.25 mm × 0.25 μm). Nonane was used as internal standard to calculate the conversion of dodecene, yield of acid and ester, chemoselectivity and linear to branched regioselectivity (l:b), expressed as the ratio of linear acid to the sum of linear and branched acid, as shown in equations 4-7.

$$X(t) = \frac{n_{t=0}(1-dodecene) - n_t(1-dodecene)}{n_{t=0}(1-dodecene)} \quad (\text{Eq. 4})$$

$$Y(t) = \frac{n_{t,product}}{n_{t=0}(1-dodecene)} \quad (\text{Eq. 5})$$

$$S_{chemo}(t) = \frac{Y_{product}(t)}{X(t)} \quad (\text{Eq. 6})$$

$$S_{l:b}(t) = \frac{Y_{linear\ product}(t)}{Y_{linear\ product}(t) + Y_{branched\ products}} \quad (\text{Eq. 7})$$

### 3.7 Determination of Catalyst Leaching and Product Distribution

After finishing the reaction, the reactor was cooled down, depressurized, and flushed with nitrogen. The reaction mixture was filled into a graduated cylinder, which was closed with a septum. After completed phase separation, GC samples were taken from both phases to determine the distribution of the product. The nonpolar phase was transferred into a round bottom flask, weighted, and distilled under reduced pressure (3.6 mbar, 180 °C). The residue was digested with 1 mL nitric acid (65 wt%), 3 mL hydrochloric acid (37 wt%) and 2 mL sulfuric acid (96 wt%) and filled up to 20 mL with water (HPLC grade). The solution was analyzed by inductively coupled plasma optical emission spectrometry (ICP-OES) for palladium and phosphorus concentration using a Varian ICP-OES 715 ES instrument. An external calibration was done with standard solutions of palladium and phosphorus. The concentration of palladium and phosphorus were measured at a wavelength of 363.5 and 213.6 nm, respectively. The results are stated as the amount of palladium and phosphorous in the nonpolar phase denoted in parts per million (ppm).

During the continuous miniplant operation, the product stream was collected for 8 h, transferred to a flask and distilled under reduced pressure (4 mbar). The residue was solubilized with hydrochloric acid (9 mL), 65 wt% nitric acid (3 mL) and sulfuric acid (6 mL) in the flask and filled up to 50 mL with water (HPLC grade). The solution was analyzed with ICP-OES as described above and results are denoted as parts per billion (ppb).

### 3.8 General procedure of the Alkaline Hydrolysis

The main part of the setup for the alkaline hydrolysis is a 40 mL double-wall reactor to adjust the temperature via a thermostat. The substrates can be injected through a two-way valve at the reaction temperature, whereby the mixture is mechanically stirred. To follow the reaction progress the conductivity is measured *in-situ*, using a conductivity electrode from the company WTW. The thermostat and the conductivity probe are connected to a computer to monitor the reaction progress. To perform the reaction, a stock solution containing the surfactant and sodium hydroxide (4 mmol, 1 eq.) was filled into the reactor, stirred mechanically and heated up to the desired reaction temperature. Immediately after reaching the reaction temperature, the substrate methyl decanoate (4 mmol, 1 eq.) was injected via a syringe into the reactor. The bulk volume was 20 mL for each experiment. The reaction was stopped when the conductivity remains constant, or latest after 24 hours.

Since the conversion depends linear on the conductivity of the mixture, the conductivity was measured to determine the conversion of methyl decanoate to sodium decanoate. For that, sodium hydroxide, which mainly contributes to the

conductivity of the mixture, and the product sodium decanoate were mixed, adapted to the concentrations from the previous section, simulating different conversions between 0% and 100%. After waiting four minutes for temperature equilibrium, the corresponding conductivity was measured at 40 °C, 60 °C and 80 °C and plotted versus the associated conversion. A two-point calibration was done for the cationic surfactants, mixing the tenfold critical micelle concentration (CMC) of the corresponding surfactant, sodium hydroxide, and sodium decanoate and measuring the conductivity at 80 °C.

## 4. Results and Discussion

### 4.1 Green Chemistry and InPROMPT

In the sense of sustainability and Green Chemistry, the collaborative research center called InPROMPT (Integrated Chemical Processes in Liquid Multiphase Systems) was established in 2010, aiming for the environmentally friendly production of chemicals. The overall aim of InPROMPT is the development of phase systems for an efficient catalyst recycling in its active form by a simple phase separation, meeting the requirements of Green Chemistry. Of special interest are surfactant-based multiphase systems, thermomorphic solvent systems, and pickering emulsions. The schematic process concept for the hydroformylation of long-chain alkenes, which was investigated as a benchmark reaction in the first funding period, is shown in Figure 8. Multiphase systems offer the possibility to separate the product by an easy phase separation. The expensive catalyst complex can be easily recycled back to the reactor for further use.

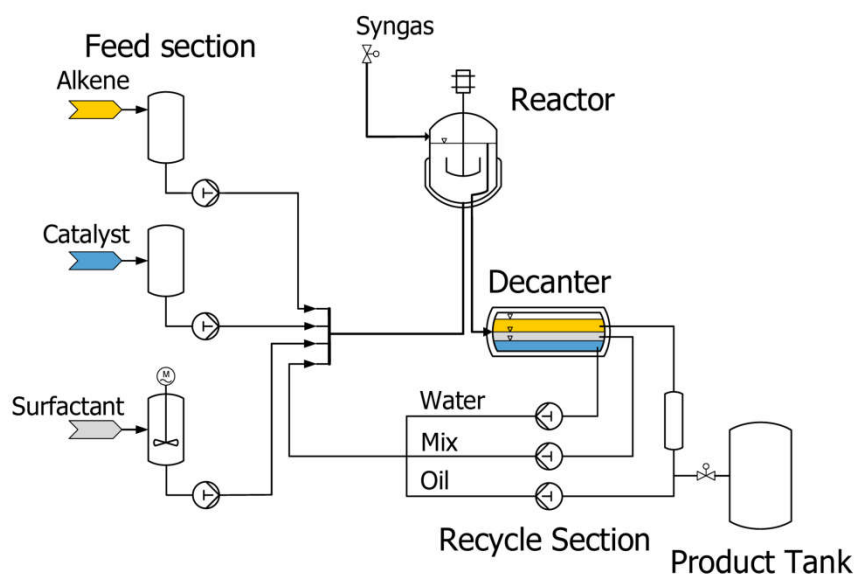


**Figure 8.** Schematic process concept for the hydroformylation of long-chain alkenes in microemulsion systems (**PAPER 5**).

Besides the chemical and physical fundamentals of the novel phase systems and the catalysis in such a system, the design and development of continuous production processes as well as their optimization and cost evaluation are in the focus of the project. As an associate member of the collaborative research center, I was involved in the development of surfactant-based multiphase systems for different homogeneously catalyzed reactions, finding suitable reaction media and appropriate reaction and separation conditions.

#### 4.1.1 Status Quo - Hydroformylation in Microemulsion Systems

The applicability of microemulsion systems as reaction media for metal-catalyzed reactions was shown in detail for the hydroformylation of 1-dodecene, mainly in the doctoral thesis of Pogrzeba.<sup>2</sup> The main focus was set on three key aims:

1. Understanding the role of the nonionic surfactant during catalysis
2. Analyzing the kinetics of the hydroformylation in microemulsion systems
3. Transferring the lab scale results in a continuously operated miniplant

The corresponding results for the hydroformylation of 1-dodecene can be found in **PAPER 3**, **PAPER 4**, **PAPER 5** and **PAPER 8**. A microemulsion system containing water, the substrate 1-dodecene and Marlipal 24/70 as phase transfer agent was found to be suitable for the hydroformylation reaction. Additionally, sodium sulfate was used to facilitate and accelerate the phase separation for catalyst recycling. In order to facilitate a fast process development for catalytic reactions in microemulsion systems, a better understanding of catalysis in such systems is necessary, which is presented in **PAPER 5** and **PAPER 8**. The results reveal that the amount and type of nonionic surfactant are crucial for the catalytic activity of the hydroformylation reaction. Interestingly, the phase behavior of the microemulsion system has no impact on the reaction performance. Instead, the catalytic activity is determined by the interfacial area between water and oil, mainly influenced by the surfactant concentration, and the local concentrations of the substrate as well as the active catalyst complex at this interface, affected by the physicochemical properties of the surfactant. Moreover, due to the surface active properties of the applied catalyst complex, the dynamic equilibrium between active and inactive catalyst species can be shifted, leading to an increased amount of active catalyst species at higher surfactant concentrations and thus, to a higher catalytic activity. Based on the mechanism for catalysis in the microemulsion system, a kinetic model was derived using a parameter estimation from experimental data. The adapted kinetic model includes the impact of the surfactant and the local catalyst concentration at the interface.

Finally, the lab-scale results were successfully transferred to a miniplant, operated continuously over a period of 150 h with a stable phase separation (see Figure 9). The corresponding results are shown in **PAPER 3**. A stable aldehyde yield of 21% was achieved and a stable phase separation was maintained by exact temperature control of the decanter during the whole operation time, which enables quantitative catalyst recycling and product separation. The loss of rhodium into the product phase was below 0.1 ppm, which is in accordance

with previous lab findings. These results show the applicability of microemulsion systems for continuously operated, catalytic reactions on a larger scale.

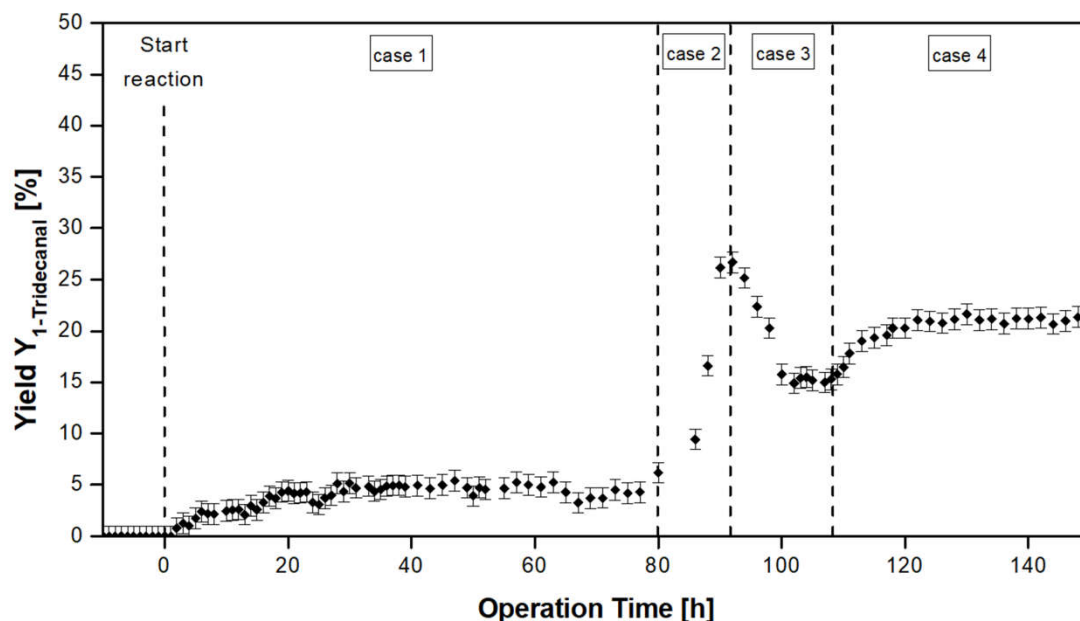


**Figure 9.** Miniplant operation results for the hydroformylation of 1-dodecene (**PAPER 3**). Case 1: continuous operation,  $\tau_{\text{Reactor}} = 0.5$  h, recycle ratio (oil:mix:water) = 0.19:0.57:0.24, Case 2: full recycle,  $\tau_{\text{Reactor}} = 3.2$  h, recycle ratio (oil:mix:water) = 0.40:0.20:0.40, Case 3: continuous operation,  $\tau_{\text{Reactor}} = 2.8$  h, recycle ratio (oil:mix:water) = 0.40:0.28:0.32, Case 4: continuous operation,  $\tau_{\text{Reactor}} = 2.8$  h, recycle ratio (oil:mix:water) = 0.24:0.52:0.24.

Not only microemulsion systems have been investigated for the hydroformylation of 1-dodecene but also the applicability of surfactant-free multiphase systems was tested, which is shown in **PAPER 4**. Ordinary aqueous-organic biphasic systems suffer from the low solubility of the substrate in the aqueous catalyst phase, leading to very low catalytic activity. An easy way to avoid the limitations by the solubility is the use of co-solvents, which enhances the reaction rate due to the higher solubility of the substrate in the catalyst phase. Hence, diethylene glycol butyl ether, a short chain amphiphile as co-solvent, has been investigated for the hydroformylation reaction, leading to a good reaction performance and enabling subsequent catalyst recycling by phase separation.

#### 4.1.2 Silylene Ligands as Alternatives

Besides the development of sustainable reaction media for metal-catalyzed reactions, the design and synthesis of new ligands are in focus of current research. The specific design of novel ligands offers the opportunity of an enhanced catalytic activity and improved selectivity, covering the challenges of Green Chemistry. In this context, the catalytic properties of monodentate and

bidentate NHSi ligands have been investigated in hydroformylation reaction for the first time (**PAPER 6**). Due to the special electronic properties of NHSi ligands, particularly the enhanced  $\sigma$ -donor/ $\pi$ -acceptor properties, these new class of ligands is a promising substitute for commercially available ligands. Unexpectedly, the hydroformylation of styrene with  $[\text{HRh}(\text{CO})(\text{PPh}_3)_3]$  and an excess of the monodentate NHSi ligands  $[\{\text{PhC}(\text{N}^t\text{Bu})_2\}\text{SiNMe}_2]$  and  $[\{\text{C}_2\text{H}_2(\text{N}^t\text{Bu})_2\}\text{Si}]$  show a lower catalytic activity to the aldehyde product compared to the benchmark system  $[\text{HRh}(\text{CO})(\text{PPh}_3)_3]$  with or without an excess of TPP. NMR studies reveal trisubstituted coordination of the NHSi ligands to the rhodium center, with or without an excess of NHSi ligand. However, the strong dative Si-Rh bond hinders the decoordination of the ligand to form the active 16-valence-electron rhodium complex, hampering the styrene coordination, resulting in low catalytic activity.

In contrast, a ferrocenediyl based bidentate NHSi, used as the ligand in hydroformylation reaction, enhances significantly the catalytic activity compared to benchmark phosphines DPPF and XantPhos (see Table 1). Due to the strong  $\sigma$ -donor ability of the bis-NHSi, the formed  $[\text{HRh}(\text{CO})(\text{PPh}_3)(\chi^2\text{-L}_2)]$  complex, evidenced by NMR experiments, facilitates the dissociation of the remained TPP and stabilizes the active 16-valence-electron complex. Furthermore, the ability of the NHSi ligand to act as  $\pi$ -acceptor promotes the hydride migration step, accelerating the reaction rate. As a result, higher conversions and TOFs are achieved.

**Table 1.** Conversion, l:b ratio and TOF of the hydroformylation with  $[\text{HRh}(\text{CO})(\text{PPh}_3)\text{L}_2]$  complexes containing bidentate ligands  $\text{L}_2$  at different temperatures (adapted from **PAPER 6**).<sup>a</sup>

Entry	Ligand $\text{L}_2$	Temperature T [°C]	Conversion $X^{\text{b,c}}$ [%]	l:b <sup>b,c</sup>	TOF <sup>b</sup> [ $\text{h}^{-1}$ ]
1	DPPF	50	traces	-	3
2	XantPhos	50	2.2	43:57	32
3	Bis-NHSi	50	10.2	16:84	83
4	DPPF	80	3.9	34:66	91
5	XantPhos	80	29.4	47:53	646
6	Bis-NHSi	80	98.9	12:88	2621
7	DPPF	100	12.5	35:65	589
8	XantPhos	100	56.4	49:51	3007
9	Bis-NHSi	100	99.7	25:75	9075

<sup>a</sup> Experimental conditions: 40 g toluene as solvent,  $n_{\text{styrene}} = 38$  mmol,  $p = 30$  bar,  $n_{[\text{HRh}(\text{CO})(\text{PPh}_3)_3]} = 0.01$  mmol,  $n_{\text{ligand}} = 3$  eq., stirrer speed = 1200 rpm.

<sup>b</sup> Determined by GC-FID.

<sup>c</sup> Determined at 50 °C after 240 min., at 80 °C after 120 min and at 100 °C after 60 min. by GC-FID.

Moreover, DFT calculations were done to confirm the differences in the catalytic activity of the bis-NHSi and XantPhos ligand, showing a lower activation barrier of the rate determining hydride migration step for the bis-NHSi ligand. The relative activation barrier between the phosphine and the bis-NHSi is 0.7 kcal/mol for the linear product and 1.7 kcal/mol for the branched product, leading to the enhanced reaction rate for the silylene ligand. Due to the enhanced catalytic activity of NHSi, this new class of ligands can be seen as green alternatives to commercially available ligands based on nitrogen or phosphorus.

## 4.2 Methoxycarbonylation in Microemulsion Systems

After successful implementation of microemulsion systems for the hydroformylation of 1-dodecene, the developed concept is to be transferred to another catalytic reaction. For this purpose, the palladium-catalyzed methoxycarbonylation is investigated to validate the previous findings and to extend the methodical toolbox for catalysis in microemulsion systems. Furthermore, the spectrum of raw materials is expanded to find a general approach. Compared to the hydroformylation reaction, the formation of the reaction mixture for the methoxycarbonylation is more challenging, which is illustrated in Figure 10.

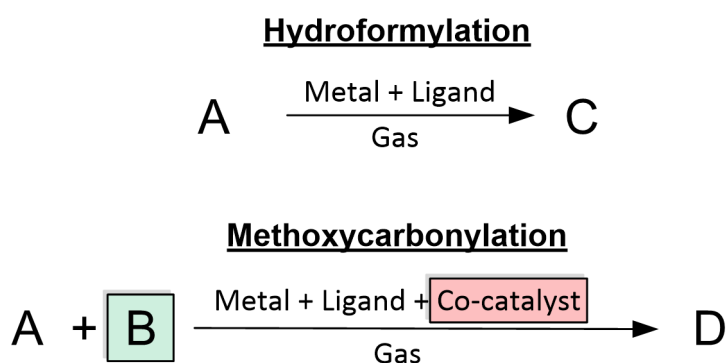


**Figure 10.** Schematic comparison between the hydroformylation and methoxycarbonylation reaction.

On the one hand, a second liquid substrate (**B**) is involved in the reaction, which is an additional amphiphilic component, affecting strongly the phase behavior of the microemulsion system. On the other hand, an acidic co-catalyst is required to form the active palladium-hydride complex. The unknown impact of the acid and the additional amphiphilic component on the catalysis and phase separation of the microemulsion system makes the methoxycarbonylation more complex. Furthermore, the formed ester (**D**) is surface active itself and behaves like a surfactant, which complicates the product separation. In order to validate the feasibility of microemulsion systems for the methoxycarbonylation, the phase separation behavior and the reaction performance was considered.

### 4.2.1 Impact of Methanol on the Phase Behavior

Initially, the impact of the additional amphiphilic reactant methanol on the phase behavior has been investigated, which is depicted in Figure 11. Based on the experiences from the hydroformylation reaction, Marlipal 24/70 as the surfactant was chosen as the benchmark. The variation of the methanol amount is expressed as the molar ratio with respect to the molar amount of 1-dodecene, whereby the oil content  $\alpha$  was fixed at 50%. Furthermore, the investigations were done without any catalyst components to exclude the impact of these additives on the phase behavior.

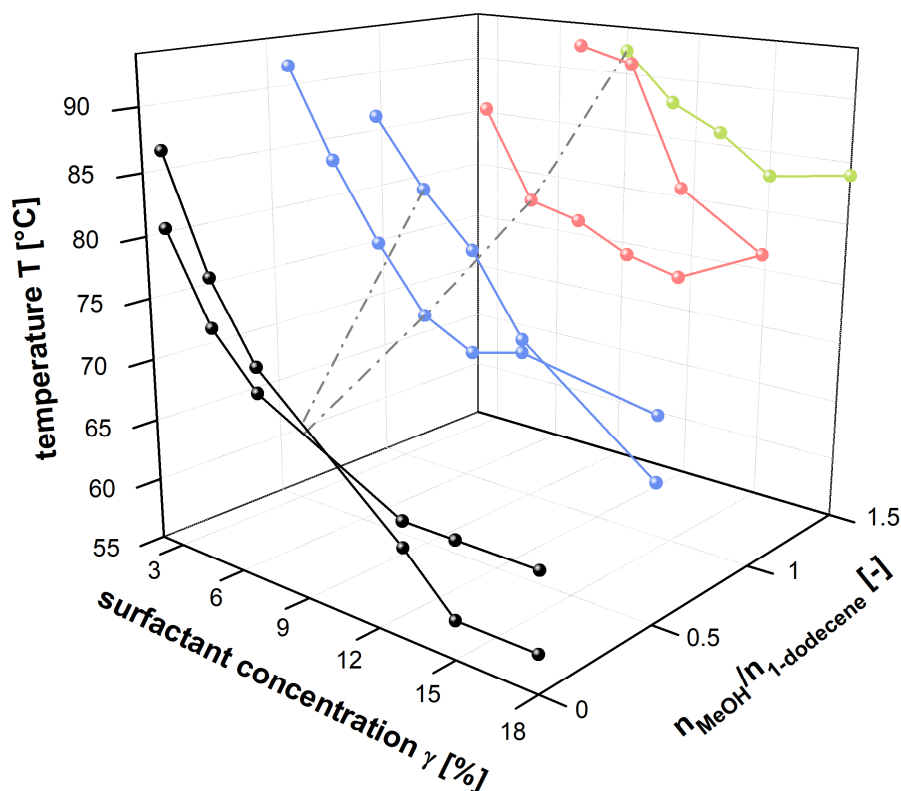


**Figure 11.** Phase boundaries for the microemulsion system consisting of water, 1-dodecene and Marlipal 24/70 with different amounts of MeOH. Experimental conditions:  $m_{1\text{-dodecene}}=12$  g,  $m_{\text{water}}=12$  g, 1wt%  $\text{Na}_2\text{SO}_4$ , Marlipal 24/70 as surfactant.

In general, although methanol was added to the microemulsion system, the phase separation is still fast and complete in the three-phase region of the microemulsion system. However, the phase boundaries are significantly shifted, even with the addition of small amounts of methanol, which can be summarized in three points. First, with an increasing amount of methanol in the microemulsion system, the three-phase region shifts to higher temperatures. Second, the minimal surfactant concentration  $\tilde{\gamma}$  shifts to higher surfactant concentrations with increasing amount of methanol. Third, the temperature range for the three-phase region of the microemulsion system enlarges. As

expected, methanol acts as a co-solvent and not as a co-surfactant, explaining the shift of the three-phase region to higher temperatures. Since methanol is a co-solvent, dissolved in the water phase, the water phase becomes more hydrophobic and thus, the surfactant inverts its solubility now at higher temperatures. All in all, despite the addition of methanol, the sensitive phase separation of the microemulsion system is feasible, which is a basic requirement for catalysis in microemulsion systems with subsequent catalyst recycling.

#### 4.2.2 Impact of Methanol on the Reaction Performance

Not only the impact of methanol on the phase behavior but also the impact of methanol on the reaction performance has been investigated to examine the feasibility of microemulsion systems for the palladium-catalyzed methoxycarbonylation. Hence, the methoxycarbonylation was carried out in the benchmark microemulsion system, using Marlipal 24/70 as the surfactant, varying the methanol amount. Preliminary investigations revealed that the composition of the catalytic system is essential to ensure catalyst stability and reaction progress. Thus, the ratio of the palladium precursor to the water-soluble ligand to co-catalyst (Pd: SX:MSA) was fixed to 1:4:40 in the following experiments. As expected, the yield of the corresponding ester methyl tridecanoate increases with increasing amount of methanol in the microemulsion system, as seen in Figure 12. The l:b regioselectivity remains nearly constant around 86:14. However, the corresponding carboxylic acid is also formed in significant amounts as high-value side product because of the availability of water in the microemulsion system. Furthermore, the hydrogenation product is also produced with low yields ( $Y_{\text{Dodecane}} < 5\%$ ), caused by the formation of hydrogen in a water-gas shift reaction. The carboxylic acid is located in the nonpolar phase, containing currently the ester, the carboxylic acid, dodecane, and unconsumed 1-dodecene, making further steps necessary to purify the nonpolar phase in order to obtain the ester as the final product. Indeed, the ester to acid ratio can be increased to 2.3 by increasing the methanol to substrate ratio to 2. However, a further increase of the methanol amount hampers the phase separation after the reaction, making catalyst recycling impossible. The impact of temperature and amount of co-catalyst on the ratio of the formed ester and carboxylic acid was also investigated but has only a minor impact. As a result, a microemulsion system is inappropriate for the methoxycarbonylation reaction. First, the formation of the carboxylic acid as side product cannot be avoided, complicating the purification of the crude product mixture. Second, the atom economy of the reaction is reduced, which is not in the sense of Green Chemistry.

In contrast, if the carboxylic acid is the desired final product, microemulsion systems are promising systems and a yield of 16% after 20 h reaction time can

be achieved. It is worth mentioning that no hydroxycarbonylation reaction can be observed in aqueous biphasic catalysis without surfactant. Hence, the methoxycarbonylation and hydroxycarbonylation are separably investigated in the following sections.

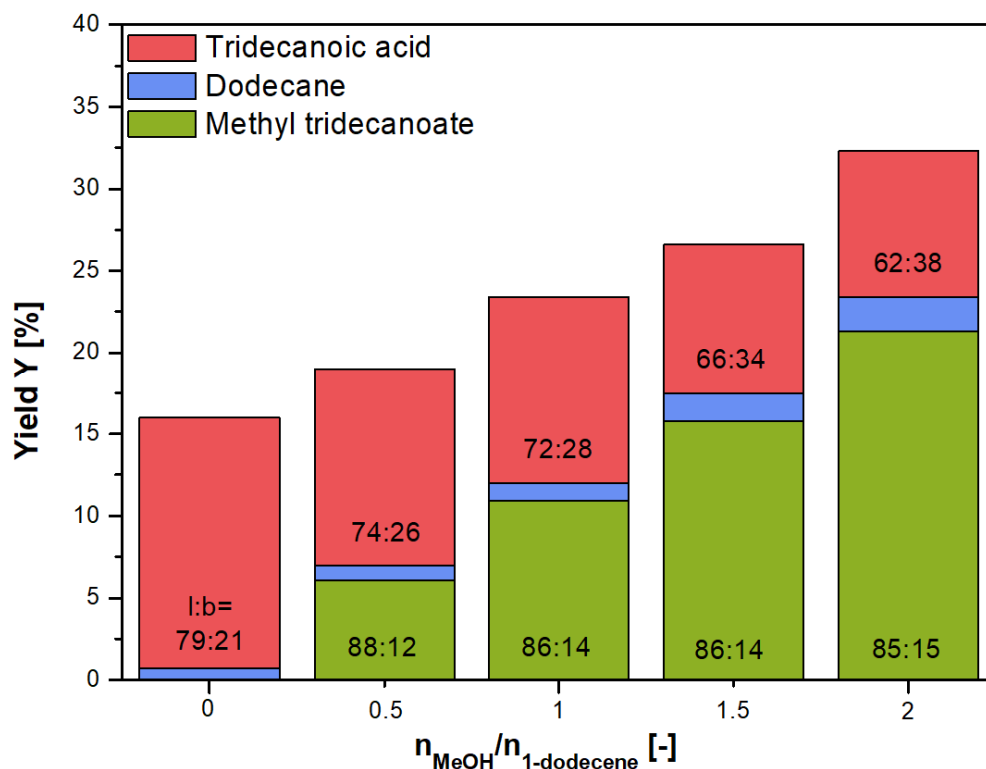


**Figure 12.** Yield of tridecanoic acid, dodecane and methyl tridecanoate for the methoxycarbonylation in microemulsion systems. Experimental conditions:  $T=110^{\circ}\text{C}$ ,  $P_{\text{CO}}=30$  bar,  $m_{\text{1-dodecene}}=12$  g,  $m_{\text{water}}=12$  g,  $n_{\text{Pd}(\text{OAc})_2}=0.16$  mmol,  $\text{Pd}:\text{SX}:\text{MSA}=1:4:40$ , 1wt%  $\text{Na}_2\text{SO}_4$ ,  $n=1200$  rpm,  $t=20$  h,  $\gamma=9\%$ , Marlipal 24/70 as surfactant.

### 4.3 Methoxycarbonylation in Biphasic Systems

In order to avoid the formation of the acid, the methoxycarbonylation has been carried out in an ordinary biphasic system, investigating the catalytic performance and separation behavior. In this section, the path toward a continuous process for the methoxycarbonylation of 1-dodecene in miniplant scale is shown, including the solvent selection in lab scale to optimize the catalyst recycling, the variation of the reaction conditions in lab experiments (temperature, pressure) to define an operation window for the miniplant and finally the proof of concept in the miniplant with continuous catalyst recycling and product separation. Furthermore, the impact of the applied substrate has been investigated to find an appropriate biphasic system for different substrates, enabling the consecutive catalyst recycling and product separation.

### 4.3.1 Solvent Selection

In the sense of Green Chemistry, a solventless system is the best option to perform metal-catalyzed organic transformations, which can be adapted to multiphase catalysis for catalyst recycling via phase separation. For the methoxycarbonylation of 1-dodecene, the simplest biphasic mixture is composed of methanol as polar phase and the substrate 1-dodecene as nonpolar phase, using no additional solvent. The catalyst can be immobilized in the methanol phase due to the water-soluble ligand SX. The experimental results for the solventless, biphasic methoxycarbonylation are shown in **PAPER 7**. It was found that the methoxycarbonylation can be performed without any additives. The variation of the catalyst concentration showed that the TOF remains constant around  $80 \text{ h}^{-1}$ , indicating a first-order dependence on the reaction rate. In contrast, the initial concentration of the catalyst is crucial for the recycling of the catalyst complex after the reaction. At low palladium concentrations, no recycling is possible via phase separation because of the formation of a one phase system after the reaction. The more hydrophilic ester, which is formed during the reaction, can solubilize the catalyst containing methanol phase, inhibiting catalyst recycling. However, phase separation takes place at high palladium concentrations, whereas the leaching of palladium and phosphorus into the nonpolar phase is 4.6 ppm and 45.7 ppm, respectively (see Table 2, entry 10). Thus, the percentage loss of palladium is 0.5%, which is too high under consideration of ecological and economic factors. Additionally, the impact of additional solvents on the reaction performance and separation properties has been investigated in **PAPER 7** to optimize catalyst recycling. It was found that modifications of both, the polar and nonpolar phase, lead to a drastic improvement of catalyst recycling.

First, it turned out that the addition of water is an easy approach to reduce the leaching of the catalyst into the organic product phase, as seen in Table 2. The palladium leaching could be drastically reduced by the addition of 15 wt% water to the polar phase from 4.6 ppm without water as a promoter (Table 2, entry 10) to 0.5 ppm (Table 2, entry 13). Moreover, the phosphorus loss could be diminished to one fiftieth adding 15 wt% of water. It is mentionable that the mass of the polar phase, which is the sum of methanol and water, was constant. The reaction mixture after the reaction (Table 2, entry 12) is exemplarily shown in Figure 13, in which a clear product phase is formed, indicating almost no catalyst leaching. In addition, the modification of the polar methanol phase by adding water increases slightly the ester amount in the nonpolar phase, resulting in quantitative separation of the product. The results prove that the addition of water increases the polarity of the polar methanol phase, leading to an improved product distribution and a decreased catalyst leaching.

**Table 2.** Methoxycarbonylation of 1-dodecene: Modification of the polar phase (adapted from PAPER 7).<sup>a</sup>

Entry	water in polar phase [wt%]	Yield (Ester) <sup>b</sup> [%]	TOF <sup>c</sup> [h <sup>-1</sup> ]	l:b <sup>b</sup>	Pd leaching <sup>d</sup> [ppm]	P leaching <sup>d</sup> [ppm]	product in nonpolar phase <sup>b</sup> [%]
10	0	97.6	63	67:33	4.6	45.7	94.7
11	5	95.1	47	68:32	1.0	4.4	96.1
12	10	93.6	31	70:30	0.8	1.7	98.7
13	15	84.6	29	69:31	0.5	0.9	99.0
14	20	44.5	14	72:28	0.1	0.3	99.4
15	50	0.9	-	80:20	0.1	0.9	99.8

<sup>a</sup> Experimental conditions: Pd(OAc)<sub>2</sub> (0.16 mmol), Pd:St:MSA:1-dodecene (1:4:40:445), polar phase (methanol and water) = 12 g, nonpolar phase (1-dodecene) = 12 g, p(CO) = 30 bar, T = 80 °C, t = 20 h, n = 1200 rpm, phase separation at room temperature.

<sup>b</sup> Determined by GC.

<sup>c</sup> Determined by gas consumption at a conversion of 20%.

<sup>d</sup> Determined by ICP-OES.

However, the modification of the polar phase with water has a negative effect on the reaction performance. The addition of water to the biphasic mixture showed that the TOF decreases significantly from 63 h<sup>-1</sup> to 14 h<sup>-1</sup> using 20 wt% water in the polar phase. Assuming a kinetically controlled biphasic reaction, which was also shown in PAPER 7 by variation of the stirrer speed having no influence on the reaction rate, the rate of methoxycarbonylation can be limited by the concentrations of the reactants 1-dodecene, carbon monoxide, and methanol in the catalyst phase. It was found that the pressure of carbon monoxide has no impact on the reaction rate (PAPER 10). However, the solubility of 1-dodecene is decreased by adding water to the polar phase, which could lead to lower reaction rates. On the other hand, the concentration of methanol is also reduced by adding water to the polar phase, which could result in the observed reduction of reaction rate, indicating the methanolysis as the RDS of the methoxycarbonylation. Interestingly, the experimental results revealed that the addition of water for recycling optimization does not lead to the formation of significant amounts of the carboxylic acid as a side product. The yield of the acid does not exceed 1.8% for the investigated reaction mixtures, meaning that the hydrolysis-equilibrium is fully shifted to the side of the ester and the ester to acid ratio is above 50. Hence, the biphasic methoxycarbonylation of 1-dodecene outperforms clearly the methoxycarbonylation in microemulsion systems, in which the ester to acid ratio is at most 2.3.

Second, it was found that the modification of the nonpolar phase by adding alkanes as co-solvents is a promising tool to reduce catalyst leaching into the

product phase. Compared to the system without co-solvent, the leaching of palladium and phosphorus can be decreased to 0.5 ppm and 2.3 ppm, respectively, using octane as co-solvent. The type of alkane as co-solvent showed no impact on the leaching and reaction performance.

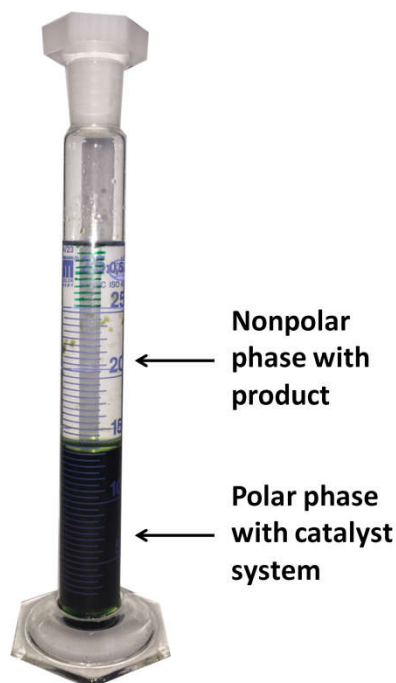


**Figure 13.** Reaction mixture after phase separation at room temperature (separation time of 10 min) for the described experiment in Table 2, entry 12 (**PAPER 7**).

As shown, good leaching results could be obtained using at least 10 wt% water in the polar phase. To investigate the impact of different substrates on the reaction performance and phase separation behavior of the methoxycarbonylation, a biphasic system with 10 wt% water in the polar methanol phase was used as a benchmark. Additionally, octane as co-solvent was added to avoid rigorous shifts because of the formation of the corresponding product, making the results better comparable. The corresponding results are shown in Table 3. Furthermore, preliminary investigations showed that solventless biphasic systems are not feasible for the methoxycarbonylation of styrene, methyl 10-undecenoate, and 1-octene, since no phase separation occurs after the reaction at room temperature, preventing subsequent catalyst recycling. As expected, the type of the substrate and its polarity has a huge impact on the reaction performance and the phase separation. Comparing the linear  $\alpha$ -olefins 1-dodecene and 1-octene (Table 3, entry 16 and 17), similar yields and l:b selectivities can be achieved after a reaction time of 20 h. However, the TOF for 1-octene is significantly higher than the TOF of 1-dodecene, which can be explained with two reasons. Firstly, the solubility of 1-octene in the polar catalyst phase is higher than that of 1-dodecene, leading to a higher concentration of 1-octene in this phase and thus, to an advanced

reaction rate. Secondly, the length of the linear  $\alpha$ -olefin has an impact on the catalytic activity. The longer the hydrocarbon chain is, the lower is the catalytic activity, due to the hampered formation of the palladium-alkyl species. Nevertheless, the phase separation proceeds very fast after the reaction, leading to a polar catalyst phase and nonpolar product phase. In both cases, the leaching of palladium and phosphorus is under the detection limit of ICP. Slight differences can be measured in the product distribution after phase separation, 97% of the product is located in the nonpolar phase for the 1-dodecene methoxycarbonylation and as expected, the content of the more polar product methyl nonanoate reaches only 89%.

**Table 3.** Methoxycarbonylation in biphasic systems: Substrate scope.<sup>a</sup>

Entry	substrate	Yield (Ester) <sup>b</sup> [%]	TOF <sup>c</sup> [h <sup>-1</sup> ]	l:b <sup>b</sup>	Pd leaching <sup>d</sup> [ppm]	P leaching <sup>d</sup> [ppm]	product in nonpolar phase <sup>b</sup> [%]
16	1-dodecene	91.7	9	68:32	-	-	97.0
17	1-octene	93.1	15	68:32	-	-	89.0
18	styrene	96.8	41	55:45	0.5	4.5	35.4
19	methyl 10-undecenoate	84.6	19	63:37	0.6	1.7	60.4
20	cyclohexene	44.5	12	-	-	-	63.5

<sup>a</sup> Experimental conditions: Pd(OAc)<sub>2</sub> (0.16 mmol), Pd:SX:MSA (1:4:40), polar phase: methanol 10.8 g, water = 1.8 g, nonpolar phase: substrate = 3 g, octane = 9 g, p(CO) = 30 bar, T = 80 °C, t = 20 h, n = 1200 rpm, phase separation at room temperature.

<sup>b</sup> Determined by GC.

<sup>c</sup> Determined by gas consumption at a conversion of 20 %.

<sup>d</sup> Determined by ICP-OES.

Similar trends can be observed for the other investigated substrates (Table 3, entries 18-20). The higher the polarity of the substrate, the higher is the reaction rate but the lower is the content of the corresponding product in the nonpolar phase. For styrene methoxycarbonylation, the content of the corresponding product is very low with 35.4%. Hence, the applied biphasic system is not suitable for styrene as the substrate. However, the biphasic system can be modified with the addition of further co-solvents, either to the polar or nonpolar phase, improving the catalyst recycling and product separation after the reaction, which was shown in **PAPER 7** for 1-dodecene.

In summary, the results reveal the feasibility of the methoxycarbonylation of different substrates in liquid/liquid biphasic systems. Considering the reaction performance and separation behavior, the biphasic system has to be selected carefully to meet the requirements of an ecological and economical biphasic reaction. Moreover, simple modifications of both, the polar and nonpolar phase,

by adding co-solvents can lead to a significant optimization of catalyst recycling and product separation properties. To transfer the methoxycarbonylation of 1-dodecene to a continuously operated process, a biphasic system was chosen composed of 10 wt% water/methanol as the polar phase and octane/1-dodecene in a mass ratio 3:1 as the nonpolar phase. The mass of the polar and nonpolar phase is the same with 12 g. Furthermore, palladium acetate as the precursor is applied with a molar amount of 0.16 mmol, in which the Pd: SX:MSA ratio was kept constant with 1:4:40, ensuring phase separation and catalyst stability.

### 4.3.2 Parameter studies

For the transfer of the lab scale results to a miniplant, not only an appropriate biphasic system is crucial, but also suitable reaction conditions to ensure the long-term stability of the catalytic system, general phase separation, and good reaction performance. Hence, the temperature and pressure have been varied in lab scale experiments with special focus on the reaction performance and phase separation behavior, which was investigated in **PAPER 10**. The applicability of the phase separation was first investigated at room temperature. It was found that both, reaction pressure and temperature, have no influence on the phase separation properties, particularly on the dynamic of phase separation, distribution of the product, and catalyst leaching. Thus, the solvent selection, which was described in the previous section, determines the quality of phase separation. Considering the described biphasic reaction mixture, the leaching of palladium and phosphorus is less than 0.1 ppm and 1 ppm, respectively. As expected, the distribution of the product into the nonpolar phase is rather high and exceeds 95%, independent from the reaction conditions.

In contrast, the variation of the reaction conditions showed a huge impact on the reaction performance. It was found that the methoxycarbonylation can already be carried out at low carbon monoxide pressure (5 bar) without loss in catalytic activity. The experimental results hint that the methanolysis step is rate determining, in which the palladium-acyl species is the resting state of the catalytic cycle. After 20 h reaction time at 5 bar carbon monoxide, the conversion of 1-dodecene was 94.8%, in which a yield to the ester of 72.6% was achieved. The l:b regioselectivity was 69:31, which was independent on the carbon monoxide pressure. However, the investigations turned out that the pressure of carbon monoxide affects strongly the isomerization of 1-dodecene. The higher the pressure, the lower is the yield of dodecene isomers, indicating a suppression of isomerization at high carbon monoxide pressure. As expected, the variation of the reaction temperature showed that the initial reaction rate increases with higher temperatures (see Table 4). An Arrhenius behavior was observed up to 80 °C, indicating a kinetically controlled biphasic reaction, which is in agreement with the investigations in **PAPER 7**. An activation energy of

203 KJ/mol could be calculated. A further increase of the reaction temperature deviates from the Arrhenius behavior, which cannot be attributed to mass transfer limitations since the formation of palladium black could be observed above 80 °C. Thus, the conversion of 1-dodecene after 20 h reaction time reaches a maximum of 94.8% at a reaction temperature of 80 °C. The influence of temperature and catalyst concentration on catalyst stability has been also studied in **PAPER 11**. Moreover, the experimental results revealed that the isomerization of 1-dodecene can be suppressed at high temperatures, improving significantly the chemoselectivity of the methoxycarbonylation up to 92% at 100 °C. The energetic barriers for the methoxycarbonylation and isomerization reaction are rather different, leading to an increase of the selectivity with higher temperature. Mecking et al. showed similar results in DFT calculations for the isomerizing methoxycarbonylation of methyl heptenoate, in which a higher activation barrier for the methoxycarbonylation was found compared to the isomerization.<sup>25</sup>

**Table 4.** Methoxycarbonylation of 1-dodecene: Variation of the temperature (adapted from **PAPER 10**).<sup>a</sup>

Entry	T [°C]	Conversion <sup>b</sup> [%]	Yield (Ester) <sup>b</sup> [%]	TOF <sup>c</sup> [h <sup>-1</sup> ]	Selectivity <sup>b</sup> [%]	l:b <sup>b</sup>	Product in nonpolar phase <sup>b</sup> [%]
<b>21</b>	60	13.9	1.7	0.1	12.2	73:27	95.2
<b>22</b>	70	38.1	12.5	0.7	32.8	71:29	97.4
<b>23</b>	80	94.8	72.6	6.4	76.6	69:31	97.7
<b>24<sup>d</sup></b>	90	85.8	72.4	11.3	84.4	68:32	97.5
<b>25<sup>d</sup></b>	100	87.2	80.2	17.8	92.0	69:31	96.7

<sup>a</sup> Experimental conditions: Pd(OAc)<sub>2</sub> (0.16 mmol), Pd: SX:MSA (1:4:40), polar phase (m<sub>methanol</sub> = 10.8 g, m<sub>water</sub> = 1.2 g), nonpolar phase (m<sub>1-dodecene</sub> = 3 g, m<sub>octane</sub> = 9 g), p(CO) = 5 bar, t = 20 h, n = 1,200 rpm, phase separation at room temperature.

<sup>b</sup> Determined by GC.

<sup>c</sup> Determined by gas consumption at a conversion of 10%.

<sup>d</sup> Pd black formation at the end of the reaction.

Based on these results, a temperature of 80 °C was chosen to transfer the results into the continuously operated miniplant, ensuring long-term catalyst stability and good reaction performance. Moreover, the pressure was set to 5 bar carbon monoxide despite enhanced isomerization at low pressures. However, isomerization can be suppressed by an appropriate choice of the operating conditions in the miniplant, which is showed in the next section.

### 4.3.3 Proof of concept in a miniplant

The proof of concept for the biphasic methoxycarbonylation was done in a miniplant, operated continuously 100 h (**PAPER 10**). Special attention was paid on the impact of the internal cycles and concentration shifts on the reaction performance and phase separation properties. Different operation modes (SP) have been applied during the continuous process, investigating the impact of residence time and stirrer speed on both, the reaction performance and separation results. Figure 14 shows the miniplant operation results for the methoxycarbonylation of 1-dodecene with respect to the reaction performance. After inertization with nitrogen, all components were introduced into the high-pressure section of the miniplant, according to the masses described in section 4.3.1. Afterward, the recycle pumps of the decanter were started, establishing stable phase separation under full recycling conditions. The reactor was heated to 80 °C and the nitrogen atmosphere was replaced by 5 bar carbon monoxide, marking the start of the reaction at operation hour 0. The miniplant was operated in full recycle mode to operation hour 20 (SP 1) in order to reach the first working point quickly. Despite the formation of more hydrophilic esters, the phase separation could be initiated at 25 °C in the decanter. At the end of SP 1, a yield to the esters of 54.9% and a conversion of 1-dodecene of 82% could be obtained. Interestingly, it was found that the l:b regioselectivity in the miniplant is constant around 82:18, which outperforms the findings in the lab scale experiments. This fact could be explained by the observed induction period in lab scale experiments (see **PAPER 7** and **PAPER 10**), which could be suppressed in the miniplant operation because of applied catalyst conditioning. Thus, the active palladium hydride species is available in sufficient amounts at operation hour 0, resulting in a higher l:b regioselectivity and higher initial reaction rates in miniplant scale. However, it was shown in **PAPER 10** that an efficient catalyst preformation can be adapted to lab scale, hampering the induction period of the methoxycarbonylation. In SP 2, the continuous operation was initiated by activating the 1-dodecene feed stream. The continuous operation could be stabilized at least for 40 hours with only small changes in the reaction performance because of the dilution of the reactor content with fresh 1-dodecene and concentration shifts due to internal recycles, indicating steady state conditions at the end of SP 2. Moreover, it was found that the reaction residence time has an impact on the chemoselectivity of the reaction. The lower the residence time, the higher is the chemoselectivity because of the hampered isomerization, which was investigated in SP 3.1 and 3.2. It is important to consider that steady state conditions could not be awaited due to lack of total operation time. Additionally, the stirrer speed was reduced in SP 3.2, increasing abruptly the chemoselectivity of methoxycarbonylation to 91%. It was shown that the absence of the catalyst

phase in the decanter due to the reduced stirring speed leads to the increase of chemoselectivity.

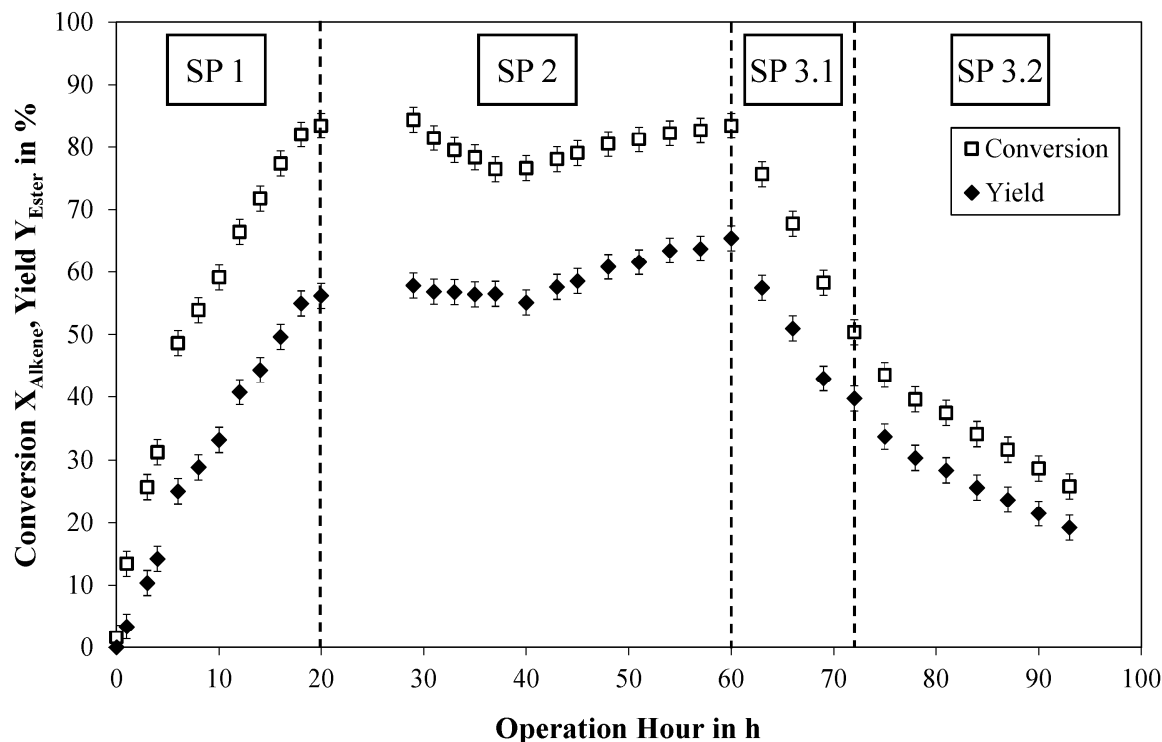


**Figure 14.** Miniplant operation results for the methoxycarbonylation of 1-dodecene (taken from **PAPER 10**). **SP 1:** Full recycle,  $\tau_{\text{Reactor}} = 0.51$  h, recycle ratio (nonpolar:polar) = 0.5:0.5, Feed rate = 0 g/h, Stirrer Speed = 1300 rpm, **SP 2:** Continuous Operation,  $\tau_{\text{Reactor}} = 0.49$  h, recycle ratio (nonpolar:polar) = 0.5:0.5, Feed rate = 30 g/h, Stirrer Speed = 1300 rpm, **SP 3:** Continuous Operation,  $\tau_{\text{Reactor}} = 0.45$  h, recycle ratio (nonpolar:polar) = 0.5:0.5, Feed rate = 100 g/h, Stirrer Speed = 1300 rpm, **SP 4:** Continuous Operation,  $\tau_{\text{Reactor}} = 0.45$  h, recycle ratio (nonpolar:polar) = 1:0, Feed rate = 100 g/h, Stirrer Speed = 700 rpm.

Furthermore, it turned out that the phase separation in the decanter could be maintained during the whole operation time. First, the palladium and phosphorus leaching into the nonpolar product phase were below 25 ppb and 250 ppb, respectively, confirming the lab results. Second, the ester content in the nonpolar product phase exceeds 99%, which is also in accordance with lab findings.

In summary, the feasibility of the process concept was shown for the methoxycarbonylation of 1-dodecene in a continuously operated miniplant in a simple biphasic system. The applicability of the applied biphasic mixture and reaction conditions was proven with long-term catalyst stability, phase separation with low catalyst leaching, and good overall reaction performance. Moreover, it was shown that the time for making new process concepts applicable in larger scale can be drastically reduced working hand in hand with constant interaction between the lab and miniplant operators.

## 4.4 Hydroxycarbonylation in Microemulsion Systems

In contrast to the methoxycarbonylation of 1-dodecene, a solventless biphasic hydroxycarbonylation, in which water act as catalyst phase and 1-dodecene as nonpolar phase, cannot be applied. Since the solubility of 1-dodecene is too low in the aqueous phase, no reaction progress could be observed. Indeed, polar organic co-solvents such as acetonitrile or dimethylformamide can be used to modify the polarity of the aqueous phase, leading to an enhanced solubility of 1-dodecene and thus, to an overall better reaction performance. However, the use of these toxic solvents is incompatible with the requirements of Green Chemistry and should be avoided. A smart and sustainable approach to overcome limitations by the solventless biphasic system is the use of surfactants as phase transfer agent for the hydroxycarbonylation of 1-dodecene, which is described in this section. Moreover, the temperature-induced switchability of the phase behavior can be used to separate the product and recycle the catalytic system via phase separation. Special attention was paid to the catalyst behavior in microemulsion systems (**PAPER 1** and **PAPER 2**) to recycle the catalyst quantitatively. Furthermore, the hydroxycarbonylation of 1-dodecene has been studied in microemulsion systems to correlate the phase behavior and reaction performance (**PAPER 11**).

### 4.4.1 Catalyst Behavior in Microemulsion Systems

Detailed knowledge of the catalyst distribution in surfactant-based systems is important for an efficient catalyst recycling as well as for evaluating the reaction performance. In contrast to ordinary biphasic systems, microstructures are formed in systems with a surfactant as phase transfer agent, affecting strongly the catalyst distribution in such a system. Hence, the impact of the type of ligand, the type of surfactant, and the temperature on the distribution of the catalyst complex has been systematically investigated. Special focus was set on the water-soluble ligands TPPTS and SX and the nonionic surfactants to exclude ionic interaction between the surfactant and ligand. Initially, the effect of the ligands on the distribution in aqueous micellar solutions has been studied to avoid interactions with the corresponding oil phase and the formation of the entire catalyst complex. As expected, it was found in **PAPER 2** that the hydrophobic ligands TPP and XantPhos show similar partition coefficients in water/octanol and aqueous micellar solutions. In contrast, the water-soluble analogs TPPTS and SX exhibit a completely different behavior in both systems. On the one hand, the logarithm of the partition coefficient is low in water/octanol for both ligands, indicating the solubility of these ligands in the water phase. On the other hand, a high partition coefficient was obtained in aqueous micellar solutions, leading to the conclusion that the ligand is incorporated into the micellar microstructure. It turned out that the surface

active properties, which were determined in investigations of the surface tension, lead to the inclusion of the water-soluble ligands in the micelle. Furthermore, a minor impact of the hydrophobicity of the surfactant was found with respect to the partition coefficient, in which a more hydrophilic surfactant increases the micelle-water partition coefficient. Besides the polarity of the ligand, further effects have to be considered to predict the partition coefficients in aqueous micellar solutions, particularly the surface active properties of the ligand and molecular interactions between ligand and surfactant.

However, to perform organic transformations in surfactant-based systems, these basic findings have to be extended to the entire catalyst complexes. Furthermore, the impact of the additional organic phase containing the substrate has to be considered. Hence, the distribution of catalyst complexes in microemulsion systems has been investigated in **PAPER 1**, in which rhodium as the metal center was chosen. In general, the same behavior could be observed for the entire catalyst complex compared to the sole ligand. Using the hydrophobic ligands TPP and XantPhos in microemulsion systems composed of water, 1-dodecene, and Marlipal 24/70 as the surfactant, most of the rhodium complex is located in the oil excess phase of the triphasic microemulsion system. In contrast, it was found that the rhodium complexes formed with TPPTS and SX are located in the surfactant-rich phase to a larger extent. Interestingly, using SX as the ligand, 96.3% of the catalyst complex are in the bicontinuous middle phase of the microemulsion system, which is due to the surface active properties of the ligand. It was concluded that the ligand determines the surface active properties of the whole catalyst complex and thus, the catalyst complex behaves like a surfactant, accumulating in the middle phase of the microemulsion system. Investigations on the surface tension of the whole catalyst complex confirm this observation. Moreover, the distribution of the SX-modified rhodium complex in the different phase regions has been studied. As expected, it was found that in the  $2\Phi$  region, 99.99% of the catalyst is located in the microemulsion phase, whereas in the  $\bar{2}\Phi$  region the catalyst is in both phases equally distributed. However, not only the catalyst distribution but also the phase separation dynamics has to be considered for the application of microemulsion systems with subsequent catalyst recycling. Thus, the time for phase separation in the different phase regions of the microemulsion system has been investigated in **PAPER 1**. It turned out that the three-phase region of the microemulsion system is of great interest for the application of metal-catalyzed reactions in microemulsion systems. First, the time for phase separation can be decreased, enabling a smaller decanter in a continuous process. Second, the oil and water excess phase allows separation of hydrophobic and hydrophilic side and main products. Changing the catalytic system from rhodium-SX to palladium-SX, the same catalyst behavior in microemulsion systems could be

observed, which is depicted in Figure 15. Due to the surface active properties of the catalyst complex, it is like a surfactant and follows the surfactant into the corresponding phase.

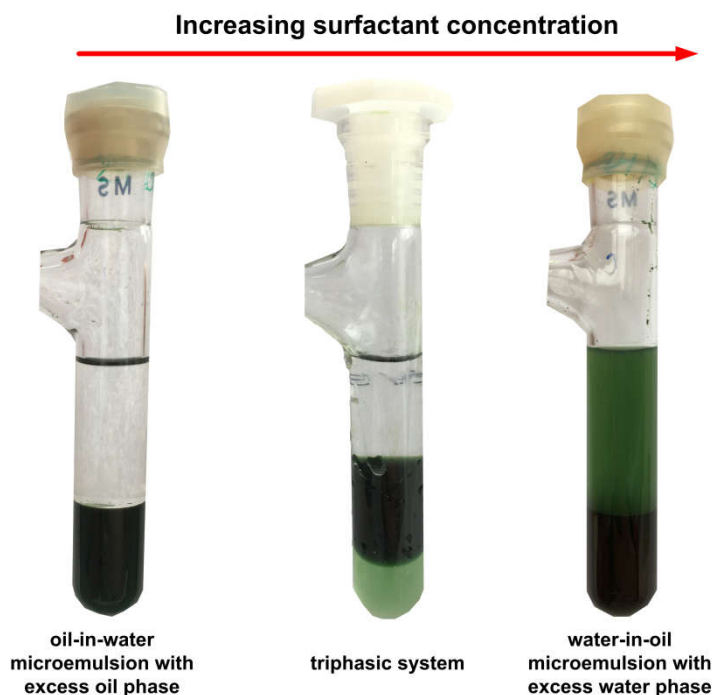


**Figure 15.** Schematic pictures of the oil-in-water microemulsion, triphasic system and water-in-oil microemulsion for the palladium-catalyzed hydroxycarbonylation of 1-dodecene (taken from **PAPER 11**). Test conditions:  $T=85\text{ }^{\circ}\text{C}$ ,  $\alpha=0.5$ , 1 wt%  $\text{Na}_2\text{SO}_4$ ,  $\text{Pd}_2(\text{allyl})_2\text{Cl}_2$  (0.02 mmol),  $\text{Pd}:\text{SX}:\text{MSA}:\text{1-dodecene}=1:4:40:110$ , mass ratio 1-dodecene to dodecane=1:3, Marlipal 24/50 as the surfactant,  $\gamma=4\%$  (left),  $\gamma=9\%$  (middle),  $\gamma=14\%$  (right).

#### 4.4.2 Nonionic Surfactants as Phase Transfer Agent

Besides the catalyst behavior, the phase behavior of microemulsion systems plays a crucial role to evaluate the reaction performance in these systems and to ensure catalyst recycling via phase separation. Particularly, the interaction between phase behavior and reaction performance is of great interest to identify crucial operation parameters such as surfactant concentration, the hydrophobicity of the surfactant, and reaction temperature, which has been investigated in **PAPER 11**. Figure 16 shows the phase diagram of the microemulsion system composed of 1-dodecene/dodecane as the nonpolar phase, water and the surfactant Marlipal 24/50. It is important to notice that all reaction components such as catalyst precursor, ligand, and co-catalyst were added to screen the phase behavior, since their addition can lead to a remarkable shift in the phase boundaries. For instance, it was found in **PAPER 1** that the addition of SX as the ligand can lead to a switch of the phase boundaries up to 10 K, dependent on the SX amount. Investigations on the phase behavior were limited to temperatures up to  $90\text{ }^{\circ}\text{C}$ , since the

formation of palladium black was observed at higher temperatures. It turned out in **PAPER 11** that the investigated microemulsion system can be characterized with a minimal surfactant concentration  $\tilde{\gamma}$  of 14% with a corresponding temperature  $\tilde{T}$  of 61 °C. Investigations on the phase behavior are the basis to find a suitable operation window for the subsequent catalyst recycling and should be considered for an efficient selection of the surfactant.

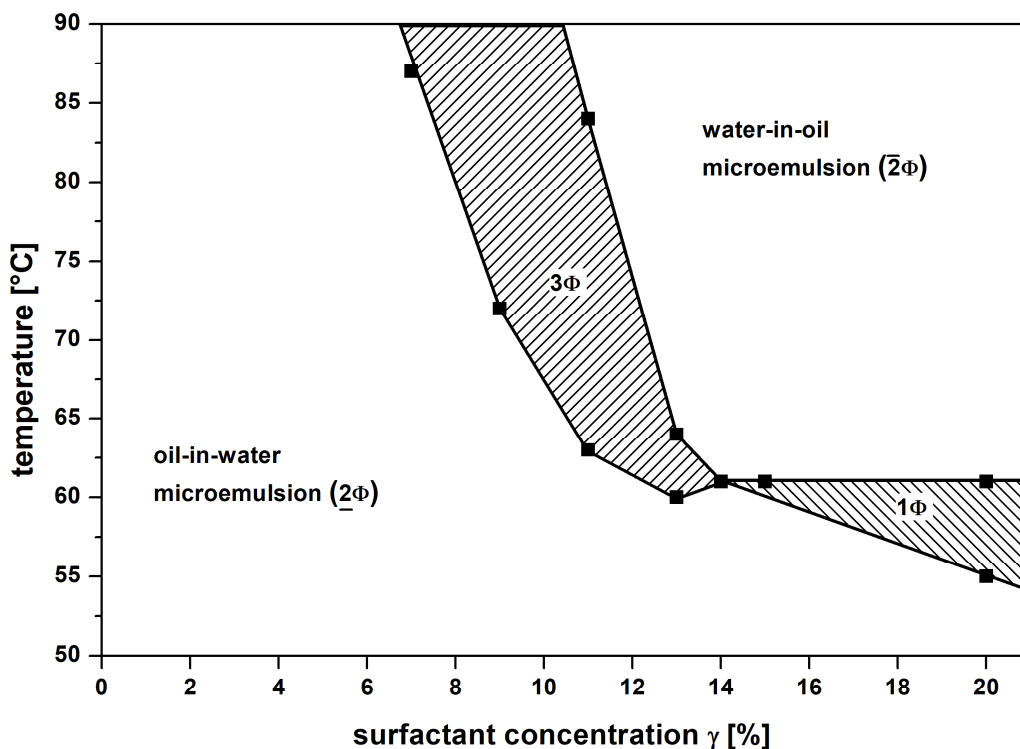


**Figure 16.** Phase diagram of a mixture of 1-dodecene, dodecane, water, and Marlipal (24/50) (taken and modified from **PAPER 11**). Test conditions:  $\alpha=0.5$ , 1 wt%  $\text{Na}_2\text{SO}_4$ ,  $\text{Pd}_2(\text{allyl})_2\text{Cl}_2$  (0.02 mmol),  $\text{Pd}:\text{SX}:\text{MSA}:\text{1-dodecene}=1:4:40:110$ , mass ratio 1-dodecene to dodecane=1:3.

With the phase behavior of the microemulsion system in mind, the impact of surfactant concentration, reaction temperature, type of surfactant, organic co-solvents and catalyst concentration on the reaction performance has been systematically studied in **PAPER 11**. It was found that the hydroxycarbonylation of 1-dodecene in microemulsion systems is a kinetically controlled multiphase reaction, indicated by a typical Arrhenius type behavior at mild reaction temperatures. However, increasing the temperature above 90 °C leads to a significant loss of catalytic activity due to the formation of palladium black which is similar to the methoxycarbonylation of 1-dodecene in biphasic mixtures (see **PAPER 10**). Variation of the surfactant concentration shows that the catalytic activity, indicated by the yield of linear acid and conversion of 1-dodecene, increases with higher amounts of surfactant (see Figure 17). As

expected, a minimal surfactant concentration ( $\gamma > 3\%$ ) is necessary to accelerate significantly the rate of hydroxycarbonylation, marked by the surfactant concentration  $\gamma_o$ , which is needed to form a microemulsion.

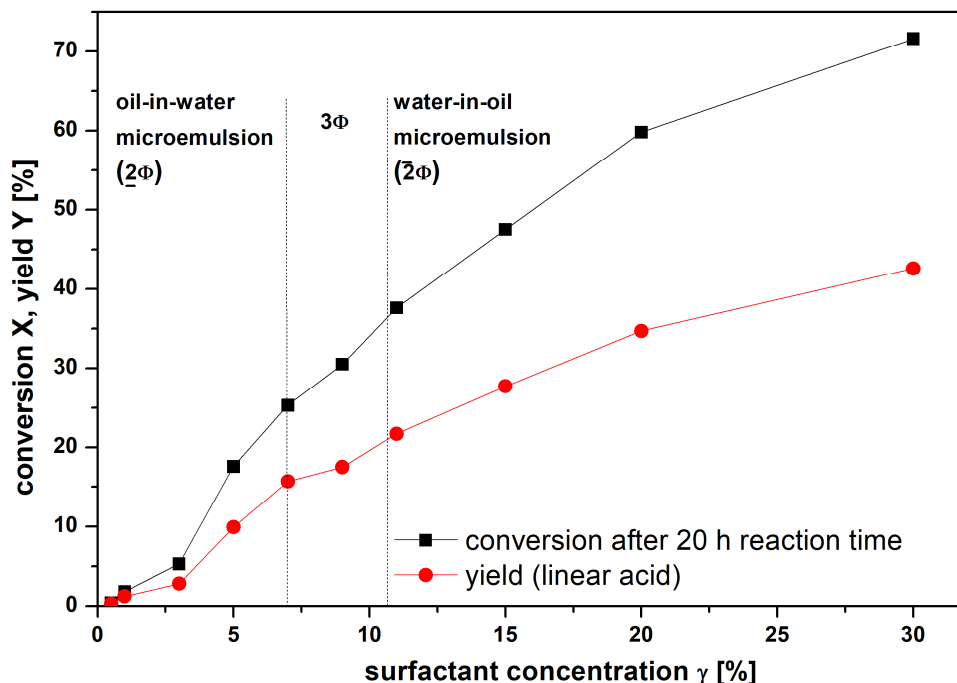


**Figure 17.** Effect of the surfactant concentration on the hydroxycarbonylation of 1-dodecene (taken from **PAPER 11**). Experimental conditions:  $\text{Pd}_2(\text{allyl})_2\text{Cl}_2$  (0.08 mmol),  $\text{Pd}:\text{SX}:\text{MSA}:\text{1-dodecene}=1:4:40:110$ ,  $\alpha=0.5$ , dodecane as the co-solvent (9 g), water (12 g), Marlipal 24/50 as the surfactant,  $\text{Na}_2\text{SO}_4$  (1 wt%),  $p(\text{CO})=30$  bar,  $T=85$  °C,  $n=1200$  rpm,  $t=20$  h.

Interestingly, the phase behavior changes from an oil-in-water microemulsion to a triphasic system at a surfactant concentration of  $\gamma=7\%$  and finally to a water-in-oil microemulsion at  $\gamma=11\%$ . However, the yield and conversion increase steadily, indicating no impact of the phase behavior on the reaction performance. Further investigations with modification of the nonpolar phase and the variation of the degree of ethoxylation confirm that the reaction performance does not care about the phase behavior of the microemulsion system. From these results, it could be concluded how catalysis, especially metal-catalyzed transformations, works in microemulsion systems. Since the applied water-soluble catalyst complex is surface active, the hydroxycarbonylation takes mainly place at the interface between the oil and water. Thus, the local concentrations of the reactants at the oil-water interface, including the concentration of the active catalyst complex, and the size of the interface are crucial for the reaction performance. Hence, it was found that amount and hydrophilicity of the surfactant should be considered as the main parameters influencing the reaction performance. First, the amount of the

surfactant provides the size of the interfacial area, affecting strongly the reaction performance. The higher the amount of surfactant, the higher is the interfacial area, the better is the catalytic activity. However, the interfacial area can only be increased to a maximum at which further effects like viscosity have to be considered. Second, the type of surfactant, particularly the degree of ethoxylation, is crucial for the reaction performance. The hydrophilicity of the surfactant determines the local concentrations of the reactants at the interface. Thus, an accumulation of the reactants at the interface by the choice of an appropriate surfactant enhances the reaction performance in microemulsion systems. These findings are in agreement with **PAPER 8**, in which the role of nonionic surfactants for the rhodium catalyzed hydroformylation has been investigated. Here, the amount and type of surfactant are also of utmost importance for the catalytic activity in microemulsion systems.

#### 4.4.3 Ionic Surfactants as Phase Transfer Agent

Additionally, ionic surfactants as phase transfer agents have been investigated for the palladium-catalyzed hydroxycarbonylation of 1-dodecene. Here, ionic interactions between the catalyst complex and the surfactant have to be considered to evaluate the reaction performance and separation behavior. Initially, the ionic surfactants SDS and CTAB were tested as a benchmark, which is shown in Table 5.

**Table 5.** Hydroxycarbonylation of 1-dodecene: Ionic surfactants as phase transfer agents.<sup>a</sup>

Entry	Surfactant	Surfactant concentration $\gamma$ [%]	Conversion <sup>b</sup> [%]	Yield (Acid) <sup>b</sup> [%]	TOF <sup>c</sup> [ $\text{h}^{-1}$ ]	l:b <sup>b</sup>	Phase separation
26	SDS	2	<1	0	0	/	No
27	CTAB	2	27.3	19.9	33.1	90:10	No
28	CTAB	1	20.7	15.8	24.0	89:11	No
29	CTAB	0.5	10.1	7.9	4.7	88:12	No
30	CTAB	0.2	2.3	1.6	0.9	84:16	Yes

<sup>a</sup> Experimental conditions:  $\text{Pd}(\text{OAc})_2$  (0.05 mmol),  $\text{Pd}:\text{SX}:\text{MSA}$  (1:4:120),  $m_{\text{water}} = 12$  g,  $m_{1\text{-dodecene}} = 12$  g,  $p(\text{CO}) = 30$  bar,  $T = 80$  °C,  $t = 6$  h,  $n = 1200$  rpm, phase separation at room temperature.

<sup>b</sup> Determined by GC.

<sup>c</sup> Determined by GC after 1 h reaction time.

Clear differences are visible comparing the cationic CTAB and anionic SDS (Table 5, entries 26 and 27) at a fixed surfactant concentration ( $\gamma=2\%$ ). A TOF of  $33.1 \text{ h}^{-1}$  and a yield to the carboxylic acid of 19.9% could be achieved with CTAB as the phase transfer agent, whereas no reaction takes place using the anionic SDS. The ligand SX is used to make the catalyst water-soluble, resulting

in a negatively charged catalyst complex. Thus, repulsive interaction between the anionic SDS and anionic catalyst complex occurs, hindering the catalyst to come to the oil-water interface. Since the hydroxycarbonylation mainly takes place at the oil-water interface, the reaction is hampered. In contrast, an attractive interaction between the surfactant and catalyst complex results using CTAB as the surfactant. Hence, the catalyst is strongly attached to the interface and the reaction takes place. However, phase separation is not possible, since a stable emulsion is formed after the reaction. Decreasing the amount of CTAB leads to a reduction of the catalytic activity from  $33.1 \text{ h}^{-1}$  at  $\gamma=2\%$  to  $0.9 \text{ h}^{-1}$  with a surfactant concentration of  $\gamma=0.2\%$  (Table 5, entries 27-30). Here, the interface between the oil and water is decreased, which leads to a retardation of the reaction rate. Nevertheless, the phase separation is possible using  $\gamma=0.2\%$ .

Promising results with respect to reaction performance and separation behavior were obtained with other cationic phase transfer agents. The ionic liquid 1-Methyl-3-octylimidazolium bromide (OMIM) outperforms clearly the cationic benchmark CTAB, leading to a high catalytic activity and quantitative catalyst recycling after the reaction (see Table 6, entry 31). To understand the role of the ionic liquid, acting as a cationic surfactant in this case, the ionic liquids of the homolog series have been investigated using a constant concentration of the phase transfer agent (0.5 M) and the fivefold CMC (see Table 6). It is mentionable that the concentration is expressed as moles of the ionic liquid in the water phase. Additionally, the CMC was measured with the bubble tensiometer at  $25 \text{ }^\circ\text{C}$ .

**Table 6.** Hydroxycarbonylation of 1-dodecene: Ionic liquids as phase transfer agents.<sup>a</sup>

Entry	Surfactant	CMC <sup>b</sup> [mM]	Yield (Acid) <sup>c</sup> [%] 5 x CMC	TOF <sup>d</sup> [h <sup>-1</sup> ] 5 x CMC	Yield (Acid) <sup>c</sup> [%] c = 0.5 M	TOF <sup>d</sup> [h <sup>-1</sup> ] c = 0.5 M
<b>31</b>	OMIM	135.3	51.4	10.5	43.8	13.1
<b>32</b>	DecMM	31.3	45.7	9.2	57.4	17.8
<b>33</b>	DodecMIM	10.0	16.7	3.1	60.5	29.9

<sup>a</sup> Experimental conditions: Pd(OAc)<sub>2</sub> (0.05 mmol), Pd: SX:TSA (1:4:40), m<sub>water</sub> = 12 g, nonpolar phase (m<sub>1-dodecene</sub> = 3 g, m<sub>octane</sub> = 9 g), p(CO) = 30 bar, T = 85 °C, t = 20 h, n = 1200 rpm.

<sup>b</sup> Determined by bubble pressure tensiometer at 25 °C.

<sup>c</sup> Determined by GC.

<sup>d</sup> Determined by gas consumption at a conversion of 20%.

As expected, the CMC decreases with increasing carbon chain length from 135.3 mM for OMIM to 10.0 mM for DodecMIM. Moreover, a significant drop of the yield and the TOF can be found using the fivefold CMC of each ionic

liquid in the hydroxycarbonylation reaction. The TOF decreases from 10.5 h<sup>-1</sup> with OMIM to 3.1 h<sup>-1</sup> with DodecMIM as the phase transfer agent. Since the fourfold CMC of each ionic liquid is responsible for the formation of the interfacial area, the oil-water interface decreases from OMIM to DodecMIM, leading to smaller TOF. In contrast, the yield and TOF increase significantly from OMIM to DodecMIM using a constant concentration of the ionic liquid of 0.5 M. Since the CMC is the lowest for DodecMIM, we assume that the interface is larger compared to the other ionic liquids, resulting in a higher TOF. Besides the impact of the homolog series of the ionic liquid, the effect of concentration has been studied. For this purpose, the OMIM concentration has been varied between 0.1 M and 1.0 M (see Table 7). No reaction takes place using 0.1 M OMIM in the water phase because the CMC was not reached (Table 7, entry 34). Increasing the OMIM concentration to 0.2 M, the conversion, yield, and TOF can be significantly enhanced which is similar to the results with nonionic surfactants as the phase transfer agent (**PAPER 11**). In general, the higher the OMIM concentration, the higher is the interfacial area between water and oil, resulting in an enhancement of conversion, yield, and TOF. The l:b selectivity remains constant at 88:12 and 89:11, respectively. Interestingly, the isomerization of 1-dodecene accelerates with increasing OMIM concentration, leading to the high conversions at high OMIM concentrations.

**Table 7.** Hydroxycarbonylation of 1-dodecene: Variation of OMIM concentration.<sup>a</sup>

Entry	Surfactant	Surfactant concentration [M]	Conversion <sup>b</sup> [%]	Yield (Acid) <sup>b</sup> [%]	TOF <sup>c</sup> [h <sup>-1</sup> ]	l:b <sup>b</sup>	Phase separation
34	OMIM	0.1	traces	traces	-	-	Yes
35	OMIM	0.2	28.3	22.1	3.6	88:12	Yes
36	OMIM	0.3	37.2	27.8	6.0	89:11	Yes
37	OMIM	0.5	51.1	34.8	7.0	89:11	Yes
38	OMIM	0.7	76.9	52.6	10.4	89:11	Yes
39	OMIM	1.0	84.3	54.9	10.7	88:12	Yes

<sup>a</sup> Experimental conditions: Pd(OAc)<sub>2</sub> (0.05 mmol), Pd: SX:TSA (1:4:40), m<sub>water</sub> = 12 g, nonpolar phase (m<sub>1-dodecene</sub> = 3 g, m<sub>octane</sub> = 9 g), p(CO) = 30 bar, T = 80 °C, t = 20 h, n = 1200 rpm, phase separation at room temperature.

<sup>b</sup> Determined by GC.

<sup>c</sup> Determined by gas consumption at a conversion of 20%.

In all cases, the phase separation was possible at room temperature after the reaction, resulting in quantitative separation into a product phase (<90% of the product) and catalyst containing water phase (Pd leaching <0.5 ppm). Furthermore, recycling runs indicate the feasibility of these systems for the hydroxycarbonylation of 1-dodecene, including a subsequent catalyst recycling

and product separation. Four runs could be performed without any loss in catalytic activity and low leaching of palladium and phosphorous.

#### 4.5 Alkaline Hydrolysis of long chain esters

As shown in the previous sections, the methoxycarbonylation and hydroxycarbonylation demand different multiphase systems to facilitate the reaction step and the subsequent catalyst recycling step. On the one hand, a simple biphasic system is sufficient for the methoxycarbonylation reaction, which enables an excellent reaction performance and quantitative catalyst recycling. The proof of concept was also shown in a continuously operated miniplant, confirming long-term catalyst stability. On the other hand, the hydroxycarbonylation reaction has to be carried out in microemulsion systems, since the reaction is hampered in aqueous organic systems because of the low solubility of the substrates in water. If the carboxylic acid is the desired final product, two reaction sequences are supposable (see Figure 18).

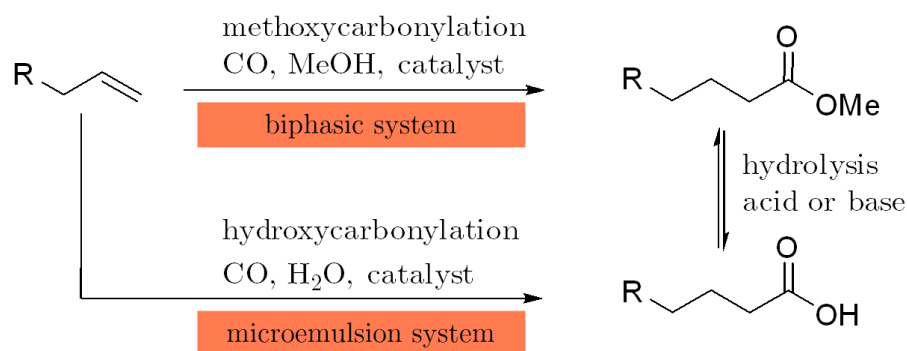


**Figure 18.** Reaction sequence for the synthesis of carboxylic acids from olefins.

First, the described one-pot synthesis in microemulsion systems. Second, a two-step sequence is possible in which the methoxycarbonylation is performed in biphasic catalysis, forming the corresponding ester, followed by an alkaline hydrolysis to produce the desired carboxylic acid. Hence, the alkaline hydrolysis of methyl decanoate has been investigated as a model reaction, which is described in detail in **PAPER 9**.

##### 4.5.1 Alkaline Hydrolysis in Water

Initially, the alkaline hydrolysis of methyl decanoate has been investigated in an aqueous sodium hydroxide solution with no further additives, varying the temperature between 40 and 80 °C (see Figure 19). For 40 and 60 °C the conversion after 20 h reaction time is 3% and 5%, respectively. As expected, the low solubility of methyl decanoate in water causes the low reaction rates, resulting in low conversions. Surprisingly, the conversion obtained after 20 h reaction time at a reaction temperature of 80 °C is 82%, although no further

additives were used. Furthermore, the slope of the conversion plot for the reaction temperature of 80° C increases as the reaction proceeds, which is an atypical trend for a second-order reaction. Obviously, the conversion of methyl decanoate to sodium decanoate accelerates the reaction. It was found that the CMC of sodium decanoate at room temperature is 0.1 mol/L, which is equal to 50% conversion of methyl decanoate. Hence, the formation of micelles, initiated by the formation of sodium decanoate during the reaction, increases the solubility of methyl decanoate, resulting in an enhancement of the reaction rate with proceeding reaction time.

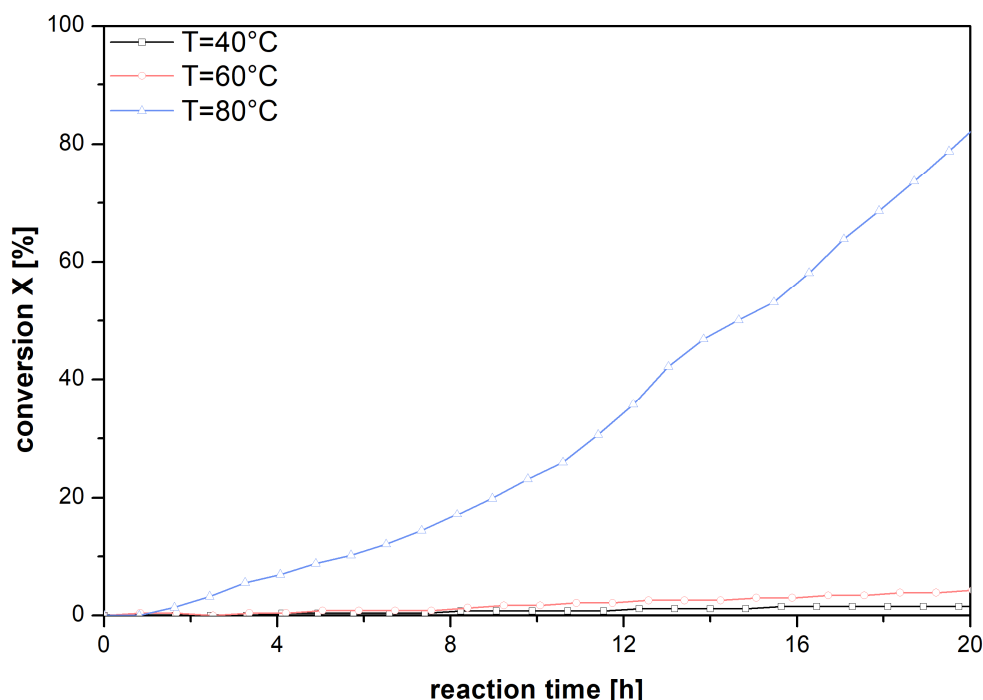


**Figure 19.** Effect of the temperature on the conversion plot of the alkaline hydrolysis of methyl decanoate in water. Experimental conditions:  $V=20$  mL,  $c_{\text{methyl decanoate}}=0.2$  mol/L,  $c_{\text{NaOH}}=0.2$  mol/L (taken from **PAPER 9**).

Obviously, the slope of the conversion plot is slightly increasing at a conversion of 40% (see Figure 19), which confirms this assumption, since the CMC of sodium decanoate is reached. We have to keep in mind that the CMC of sodium decanoate is slightly temperature-dependent, which could lead to a small mismatch.

#### 4.5.2 Alkaline Hydrolysis in Surfactant-Based Systems

To enhance the reaction performance compared to the unmodified system, surfactant-based systems has been studied. It was found that both, ionic and nonionic surfactants, increase significantly the initial reaction rate (see Table 8). However, the application of cationic surfactants outperforms clearly the results

with the nonionic benchmark TX100. Since the head groups of the applied alkyl trimethylammonium bromides carry a positive charge, an electrostatic attraction of the hydroxide ions is obtained, increasing the local concentration of hydroxide ions at the water-oil interface, which enhances the initial rate of hydrolysis.

**Table 8.** CMC values and initial reaction rates for the alkaline hydrolysis in surfactant-based systems (taken and modified from **PAPER 9**).<sup>a</sup>

Entry	Surfactant	CMC <sup>b</sup> [mM]	Initial rate $r_0^c$ [mmol/(L·h)] 10 x CMC	Normalized rate [%]	Initial rate $r_0^c$ [mmol/(L·h)] c-CMC = 10 mM	Normalized rate [%]
40	DeTAB	61.1	3839	11.9	1023	3.5
41	DTAB	14.4	2813	8.7	632	2.2
42	TTAB	5.8	703	2.2	461	1.6
43	CTAB	1.4	322	1	291	1
44	TX100	0.4	81.3	0.252	/	/
45	/	/	5	0.015	/	/

<sup>a</sup> Experimental conditions:  $V = 20$  mL,  $c_{\text{methyl decanoate}} = 0.2$  mol/L,  $c_{\text{NaOH}} = 0.2$  mol/L.

<sup>b</sup> Determined by bubble pressure tensiometer at 25 °C.

<sup>c</sup> Determined from the conversion plot at  $X = 10\%$ .

Additionally, the effect of the CMC towards the reaction performance has been investigated for the cationic surfactants. Therefore, the amount of surfactant was varied in two series of experiments, in which firstly the tenfold CMC and secondly a constant c-CMC value of 10 mM was used. The results are given in Table 8 expressed as the initial rates and normalized rates based on CTAB as the benchmark. Moreover, the CMC values were determined by bubble pressure tensiometer. As expected, with increasing chain length of the alkyl chain from 10 to 16, the CMC decreases significantly from 61.1 mmol/L to 1.4 mmol/L, indicating a higher hydrophobicity of the cationic surfactant. Using the tenfold CMC, the initial rate of hydrolysis decreases from 3839 mmol/(L·h) with DeTAB to 322 mmol/(L·h) with CTAB as the surfactant. Since the CMC increases from CTAB to DeTAB, the amount of surfactant in the reaction mixture increases drastically using the tenfold CMC, resulting in higher solubilization of methyl decanoate and thus, in a much higher initial reaction rate. Hence, experiments were carried out using the same concentration of the surfactant but corrected with the determined CMC (c-CMC = 10 mM). As a result, the molar concentration for micellization is constant which allows for a fairer comparison of the used cationic surfactants. Interestingly, the same trend can be observed whereby the initial rate decreases from 1023 mmol/(L·h) for DeTAB to 291 mmol/(L·h) for CTAB. From the normalized reaction rates, it is obvious that for the same micellar concentration, the rates are closer together,

showing that the CMC cannot be neglected in the screening of ionic surfactants. After correction of the surfactant concentration by its CMC, the more hydrophilic cationic surfactant still shows a higher reaction rate. Two more effects have to be considered for the discussion of the observed reactions rates: (a) the solubilization of methyl decanoate and (b) the local concentration of hydroxide ions at the water-oil interface. Considering the aggregation number for the investigated surfactants, which decreases from CTAB to DeTAB by a factor of about two, the number of micelles for DeTAB as the phase transfer agent is higher. Hence, the concentration of methyl decanoate is higher in the water phase which explains the higher initial reaction rate. As a result, to understand the role of the surfactant in detail, investigations of the aggregation behavior, solubilization capacity and phase behavior is essential.

## 5. Conclusion

Sustainability, recycling and Green Chemistry are not only words circling in people's minds, these words are an inherent part of our life, anchored in all areas of our society. Particularly in chemical research, much effort is done to meet the requirements of sustainability, which has opened the doors to a lot of new fields in research, fulfilling the demands of the society. This thesis is part of these efforts, showing the applicability of alternative reaction systems for chemical synthesis, which makes the production of chemicals more sustainable, more ecological and even more economical. In general, the feasibility of multiphase systems for the palladium-catalyzed methoxy- and hydroxycarbonylation of different substrates is shown in this thesis, facilitating an easy recycling of the expensive homogeneous catalyst system in its active form and the separation of the product via phase separation.

The first research focus aimed the design of a multiphase system for the palladium-catalyzed methoxycarbonylation of 1-dodecene and its implementation in a continuously operated miniplant. For this purpose, an ordinary liquid/liquid biphasic system consisting of methanol as polar catalyst containing phase and 1-dodecene/octane as nonpolar phase fulfils the requirements of a good reaction performance and phase separation. It was shown that the modification of the polar phase with small amounts of water improves drastically the quality of catalyst recycling. Parameter studies indicate that the methoxycarbonylation of 1-dodecene in the liquid/liquid biphasic system is kinetically controlled. Moreover, the transfer of the lab scale results to a continuously operated miniplant was successfully presented (reaction volume scale up factor: 19), operating continuously over 100 h with stable phase separation (Pd leaching < 25 ppb) and under steady state conditions. A substrate scope was done to identify the limitations of the applied biphasic system, showing a strong impact of the hydrophobicity of the substrate and the catalyst concentration on the quality of product separation and catalyst recycling.

The second research focus was set on the hydroxycarbonylation of 1-dodecene in multiphase systems. Although just water is used instead of methanol, compared to the methoxycarbonylation, the design of the multiphase system becomes much more complicated. The solubility of 1-dodecene in the catalyst containing water phase is too low, suppressing the hydroxycarbonylation in ordinary liquid/liquid biphasic systems. This part focused on the addition of surfactants as phase transfer agents, accelerating the reaction rate and facilitating the temperature-induced phase separation for catalyst recycling and product separation. While anionic surfactants like SDS hamper the

hydroxycarbonylation due to repulsive interaction of the applied catalyst complex and the surfactant, cationic and nonionic surfactants showed promising results in terms of reaction performance and phase separation. With the ionic liquid OMIM as phase transfer agent, the hydroxycarbonylation could be successfully performed in four consecutive runs without loss in activity and stable phase separation. Moreover, the complex role of nonionic surfactants in the palladium-catalyzed hydroxycarbonylation of 1-dodecene was investigated. Due to the surface active properties of the applied catalytic system consisting of palladium and SulfoXantPhos, it was concluded that the reaction takes place at the interface between the oil and water. Hence, not the phase behavior of the microemulsion system but the size and properties of the oil-water interface determine the reaction performance, which is mainly influenced by the kind and amount of surfactant. In addition, the alkaline hydrolysis of methyl decanoate in surfactant-based systems was investigated, which can be used to form the corresponding carboxylic acid as a consecutive step after the methoxycarbonylation reaction. The reaction rate can be significantly accelerated by the addition of nonionic and cationic surfactants, whereby the electrostatic interaction between the cationic surfactants and hydroxide ions lead to a stronger improvement of the reaction performance.

All things summarized, multiphase systems are a promising tool for the recycling of homogeneously dissolved catalyst complexes. However, the selection of a suitable reaction system is a challenging task, since a lot of aspects like the catalytic system, reaction itself, applied substrates, distribution coefficients and possible side reactions have to be considered to achieve good reaction performance and complete phase separation for catalyst recycling. With that in mind, multiphase systems can be an important contribution to Green Chemistry, helping to change the world.

## References

- (1) Anastas, P. T.; Warner, J. C. *Green Chemistry Theory and Practice*, Oxford University Press: New York, 1998.
- (2) Pogrzeba, T. Rhodium-Catalysed Hydroformylation of Long-Chain Alkenes in Aqueous Multiphase Systems : Kinetic Studies and Systematic Process Development, Technische Universität Berlin, 2018.
- (3) Hamerla, T. Hydroformylierung Langkettiger Olefine Mit Zweizähligen Rhodium-Komplexen in Mizellaren Lösungen Und Mikroemulsionen (Dissertation). **2014**, No. September 2014, 132.
- (4) Beller, M.; Cornils, B.; Frohning, C. D.; Kohlpaintner, C. W. Progress in Hydroformylation and Carbonylation. *J. Mol. Catal. A. Chem.* **1995**, *104* (1), 17.
- (5) Brennführer, A.; Neumann, H.; Beller, M. Palladium-Catalyzed Carbonylation Reactions of Alkenes and Alkynes. *ChemCatChem* **2009**, *1* (1), 28.
- (6) Kiss, G. Palladium-Catalyzed Reppe Carbonylation. *Chem. Rev.* **2001**, *101* (11), 3435.
- (7) Reppe, W. Carbonylierung I. Über Die Umsetzung von Acetylen Mit Kohlenoxyd Und Verbindungen Mit Reaktionsfähigen Wasserstoffatomen Synthesen  $\alpha,\beta$ -Ungesättigter Carbonsäuren Und Ihrer Derivate. *Justus Liebigs Ann. Chem.* **1953**, *582* (1), 1.
- (8) Reppe, W.; Kröper, H. Carbonylierung II. Carbonsäuren Und Ihre Derivate Aus Olefinischen Verbindungen Und Kohlenoxyd. *Justus Liebigs Ann. Chem.* **1953**, *582* (1), 38.
- (9) Reppe, W.; Kröper, H.; v. Kutepow, N.; Pistor, H. J. Carbonylierung III. Umsetzung von Alkoholen Und Offenen Äthern Mit Kohlenoxyd Zu Carbonsäuren. *Justus Liebigs Ann. Chem.* **1953**, *582* (1), 72.
- (10) Reppe, W.; Kröper, H.; Pistor, H. J.; Weissbarth, O. Carbonylierung IV. Einwirkung von Kohlenoxyd Und Wasser Auf Cyclische Äther. *Justus Liebigs Ann. Chem.* **1953**, *582* (1), 87.
- (11) Reppe, W. Carbonylierung V. Zur Kenntnis Der Metallcarbonyle Und Metallcarbonylwasserstoffe. *Justus Liebigs Ann. Chem.* **1953**, *582* (1), 116.
- (12) Reppe, W.; Vetter, H. Carbonylierung VI. Synthesen Mit Metallcarbonylwasserstoffen. *Justus Liebigs Ann. Chem.* **1953**, *582* (1), 133.
- (13) Mika, L. T.; Tuba, R.; Tóth, I.; Pitter, S.; Horváth, I. T. Molecular Mapping of the Catalytic Cycle of the Cobalt-Catalyzed

- Hydromethoxycarbonylation of 1,3-Butadiene in the Presence of Pyridine in Methanol. *Organometallics* **2011**, *30* (17), 4751.
- (14) Morimoto, T.; Kakiuchi, K. Evolution of Carbonylation Catalysis: No Need for Carbon Monoxide. *Angew. Chemie - Int. Ed.* **2004**, *43* (42), 5580.
- (15) de la Fuente, V.; Waugh, M.; Eastham, G. R.; Iggo, J. A.; Castellón, S.; Claver, C. Phosphine Ligands in the Palladium-Catalysed Methoxycarbonylation of Ethene: Insights into the Catalytic Cycle through an HP NMR Spectroscopic Study. *Chem. - A Eur. J.* **2010**, *16* (23), 6919.
- (16) Holzapfel, C.; Bredenkamp, T. An Empirical Study of Phosphine Ligands for the Methoxycarbonylation of Medium-Chain Alkenes. *ChemCatChem* **2015**, *7* (17), 2598.
- (17) del Río, I.; Ruiz, N.; Claver, C.; Van Der Veen, L. A.; Van Leeuwen, P. W. N. M. Hydroxycarbonylation of Styrene with Palladium Catalysts: The Influence of the Mono- and Bidentate Phosphorus Ligand. *J. Mol. Catal. A Chem.* **2000**, *161* (1–2), 39.
- (18) Konrad, T. M.; Durrani, J. T.; Cobley, C. J.; Clarke, M. L. Simultaneous Control of Regioselectivity and Enantioselectivity in the Hydroxycarbonylation and Methoxycarbonylation of Vinyl Arenes. *Chem. Commun.* **2013**, *49* (32), 3306.
- (19) Eastham, G. R.; Heaton, B. T.; Iggo, J. A.; Tooze, R. P.; Whyman, R.; Zacchini, S. Synthesis and Spectroscopic Characterisation of All the Intermediates in the Pd-Catalysed Methoxycarbonylation of Ethene. *Chem. Commun.* **2000**, No. 7, 609.
- (20) Drent, E.; Budzelaar, P. H. M. Palladium-Catalyzed Alternating Copolymerization of Alkenes and Carbon Monoxide. *Chem. Rev.* **1996**, *96* (2), 663.
- (21) Clegg, W.; Eastham, G. R.; Elsegood, M. R. J.; Heaton, B. T.; Iggo, J. A.; Tooze, R. P.; Whyman, R.; Zacchini, S. Characterization and Dynamics of  $[\text{Pd}(\text{L-L})\text{H}(\text{Solv})]^+$ ,  $[\text{Pd}(\text{L-L})(\text{CH}_2\text{CH}_3)]^+$ , and  $[\text{Pd}(\text{L-L})(\text{C}(\text{O})\text{Et})(\text{THF})]^+$  ( $\text{L-L} = 1,2\text{-CH}_2\text{P}(\text{Bu})_2\text{C}_6\text{H}_4$ ): Key Intermediates in the Catalytic Methoxycarbonylation of Ethene to Methylpropanoate. *Organometallics* **2002**, *21* (9), 1832.
- (22) Eastham, G. R.; Tooze, R. P.; Kilner, M.; Foster, D. F.; Cole-Hamilton, D. J. Deuterium Labelling Evidence for a Hydride Mechanism in the Formation of Methyl Propanoate from Carbon Monoxide, Ethene and Methanol Catalysed by a Palladium Complex. *J. Chem. Soc. Dalt. Trans.* **2002**, *8*, 1613.
- (23) Clegg, W.; Eastham, G. R.; Elsegood, M. R. J.; Heaton, B. T.; Iggo, J. A.; Tooze, R. P.; Whyman, R.; Zacchini, S. Synthesis and Reactivity of

- Palladium Hydrido-Solvento Complexes, Including a Key Intermediate in the Catalytic Methoxycarbonylation of Ethene to Methyl Propanoate. *J. Chem. Soc. Dalton Trans.* **2002**, 0 (17), 3300.
- (24) Roesle, P.; Dürr, C. J.; Möller, H. M.; Cavallo, L.; Caporaso, L.; Mecking, S. Mechanistic Features of Isomerizing Alkoxy carbonylation of Methyl Oleate. *J. Am. Chem. Soc.* **2012**, *134* (42), 17696.
- (25) Roesle, P.; Caporaso, L.; Schütte, M.; Goldbach, V.; Cavallo, L.; Mecking, S. A Comprehensive Mechanistic Picture of the Isomerizing Alkoxy carbonylation of Plant Oils. *J. Am. Chem. Soc.* **2014**, *136* (48), 16871.
- (26) Seayad, A.; Kelkar, A. A.; Toniolo, L.; Chaudhari, R. V. Hydroesterification of Styrene Using an in Situ Formed Pd(OTs)<sub>2</sub>(PPh<sub>3</sub>)<sub>2</sub> Complex Catalyst. *J. Mol. Catal. a-Chemical* **2000**, *151* (1–2), 47.
- (27) Liu, J.; Heaton, B. T.; Iggo, J. A.; Whyman, R. The Complete Delineation of the Initiation, Propagation, and Termination Steps of the Carbomethoxy Cycle for the Carboalkoxylation of Ethene by Pd-Diphosphane Catalysts. *Angew. Chemie - Int. Ed.* **2004**, *43* (1), 90.
- (28) Zuidema, E.; Bo, C.; Van Leeuwen, P. W. N. M. Ester versus Polyketone Formation in the Palladium-Diphosphine Catalyzed Carbonylation of Ethene. *J. Am. Chem. Soc.* **2007**, *129* (13), 3989.
- (29) Del Río, I.; Claver, C.; Van Leeuwen, P. W. N. M. On the Mechanism of the Hydroxycarbonylation of Styrene with Palladium Systems. *Eur. J. Inorg. Chem.* **2001**, No. 11, 2719.
- (30) Crabtree, R. H. Deactivation in Homogeneous Transition Metal Catalysis: Causes, Avoidance, and Cure. *Chem. Rev.* **2015**, *115* (1), 127.
- (31) Portnoy, M.; Milstein, D. A Binuclear Palladium(I) Hydride. Formation, Reactions, and Catalysis. *Organometallics* **1994**, *13* (2), 600.
- (32) Grushin, V. V. Hydrido Complexes of Palladium. *Chem. Rev.* **1996**, *96* (6), 2011.
- (33) Rünzi, T.; Tritschler, U.; Roesle, P.; Göttker-Schnetmann, I.; Möller, H. M.; Caporaso, L.; Poater, A.; Cavallo, L.; Mecking, S. Activation and Deactivation of Neutral Palladium(II) Phosphinesulfonato Polymerization Catalysts. *Organometallics* **2012**, *31* (23), 8388.
- (34) Besora, M.; Maseras, F. Microkinetic Modeling in Homogeneous Catalysis. *Wiley Interdiscip. Rev. Comput. Mol. Sci.* **2018**, No. March, e1372.
- (35) Kiedorf, G.; Hoang, D. M.; Müller, A.; Jörke, A.; Markert, J.; Arellano-García, H.; Seidel-Morgenstern, A.; Hamel, C. Kinetics of 1-Dodecene Hydroformylation in a Thermomorphic Solvent System Using a Rhodium-Biphospho Catalyst. *Chem. Eng. Sci.* **2014**, *115*, 31.

- 
- (36) Galvanin, F.; Psyraki, C.; Morris, T.; Gavriilidis, A. Development of a Kinetic Model of Ethylene Methoxycarbonylation with Homogeneous Pd Catalyst Using a Capillary Microreactor. *Chem. Eng. J.* **2017**, *329*, 25.
- (37) Vavasori, A.; Toniolo, L.; Cavinato, G. Hydroesterification of Cyclohexene Using the Complex Pd(PPh<sub>3</sub>)<sub>2</sub>(TsO)<sub>2</sub> as Catalyst Precursor: Effect of a Hydrogen Source (TsOH, H<sub>2</sub>O) on the TOF and a Kinetic Study (TsOH: P-Toluenesulfonic Acid). *J. Mol. Catal. A Chem.* **2003**, *191* (1), 9.
- (38) Averyanov, V. A.; Sevostyanova, N. T.; Batashev, S. A.; Vorobiev, A. A.; Rodionova, A. S. Kinetics and Mechanism of Cyclohexene Hydrocarbomethoxylation Catalyzed by the Pd(OAc)<sub>2</sub>-PPh<sub>3</sub>-p-Toluenesulfonic Acid System. *Russ. J. Phys. Chem. B* **2014**, *8* (2), 140.
- (39) Rosales, M.; Pacheco, I.; Medina, J.; Fernández, J.; González, Á.; Izquierdo, R.; Melean, L. G.; Baricelli, P. J. Kinetics and Mechanisms of Homogeneous Catalytic Reactions. Part 12. Hydroalcoxycarbonylation of 1-Hexene Using Palladium/Triphenylphosphine Systems as Catalyst Precursors. *Catal. Lett.* **2014**, *144* (10), 1717.
- (40) Gerlach, M.; Kirschtowski, S.; Seidel-Morgenstern, A.; Hamel, C. Kinetic Modeling of the Palladium-Catalyzed Isomerizing Methoxycarbonylation of 1-Decene. *Chemie-Ingenieur-Technik* **2018**, *90* (5), 673.
- (41) Harris, B. Acrylics for the Future. *Ingenia* **2010**, No. 45, 18.
- (42) Sumitomo Chemical Co. Ltd. Trends and Future of Monomer- MMA Technologies <https://www.sumitomo-chem.co.jp/english/rd/report/theses/2004-2.html> (accessed Aug 23, 2018).
- (43) Walther, G. High-Performance Polymers from Nature: Catalytic Routes and Processes for Industry. *ChemSusChem* **2014**, *7* (8), 2081.
- (44) Neumann, H.; Brennführer, A.; Beller, M. An Efficient and Practical Sequential One-Pot Synthesis of Suprofen, Ketoprofen and Other 2-Arylpropionic Acids. *Adv. Synth. Catal.* **2008**, *350* (14–15), 2437.
- (45) Jang, E. J.; Lee, K. H.; Lee, J. S.; Kim, Y. G. Regioselective Synthesis of Ibuprofen via the Palladium Complex Catalyzed Hydrocarboxylation of 1-(4-Isobutylphenyl) Ethanol. *J. Mol. Catal. A Chem.* **1999**, *138* (1), 25.
- (46) Sheldon, R. A. Fundamentals of Green Chemistry: Efficiency in Reaction Design. *Chem. Soc. Rev.* **2012**, *41* (4), 1437.
- (47) de Pater, J. J. M.; Deelman, B.-J.; Elsevier, C. J.; Van Koten, G. Multiphase Systems for the Recycling of Alkoxycarbonylation Catalysts. *Adv. Synth. Catal.* **2006**, *348* (12–13), 1447.
- (48) Vural Gürsel, I.; Noël, T.; Wang, Q.; Hessel, V. Separation/Recycling Methods for Homogeneous Transition Metal Catalysts in Continuous Flow. *Green Chem.* **2015**, *17* (4), 2012.
-

- (49) Kohlpaintner, C. W.; Fischer, R. W.; Cornils, B. Aqueous Biphasic Catalysis: Ruhrchemie/Rhône-Poulenc Oxo Process. *Appl. Catal. A Gen.* **2001**, *221* (1–2), 219.
- (50) Tilloy, S.; Monflier, E.; Bertoux, F.; Castanet, Y.; Mortreux, A. A New Fruitful Development in Biphasic Catalysis: The Palladium-Catalyzed Hydrocarboxylation of Alkenes. *New J. Chem.* **1997**, *21* (5), 529.
- (51) Papadogianakis, G.; Verspui, G.; Maat, L.; Sheldon, R. A. Catalytic Conversions in Water. Part 6. A Novel Biphasic Hydrocarboxylation of Olefins Catalyzed by Palladium TPPTS Complexes (TPPTS=P(C<sub>6</sub>H<sub>4</sub>-m-SO<sub>3</sub>Na) <sub>3</sub>). *Catal. Letters* **1997**, *47* (1), 43.
- (52) Jayasree, S.; Seayad, A.; Chaudhari, R. V. Highly Active Water-Soluble Palladium Catalyst for the Regioselective Carbonylation of Vinyl Aromatics to 2-Arylpropionic Acids. *Chem. Commun.* **2000**, No. 14, 1239.
- (53) Verspui, G.; Feiken, J.; Papadogianakis, G.; Sheldon, R. A. Catalytic Conversions in Water. Part 11: Highly Active Water-Soluble Palladium-Catalysts in the Hydrocarboxylation of Olefins and the Alternating Copolymerization of CO and Olefins in Water. *J. Mol. Catal. A Chem.* **1999**, *146* (1–2), 299.
- (54) Schreuder Goedheijt, M.; N. H. Reek, J.; C. J. Kamer, P.; W. N. M. van Leeuwen, P. A Highly Selective Water-Soluble Dicationic Palladium Catalyst for the Biphasic Hydroxycarbonylation of Alkenes. *Chem. Commun.* **1998**, No. 22, 2431.
- (55) Miquel-Serrano, M. D.; Aghmiz, A.; Diéguez, M.; Masdeu-Bultó, A. M.; Claver, C.; Sinou, D. Recoverable Chiral Palladium-sulfonated Diphosphine Catalysts for the Asymmetric Hydrocarboxylation of Vinyl Arenes. *Tetrahedron: Asymmetry* **1999**, *10* (23), 4463.
- (56) Pruvost, R.; Boulanger, J.; Léger, B.; Ponchel, A.; Monflier, E.; Ibert, M.; Mortreux, A.; Sauthier, M. Biphasic Palladium-Catalyzed Hydroesterification in a Polyol Phase: Selective Synthesis of Derived Monoesters. *ChemSusChem* **2015**, *8* (12), 2133.
- (57) Pruvost, R.; Boulanger, J.; Léger, B.; Ponchel, A.; Monflier, E.; Ibert, M.; Mortreux, A.; Chenal, T.; Sauthier, M. Synthesis of 1,4:3,6-Dianhydrohexitols Diesters from the Palladium-Catalyzed Hydroesterification Reaction. *ChemSusChem* **2014**, *7* (11), 3157.
- (58) Nowothnick, H.; Blum, J.; Schomäcker, R. Suzuki Coupling Reactions in Three-Phase Microemulsions. *Angew. Chemie Int. Ed.* **2011**, *50* (8), 1918.
- (59) Nishikata, T.; Abela, A. R.; Lipshutz, B. H. Room Temperature C À H Activation and Cross-Coupling of Aryl Ureas in Water \*\*. **2010**, 781.
- (60) Lipshutz, B. H.; Ghorai, S. PQS-2: Ring-Closing- and Cross-Metathesis Reactions on Lipophilic Substrates; in Water Only at Room Temperature, with in-Flask Catalyst Recycling. *Tetrahedron* **2010**, *66* (5), 1057.

- 
- (61) Bunton, C. A. Micellar Charge Effects as Mechanistic Criteria in Spontaneous Hydrolyses of Acid Chlorides. *J. Phys. Org. Chem.* **2005**, *18* (2), 115.
- (62) Milano-Brusco, J. S.; Schwarze, M.; Djennad, M.; Nowothnick, H.; Schomäcker, R. Catalytic Hydrogenation of Dimethyl Itaconate in a Water–Cyclohexane–Triton X-100 Microemulsion in Comparison to a Biphasic System. *Ind. Eng. Chem. Res.* **2008**, *47* (20), 7586.
- (63) Schwarze, M.; Milano-Brusco, J. S.; Stempel, V.; Hamerla, T.; Wille, S.; Fischer, C.; Baumann, W.; Arlt, W.; Schomäcker, R. Rhodium Catalyzed Hydrogenation Reactions in Aqueous Micellar Systems as Green Solvents. *RSC Adv.* **2011**, *1* (3), 474.
- (64) Lipshutz, B. H.; Ghorai, S.; Cortes-Clerget, M. The Hydrophobic Effect Applied to Organic Synthesis: Recent Synthetic Chemistry “in Water.” *Chem. - A Eur. J.* **2018**, *24* (26), 6672.
- (65) Dwars, T.; Paetzold, E.; Oehme, G. Reactions in Micellar Systems. *Angew. Chemie - Int. Ed.* **2005**, *44* (44), 7174.
- (66) La Sorella, G.; Strukul, G.; Scarso, A. Recent Advances in Catalysis in Micellar Media. *Green Chem.* **2015**, *17* (2), 644.
- (67) Gallou, F.; Isley, N. A.; Ganic, A.; Onken, U.; Parmentier, M. Surfactant Technology Applied toward an Active Pharmaceutical Ingredient: More than a Simple Green Chemistry Advance. *Green Chem.* **2016**, *18* (1), 14.
- (68) Hapiot, F.; Manuel, S.; Ferreira, M.; Léger, B.; Bricout, H.; Tilloy, S.; Monflier, E. Catalysis in Cyclodextrin-Based Unconventional Reaction Media: Recent Developments and Future Opportunities. *ACS Sustain. Chem. Eng.* **2017**, *5* (5), 3598.
- (69) Hapiot, F.; Bricout, H.; Manuel, S.; Tilloy, S.; Monflier, E. Recent Breakthroughs in Aqueous Cyclodextrin-Assisted Supramolecular Catalysis. *Catal. Sci. Technol.* **2014**, *4* (7), 1899.
- (70) Six, N.; Guerriero, A.; Landy, D.; Peruzzini, M.; Gonsalvi, L.; Hapiot, F.; Monflier, E. Supramolecularly Controlled Surface Activity of an Amphiphilic Ligand. Application to Aqueous Biphasic Hydroformylation of Higher Olefins. *Catal. Sci. Technol.* **2011**, *1* (8), 1347.
- (71) Tilloy, S.; Bertoux, F.; Mortreux, A.; Monflier, E. Chemically Modified  $\beta$ -Cyclodextrins in Biphasic Catalysis: A Fruitful Contribution of the Host-Guest Chemistry to the Transition-Metal Catalyzed Reactions. *Catal. Today* **1999**, *48* (1–4), 245.
- (72) Behr, A.; Toslu, N. Einphasige Und Zweiphasige Reaktionsführung Der Hydrosilylierungsreaktion. *Chemie Ing. Tech.* **1999**, *71* (5), 490.
- (73) Behr, A.; Vorholt, A. J.; Rentmeister, N. Recyclable Homogeneous Catalyst for the Hydroesterification of Methyl Oleate in Thermomorphic
-

- Solvent Systems. *Chem. Eng. Sci.* **2013**, *99*, 38.
- (74) Gaide, T.; Behr, A.; Arns, A.; Benski, F.; Vorholt, A. J. Hydroesterification of Methyl 10-Undecenoate in Thermomorphic Multicomponent Solvent Systems—Process Development for the Synthesis of Sustainable Polymer Precursors. *Chem. Eng. Process. Process Intensif.* **2016**, *99*, 197.
- (75) Jessop, P. G. Homogeneous Catalysis Using Supercritical Fluids: Recent Trends and Systems Studied. *J. Supercrit. Fluids* **2006**, *38* (2), 211.
- (76) Bhanage, B. M.; Shirai, M.; Arai, M.; Ikushima, Y. Multiphase Catalysis Using Water-Soluble Metal Complexes in Supercritical Carbon Dioxide. *Chem. Commun.* **1999**, No. 14, 1277.
- (77) Koch, D.; Leitner, W. Rhodium-Catalyzed Hydroformylation in Supercritical Carbon Dioxide. *J. Am. Chem. Soc.* **1998**, *120* (51), 13398.
- (78) Estorach, C. T.; Masdeu-Bultó, A. M. Hydroesterification of 1-Alkenes in Supercritical Carbon Dioxide. *Catal. Letters* **2008**, *122* (1–2), 76.
- (79) Jia, L.; Jiang, H.; Li, J. Selective Carbonylation of Norbornene in ScCO<sub>2</sub>. *Green Chem.* **1999**, *1* (2), 91.

## Acknowledgement

Diese Arbeit hat viel Zeit und Nerven gekostet, aber auch extrem viel Spaß und Freude bereitet. Weiteres liegt an der tollen Unterstützung von Prof. Schomäcker, der nicht nur wissenschaftliche Freiräume zugelassen hat, sondern auch durch viele Diskussionen zum Gelingen dieser Arbeit beigetragen hat.

Ich möchte mich auch bei Prof. Vogt bedanken, der nicht nur das Zweitgutachten übernommen hat, sondern auch durch hervorragenden fachlichen Input bei verschiedenen Seminaren einen großen Beitrag geleistet hat.

Für die Übernahme des Vorsitzes des Promotionsausschusses möchte ich mich bei Prof. Friedrich bedanken.

Unzählige Stunden wurden im Labor verbracht, was jedoch durch meine beiden blonden Engel Ariane und Caro erheblich vereinfacht wurde, da eigentlich Sie ja die ganze Arbeit gemacht haben und mich mit Daten zugeschüttet haben. Danke dafür! ;) Auch wenn sie mich manchmal an den Rand eines Nervenzusammenbruchs gebracht haben, weil Sie per Geisterhand meine Computermaus steuerten oder gefühlte 15 000 Kopien einer Masterarbeit auf meinen Desktop verteilt haben, vermisse ich schon jetzt die Büroregeln, Fluchkasse, komische Schreigeräusche und alle anderen Bürospäße. Ihr seid die Besten!

Besonders möchte ich mich auch bei Tobi bedanken, der nicht durch fachliche Diskussionen extrem geholfen hat, sondern auch in allen anderen Lebenssituationen da war.

Ich möchte mich auch bei allen Kollegen des Sonderforschungsbereiches TRR 63 bedanken, besonders aber bei Markus für die hervorragende Zusammenarbeit während des letzten Jahre.

Auch bei meinen Studenten Frank, André, Svenja, Johannes und Philipp möchte ich mich bedanken, die meine Ideen in Form von Abschlussarbeiten umgesetzt haben und somit auch einen großen Beitrag dieser Arbeit geleistet haben.

Ein Dank gehört auch allen Kollegen des AK Schomäcker – Gabi, die immer zur Stelle war, wenn die GC nicht so wollte wie ich – Frau Löhr, die die unliebsame Bürokratie der Uni für mich übernommen hat – Micha, der immer für neue Ideen zu begeistern ist – Samira, dass sie auch mal einen Burani geholt hat – Max und Lukas für die verrückten Diskussionen – Natasa und Martin, dass sie oft Zuflucht auf unserer Couch gesucht haben, um eine Kaffeepause zu machen und Julian, den ich seit dem ersten Tag des Studiums kenne und nun auch wieder bei mir im Büro ist. :)

Zu guter Letzt möchte ich mich bei meinen Eltern bedanken, da sie immer für mich da sind und bei meiner Michi, dass sie zum Einen schon seit 3 Jahren wöchentlich fragt, wann ich denn endlich mit der Promotion fertig sei ;) und zum Anderen, dass Sie mich immer unterstützt hat, die Doktorarbeit versucht hat zu verstehen ;) und einfach immer für mich da ist. Ich hab dich lieb! ;)

## Appendix

**Table A1. Applied catalyst components, supplier and purity.**

Catalyst precursors and ligands	Supplier	Purity [%]
2,7-Bis(SO <sub>3</sub> Na)-4,5-Bis(diphenylphosphino)-9,9-dimethylxanthene (SulfoXantPhos)	Molisa GmbH	-
3,3',3''-Phosphanetriyltris(benzenesulfonic acid) trisodium salt (TPPTS)	ABCR	95
4,5-Bis(diphenylphosphino)-9,9-dimethylxanthene (XantPhos)	Sigma-Aldrich	97
Dicarbonyl(acetylacetonato)rhodium(I)	Umicore	
Dichloro-(1,5-cyclooctadiene)-palladium(II)	Sigma-Aldrich	99
Methane sulfonic acid	Sigma-Aldrich	99.5
Palladium acetate	Sigma-Aldrich	99.9
Allylpalladium(II) chloride dimer	Sigma-Aldrich	98
<i>p</i> -Toluene sulfonic acid	Sigma-Aldrich	98
Triphenylphosphine (TPP)	Sigma-Aldrich	99

**Table A2. Applied substrates, supplier and purity.**

Substrates	Supplier	Purity [%]
1-Dodecene	Merck	94
1-Octene	Sigma-Aldrich	98
10-Undecenoic acid methylester	Sigma-Aldrich	96
Cyclohexene	Sigma-Aldrich	99
Methyl decanoate	Sigma-Aldrich	99
Styrene	Sigma-Aldrich	99

**Table A3. Applied solvents, supplier and purity.**

Solvents	Supplier	Purity [%]
1-octanol	Roth	99
n-octane	ABCR	98
n-decane	Merck	94
n-dodecane	Fluka	98
n-tetradecane	Sigma-Aldrich	92
n-hexadecane	Merck	99
methanol	VWR	HPLC grade
water	VWR	HPLC grade

**Table A4. Applied surfactants, supplier and purity.**

Surfactants	Supplier	Purity [%]
Marlipal 24/20-90	Sasol	technical grade
Marlipal 24/20-90	Sasol	technical grade
Sodium dodecyl sulfate (SDS)	Sigma-Aldrich	99
Tetradecyltrimethylammonium bromide (TTAB)	Sigma-Aldrich	99
Triton X-100	Sigma-Aldrich	technical grade
Triton X-114	Sigma-Aldrich	technical grade
Decyltrimethylammonium bromide (DeTAB)	ABCR	99
1-Methyl-3-decylimidazolium bromide (DecMIM)	Iolitec	99
1-Methyl-3-dodecylimidazolium bromide (DodecMIM)	Iolitec	99
1-Methyl-3-octylimidazolium bromide (OMIM)	ABCR	99
Dodecyltrimethylammonium bromide (DTAB)	Sigma-Aldrich	98
Hexadecyltrimethylammonium bromide (CTAB)	Roth	99



# PAPER 1

## **Superior catalyst recycling in surfactant based multiphase systems - Quo vadis catalyst complex?**

Tobias Pogrzeba, David Müller, Markus Illner, Marcel Schmidt, Yasemin Kasaka, Ariane Weber, Günter Wozny, Reinhard Schomäcker, Michael Schwarze

Chemical Engineering and Processing: Process Intensification, 2016, 99, 155-166

Online Article:

<https://www.sciencedirect.com/science/article/pii/S0255270115300957>

Reprinted with permission from “Superior catalyst recycling in surfactant based multiphase systems – Quo vadis catalyst complex?; Tobias Pogrzeba, David Müller, Markus Illner, Marcel Schmidt, Yasemin Kasaka, Ariane Weber, Günter Wozny, Reinhard Schomäcker, and Michael Schwarze. Chemical Engineering and Processing, 2016, 99, 155-166.” Copyright (2015) Elsevier B.V.





## Superior catalyst recycling in surfactant based multiphase systems – Quo vadis catalyst complex?



T. Pogrzeba<sup>a,\*</sup>, D. Müller<sup>b</sup>, M. Illner<sup>b</sup>, M. Schmidt<sup>a</sup>, Y. Kasaka<sup>a</sup>, A. Weber<sup>a</sup>, G. Wozny<sup>b</sup>, R. Schomäcker<sup>a</sup>, M. Schwarze<sup>c</sup>

<sup>a</sup> Technische Universität Berlin, Department of Chemistry, TC-8, Str. des 17. Juni 124, 10623 Berlin, Germany

<sup>b</sup> Technische Universität Berlin, Chair of Process Dynamics and Operation, KWT 9, Str. des 17. Juni 135, 10623 Berlin, Germany

<sup>c</sup> Technische Universität Berlin, Chair of Plant and Process Safety, TK-01, Straße des 17. Juni 135, 10623, Berlin, Germany

### ARTICLE INFO

#### Article history:

Received 9 March 2015

Received in revised form 7 July 2015

Accepted 3 September 2015

Available online 9 September 2015

#### Keywords:

Microemulsion systems

Surfactants

Catalyst Recycling

Process Design

Separation

### ABSTRACT

Microemulsion systems are smart solvent systems which can be applied in homogeneous catalysis. We investigate these multiphase systems to exploit their characteristics for catalytic gas/liquid reactions and processes in aqueous media. One critical aspect from an economic perspective is the quantitative recycling of the catalyst complex dissolved in the multiphase system. Therefore, it is important to know the distribution of the catalyst complex in each of the single phases. In this contribution we analyse the different parameters/factors that may have an influence on the distribution of catalyst complexes in microemulsion systems, e.g. temperature, type of ligand, structure of surfactant, and chain length of surfactant. Afterwards, the derived information is used for the design of a real, industry-oriented application: hydroformylation of long chained alkenes. Hereby, special attention is given to the separation step of a process, which is performed after a homogeneously catalyzed reaction step in a microemulsion system. Process and economic constraints are briefly outlined and compared with operation data, aiming for the reuse of the catalyst in the reaction step and reduced leaching into product streams, even in the case of operational disturbances and shifts in the catalyst distribution.

© 2015 Elsevier B.V. All rights reserved.

## 1. Introduction

Expensive noble metal catalysts are often applied in homogeneous catalysis. The aims hereby are high activity and selectivity at moderate reaction conditions. However, to establish a large-scale process, the quantitative recovery of these catalysts is crucial and should be possible without loss in activity/selectivity. Hence, reaction media that combine the advantages of homogenous catalysis (high turnover frequencies and high selectivity) and two-phase-catalysis (easy separation of catalyst and product) are of great interest. Beside the classical aqueous-organic two-phase systems, i.e. for the hydroformylation of 1-propene to n-butanal in the Ruhrchemie/Rhône-Poulenc Process [1], many new systems have been developed during the last decades. Well known examples are ionic liquids [2,3], supercritical media based on CO<sub>2</sub> [4,5], thermomorphic solvent mixtures [6], supported ionic liquid-phase (SILP) [7], or sol-gel immobilized catalyst systems [8]. An alternative approach is the application of microemulsion systems as tuneable solvents for the

recycling of water-soluble catalysts. Microemulsion systems are ternary mixtures consisting of a non-polar compound (oil), a polar compound (water), and a surfactant (often non-ionic surfactants are chosen in this context). They provide a high interfacial area between the polar and non-polar domains during the reaction. Additionally, their phase separation behaviour can be manipulated through temperature changes. However, for the application of microemulsion systems their phase behaviour, which not only depends on temperature but also on their composition and the interaction between the surfactant and the catalyst/reactants, has to be studied in detail [9]. Among the available green solvents, microemulsion systems, easily tuneable by the selection of an appropriate surfactant, show superior characteristics for catalytic reactions and processes in aqueous media. Furthermore, they fulfil all requirements needed for successful and efficient catalyst recycling. Examples for the application of microemulsions as reaction system are the hydrogenation of dimethyl itaconate with Rh/TPPTS [10], the Suzuki coupling of 2-bromobenzonitrile and 4-methylbenzeneboronic acid with Pd/TPPTS [11] and the hydroformylation of 1-dodecene with Rh/SX [12]. For further examples see also [9].

In this contribution we will evaluate and discuss the distribution of homogeneous catalyst complexes in microemulsion

\* Corresponding author.

E-mail address: [tobias.pogrzeba@tu-berlin.de](mailto:tobias.pogrzeba@tu-berlin.de) (T. Pogrzeba).

systems by the variation of different parameters, e.g. temperature, ligand, structure of surfactant, and chain length of surfactant. We will also discuss several aspects which are important for the application of microemulsion systems for a closed recycle catalytic process with respect to the choice of the surfactant. In addition, we will present a case study to design a process for homogeneous catalysis in a microemulsion system with efficient catalyst recycling based on the results of the first part of this contribution.

## 2. Aqueous surfactant media

Water can act as a solvent for water-soluble catalysts and enables the biphasic extraction of non-polar products as well as the recycling of catalysts. However, in case of hydrophobic reactants it has the disadvantage of poor reactant solubility. The addition of a surfactant increases the solubility of non-polar reactants in the aqueous phase. Generally, there are two different approaches to create aqueous surfactant media for homogeneously catalysed reactions.

The first approach is to create an aqueous–micellar solution by the addition of a surfactant to water, which exceeds the critical micelle concentration (cmc). Micelles are nano-scale aggregates of surfactant monomers, which are able to solubilize organic components in their cores. Since the size of micelles is usually very small, the concentration of substrate in an aqueous–micellar solution is often lower than in conventional organic solvents. The cmc and the size of micelles depend on the type of surfactant. In general, non-ionic surfactants form larger micelles and have a low cmc in comparison to ionic surfactants.

The second approach is the use of microemulsion systems, which are formed at surfactant concentrations much higher than the cmc. By the addition of a non-ionic surfactant of the type  $C_iE_j$  to a biphasic mixture of water and oil, usually four different states can be observed that were classified by Winsor (Winsor systems I–IV). In  $C_iE_j$ ,  $i$  is the number of hydrocarbon groups of the surfactant's hydrophobic part, and  $j$  is the number of ethoxylate groups of its hydrophilic part. Important parameters to characterize the mixture are the weight fractions  $\alpha$  and  $\gamma$ . In Eq. (1)  $m_{oil}$  is the mass of oil,  $m_{water}$  is the mass of water and  $m_{surf}$  is the mass of non-ionic surfactant.

$$\alpha = \frac{m_{oil}}{m_{oil} + m_{water}} \quad \gamma = \frac{m_{surf}}{m_{oil} + m_{water} + m_{surf}} \quad (1)$$

In Fig. 1 the phase behaviour of a ternary mixture of oil, water and non-ionic surfactant is schematically shown for a constant value of  $\alpha$ .

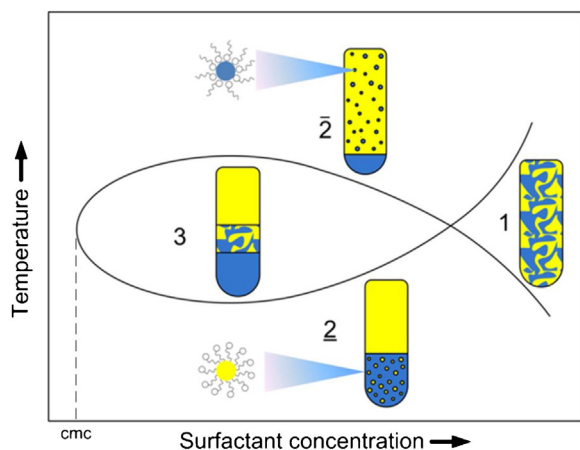


Fig. 1. Phase diagram (commonly called fish-diagram) for a ternary mixture of oil, water, and non-ionic surfactant at a constant ratio of oil and water with normal (bottom) and inverse (top) micelles. The figure has been modified from [13].

At low temperatures the surfactant is mainly solubilized in water, whereas its solubility in oil increases at higher temperatures. Thus, the illustrated sequence of phases as a function of temperature is the result of the gradual change in the surfactant's solubility from hydrophilic to hydrophobic. The phase sequence generally starts at low temperatures with an oil-in-water (o/w) microemulsion ( $\underline{2}$ , Winsor I). This microemulsion consists of oil-bearing micelles in a continuous water phase which is in equilibrium with an organic excess phase. At intermediate temperatures a three-phase region (3, Winsor III) exists, where the surfactant is almost equally soluble in both liquids and forms a surfactant rich microemulsion phase in the middle of two excess phases. For even higher temperatures a water-in-oil (w/o) microemulsion ( $\bar{2}$ , Winsor II) is formed. Here, water-bearing inverse micelles exist in a continuous oil phase, which is in equilibrium with a water excess phase. If the concentration of surfactant in the ternary mixture is high enough for the complete solubilization of oil and water, a one-phase microemulsion (1, Winsor IV) of the entire volume will be formed, which can be an o/w-, bicontinuous- or w/o-microemulsion depending on the oil content in the mixture.

In general, each of the four Winsor states can be applied as a reaction medium for homogeneous catalysis. Since the phase behaviour of a microemulsion system can be changed as a function of temperature and surfactant concentration, it is possible to adjust the reaction system between different process steps with varying requirements [13]. The choice of the applied surfactant has to be made carefully so that the requirements for a homogeneously catalysed reaction with subsequent product separation and catalyst recycling, can be fulfilled. Besides its influence on the phase behaviour, the surfactant will have a strong impact on the distribution of reactants and catalysts between the aqueous and the organic phase. For the quantitative recycling of a homogeneously dissolved catalyst complex from multiphase systems as well as the evaluation of the reaction kinetics it is important to know the distribution of the catalyst complex between the single phases. In general, based on the experience with conventional organic–aqueous two-phase systems, water-soluble catalyst complexes are preferentially dissolved in the aqueous phase (see e.g. the Rh/TPPTS complex in the RCH/RP process) and hydrophobic counterparts are dissolved in the oil phase. For microemulsion systems, the interactions between the surfactant and the catalyst complex can influence the solubility of the latter considerably. In many cases the catalyst follows the surfactant into the corresponding microemulsion phase, which results in different separation tasks for the catalyst recycling during a process step depending on the phase behaviour of the microemulsion system. Therefore, it is necessary to indicate the parameters which are responsible for the catalyst distribution in such surfactant based multiphase systems to select the best surfactant as well as ideal operating conditions that result in a quantitative catalyst recycling and an optimal separation process.

## 3. Catalyst distribution in multiphase systems

To analyse the effects of the different parameters on the catalyst distribution multiple experiments were carried out. The obtained information from these experiments was then used for an actual industry-oriented application. In the following, details on these experiments as well as the results are presented.

### 3.1. Experimental

#### 3.1.1. Chemicals

The solvents 1-dodecene (94%), water (HPLC grade), and tetrahydrofuran (THF, 99.5%) were purchased from VWR. The

surfactants Marlipal 24/50, Marlipal 24/60 and Marlipal 24/70 were a donation from Sasol. The surfactant Triton X-114, the amphiphiles C<sub>4</sub>E<sub>1</sub> (99%) and C<sub>4</sub>E<sub>2</sub> (99.2%), the hydrophobic ligands triphenylphosphine (TPP, 99%) and Xantphos (97%) and the rhodium standard solution (1011 mg/L) for ICP-OES analysis were received from Sigma–Aldrich. The water-soluble ligands 3,3',3''-phosphanetriyltris(benzenesulfonic acid) trisodium salt (sodium triphenylphosphine trisulfonate, TPPTS, 95%) and sulfonated 4,5-bis(diphenylphosphino)-9,9-dimethylxanthene (SulfoXantphos, SX) were purchased from ABCR and Molisa GmbH, respectively. The rhodium precursor Rh(acac)(CO)<sub>2</sub> was a donation from Umicore. To adjust the ionic strength we used sodium sulfate (Na<sub>2</sub>SO<sub>4</sub>, 99%) purchased from Merck. All the chemicals were used without further purification.

### 3.1.2. Preparation of the catalyst complex

For the preparation of the catalyst complex, 12.9 mg (0.05 mmol, 1 eq.) Rh(acac)(CO)<sub>2</sub> and the investigated ligand (10 eq. for the monodentate ligands and 5 eq. for the bidentate ligands) were evacuated three times in a Schlenk tube and flushed with argon. The solvent (2 g degassed water for the hydrophilic ligands and 3 g THF for the hydrophobic ligands) was added through a septum. Then the catalyst solution was stirred over night at room temperature to ensure the formation of the catalyst complex.

### 3.1.3. Investigation of the phase behaviour

Standard experiments were carried out by using a microemulsion system consisting of water as the hydrophilic compound, 1-dodecene as the hydrophobic oil ( $\alpha = 50\%$ ), the investigated non-ionic surfactant ( $\gamma = 8\%$ ) and a sodium sulfate amount of 1 wt%. To ensure the three phase region for the other amphiphiles, C<sub>4</sub>E<sub>1</sub> and C<sub>4</sub>E<sub>2</sub>, the concentration had to be increased to  $\gamma = 20\%$ . The compounds were weighted into a glass reactor with a heating jacket. The lid of the reactor offers connections for sampling, for vacuum establishment, and argon inertisation. The samples were evacuated and flushed with argon three times. Then the catalyst solution was injected with a syringe. We studied the phase behaviour from 25 °C to 91 °C in 1 °C steps. For this purpose, we adjusted the temperature with a thermostat while stirring the microemulsion. After the desired temperature was reached, the

stirrer was stopped and the phase separation was observed. Samples of the different phases were taken to determine the rhodium concentration in each.

### 3.1.4. Determination of the rhodium concentration

The concentration of rhodium in the different phases was determined by inductively coupled plasma optical emission spectrometry (ICP-OES) using a Varian ICP-OES 715 ES instrument. In each case, we analysed the aqueous phase and the middle phase of the three phase system. Therefore, 2 mL of the water or 1 mL of the middle phase were added to an ICP tube and treated with freshly prepared aqua regia. Afterwards, the samples were diluted with degassed water and the rhodium concentration was measured at a wavelength of 369 nm. A calibration of the setup was performed with rhodium standard solutions having concentrations of 1, 5, 20, 50, and 150 mg/L.

## 3.2. Phase behaviour of the investigated microemulsion systems

To ensure an efficient recycling of the catalyst complex after the reaction, it is of utmost importance to know the phase behaviour of the reaction mixture. This phase behaviour strongly depends on the selected amphiphile. Several publications generalize observed effects [14,15], but to date and to the best of our knowledge the influence of the used catalyst complex has not been studied in detail. Therefore, we firstly tested different amphiphiles to obtain the influence of the chain length, structure, and the hydrophobic character of the amphiphiles towards the position of the three phase region on the temperature scale (see Fig. 2). Based on this information, the next step was to investigate the influence of ligands and thus the catalyst complex in particular in the subsequent sections. For the sake of completeness it has to be mentioned, that some of the applied chemicals are technical grade and may contain impurities which can have an impact on the phase behaviour of the investigated microemulsion systems and therefore have to be considered.

### 3.2.1. Hydrophobicity influence

It is well known that the three phase region for short chained amphiphiles, such as C<sub>4</sub>E<sub>1</sub> and C<sub>4</sub>E<sub>2</sub>, has a broad temperature range. As expected, for the hydrophilic amphiphiles the position of the

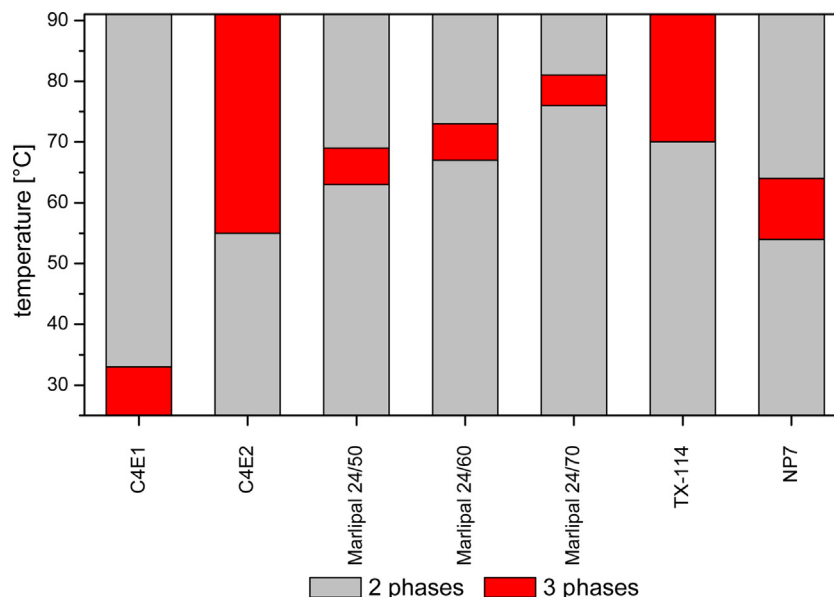


Fig. 2. Phase behaviour for different surfactants ( $\alpha = 50\%$ ,  $\gamma = 8\%$  ( $\gamma = 20\%$  for C<sub>4</sub>E<sub>1</sub> and C<sub>4</sub>E<sub>2</sub>), 1 wt.% sodium sulfate,  $n_{\text{Rh(acac)CO}_2} = 0.05$  mmol,  $n_{\text{SX}} = 5$  eq.).

three phase region is shifted to higher temperatures. The same effect of the three phase region being shifted to higher temperatures with increasing hydrophobicity exists for technical grade surfactants of the Marlipal series, which are long chain aliphatic surfactants (see Fig. 3). It is characteristic for these surfactants that they form micelles as a microstructure. By increasing the degree of ethoxylation from 5 in Marlipal 24/50 to 7 in Marlipal 24/70 the hydrophilic character increases and the three phase region is shifted to higher temperatures. In comparison to the short chained amphiphiles the temperature range of the three phase region is often limited to 5–10 K. It must be kept in mind that short chained amphiphiles only act as solubilisers and do not form micellar structures.

### 3.2.2. Chain length influence

The difference in the size of the temperature range of the three phase region of short compared to long chain amphiphiles is due to their different solubilisation properties in oil and water. Short chained amphiphiles, which act as an additional solvent, can dissolve more oil and water in their own phase compared to the technical grade surfactant Marlipal. This leads to a broad range of the three phase region.

### 3.2.3. Surfactant structure

Of special interest is the influence of the structure of the surfactant towards the position of the three phase region. Therefore, we compared different surfactants with the same degree of ethoxylation which are illustrated in Fig. 3: Marlipal 24/70 with a linear hydrophobic carbon chain, Triton X-114 holding a branched carbon chain with a phenyl unit as linker, and NP7, which also has a phenyl unit as linker, but a linear carbon chain. Due to the different properties of the hydrophobic part of the surfactants, we obtain variable positions of the three phase region. Triton X-114 and NP7 have the same number of carbon atoms, but Triton X-114 is branched. Hence Triton X-114 is more hydrophilic than NP7 and so the three phase region is established at higher temperatures.

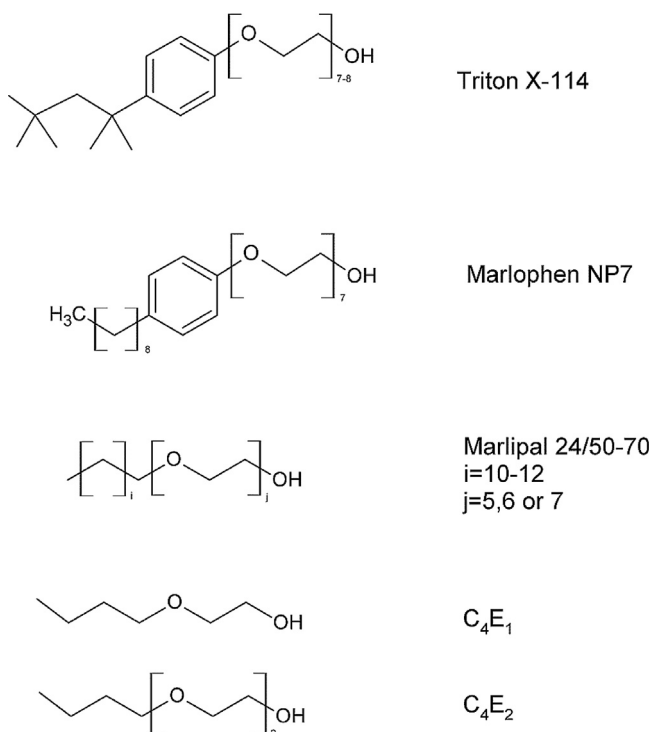


Fig. 3. Structures of the different investigated surfactants.

### 3.2.4. Ligand influence

Another important influence factor on the position of the three phase region is the type of applied ligand. The experimental results are shown in Fig. 4. The reference is a mixture with rhodium precursor without any ligand. We tested the monodentate ligands TPP and TPPTS and the bidentate ligands Xantphos and SulfoXantphos (see Fig. 5). At first glance, the water-soluble ligands TPPTS and SulfoXantphos shift the three phase region to higher temperatures. This is a result of the catalyst preparation though. The hydrophobic catalyst complexes were prepared using little amounts of THF, which is more hydrophilic in comparison to 1-dodecene. It is well known that the hydrophobicity of the oil influences the position of the three phase region [15]. The less hydrophobic the oil, the lower the position of the three phase region is. The difference of the position of the three phase region for TPPTS and SulfoXantphos is due to the ligand concentration. We used 10 eq. of the monodentate TPPTS and 5 eq. of the bidentate SulfoXantphos. As a result the water solubility of the surfactant decreases according to the salting out phenomenon of the sulfate anions [16], thus shifting the position of the three phase region to lower temperatures [14].

Based on these results, we moved on to investigate the parameters influencing the distribution of the whole catalyst complex.

### 3.3. Distribution of the catalyst complex

Not only is the temperature range for the different phases crucial for the separation process, but also the distribution of the catalyst complex between the different phases. For a feasible and economic process it is necessary to achieve a quantitative separation of the expensive catalyst complex. Therefore, it is essential to estimate or manipulate the interactions between the catalyst complex and the amphiphile. For this reason we investigated different amphiphiles and different ligands, which have an influence on the distribution characteristics of the catalyst complex. Qualitatively speaking, the distribution can be estimated visually by the colour of the different phases (see Fig. 6), but for quantification we measured the amount of rhodium by ICP-OES. In Fig. 7 the influence of different amphiphiles on the distribution of the water-soluble Rh/SX complex is shown. The rhodium content in the oil phase is negligible because of the water-soluble SulfoXantphos ligand as shown in [17,18]. So for the investigation of the catalyst complex distribution only the rhodium amount in the aqueous phase and the middle phase was considered. However, it should be mentioned that minor rhodium leaching into the oil phase was found in the order of 0.1 ppm [18] so that post-treatment of the organic phase would be necessary for complete rhodium recovery.

For the short chain amphiphiles  $C_4E_1$  and  $C_4E_2$  a high amount of the rhodium complex is present in the aqueous phase. The distribution of the rhodium complex depends on the partition coefficient between the phases. For the short chain amphiphiles, the major reason for the catalyst distribution is the different polarity of the phases, which increases from the oil phase over the amphiphile rich middle phase to the water phase. For the amphiphile  $C_4E_1$ , the middle phase is too non-polar to dissolve the catalyst complex to a sufficient extent and only 34% of the rhodium is located in the middle phase. For the amphiphile  $C_4E_2$ , the middle phase is more hydrophilic and allows for about 82% of the catalyst complex to be located there. As a consequence, the amount of rhodium in the aqueous phase is higher in the  $C_4E_1$  system in comparison to the  $C_4E_2$  system. In contrast, the rhodium amount in the aqueous phase of the Marlipal systems is only between 1.7% and 3.7% of the overall amount of rhodium in the system. Apparently, the catalyst complex follows the surfactant

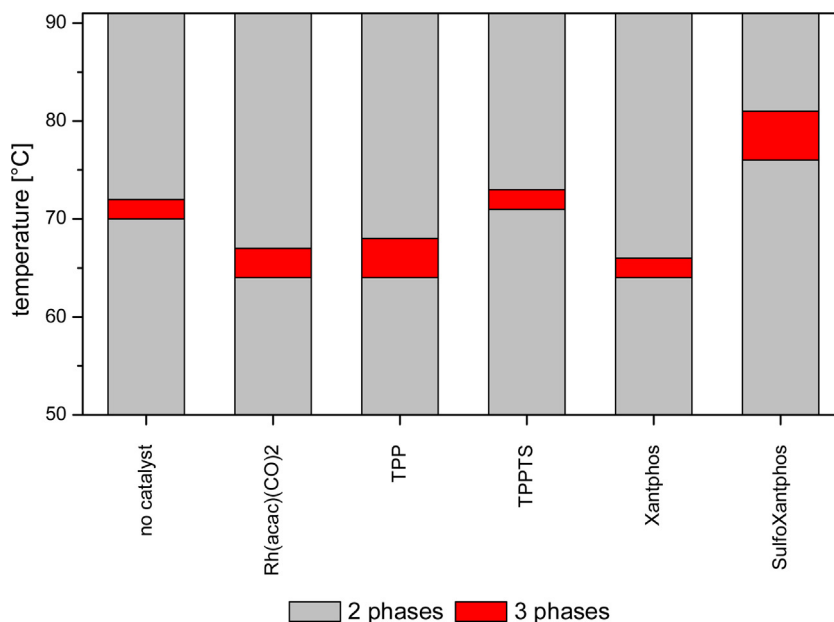


Fig. 4. Phase behaviour of Marlipal 24/70 in the presence of different ligands ( $\alpha = 50\%$ ,  $\gamma = 8\%$ , 1 wt% sodium sulfate,  $n_{\text{Rh(acac)CO}_2} = 0.05$  mmol,  $n_{\text{Ligand}} = 5$  or 10 eq.).

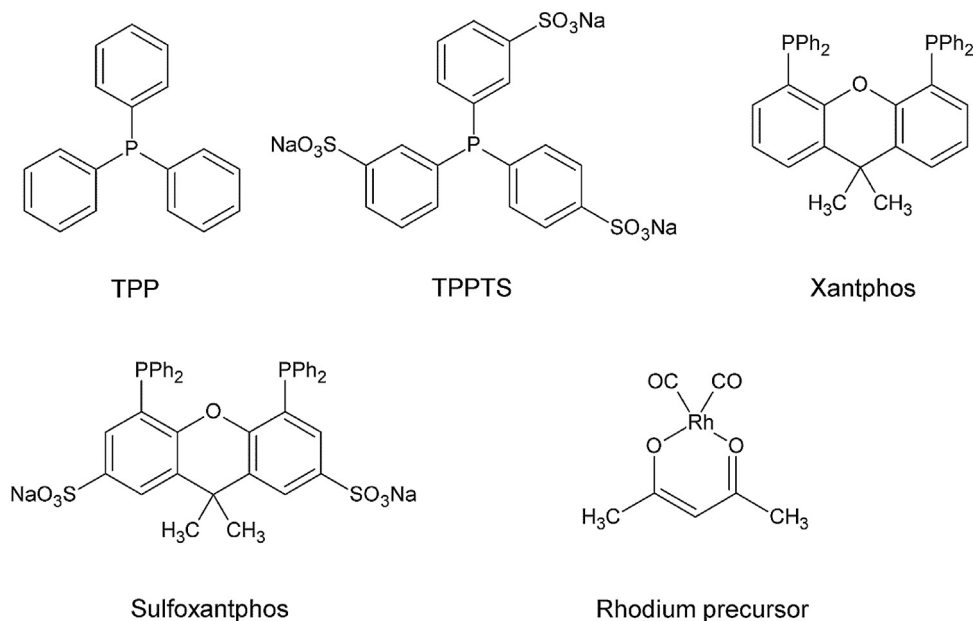


Fig. 5. Structures of the investigated ligands.

into the surfactant rich middle phase of the microemulsion systems. We assume that the water-soluble catalyst complex is also surface active and attaches itself to the oil-water interface of the bicontinuous phase of the microemulsion system.

Besides the amphiphile the kind of ligand has a strong influence on the distribution of the catalyst complex. In Fig. 8 the distribution of rhodium in the presence of different ligands is shown. It is clear that the hydrophobicity of the ligand is crucial for the distribution of the rhodium. For the water-soluble ligands TPPTS and SulfoXantphos the rhodium complex is located in the middle phase to a larger extent. The high amount of Rh/TPPTS in the aqueous phase (40%) is due to the high number of sulfonate groups per complex. In comparison to the water-insoluble ligands TPP and Xantphos, as well as for the unmodified rhodium precursor, the rhodium species is mainly located in the oil phase.

Here, only 10% of the Rh/TPP complex and 26% of the Rh/Xantphos complex are located in the middle phase. The comparison of mono- and bidentate ligands with respect to the distribution of the rhodium complex is difficult, because a different number of complex species can be formed. The number of coordinated ligands is important for the hydrophilic or hydrophobic character of the catalyst complex.

Furthermore, we investigated the distribution of the Rh/SulfoXantphos catalyst in a Winsor I and II system with the surfactant Marlipal 24/70, since this catalyst complex is of high interest for the discussion in Section 4. We found that in a Winsor I system over 99.99% of the catalyst is located in the microemulsion phase, whereas in a Winsor II system the catalyst is equally distributed between both phases.

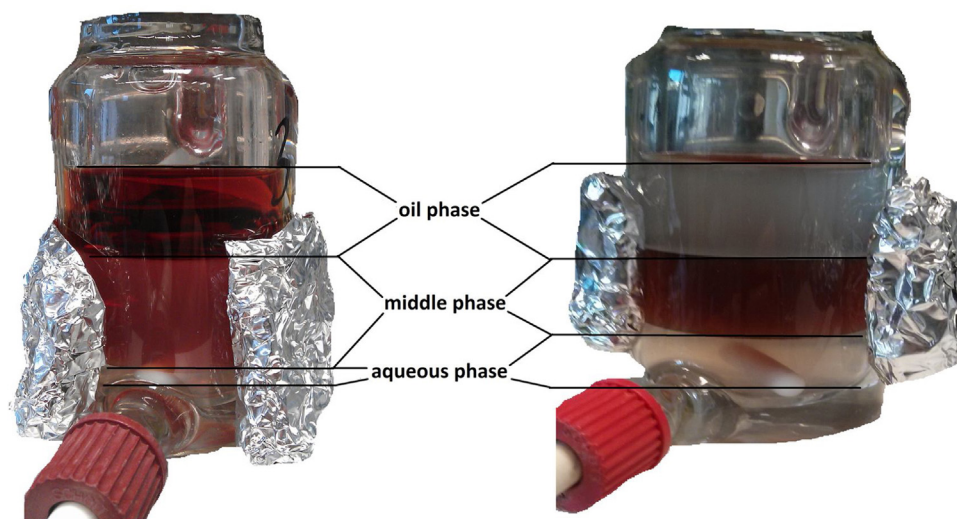


Fig. 6. Examples of catalyst distribution obtained for the three phase microemulsion system: Marlipal 24/70 and Rh/Xantphos (left) and Marlophen NP7 and Rh/SX (right).

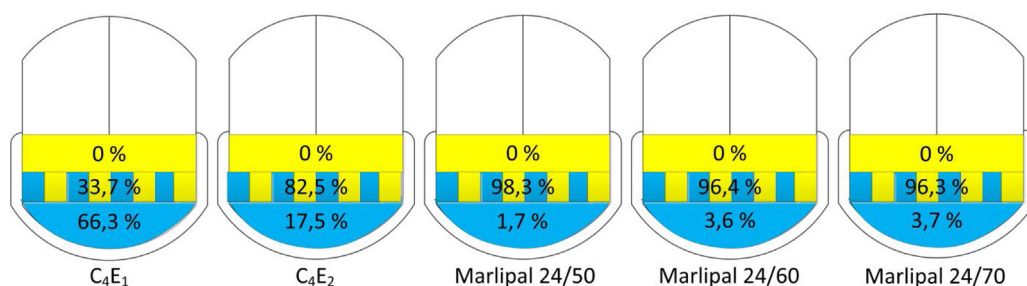


Fig. 7. Rh-content in the aqueous phase by the use of different amphiphiles ( $\alpha = 50\%$ ,  $y = 8\%$  ( $\gamma = 20\%$  for  $C_4E_1$  and  $C_4E_2$ ), 1 wt% sodium sulfate,  $n_{Rh(acac)CO_2} = 0.05$  mmol,  $n_{SX} = 5$  eq.).

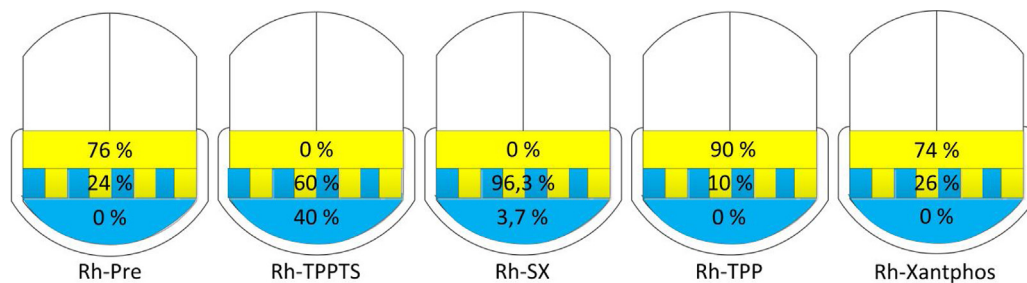


Fig. 8. Distribution of the Rh catalyst for different ligands ( $\alpha = 50\%$ ,  $y = 8\%$  (Marlipal 24/70), 1 wt% sodium sulfate,  $n_{Rh(acac)CO_2} = 0.05$  mmol,  $n_{bidentate} = 5$  eq.,  $n_{monodentate} = 10$  eq.).

However, concluding from these results it is clear that only water-soluble ligands should be used in connection with three-phase microemulsion systems, if an efficient recycling of the catalyst combined with a hydrophobic product isolation are desired.

### 3.4. Temperature influence

The prior results show that the distribution of the rhodium complex in a microemulsion system strongly depends on the hydrophobicity of the ligand and on the kind of the amphiphile. It

**Table 1**  
Rhodium content in the aqueous phase at different temperatures with the amphiphile  $C_4E_2$  ( $\alpha = 50\%$ ,  $y = 20\%$ , 1 wt% sodium sulfate,  $n_{Rh(acac)CO_2} = 0.05$  mmol ( $m_{Rh} = 5145$  mg),  $n_{SX} = 5$  eq.).

Temperature ( $^{\circ}C$ )	Volume aqueous layer (mL)	Volume middle layer (mL)	Volume oil layer (mL)	Rh-concentration aqueous layer (ppm)	Rh-content aqueous layer (mg)
60	16.0	10.4	24.6	34.5	0.55
70	17.0	9.0	25.0	52.7	0.90
80	17.0	8.0	26.0	60.3	1.03

is well known that the temperature shows a tremendous influence on the partition coefficient of salts like the catalyst complex. Hence, we investigated the rhodium content in the aqueous phase at different temperatures (see Table 1). Since most of the systems are extremely temperature sensitive, we decided to choose the microemulsion system formulated with of the amphiphile  $C_{4}E_{2}$ . As illustrated in Fig. 2 it has a broad three phase region, which allows us to study the effect of temperature without changing other experimental conditions.

The results listed in Tab. 1 state that the temperature has a strong influence on the distribution of the catalyst complex. The results are comparable, because the volume of the three layers stays almost constant. There is only a small reduction of the middle phase due to the fact that the solubility of the amphiphile in the oil phase increases with increasing temperature. Hence, the volume of the oil phase increases and that of the middle phase decreases. However, we can clearly show that the rhodium content in the aqueous layer is a function of the temperature. The higher the temperature, the higher is the rhodium content in the aqueous layer. The amount of rhodium was almost doubled by increasing the temperature from 333 K to 353 K. The results verify the typical properties for the solubility of a salt. Most salts (the water-soluble catalyst complex is an organic salt) show an increasing solubility in water with temperature. Thus, the separation temperature is also an important factor besides the kind of amphiphile and ligand to obtain a quantitative recycling of the catalyst complex.

### 3.5. Transfer of the lab results to a continuous process

The experimental results for the distribution of homogeneous catalyst complexes in microemulsion systems in the first part of this contribution demonstrate several possibilities to tune a reaction system with respect to an optimal catalyst recycling and separation process. The interactions between the surfactant and the catalyst complex influence the solubility of the latter and thus enable the control of catalyst distribution in the different phases by the choice of surfactant. For a fixed microemulsion system the application of different ligands has a strong influence on the distribution of the catalyst complex as well. However, a change of the applied ligand is rather unusual for an established reaction process and may result in a modification of the reaction kinetics. Therefore, the adjustment of the catalyst distribution by the choice of surfactant and the determination of the optimal

temperature range for the phase separation of the applied microemulsion system should be the preferred option for optimization of catalyst recycling.

In order to establish a closed recycle catalytic process, the Winsor III system is of great interest due to its two excess phases allowing for separation of hydrophobic products and hydrophilic side-products in the same separation step. Since the phase separation requires a certain amount of time depending on the state and temperature of the system, the reaction and catalyst recycling should be performed in different process steps to enable a continuous process.

Process design for homogeneous catalysis and catalyst recovery in microemulsion systems enables new paths in chemical engineering. Exemplarily, the homogeneously catalysed conversion of long chained olefins becomes feasible, as the surfactant compensates the miscibility gap between the olefin and a catalyst solved in an aqueous phase. As part of the Collaborative Research Center/Transregio 63, "Integrated Chemical Processes in Liquid Multiphase Systems" (InPROMPT) such a novel process concept is being investigated. One aim is to design, construct, and operate a mini-plant for the continuous hydroformylation in such a multicomponent system. Primary target is the combined homogeneous catalysis and catalyst recovery using this multiphase surfactant system. In the following, the task, the constraints, and the applied system is presented as well as an actual application in the mentioned mini-plant.

### 3.6. Task formulation

The task is to design a process in which the catalyst is recycled reliably in order to be reused in the reaction step and leaching via product streams is minimized or even eliminated. After the determination of a suitable tuned micellar solvent system, arising process constraints in terms of remaining catalyst leaching, catalyst stability, and separation dynamics have to be outlined, leading to the development of separation unit design for the given task. To keep things focussed, we consider that the product is always an oily component, thus forming the upper excess phase, and that the catalyst complex is hydrophilic. However, parts of the metal complex structure could be hydrophobic and thus inducing side effects, which have to be considered for the separation step. The thermomorphic behaviour of the microemulsion system and the catalyst behaviour described in Section 3 are summarized in

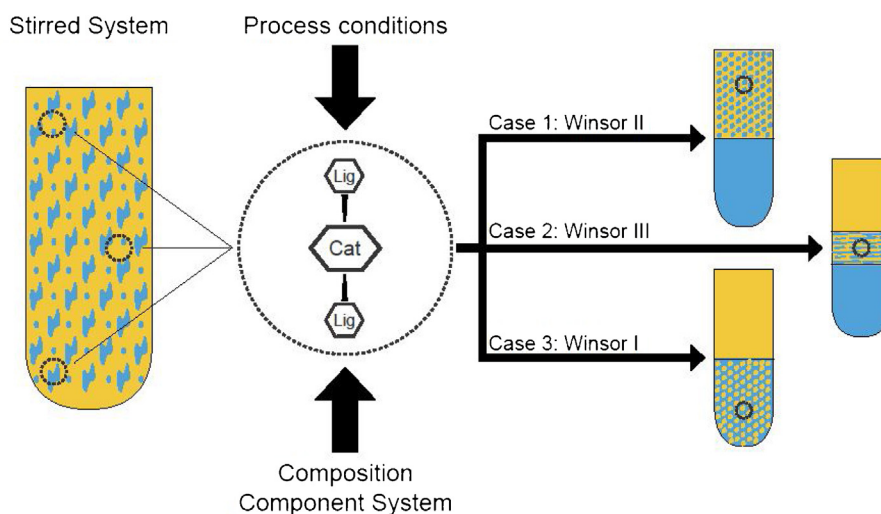


**Fig. 9.** Catalyst distribution and formed excess phases in the different phase separation systems for a microemulsion system tuned towards oily product separation and hydrophilic catalysts. Blue: aqueous excess phase, yellow: oily excess phase. The cycle indicates the location of the hydrophilic catalyst complex. (For interpretation of the references to colour in this figure legend, the reader is referred to the web version of this article.)

Fig. 9, showing the main catalyst position in the described Winsor systems, as well as formed excess phases.

We assume that the corresponding phase shows the major catalyst concentration. However, small amounts of catalyst could still remain in the directly neighbouring phases. The starting point for the separation process is right after a reaction step, in which a homogeneous emulsion is created.

### 3.6.1. Phase separation dynamics

An important issue which has to be considered in terms of operation conditions and equipment sizing (costs) is that of the phase separation dynamics. In the example shown in Fig. 10 the dependence of the separation time  $t_{\text{sep}}$  on the temperature can be seen. Fortunately, the Winsor III state shows a fast phase separation as opposed to the other states. This means, a short residence time in the separation step is possible. From an economic point of view this means a smaller settler, the operation unit in which the phase separation will take place, can be built or the through-put can be increased. Outside of the Winsor III temperature interval the separation time increases drastically. For the applied system, a separation in the Winsor I or Winsor II temperature interval was not observed, even after several hours. Other experimental results as well as a discussion on this issue regarding process applicability can be found in [19].

### 3.6.2. Process constraints

In addition to the determination of catalyst distribution and the overall phase separation dynamics, process constraints depending on the applied substances and microemulsion system need to be specified.

To maintain a viable lifetime of the active catalyst species in a continuous process, operation temperatures should be low, as the ligand-metal-complex is likely to decompose or initiate various side reactions at too high temperatures. This implies limitations for applicable thermal separation processes or prevents for example the use of distillation steps, as the catalyst complex would be completely deactivated and mainly transformed into metal particles in the reboiler. The system pressure should be kept constant or shifted smoothly for the overall process. Failing that, irreversible clustering of the metal-complexes may be observed, as shown in investigations of [20]. Moreover, aspects of chemical stability, such as degradation through the presence of oxygen, as well as electro chemical stability of the catalyst complex have to be

considered. Regarding the formation and thermomorphic behaviour of microemulsions, a variety of side effects could influence the separation dynamics [9]. It is obvious that for the surfactant concentration certain upper and lower bounds are required to maintain a microemulsion system. Impurities (salts) cause shifts in the observed temperature domains of the emulsion systems, as shown by Pfenning et al. [21]. Additionally, process pressure, stirrer speed in the reactor, and in general the occurring chemical reactions influence the phase separation dynamics and feasible temperature domains for the separation [19].

The previous findings are summarized in Fig. 11, which outlines feasible operation conditions and critical aspects of the phase separation states. At this point we define a critical rhodium loss, the rhodium mass fraction within the oil phase, which exits the plant as a product stream. Considering only rhodium precursor prices as catalyst costs, a value of 0.1 ppm equals monthly costs of around 200,000 for the catalyst (Rhodium price of 287/g [22], industrial scale product stream 10 t/h). This underlines the necessity for a low rhodium loss. According to the catalyst distribution in the Winsor system, the Winsor II state is highly economical infeasible, as high rhodium leaching would occur. Additionally, the separation dynamics are expected to be very slow, impairing the productivity of the plant. This fact also excludes the Winsor I system for operating points of a separator unit, because massively large units with high residence times would be necessary, although the rhodium loss poses to be optimally low. Therefore, only the Winsor III system seems economically feasible, concerning both criteria and is in scope for separator unit design and operating conditions.

### 3.7. Application example

The general process concept is depicted in Fig. 12 and consists of 2 main unit operations: mixing and settling. In the mixer part, the olefin, the surfactant, and an aqueous catalyst solution are mixed. By introducing syngas into the system, the hydroformylation reaction is initiated, thus forming aldehydes and byproducts [23]. Afterwards the reaction media is heated or cooled down to a desired temperature and separated accordingly. The idea is to exploit the thermomorphic behaviour and catalyst distribution according to Figs. 1 and 9. The goal is to obtain a catalyst-free oil phase, in which the product can be found, and a mixed phase, containing the vast majority of the dissolved catalyst. The mixed

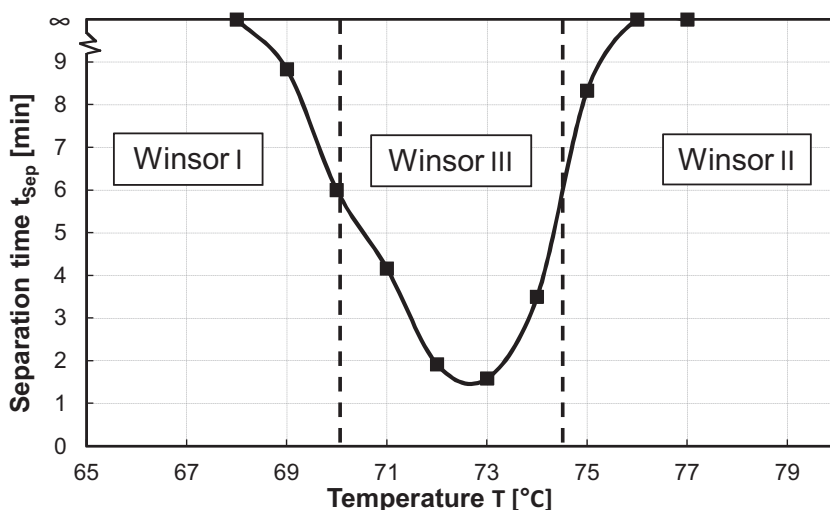
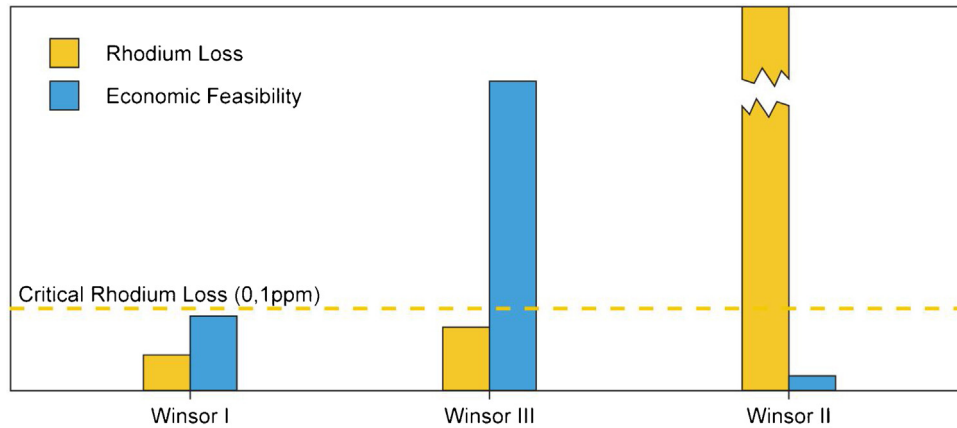
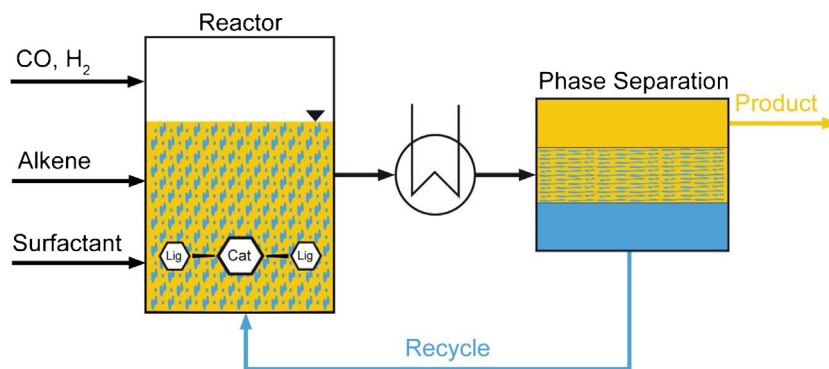


Fig. 10. Temperature dependency of the phase separation time and occurring phase states of a microemulsion system consisting of 1-dodecene/water/Marlipal 24/70 ( $\alpha = 50\%$ ,  $y = 8\%$ , 1 wt% sodium sulphate,  $n_{\text{Rh(acac)CO}_2} = 0.05$  mmol,  $n_{\text{SX}} = 5$  eq.).



**Fig. 11.** Qualitative evaluation of the rhodium loss via the product phase and the economic feasibility of a settler operation in the corresponding Winsor systems. Phase separation dynamics are considered for the feasibility evaluation.



**Fig. 12.** Process concept for the hydroformylation of long-chained aldehydes in microemulsion systems [24].

phase is then recycled, thus enabling the reuse of catalyst and surfactant mixture.

For the investigated reaction system the hydrophilic catalyst complex, consisting of the rhodium precursor  $\text{Rh}(\text{acac})(\text{CO})_2$  and the ligand SulfoXantphos, is applied. Hamerla et al. [12] have

shown that with this complex good reaction rates as well as a high selectivity regarding the linear aldehyde are achievable. Moreover, the application of a suitable surfactant is outlined, whereby according to experimental data the use of Marlipal 24/70 is

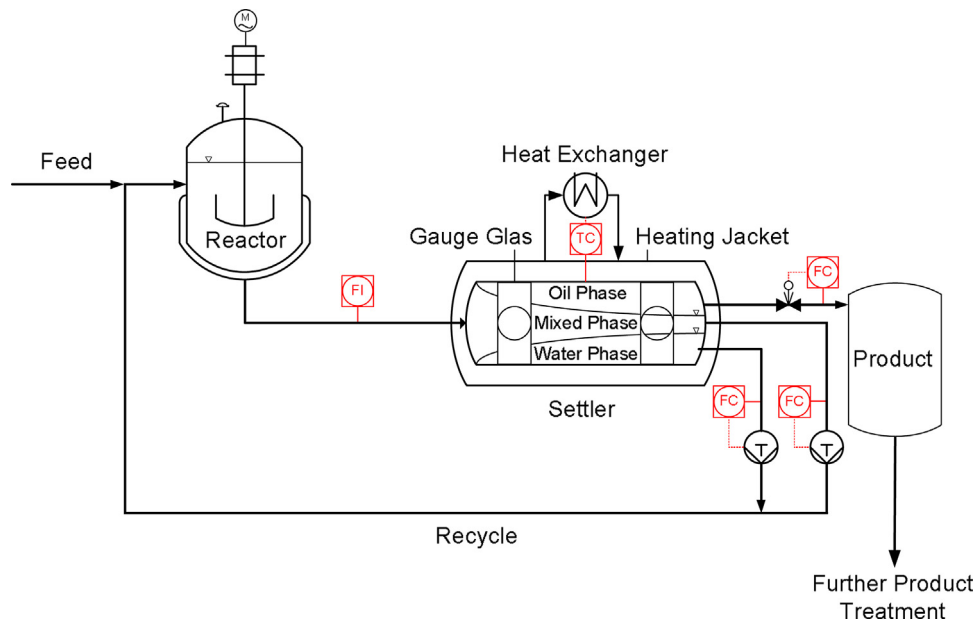


**Fig. 13.** General mixer-settler setup for the separation of up to three liquid phases.

preferential due to its applicability for the reaction and separation purposes [25].

### 3.8. Separation unit design and experimental data

Focussing on the separation step, the results from the first part of this contribution, together with outlined process constraints and challenges are applied for a separation unit design. Operational and economic aspects are then discussed on basis of experimental data of the respective unit.

#### 3.8.1. Settler development

The pre-setting of a thermomorphic multiphase system, containing an oily component, water, and a surfactant for the regarded application offers the exploitation of suitable phase states. Due to the density differences of the components, a separation of the emulsion takes place in a composition dependent temperature domain, forming the three defined phases.

Fast phase separation dynamics for the Winsor III state and a suitable catalyst distribution (see Figs. 10 and 11) with almost no catalyst located in the oily product could be used in a simple settler setup. With the knowledge of the component concentration range in the reactor outlet and corresponding useful separation temperatures, we propose a temperature controlled settler setup, depicted in Fig. 13, for which the desired phase behaviour could be easily achieved. In this case a cylindrical tank with heating jacket, feed inlet, and 3 outlets for the corresponding phases is applicable. Adjusting the residence time via flow controllers and pumps and controlling the separation temperature, a phase split could be realized, gaining a pure oily product stream at the upper settler outlet. Lacking the input of mechanical and large quantities of thermal energy, along with needed internal, this set up offers low investment and operational costs.

In [19] a workflow is presented on how to systematically analyse surfactant containing multiphase systems regarding their applicability for mixer-settler processes. With respect to operational criteria, controllability and modularization a settler construction is presented, which was realised and integrated in the regarded mini-plant.

#### 3.8.2. Settler operation

Given a settler design, as well as a specific microemulsion system, the economic and operational feasibility has to be validated. Therefore, experimental results of a mini-plant run will

be discussed in this section. Additional information about the hydroformylation mini-plant operation is given by Müller et al. [26].

The operating point for the reaction step of the hydroformylation in microemulsions was set to a pressure of 15 bar (g), temperature of 95 °C and a composition of  $\alpha = 50\%$ ,  $y = 8\%$ ,  $w_{RH}(\text{acac})\text{CO}_2 = 298 \text{ g/g}$ ,  $w_{SX} = 4500 \text{ g/g}$ , using Marlipal 24/70 as a technical grade surfactant. The plant was operated mostly in steady state condition (residence time settler approx. 40 min), using a settler with no internals.

For the observation of the phase separation state, samples at the outlet of the upper oily phase and the lower water phase were taken and analysed using offline gas chromatography. Taking a closer look at Fig. 14, it is possible to identify time periods where the separation was adequately. This is shown by the sum of the mass fraction of oily components, which reaches values close to 100% for the oily phase and simultaneously low values in the water phase. However, due to concentration shifts, caused by the ongoing reaction, the phase separation was partly lost.

It has to be mentioned that for the case of equal mass fractions in oil and water phase basically no separation took place and large amounts of surfactant and catalyst solution are introduced into the oil outlet stream. The overall high oil concentrations in both phases at these points indicate temporary shifts in the oil content of the settler, caused by inappropriate recycle ratios. By adjusting relevant process parameters, as temperature, recycle-ratio and surfactant concentration, the re-establishment of the separation was achieved, showing feasible settler operation for different operational states of the mini-plant.

In addition, Fig. 15 depicts the mass fraction of rhodium in the oil outlet stream of the settler. As this is the product stream, high rhodium contents cause a high economic loss.

Assuming a critical rhodium fraction of 0.1 ppm related to the oil phase, feasible operation periods are shown. For established phase separation, identified by a significant difference in the oil content of the regarded phases (Fig. 14), rhodium contents below 0.05 ppm were achieved (Operation time 35–60 h). With lost phase separation within the next 5 h of operation, the rhodium fraction increases immediately. Referring to the sampling point for operation time 63 h this behaviour is indicated and even higher rhodium contents are expected in the period of totally lost phase separation. Given the plant data, it could be seen that concentration shifts led to a drift towards the Winsor I state, where separation time increase massively. Interestingly no significant

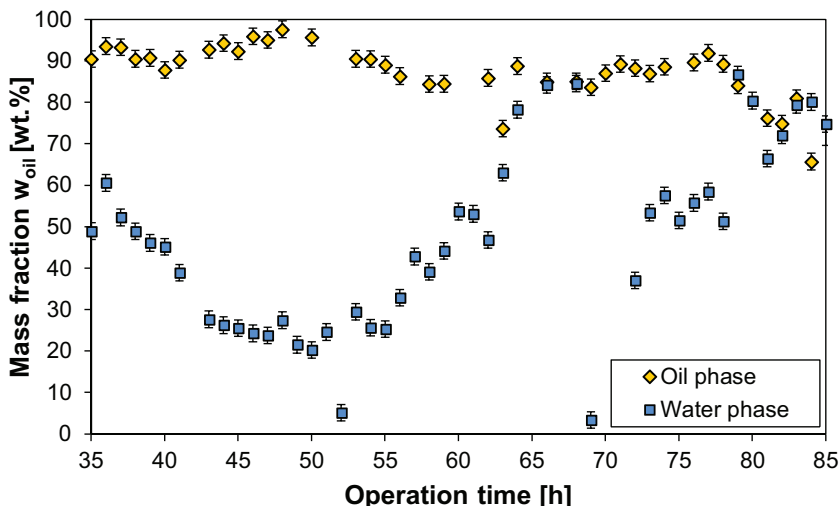
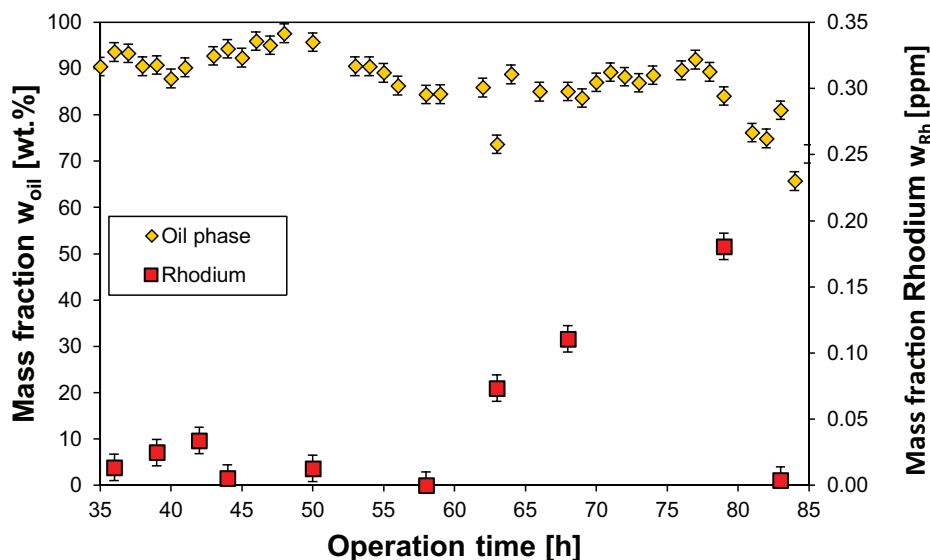


Fig. 14. Mini-plant operation data: mass fraction of total oily components in the upper oily phase and lower water phase.



**Fig. 15.** Mini-plant operation data: mass fraction of total oily components (educt, products) in the upper oily phase and mass fraction of rhodium in the oily phase (product stream). Rhodium was measured using ICP-OES with a Varian ICP-OES 715 ES instrument, oil component data was gathered from gas chromatography.

decrease of rhodium concentration was achieved with re-established phase separation (70–80 h). In this case the settler temperature was set to high and the system moved towards the Winsor II state, whereas phase separation slowed down again and was subsequently lost.

Concluding, it is obvious that the expected behaviour for the catalyst distribution and phase separation dynamics is successfully confirmed in a mini-plant operation. However, challenges still exist to control the phase separation throughout all operational states and under process disturbances. For these cases different options for an advanced process concept seem possible and are in the scope of future investigations. Among these are liquid–liquid extraction for catalyst and surfactant separation from an oily phase or micellar enhanced ultrafiltration techniques, as described in [27,28].

#### 4. Conclusions

The aim of this contribution was to analyse the effects that can have an influence on the distribution of homogeneous catalyst complexes between the different phase layers of microemulsion systems to ensure an efficient catalyst recycling for processes applying these multiphase systems. A profound knowledge of the thermodynamics of microemulsion systems and their phase behaviour as a function of temperature and composition is necessary to get a quantitative separation of the expensive catalyst complex. Especially the three-phase region is of great interest for a mixer-settler process due to its two excess phases allowing for separation of hydrophobic products and hydrophilic side-products in the same separation step. We have shown that the distribution of catalyst in a microemulsion system can be manipulated by the choice of the surfactant, the applied ligand, and the temperature. The surfactant seems to attract the catalyst complex, which follows the surfactant into the corresponding microemulsion phase. However, the higher the hydrophilicity of the ligand, the higher is the amount of catalyst that remains in the aqueous phase. In contrast, catalyst complexes involving hydrophobic ligands stay almost in the oil phase and should not be used in the presence of hydrophobic reactants as the separation is more challenging and requires further process steps. In addition, an increase of temperature improves the solubility of the catalyst complex in the aqueous phase as well. In summary, these results establish the

base for integrated processes using microemulsion systems. We presented a case study for the design of a continuous mixer-settler process, realized in a mini-plant for the Rh/SX catalysed hydroformylation of 1-dodecene to tridecanal in a microemulsion system. Analysing operation data, a temperature controlled settler is shown to be a feasible concept for a separation step, gaining an oily product phase and recycle a valuable catalyst rich phase. Due to disturbances, temporary high rhodium losses have to be tackled. Here, different process options like liquid–liquid extraction and membrane processes exist, which are of future research interest. However, summarizing the existing options for manipulating the phase behaviour of the microemulsion system for the application example, maintaining the three phase condition is desirable due to beneficial separation dynamics and moderate rhodium losses. Regarding microemulsion systems in general, this contribution gives information for a reasoned tailoring of the component system for an optimal catalyst distribution within the system, where a catalyst rich aqueous phase and fast separation dynamics is the desired situation for an easy and quantitative catalyst recycling.

#### Acknowledgements

This work is part of the Collaborative Research Centre “Integrated Chemical Processes in Liquid Multiphase Systems” coordinated by the Technische Universität Berlin. Financial support by the Deutsche Forschungsgemeinschaft (DFG) is gratefully acknowledged (TRR 63).

#### References

- [1] B. Cornils, J. Hibbel, W. Konkol, B. Lieder, J. Much, V. Schmidt, E. Wiebus, Verfahren Zur Herstellung von Aldehyden DE234701 (1982).
- [2] P.B. Webb, M.F. Sellin, T.E. Kunene, S. Williamson, A.M.Z. Slawin, D.J. Cole-Hamilton, *J. Am. Chem. Soc.* 125 (2003) 15577.
- [3] L. Leclercq, I. Suisse, F. Agbossou-Niedercorn, *Chem. Commun.* (2008) 311.
- [4] W. Leitner, *Acc. Chem. Res.* 35 (2002) 746.
- [5] P.G. Jessop, Y. Hsiao, T. Ikariya, R. Noyori, *J. Am. Chem. Soc.* 118 (1996) 344.
- [6] E. Schäfer, Y. Brunsch, G. Sadowski, A. Behr, *Ind. Eng. Chem. Res.* 51 (2012) 10296.
- [7] A. Riisager, P. Wasserscheid, R. Van Hal, R. Fehrmann, *J. Catal.* 219 (2003) 452.
- [8] I. Volovych, M. Schwarze, T. Hamerla, J. Blum, R. Schomäcker, *J. Mol. Catal. Chem.* 366 (2013) 359.
- [9] M. Schwarze, T. Pogrzeba, I. Volovych, R. Schomäcker, *Catal. Sci. Technol.* 5 (2015) 24.

- [10] J.S. Milano-Brusco, M. Schwarze, M. Djennad, H. Nowothnick, R. Schomäcker, *Ind. Eng. Chem. Res.* 47 (2008) 7586.
- [11] H. Nowothnick, J. Blum, R. Schomäcker, *Angew. Chem. Int. Ed. Engl.* 50 (2011) 1918.
- [12] T. Hamerla, A. Rost, Y. Kasaka, R. Schomäcker, *ChemCatChem* 5 (2013) 1854.
- [13] R. Schomäcker, M. Schwarze, H. Nowothnick, A. Rost, T. Hamerla, *Chem. Ing. Tech.* 83 (2011) 1.
- [14] M.-J. Schwuger, K. Stickdorn, R. Schomäcker, *Chem. Rev.* 95 (1995) 849.
- [15] M. Kahlweit, E. Lessner, R. Strey, *J. Phys. Chem.* 87 (1983) 5032.
- [16] A. Kabalnov, U. Olsson, H. Wennerström, *J. Phys. Chem.* 99 (1995) 6220.
- [17] L. Wang, H. Chen, Y.E. He, Y. Li, M. Li, X. Li, *Appl. Catal. A Gen.* 242 (2003) 85.
- [18] H. Nowothnick, A. Rost, T. Hamerla, R. Schomäcker, C. Müller, D. Vogt, *Catal. Sci. Technol.* 3 (2013) 600.
- [19] D. Müller, E. Esche, T. Pogrzeba, M. Illner, F. Leube, R. Schomäcker, G. Wozny, *Ind. Eng. Chem. Res.* 54 (2015) 3205.
- [20] R.H. Crabtree, *Chem. Rev.* 115 (2015) 127.
- [21] A. Pfennig, A. Schwerin, *Ind. Eng. Chem. Res.* 37 (1998) 3180.
- [22] [www.sigmaaldrich.com/catalog/product/aldrich/288101?lang=de&region=D](http://www.sigmaaldrich.com/catalog/product/aldrich/288101?lang=de&region=D), 2015, (access 02.06.2015).
- [23] J. Markert, Y. Brunsch, T. Munkelt, G. Kiedorf, A. Behr, C. Hamel, A. Seidel-Morgenstern, *Appl. Catal. A Gen.* 462–463 (2013) 287.
- [24] D. Müller, E. Esche, M. Müller, G. Wozny, *Present. AIChE 2012, Pittsburgh, 2012*.
- [25] T. Hamerla, *Hydroformylierung Langkettiger Olefine Mit Zweizähligen Rhodium-Komplexen, Mizellaren Lösungen Und Mikroemulsionen (Dissertation)*, Technische Universität Berlin, 2014, 2015.
- [26] D. Müller, E. Esche, T. Pogrzeba, T. Hamerla, T. Barz, R. Schomäcker, G. Wozny, *20th Int. Conf. Process Eng. Chem. Plant Des.*, ISBN: 978-3-00-047364-7, Berlin, 2014.
- [27] M. Schwarze, M. Schmidt, L.A.T. Nguyen, A. Drews, M. Kraume, R. Schomäcker, *J. Membr. Sci.* 421–422 (2012) 165.
- [28] M. Schwarze, A. Rost, T. Weigel, R. Schomäcker, *Chem. Eng. Process. Process Intensif.* 48 (2009) 356.

# PAPER 2

## Verteilungsgleichgewichte von Liganden in mizellaren Lösungsmittelsystemen

Marcel Schmidt, Tobias Pogrzeba, Dmitrij Stehl, René Sachse, Michael Schwarze, Regine von Klitzing, Reinhard Schomäcker

Chemie Ingenieur Technik, 2016, 88, 119-127

Online Article:

<https://onlinelibrary.wiley.com/doi/full/10.1002/cite.201500125>

Reprinted with permission from “Verteilungsgleichgewichte von Liganden in mizellaren Lösungsmittelsystemen; Marcel Schmidt, Tobias Pogrzeba, Dmitrij Stehl, René Sachse, Michael Schwarze, Regine von Klitzing, and Reinhard Schomäcker. Chemie Ingenieur Technik, 2016, 88, 119-127.” Copyright (2016) Wiley-VCH.



# Verteilungsgleichgewichte von Liganden in mizellaren Lösungsmittelsystemen

Marcel Schmidt<sup>1,\*</sup>, Tobias Pogrezba<sup>1</sup>, Dmitrij Stehl<sup>1</sup>, René Sachse<sup>1</sup>, Michael Schwarze<sup>2</sup>, Regine von Klitzing<sup>1</sup> und Reinhard Schomäcker<sup>1</sup>

DOI: 10.1002/cite.201500125

*Herrn Prof. Dr.-Ing. Matthias Kraume zum 60. Geburtstag gewidmet*

Im Rahmen des Sonderforschungsbereichs SFB/TRR 63 „InPROMPT“ (Integrierte chemische Prozesse in flüssigen Mehrphasensystemen) wird der Einsatz mizellarer Lösungsmittelsysteme als schaltbare mehrphasige Reaktionsmedien für die homogene Katalyse untersucht. In diesem Beitrag wird das Verteilungsgleichgewicht von vier repräsentativen Liganden in unterschiedlichen wässrig-mizellaren Systemen analysiert und die Abhängigkeit ihrer Verteilung – und damit auch der eines homogen gelösten Katalysators – in den einzelnen Phasen dieser Mehrphasensysteme diskutiert. Die Kenntnis der Verteilungskoeffizienten ist von entscheidender Bedeutung für eine effiziente und quantitative Katalysatorrückführung in wässrig-mizellaren Systemen.

**Schlagwörter:** Liganden, Mizellen, Tenside, Verteilungskoeffizient

*Eingegangen:* 14. August 2015; *akzeptiert:* 29. September 2015

## Equilibrium Distribution of Ligands in Micellar Solutions

The applicability of micellar solvent systems as tuneable multiphase reaction media for homogeneous catalysis is being examined within the framework of the collaborative research centre SFB/TRR 63 “InPROMPT” (Integrated Chemical Processes in Liquid Multiphase Systems). In this contribution the equilibrium distribution of four representative ligands in different aqueous-micellar systems was investigated and the dependency of their distribution – and thereby the distribution of a homogeneously dissolved catalyst – in the different phases of these multiphase systems is discussed. The knowledge of the distribution coefficients is of utmost importance for an efficient and quantitative catalyst recycling in aqueous-micellar systems.

**Keywords:** Equilibrium distribution, Ligands, Micelles, Surfactants

## 1 Einleitung

Für die Wirtschaftlichkeit eines chemischen Prozesses in der homogenen Katalyse ist vor allem die quantitative Rückführung der teuren Edelmetall-Katalysatoren von entscheidender Bedeutung. Den Idealfall für homogene Reaktionsmedien stellen deshalb sogenannte schaltbare Reaktionssysteme dar, deren Phasenverhalten sich zwischen den

verschiedenen Prozessschritten verändern lässt. So sollte ein Reaktionsmedium während der Reaktion homogen sein, um Stofftransporthemmungen zu vermeiden, und für die Katalysatorabtrennung in ein Zweiphasensystem umschaltbar sein, in dem Produkt und Katalysator in unterschiedlichen Phasen vorliegen. Zur vollständigen Abtrennung des Katalysators vom Produkt empfiehlt sich der Einsatz von Zweiphasensystemen mit sehr breiten Mischungslücken, da darin die Verteilungskoeffizienten der Katalysatoren häufig große Werte zugunsten einer der beteiligten Phase annehmen. So bieten z. B. wässrig-organische Systeme oft optimale Verhältnisse für die Katalysatorabtrennung, da die Liganden für die Katalysatoren durch funktionelle Gruppen sehr gut in ihrer Löslichkeit (polar/unpolar) eingestellt werden können (s. Abb. 1). Durch einfache Modifikationen am Liganden (z. B. das Anbringen von Sulfonat-Gruppen zur

<sup>1</sup>Marcel Schmidt (marcel.schmidt@tu-berlin.de), Tobias Pogrezba, Dmitrij Stehl, René Sachse, Prof. Regine von Klitzing, Prof. Reinhard Schomäcker, Technische Universität Berlin, Institut für Chemie, Straße des 17. Juni 124, 10623 Berlin, Deutschland; <sup>2</sup>Prof. Michael Schwarze, Technische Universität Berlin, Fachgebiet Anlagen- und Sicherheitstechnik, Straße des 17. Juni 135, 10623 Berlin, Deutschland.

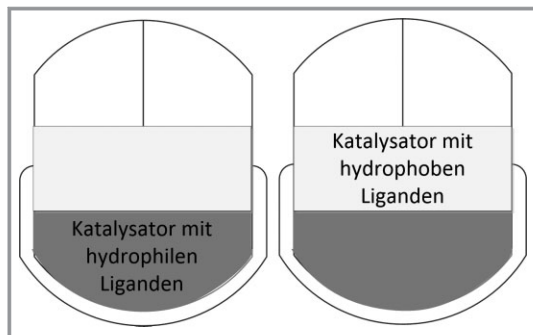


**Abbildung 1.** Schematische Darstellung zur Verteilung von Katalysatoren mit verschiedenen Liganden in einem flüssig-flüssig-Mehrphasensystem.

Erhöhung der Wasserlöslichkeit) kann somit dafür gesorgt werden, dass der Katalysator quantitativ in nur einer Phase vorliegt.

Das Hauptproblem der Anwendung von Wasser in der organischen Synthese ist die Unlöslichkeit vieler Reagenzien in diesem Medium. Neben zahlreichen Möglichkeiten wie dem Zusatz von hydrophilen Lösevermittlern, dem Einsatz von Phasentransfer-Katalysatoren oder pH-Regulierung der Reaktionslösung, bietet der Einsatz von Tensiden eine weitere Option zur Behebung des Löslichkeitsproblems. Hierbei übertragen Mizellen unpolare Reaktanden in die wässrige Phase oder polare Komponenten in die organische Phase. Diese Variante zur Modifikation von Zweiphasensystemen bietet eine hohe Flexibilität in ihrer Anwendung, da eine breite Palette an Tensiden auf dem Markt verfügbar ist. Außerdem eröffnet der Einsatz von Tensiden durch die Bildung von Mikroemulsionen den Zugang zu schaltbaren Reaktionsmedien, deren Phasenverhalten stark von der Zusammensetzung und Temperatur abhängig ist.

In den folgenden Kapiteln wird der Einfluss von unterschiedlichen Liganden und Tensiden auf die Katalysatorrückführung in mizellaren Systemen diskutiert. Für ausgewählte repräsentative Liganden wurden die Verteilungskoeffizienten in diesen Systemen experimentell und rechnerisch ermittelt. Auf Basis dieser Ergebnisse wird die Aussagekraft der Verteilungskoeffizienten zur Vorhersage der Qualität der Katalysatorrückführung in wässrigen Mehrphasensystemen überprüft.

## 2 Grundlagen und Methoden

Für die Bestimmung des polaren Charakters eines Substrates kann der Oktanol/Wasser-Verteilungskoeffizient  $P_{OW}$ , der nach Gl. (1) definiert ist, herangezogen werden.

$$P_{OW} = \frac{c_O^i}{c_W^i} \quad (1)$$

In Gl. (1) steht  $c_O^i$  für die Konzentration des Substrats in der Oktanolphase und  $c_W^i$  für die Konzentration in der Wasserphase. Für die Bestimmung des Wertes wird in der

Regel die Shake-Flask-Methode (OECD-Richtlinie 107) eingesetzt, bei der Oktanol und Wasser intensiv gemischt werden, wobei die zu verteilende Substanz in einer der Phasen vorgelöst wird. Nach erfolgter Phasentrennung wird die Konzentration der Substanz in den einzelnen Phasen bestimmt. Der Vorteil der Methode besteht darin, dass die Phasentrennung zumeist sehr schnell verläuft und die Versuche einfach zu realisieren sind. Für die Bestimmung von Verteilungskoeffizienten im Allgemeinen existieren aber auch andere experimentelle Methoden, z. B. über die Bestimmung von Löslichkeiten oder die Flüssigkeitschromatographie. Eine Übersicht ist in [1] gegeben. Anstelle der Konzentrationen kann der Verteilungskoeffizient auch über die Molenbrüche als  $K_{OW}$  (Gl. (2)) definiert werden.

$$K_{OW} = \frac{v_O}{v_W} \frac{c_O^i}{c_W^i} = 6,63P_{OW} \quad (2)$$

In Gl. (2) steht  $v_O$  für das molare Volumen der Oktanolphase und  $v_W$  für das molare Volumen der Wasserphase. Da nach der Phasentrennung die Oktanolphase ca. 28 % Wasser enthält, während die Wasserphase nahezu rein vorliegt, muss dies bei der Berechnung berücksichtigt werden, weshalb sich ein Vorfaktor von 6,63 ergibt. Neben der experimentellen Bestimmung der Verteilungskoeffizienten kann auch eine Vorhersage durch Simulationsrechnung erfolgen. Hierfür bietet sich das freiverfügbare Programm ALOGPS2.1 an, das mithilfe künstlicher neuronaler Netze arbeitet. Dabei werden Modelle für die Lipophilie von chemischen Substanzen und die Löslichkeit in einer wässrigen Lösung kombiniert, um dies auf unbekannte Stoffe zu übertragen. So können Verteilungskoeffizienten anhand der chemischen Struktur kalkuliert werden – für weitere Informationen s. [2]. Dieses Programm eignet sich gut zur Vorhersage der Verteilungskoeffizienten von nicht-ionischen Verbindungen, wie z. B. Itaconsäureester [3]. Weiterhin bietet das Programm den Vorteil, dass auch Verteilungskoeffizienten bestimmt werden können, wo die experimentelle Erfassung sehr aufwendig ist, z. B. bei Substanzen deren Konzentration in einer Phase so gering ist, dass sie analytisch kaum erfassbar ist. Da die Verteilungskoeffizienten in der Regel über mehrere Zehnerpotenzen variieren können, wird zumeist der  $\log P_{OW}$  bzw.  $\log K_{OW}$  angegeben.

Auch in Tensidsystemen erfolgt die Verteilung eines Substrats zwischen Domänen unterschiedlicher Hydrophobizität. Im Vergleich zu den Oktanol/Wasser-Verteilungskoeffizienten ist jedoch die experimentelle Bestimmung der Verteilung in Tensidsystemen aufwendiger, da z. B. für wässrig-mizellare Lösungen oder Mikroemulsionen makroskopisch einphasige Systeme vorliegen. Weiterhin können in diesen Systemen, bedingt durch die Anwesenheit des Tensids, zusätzliche Effekte die Verteilung stark beeinflussen. Für wässrig-mizellare Lösungen findet man in der Literatur unterschiedliche Methoden zur Bestimmung des Verteilungskoeffizienten, die im Folgenden erläutert werden. Eine Methode, die sich gut für Feststoffe eignet, ist die Methode der erhöhten Löslichkeit (ESM; enhanced solubility

method). Dabei steigt die Löslichkeit eines Stoffes mit der Tensidkonzentration aufgrund einer größeren Anzahl an Mizellen, die für die Solubilisierung zur Verfügung stehen. Wie in [4] beschrieben, lässt sich der Verteilungskoeffizient aus Gl. (3) berechnen.

$$K_{MW} = \frac{(S_M - S_W)V_W}{S_W(C - \text{cmc})} \quad (3)$$

In Gl. (3) ist  $S_M$  die Löslichkeit des Substrates in der wässrig-mizellaren Lösung,  $S_W$  die Löslichkeit in Wasser,  $C$  die Tensidkonzentration,  $\text{cmc}$  die kritische Mizellbildungskonzentration und  $V_W$  das molare Volumen von Wasser ( $55,55 \text{ mol L}^{-1}$ ). Die Methode ist einfach durchzuführen, da der Bodensatz des nicht gelösten Substrates abfiltriert und nur die gesättigte Lösung analysiert wird. Für nicht-ionische Tenside wird oft die Trübungspunktextraktion (CPE; cloud point extraction) angewendet. Dabei wird eine, mit dem Substrat gesättigte, wässrig-mizellare Lösung oberhalb der Trübungstemperatur in eine wasserreiche und tensidreiche Phase aufgespalten. Durch Bilanzierung der einzelnen Phasen kann der Verteilungskoeffizient aus Gl. (4) erhalten werden.

$$K_{MW} = \frac{x_M^i}{x_W^i} \quad (4)$$

In Gl. (4) ist  $x_M^i$  der Molenbruch des Substrates in der tensidreichen Phase und  $x_W^i$  der Molenbruch in der wasserreichen Phase. Da die CPE nur für nicht-ionische Tenside geeignet ist, können Verteilungen für ionische Tenside damit nicht bestimmt werden. Eine Methode, die für alle Tenside gleichermaßen geeignet ist, ist die Ultrafiltration wässrig-mizellarer Lösungen (MEUF; micellar enhanced ultrafiltration). Dabei wird eine mit dem Substrat gesättigte, wässrig-mizellare Lösung durch eine Membran mit einem Porendurchmesser unterhalb der Mizellgröße filtriert, wobei die Mizellen von der Membran zurückgehalten werden. Nur der Anteil an Substrat, der in der kontinuierlichen Wasserphase gelöst vorliegt, sowie das Tensid in monomerer Form passieren ungehindert die Membran. Durch Bilanzierung des Tensidsystems vor und nach der Filtration lässt sich der Verteilungskoeffizient, wie von Schwarze et al. in [3] gezeigt, bestimmen. Da die experimentellen Methoden sehr aufwendig sind, wurden Methoden zur Vorhersage der Verteilungskoeffizienten für Tensidsysteme untersucht. Eine Methode, die gute Vorhersagen liefert, ist COSMO-RS (conductor-like screening model for real solvents). Diese Methode konnte bereits anhand von Verteilungskoeffizienten aus CPE [5] oder MEUF [3] validiert werden.

## 3 Experimentelles

### 3.1 Chemikalien

Die Lösungsmittel 1-Dodecen (94 %) und Wasser (HPLC grade) wurden von VWR bezogen. 1-Oktanol (99 %) wurde von Roth erhalten. Die technischen Tenside Marlipal 24/40,

24/50 und 24/70 sind eine Spende der Firma Sasol. Die Tenside Triton X-114 und Triton X-100, sowie die Liganden Triphenylphosphin (TPP, 99 %), 4,5-Bis(diphenylphosphino)-9,9-dimethylxanthene (XantPhos, 97 %) und Tri-(natrium-meta-sulfonatophenyl)-phosphan (TPPTS, 95 %) wurden von Sigma-Aldrich erhalten. Das sulfonierte Analogum zum XantPhos Ligand, SulfoXantPhos, wurde von der Molisa GmbH hergestellt. Der Rhodium-Vorläufer  $\text{Rh}(\text{acac})(\text{CO})_2$  ist eine Spende von Umicore. Alle Chemikalien wurden ohne Aufreinigung verwendet.

### 3.2 Methoden

#### *Bestimmung des Oktanol/Wasser Verteilungskoeffizienten*

Zur Bestimmung des Oktanol/Wasser-Verteilungskoeffizienten wurden jeweils 5 mL von mit Wasser gesättigtem Oktanol und mit Oktanol gesättigtem Wasser gemischt. Anschließend wurden 100 mg SulfoXantPhos bzw. TPPTS hinzugegeben und über Nacht auf einer Rüttelplatte vermischt. Die Konzentration der Liganden in den einzelnen Phasen wurde nach der Phasentrennung mit einer HPLC-Anlage der Serie 1200 von Agilent untersucht. Als Säule wurde eine Multospher 120 RP18-5  $\mu\text{L}$  verwendet. Die Proben wurden bei einer Flussrate von  $1 \text{ mL min}^{-1}$  mit einem Lösemittelgemisch aus Wasser/Acetonitril von 30:70 vermessen.

#### *Erhöhte Löslichkeitsmethode*

Zur Bestimmung des Mizelle/Wasser-Verteilungskoeffizienten mittels der Methode der erhöhten Löslichkeit (ESM) wurden verschiedene tensidhaltige Lösungen hergestellt und der zu untersuchende Ligand bis zur Bodensatzbildung hinzugegeben. Die mizellare Lösung wurde über Nacht auf einer Rüttelplatte gemischt, anschließend filtriert und das Filtrat auf die Konzentration des Liganden analysiert.

#### *Trübungspunkt-Extraktion*

Für die Trübungspunkt-Extraktion (CPE) wurden 5 Gew.-% des Tensids mit den zu untersuchenden Liganden in einer wässrigen Lösung gemischt. Die Temperatur wurde schrittweise erhöht, bis der Trübungspunkt erreicht wurde. Nach erfolgter Phasentrennung wurden die einzelnen Phasen mittels HPLC hinsichtlich der Ligandenkonzentration untersucht. Für den Liganden XantPhos wurde die Konzentration mittels induktiv gekoppeltem Plasma mit optischer Emissionsspektroskopie (ICP-OES) bestimmt. Für die analytische Messung wurde das ICP-OES Varian 714 ES verwendet und zur Kalibrierung wurden Phosphorlösungen mit 1, 10, 100 und  $1000 \text{ mg L}^{-1}$  hergestellt. Die Auswertung erfolgte bei einer Wellenlänge von 213 nm.

#### *Bestimmung der Oberflächenspannung der Liganden*

Die Messungen zur Oberflächenspannung der Ligandenlösungen wurden mit einem DCAT 11 der Firma

DATAPHYSICS durchgeführt. Der Messkörper war ein Du Noüy-Ring bestehend aus einer Platin-Iridium-Legierung mit einer Ringhöhe von 25 mm, einen Ringdurchmesser von 18,7 mm und einer Drahtdicke von 0,37 mm. Es wurden verschieden konzentrierte Lösungen der Liganden TPPTS und SulfoXantPhos hergestellt und vermessen. Nach jeder Messung wurde der Messring mit einer Butangasflamme gereinigt.

#### Bestimmung der Verteilung des Katalysators in der Mikroemulsion

Die Konzentration von Rhodium in den unterschiedlichen Phasen eines mehrphasigen Mikroemulsionssystems wurde mittels ICP-OES bestimmt. Es wurde jeweils die wässrige Phase und die Mittelphase des Mikroemulsionssystems untersucht. Dazu wurden 2 mL der wässrigen bzw. 1 mL der Mittelphase mit Königswasser versetzt und mit destilliertem Wasser verdünnt. Die Rhodiumkonzentration wurde bei einer Wellenlänge von 369 nm gemessen. Die Kalibrierung erfolgte mit Rhodiumstandard-Lösungen der Konzentration 1, 5, 20, 50 und 150 mg L<sup>-1</sup>.

## 4 Ergebnisse und Diskussion

Für die effektive Abschätzung der Verteilung von homogenen Katalysatorkomplexen in tensidmodifizierten Flüssig/flüssig-Mehrphasensystemen spielt die Polarität des Komplexes eine entscheidende Rolle. Diese kann maßgebend durch die Löslichkeitseigenschaften des verwendeten Liganden gesteuert werden. Das Wissen über die Verteilung des Liganden ist somit essentiell für die quantitative Abtrennung des homogenen Katalysatorkomplexes.

Das Verteilungsgleichgewicht eines homogenen Katalysatorkomplexes soll für mizellare Lösungsmittelsysteme qualitativ vorhergesagt werden, wobei ein besonderes Augenmerk auf die Art der Liganden und die Struktur des Tensids gelegt wird. Dazu wird schrittweise die Komplexität des Flüssig/flüssig-Mehrphasensystems erhöht um eine aussagekräftige Beurteilung zu gewährleisten.

### 4.1 Verteilungskoeffizienten für verschiedene Liganden zwischen 1-Oktanol und Wasser

Für die Auswahl eines Katalysatorkomplexes für Flüssig/flüssig-Mehrphasensysteme spielt der Verteilungskoeffizient des Liganden zwischen den nicht mischbaren Phasen eine entscheidende Rolle. Auf der einen Seite muss die lokale Konzentration aller Reaktionsteilnehmer so hoch sein, dass eine wirtschaftlich sinnvolle Reaktionsgeschwindigkeit resultiert. Auf der anderen Seite muss sichergestellt werden, dass ein Recycling des ligand-modifizierten, meist teuren Katalysatorkomplexes und eine Trennung des Reaktionsproduktes durch eine Phasenseparation ermöglicht wird.

Die Verteilungskoeffizienten von nicht-ionischen Liganden sind für Flüssig/flüssig-Mehrphasensysteme wie Oktanol/Wasser bekannt bzw. können mit verschiedenen Methoden berechnet werden, jedoch findet man kaum Informationen für ionische Liganden, die sulfoniert und somit wasserlöslich sind. Deshalb wurden die Oktanol/Wasser-Verteilungskoeffizienten  $K_{OW}$  für TPPTS und SulfoXantPhos – die sulfonierten Analoga zu TPP und XantPhos – bestimmt (Tab. 1). Für die Berechnung der Verteilungskoeffizienten wurde das Programm ALOGPS2.1 verwendet, das für nicht-ionische und nicht-geladene Moleküle gute Vorhersagen liefert.

**Tabelle 1.** Experimentelle und berechnete Oktanol-Wasser-Verteilungskoeffizienten  $K_{OW}$  für verschiedene Liganden (berechnet mit ALOGPS2.1).

Ligand	$\log(K_{OW})$ exp.	$\log(K_{OW})$ ber.
TPP	6,02 [6]	6,2 ± 0,5
TPPTS	-3,07	-
XantPhos	-	11,1 ± 1,4
SulfoXantPhos	-1,21	-

Die berechneten Oktanol/Wasser-Verteilungskoeffizienten zeigen, dass das bidentate XantPhos im Vergleich zu TPP viel hydrophober ist, was auf die größere Anzahl an Phenylringen zurückzuführen ist (Abb. 2). Der berechnete Wert für TPP stimmt dabei mit dem experimentell ermittelten Literaturwert überein. Eine Berechnung für die wasserlöslichen Analoga konnte aufgrund ihres ionischen Charakters nicht durchgeführt werden. Die experimentellen Daten zeigen jedoch deutlich, dass die Sulfonierung eine Umkehrung der Löslichkeit hervorruft und TPPTS bzw. SulfoXantPhos sich vorwiegend in der Wasserphase lösen. Dabei zeigt TPPTS im Vergleich zu SulfoXantPhos einen kleineren Oktanol/Wasser-Verteilungskoeffizienten, da drei

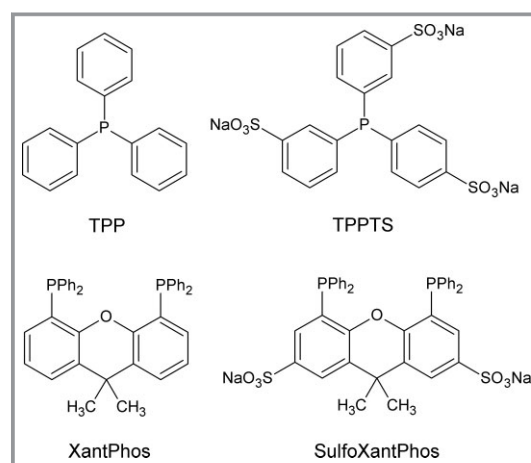


**Abbildung 2.** Strukturformeln der Liganden TPP, TPPTS, XantPhos und SulfoXantPhos.

statt zwei Sulfonat-Gruppen für eine größere Hydrophilie im Molekül sorgen. Außerdem besitzt SulfoXantPhos eine größere Anzahl an Phenylgruppen.

#### 4.2 Verteilungskoeffizienten für verschiedene Liganden in einem mizellaren Lösungsmittelsystem

Ein basiertes Wissen über den Mizelle/Wasser-Verteilungskoeffizienten  $K_{MW}$  ist entscheidend, um den Trennungsprozess für homogene Katalysatorkomplexe in mizellaren Lösungsmittelsystemen zu verstehen und das Recycling zu optimieren. Für neutrale, nicht oberflächenaktive Komponenten besteht ein linearer Zusammenhang zwischen den Oktanol/Wasser- und Mizelle/Wasser-Verteilungskoeffizienten [7], der durch die Collander-Gleichung [8] beschrieben werden kann (Gl. (5)). Collander beobachtete in verschiedenen zweiphasigen Systemen einen linearen Zusammenhang zwischen den logarithmierten Verteilungskoeffizienten einer Komponente, wobei  $K_1$  und  $K_2$  die Verteilungskoeffizienten in den Systemen 1 und 2 widerspiegelt und  $a$  und  $b$  empirische Konstanten sind.

$$\log(K_1) = a \log(K_2) + b \quad (5)$$

Jedoch ist dieser Zusammenhang für ionische Spezies nicht nachweisbar, so dass dort zusätzliche Effekte bei der Verteilung in einem mizellaren Lösungsmittelsystem eine wesentliche Rolle spielen und untersucht werden müssen. Im Folgenden wird der Verteilungskoeffizient für einige Modell-Liganden, die häufig in Metallkomplexen eingesetzt werden, diskutiert, wobei ein Augenmerk auf die Tensidauswahl sowie auf die Struktur des Liganden gelegt wird.

##### 4.2.1 Tensideinfluss

Zunächst wurde der Einfluss des Tensids auf die Verteilung des hydrophoben Liganden TPP und des hydrophilen Liganden SulfoXantPhos untersucht (Abb. 3). Dazu wurden die nichtionischen Tenside NP9, Triton X-100, Triton X-114, Marlipal 24/40, 24/50 und 24/70, und das anionische Tensid Natriumdodecylsulfat (SDS) verwendet. Typische Eigenschaften der Tenside sind in Tab. 2 aufgelistet und die Tensidstrukturen sind in Abb. 4 gezeigt.

Der Mizelle/Wasser-Verteilungskoeffizient  $K_{MW}$  von TPP liegt in der Größenordnung von  $K_{OW}$  für TPP. Demnach wird TPP vorwiegend innerhalb des hydrophoben Kerns der gebildeten Mizellen eingelagert. Des Weiteren war die Struktur des Tensids hinsichtlich des Mizelle/Wasser-Verteilungskoeffizienten von Interesse, weshalb zwei Tenside mit

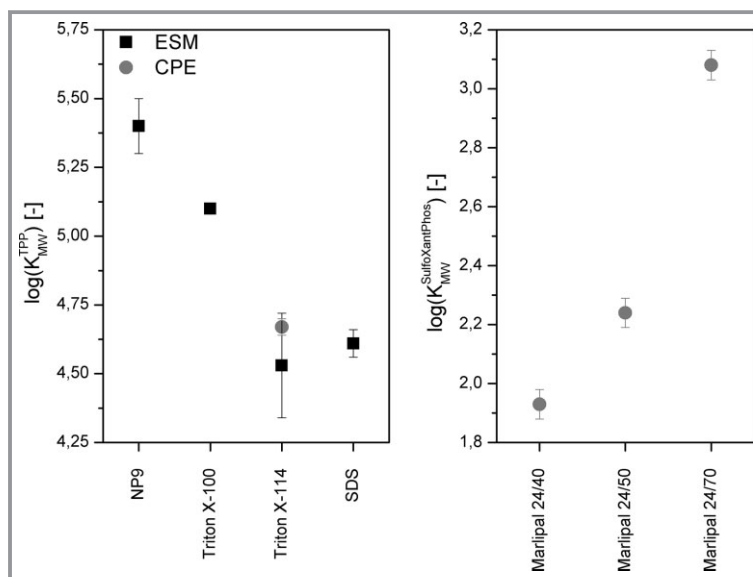


**Abbildung 3.** Verteilungskoeffizienten von TPP (links) und SulfoXantPhos (rechts) in mizellaren, wässrigen Lösungen mit der Methode nach der erhöhten Löslichkeit (ESM) und der Trübungspunkt Extraktion (CPE).

**Tabelle 2.** Molare Masse, Trübungspunkt, cmc und HLB-Wert der verwendeten Tenside.

Tensid	Molare Masse [g mol <sup>-1</sup> ]	Trübungspunkt [°C]	cmc [mol L <sup>-1</sup> ]	HLB-Wert
Triton X-100	≈ 625	65	2 · 10 <sup>-4</sup>	13,5
Triton X-114	≈ 537	23	2 · 10 <sup>-4</sup>	12,4
Marlophen NP9	≈ 600	52 – 56 <sup>a)</sup>	6,7 · 10 <sup>-5</sup>	–
SDS	288,38	–	8,2 · 10 <sup>-3</sup>	40 <sup>d)</sup>
Marlipal 24/40	≈ 376	66 – 68 <sup>b)</sup>	–	–
Marlipal 24/50	≈ 420	72 – 74 <sup>b)</sup>	–	–
Marlipal 24/70	≈ 508	53 – 56 <sup>c)</sup>	–	–

a) 1 % in deionisiertem Wasser, b) 10 % in 25 % BDG-Lösungen, c) 2 % in deionisiertem Wasser, d) nach der Methode von Davies.

identischen Ethoxylierungsgrad, aber unterschiedlichem hydrophoben Rest verglichen wurden: Triton X-100 besitzt einen verzweigten hydrophoben Rest und Marlophen NP9 weist eine lineare Alkylkette mit vergleichbarer Kohlenstoffanzahl auf. Es wurden bedingt durch die unterschiedlichen Alkylketten leicht unterschiedliche Verteilungskoeffizienten bestimmt. Durch die verzweigte Alkylkette ist der Kern der gebildeten Triton X-100-Mizelle hydrophiler im Vergleich zu Marlophen NP9. Dadurch ist der Verteilungskoeffizient geringer, da das stark hydrophobe TPP somit den Kern der Mizelle von Marlophen NP9 präferiert.

Weiterhin wurde der Einfluss des Ethoxylierungsgrad untersucht, wobei die Tenside Triton X-100 (9 – 10 Ethoxyeinheiten) und Triton X-114 (7 – 8 Ethoxyeinheiten)

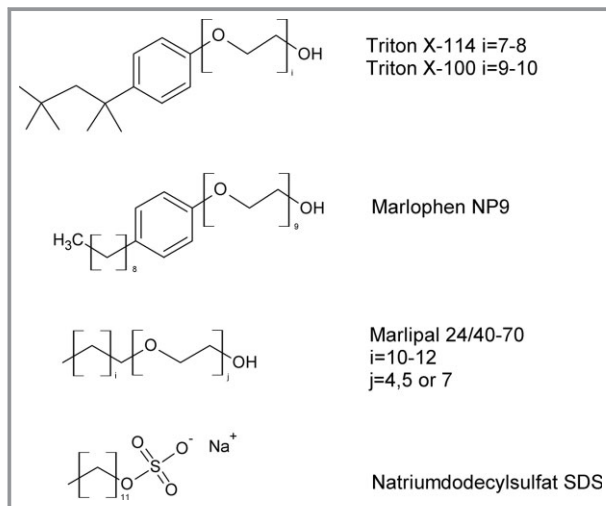


**Abbildung 4.** Strukturformeln der Tenside Triton X-100, Triton X-114, Marlophen NP9, Marlipal 24/40, 24/50 und 24/70 und SDS.

mit identischer hydrophober Alkylkette, jedoch unterschiedlicher Anzahl an Ethoxyeinheiten verglichen wurden. Die Schicht der hydrophilen Kopfgruppen von Triton X-100 ist im Vergleich zu Triton X-114 aufgrund der höheren Anzahl an Ethoxyeinheiten hydrophiler. Als Folge wird der Ligand TPP zusätzlich aus der kontinuierlichen wässrigen Phase verdrängt und es resultiert bei Triton X-100 ein höherer Verteilungskoeffizient im Vergleich zu Triton X-114. Für Triton X-100 und den Liganden TPP wurde mittels COSMO-RS ein Mizelle/Wasser-Verteilungskoeffizient von 7,1 bestimmt, der sich zwei Größenordnungen von den experimentellen unterscheidet [9]. Der Verteilungskoeffizient für SulfoXantPhos  $P_{MW}$ , bestimmt durch eine Trübungspunkt-Extraktion, zeigt eine identische Tendenz. Je hydrophiler das Tensid ist, desto höher ist der Verteilungskoeffizient. Demzufolge reichert sich SulfoXantPhos, abhängig von der Hydrophilie des Tensids, bevorzugt in der tensidreichen Phase an, wobei jedoch zusätzliche Effekte eine entscheidende Rolle spielen, die im nächsten Abschnitt diskutiert werden. Überraschend ist dabei der positive Wert des Mizelle/Wasser-Verteilungskoeffizienten, da der Oktanol/Wasser-Verteilungskoeffizient  $\log K_{OW}$  für SulfoXantPhos stark negativ war. Für Triton X-114 ist exemplarisch gezeigt, dass die gewählte Methode für die Bestimmung des Verteilungskoeffizienten keine Rolle für das Ergebnis spielt, da sich die  $\log K_{MW}$ -Werte innerhalb der Messgenauigkeit decken. Zusätzlich wurde der Einfluss eines ionischen Tensids (SDS) auf den Verteilungskoeffizienten von TPP untersucht. Im Vergleich zu den anderen Tensiden erhält man hier einen ähnlichen Verteilungskoeffizienten wie für TX-114. Da TPP keine Ladung trägt, kann nur eine Wechselwirkung mit dem hydrophoben Mizellkern des SDS erfolgen und nicht zusätzlich mit den ionischen Kopfgruppen. Jedoch kann es zu attraktiven Wechselwirkungen kommen, wenn das Substrat ebenfalls Ladungen trägt.

Aus der Wasseraufbereitung mittels mizellgestützter Ultrafiltration (MEUF) ist bekannt, dass sich Metallionen an die negativen Kopfgruppen von anionischen Tensiden anbinden, wodurch aufgrund der vorliegenden Komplexbildung der Verteilungskoeffizient zugunsten der Mizelle verschoben wird. Dadurch können die Metallionen leicht abgetrennt werden [10,11]. Dasselbe Prinzip gilt auch für gelöste Anionen und kationische Tenside. So wurde in früheren Arbeiten zur Hydroformulierung von Olefinen in Gegenwart des kationischen Tensids Cetyltrimethylammoniumbromid (CTAB) unter Verwendung des hydrophilen Liganden TPPTS oft höhere Aktivitäten beobachtet, die sich neben einer höheren Eduktkonzentration im Mizellkern auch durch einen höheren Verteilungskoeffizienten von TPPTS erklären lassen; auch wenn dieser nie bestimmt wurde [12].

#### 4.2.2 Ligandeneinfluss

Während in Abschn. 4.2.1 gezeigt wurde, dass sich durch die Auswahl des Tensids Einfluss auf die Verteilung des Liganden nehmen lässt, wird nun der Einfluss des Liganden selbst diskutiert. Für die beiden nicht-ionischen Tenside TX-100 und TX-114 sind die Verteilungskoeffizienten der untersuchten Liganden in Abb. 5 gezeigt.

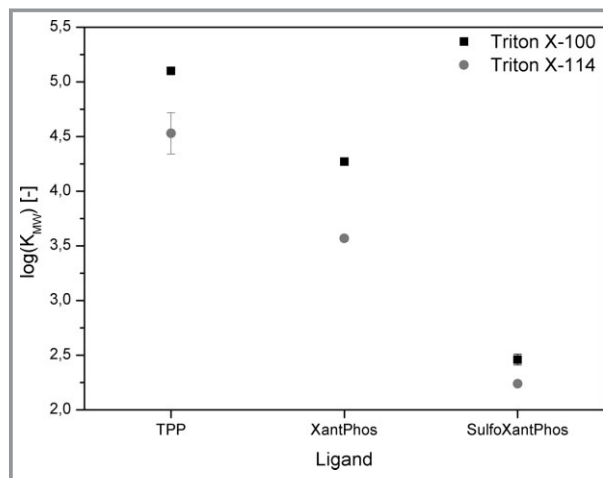


**Abbildung 5.** Verteilungskoeffizienten von TPP, XantPhos und SulfoXantPhos in mizellaren, wässrigen Lösungen mit Triton X-100 und Triton X-114, bestimmt mittels ESM.

Wie schon zuvor diskutiert, ist bei allen Liganden ein kleinerer Verteilungskoeffizient bei Triton X-114 zu beobachten. Überraschend ist, dass der Verteilungskoeffizient von XantPhos im Vergleich zu TPP kleiner ist, obwohl  $K_{OW}$  für XantPhos deutlich über den von TPP liegt. Weiterhin ist interessant, dass für das wasserlösliche SulfoXantPhos ein experimenteller Verteilungskoeffizient  $\log K_{MW}$  von ca. 2,4 ermittelt wurde. Dies bedeutet, dass SulfoXantPhos vorwiegend in oder an der Mizelle eingelagert ist, was in Kontrast zu den Ergebnissen für  $K_{OW}$  steht. Erwartungsgemäß hätte

auch für den Mizelle/Wasser-Verteilungskoeffizienten aufgrund der Polarität von SulfoXantPhos ein negativer Wert resultieren müssen. Jedoch scheinen hier zusätzliche Effekte eine entscheidende Rolle zu spielen. Da das Molekül SulfoXantPhos ähnlich wie ein Tensid über einen hydrophoben und hydrophilen Teil verfügt, ist anzunehmen, dass SulfoXantPhos eine oberflächenaktive Substanz ist, die somit als Tensid fungieren kann. Demnach lagert sich SulfoXantPhos, bedingt durch dessen Oberflächenaktivität, an der Mizelle an und es ergibt sich ein vergleichsweise hoher Mizelle/Wasser-Verteilungskoeffizient. Dies wird auch durch die Messung der Oberflächenspannung von wässrigen Lösungen der Liganden bestätigt. Die sulfonierten Liganden SulfoXantPhos und TPPTS zeigen beide oberhalb einer Konzentration von  $1 \cdot 10^{-4} \text{ mol L}^{-1}$  einen Abfall der Oberflächenspannung (Abb. 6). Dies erklärt den großen Mizelle/Wasser-Verteilungskoeffizienten von SulfoXantPhos.

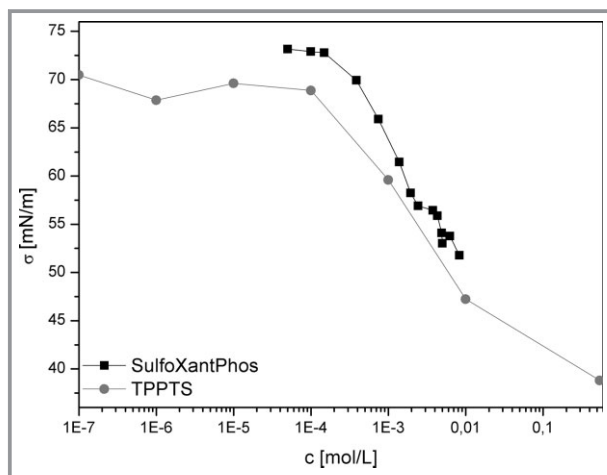


**Abbildung 6.** Oberflächenspannung  $\sigma$  von wässrigen TPPTS- und SulfoXantPhos-Lösungen in Abhängigkeit der Konzentration.

### 4.3 Verteilung des Katalysatorkomplexes in einem Mikroemulsionssystem

Die Wechselwirkungen zwischen verschiedenen Liganden und den Komponenten eines mizellaren Lösungsmittelsystems sind nun weitestgehend bekannt. Jedoch erhöht sich die Komplexität des Lösungsmittelsystems, wenn ein hydrophobes Lösungsmittel hinzukommt und eine Mikroemulsion gebildet wird. In Abb. 7 sind schematisch die Verteilungsgleichgewichte eines homogenen Katalysatorkomplexes zwischen den einzelnen Phasen eines Mikroemulsionssystems im Dreiphasengebiet aufgezeigt. Es wird angenommen, dass die Verteilung des Katalysatorkomplexes vorwiegend durch die Eigenschaften der Liganden bestimmt wird.

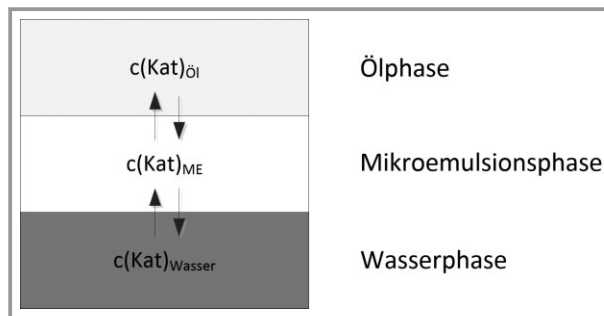


**Abbildung 7.** Schematische Darstellung des Verteilungsgleichgewichtes eines Katalysators in einer Mikroemulsion.

Durch die zusätzliche Ölkomponente spielt nicht nur die Verteilung des Katalysators zwischen der wässrigen und tensidreichen Phase, sondern auch die Verteilung zwischen der tensidreichen und öligen Phase eine Rolle. Für eine quantitative Abtrennung der teuren homogenen Katalysatoren ist es somit essentiell, die Verteilungsgleichgewichte zu kennen bzw. vorhersagen zu können. In Abb. 8 ist die Verteilung des Rhodium-Katalysators für die Liganden XantPhos und SulfoXantPhos in einem Mikroemulsionssystem dargestellt. Als Tensid wurde Marlipal 24/70 verwendet.

Es ist deutlich zu erkennen, dass die Hydrophilie und Grenzflächenaktivität des Liganden entscheidend für die Verteilung des Katalysatorkomplexes ist. Für den hydrophoben Liganden XantPhos ist der Katalysatorkomplex zu 74 % in der Ölphase enthalten, was auch optisch durch die intensive Rotfärbung der Ölphase ersichtlich ist. Der restliche Anteil befindet sich in der tensidreichen Mittelphase, die selbst ca. 1/4 der organischen Phase enthält. Interessant ist, dass für den wasserlöslichen Katalysatorkomplex mit SulfoXantPhos eine klare wässrige Phase vorhanden ist und sich der Großteil (96,3 %) des Katalysatorkomplexes in der tensidreichen Mittelphase anreichert. Dies ist, belegt durch die Mizelle/Wasser-Verteilungskoeffizienten  $K_{MW}$  von SulfoXantPhos, auf die attraktiven Wechselwirkungen und die Grenzflächenaktivität des Liganden mit dem Tensid zurückzuführen, wodurch der gesamte Katalysatorkomplex in die

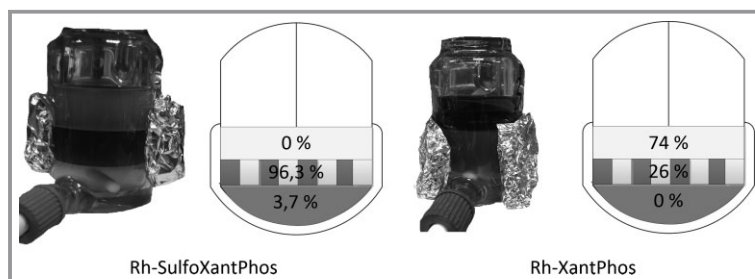


**Abbildung 8.** Verteilung des Rhodium-Katalysators bei Verwendung von SulfoXantPhos (links) und XantPhos (rechts) mit dem Tensid Marlipal 24/70 und 1-Dodecan als Lösungsmittel ( $m_{\text{Wasser}} = m_{1\text{-Dodecan}} = 20 \text{ g}$ ,  $m_{\text{Marlipal 24/70}} = 3,47 \text{ g}$ , 1 Gew.-% Natriumsulfat,  $n_{\text{Rh(acac)(CO)}_2} = 0,05 \text{ mmol}$ ,  $n_{\text{Ligand}} = 5 \text{ eq.}$ ).

tensidreiche Mittelphase eingelagert wird. Somit können die Mizelle/Wasser-Verteilungskoeffizienten genutzt werden, um erste Hinweise über die Verteilung von Katalysatorkomplexen in einem Mikroemulsionssystem zu erhalten.

Die Ergebnisse für die Anreicherung des Rh/SulfoXanthphos-Komplexes in der tensidreichen Phase lassen sich auch auf einen kontinuierlichen Versuch in einer Miniplant übertragen, in der 1-Dodecen zu Tridecanal in einem Mikroemulsionssystem bestehend aus 1-Dodecen, Wasser und Marlupal 24/70 hydroformuliert wurde. Die Phasentrennung des Reaktionsgemisches wurde bei der kontinuierlichen Prozessführung von ca. 200 h in einem Dekanter realisiert. Dabei separierte das Reaktionsgemisch in eine Produktphase, die abgeführt wurde, und eine katalysatorreiche Phase, die zurück in den Reaktor geführt wurde. Über 99,99 % des Katalysators blieben in der Katalysatorphase im aktiven Zustand erhalten [13]. Die gute Trennung und hohe Rückführrate bestätigen die Vorhersagen zur Katalysatorverteilung auf der Grundlage der Verteilung des Liganden.

## 5 Zusammenfassung

Für Flüssig/flüssig-Zweiphasenreaktionen bieten sich tensidmodifizierte Reaktionsmedien an, da diese nicht nur zu wirtschaftlich sinnvollen Reaktionsgeschwindigkeiten führen, sondern es auch ermöglichen, homogene Katalysatoren vom Produkt abzutrennen und nochmals zu verwenden. Ein entscheidender Faktor für die quantitative Abtrennung des Katalysators ist die Wahl eines geeigneten Liganden und die Art des verwendeten Tensids. Es konnte gezeigt werden, dass die Struktur und Art des Tensids nur einen geringen Einfluss auf den Verteilungskoeffizienten von nichtionischen Liganden in einem mizellaren Reaktionssystem hat. Ausschlaggebenden Einfluss auf den Verteilungskoeffizienten in mizellaren Systemen hat nicht nur wie erwartet die Hydrophobizität der Liganden, sondern auch deren Grenzflächenaktivität. Für grenzflächenaktive sulfonierte Phosphinliganden konnte gezeigt werden, dass sich diese an die Tensidphase anlagern, wodurch ein unerwartet hoher Mizelle/Wasser-Verteilungskoeffizient resultiert.

Diese Arbeiten sind Teil des von der TU Berlin koordinierten Sonderforschungsbereichs/Transregio 63 „Integrierte chemische Prozesse in flüssigen Mehrphasensystemen“. Die Autoren bedanken sich bei der DFG für die finanzielle Unterstützung des Projektes (TRR63).

## Formelzeichen

$c_{\text{O}}^i$	[mol L <sup>-1</sup> ]	Konzentration des Substrats <i>i</i> in der Oktanolphase
$c_{\text{W}}^i$	[mol L <sup>-1</sup> ]	Konzentration des Substrats <i>i</i> in der Wasserphase
cmc	[mol L <sup>-1</sup> ]	kritische Mizellbildungskonzentration
$K_{\text{OW}}$	[-]	Verteilungskoeffizient Oktanol-Wasser, berechnet aus den Molenbrüchen
$K_{\text{MW}}$	[-]	Verteilungskoeffizient Mizelle-Wasser
<i>m</i>	[kg]	Masse
<i>n</i>	[mol]	Stoffmenge
$P_{\text{OW}}$	[-]	Verteilungskoeffizient Oktanol-Wasser, berechnet aus den Konzentrationen
$S_{\text{M}}$	[mol L <sup>-1</sup> ]	Löslichkeit des Substrats in der mizellaren Lösung
$S_{\text{W}}$	[mol L <sup>-1</sup> ]	Löslichkeit des Substrats in Wasser
$V_{\text{W}}$	[m <sup>3</sup> mol <sup>-1</sup> ]	molares Volumen von Wasser
$x_{\text{M}}^i$	[-]	Molenbruch des Substrats <i>i</i> in der mizellaren Phase
$x_{\text{W}}^i$	[-]	Molenbruch des Substrats <i>i</i> in der Wasserphase
$\nu_{\text{O}}$	[m <sup>3</sup> mol <sup>-1</sup> ]	molares Volumen der Oktanolphase
$\nu_{\text{W}}$	[m <sup>3</sup> mol <sup>-1</sup> ]	molares Volumen der Wasserphase
$\sigma$	[mN m <sup>-1</sup> ]	Oberflächenspannung

## Abkürzungen

BDG	2-(2-Butoxyethoxy)ethanol
COSMO-RS	conductor-like screening model for real solvents
CPE	Trübungspunkt-Extraktion
CTAB	Cetyltrimethylammoniumbromid
ESM	erhöhte Löslichkeitsmethode
HLB	hydrophilic-lipophilic balance
ICP-OES	Optische Emissionsspektrometrie mit induktiv gekoppeltem Plasma
ME	Mikroemulsion
MEUF	micellar enhanced ultrafiltration
OECD	Organisation for Economic Cooperation and Development
SDS	Natriumdodecylsulfat
TPP	Triphenylphosphin
TPPTS	Tri-(natrium-meta-sulfonatophenyl)-phosphan
XantPhos	4,5-Bis(diphenylphosphino)-9,9-dimethylxanthene

## Literatur

- [1] J. Sangster, *J. Phys. Chem. Ref. Data* **1989**, *18* (3), 1111 – 1229. DOI: 10.1063/1.555833
- [2] J. Dallos, A. Liszi, *J. Chem. Thermodyn.* **1995**, *27* (4), 447 – 448.
- [3] M. Schwarze, I. Volovych, S. Wille, L. Mokrushina, W. Arlt, R. Schomäcker, *Ind. Eng. Chem. Res.* **2011**, *51* (4), 1846 – 1852. DOI: 10.1021/ie2006565
- [4] K. Hanna, R. Denoyel, I. Beurroies, J. P. Dubès, *Colloids Surf., A* **2005**, *254* (1 – 3), 231 – 239. DOI: 10.1016/j.colsurfa.2004.12.016
- [5] T. Mehling, T. Ingram, I. Smirnova, *Langmuir* **2011**, *28*, 118 – 124. DOI: 10.1021/la2028274
- [6] *Flame Retardants* (Eds: P. M. Visakh, Y. Arao), Springer International Publishing, Cham **2015**.
- [7] N. Chen, Y. Zhang, S. Terabe, T. Nakagawa, *J. Chromatogr. A* **1994**, *678*, 327 – 332. DOI: 10.1016/0021-9673(94)80480-X
- [8] R. Collander, *Acta Physiol. Scand.* **1947**, *13* (4), 363 – 381.
- [9] S. Wille, L. Mokrushina, M. Schwarze, I. Smirnova, R. Schomäcker, W. Arlt, *Chem. Eng. Technol.* **2011**, *34* (11), 1899 – 1908. DOI: 10.1002/ceat.201100359
- [10] M. Schwarze et al., *J. Membr. Sci.* **2015**, *478*, 140 – 147. DOI: 10.1016/j.memsci.2015.01.010
- [11] M. Schwarze, L. Chiappisi, S. Prévost, M. Gradzielski, *J. Colloid Interface Sci.* **2014**, *421*, 184 – 190. DOI: 10.1016/j.jcis.2014.01.037
- [12] P. Baricelli et al., *Appl. Catal., A* **2015**, *490*, 163 – 169. DOI: 10.1016/j.apcata.2014.11.028
- [13] D. Müller, E. Esche, T. Pogrzeba, T. Hamerla, T. Barz, R. Schomäcker, G. Wozny, in *20th Int. Conf. of Process Engineering and Chemical Plant Design* (Eds: M. Kraume, G. Wehinger), Copy Print, Berlin **2014**.



# PAPER 3

## **Hydroformylation in microemulsions: Proof of concept in a miniplant**

Markus Illner and David Müller, Erik Esche, Tobias Pogrzeba, Marcel Schmidt, Reinhard Schomäcker, Günter Wozny, Jens-Uwe Repke

Industrial & Engineering Chemistry Research, 2016, 55, 8616-8626

Online Article:

<https://pubs.acs.org/doi/abs/10.1021/acs.iecr.6b00547>

Reproduced (or 'Reproduced in part') with permission from “Hydroformylation in Microemulsions: Proof of Concept in a Miniplant; Markus Illner, David Müller, Erik Esche, Tobias Pogrzeba, Marcel Schmidt, Reinhard Schomäcker, and Jens-Uwe Repke. Industrial & Engineering Chemistry Research, 2016, 55, 8616-8626.” Copyright (2016) American Chemical Society.





catalyst are lost via the product phase, no side reactions are observed in subsequent distillation steps. However, a major drawback of the process lies in its limitation to short-chain alkenes. Since alkenes longer than hexene have a limited solubility in the aqueous phase, which results in a severe decrease of reactivity, they are inadequate for the RCH/RP process.<sup>11</sup> For longer-chain alkenes Börner et al.<sup>5</sup> report that the conversion is carried out in single phase reactions at severe process conditions (up to 300 bar and 200 °C), using mainly cobalt catalysts. Modifying the catalysts with phosphines, these process conditions can be lowered significantly. Nevertheless, these processes suffer from lower selectivities toward the desired aldehydes and thus a rather costly product separation. Consequently, switching the feedstock toward long-chain alkenes remains challenging for the chemical industry to date.

To overcome this hurdle, a novel process concept is currently under investigation within the Collaborative Research Center InPROMPT/TRR 63 and presented in this contribution. Therein, a surfactant is added to the system, to enhance the miscibility between the long-chain alkene and an aqueous catalyst solution leading to the formation of a microemulsion. A highly hydrophilic ligand-modified rhodium catalyst is used to achieve high selectivities at mild process conditions.<sup>2</sup>

To carry out the hydroformylation reaction, the catalyst needs to be activated. This is done by introducing synthesis gas into the system. Carbon monoxide transforms the catalyst into its active species.<sup>12</sup> With carbon monoxide and hydrogen as reactants present, the formation of aldehydes starts immediately. After the reaction step, the mixture is led into a phase separation unit, within which the thermomorphic behavior of the micellar system can be exploited to separate and recycle the catalyst from the oily product. The process concept can thus be summarized as a mixer–settler concept shown in Figure 2.

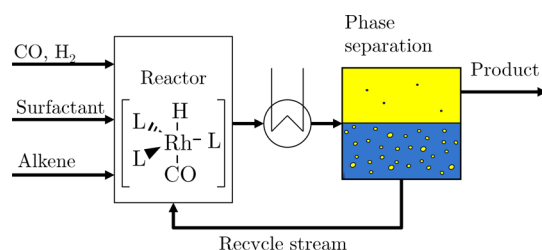


**Figure 2.** Process concept for the hydroformylation of long-chain alkenes in microemulsions.<sup>13</sup>

In order to investigate this novel concept at a larger scale, a miniplant has been designed, constructed, and operated at Technische Universität Berlin (TU Berlin). Therein, the hydroformylation of 1-dodecene as a model, biobased olefin using a nonionic surfactant is carried out.

The aim of this contribution is to present the results from long-term miniplant operation and to discuss the applicability of such a process concept. Keeping an eye on economic viability and sustainability, the presented results are analyzed regarding specific targets:

- long-term stable application of ligand-modified rhodium-based catalysts for high reaction activity and normal:iso selectivity
- realization of a homogeneous catalysis at mild reaction conditions (low pressures and low temperatures)

- adequate separation of the catalyst complex from the product phase after the reaction

Additionally, special attention is given to challenges which have arisen during the implementation of this concept as well as strategies to overcome these challenges.

## 2. BACKGROUND INFORMATION

The following sections discuss the state of the art of microemulsions as reaction media and their capabilities for catalyst recovery. Consequently, characteristics of oil–water–surfactant systems and phenomena exploited to achieve the desired process steps are highlighted.

### 2.1. State of the Art and Preliminary Investigations.

To date, various applications of surfactant containing reaction systems have been reported. Among them, several organic applications such as reduction, oxidation, and coupling reactions at C=C bonds can be found.<sup>14,15</sup> For long-chain alkenes of chain lengths up to C<sub>16</sub>, a feasible application of homogeneously catalyzed hydroformylation using micellar reaction media was presented by Van Vyve and Renken in 1999<sup>16</sup> for alkenes. Also, Li et al.<sup>17</sup> reported increased selectivities and higher reaction yields for the conversion of 1-dodecene in biphasic mixed micelle systems, depending on the surfactant composition and micellar state. The direct influence of surfactants on the reaction performance was the main focus of the studies of Haumann et al. in 2002.<sup>10</sup> They reported the hydroformylation of 1-dodecene in microemulsions using water-soluble ligands. Compared to those, biphasic water–oil systems showed no significant conversion of long-chain alkenes to aldehydes. The addition of a surfactant, however, enables the reaction. The main challenge lies in determining an appropriate surfactant. The surfactant selection is crucial for both the reaction performance and the subsequent product separation.<sup>18</sup> The thermomorphic behavior of micellar systems (see section 2.2) and therefore also the distribution of the catalyst between all formed phases strongly depend on the surfactant's properties.<sup>19</sup> Furthermore, high reaction rates, clear phase separation, and catalyst recovery also have to be realized as continuous operations in a technical system to estimate economic viability. Regarding the process concept in Figure 2, no continuous operation on a miniplant or any comparable scale was reported until now.

**2.2. General Phase Separation Characteristics of Oil–Water–Surfactant Systems.** The addition of sufficient amounts of surfactant to an oil and water mixture leads to the formation of a microemulsion. From a macroscopic point of view a microemulsion can be regarded as homogeneous. On a microscopic scale it is heterogeneous with coexisting, nanometer-thin hydrophobic and hydrophilic layers.<sup>20,21</sup> For the application here, a microemulsion can be used in two ways. It acts as a tunable solvent, which on the one hand increases the interfacial area during the reaction, and on the other hand changes its phase separation behavior dependent on temperature.<sup>22</sup> Thus, the reaction can be carried out in a homogeneous mixture followed by a fast and pure phase separation in a settler.<sup>23</sup> However, for this purpose the phase separation characteristics of oil–water–surfactant systems must be well understood.<sup>24</sup>

The phase separation characteristics of a microemulsion system formed with nonionic surfactants can be described by Kahlweit's fish diagram. The diagram is created by slicing Gibbs' phase prism of an oil–water–surfactant system at an oil

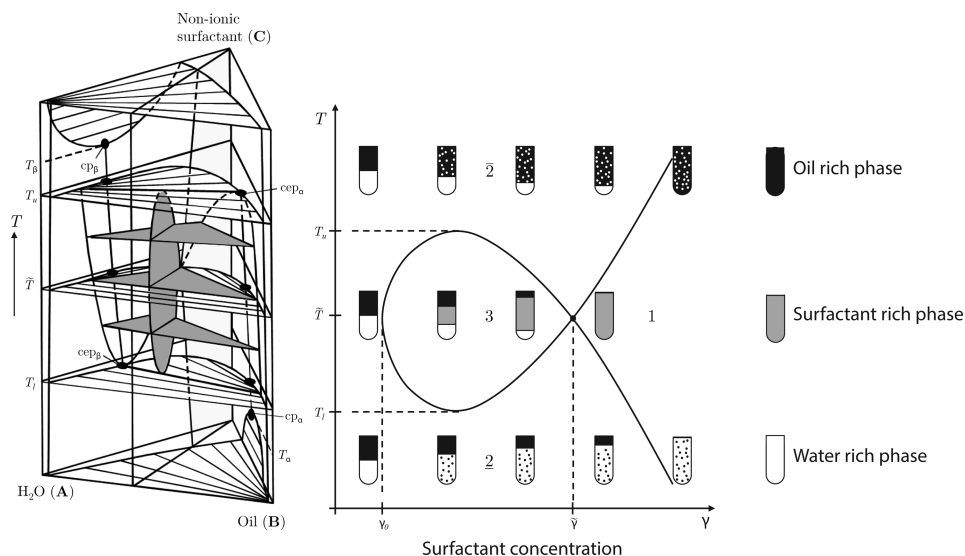


**Figure 3.** Gibbs' phase prism of oil–water–surfactant mixtures at different temperatures (left) and Kahlweit's fish (right). The figures are based on and partially redrawn in accordance with the original images presented in ref 25.

to water ratio of 1:1. Thus, the various phase states at different temperatures and surfactant concentrations become visible. Figure 3 shows a qualitative sketch of Gibbs' phase prism for an arbitrary oil–water–surfactant system and Kahlweit's fish therein.

A closer look at Kahlweit's fish reveals several distinct phase states. The fish's body (micellar system) is established in case a sufficient amount of surfactant is present (greater than the critical micellar concentration,  $\gamma_0$ ). A two-phase regime (2) is created at low surfactant concentrations and low temperatures. This is governed by a water and surfactant rich emulsions phase at the bottom and an oily excess phase on top. As mentioned by Müller et al., "the surfactant is mainly dissolved in the water-rich phase due to its higher solubility there at lower temperatures. Hence, an oil-in-water (o/w) microemulsion is formed. This regime can be desired for the product separation step of a mixer–settler process as a pure product phase can be removed while recycling the surfactant and water (aqueous catalyst solution)."<sup>26</sup> By increasing the temperature, a three-phase region (3) is established in which the bulk of the surfactant is located in a middle phase. In coexistence with this middle phase an oil-rich top phase and a water-rich bottom phase appear. Here, the catalyst is also mainly located in the middle phase, whereas the oily excess phase still remains free of catalyst.<sup>19</sup> Given its pure oil phase, this region is desirable for the separation step. Two more regions are shown in Figure 3. The first is the single-phase region on the right-hand side (fish's fin). Obviously this region may be suitable for the reaction, but inadequate for separation purposes. The second undesired region is the upper two-phase (2) region. There, the surfactant lies dissolved in the top phase. This may be problematic, because phase separation would lead to drastic surfactant and water loss with the product phase. The surfactant as well as the water (catalyst solution) trapped therein would have to be replenished and separated in additional separation steps from the product.<sup>19</sup>

Regarding the phase separation dynamics, microemulsion systems show a distinct reduction of the separation time in the three-phase region (3) compared to the two-phase regions (2, 2). Depending on the applied surfactant, the required time for achieving an equilibrium state increases by several orders of

magnitude on leaving this area.<sup>19</sup> Hence, for the construction of a decanter with reasonable residence time, solely the three-phase region is of interest. However, this causes two major challenges toward process design and control. First, the concentration dependent location of Kahlweit's fish needs to be intensively investigated for the considered component system in the miniplant. Second, the temperature only offers a small operational window regarding the temperature in the decanter. Using this information on the general phase separation characteristics, the miniplant, and the settler in particular, was constructed and operated. Here, an approach described by Müller et al.<sup>26</sup> was applied, to systematically tackle the unit design for such a multiphase system.

### 3. MATERIALS AND METHODS

At this point, the applied substances as well as the constructed miniplant are introduced. A miniplant operation schedule is presented to highlight applied operation strategies and discuss their influence on the system. Additionally, operational challenges and solution approaches are discussed.

**3.1. Materials.** The applied substances can be categorized into several groups: reactants, catalyst compounds, solubilizing substances, and products.

The first reactant is 1-dodecene (CAS Registry Number 112-41-4, purchased from VWR), a  $C_{12}$  alkene, which is used as an exemplary unsaturated, long-chain hydrocarbon. The second reactant is synthesis gas with a composition of 1:1 mol % CO:H<sub>2</sub> with a purity of 5.0 purchased from Linde.

The applied catalyst consists of a rhodium-based precursor [Rh(acac)(CO)<sub>2</sub>] (CAS Registry Number 14874-82-9), sponsored by Umicore, and the water-soluble ligand SulfoXantPhos (sulfonated form of XantPhos, CAS Registry Number 161265-03-8), purchased from MOLISA GmbH. Both precursor and ligand are dissolved in water.

The miscibility of 1-dodecene and the catalyst solution is enabled by the nonionic surfactant Marlipal 24/70 (CAS Registry Number 68439-50-9), sponsored by Sasol Germany GmbH. Additionally, Na<sub>2</sub>SO<sub>4</sub>, purchased from Th. Geyer, is added in small amounts as a separation enhancing additive.

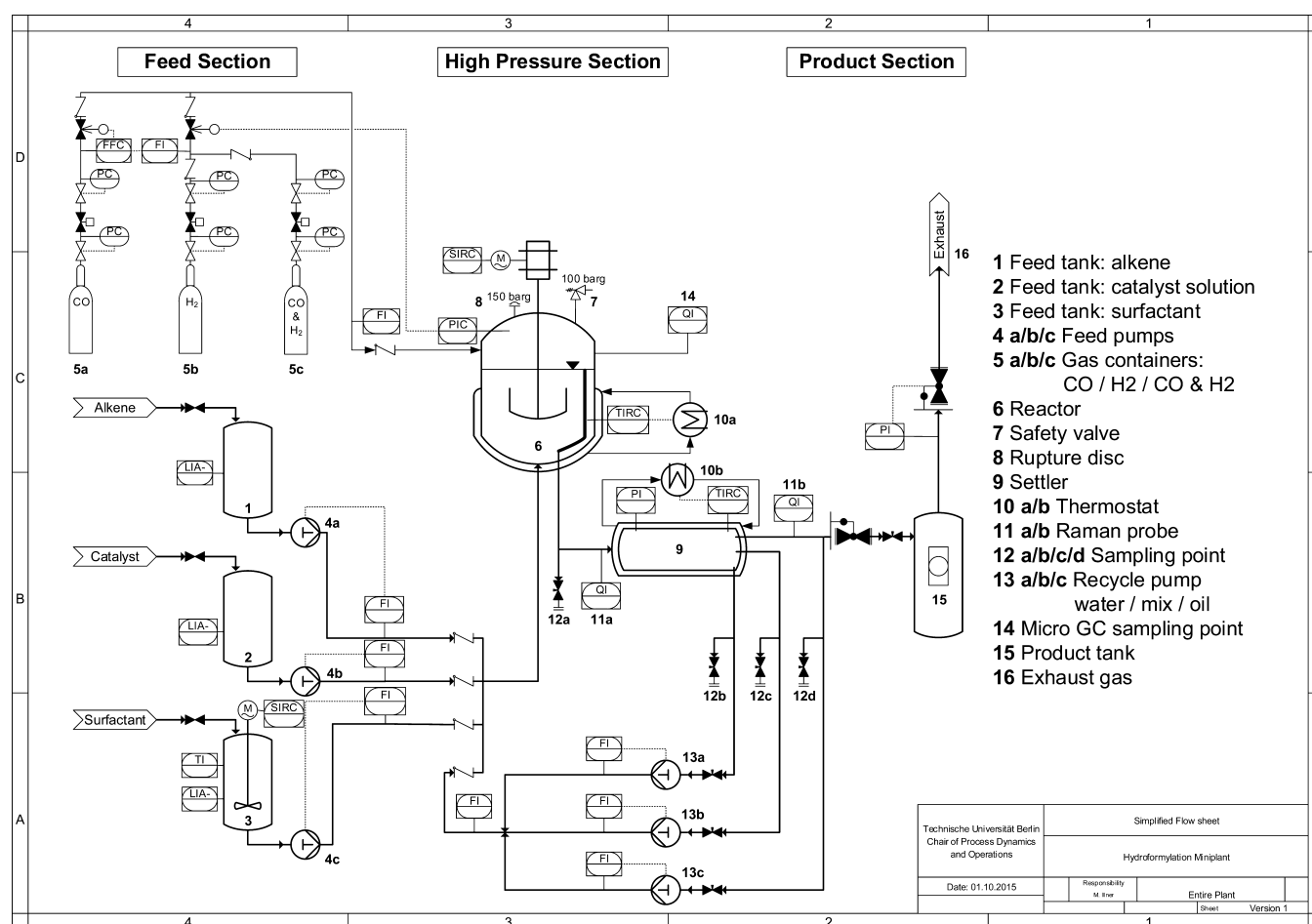


Figure 4. P&ID of the miniplant at TU Berlin.

For the initial mixture of the miniplant operation campaign mass fractions of roughly  $44.52 \times 10^{-2}$  g/g water,  $46.00 \times 10^{-2}$  g/g alkene, and  $8.00 \times 10^{-2}$  g/g surfactant were used. Additionally,  $1.00 \times 10^{-2}$  g/g  $\text{Na}_2\text{SO}_4$ ,  $0.03 \times 10^{-2}$  g/g precursor, and  $0.45 \times 10^{-2}$  g/g were applied.

### 3.2. Technical Realization: Miniplant at TU Berlin.

**3.2.1. Process Design.** A simplified piping and instrumentation diagram (P&ID) of the miniplant at TU Berlin is shown in Figure 4. As described by Müller,<sup>27</sup> the miniplant consists of three sections. The feed section contains the feed tanks and feed pumps for the liquid components 1-dodecene, catalyst solution, and surfactant.<sup>27</sup> Additionally, the feed section holds the gas bottles for synthesis gas, pure hydrogen, and pure carbon monoxide. The feeds of 1-dodecene (4a), catalyst solution (4b), and nonionic surfactant (4c) can be regulated to a maximum values of 840, 400, and 200 g/h, respectively.

The lower part of Figure 5 shows a three-dimensional (3-D) image created with Solid Edge and a photo of the feed section with the tanks and pumps for the liquids.

The mixer-settler section consists of a reactor and a decanter. The reactor has a maximum volume of 1500 mL. The liquid mixture is stirred with a gassing stirrer featuring a Rushton turbine with a maximum speed of 2880 rpm. Within the reactor, baffles are installed to avoid vortex formation and a drain is positioned at roughly 70% height to guarantee a constant liquid level. The second unit, the decanter or settler, consists of several modules with three separate drains. These drains are located at the bottom (water phase), in the middle

(surfactant-rich middle phase), and at the top (oil phase). Each drain is connected to a separate pump (13a–c) so that each of the phases can be recycled differently back into the reactor with maximum flow rates of up to 1000 g/h. The bottom part of Figure 5 shows a 3-D image and a photo of the mixer-settler section. Figure 6 shows the custom-made settler. Two cylindrical gauge glasses enable the observation of the phase separation before and after passing through a knitted wire section in the middle of the settler. A detailed description of the settler and the knitted wire for enhancement of the phase separation can be found in the contribution by Müller et al.<sup>26</sup>

The third section, the product storage section, consists of a product container for the liquid components and a depressurization unit for the removal of synthesis gas from the system. To remove oxygen from the system before the reaction, a vacuum pump is installed above the depressurization unit.

**3.2.2. Automation and Analytics.** The miniplant is fully automated with SIEMENS PCS 7 allowing for the online monitoring of more than 50 sensors from the control room. From there, operators are also able to control the process with several actuators (pumps, control valves, magnetic valves).

Regarding the analytics, two offline gas chromatographs (Agilent HP-5 column with an FID analyzer) are employed for an accurate hourly composition analysis. Second, an offline inductively coupled plasma optical emission spectrometer (ICP-OES; Varian ICP-OES 715 ES) is used to estimate the rhodium amount in the product phase. The sample positions of the liquids are located at the top, middle, and bottom drains of

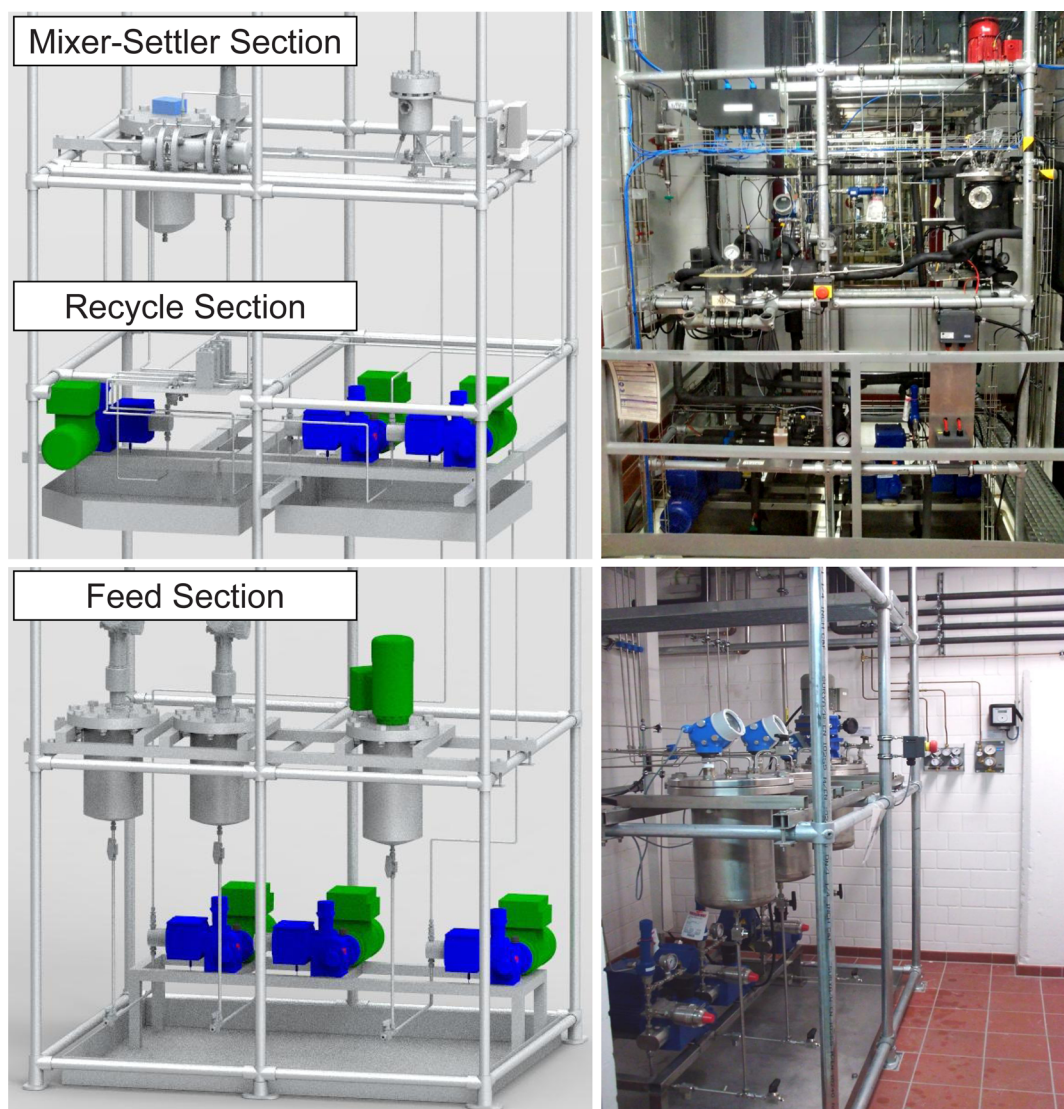


**Figure 5.** (top) Three-dimensional image (left) and photo (right) of the mixer–settler and recycle section. (bottom) Three-dimensional image (left) and photo (right) of the feed section of the miniplant at TU Berlin.<sup>27</sup>

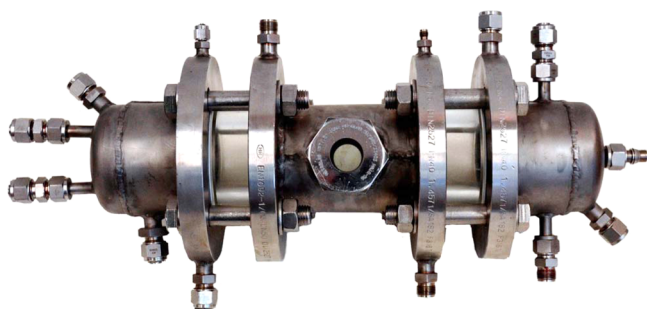


**Figure 6.** Self-constructed decanter/settler installed in the miniplant. The depicted setup contains a gauge glass, a knitted fabric from Rhodius GmbH (inside, not visible), and two cylindrical sight glasses.<sup>26</sup> The center piece with the small gauge glass is one of several modules. The settler length and volume can thus be increased by attaching additional modules in the middle.

the settler and of the reactor (see 12a–d in Figure 4). The gas composition is measured online with a micro gas chromatograph (micro-GC; molecular sieve 5 Å column). Additionally, an online Raman spectrometer (Kaiser Optical Systems RXN1,

NIR probe) has been installed for a fast analysis of the liquids entering the settler.

**3.2.3. Safety Concept.** Finally, it must be mentioned that considerable efforts have been made to guarantee a safe operation of the miniplant. The surrounding area of the plant is classified as an “explosion zone II” seeing that hazardous and explosive components are used during the reaction which may leak into the surroundings. Therefore, an extensive HAZOP analysis has been carried out during which technical and operative countermeasures to potential hazards were defined.

Following the concept of multiple layers of protection described by Seborg et al.<sup>28</sup> and based on the proceedings of the American Institute of Chemical Engineers from 1993,<sup>29</sup> these countermeasures are systematically applied. At the process design layer, all units are constructed or bought according to the regulations for an explosion zone II and according to the regulations for the temperature classes for 1-dodecene and synthesis gas. The necessary auxiliary equipment, such as thermostats, the offline gas chromatographs, online Raman spectrometers, gas feeds, and control cabinet of the process control system, not designated for an “explosion zone

Table 1. Simplified Miniplant Operation Schedule with Applied Process Parameters for Several Operation Modes (Cases 1–4)

	case 1	case 2	case 3	case 4
operation hours [h]	0–80	80–92	92–108	108–150
operation mode	continuous	full recycle	continuous	continuous
residence time reactor [h]	0.50	3.18	2.80	2.80
residence time settler [h]	0.58	3.53	3.15	3.15
recycle rate [g/h]	1500	250	250	250
recycle ratio (oil:mix:water)	0.19:0.57:0.24	0.40:0.20:0.40	0.40:0.28:0.32	0.24:0.52:0.24
feed rate dodecene [g/h]	100	0	30	30
gas supply	synthesis gas	synthesis gas	synthesis gas	synthesis gas

II", are located outside of the miniplant's housing. Basic process control features allow for indication of alarms in case of sensor malfunction or violated process value limits. As a safety interlock, H<sub>2</sub> and CO concentrations are monitored with gas detectors on each floor. Additionally, critical process values, such as reactor pressure and temperature, are tracked with the process control system. In case of emergency, nitrogen is automatically flooded into the plant and simultaneously all liquid and other gas feeds are shut down. The physical protection layer is equipped with pressure relief valves, venting synthesis gas to the flare. To prevent the spread of a fire, the miniplant has been set up in a separate three-story high room. In case of an explosion, magnetic flaps open to the outside to prevent structural damage to the miniplant's housing. On top of that, a ventilation system is installed to prevent an accumulation of synthesis gas in the room, which guarantees a 10-fold air exchange per hour. For liquid leakage multiple collection basins are in place to contain hazardous components.

**3.3. Miniplant Operation Challenges.** Prior to the miniplant operation, a number of preliminary experiments and shorter miniplant operations were carried out,<sup>26,30</sup> which led to the identification of several challenges and methods to overcome them.

The first challenge was foaming in several sections of the miniplant, especially during the depressurization. The applied oil–water–surfactant system tends to foam whenever stronger degassing occurs. This undesirable effect has been described by several authors.<sup>8,31</sup> Foaming in general can cause problems, since mass and heat transfer is limited by foam itself. This issue can be avoided though by degassing more slowly or expansion into tanks with a large surface to volume ratio and an appropriate gas holdup. Additionally, it has been observed that certain oil–water–surfactant mixtures with a high water content tend to establish a foam that remains stable for a longer period of time. Therefore, a water concentration below a critical level of 35 wt % was ensured for all conducted plant operations and the original depressurization unit was replaced by a suitably larger one.

The second issue was an inseparable liquid mixture in the decanter after catalyst activation with synthesis gas.<sup>32,33</sup> The phase separation of the oil–water–surfactant system with catalyst present was investigated in multiple steps in the lab. Without synthesis gas, the separation takes place as desired. Once synthesis gas is added to the system, a separation can take multiple hours or even last indefinitely. A reason for this is the strong surface activity of the catalyst complex and changing electric charges of the molecule once CO is attached to it. We assume that the appearing surface activity of the catalyst complex is due to a change in geometry between the nonactivated and activated complex, which was recently discussed by Pogrzeba et al.<sup>34</sup> This stops micelles from

coalescing and thus hinders the phase separation. To counter this issue, the addition of small amounts of Na<sub>2</sub>SO<sub>4</sub> (same quantity as catalyst, 300 ppm) has proven to be successful. It was decided to introduce a larger mass fraction of Na<sub>2</sub>SO<sub>4</sub> of 1 wt % to ensure the countereffect at all times.

The third challenge was that, despite the presence of Na<sub>2</sub>SO<sub>4</sub> in the plant, the kinetics of the phase separation was too slow. Consequently, coalescence accelerators (knitted fabrics) were implemented in the settler. A more detailed discussion can be found in ref 26.

**3.4. Process Conditions and Operation Schedule.** The following section introduces a description of reaction conditions and modes of operation for the subsequent discussion of long-term miniplant results. The overall duration of the miniplant operation including start-up and shutdown was more than 200 h long. The plant was operated in a three-shift system with a team of overall 17 operators and lab assistants.

**3.4.1. Reaction.** According to lab-scale experiments, the reaction pressure was set to 15 bar gauge pressure, along with a constant reactor temperature of 95 °C.<sup>34,35</sup> The stirrer speed has been varied between 600 and 1500 rpm depending on the emulsion state. Within this range, it was guaranteed that the stirrer operates in gassing mode, thus ensuring sufficient dissolution of synthesis gas in the reaction mixture. The reaction conditions were not changed throughout the operation campaign. Thus, influences on the reaction rates were not related to temperature or pressure.

Several products were created during the reaction. The desired product was the linear aldehyde 1-tridecanal. Possible byproducts of the reaction mechanism are the isomers of tridecanal, the hydrogenated form of 1-dodecene (*n*-dodecane), and *cis/trans* isomers of 1-dodecene. A detailed description of the reaction network is given by Markert et al.<sup>36</sup>

To evaluate the reaction performance, the yield of the main product 1-tridecanal is defined as the ratio of the *n*-aldehyde mass fraction to the mass fraction of all reaction educts and products, i.e. the 1-tridecanal mass fraction divided by the mass fraction of all oily components. Given that 1-dodecene is the main reactant and all reaction products are formed from this component, the total mass fraction of all oily components corresponds to the theoretical mass of product.

$$Y_{1\text{-tridecanal}} = \frac{w_{1\text{-tridecanal}}}{w_{\text{oil}}}$$

**3.4.2. Modes of Operation.** The miniplant operation was divided into several operation modes, in order to influence the reaction by manipulating feed rate, product purge, and residence time. After inertization of the system with N<sub>2</sub>, alkene, catalyst solution, and surfactant were fed into the plant with feed streams set to meet the concentrations described in section 3.1. Subsequently, the plant was operated in full recycle mode

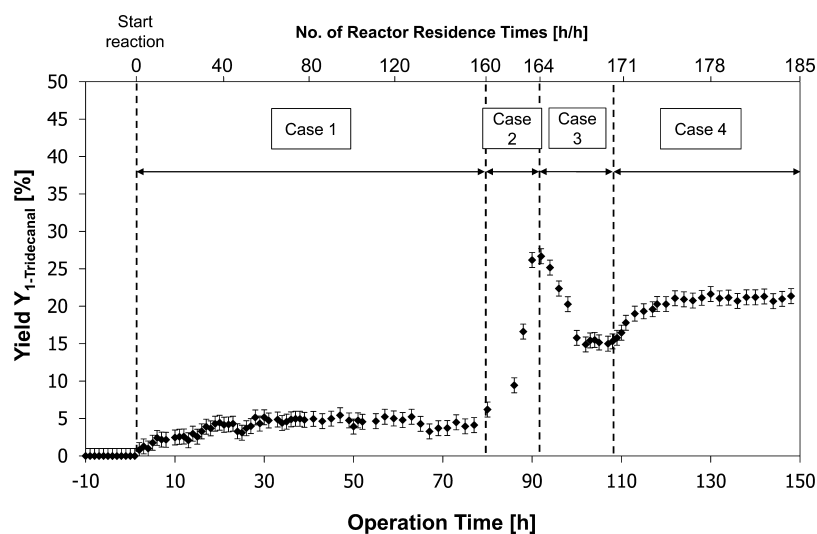


**Figure 7.** Miniplant operation results. Yield of 1-tridecanal in the reactor over time. Reactor residence times as ratio of operation time to the current residence time in the reactor are indicated to assess process stability.

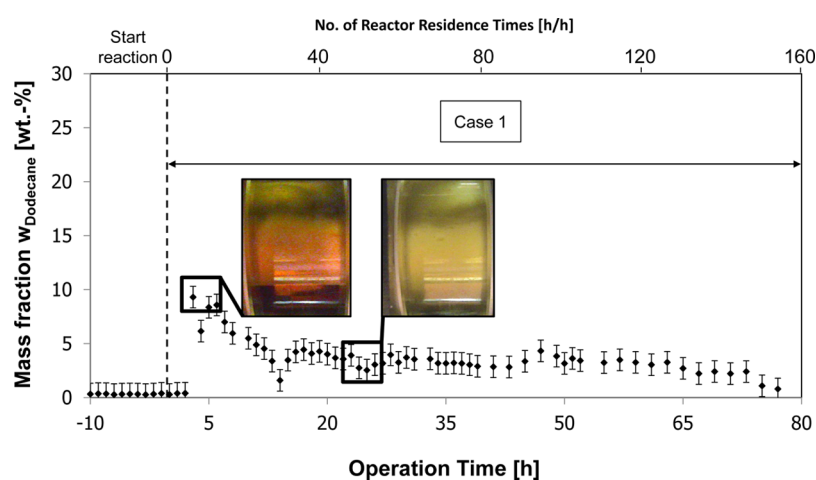


**Figure 8.** Miniplant operation results of case 1. Mass fraction of the hydrogenation byproduct *n*-dodecane. Settler's sight glass pictures given above indicate the activity of the catalyst (red, inactive; yellow, active).

without activation of the catalyst with synthesis gas. Therefore, no reaction took place. During this start-up phase, different settler residence times were implemented by manipulating the recycle stream rates with the aim of determining optimal phase separation conditions and to stabilize the process before initiating the reaction.

After this phase, the system was pressurized with synthesis gas. This defines the start of the actual operation (operation time = 0 h) for all further discussions. With stable phase separation and *n*-aldehyde yield being the main targets for the miniplant operation, different scenarios were performed within the operation schedule. Table 1 shows relevant process parameter sets for those scenarios (cases) allowing to relate changes in, e.g., residence times or recycle ratios to given results in the next section.

Case 1 represents a continuous operation mode with reaction, during which a low reactor residence time was chosen to demonstrate a stable aldehyde yield over a reasonable number of residence times. Based on the reactor's residence time of 0.5 h, a 1-tridecanal yield of 7% was expected from lab scale investigations.<sup>34,35</sup>

A full recycle operation in case 2 was used to increase the aldehyde yield in the reactor. In this mode, settler outlet streams were fed back into the reactor, with the alkene feed turned off. Synthesis gas though was fed into the system and partially purged to maintain the ideal ratio of CO to H<sub>2</sub>. The operation mode was changed from continuous to full recycle operation to shorten the time needed to achieve higher yields and thus also shorten the required length of the plant operation. Apart from the deactivated alkene feed, the yield increase was achieved with an increased reactor residence time.

Subsequently, a stable continuous operation with the aim of a higher yield compared to case 1 was established in case 3. Given the data in Table 1, a total recycle flow rate of 250 g/h was established, causing a reactor residence time of approximately 2.8 h in the reactor. This corresponds to a yield of 25%, which was expected according to lab experiments.

Case 4 investigated the influence of the ratio between the settler outlet streams—and thus the residence times of the corresponding phases inside the settler—on yield and process viability.

Note that reaction temperature and pressure were kept constant at 95 °C and 15 bar throughout all described cases.

**3.4.3. Disturbances.** In order to evaluate the recorded experimental data, unavoidable systematic or random disturbances and their impact on the process have to be considered.

Concentration measurements of reactants, products, and byproducts were carried out via offline gas chromatography implying manual sampling. Hence, the total liquid amount inside the plant was reduced each time and needed to be replenished systematically according to the extracted components. With three samples (reactor, oil phase, water phase) a total of 30 g was extracted every hour. This equals roughly 1.2% of the total liquid amount in the plant's high pressure section. Given the analysis result, the specific amounts of pure components were calculated. Hence, these component masses were re-fed to diminish the influence on the overall component concentrations inside the plant, especially the loss of catalyst.

## 4. RESULTS OF THE MINIPLANT OPERATION

In this section, long-term miniplant operation results are presented. Here, the two major aspects of the reaction and phase separation performance are evaluated and linked to the operation schedule.

**4.1. Reaction Performance and Product Yield.** The product yield is one of the main performance indicators of the reaction. Based on the GC results of the reactor samples (position 12a in the P&ID diagram in Figure 4), the 1-tridecanal yield for all operational modes is depicted in Figure 7.

Referring to operation time 0 h in Figure 8, an increase of the yield is visible, as this marks the start of the reaction. During a period of 20 h the yield increased to an average maximum value of 6.8% for the reaction mode of case 1. This value is consistent with preliminary lab experiments.<sup>35</sup> Temporary decreases in reaction yield were observable at operation hours 25 and 68. This was mainly caused by extended sampling for additional tests, whereas 1-dodecene was re-fed to maintain a constant amount of reaction mass. Overall, a stable yield over an uninterrupted period of more than 100 residence times was achieved for operation case 1. This generally highlights the catalyst stability as no decomposition and according reaction slowdown were observed. Therefore, unknown effects in the technical system (contaminants, side reactions), which are prone to trigger catalyst decomposition, were not observable.

As a next step, an operation mode with higher yield was desired to increase profitability. Here, a yield increase of 20 percentage points was achieved within 12 h (case 2). The reaction rate during that time frame is again in accordance with lab experiments.

Subsequently, the continuous operation was reestablished (case 3). Here, the 1-tridecanal yield declined drastically and evened out to a new steady-state point at a yield of 15%. However, for case 4 an immediate increase of 6 percentage points and stabilization of the 1-tridecanal yield was observed. Figure 7 depicts a continuous operation for operation hours 120–150. The extent of the yield increase is not solely explicable with perturbations given that the residence time was kept constant. In this case the increase was caused by a changed ratio between the recycle streams for oil, water, and surfactant. Referring to Table 1, the middle phase recycle stream, in which the majority of surfactant is located, was proportionally increased. The streams of oil and water phase recycle were at comparable levels for this part of the operation.

A higher recycle rate for the surfactant compared to the catalyst solution and oil phase could have caused surfactant concentration shifts or reduced surfactant accumulations in the settler. Thus, the surfactant concentration in the reactor could have increased. Linking yield and higher surfactant concentrations in the reactor, a positive effect of the surfactant concentration on the reaction yield is assumed.

**4.2. Byproduct Formation.** The reaction in Figure 1 represents a complex reaction network, which contains the formation of several byproducts.<sup>12,36</sup> One major side reaction is the hydrogenation of *n*-dodecene toward *n*-dodecane. Therefore, the formation of this component is shown exemplarily in Figure 8, to discuss the selectivity of the reaction.

On initiating the reaction, a significant formation of *n*-dodecane was observed with mass fractions of up to 10 wt %. For this initial period the dodecane yield actually exceeded the 1-tridecanal yield. Later, the amount of *n*-dodecane declined to values below 1 wt % as it was slowly purged from the process and was led into the product container (position 15 in Figure 4). It is assumed that the hydrogenation took place during the first hours of the operation and was then successfully suppressed by full catalyst activation. Supporting this hypothesis, photos showing the separated reaction medium in the settler are given in Figure 8. Preliminary lab scale investigations showed that the inactive catalyst (no synthesis gas in the system) shows a deep red color, while the activated form is bright yellow. Given that, it is assumed that the catalyst was not completely activated with synthesis gas during the first hours after the reaction initiation, since a red colored reaction medium was observed. A possible intermediate species of the catalytic cycle might be prone to support hydrogenation reactions.<sup>12</sup> With the applied low residence times for case 1, a sufficient activation was achieved in a short time frame.

The other byproducts of interest are all isomers of 1-tridecanal. In this contribution they are summarized as isotridecanal. Negligible to no amounts of isotridecanal were measured during the entire operation.

**4.3. Phase Separation.** The investigation of the phase separation behavior for the miniplant operation is the second main result of interest. As stated before, efficient recovery and recycle of the catalyst as well as product isolation are crucial for the shown process concept. Referring to Kahlweit's fish in Figure 3 and the subsequent discussion, this can be reached by maintaining a three-phase separation state. Figure 9 depicts this, marking the three relevant phases.

To evaluate the separation performance, Figure 10 depicts the total amount of oily components in the oil phase outlet of the settler. Here, the sum of mass fractions of all reaction educts and products is considered. The data was gathered from GC analysis of oil phase samples (position 12d in PI diagram Figure 4). Here, total oil mass fractions close to 1 mark an ideal phase separation with almost no catalyst solution or surfactant contained in the oily phase.

As an overall result, it can be stated that the phase separation was stable throughout all discussed operation modes (cases 1–4), in total, for an operation time of more than 150 h.

The optimal separation temperature for maintaining a three-phase system as depicted in Figure 9 is influenced by component concentrations in the system and changed flow rates, which can induce concentration shifts or accumulations. Therefore, control actions on the settler temperature had to be carried out accordingly to maintain a stable phase separation. For this, a prediction model for the optimal separation

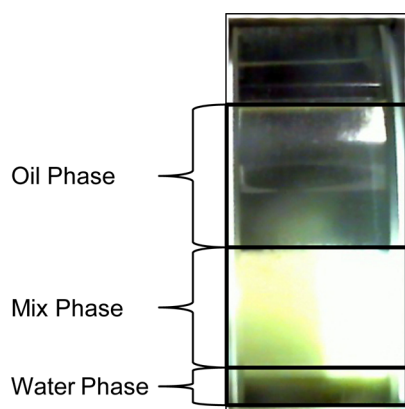


**Figure 9.** Photo of settler's sight glass with an ideal phase separation state. A surfactant rich phase is surrounded by a clear oily product phase and a catalyst containing water phase.

temperature, as described by Müller et al.,<sup>26</sup> was used. With this, a minimum oil content of 95 wt % could be achieved for all operational modes. Deviations from an ideal pure oil phase were caused by partial solubilization of surfactant in the oil phase and drastic changes in process operation conditions.

To this end, especially the change between batch and continuous operation caused highly dynamic disturbances, leading to a reduced separation quality (see start of case 1 in Figure 10, switching from case 1 to case 2 and switching from case 2 to case 3). Additionally, the necessary refeeding of surfactant and catalyst solution due to sample losses caused temporary perturbations at some operational points (see middle of case 1 and end of case 4). These dynamic concentration shifts impede tracking the optimal temperature for the phase separation and several control actions needed to be performed to regain an optimal separation state.

The separation behavior in dependence of the settler temperature showed the expected correlations. Referring to results obtained by Müller et al.,<sup>26</sup> increasing product concentrations lead to lower separation temperatures required to maintain a three-phase separation. The observation was verified throughout the campaign. Thus, the applicability of the prediction model was given.

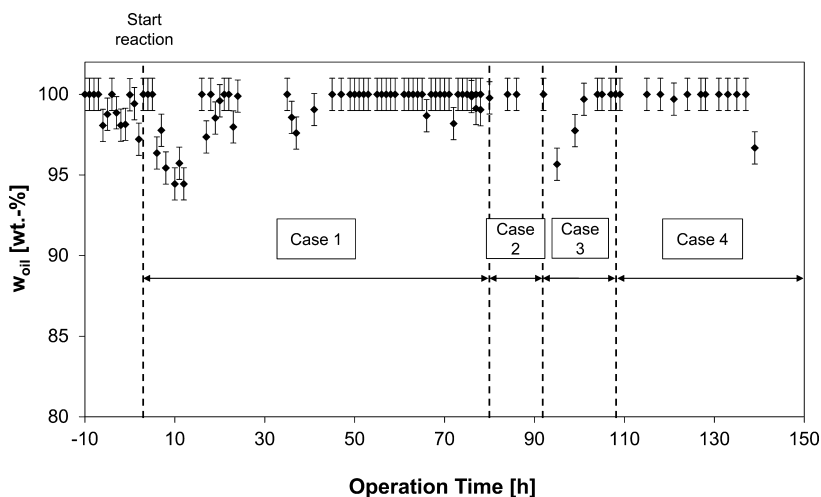


**Figure 10.** Miniplant operation. Phase separation quality depicted as the total amount of oily components in the oil phase of the settler. Results are given for the total time of operation.

Interestingly, the coalescence support with knitted wire fabrics led to overall excellent phase separation dynamics. This was observed with gauge glasses before and after the settler internals. The improved coalescence achieved with the knitted wire fabrics resulted in a successful separation, regardless of the emulsion's state at the settler inlet.

Concerning the rhodium loss, ICP-OES measurements confirmed results from previous miniplant operations. In case an almost pure oil phase was established, rhodium concentrations of around 0.1 ppm and below were observed. The rhodium concentrations in most of our samples lay below the detectability limit of the ICP-OES. This result is similar to lab-scale test tube results.

## 5. CONCLUSIONS AND OUTLOOK

With this contribution a long-term miniplant operation is presented for the hydroformylation of long-chain alkenes ( $C_{12}$  alkene) in micellar systems. Here, the applicability of a proposed process concept using a microemulsion system is demonstrated with a stable phase separation and an efficient catalyst recovery. Moreover, a stable product yield of 21% was achieved. The surfactant-supported reaction system enabled the hydroformylation of long-chain alkenes at mild reaction conditions (95 °C and 15 bar). Hence, this contribution presents the proof of concept for realizing a homogeneously catalyzed hydroformylation in microemulsions during a 200 h long miniplant operation.

However, some challenges still remain. Based on the results, it can be seen that there are critical process parameters which have a drastic influence on the performance of the plant and the dynamics of the system. Among these are the recycle ratio of the three streams in the settler and the accumulation of certain components, such as catalyst and surfactant, in the settler. Throughout the miniplant operation the latter led to reduced reaction rates as phase mediation and catalytic mass were reduced.

In terms of profitability, higher yields should be strived for. This is to be achieved by increasing the reactor residence time and simultaneously manipulating the recycle flows of the three phases. This effect outlines one field for future research. Additionally, the introduction of larger amounts of catalyst into the system, increasing the reactor pressure from 15 to 20 bar, or

raising the temperature are possible and planned options for future investigations. Moreover, the catalyst stability is to be proven in a long-term operation without sampling and hence, no replenishing.

Concluding, in this contribution it was successfully shown how surfactants can under realistic conditions be employed to enable homogeneous catalysis and simultaneously enable pure phase separation in a multiphase system. The authors hope to have inspired ideas and presented possible solutions for similar process concepts, in which comparable challenges of reactions followed by catalyst separation and product isolation are being tackled.

## AUTHOR INFORMATION

### Corresponding Authors

\*E-mail: [markus.illner@tu-berlin.de](mailto:markus.illner@tu-berlin.de).

\*E-mail: [david-nicolas.mueller@evonik.de](mailto:david-nicolas.mueller@evonik.de).

### Author Contributions

||Markus Illner and David Müller have contributed equally to this article and are both considered primary authors.

### Notes

The authors declare no competing financial interest.

## ACKNOWLEDGMENTS

This work is part of the Collaborative Research Center "Integrated Chemical Processes in Liquid Multiphase Systems" (Subproject B4) coordinated by the Technische Universität Berlin. Financial support by the German Research Foundation (Deutsche Forschungsgemeinschaft, DFG) is gratefully acknowledged (TRR 63). Furthermore, the authors gratefully acknowledge the support of Umicore N.V. for sponsoring the rhodium catalyst precursor "acetylacetonatodicarbonylrhodium(I) (CAS Registry Number 14874-82-9)", Sasol Ltd. for the surfactant used in the described experiments, the support of SIEMENS AG for sponsoring the entire process control system SIMATIC PCS7 for the automation of the miniplant, and Rhodius GmbH for sponsoring the knitted fabrics. Finally, the support of the Federal Institute for Materials Research and Testing (BAM) is gratefully acknowledged. A special thanks is given to Dr. Michael Maiwald and his team of the Federal Institute for Materials Research and Testing (BAM) for lending the Raman spectrometer for the miniplant campaign.

## REFERENCES

- (1) Kummer, R. *New Synthesis with Carbon Monoxide*. Herausgegeben von J. Falbe, Springer-Verlag, Berlin 1980. XIV, 465 S., Geb. DM 244.00. *Angew. Chem.* **1982**, *94*, 156.
- (2) Hamerla, T.; Rost, A.; Kasaka, Y.; Schomäcker, R. Hydroformylation of 1-Dodecene with Water-Soluble Rhodium Catalysts with Bidentate Ligands in Multiphase Systems. *ChemCatChem* **2013**, *5* (7), 1854.
- (3) Kohlpaintner, C. W.; Fischer, R. W.; Cornils, B. Aqueous Biphasic Catalysis: Ruhrchemie/Rhône-Poulenc Oxo Process. *Appl. Catal., A* **2001**, *221* (1–2), 219.
- (4) Wiese, K.-D.; Obst, D. Catalytic Carbonylation Reactions: Hydroformylation. In *Topics in Organometallic Chemistry*; Springer: Berlin, 2006; pp 1–33.
- (5) Franke, R.; Selent, D.; Börner, A. Applied Hydroformylation. *Chem. Rev.* **2012**, *112* (11), 5675.
- (6) Cornils, B.; Herrmann, W. a.; Rasch, M. Otto Roelen, Pioneer in Industrial Homogeneous Catalysis. *Angew. Chem., Int. Ed. Engl.* **1994**, *33*, 2144.
- (7) Kupka, J. *Hydroformylierung von 1-Octen in Mikroemulsion*. Ph.D. Dissertation, Technische Universität Braunschweig, 2006.

- (8) Miyagawa, C. C.; Kupka, J.; Schumpe, A. Rhodium-Catalyzed Hydroformylation of 1-Octene in Micro-Emulsions and Micellar Media. *J. Mol. Catal. A: Chem.* **2005**, *234* (1–2), 9.

- (9) Fell, B.; Papadogianakis, G. Rhodiumkatalysierte Mizellare Zweiphasenhydroformylierung von N-Tetradecen-1 Mit Grenzflächenaktiven Sulfobetainderivaten Des Tris(2-Pyridyl)phosphans Als Wasserlösliche Komplexliganden. *J. Mol. Catal.* **1991**, *66* (2), 143.

- (10) Haumann, M.; Koch, H.; Hugo, P.; Schomäcker, R. Hydroformylation of 1-Dodecene Using Rh-TPPTS in a Microemulsion. *Appl. Catal., A* **2002**, *225* (1–2), 239.

- (11) Wachsen, O.; Himmler, K.; Cornils, B. Aqueous Biphasic Catalysis: Where the Reaction Takes Place. *Catal. Today* **1998**, *42* (4), 373.

- (12) Kiedorf, G.; Hoang, D. M.; Müller, A.; Jörke, A.; Markert, J.; Arellano-Garcia, H.; Seidel-Morgenstern, A.; Hamel, C. Kinetics of 1-Dodecene Hydroformylation in a Thermomorphic Solvent System Using a Rhodium-Biphospho Catalyst. *Chem. Eng. Sci.* **2014**, *115*, 31.

- (13) Müller, M.; Kasaka, Y.; Müller, D.; Schomäcker, R.; Wozny, G. Process Design for the Separation of Three Liquid Phases for a Continuous Hydroformylation Process in a Miniplant Scale. *Ind. Eng. Chem. Res.* **2013**, *52* (22), 7259.

- (14) Dwars, T.; Paetzold, E.; Oehme, G. Reactions in Micellar Systems. *Angew. Chem., Int. Ed.* **2005**, *44* (44), 7174.

- (15) Yonehara, K.; Ohe, K.; Uemura, S. Highly Enantioselective Hydrogenation of Enamides and Itaconic Acid in Water in the Presence of Water-Soluble Rhodium(I) Catalyst and Sodium Dodecyl Sulfate. *J. Org. Chem.* **1999**, *64* (26), 9381.

- (16) Van Vyve, F.; Renken, A. Hydroformylation in Reverse Micellar Systems. *Catal. Today* **1999**, *48* (1–4), 237.

- (17) Li, M.; Li, Y.; Chen, H.; He, Y.; Li, X. Studies on 1-Dodecene Hydroformylation in Biphasic Catalytic System Containing Mixed Micelle. *J. Mol. Catal. A: Chem.* **2003**, *194* (1–2), 13.

- (18) Schwarze, M.; Pogrzeba, T.; Seifert, K.; Hamerla, T.; Schomäcker, R. Recent Developments in Hydrogenation and Hydroformylation in Surfactant Systems. *Catal. Today* **2015**, *247*, 55.

- (19) Pogrzeba, T.; Müller, D.; Illner, M.; Schmidt, M.; Kasaka, Y.; Weber, a.; Wozny, G.; Schomäcker, R.; Schwarze, M. Superior Catalyst Recycling in Surfactant Based Multiphase Systems – Quo Vadis Catalytic Complex? *Chem. Eng. Process.* **2016**, *99*, 155.

- (20) Holmberg, K. Organic Reactions in Microemulsions. *Eur. J. Org. Chem.* **2007**, *2007*, 731.

- (21) Schomäcker, R.; Holmberg, K. Reactions in Organised Surfactant Systems. In *Microemulsions: Background, New Concepts, Applications, Perspectives*; Subenrauch, C., Ed.; John Wiley & Sons Ltd.: Chichester, U.K., 2009; pp 148–177.

- (22) Schwarze, M.; Pogrzeba, T.; Volovych, I.; Schomäcker, R. Microemulsion Systems for Catalytic Reactions and Processes. *Catal. Sci. Technol.* **2015**, *5* (1), 24.

- (23) Müller, D.; Minh, D. H.; Merchan, V. A.; Arellano-Garcia, H.; Kasaka, Y.; Müller, M.; Schomäcker, R.; Wozny, G. Towards a Novel Process Concept for the Hydroformylation of Higher Alkenes: Mini-Plant Operation Strategies via Model Development and Optimal Experimental Design. *Chem. Eng. Sci.* **2014**, *115*, 127.

- (24) Kahlweit, M.; Strey, R.; Haase, D.; Kunieda, H.; Schmeling, T.; Faulhaber, B.; Borkovec, M.; Eicke, H.-F.; Busse, G.; Eggers, F.; et al. How to Study Microemulsions. *J. Colloid Interface Sci.* **1987**, *118* (2), 436.

- (25) Stubenrauch, C. *Microemulsions: Background, New Concepts, Applications, Perspectives*; Stubenrauch, C., Ed.; John Wiley & Sons, Ltd.: Chichester, U.K., 2009.

- (26) Müller, D.; Esche, E.; Pogrzeba, T.; Illner, M.; Schomäcker, R.; Wozny, G.; Leube, F. Systematic Phase Separation Analysis of Surfactant Containing Systems for Multiphase Settler Design. *Ind. Eng. Chem. Res.* **2015**, *54* (12), 3205.

- (27) Müller, D. *Development of Operation Trajectories Under Uncertainty for a Hydroformylation Mini-Plant*. Ph.D. Dissertation, Technische Universität Berlin, 2015.

(28) Seborg, D. E.; Mellichamp, D. A.; Edgar, T. F.; Doyle, F. J., III. *Process Dynamics and Control*; John Wiley & Sons: Chichester, U.K., 2011.

(29) AIChE Center for Chemical Process Safety. *Guidelines for Safe Automation of Chemical Processes*; AIChE: New York, 1993.

(30) Müller, D.; Esche, E.; Hamerla, T.; Rost, A.; Kasaka, Y. Enabling Hydroformylation in Micro-Emulsion Systems: Long-Term Performance of a Continuously Operated Mini-Plant. Presented at the AIChE Annual Meeting, San Francisco, CA, 2013.

(31) Torres, R.; Podzimek, M.; Friberg, S. E. E. Foaming of Microemulsions I. Microemulsions with Ionic Surfactants. *Colloid Polym. Sci.* **1980**, 258, 855.

(32) Ding, H.; Bartik, B.; Hanson, B. E. Surface Active Phosphines for Catalysis under Two-Phase Reaction Conditions. P(menthyl)  $[(\text{CH}_2)_8\text{C}_6\text{H}_4\text{-}p\text{-SO}_3\text{Na}]_2$  and the Hydroformylation of Styrene. *J. Mol. Catal. A: Chem.* **1995**, 98 (95), 117.

(33) Karakhanov, E. a.; Kardasheva, Y. S.; Runova, E. a.; Semernina, V. a. Surface Active Rhodium Catalysts for Hydroformylation of Higher Alkenes in Two-Phase Systems. *J. Mol. Catal. A: Chem.* **1999**, 142 (3), 339.

(34) Pogrzeba, T.; Müller, D.; Hamerla, T.; Esche, E.; Paul, N.; Wozny, G.; Schomaecker, R. Rhodium Catalysed Hydroformylation of Long-Chain Olefins in Aqueous Multiphase Systems in a Continuously Operated Miniplant. *Ind. Eng. Chem. Res.* **2015**, 54, 11953.

(35) Hamerla, T. *Hydroformylierung Langkettiger Olefine Mit Zweizähnigen Rhodium-Komplexen in Mizellaren Lösungen Und Mikroemulsionen*. Ph.D. Dissertation, Technische Universität Berlin, 2014; p 132.

(36) Markert, J.; Brunsch, Y.; Munkelt, T.; Kiedorf, G.; Behr, A.; Hamel, C.; Seidel-Morgenstern, A. Analysis of the Reaction Network for the Rh-Catalyzed Hydroformylation of 1-Dodecene in a Thermomorphic Multicomponent Solvent System. *Appl. Catal., A* **2013**, 462–463, 287.



# PAPER 4

## Catalytic Reactions in aqueous surfactant-free multiphase emulsions

Tobias Pogrzeba, Marcel Schmidt, Lena Hohl, Ariane Weber, Georg Buchner, Joschka Schulz, Michael Schwarze, Matthias Kraume, Reinhard Schomäcker

Industrial & Engineering Chemistry Research, 2016, 55, 12765-12775

Online Article:

<https://pubs.acs.org/doi/abs/10.1021/acs.iecr.6b03384>

Reproduced (or 'Reproduced in part') with permission from “Catalytic Reactions in Aqueous Surfactant-Free Multiphase Emulsions; Tobias Pogrzeba, Marcel Schmidt, Lena Hohl, Ariane Weber, Georg Buchner, Joschka Schulz, Michael Schwarze, Matthias Kraume, and Reinhard Schomäcker. Industrial & Engineering Chemistry Research, 2016, 55, 12765-12775.” Copyright (2016) American Chemical Society.



# Catalytic Reactions in Aqueous Surfactant-Free Multiphase Emulsions

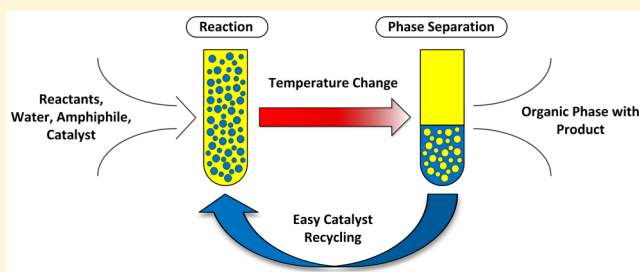
Tobias Pogrzeba,<sup>\*,†</sup> Marcel Schmidt,<sup>†</sup> Lena Hohl,<sup>‡</sup> Ariane Weber,<sup>†</sup> Georg Buchner,<sup>†</sup> Joschka Schulz,<sup>‡</sup> Michael Schwarze,<sup>§</sup> Matthias Kraume,<sup>‡</sup> and Reinhard Schomäcker<sup>†</sup>

<sup>†</sup>Department of Chemistry, Technische Universität Berlin, Straße des 17. Juni 124, Sekr. TC-8, D-10623 Berlin, Germany

<sup>‡</sup>Chemical and Process Engineering, Technische Universität Berlin, Ackerstraße 76, D-13355 Berlin, Germany

<sup>§</sup>Plant and Process Safety, Technische Universität Berlin, Straße des 17. Juni 135, TK-01, D-10623 Berlin, Germany

**ABSTRACT:** The first applications of aqueous surfactant-free multiphase emulsions as reaction media for rhodium-catalyzed hydroformylation of 1-dodecene and Suzuki coupling reaction of 1-chloro-2-nitrobenzene and 4-chlorobenzeneboronic acid are herein reported. The reaction systems were formulated from oil (reactant and solvent), aqueous catalyst solution, and diethylene glycol butyl ether [C<sub>4</sub>H<sub>9</sub>(C<sub>2</sub>H<sub>4</sub>O)<sub>2</sub>OH]. We investigated these multiphase systems with respect to reaction engineering and catalyst recycling to evaluate their application potential for new chemical processes based on switchable solvents. For the hydroformylation, conversion of 23.4% after 4 h reaction time could be achieved at mild reactions conditions of 95 °C and 15 bar syngas pressure. The applied Rhodium-SulfoXantPhos catalyst could be successfully recycled for four times, maintaining its very high linear-to-branched selectivity of 99:1. For the Suzuki coupling reaction yields up to 90% were achieved within a single run. The Pd/SPhos catalyst could be recycled three times, but activity decreased at almost stable selectivity due to higher ligand leaching during the separation steps.



## 1. INTRODUCTION

In the course of the development of new sustainable industrial chemical processes the exploitation of switchable solvent systems is increasingly investigated in various fields. Several different approaches of switchable solvent systems have already been reported in the literature, like supercritical media based on CO<sub>2</sub>,<sup>1</sup> switchable-polarity solvents,<sup>2</sup> thermomorphic multi-component solvents (TMS),<sup>3</sup> or microemulsion systems (MES).<sup>4</sup> Switchable solvents are liquids that can be reversibly switched from one state (or form) to another by the use of a simple trigger, for instance a change in temperature like for TMS and MES. The idea behind the application of these solvents in a chemical process is that they would meet the needs of one process step and could then be switchable to serve in the following step. For water-soluble catalysts, aqueous solutions can be applied as switchable solvent systems by the use of surfactants to formulate microemulsion systems. According to Winsor, microemulsions are thermodynamically stable and can be either a one-phase system (Winsor IV) or part of a multiphase system (Winsor I, II, or III) in which the microemulsion can be of three different types: water-in-oil (w/o), oil-in-water (o/w), or bicontinuous; the phase behavior is described in detail in the literature.<sup>4–7</sup> It is believed that the surfactant is in any case necessary to stabilize the system by formation of an interfacial film between the aqueous and oil phases. However, in terms of sustainable processing it would be desirable to achieve aqueous two-phase systems that have a switchability similar to microemulsion systems but would not

need to be modified with a surfactant. Smith et al.<sup>8</sup> reported in 1977 an oil-continuous (w/o) (micro)emulsion composed of hexane, 2-propanol, and water which could be considered as the first surfactant-free multiphase emulsion (denoted as SFME), since no traditional surfactant was involved in the system. Subsequently, the SFMEs have attracted much attention especially in physical chemistry,<sup>9–16</sup> but besides their interesting physical properties SFMEs provide the possibility to create new chemical processes based on the concept of temperature-induced phase transition similar to TMS or MES systems. In addition, they offer the advantage of an easily handled and removable additive instead of nonenvironmentally friendly solvents or usually highly viscous and high-boiling long-chained surfactants.

In order to understand aqueous surfactant-free multiphase systems better for their application as switchable solvents in homogeneous catalysis, we decided to test these new multiphase systems using two model reactions, namely the hydroformylation of a long-chain olefin (1-dodecene) and the Suzuki coupling reaction of 1-chloro-2-nitrobenzene and 4-chlorobenzeneboronic acid in these systems. The applied reaction systems consist of oil (reactant and solvent), aqueous catalyst solution, and diethylene glycol butyl ether

**Received:** September 2, 2016

**Revised:** November 2, 2016

**Accepted:** November 28, 2016

**Published:** November 28, 2016

[C<sub>4</sub>H<sub>9</sub>(C<sub>2</sub>H<sub>4</sub>O)<sub>2</sub>OH, denoted as C4E2]. Since the main goal of this work was to understand this new type of aqueous multiphase systems, we focused our experimental work on parametric studies and recycling experiments. In addition, we investigated the phase behavior of the resulting SFMEs and analyzed their structure by endoscopic measurement. The obtained results allow a characterization of the solvent properties of SFME and an evaluation of their application potential for new chemical processes.

## 2. MATERIALS AND METHODS

**2.1. Materials. Chemicals for Hydroformylation Reactions.** The reactant 1-dodecene was purchased from VWR with a purity of 95%. The precursor (acetylacetonato)-dicarbonylrhodium(I) (Rh(acac) (CO)<sub>2</sub>) was contributed by Umicore, Germany. The water-soluble ligand 2,7-bisulfonate-4,5-bis(diphenylphosphino)-9,9-dimethylxanthene (SulfoXantPhos, SX) was purchased from Molisa, where it was synthesized according to a procedure described by Goedheijt et al.<sup>17</sup> The syngas (1:1 mixture of CO and H<sub>2</sub>, purity 2.1 for CO and 2.1 for H<sub>2</sub>) was purchased from Air Liquide.

**Chemicals for Suzuki Coupling Reactions.** The reactants 1-chloro-2-nitrobenzene (purity 99.0%) and 4-chlorobenzenboronic acid (purity 98.0%) were received from ABCR and Sigma-Aldrich, respectively. The precursor palladium(II) acetate (Pd(OAc)<sub>2</sub>, purity 99.0%) was received from ABCR. The water-soluble ligand 2'-dicyclohexylphosphino-2,6-dimethoxy-sodium salt (SPhos, purity 97.0%) was received from Sigma-Aldrich. The base potassium carbonate (K<sub>2</sub>CO<sub>3</sub>, purity 98.0%) was received from Carl-Roth.

**Miscellaneous Chemicals.** The short-chain amphiphile diethylene glycol butyl ether (purity >99.0%) was purchased from Sigma-Aldrich. The solvent *n*-heptane (purity >99.0%) was received from Carl Roth. The solvents acetonitrile (HPLC, 99.9% purity) and water (HPLC, > 99.9% purity) were received from VWR. The ICP standards Rh (1011 ppm in 4.9 wt % HCl) and Pd (1011 ppm in 5.1 wt % HCl) were received from Sigma-Aldrich.

**2.2. Investigation on Phase Behavior.** Investigations on the phase behavior of the multiphase systems were performed by using tubes in a heatable water bath. Samples with different amounts of oil, water, and the particular amphiphile were prepared and heated up to the desired temperature. After reaching the temperature the test tubes were shaken to ensure homogeneity of mixture and put back into the water bath, and then phase separation was awaited. A phase diagram was constructed from the observed phase behavior as a function of amphiphile and temperature.

The important composition parameters to characterize the SFMEs are the weight fractions of oil ( $\alpha$ ) and amphiphile ( $\gamma$ ) (eq 1), which are calculated with the mass  $m$  of the corresponding component:

$$\alpha = \frac{m_{\text{oil}}}{m_{\text{oil}} + m_{\text{H}_2\text{O}}} \quad \gamma = \frac{m_{\text{Amph}}}{m_{\text{oil}} + m_{\text{H}_2\text{O}} + m_{\text{Amph}}} \quad (1)$$

**2.3. Endoscope Measurements.** The experimental setup used for the endoscope measurements (Figure 1) consisted of a double-walled glass tank (DN 150, H/D = 1) equipped with four rectangular baffles and a Rushton turbine (stirrer diameter  $d_{\text{st}} = 50$  mm, height of stirrer blade  $h_{\text{st}} = 12.5$  mm). The Rushton turbine was installed at a constant bottom clearance ( $h = 75$  mm). The temperature was maintained via an external

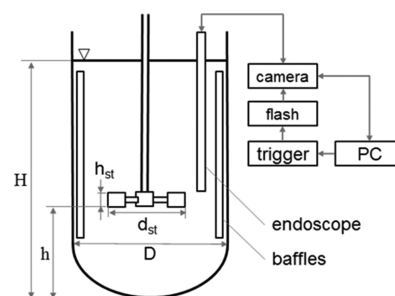


Figure 1. Experimental setup and endoscope measurement technique.

thermostat. The images were acquired using an endoscope, camera (GX 2750, Allied Visions Technology), trigger, and stroboscope at stirrer blade height. The drop sizes were determined using an automated image acquisition and drop detection software (SOPAT GmbH). Only spherical drops were taken into consideration. The minimum detectable drop size was 8–10  $\mu\text{m}$ . Deviations of Sauter mean diameter were  $\pm 10\%$ .

**2.4. Hydroformylation and Suzuki Coupling Experiments.** **2.4.1. Catalyst Preparation.** For the preparation of the hydroformylation catalyst complex, 12.9 mg (0.05 mmol) of the rhodium precursor [Rh(acac) (CO)<sub>2</sub>] and the ligand SulfoXantPhos (0.05–0.5 mmol) were dissolved in 4 mL of distilled water (degassed and flushed with nitrogen for at least 30 min) by using the Schlenk technique and stirred under argon atmosphere for a minimum of 12 h.

The homogeneous Pd/SPhos catalyst complex applied in Suzuki coupling reactions was prepared *ex situ* by stirring 7.5 mg (0.03 mmol) of the Pd(OAc)<sub>2</sub> catalyst precursor and 51.4 mg (0.10 mmol) of the water-soluble ligand SPhos in 3–5 mL of distilled water (degassed and flushed with nitrogen for at least 30 min) for 20 h under argon as inert gas.

**2.4.2. Reaction Procedure.** The hydroformylation reactions in lab-scale are performed in a 100 mL stainless steel high-pressure vessel from Premex Reactor AG, equipped with a gas dispersion stirrer and mounted in an oil thermostat from Huber (K12-NR). Reactor setup is illustrated in Figure 2. Mass flow controller (3) and a pressure transmitter (4) in the syngas feed line enable isobaric reaction management (semibatch mode). A connection for the inertization of reaction mixture is implemented as well (7).

The typical reaction conditions for the hydroformylation were 1–30 bar pressure of syngas, an internal reactor temperature of 75–100 °C, and a stirring speed of 1200 rpm, using a gas dispersion stirrer. The reaction mixture usually consisted of 1-dodecene, water (HPLC grade), C4E2, rhodium precursor [Rh(acac) (CO)<sub>2</sub>], and the ligand SulfoXantPhos.

The reaction was performed as described in the following. At first the reactor was filled with the desired amounts of olefin, water, and C4E2. Then the catalyst solution was transferred with a syringe to the reactor. The reactor was closed and evacuated and purged with nitrogen for at least three times. The stirrer was started at a rate of 500 rpm, and the reactor was heated up to the desired temperature. After reaching the temperature the stirring was slowed down (200–300 rpm), and the reactor was pressurized with syngas. Then the reaction was started by increasing the stirring speed again to 1200 rpm.

For the evaluation of reaction progress, samples were withdrawn at several time intervals via a sampling valve (Figure 2, (6)) and analyzed by gas chromatography (GC). To ensure

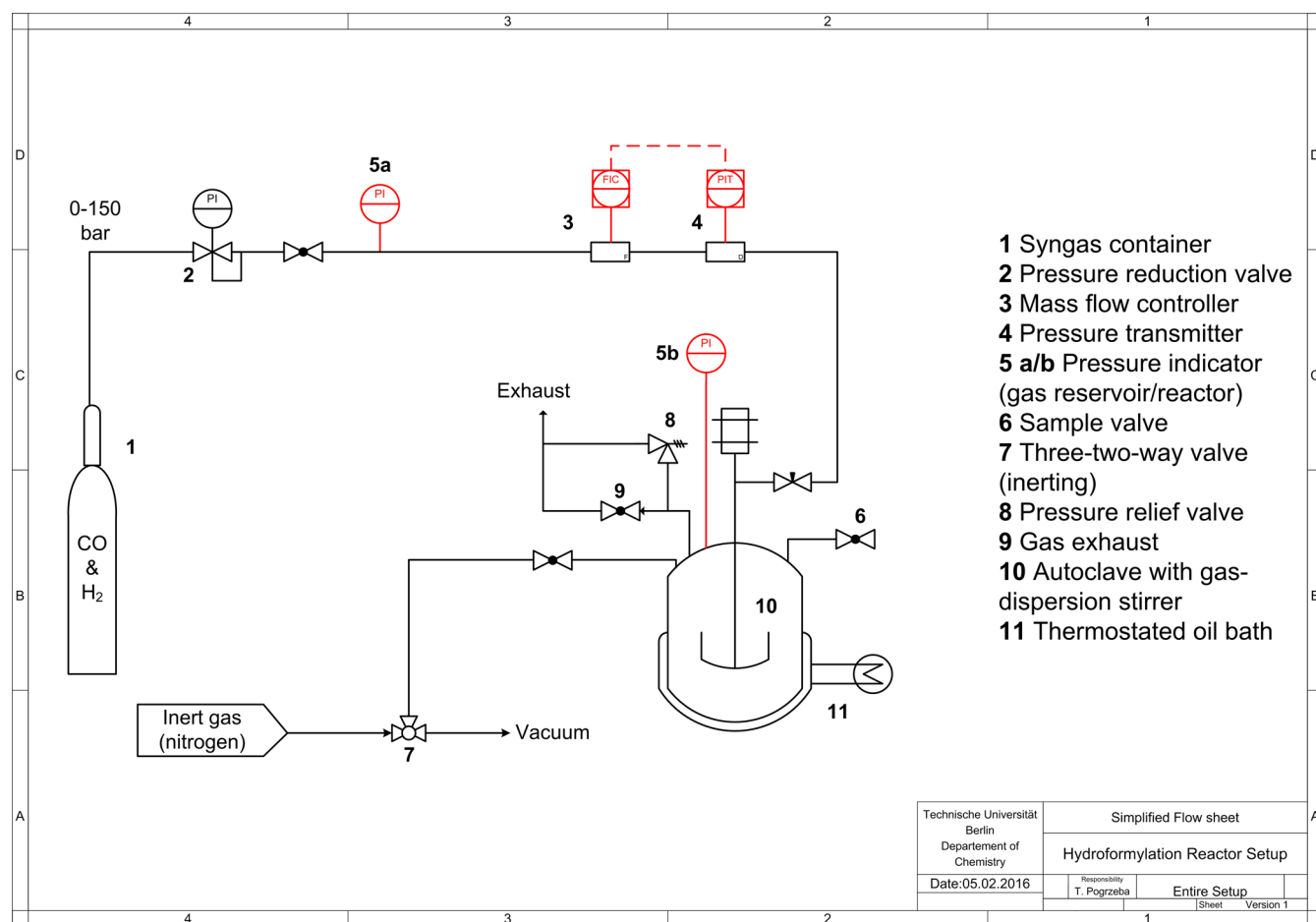


Figure 2. Reactor setup for hydroformylation experiments.

homogeneous liquid sampling, the stirring speed was not changed, while the samples were taken from the reactor. In addition, consumption of syngas during the experiments has been recorded via the mass flow controller.

The important parameters (conversion  $X$ , yield  $Y$ , selectivity  $S$ , and TOF) for the evaluation of experimental data were calculated as shown in eqs 2–5, where  $n$  is the amount of substance, 1-dodecene is the substrate, and 1-tridecanal is the product.

$$X(t) = \frac{n_{t=0, \text{Substrate}} - n_{t, \text{Substrate}}}{n_{t=0, \text{Substrate}}} \quad (2)$$

$$Y(t) = \frac{n_{t, \text{Product}}}{n_{t=0, \text{Substrate}}} \quad (3)$$

$$S(\text{n:iso}) = \frac{n_{\text{Product}}}{n_{\text{iso Aldehydes}}} \quad (4)$$

$$\text{TOF}_{\text{Ald}} = \frac{n_{t=0, \text{Substrate}} \cdot Y_{\text{Ald}}(t)}{n_{\text{cat}} \cdot t} \quad (5)$$

The Suzuki coupling reactions were performed in a double-walled glass reactor equipped with a condenser under nitrogen atmosphere. First, the reactor was evacuated and flushed with nitrogen. Second, the reactants were added under nitrogen flow (3 mmol of 4-chlorobenzenboronic acid, 3 mmol of 1-chloro-2-nitrobenzene, and 4 mmol of  $\text{K}_2\text{CO}_3$ ) followed by water, C4E2, and heptane. The total mass was about 100 g. After

stirring at the desired reaction temperature, the reaction was started by the addition of the previously prepared Pd/SPhos catalyst. The reaction progress was followed by withdrawing samples which were analyzed by HPLC.

**2.4.3. Analysis. GC Measurements.** Reaction progress and selectivity of hydroformylation reactions were analyzed by gas chromatography on a Shimadzu model GC-2010, equipped with a Supelcowax 10 capillary column, a flame ionization detection analyzer, and nitrogen as carrier gas.

**HPLC Measurements.** The conversion and selectivity in all coupling reactions were determined by high performance liquid chromatography (HPLC) using an Agilent instrument 1200 series with  $250 \times 4$  mm chromatographic column Multospher 120 RP18-5  $\mu$  from Ziemer Chromatographie Langerwehe/Germany. A mixture of acetonitrile/water (70 vol %/30 vol %) was used as eluent with a flow rate of 1 mL/min,  $T = 25$  °C,  $\lambda = 225$  nm, injection volume = 10  $\mu\text{L}$ ,  $p = 110$  bar, and  $t = 15$  min. All samples were dissolved in acetonitrile ( $F = 100$ ).

**ICP-OES Measurements.** The residue solutions from different coupling reactions were analyzed for palladium and phosphorus content using a Varian 715-ES Optical Emission Spectrometer (ICP-OES) to determine catalyst leaching. Calibration of the instrument was performed with commercial palladium and phosphorus standards from Sigma-Aldrich.

### 3. RESULTS AND DISCUSSION

**3.1. Hydroformylation Reaction.** As a benchmark for the rhodium-catalyzed hydroformylation in aqueous multiphase

systems (Figure 3) we selected the 1-dodecene/water/Marlipal (24/70) microemulsion system, which was recently presented

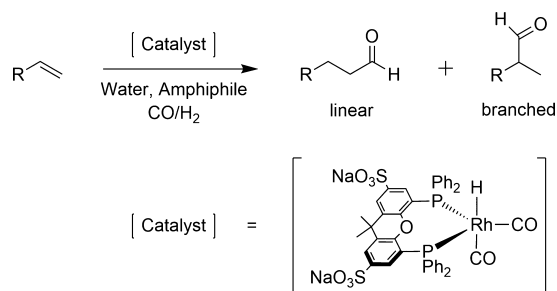


**Figure 3.** Hydroformylation reaction with the applied rhodium catalyst.

by our working group.<sup>18</sup> The following parameters were found to be optimal for the reaction:  $\alpha = 0.5$ ,  $\gamma = 0.08$ , 95 °C reaction temperature, 15 bar syngas pressure, 1200 rpm stirring speed, and 1:4 metal-to-ligand ratio. Hence we started the investigation of hydroformylation in the SFME system with these settings and subsequently optimized the parameters in several kinetic experiments. The results of these experiments are presented in the following chapters.

**Investigation on Phase Behavior.** At the beginning of our investigation the phase behavior of the applied 1-dodecene/water/C4E2 multiphase system was studied. For this purpose, several mixtures with different values for  $\alpha$  (0.4, 0.5, 0.6) and  $\gamma$  (0.05 to 0.3) have been prepared. The phase behavior of the resulting emulsions was investigated from 25 to 95 °C in 2 °C steps (experimental procedure is described in section 2.2). Since the phase behavior was found to be similar for every investigated  $\alpha$  value, in Figure 4 only the results for  $\alpha$

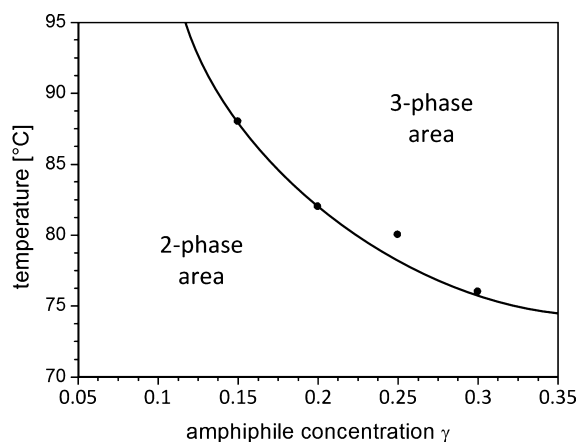


**Figure 4.** Phase diagram of the 1-dodecene/water/C4E2 multiphase system ( $\alpha = 0.5$ ): 2-phase area = oil phase + aqueous phase, 3-phase area = oil phase, C4E2-rich middle phase, and aqueous phase.

$\alpha = 0.5$  are presented. A broad 3-phase area was found for the SFME beginning at 77 °C for  $\gamma = 0.3$ , at lower temperatures a 2-phase system was observed. The separation time of the system was less than 1 min in each case. With lower amphiphile concentration the phase transition temperature increased, for  $\gamma = 0.15$  it was found at 88 °C. For  $\gamma = 0.05$  and  $\gamma = 0.1$  no 3-phase area could be observed. We assume that the required temperature for phase transition in these two systems is higher

than 95 °C, which was the maximal temperature we could adjust in the water bath.

Furthermore, the experiment for  $\alpha = 0.5$  was repeated with rhodium-SX catalyst in the mixture to investigate the influence of the catalyst on phase behavior and the catalyst distribution in the multiphase system. As a result, no change of phase behavior could be detected with catalyst in the solution. However, the catalyst distribution between the phases changed with the phase behavior of the system. In the 2-phase area (depicted gray in Figure 4) all the catalyst was located in the aqueous phase. When the 3-phase area was adjusted by temperature, large amounts of the catalyst (82.5%) followed the amphiphile into the middle phase which was proved by ICP-OES measurements. The rest of the catalyst (17.5%) remained in the aqueous phase.

Furthermore, we observed decomposition of the catalyst for  $\gamma > 0.2$  after several hours of experiment. The catalyst containing phase(s) changed color from yellow to brown and black rhodium particles adsorbed at the water–oil interface. Interestingly, this observation could not be verified for lower amphiphile concentrations. We heated and shook all emulsions for several days without observing any sign of catalyst decomposition. An explanation for this could be that if the amount of C4E2 reaches a certain level, the equilibrium of rhodium-SX complex formation gets misaligned and the short-chained amphiphile replaces SX as ligand. The resulting complex should be very instable, which in consequence would lead to a facilitated oxidation of rhodium by dissolved oxygen or the formation of hardly soluble rhodium clusters. Thus, we decided to apply a maximum of  $\gamma = 0.2$  in the hydroformylation experiments.

**Investigation on Phase Volumina.** The influence of the oil/water ratio and amphiphile concentration on the phase volume fractions of the applied 1-dodecene/water/C4E2 system was studied (see Figure 5). For this purpose, different mixtures for  $\alpha$  (0.3–0.5) and  $\gamma$  (0.175–0.225) were prepared, and the phase volume fractions were determined at two different temperatures. An increase of amphiphile concentration resulted in a larger middle phase volume fraction. Correspondingly, a decrease of the organic and aqueous volume fractions occurred. This effect was more pronounced at 83 °C, where the middle phase volume fraction also was slightly larger compared to 95 °C. A variation of the oil/water ratio  $\alpha$  did not affect the microemulsion phase considerably.

**Investigation on Drop Size Distribution.** The occurrence of the third liquid phase was also visualized using the endoscope measurement technique. Figure 6 depicts the droplet appearance inside the stirred tank under 2-phase (left) and 3-phase conditions (right). Under two-phase conditions (e.g.,  $T = 60$  °C) an o/w emulsion occurs. An increase of the temperature led to the formation of the 3-phase system, where the third phase occurred. The third liquid phase changed the dispersion conditions of the system toward multiple emulsions, where the middle phase is dispersed inside the dispersed aqueous phase. Details about the identification of the phases are given in previous studies.<sup>19,20</sup>

The drop size distribution under both conditions can be determined using image analysis. Figure 7 (left) depicts the drop size distributions in the 2-phase area (o/w emulsion) and the overall drop size distribution of the 3-phase area (multiple emulsion). An increase of the droplet size and widening of the drop size distribution can be observed as a function of temperature. The droplet sizes in the 3-phase area were also

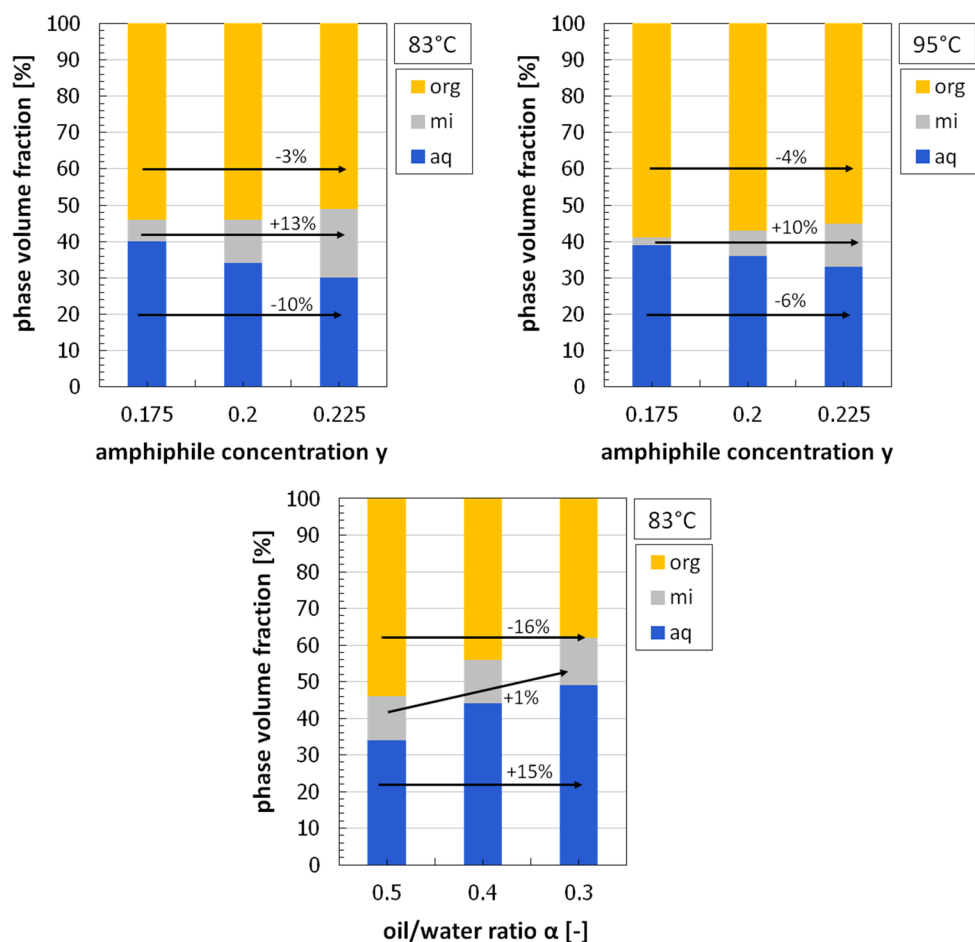


**Figure 5.** Phase volume fractions for different mixtures of 1-dodecene/water/C4E2. Top: At 83 and 95 °C with constant  $\alpha = 0.5$ . Bottom: At 83 °C with constant  $\gamma = 0.2$ . Phase volume fractions (phase heights) were determined by optical methods.

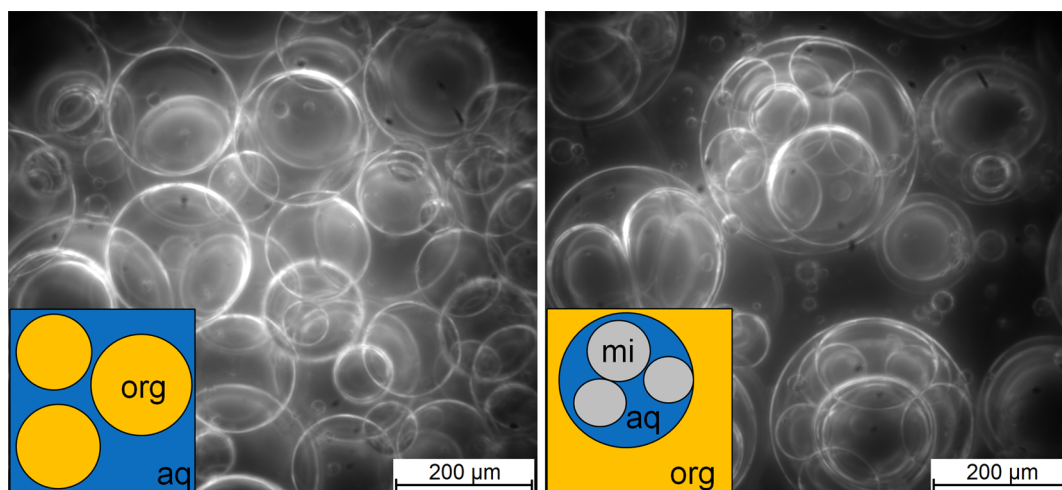


**Figure 6.** Drop images of the 1-dodecene/water/C4E2 multiphase system at 60 °C (2-phase area) and 83 °C (3-phase area).

determined separately: outer droplets = aqueous phase, inner droplets = emulsion phase (Figure 7, right).

**Influence of Amphiphile Concentration on Hydroformylation.** The reaction was tested with different C4E2 concentrations to identify the optimal amount of amphiphile. Due to the findings for the decomposition of catalyst at higher amphiphile concentrations (during investigation of phase behavior, see above),  $\gamma$  was not raised above 0.2 in these

experiments. In general, an increased amount of C4E2 in the mixture (and by that a larger emulsion phase, see Figure 5) benefits the reaction. For concentrations below  $\gamma = 0.1$  the hydroformylation performed very poorly, resulting in almost no conversion after a 4 h reaction time (Figure 8). For  $\gamma = 0.1$  a conversion of 3.5% was reached with a 1.4% yield in linear aldehyde (TOF = 7.3  $\text{h}^{-1}$ ). The yield could be increased to 9.1% (TOF = 53.8  $\text{h}^{-1}$ ) with a  $\gamma$  of 0.2, whereas formation of

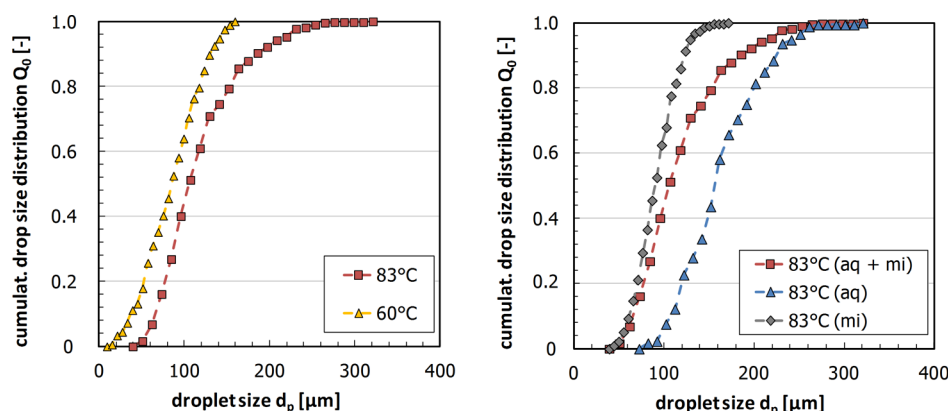


**Figure 7.** Overall drop size distribution in the 2-phase area at 60 °C and the 3-phase area at 83 °C (left). Overall and separated drop size distribution in the 3-phase area (right) at 500 rpm stirring speed in steady state.

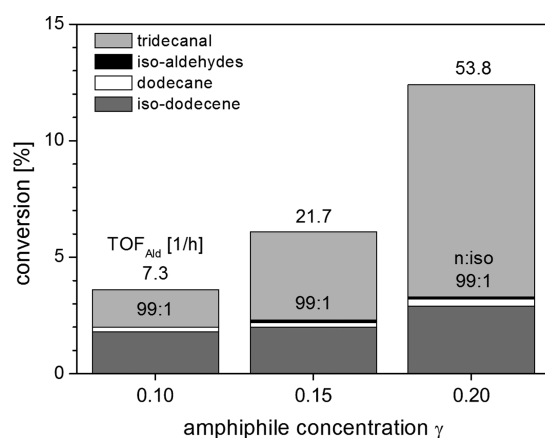


**Figure 8.** Effect of amphiphile concentration. Test conditions:  $[\text{Rh}(\text{acac}) (\text{CO})_2] = 0.05 \text{ mmol}$ , SulfoXantPhos = 0.2 mmol, 1-dodecene = 120 mmol, water ( $\alpha = 0.5$ ),  $V_R = 50 \text{ mL}$ ,  $T = 95 \text{ }^\circ\text{C}$ ,  $p = 15 \text{ bar}$ , stirring speed = 1200 rpm,  $t_R = 4 \text{ h}$ . Statistic deviation of conversion:  $\pm 3\%$ .

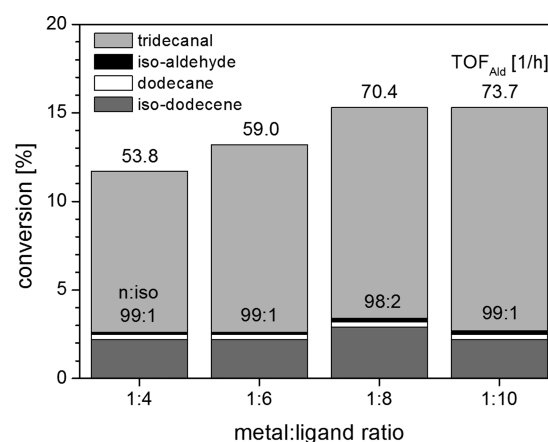


**Figure 9.** Effect of metal-to-ligand ratio. Test conditions:  $[\text{Rh}(\text{acac}) (\text{CO})_2] = 0.05 \text{ mmol}$ , 1 dodecene = 120 mmol, water ( $\alpha = 0.5$ ),  $\gamma = 0.2$ ,  $V_R = 50 \text{ mL}$ ,  $T = 95 \text{ }^\circ\text{C}$ ,  $p = 15 \text{ bar}$ , stirring speed = 1200 rpm,  $t_R = 4 \text{ h}$ . Statistic deviation of conversion:  $\pm 3\%$ .

side products increased only slightly. The n:iso selectivity in the hydroformylation remained unchanged at 99:1 for each experiment, indicating that catalyst decomposition was not an issue for the applied C4E2 concentrations. In consequence we chose to apply a  $\gamma$  of 0.2 in all following experiments.

**Influence of Catalyst Composition.** Different metal-to-ligand ratios were tested to identify the optimal catalyst composition in terms of activity and long-term stability. The results are displayed in Figure 9. The selectivity of the catalyst was almost the same in each experiment. We found that an increase of metal-to-ligand ratio from 1:4 to 1:10 had a beneficial effect on the activity of catalyst. For a ratio of 1:10 approximately 15.3% of 1-dodecene was converted after 4 h reaction time with a yield of 12.6% in linear aldehyde, compared to 11.8% conversion (9.1% linear aldehyde) for a ratio of 1:4 (TOFs = 73.7 h<sup>-1</sup> and 53.8 h<sup>-1</sup>, respectively). These results were in contradiction to our assumption that a higher concentration of ligand should reduce the reaction rate due to the increased formation of inactive catalyst species bearing more than one SulfoXantPhos ligand. This partial deactivation of the applied rhodium-SulfoXantPhos catalyst was found by Hamerla et al.<sup>21</sup> for the hydroformylation of 1-dodecene in microemulsion systems with nonionic surfactants. We assume that in the case of SFMEs this deactivation might be compensated by an enhancement in stability of the applied

emulsions due to higher amounts of ligand. Since SulfoXantPhos is surface active by itself<sup>22</sup> it could have an additional stabilizing effect on the droplets in the SFME, which would be beneficial for mass transport and hence for the reaction rate. According to these results, a metal-to-ligand ratio of 1:10 was used for further investigation.

**Influence of Oil Fraction.** We investigated the influence of oil fraction on the hydroformylation in the applied SFME, to determine the optimal amount of oil with respect to reaction rate and yield. The oil fraction was varied between  $\alpha = 0.3$  and  $\alpha = 0.7$  (see Table 1). Interestingly the amount of oil seems to have only a slight but indistinct impact on the reaction rate. For

**Table 1. Results for Different Weight Fractions of Oil**

alpha (1-dodecene/water)	TOF <sub>Ald</sub> [h <sup>-1</sup> ]	m(tridecanal) [g] <sup>a</sup>	selectivity (n:iso aldehyde)
0.3	68.6	2.33	99:1
0.4	77.5	2.66	99:1
0.5	73.7	2.52	99:1
0.6	51.9	1.78	99:1
0.7	71.2	2.41	99:1

<sup>a</sup>After 4 h reaction time.  $[\text{Rh}(\text{acac}) (\text{CO})_2] = 0.05 \text{ mmol}$ , SulfoXantPhos = 0.5 mmol,  $\gamma = 0.2$ ,  $V_R = 50 \text{ mL}$ ,  $T = 95 \text{ }^\circ\text{C}$ ,  $p = 15 \text{ bar}$ , stirring speed = 1200 rpm.

the lowest  $\alpha$  value of 0.3, reaction performed slightly slower (TOF = 68.6 h<sup>-1</sup>) than for  $\alpha = 0.5$  (TOF = 73.7 h<sup>-1</sup>), whereas the TOF was found to be the highest at  $\alpha = 0.4$  (TOF = 77.5 h<sup>-1</sup>). With the exception of the experiment for  $\alpha = 0.6$  (TOF = 51.9 h<sup>-1</sup>) all TOFs lie in the range of  $\pm 10\%$ . Together with the results from the experiments with varying C4E2 concentration (see Figure 8), this ultimately leads us to the assumption that the reaction mainly takes place in the middle phase and at the interfacial area of the multiple emulsion droplets. Since the size of middle phase can only be adjusted by the amount of amphiphile in the system, as depicted in Figure 5, the concentration of substrate in this phase should not have changed between the experiments with different  $\alpha$  (and therefore the reaction rate too). Due to slightly better results, we finally chose to apply  $\alpha = 0.4$  instead of  $\alpha = 0.5$  for further investigation.

**Influence of Syngas Pressure.** After optimization of the composition of the reaction medium the influence of syngas pressure on the hydroformylation was tested in the range of 2 to 25 bar. The results are displayed in Figure 10. The

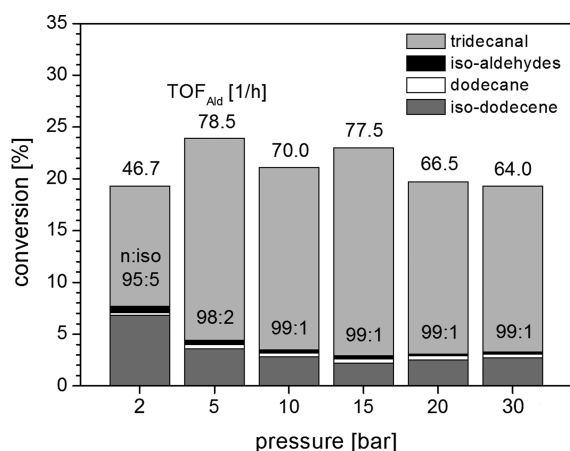


**Figure 10.** Effect of syngas pressure. Test conditions: [Rh(acac)(CO)<sub>2</sub>] = 0.05 mmol, SulfoXantPhos = 0.5 mmol, 1-dodecene = 80 mmol, water ( $\alpha = 0.4$ ),  $\gamma = 0.2$ ,  $V_R = 50$  mL,  $T = 95$  °C, stirring speed = 1200 rpm,  $t_R = 4$  h. Statistic deviation of conversion:  $\pm 3\%$ .

experiments showed that the hydroformylation performs best at 5 and 15 bar with conversions of roughly 24% after 4 h reaction time (TOFs = 78.5 h<sup>-1</sup> and 77.5 h<sup>-1</sup>, respectively) and slightly slower at 10 bar (21% conversion, TOF = 70.0 h<sup>-1</sup>). At a pressure of 2 bar the catalyst activity was comparably high but featured rather low reaction selectivity. The n:iso selectivity decreased to 95:5, and approximately 40% of converted 1-dodecene were isomerization products. An explanation for this finding could be the low partial pressure of CO. Markert et al.<sup>23</sup> showed for the hydroformylation of 1-dodecene with a rhodium-biphephos catalyst that a reduced partial pressure of carbon monoxide leads to an increase of the rate of the reversible isomerization reaction as well as the rate of hydrogenation. At syngas pressures higher than 15 bar the reaction rate seems to decrease slowly with an increase of pressure. At 25 bar the TOF value was only 64.0 h<sup>-1</sup>, whereas selectivity remained unchanged. This result was expected and is a well-known effect in hydroformylation reactions.<sup>23,24</sup> The inhibition of the reaction rate can be explained by increased formation of several inactive catalyst species with increasing CO concentration. As conclusion from these experiments we

decided to keep the pressure at 15 bar for further investigation. Although the reaction performed slightly faster at 5 bar and thus might be preferential from an economic point of view, we also considered selectivity and long-term stability of the catalyst for our decision.

**Influence of Temperature.** Different reaction temperatures were tested from 75 to 95 °C in 5 °C steps. The results show very clearly an increase of reaction rate with the temperature: After 4 h reaction time at 75 °C conversion of 1-dodecene was found to be 12.8% (TOF = 41.0 h<sup>-1</sup>) which linearly increased to 23.4% at 95 °C (TOF = 77.5 h<sup>-1</sup>) while selectivity of the catalyst remained on the same value in all experiments (Figure 11). The experimental data show that the

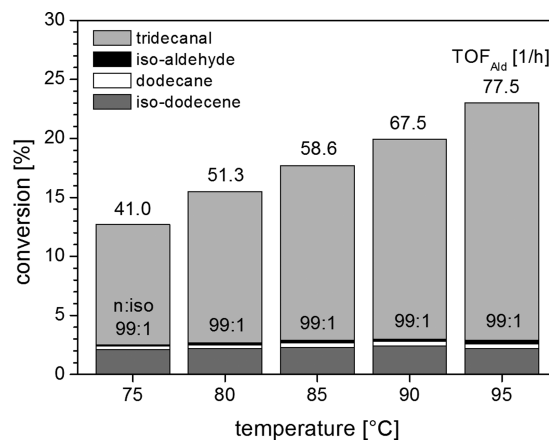


**Figure 11.** Effect of reaction temperature. Test conditions: [Rh(acac)(CO)<sub>2</sub>] = 0.05 mmol, SulfoXantPhos = 0.5 mmol, 1-dodecene = 80 mmol, water ( $\alpha = 0.4$ ),  $\gamma = 0.2$ ,  $V_R = 50$  mL,  $p = 15$  bar, stirring speed = 1200 rpm,  $t_R = 4$  h. Statistic deviation of conversion:  $\pm 3\%$ .

phase behavior of the applied SFME has no influence on reaction rate and a simple Arrhenius approach is sufficient to describe temperature dependency. The initial rates of the experiments were calculated and plotted in an Arrhenius diagram (Figure 12). Activation energy of the hydroformylation was calculated to be 53.9 kJ/mol which is in good accordance to the literature data collected with single phase systems.<sup>25</sup>

**Recycling Experiment.** The gathered data from the previous experiments were used to optimize the reaction parameters for the rhodium-catalyzed hydroformylation in the

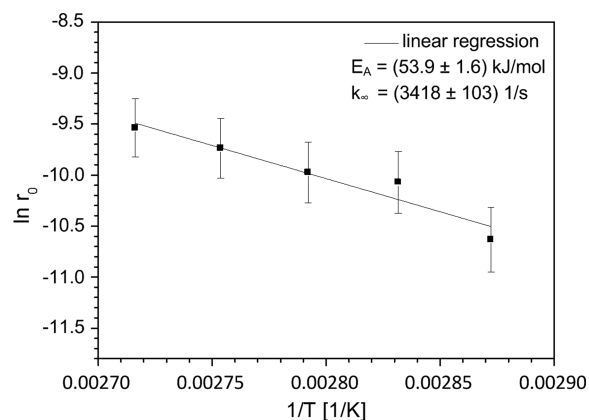


**Figure 12.** Arrhenius plot for the investigated reaction system.  $r_0$  was calculated from syngas consumption at the start of the reaction.

applied SFME. To finally investigate and prove the applicability of SFMEs for chemical processing we performed a recycling experiment over 5 cycles including all optimal reaction settings. For this purpose the reactor was cooled down to room temperature and depressurized after each run. Next, the reactor was opened, the oil phase was decanted (after complete phase separation), and then the new substrate was added. In addition, we had to add some C4E2 after each run since GC measurements showed that small amounts of C4E2 leave the reactor together with the oil phase (roughly 1 g per recycle, which is 11 wt % of the applied amphiphile). After replenishing the reactor, it was closed and heated up again for the next run.

Following this procedure, the catalyst could be successfully recycled for four times and performed the hydroformylation reaction in a total of five runs with very high selectivity toward the desired product (Figure 13). Thus, the proof of concept for

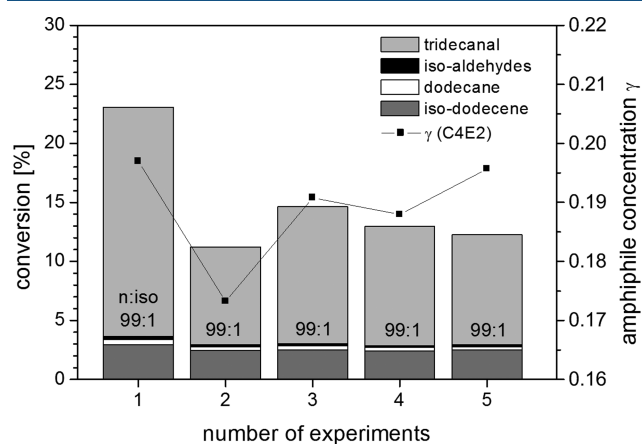


**Figure 13.** Recycling experiment. Test conditions:  $[\text{Rh}(\text{acac})(\text{CO})_2] = 0.05 \text{ mmol}$ , SulfoXantPhos = 0.5 mmol, 1-dodecene = 80 mmol, water ( $\alpha = 0.4$ ),  $\gamma = 0.2$ ,  $V_R = 50 \text{ mL}$ ,  $T = 95 \text{ }^\circ\text{C}$ ,  $p = 15 \text{ bar}$ , stirring speed = 1200 rpm,  $t_R = 4 \text{ h}$ . Statistic deviation of conversion:  $\pm 3\%$ .

the application of SFMEs as switchable reaction media in homogeneous catalysis is given. However, the results show a considerable decrease in activity of the catalyst after the first recycle. The TOF decreases by nearly 50% from  $73.4 \text{ h}^{-1}$  to  $38.0 \text{ h}^{-1}$  between the first and second run. The decrease is mainly due to the low C4E2 concentration in this run, since the loss of C4E2 in the extracted oil phase had been higher than expected. Thus, the value of  $\gamma$  decreased from 0.20 to roughly 0.175, which has a considerable impact on the rate of reaction

as already shown in Figure 8. The C4E2 concentration could be increased for the subsequent runs, leading to higher conversions. However, the activity of catalyst still decreased slightly with every new recycling step. We assume that this decrease could be due to catalyst deactivation by decomposition which had been already observed during the first phase separation experiments (see discussion of Figure 4). Oxidation of the catalyst by oxygen could also be part of the reason for catalyst deactivation, since the reactor had to be opened between the runs for the renewal of the oil phase. An indication for this assumption could be that the catalyst solution lost its characteristic yellow color during the recycling experiment and changed to light brown. Unfortunately, we have no evidence of the quantitative amount of remaining active catalyst after the fifth run, since this information would require the implementation of highly extensive in situ measurement techniques.

#### 4. SUZUKI COUPLING

The Pd/SPhos catalyzed Suzuki coupling of 1-chloro-2-nitrobenzene and 4-chlorobenzeneboronic acid to 4'-chloro-2-nitrobiphenyl was carried out in heptane/water/C4E2 as reaction medium (Figure 14).

In contrast to the hydroformylation reaction, where 1-dodecene is used as a reactant and oily compound at the same time, heptane was used as a nonpolar component to dissolve the hydrophobic reactants. Suzuki coupling reactions have already been investigated in microemulsion systems of technical grade surfactants. It was demonstrated that  $3\phi$  microemulsion systems provide the best conditions for the reaction and the simultaneous separation of hydrophobic products, the catalyst complex, and salts produced during the reaction from the inorganic base.<sup>26,27</sup>

At first, the phase behavior for the reaction mixture with C4E2 as the amphiphile was studied, and the obtained phase diagram after the coupling reaction is shown in Figure 15. Between an amphiphile concentration of 0 and 0.6 the  $2\Phi$  and  $3\phi$  states are observed. In comparison to Figure 4, for the Suzuki coupling reaction the  $3\Phi$  region is shifted to lower temperatures and covers a range of about 30–40 °C.

If classical surfactants are applied to formulate a microemulsion system, the range for the  $3\phi$  region is often very small (about 5–10 °C); therefore, a change in the composition of the reaction mixture can easily lead to a change in the phase behavior, e.g. from  $3\phi$  to  $2\phi$  state. This is a challenge, if a continuous process is aspired, but a successful example for a

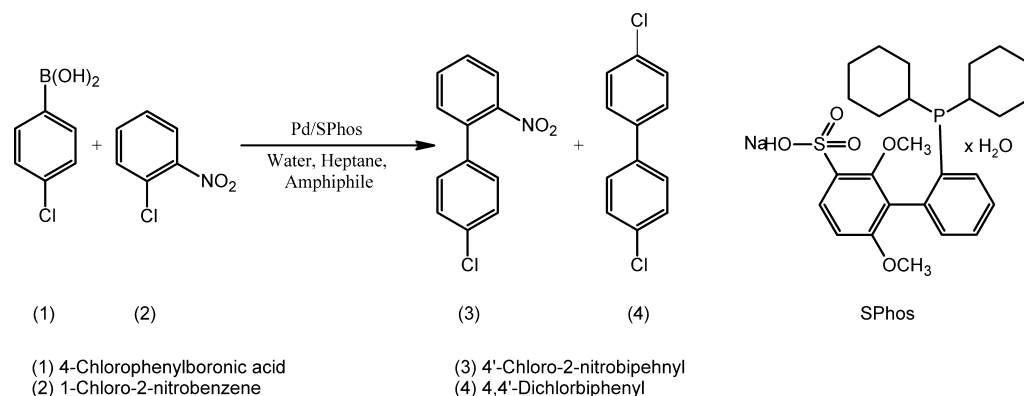


**Figure 14.** Suzuki coupling reaction with the applied water-soluble ligand.

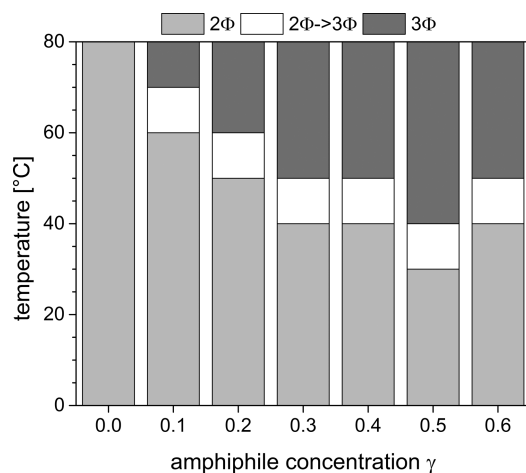


**Figure 15.** Phase behavior after reaction of 1-chloro-2-nitrobenzene (3 mmol) and 4-chlorobenzeneboronic acid (3 mmol) with  $K_2CO_3$  (4 mmol) as base and Pd/SPhos as catalyst complex (Pd/SPhos = 1/3, 33.42  $\mu$ mol Pd) in heptane/water/C4E2 ( $\alpha = 0.5$ ).

continuous operation of a hydroformylation reaction in a miniplant using 1-dodecene/water/Marlipal 24/70 as reaction medium is presented in refs 18 and 28. This example shows that it is possible to apply a microemulsion system in a combined reaction and separation process. However, the lower sensitivity of the phase behavior for the C4E2 based SFME toward smaller changes in the composition of the reaction mixture is of advantage. In addition, phase separation is much faster than in microemulsion systems, where the time for phase separation increases significantly when approaching the phase boundaries, but there are new challenges when C4E2 is used as an amphiphile instead of a conventional surfactant. The properties of the microemulsions system which are needed to have a favorable interaction with the catalyst complex, as we have already shown in ref 29 for microemulsion systems, are missed. For the  $3\Phi$  microemulsion system, we would expect a higher catalyst concentration in the middle phase if water-soluble ligands are used. In contrary, we found for the C4E2 system that the Pd/SPhos catalyst complex used for the Suzuki coupling reaction accumulates in the middle phase, whereby a Pd/TPPTS complex accumulates mainly in the aqueous-excess phase. The short-chained amphiphilic structure of C4E2 is responsible for a more solvent-like behavior of the middle phase so that now the polarity of the catalyst complex is more important than its amphiphilic nature.

The Suzuki coupling reaction was performed at different C4E2 concentrations. As shown in Figure 16, the conversion and selectivity are slightly lower for the  $2\Phi$  system but increase when the  $3\phi$  system is obtained, where yields up to 90% are achievable. When the amphiphile concentration is increased further, conversion and yield decrease again. As shown in Figure 5, the volume fractions within the  $3\phi$  system depend on the amphiphile concentration, whereby in the case of heptane, the volume of the middle phase increases and the volumes of the water and oil excess phase decrease. As the Pd/SPhos catalyst is located in the middle phase, its concentration will decrease with C4E2 concentration (dilution) and the reaction will slow down.

Although the  $3\phi$  system is the desired state for separation, the higher volume fraction of the middle phase is disadvantageous for the Suzuki coupling reaction. As already mentioned, for this reaction the oily phase is composed by heptane and the

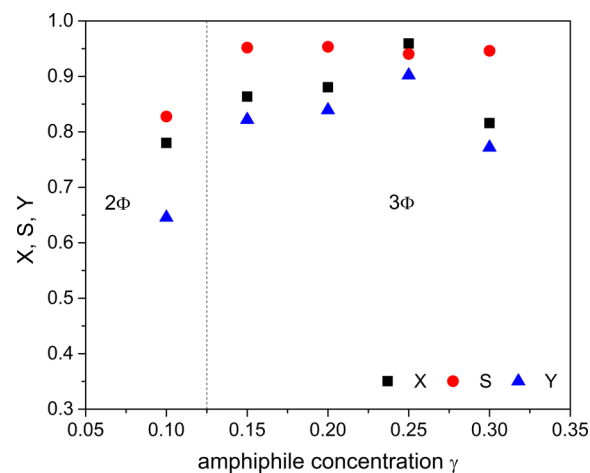


**Figure 16.** Conversion, selectivity, and yield as a function of the C4E2 concentration for the Suzuki coupling of 1-chloro-2-nitrobenzene (3 mmol) and 4-chlorobenzeneboronic acid (3 mmol) with  $K_2CO_3$  (4 mmol) as base and Pd/SPhos as catalyst complex (Pd/SPhos = 1/3, 33.42  $\mu$ mol Pd) in heptane/water/C4E2 ( $\alpha = 0.5$ ). Reaction temperature = 60 °C and reaction time = 120 min.

reactants/products within. Therefore, we have to consider the partitioning of the product between the individual phases. As shown by Volovych et.<sup>27</sup> for a C4E2 concentration of 15% only 56% of the product is located in the oil excess phase and the rest accumulates in the middle phase. Since heptane is not as hydrophobic as 1-dodecene, more heptane is dissolved in the middle phase with increasing C4E2 concentration so that the middle phase becomes more hydrophobic. If the oil excess phase should be used further, e.g. in tandem reactions, or high product removal is desired after one single reaction, the C4E2 concentration should be kept low. Again, we found an optimum in C4E2 concentration of 20%. The obtained yields for the Suzuki coupling reaction were already sufficient; therefore, we investigated the catalyst recycling and the increase in reactant concentration to achieve a higher space-time yield. For the recycling experiments, the oil and water excess phases after reaction containing the product and the salts were replaced by the same amount of heptane, water, and fresh reactants. As in the hydroformylation experiments, we found that C4E2 also leaches into the excess phases and has to be replaced in order to stabilize the phase behavior. Without any other modification, three runs could be carried out with the same catalyst, whereby the reaction time for each run was reduced to 20 min. The results are shown in Table 2.

Obviously, there is a strong decrease in the catalytic activity between the runs. To find the reason, we determined the catalyst leaching into the excess phases. We found a minor

**Table 2.** Conversion, Selectivity, and Yield for the Pd/SPhos Catalyzed Suzuki Coupling with Catalyst Recycling<sup>a</sup>

run	conversion (X)	selectivity (S)	yield (Y)
1	0.87	0.91	0.79
2	0.41	0.86	0.35
3	0.22	0.81	0.18

<sup>a</sup>1-Chloro-2-nitrobenzene (3 mmol) and 4 chlorobenzeneboronic acid (3 mmol) with  $K_2CO_3$  (4 mmol) as base and Pd/SPhos as catalyst complex (Pd/SPhos = 1/3, 33.42  $\mu$ mol Pd) in heptane/water/C4E2 ( $\alpha = 0.5$ ). Reaction temperature = 60 °C and reaction time = 20 min.

leaching of about 8% of Pd in three runs, but about 25% of SPhos already leached in a single run. A strong ligand leaching was also observed earlier by Nowothnick et al. for TPPTS.<sup>26</sup> Based on the Pd and SPhos losses, there are several possibilities to explain the lower activity, e.g. change in the Pd/SPhos ratio. However, the selectivity changes only slightly, and we can assume that the main reaction is still carried out by the Pd/SPhos complex but only at lower concentrations. It might be possible that some Pd is reduced but stabilized by the C4E2, which can explain that still 92% of Pd are present. As the C4E2 system is relatively new, further investigations are necessary. As this trend was also observed for the microemulsion systems<sup>27</sup> and could finally be solved by adding fresh ligand after a single run, we can expect the same behavior for the SFME.

Finally, we were interested in an increased productivity of the reaction system for which the reactant amounts were increased by a factor of 5 from 3 to 15 mmol. Within 15 min 98% conversion was achieved, but the selectivity decreased to 87% attributed to the high concentration of activated boronic acid able to perform the homocoupling reaction. It should be mentioned that the reaction at 60 °C was carried out in the upper 2 $\Phi$  region due to a hydrophilic shift at higher reactant concentrations. To re-establish the 3 $\Phi$  region, a reaction solution must be cooled down to 30 °C. We performed the reaction at 30 °C so that after the reaction separation can be done without a change in temperature; but activity was lower than expected, and 94% conversion and 85% selectivity were obtained after a reaction time of 120 min. We can summarize that the SFME can also be used for a combined reaction and separation process for the Suzuki coupling reaction, but further investigation is necessary to optimize the performance.

## 5. CONCLUSION AND OUTLOOK

In this contribution, we have shown that aqueous surfactant-free multiphase emulsions are feasible reaction media for homogeneously catalyzed reactions. A short-chain amphiphile, like diethylene glycol butyl ether (C4E2), is able to solubilize hydrophobic substrates in an aqueous environment and thus support the catalytic reaction and facilitate catalyst recycling in its active form. Preliminary investigations by the use of an endoscope measurement technique shown, that the applied reaction mixture for hydroformylation reaction consisting of 1-dodecene, water, and the amphiphile C4E2, formulates a multiphase system that has temperature dependent phase behavior similar to microemulsion systems (MES). Moreover, the switch from 2-phase to 3-phase conditions changed the dispersion conditions of the system from o/w emulsion toward multiple emulsions, where the emulsion phase was dispersed inside the continuous phase. Semibatch experiments for the rhodium-catalyzed hydroformylation of 1-dodecene in these systems showed under optimized reaction conditions a conversion of 23.4% (TOF = 77.5 h<sup>-1</sup>) after 4 h reaction time. Interestingly, the results from the kinetic experiments let us assume that the reaction behavior of hydroformylation in SFMEs is more comparable to reactions in thermomorphic multicomponent systems (TML) than in MES. It seems like the reaction mainly takes place in the middle phase, and the reaction rate is strongly dependent on the amount of amphiphile in the system. This indicates the solvent properties of a medium polarity solvent mixture, rather than a highly dispersed MES. In recycling experiments the applied Rhodium-SulfoXantPhos catalyst could be successfully recycled for four times, maintaining its very high linear-to-branched selectivity of

99:1. The Suzuki coupling reaction of 1-chloro-2-nitrobenzene and 4-chlorobenzeneboronic acid could also be successfully performed in aqueous SFMEs at yields up to 90%. Catalyst recycling was proven in general but needs further investigation in order to optimize the performance.

In summary, the results of the lab-scale experiments demonstrated the potential of surfactant-free multiphase emulsions as switchable reaction media for homogeneous catalysis and established the basis for more research using these systems, including the prospect of the design of a continuous process.

## AUTHOR INFORMATION

### Corresponding Author

\*E-mail: tobias.pogrzeba@tu-berlin.de.

### ORCID

Tobias Pogrzeba: 0000-0003-3727-9589

### Notes

The authors declare no competing financial interest.

## ACKNOWLEDGMENTS

This work is part of the Collaborative Research Center/Transregio 63 “Integrated Chemical Processes in Liquid Multiphase Systems” (subprojects A2 and B8). Financial support by the Deutsche Forschungsgemeinschaft (DFG, German Research Foundation) is gratefully acknowledged (TRR 63). Furthermore, the authors gratefully acknowledge the support of the company Umicore for sponsoring the rhodium catalyst “Acetylacetonato-dicarbonylrhodium(I) (CAS: 14874-82-9)”.

## ABBREVIATIONS

2 $\phi$  = two phase

3 $\phi$  = three phase

C4E2 = diethylene glycol butyl ether, C<sub>4</sub>H<sub>9</sub>(C<sub>2</sub>H<sub>4</sub>O)<sub>2</sub>OH

MES = microemulsion system

SFME = surfactant-free multiphase emulsion

SPhos = 2'-dicyclohexylphosphino-2,6-dimethoxy-sodium salt

SX = SulfoXantphos, 4,5-bis(diphenylphosphino)-9,9-dimethylxanthene

TMS = thermomorphic multicomponent solvent

TOF = turnover frequency

## REFERENCES

- (1) Leitner, W. Supercritical Carbon Dioxide as a Green Reaction Medium for Catalysis. *Acc. Chem. Res.* **2002**, *35*, 746.
- (2) Jessop, P. G.; Mercer, S. M.; Heldebrant, D. J. CO<sub>2</sub>-Triggered Switchable Solvents, Surfactants, and Other Materials. *Energy Environ. Sci.* **2012**, *5*, 7240.
- (3) Schäfer, E.; Brunsch, Y.; Sadowski, G.; Behr, A. Hydroformylation of 1-Dodecene in the Thermomorphic Solvent System Dimethylformamide/Decane. Phase Behavior – Reaction Performance – Catalyst Recycling. *Ind. Eng. Chem. Res.* **2012**, *51*, 10296.
- (4) Schwarze, M.; Pogrzeba, T.; Volovych, I.; Schomäcker, R. Microemulsion Systems for Catalytic Reactions and Processes. *Catal. Sci. Technol.* **2015**, *5*, 24.
- (5) Winsor, P. A. Hydrotrophy, Solubilisation and Related Emulsification Processes. Part I. *Trans. Faraday Soc.* **1948**, *44*, 376.
- (6) Kahlweit, M.; Strey, R.; Busse, G. Microemulsions: A Qualitative Thermodynamic Approach. *J. Phys. Chem.* **1990**, *94*, 3881.
- (7) Sottmann, T.; Stubenrauch, C. *Microemulsions: Background, New Concepts, Applications, Perspectives*; John Wiley & Sons: Chichester, 2009.

- (8) Smith, G. D.; Donelan, C. E.; Barden, R. E. Oil-Continuous Microemulsions Composed of Hexane, Water, and 2-Propanol. *J. Colloid Interface Sci.* **1977**, *60*, 488.
- (9) Keiser, B. A.; Varie, D.; Barden, R. E.; Holt, S. L. Detergentless Water Oil Microemulsions Composed of Hexane, Water, and 2-Propanol. 2. Nuclear Magnetic Resonance Studies, Effect of Added NaCl. *J. Phys. Chem.* **1979**, *83*, 1276.
- (10) Borys, N. F.; Holt, S. L.; Barden, R. E. Detergentless Water/oil Microemulsions. III. Effect of KOH on Phase Diagram and Effect of Solvent Composition on Base Hydrolysis of Esters. *J. Colloid Interface Sci.* **1979**, *71*, 526.
- (11) Knickerbocker, B. M.; Pesheck, C. V.; Davis, H. T.; Scriven, L. E. Patterns of Three-Liquid-Phase Behavior Illustrated by Alcohol-Hydrocarbon-Water-Salt Mixtures. *J. Phys. Chem.* **1982**, *86*, 393.
- (12) Khmel'nitsky, Y. L.; Van Hoek, A.; Veeger, C.; Visser, A. J. W. G. Detergentless Microemulsions as Media for Enzymatic Reactions: Spectroscopic and Ultracentrifugation Studies. *J. Phys. Chem.* **1989**, *93*, 872.
- (13) Klossek, M. L.; Touraud, D.; Zemb, T.; Kunz, W. Structure and Solubility in Surfactant-Free Microemulsions. *ChemPhysChem* **2012**, *13*, 4116.
- (14) Xu, J.; Yin, A.; Zhao, J.; Li, D.; Hou, W. Surfactant-Free Microemulsion Composed of Oleic Acid, N-Propanol, and H<sub>2</sub>O. *J. Phys. Chem. B* **2013**, *117*, 450.
- (15) Fischer, V.; Marcus, J.; Touraud, D.; Diat, O.; Kunz, W. Toward Surfactant-Free and Water-Free Microemulsions. *J. Colloid Interface Sci.* **2015**, *453*, 186.
- (16) Marcus, J.; Touraud, D.; Prévost, S.; Diat, O.; Zemb, T.; Kunz, W. Influence of Additives on the Structure of Surfactant-Free Microemulsions. *Phys. Chem. Chem. Phys.* **2015**, *17*, 32528.
- (17) Goedheijt, M. S.; Kamer, P. C. J.; van Leeuwen, P. W. N. M. A Water-Soluble Diphosphine Ligand with a Large "Natural" Bite Angle for Two-Phase Hydroformylation of Alkenes. *J. Mol. Catal. A: Chem.* **1998**, *134*, 243.
- (18) Pogrzeba, T.; Müller, D.; Hamerla, T.; Esche, E.; Paul, N.; Wozny, G.; Schomäcker, R. Rhodium-Catalyzed Hydroformylation of Long-Chain Olefins in Aqueous Multiphase Systems in a Continuously Operated Miniplant. *Ind. Eng. Chem. Res.* **2015**, *54*, 11953.
- (19) Hohl, L.; Paul, N.; Kraume, M. Dispersion Conditions and Drop Size Distributions in Stirred Micellar Multiphase Systems. *Chem. Eng. Process.* **2016**, *99*, 149.
- (20) Hohl, L.; Schulz, J.; Paul, N.; Kraume, M. Analysis of Physical Properties, Dispersion Conditions and Drop Size Distributions in Complex Liquid/liquid Systems. *Chem. Eng. Res. Des.* **2016**, *108*, 210.
- (21) Hamerla, T.; Rost, A.; Kasaka, Y.; Schomäcker, R. Hydroformylation of 1-Dodecene with Water-Soluble Rhodium Catalysts with Bidentate Ligands in Multiphase Systems. *ChemCatChem* **2013**, *5*, 1854.
- (22) Schmidt, M.; Pogrzeba, T.; Stehl, D.; Sachse, R.; Schwarze, M.; von Klitzing, R.; Schomäcker, R. Verteilungsgleichgewichte von Liganden in Mizellaren Lösungsmittelsystemen. *Chem. Ing. Tech.* **2016**, *88*, 1.
- (23) Markert, J.; Brunsch, Y.; Munkelt, T.; Kiedorf, G.; Behr, A.; Hamel, C.; Seidel-Morgenstern, A. Analysis of the Reaction Network for the Rh-Catalyzed Hydroformylation of 1-Dodecene in a Thermomorphic Multicomponent Solvent System. *Appl. Catal., A* **2013**, *462–463*, 287.
- (24) Deshpande, R. M.; Kelkar, A. A.; Sharma, A.; Julcour-lebigue, C.; Delmas, H. Kinetics of Hydroformylation of 1-Octene in Ionic Liquid-Organic Biphasic Media Using Rhodium Sulfoxantphos Catalyst. *Chem. Eng. Sci.* **2011**, *66*, 1631.
- (25) Bhanage, B. M.; Divekar, S. S.; Deshpande, R. M.; Chaudhari, R. V. Kinetics of Hydroformylation of 1-Dodecene Using Homogeneous HRh(CO) (PPh<sub>3</sub>)<sub>3</sub> Catalyst. *J. Mol. Catal. A: Chem.* **1997**, *115*, 247.
- (26) Nowothnick, H.; Blum, J.; Schomäcker, R. Suzuki Coupling Reactions in Three-Phase Microemulsions. *Angew. Chem., Int. Ed.* **2011**, *50*, 1918.
- (27) Volovych, I.; Neumann, M.; Schmidt, M.; Buchner, G.; Yang, J.-Y.; Wölk, J.; Sottmann, T.; Strey, R.; Schomäcker, R.; Schwarze, M. A Novel Process Concept for the Three Step Boscalid® Synthesis. *RSC Adv.* **2016**, *6*, 58279.
- (28) Illner, M.; Müller, D.; Esche, E.; Pogrzeba, T.; Schmidt, M.; Schomäcker, R.; Wozny, G.; Repke, J.-U. Hydroformylation in Microemulsions: Proof of Concept in a Miniplant. *Ind. Eng. Chem. Res.* **2016**, *55*, 8616.
- (29) Pogrzeba, T.; Müller, D.; Illner, M.; Schmidt, M.; Kasaka, Y.; Weber, A.; Wozny, G.; Schomäcker, R.; Schwarze, M. Superior Catalyst Recycling in Surfactant Based Multiphase Systems – Quo Vadis Catalyst Complex ? *Chem. Eng. Process.* **2016**, *99*, 155.



# PAPER 5

## **Microemulsion systems as switchable reaction media for the catalytic upgrading of long-chain alkenes**

Tobias Pogrzeba, Markus Illner, Marcel Schmidt, Jens-Uwe Repke, Reinhard Schomäcker

Chemie Ingenieur Technik, 2017, 89, 459-463

Online Article:

<https://onlinelibrary.wiley.com/doi/full/10.1002/cite.201600140>

Reprinted with permission from “Microemulsion Systems as Switchable Reaction Media for the Catalytic Upgrading of Long-Chain Alkenes; Tobias Pogrzeba, Markus Illner, Marcel Schmidt, Jens-Uwe Repke, and Reinhard Schomäcker. Chemie Ingenieur Technik, 2017, 89, 459-463.” Copyright (2017) Wiley-VCH.



# Microemulsion Systems as Switchable Reaction Media for the Catalytic Upgrading of Long-Chain Alkenes

Tobias Pogrzeba<sup>1,\*</sup>, Markus Illner<sup>2</sup>, Marcel Schmidt<sup>1</sup>, Jens-Uwe Repke<sup>2</sup>, and Reinhard Schomäcker<sup>1</sup>

DOI: 10.1002/cite.201600140

The application of microemulsion systems as switchable reaction media for the rhodium-catalyzed hydroformylation of 1-dodecene is herein reported. The influence of temperature and the selected surfactant on the reaction kinetics was investigated. In addition, the feasibility of a process concept for these reaction systems was tested within 100 hours continuous mini-plant operation, showing similar product yield and reaction selectivity as on the lab-scale. Alongside, a stable steady state operation was achieved, showing an efficient phase separation and recycling of surfactant and catalyst.

**Keywords:** Hydroformylation, Microemulsions, Mini-plant, Process design, Switchable solvents

*Received:* September 29, 2016; *revised:* January 27, 2017; *accepted:* February 03, 2017

## 1 Introduction

The selection of an appropriate solvent is certainly one of the biggest obstacles for the development of chemical processes. Since an optimal yield is not a solely satisfying objective in terms of green chemical processing, the selection criteria for solvents imply an integrated consideration of the process, including aspects of resource and energy efficiency as well as sustainability. Unfortunately, most industrial applications involve more than one step, especially in downstream processing, where typically each step requires a different solvent that has to be removed again once its task is done. In terms of process sustainability, that strategy is highly wasteful and contributes to wastage of energy and materials. To overcome this, one would need a solvent that can transform itself, changing its properties to enable several applications. Fortunately, these systems do already exist: Switchable solvents, meaning liquids that can be reversibly switched from one state to another, could unfold a great potential for process intensification, if applied in a subtle way. Several different approaches of switchable solvent systems have already been reported in literature, like supercritical media based on CO<sub>2</sub> [1], switchable-polarity solvents [2], thermomorphic multicomponent solvents [3] or microemulsion systems (further denoted as MES) [4].

In terms of green processing the application of water as solvent is highly desirable but carries the issue of poor reactant solubility in case of hydrophobic reactants. A way to bring organic substrates and water together is to add a surfactant to the reaction mixture, which enables many interesting applications for water-soluble catalysts in homogeneous catalysis. For example performing catalytic reactions in microemulsion systems, which are ternary mixtures consist-

ing of oil, water, and a surfactant (often non-ionic surfactants are chosen in this context). Microemulsions provide a high interfacial area between the polar and non-polar domains during the reaction. Additionally, their phase separation behaviour can be manipulated through temperature changes and thus makes them switchable solvent systems. According to Winsor, microemulsions are thermodynamically stable and can be either a one-phase system (Winsor IV) or part of a multiphase system (Winsor I, II, or III) in which the microemulsion can be of three different types: water-in-oil (w/o), oil-in-water (o/w) or bicontinuous; the phase behaviour is described in detail in literature [4–6].

The switchability of MES enables chemical processes in aqueous media with high reaction rates and efficient catalyst recycling. To proof the applicability of MES as switchable reaction media, an integrated process concept for the rhodium-catalyzed hydroformylation of 1-dodecene on a mini-plant scale is currently under investigation. In this contribution the results of a long-term operation, in which a highly selective reaction as well as a stable phase separation with feasible catalyst recycling could be achieved continuously for 100 hours in total, are presented. Also a number of results from kinetic lab-scale experiments that show an interesting reaction behavior dependent on temperature

<sup>1</sup>Tobias Pogrzeba, Marcel Schmidt, Prof. Reinhard Schomäcker  
tobias.pogrzeba@tu-berlin.de  
Technische Universität Berlin, Department of Chemistry, Straße  
des 17. Juni 124, 10623 Berlin, Germany.

<sup>2</sup>Markus Illner, Prof. Jens-Uwe Repke  
Technische Universität Berlin, Department of Process Dynamics and  
Operation, Straße des 17. Juni 135, 10623 Berlin, Germany.

and surfactant chain-length are highlighted. The obtained results are of great importance for understanding these complex reaction systems and contribute to further development and enhancement of chemical processes in MES.

## 2 Experimental

In lab-scale the hydroformylation reactions were performed in a 100 mL stainless steel high-pressure vessel (Premex Reactor AG) equipped with a gas dispersion stirrer and mounted in an oil thermostat (Huber, K12-NR). The typical reaction conditions for the hydroformylation were 15 bar of synthesis gas (1:1 mixture, purity 2.1), an internal reactor temperature of 65–110 °C, and a stirring speed of 1200 rpm. The reaction mixture usually consisted of 1-dodecene (VWR, 95 %), water (HPLC grade), a non-ionic surfactant from the Marlipal® 24 series (Sasol), the rhodium precursor [Rh(acac)(CO)<sub>2</sub>] (Umicore), and the ligand SulfoXantphos (Molisa). A more detailed description of experimental set-up and reaction procedure can be found in [7]. The important parameters (oil content  $\alpha$ , surfactant concentration  $\gamma$ , selectivity  $S$ , and TOF) for the evaluation of experimental data were calculated as shown in Eqs. (1)–(4), where  $m$  is the mass,  $n$  is the amount of substance, 1-dodecene is the substrate and tridecanal is the product.

$$\alpha = \frac{m_{\text{Oil}}}{m_{\text{Oil}} + m_{\text{Water}}} \quad (1)$$

$$\gamma = \frac{m_{\text{Surfactant}}}{m_{\text{Oil}} + m_{\text{Water}} + m_{\text{Surfactant}}} \quad (2)$$

$$S(n : \text{iso}) = \frac{n_{\text{Product}}}{n_{\text{iso-Aldehydes}}} \quad (3)$$

$$\text{TOF} = \frac{n_{t=0, \text{Substrate}} Y(t)}{n_{\text{cat}} t} \quad (4)$$

The mini-plant system, which is schematically depicted in Fig. 1, consists of a feed section holding containers for the applied substances, a main reaction section holding the

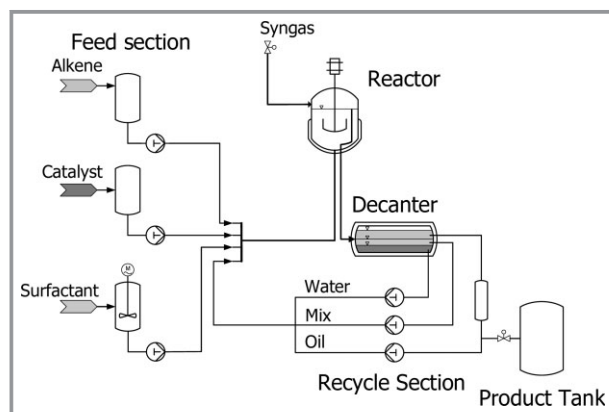


**Figure 1.** Schematic setup of the mini-plant system for the continuous hydroformylation of 1-dodecene in MES.

reactor (1.5 L), and a separation unit (decanter, 0.5 L). Here, a decanter with three drains was installed to adjust the phase separation for the MES and enable a reliable separation of the product containing oil phase from the surfactant and catalyst rich mix phase and the lower aqueous solution [8]. The mini-plant is fully automatized with SIEMENS PCS7 and meets ATEX zone 2 specifications [9]. Offline gas chromatography (Agilent HP-5 column, FID) and online raman spectroscopy (RXN1 NIR, Kaiser Optical Systems) were used for liquid sampling and thus, evaluating separation success and reaction performance. Rhodium leaching into the product phase is determined by an ICP-OES (Varian ICP-OES 715 ES).

## 3 Results and Discussion

The rhodium-catalysed hydroformylation of 1-dodecene in microemulsion systems (Fig. 2) is investigated by our research group for several years [7, 10, 11]. In previous experiments it was found that the aliphatic surfactants from the Marlipal® series provide good results as emulsifier for the applied reaction mixture. By the application of the surfactant Marlipal® 24/70, 31.3 % yield of aldehyde (98 % linear product) were obtained after 4 h reaction time under optimized reaction conditions:  $\alpha = 0.5$ ,  $\gamma = 0.08$ , 95 °C reaction temperature, 15 bar syngas pressure, 1200 rpm stirring speed, and 1:4 metal-to-ligand ratio.

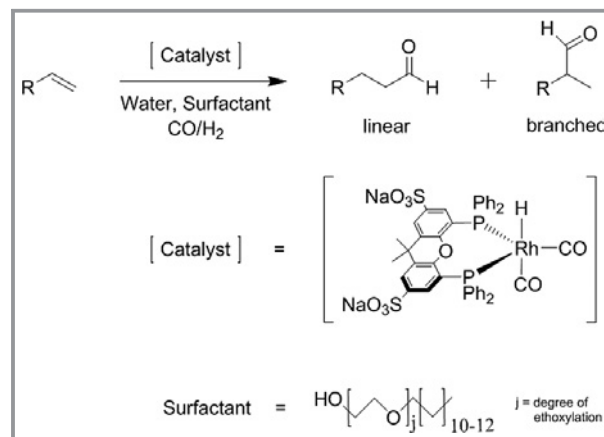


**Figure 2.** Hydroformylation reaction in microemulsion systems, structures of the applied rhodium catalyst and of the non-ionic surfactants (Marlipal® 24 series).

To gain deeper understanding of the mechanisms behind homogeneous catalysis in MES, it is highly necessary to thoroughly investigate the influence of surfactants and temperature on catalytic reactions in these systems, since both have simultaneous impact on reaction rate and phase behaviour. In order to do this, the influence of temperature on the hydroformylation of 1-dodecene with respect to reaction rate and selectivity for a fixed composition of the reaction mixture was investigated. The results are depicted

in Fig. 3. Interestingly, the reaction rate increased exponentially within the investigated temperature range and indicated a simple Arrhenius behaviour. At 68 °C a TOF of 50 h<sup>-1</sup> was achieved which could be raised to 380 h<sup>-1</sup> at 110 °C, while the selectivity towards the linear product remained at very high value of 98 %. These results were slightly unexpected, since the MES underwent two phase transitions between 68 and 82 °C that completely changed the type of microemulsion (oil-in-water → bicontinuous → water-in-oil). As it was already shown, the switch in phase behaviour leads to a noticeable change of mass transfer in the MES [12]. In addition, the type of microemulsion dictates the continuous phase for the reaction mixture since the catalyst follows the surfactant into the corresponding microemulsion phase due to its amphiphilic character. However, that all seems to have no immediate influence on the reaction rate in the presented experiment. Hence it was assumed that MES feature kinetically controlled two-phase reactions, which is also indicated by the Arrhenius behaviour of the hydroformylation (Fig. 3). In addition, an activation energy of 59 kJ mol<sup>-1</sup> could be calculated for the reaction which is in good accordance to literature data collected for the applied catalyst in single phase systems. Considering a two-phase reaction, the surfactant should play an even greater role for the reaction conditions in MES than expected since catalysis mainly takes place at the oil-water interface, where all the reactants are located and bound by the surfactant. Thus the ability of the surfactant to work as emulsifier for the applied reaction system determines the size of the interfacial area for the reaction and, in addition, also the local concentrations of reactants at the interface that are relevant for catalysis. Simply said, the better the surfactant performs, the higher is the possible outcome of the reaction.

To further investigate this matter, an experiment was performed in which the hydroformylation was carried out with

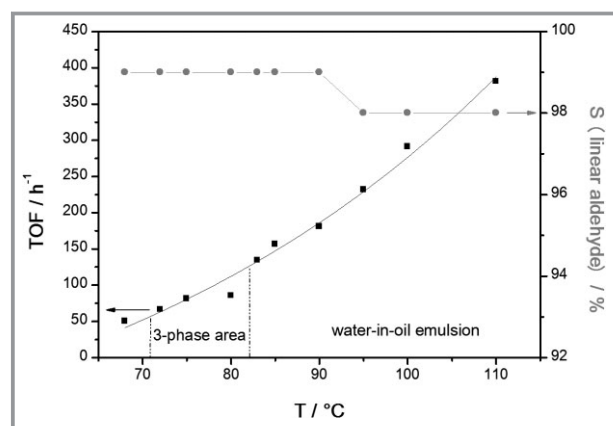


**Figure 3.** Turnover frequency and selectivity as function of temperature. Test conditions: 15 bar, 1200 rpm, 120 mmol 1-dodecen,  $\alpha = 0.5$ ,  $\gamma = 0.08$  (Marlipal 24/70), 1 wt % Na<sub>2</sub>SO<sub>4</sub>, 0.05 mmol (0.04 mol %) Rh(acac)(CO)<sub>2</sub>, 0.2 mmol SulfoXantphos, V<sub>R</sub> = 50 mL. TOFs were calculated after 1 h reaction time. Arrows indicate the corresponding axis.

several related surfactants from the Marlipal<sup>®</sup> series (the results are shown in Fig. 4). All reaction parameters were kept constant for every run to ensure that the degree of ethoxylation of the surfactant was the only essential variable for the reaction. The degree of ethoxylation, meaning the amount of ethoxylate groups in the surfactant-chain, was varied between 5 and 9 (Marlipal<sup>®</sup> 24/70 has an average of 7). The experimental results indicate that the applied surfactant indeed plays a greater role for the reaction than just emulsifying the two-phase systems. In case of the investigated hydroformylation an enhanced hydrophilicity of surfactant (meaning a higher ethoxylation degree) seems to be beneficial. The reaction rate was found to be the highest at an ethoxylation degree of 9 (Marlipal<sup>®</sup> 24/90). A TOF of 309 h<sup>-1</sup> was calculated for this surfactant which is an increase of 51 % in comparison to 205 h<sup>-1</sup> for an ethoxylation degree of 5 (Marlipal<sup>®</sup> 24/50). This finding could be explained by a higher density of the surfactant film that enhances the adsorption of reactants at the oil-water interface and, by that, increases the reaction rate. In the same time, a change in the degree of ethoxylation has an impact on the resulting phase behaviour of the applied MES. However, the change in phase behaviour had again no noticeable influence on the reaction since the results show only a slight linear increase of the reaction rate without an abrupt rising in between that would indicate a major change of mass transfer conditions. All things considered, these results alone are not sufficient for an accurate explanation of the impact of surfactants on homogeneous catalysis and thus this topic requires more investigation. But they do point out the high optimization potential of chemical processes in microemulsion systems with respect to higher space-time yields.

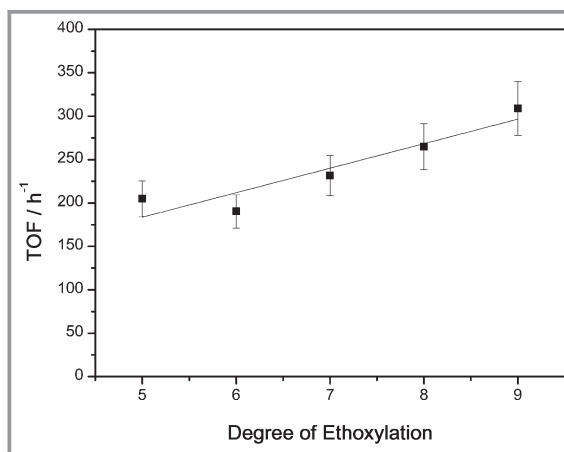


**Figure 4.** Turnover frequency vs degree of ethoxylation. Test conditions: 95 °C, 15 bar, 1200 rpm, 120 mmol 1-dodecen,  $\alpha = 0.5$ ,  $\gamma = 0.08$  (Marlipal 24/XX), 1 wt % Na<sub>2</sub>SO<sub>4</sub>, 0.05 mmol (0.04 mol %) Rh(acac)(CO)<sub>2</sub>, 0.2 mmol SulfoXantphos, V<sub>R</sub> = 50 mL. TOFs were calculated after 1 h reaction time.

### 3.1 Mini-Plant Operation

The proof of concept for the hydroformylation in MES is performed within the technical mini-plant system. The conducted mini-plant campaign was carried out as 100 hours continuous operation, covering different operational modes from start-up, full recycle mode to increase product yield and long-term steady state continuous operation. Referring to the lab-scale results an initial mixture of 50 %  $\alpha$  and 8 %  $\gamma$  was applied, including 0.04 mol % rhodium precursor, 0.2 mol % SulfoXantphos and 1.00 wt %  $\text{Na}_2\text{SO}_4$ . The reaction conditions, determined on the lab-scale as well, were set to 15 bar(g) pressure and 95 °C.

A trajectory for the total conversion of 1-dodecene and yield of tridecanal was obtained from the mini-plant campaign, depicted in Fig. 5. After feeding and starting up the plant, the reaction was successfully initiated. From here on a full recycle operation was performed to quickly increase yield. At operation hour 35, the continuous operation was started with the introduction of fresh 1-dodecene and extraction of the product-containing organic phase. Consequently, the conversion slightly decreased and stabilized at a new level of 41 %, which could be sustained during the steady-state operation for more than 50 hours. With a reaction residence time of 6.5 hours for the continuous operation, these results are in good accordance to lab-scale find-

ings. The product yield stabilized at around 39 %, showing an excellent overall reaction selectivity of 95 % towards the desired aldehyde. In addition, the product was obtained with a linear to branched selectivity of 99 %. Again, this is in very good accordance to previous findings in lab. Moreover, a continuous phase separation could be accomplished, leading to a remarkably pure organic phase (educt and product content of 99.8 %) and very low rhodium leaching into the product phase (lower than 0.1 ppm). Thus, an efficient separation and recycling of surfactant and catalyst could be shown by the mini-plant operation, which demonstrates the applicability of MES as reaction media in continuous chemical processes.

### 4 Conclusions and Outlook

In this contribution, it is shown that microemulsion systems are feasible reaction media for homogeneously catalysed reactions and continuous chemical processes in aqueous media. The mini-plant experiments proved the applicability of MES and demonstrated that their switchability can be exploited in an integrated process with reaction and subsequent recycling of surfactant and catalyst. However, these multiphase systems require a profound knowledge of the influence of parameters regarding reaction

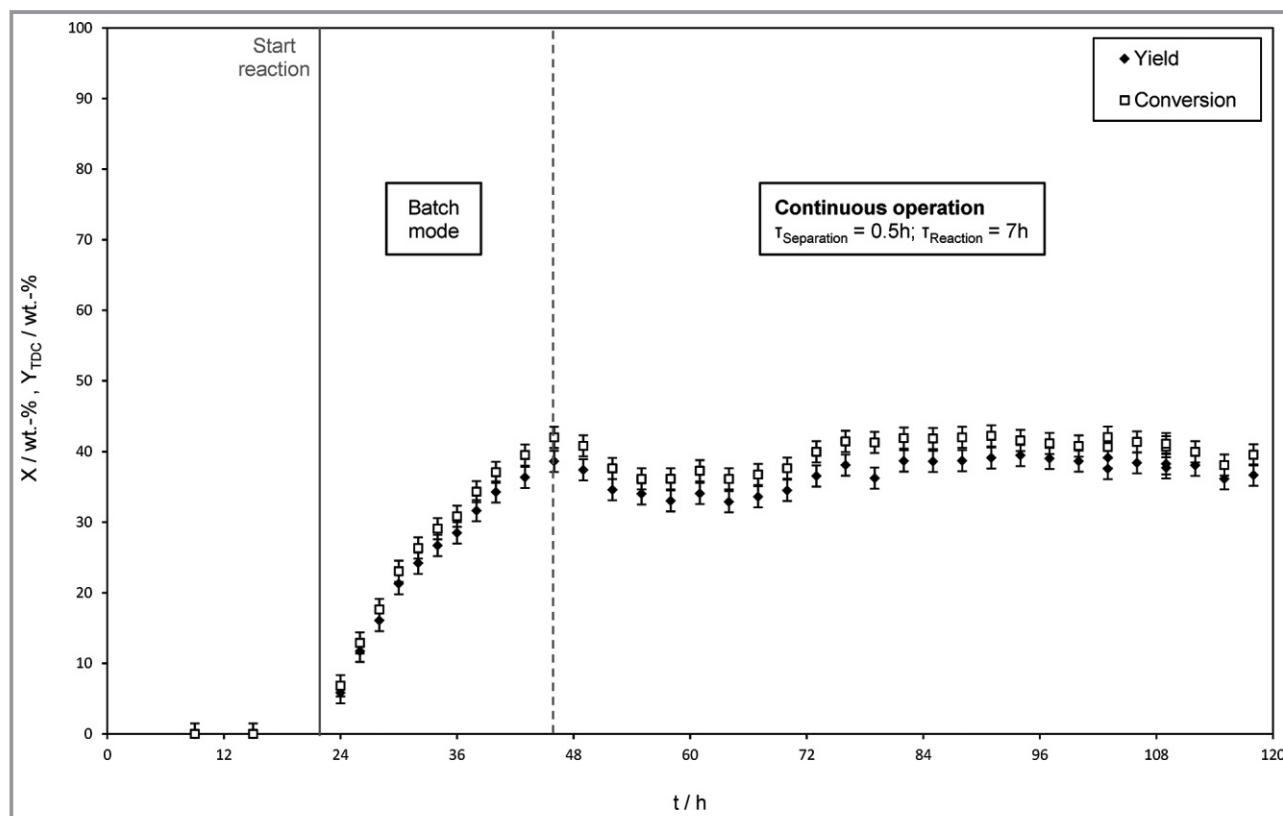


**Figure 5.** Mini-plant operation results, total conversion of 1-dodecene and yield of tridecanal over time. Reaction residence time indicates equivalent reaction time of a batch experiment.

and separation. In particular, the applied surfactant has a strong impact on the outcome of a reaction. Further investigations on this matter are mandatory to fully understand the role of the surfactant and, by that, enhance the operability of MES in technical systems.

This work is part of the Collaborative Research Center/Transregio 63 "Integrated Chemical Processes in Liquid Multiphase Systems" (subprojects A2 and B4). Financial support by the Deutsche Forschungsgemeinschaft (DFG, German Research Foundation) is gratefully acknowledged (TRR 63). Furthermore, the authors gratefully acknowledge the support of the company Umicore for sponsoring the rhodium catalyst "Acetylacetonato-dicarbonylrhodium(I)" (CAS: 14874-82-9).

### Symbols used

$m$	[kg]	mass
$n$	[mol]	amount of substance
$S$	[-]	selectivity
$t$	[h]	time
$T$	[°C]	temperature
TOF	[h <sup>-1</sup> ]	turnover frequency
$X$	[-]	conversion
$Y$	[-]	yield
$\alpha$	[-]	oil-to-water ratio
$\gamma$	[-]	surfactant concentration

### Abbreviations

MES	Microemulsion system
SulfoXantphos	4,5-Bis(diphenylphosphino)-9,9-dimethylxanthene

### References

- [1] W. Leitner, *Acc. Chem. Res.* **2002**, *35* (9), 746 – 56.
- [2] P. G. Jessop, S. M. Mercer, D. J. Heldebrant, *Energy Environ. Sci.* **2012**, *5* (6), 7240 – 7253.
- [3] E. Schäfer, Y. Brunsch, G. Sadowski, A. Behr, *Ind. Eng. Chem. Res.* **2012**, *51* (31), 10296 – 10306.
- [4] M. Schwarze, T. Pogrzeba, I. Volovych, R. Schomäcker, *Catal. Sci. Technol.* **2015**, *5* (1), 24 – 33.
- [5] M. Kahlweit, R. Strey, G. Busse, *J. Phys. Chem.* **1990**, *94* (10), 3881 – 3894.
- [6] P. A. Winsor, *Trans. Faraday Soc.* **1948**, *44*, 376 – 398.
- [7] T. Pogrzeba, D. Müller, T. Hamerla, E. Esche, N. Paul, G. Wozny, R. Schomäcker, *Ind. Eng. Chem. Res.* **2015**, *54* (48), 11953 – 11960.
- [8] D. Müller, E. Esche, T. Pogrzeba, M. Illner, F. Leube, R. Schomäcker, G. Wozny, *Ind. Eng. Chem. Res.* **2015**, *54* (12), 3205 – 3217.
- [9] M. Müller, Y. Kasaka, D. Müller, R. Schomäcker, G. Wozny, *Ind. Eng. Chem. Res.* **2013**, *52* (22), 7259 – 7264.
- [10] T. Hamerla, A. Rost, Y. Kasaka, R. Schomäcker, *ChemCatChem* **2013**, *5* (7), 1854 – 1862.
- [11] A. Rost, M. Müller, T. Hamerla, Y. Kasaka, G. Wozny, R. Schomäcker, *Chem. Eng. Process.* **2013**, *67*, 130 – 135.
- [12] T. Hamerla, N. Paul, M. Kraume, R. Schomäcker, *Chem. Ing. Tech.* **2013**, *85* (10), 1530 – 1539.



# PAPER 6

## **Improving the catalytic activity in the rhodium-mediated hydroformylation of styrene by a Bis(N-heterocyclic silyene) ligand**

Marcel Schmidt, Burgert Blom, Tibor Szilvási, Reinhard Schomäcker, Matthias Driess

European Journal of Inorganic Chemistry, 2017, 9, 1284-1291

Online Article:

<https://onlinelibrary.wiley.com/doi/full/10.1002/ejic.201700148>

Reprinted with permission from “Improving the catalytic activity in the rhodium-mediated hydroformylation of styrene by a Bis(N-heterocyclic silyene) ligand; Marcel Schmidt, Burgert Blom, Tibor Szilvási, Reinhard Schomäcker, and Matthias Driess. European Journal of Inorganic Chemistry, 2017, 9, 1284-1291.” Copyright (2017) Wiley-VCH.



## Successful Silicon Bite

## Improving the Catalytic Activity in the Rhodium-Mediated Hydroformylation of Styrene by a Bis(N-heterocyclic silylene) Ligand

Marcel Schmidt,<sup>[a]</sup> Burgert Blom,<sup>[b,c]</sup> Tibor Szilvási,<sup>[d]</sup> Reinhard Schomäcker,\*<sup>[a]</sup> and Matthias Driess\*<sup>[c]</sup>

**Abstract:** For the first time, a significant boost in catalytic activity in the rhodium-catalysed hydroformylation of an alkene by using a bidentate bis(N-heterocyclic silylene) ligand is reported. This is shown by the hydroformylation of styrene at 30 bar CO/H<sub>2</sub> pressure in the presence of [HRh(CO)(PPh<sub>3</sub>)<sub>3</sub>] with an excess of the ferrocenediyl-based bis-NHSi ligand **4**, [(η<sup>5</sup>-C<sub>5</sub>H<sub>4</sub>{PhC(NtBu)<sub>2</sub>}Si)<sub>2</sub>Fe], which results in superior catalytic activity, compared with the bidentate diphosphines DPPF (**3a**) and xantphos (**3b**). In contrast, the hydroformylation of styrene in the presence of [HRh(CO)(PPh<sub>3</sub>)<sub>3</sub>] with excesses of the monodentate NHSi ligands [(PhC(NtBu)<sub>2</sub>)SiNMe<sub>2</sub>] (**1**) and [(C<sub>2</sub>H<sub>2</sub>(NtBu)<sub>2</sub>)Si:] (**2**) at 30 bar CO/H<sub>2</sub> pressure revealed consid-

erably slower conversion to the aldehyde products than [HRh(CO)(PPh<sub>3</sub>)<sub>3</sub>], with or without an excess of PPh<sub>3</sub>, showing catalyst deactivation. Surprisingly, the germanium analogue of **4** is shown to be virtually catalytically inactive. The superior activity of **4**, compared with the xantphos-containing benchmark system, is rationalized on the basis of solution NMR spectroscopic studies, and the comparative catalyst cycles are elucidated using density functional theory (DFT) methods. The latter quantum-chemical studies explain very well the favourable energy pathway for the hydroformylation of styrene using **4** versus xantphos.

## Introduction

Otto Roelen's early discovery of the hydroformylation of olefins to aldehydes in the 1930s has emerged as one of the most important industrial processes worldwide.<sup>[1]</sup> Nowadays, the total volume of produced aldehydes by the hydroformylation process is over 10 million tons per year.<sup>[2]</sup> Over the last few decades, mammoth efforts have been made to optimize the Rh-catalysed hydroformylation reaction.<sup>[1–4]</sup> The choice of an appropriate ligand is crucial for the performance and selectivity of the hydroformylation process; thus, the synthesis and appli-

cation of new ligands with novel properties are the centres of interest. Ligands with Group 15 elements as donor atoms have been widely studied in this regard, and it has been shown that phosphines outperform analogous nitrogen-coordinating ligands in catalytic activity.<sup>[5,6]</sup> Phosphites have also been shown to exhibit higher activity than phosphines, due to the fact that they have a stronger π-acceptor character and decrease the energy barrier of the rate-determining step.<sup>[7–13]</sup> Nowadays, bidentate phosphine ligands such as xantphos (**3b**; Scheme 1) are widely used, because its specific bite angle can improve the selectivity and avoid undesired branched products.<sup>[14–16]</sup>

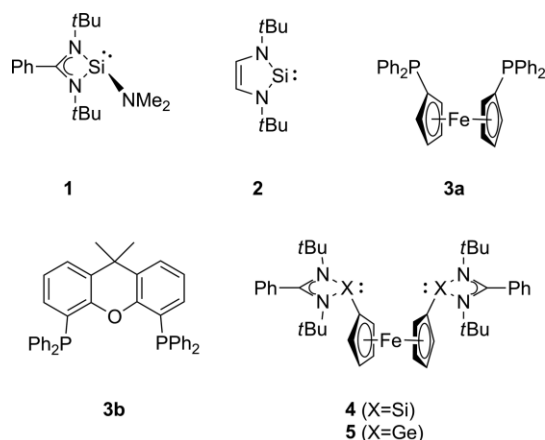
[a] Department of Chemistry: Technical Chemistry, Technische Universität Berlin, Straße des 17. Juni 124, 10623 Berlin, Germany  
E-mail: schomaecker@tu-berlin.de  
[https://www.chemie.tu-berlin.de/menue/about\\_us/staff/personen/s/schomaecker/](https://www.chemie.tu-berlin.de/menue/about_us/staff/personen/s/schomaecker/)

[b] Maastricht Science Program, Faculty of Humanities and Sciences, Maastricht University, P. O. Box 616, 6200 MD Maastricht, The Netherlands

[c] Department of Chemistry: Metalorganics and Inorganic Materials, Technische Universität Berlin, Straße des 17. Juni 135, 10623 Berlin, Germany  
E-mail: matthias.driess@tu-berlin.de  
[http://www.metalorganik.tu-berlin.de/menue/metalorganics\\_and\\_inorganic\\_materials/parameter/en/](http://www.metalorganik.tu-berlin.de/menue/metalorganics_and_inorganic_materials/parameter/en/)

[d] Department of Chemical & Biological Engineering, University of Wisconsin–Madison, 1415 Engineering Drive, Madison, WI 53706, USA

Supporting information and ORCID(s) from the author(s) for this article are available on the WWW under <http://dx.doi.org/10.1002/ejic.201700148>.



Scheme 1. Ligands employed for the rhodium-catalysed hydroformylation of styrene in this work.

Recently, N-heterocyclic carbenes (NHC) have also been introduced as ligands in hydroformylation, showing high activity.<sup>[17–19]</sup> Due to the stable metal–C<sup>II</sup> (NHC) bond, the complexes are also robust under hydroformylation conditions and CO- or P-based ligands do not eliminate the NHC.<sup>[20]</sup>

To explore NHC-analogous ligands bearing heavier divalent Group 14 elements (Si, Ge, Sn, Pb), we set our focus on N-heterocyclic silylene ligands (NHSi), which, to our surprise, have escaped testing for hydroformylation catalysis. The synthesis and isolation of the first N-heterocyclic silylene (NHSi, **2**; Scheme 1) by Denk and West in the early 1990s introduced the possibility of incorporating isolable low-valent silicon-based ligands in catalysis.<sup>[21]</sup>

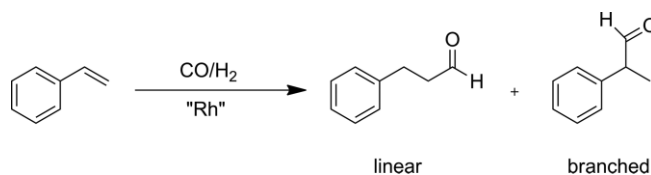
For the last 20 years, the synthesis and characterization of new and stable NHSi complexes has received considerable attention.<sup>[22,23]</sup> Nowadays, there is a range of different stable NHSi ligands with different electronic and steric features. The potential of NHSi-supported transition-metal compounds as catalysts is enormous, because of their unique properties – in particular, their enhanced  $\sigma$ -donor/ $\pi$ -acceptor properties.<sup>[24–28]</sup> A relatively large number of transition-metal NHSi complexes have been synthesized, characterized and tested in different catalytic and stoichiometric reactions, but compared with their NHC counterparts, this is still an emerging field, with many avenues still left open to explore, particularly in the realm of metal-complex-mediated homogeneous catalysis. The donor-stabilized heteroleptic  $\{[\text{PhC}(\text{NtBu})_2](\text{NMe}_2)\text{Si}\}$  (**1**; Scheme 1) silylene is especially promising, because it has been shown to exhibit a higher  $\sigma$ -donor strength than NHCs and phosphines.<sup>[29,30]</sup> In addition, a closely related bidentate analogue has also been studied (**4**; Scheme 1), together with the germanium counterpart (**5**; Scheme 1). Both of them can potentially serve as alternatives to benchmark diphosphine ligands, such as DPPF or xantphos (**3a** or **3b**; Scheme 1), in hydroformylation, inspiring us to investigate this hitherto unexplored area.<sup>[31]</sup>

Herein, we report the first application of NHSi ligands in hydroformylation, using styrene as a substrate. The remarkable activity and selectivity of respective Rh complexes are compared with the current benchmark complexes containing diphosphine ligands. We observed that, in terms of activity, the use of the bis-NHSi ligand **4** with a 1,1'-ferrocenediyl backbone outperforms that containing the diphosphines DPPF (**3a**) and xantphos (**3b**).

## Results and Discussion

To learn about the steering properties of NHSi ligands in rhodium-catalysed hydroformylation, we probed styrene as a substrate. Styrene is often used as model substrate, because isomerisation of the double bond does not occur. Scheme 2 shows the hydroformylation of styrene with a homogeneously catalysed rhodium complex under synthesis gas (CO/H<sub>2</sub>), yielding the corresponding linear and branched aldehyde products.

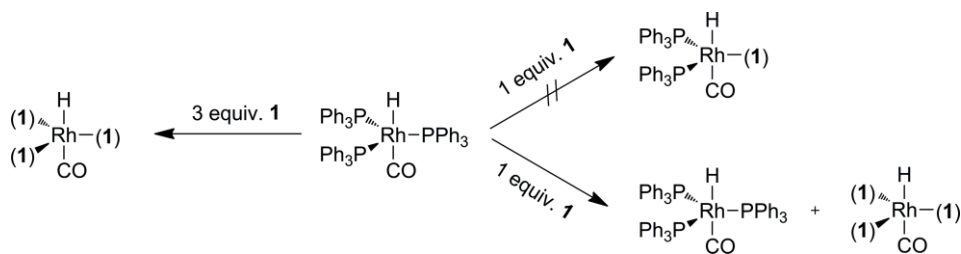
We employed the commercially available  $[\text{HRh}(\text{CO})(\text{PPh}_3)_3]$  complex as a precursor for our investigations. The starting point of our investigations was focussed on monodentate NHSi ligand systems **1** and **2** (Scheme 1). We tested the heteroleptic silylene



Scheme 2. Rh-catalysed hydroformylation of styrene to give the linear and branched aldehydes.

$\{[\text{PhC}(\text{NtBu})_2](\text{NMe}_2)\text{Si}\}$  (**1**),<sup>[29]</sup> which exhibits a strong  $\sigma$ -donor capacity, and the homoleptic  $\{[\text{C}_2\text{H}_2(\text{NtBu})_2]\text{Si}\}$  (**2**).<sup>[21]</sup>

First, we explored the coordination ability of the ligands **1** and **2** towards Rh<sup>I</sup> in the precursor  $[\text{HRh}(\text{CO})(\text{PPh}_3)_3]$  by NMR spectroscopic experiments. Scheme 3 illustrates the formed rhodium complexes with different molar amounts of **1**. As expected, there was a substitution reaction of the triphenylphosphine (TPP) ligand by the NHSi **1**, when **1** (3 equiv.) was added to the precursor  $[\text{HRh}(\text{CO})(\text{PPh}_3)_3]$ . This indicates a strong interaction of **1** with the Rh<sup>I</sup> centre, due to the stronger  $\sigma$ -donor ability of **1** than of TPP, facilitating the substitution. The <sup>1</sup>H NMR spectrum (in C<sub>6</sub>D<sub>6</sub>) shows the clean formation of the trisubstituted  $[\text{HRh}(\text{CO})(\mathbf{1})_3]$  product, consistent with the absence of <sup>31</sup>P-coupling for the resonance signal of the hydride ligand at  $\delta = -10.45$  ppm (d, <sup>1</sup>J<sub>H,Rh</sub> = 9.2 Hz, 1 H). Accordingly, the <sup>31</sup>P{<sup>1</sup>H} NMR spectrum (C<sub>6</sub>D<sub>6</sub>) shows only “free” PPh<sub>3</sub>. Moreover, the <sup>29</sup>Si{<sup>1</sup>H} NMR spectrum exhibits a clean doublet resonance signal at  $\delta = 62.8$  ppm (d, <sup>1</sup>J<sub>Si,Rh</sub> = 80.4 Hz), further confirming the fully NHSi-substituted product. The observation of a clean doublet resonance signal in the <sup>29</sup>Si NMR spectrum suggests equatorial substitution of the NHSi ligands in the trigonal-bipyramidal-coordinated Rh centre, but Berry pseudorotation is another possibility to explain the highly symmetrical spectrum. Variable-temperature NMR spectroscopic experiments show that  $[\text{HRh}(\text{CO})(\mathbf{1})_3]$  is stable in the presence of PPh<sub>3</sub>, and no evidence of reversion to the  $[\text{HRh}(\text{CO})(\text{PPh}_3)_3]$  precursor could be observed over a range of temperatures (298–378 K). Strikingly, addition of **1** (1 equiv.) to  $[\text{HRh}(\text{CO})(\text{PPh}_3)_3]$  precludes the formation of the expected monosubstituted species  $[\text{HRh}(\text{CO})(\text{PPh}_3)_2(\mathbf{1})]$ , and a mixture consisting of  $[\text{HRh}(\text{CO})(\mathbf{1})_3]$  and  $[\text{HRh}(\text{CO})(\text{PPh}_3)_3]$  is formed instead, as evidenced by the NMR spectroscopic studies. This observation can be explained by the stronger  $\sigma$ -donor capacity of **1**, kinetically labilizing the PPh<sub>3</sub> ligands in the intermediate species  $[\text{HRh}(\text{CO})(\text{PPh}_3)_2(\mathbf{1})]$  and resulting in their rapid dissociation, facilitating the formation of  $[\text{HRh}(\text{CO})(\mathbf{1})_3]$ . In close analogy, monitoring the reaction of  $[\text{HRh}(\text{CO})(\text{PPh}_3)_3]$  with ligand **2** by NMR spectroscopy shows an identical reactivity pattern: reaction of  $[\text{HRh}(\text{CO})(\text{PPh}_3)_3]$  with ligand **2** (3 equiv.) affords, as expected, the trisubstituted  $[\text{HRh}(\text{CO})(\mathbf{2})_3]$  product with concomitant PPh<sub>3</sub> elimination. The rhodium-bound hydride shows a resonance signal at  $\delta = -9.68$  ppm (d, <sup>1</sup>J<sub>H,Rh</sub> = 5.2 Hz, 1 H) with no <sup>31</sup>P coupling, evidencing again complete substitution of PPh<sub>3</sub>. Correspondingly, the <sup>29</sup>Si{<sup>1</sup>H} NMR spectrum exhibits a clean doublet resonance signal at  $\delta = 106.0$  ppm (d, <sup>1</sup>J<sub>Si,Rh</sub> = 72.0 Hz) in C<sub>6</sub>D<sub>6</sub>. As before, the observation of only one doublet resonance signal suggests equatorial substitution in the trigonal-bipyramidal geometry around the Rh centre or Berry pseudorotation. The reaction of



Scheme 3. Reactivity of the NHSi ligand **1** towards  $[\text{HRh}(\text{CO})(\text{PPh}_3)_3]$ . Analogous products were obtained for the NHSi ligand **2**, detected by means of multinuclear NMR spectroscopy.

$[\text{HRh}(\text{CO})(\text{PPh}_3)_3]$  with only 1 equiv. of **2** yields a mixture of unreacted  $[\text{HRh}(\text{CO})(\text{PPh}_3)_3]$  with  $[\text{HRh}(\text{CO})(\mathbf{2})_3]$ , with no sign of the expected intermediate  $[\text{HRh}(\text{CO})(\text{PPh}_3)_2(\mathbf{2})]$ . Our efforts to isolate the  $[\text{HRh}(\text{CO})(\mathbf{1})_3]$  and  $[\text{HRh}(\text{CO})(\mathbf{2})_3]$  complexes failed, because the eliminated  $\text{PPh}_3$  could not be completely removed, even after several recrystallization procedures.

We compared the activity and selectivity of the in-situ-generated NHSi–rhodium complexes  $[\text{HRh}(\text{CO})(\mathbf{1})_3]$  and  $[\text{HRh}(\text{CO})(\mathbf{2})_3]$  with that of the phosphine-modified rhodium precursor  $[\text{HRh}(\text{CO})(\text{PPh}_3)_3]$  in the hydroformylation of styrene at 30 bar syngas pressure at 50 and 80 °C, respectively. In Figure 1, the conversion  $X$  of the hydroformylation reaction is plotted against the reaction time reflecting these catalyst runs. At both reaction temperatures, the unmodified precursor complex  $[\text{HRh}(\text{CO})(\text{PPh}_3)_3]$  is more active than the NHSi-modified rhodium complexes  $[\text{HRh}(\text{CO})(\mathbf{1})_3]$  and  $[\text{HRh}(\text{CO})(\mathbf{2})_3]$ , respectively. However, the linear/branched ( $l/b$ ) selectivity ratios of all catalysts are comparable. Additionally, we tested the unmodified  $[\text{Rh}(\text{CO})_2(\text{acac})]$  catalyst at 50 °C and 30 bar syngas pressure. As expected, the unmodified catalyst shows the highest conversion, because there is no ligand preventing the styrene coordination. According to the literature, the  $l/b$  ratio of the unmodified catalyst is rather low ( $l/b = 16:84$ ) and comparable with that of the modified ones.<sup>[32]</sup>

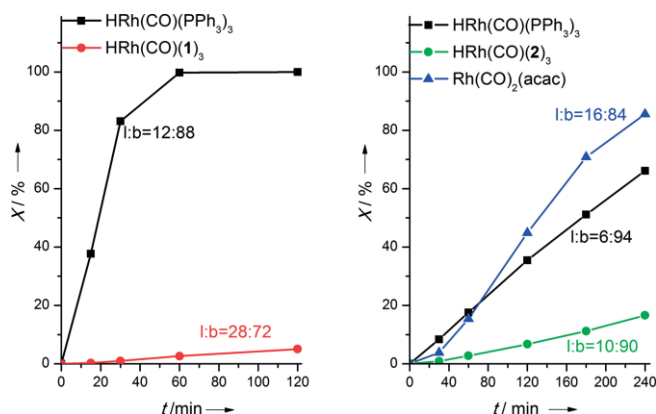


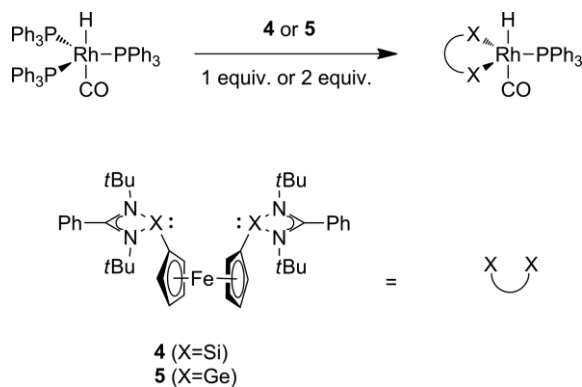
Figure 1. Hydroformylation with  $[\text{HRh}(\text{CO})(\text{PPh}_3)_3]$ ,  $[\text{HRh}(\text{CO})(\mathbf{1})_3]$ ,  $[\text{HRh}(\text{CO})(\mathbf{2})_3]$  and  $[\text{Rh}(\text{CO})_2(\text{acac})]$  at 80 °C (left) and 50 °C (right). Reaction conditions: 40 g of toluene,  $n_{\text{styrene}} = 38$  mmol,  $n_{\text{Rh}} = 0.01$  mmol,  $n_1 = 4$  equiv.,  $n_2 = 3$  equiv.,  $p = 30$  bar, stirrer speed = 1200 rpm. The conversion  $X$  and  $l/b$  ratios were determined by GC-FID.

The low activity of the in-situ-generated NHSi–rhodium complexes  $[\text{HRh}(\text{CO})(\mathbf{1})_3]$  and  $[\text{HRh}(\text{CO})(\mathbf{2})_3]$  is potentially due to the

increased  $\sigma$ -donor strength of the NHSi ligands, compared with that of TPP, which reduces their overall activity compared with  $[\text{HRh}(\text{CO})(\text{PPh}_3)_3]$ . On the one hand, the formation of the active 16-valence-electron rhodium complex by de-coordination of an NHSi ligand might be hindered, because of the strong dative  $\text{Si} \rightarrow \text{Rh}$  bond. On the other hand, the coordination-insertion step of styrene to the rhodium centre, which is the initial step of the catalytic cycle,<sup>[32,33]</sup> was found to be rate-determining for electron-donating monodentate ligands.<sup>[13]</sup> Probably, the strong  $\sigma$ -donor capacity of the NHSi ligands hampers styrene coordination, leading to deleterious catalytic performance. Moreover, the sterically demanding *tert*-butyl groups in both ligands **1** and **2** might also hinder the styrene coordination, decreasing the activity in hydroformylation.

Clearly, the monodentate NHSi ligands decelerate the reaction rate of the rhodium-catalysed hydroformylation, in part due to the full substitution observed in the NMR spectroscopic studies (see above). To avoid the formation of a trisubstituted and kinetically inert NHSi–rhodium complex, we next envisaged the use of a bidentate NHSi ligand. We reasoned that the use of such a ligand might preclude trisubstitution of the  $\text{PPh}_3$  ligands, as observed with the monodentate ligands, affording a complex of the type  $[\text{HRh}(\text{CO})(\text{PPh}_3)(\kappa^2\text{-L}_2)]$  ( $\text{L}_2 = \text{bis-NHSi ligand}$ ). This should enhance the catalytic activity, since the higher  $\sigma$ -donor capacity of the bidentate ligand, in turn, facilitates the dissociation of the remaining  $\text{PPh}_3$  ligand and thereby promotes coordination of the substrate. For this purpose, we decided to employ the bidentate ligand **4** (Scheme 1), linked with a ferrocenediyl bridge, which was previously synthesized in our group.<sup>[31]</sup> To compare the catalytic activity, we decided to include the analogous bis-germylene ligand (bis-NHGe) **5** (Scheme 1) in our investigations and to compare them with the ability of the bidentate phosphine xantphos (**3b**; Scheme 1), typically employed in Rh-mediated hydroformylation. Furthermore, we tested DPPF (**3a**; Scheme 1) as a ligand, because its backbone is the same as those of ligands **4** and **5**.

The coordination behaviour of diphosphines is well known and has been investigated in detail.<sup>[34]</sup> To understand the coordination behaviour of the related bis-NHSi–Rh and bis-NHGe–Rh complexes, we performed several NMR spectroscopic experiments as before with the monodentate ligands **1** and **2**. These studies categorically show that the bidentate ligands **4** and **5** form the desired and expected complexes  $[\text{HRh}(\text{CO})(\text{PPh}_3)(\kappa^2\text{-4})]$  and  $[\text{HRh}(\text{CO})(\text{PPh}_3)(\kappa^2\text{-5})]$  by the substitution process shown in Scheme 4.



Scheme 4. Coordination behaviour of the bis-NHSi (**4**) and -NHGe (**5**) ligands with the rhodium precursor  $[\text{HRh}(\text{CO})(\text{PPh}_3)_3]$ .

Even with an excess of the ligands **4** and **5**, the same products were afforded with unreacted bidentate **4** and **5** present. In the case of  $[\text{HRh}(\text{CO})(\text{PPh}_3)(\kappa^2\text{-4})]$ , an NMR spectroscopic experiment with a ratio of  $[\text{HRh}(\text{CO})(\text{PPh}_3)_3]/\mathbf{4} = 1:1$  showed the clean formation of  $[\text{HRh}(\text{CO})(\text{PPh}_3)(\kappa^2\text{-4})]$  with a characteristic signal of the hydride ligand in the  $^1\text{H}$  NMR spectrum ( $[\text{D}_8]\text{THF}$ ) at  $\delta = -9.43$  ppm, which appears as a triplet resonance signal (two overlapping doublets;  $^1J_{\text{H,Rh}}$  and  $^2J_{\text{H,P}} = 11.4$  Hz), in accordance with the expectations for  $[\text{HRh}(\text{CO})(\text{PPh}_3)(\kappa^2\text{-4})]$ . Moreover, the  $^{31}\text{P}\{^1\text{H}\}$  NMR spectrum shows a doublet resonance signal at  $\delta = 44.7$  ppm (d,  $^1J_{\text{P,Rh}} = 98.7$  Hz), providing further evidence of the fact that one  $\text{PPh}_3$  ligand is still bound to the Rh centre. In close analogy, NMR spectroscopic experiments of  $[\text{HRh}(\text{CO})(\text{PPh}_3)_3]$  with the bidentate NHGe ligand **5** in a 1:1 ratio revealed a similar picture: in the  $^1\text{H}$  NMR spectrum ( $\text{C}_6\text{D}_6$ ), the hydride ligand resonates as a quintet signal at  $\delta = -9.91$  ppm ( $^1J_{\text{H,Rh}} = 10.4$ ,  $^2J_{\text{H,P}} = 5.0$  Hz), whilst in the  $^{31}\text{P}\{^1\text{H}\}$  spectrum, a new signal, corresponding to  $[\text{HRh}(\text{CO})(\text{PPh}_3)(\kappa^2\text{-5})]$ , is seen at  $\delta = 49.7$  ppm (d,  $^1J_{\text{P,Rh}} = 164.2$  Hz), along with concomitantly liberated  $\text{PPh}_3$ . The attempted crystallization of  $[\text{HRh}(\text{CO})(\text{PPh}_3)(\kappa^2\text{-3b/4/5})]$  for single-crystal X-ray diffraction analysis failed, due to the inability to remove triphenylphosphine, despite several procedures.

Hydroformylation reactions were again carried out with in situ-generated  $[\text{HRh}(\text{CO})(\text{PPh}_3)(\kappa^2\text{-4})]$  and  $[\text{HRh}(\text{CO})(\text{PPh}_3)(\kappa^2\text{-5})]$  and compared with the benchmark systems  $[\text{HRh}(\text{CO})(\text{PPh}_3)(\kappa^2\text{-3a/3b})]$ . Interestingly, there are clear differences in the catalytic performance of the four bidentate ligands, as shown in Table 1. As expected, the bis-NHSi complex  $[\text{HRh}(\text{CO})(\text{PPh}_3)(\kappa^2\text{-4})]$  is the most active catalyst at all temperatures. Due to the enhanced  $\sigma$ -donor ability of the bis-NHSi ligand, the electron density at the metal centre is increased, facilitating the dissociation of  $\text{PPh}_3$  and stabilizing the active rhodium complex. The enhanced  $\sigma$ -donor strength of the bidentate NHSi ligands, compared with the analogous bidentate phosphines, was clearly shown in the literature for iridium<sup>[35]</sup> and most recently also for nickel complexes.<sup>[27]</sup> However, it is not only its strong  $\sigma$ -donor ability that causes the high activity of  $[\text{HRh}(\text{CO})(\text{PPh}_3)(\kappa^2\text{-4})]$ , but also its ability to act as a  $\pi$ -acceptor, which accelerates the hydride-migration step. The  $\pi$ -acceptor properties of NHSi ligands of this type have been documented in the literature.<sup>[28,36]</sup> Hence,  $[\text{HRh}(\text{CO})(\text{PPh}_3)(\kappa^2\text{-4})]$  is more ac-

tive, and we achieve a higher conversion and higher turnover frequencies (TOFs) than with the catalysts  $[\text{HRh}(\text{CO})(\text{PPh}_3)(\kappa^2\text{-3a/3b})]$  and the Ge analogue  $[\text{HRh}(\text{CO})(\text{PPh}_3)(\kappa^2\text{-5})]$ . Furthermore, because of the structural similarity of ligands **3a**, **4** and **5** due to their ferrocenediyl bridge, the electronic properties, particularly the  $\sigma$ -donor/ $\pi$ -acceptor properties of the ligand, play the major role concerning the different activities. Surprisingly, employing  $[\text{HRh}(\text{CO})(\text{PPh}_3)(\kappa^2\text{-5})]$  as a potential precatalyst, the hydroformylation is hampered, and almost no product formation is observed. Similar results have been shown in cobalt-mediated [2+2+2] cycloaddition with the same ligands **4** and **5**.<sup>[31]</sup> Consequently, the activity of the respective  $[\text{HRh}(\text{CO})(\text{PPh}_3)(\text{L}_2)]$  complexes increases in the following order for the bidentate ligands,  $\text{L}_2$ :



Table 1. Conversion  $X$ ,  $l/b$  ratio and turnover frequency of the hydroformylation with  $[\text{HRh}(\text{CO})(\text{PPh}_3)(\text{L}_2)]$  complexes containing bidentate ligands  $\text{L}_2$  at different temperatures. Reaction conditions: 40 g of toluene,  $n_{\text{styrene}} = 38$  mmol,  $n_{\text{Rh}} = 0.01$  mmol,  $n_{\text{ligand}} = 3$  equiv.,  $p = 30$  bar, stirrer speed = 1200 rpm. The conversion  $X$ ,  $l/b$  ratio and the TOF were determined by GC-FID.

Ligand $\text{L}_2$	$T$ [°C]	Conversion $X$ <sup>[a]</sup> [%]	$l/b$ ratio	TOF <sup>[b]</sup> [ $\text{h}^{-1}$ ]
<b>3a</b>	50	traces	–	3.0
<b>3b</b>	50	2.2	43:57	32
<b>4</b>	50	10	16:84	83
<b>5</b>	50	traces	–	1.1
<b>3a</b>	80	3.9	34:66	91
<b>3b</b>	80	29	47:53	650
<b>4</b>	80	99	12:88	2600
<b>3a</b>	100	13	35:65	590
<b>3b</b>	100	56	49:51	3000
<b>4</b>	100	100	25:75	9100
<b>5</b>	100	2.2	14:86	100

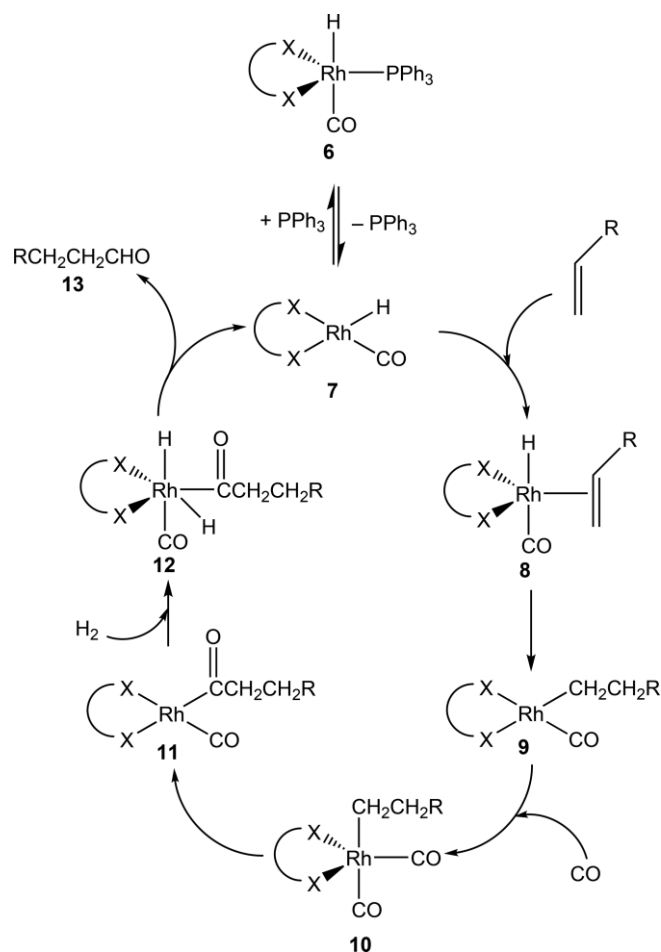
[a] Determined at 50 °C after 240 min, at 80 °C after 120 min and at 100 °C after 60 min. [b] Determined at 50 °C after 60 min, at 80 °C after 30 min and at 100 °C after 10 min.

Moreover, some results concerning the selectivity of the styrene hydroformylation are worth noting. Firstly, the linear/branched ratio increases by raising the temperature for all the catalysts employed. According to the literature, the formation of the alkyl–rhodium bond is crucial for the selectivity, and this step becomes reversible at higher temperatures, which leads to a higher  $l/b$  ratio at high temperatures.<sup>[37,38]</sup> The bite angle of the formed complex and the steric hindrance are the crucial parameters for the  $l/b$  selectivity of bidentate ligands. Comparing the applied bidentate ligands, the  $l/b$  selectivity increases in the following order:



Obviously, the benchmark xantphos system has the best steric conditions to increase the formation of the linear product. Interestingly, although the ligands **3a**, **4** and **5** are structurally similar, due to their ferrocenediyl-bridge backbones, the  $l/b$  selectivity differs. Presumably, the sterically demanding *tert*-butyl groups at the NHSi and NHGe ligands, compared with the phenyl group in DPPF, also affect the  $l/b$  selectivity of the reaction.

The general catalytic cycle of the rhodium-catalysed hydroformylation is well established and consistent with the experi-



Scheme 5. Proposed catalytic cycle for the hydroformylation with bidentate ligands bearing two donor atoms X (X = P, Si), leading to the major branched product. The same numbering scheme of the intermediates is employed as in Figure 2.

mental and theoretical data.<sup>[39,40]</sup> Scheme 5 illustrates the proposed catalytic cycle for the hydroformylation of alkenes with diphosphine ligands. Starting from the trigonal-bipyramidal hydride species **6**, which is an 18-valence-electron rhodium complex generated in situ, the formation of the active complex **7** is initiated by dissociation of a PPh<sub>3</sub> ligand. The  $\pi$ -coordination of the alkene substrate to the unsaturated rhodium complex **7** results in the formation of **8**, which is converted through the migration of the hydride into the corresponding rhodium-alkyl complex **9**. After the coordination of an additional CO molecule to give **10**, the insertion of CO into the rhodium-alkyl bond affords the rhodium-acyl complex **11**. Finally, the coordination of hydrogen, resulting in complex **12**, a reductive elimination step, generates the aldehyde, along with the regeneration of the active 16-valence-electron hydrido-rhodium complex **7**.

To gain further insight into the catalytic process facilitated by rhodium complexes supported by the bis-NHSi ligand **4**, we performed density functional theory (DFT) calculations at the  $\omega$ B97X-D/cc-pVTZ(-PP)(SMD=toluene)//B97-D/6-31G(d)[Rh:cc-pVTZ-PP] level; these calculations have been previously successfully applied to explore the reactivity of transition-metal-silylene complexes.<sup>[27,41,42]</sup> We wanted to show that employing **4** is energetically more favourable than using the benchmark ligand xantphos (**3b**) and that it is easier to form the branched product than the linear, as we observed experimentally (see above). The calculated reaction profiles revealed that the general rhodium hydroformylation mechanism applies to Rh complexes supported by both **3b** and **4**, using styrene as the substrate (Scheme 5). Moreover, it is clearly visible that the styrene hydroformylation, catalysed by [HRh(CO)(PPh<sub>3</sub>)( $\kappa^2$ -**4**)], proceeds along a pathway notably lower in energy than that of [HRh(CO)(PPh<sub>3</sub>)( $\kappa^2$ -**3b**)] (Figure 2).

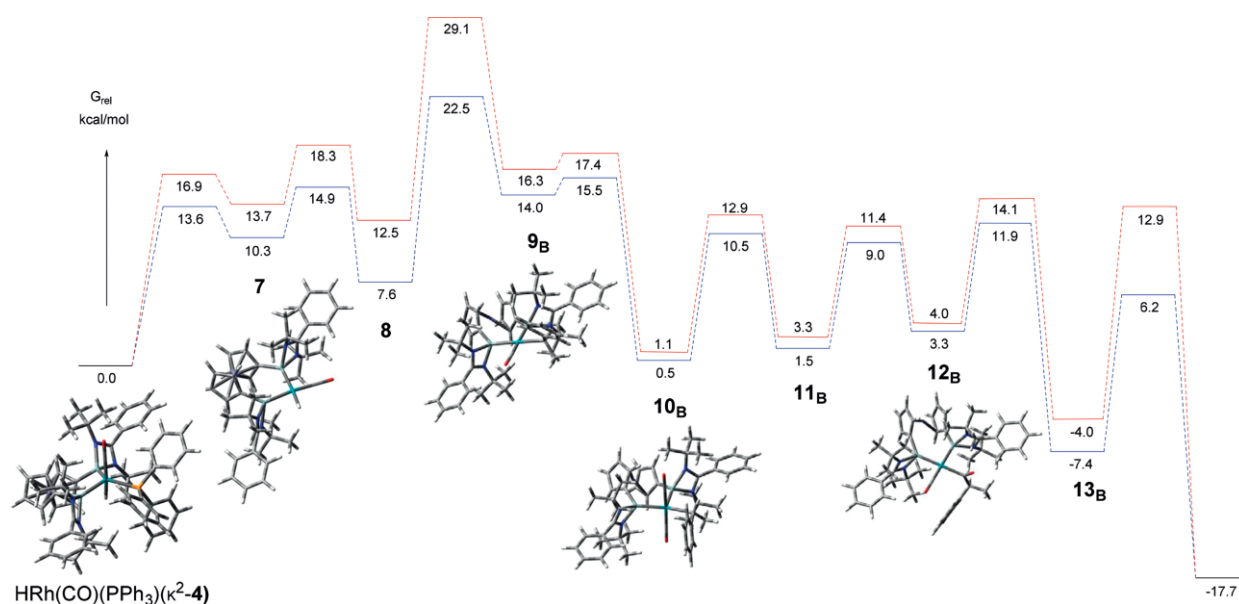


Figure 2. Reaction profile of the full catalytic process with the bidentate ligands **3b** and **4**, respectively. The red line is for [HRh(CO)(PPh<sub>3</sub>)( $\kappa^2$ -**3b**)], and the blue line is for [HRh(CO)(PPh<sub>3</sub>)( $\kappa^2$ -**4**)], the latter clearly following a slightly lower energy pathway. Selected intermediates (**7**, **9**, **10**, **12**) along the catalyst pathway for the [HRh(CO)(PPh<sub>3</sub>)( $\kappa^2$ -**4**)] precursor are shown.

The results from the DFT calculations further indicate that the formation of the active Rh complex **7** is energetically more favourable in the presence of NHSi **4** than that of xantphos (**3b**). The activation barrier leading to **7** is only 13.6 kcal mol<sup>-1</sup> for [HRh(CO)(PPh<sub>3</sub>)(κ<sup>2</sup>-**4**)], while it is 16.9 kcal mol<sup>-1</sup> for [HRh(CO)(PPh<sub>3</sub>)(κ<sup>2</sup>-**3b**)]. This 3.3 kcal mol<sup>-1</sup> difference can be attributed to the stronger σ-donor strength of the NHSi, and it can result in a higher concentration of the catalytically active Rh-silylene species, which might be one cause of the experimentally observed higher TOF (see above). The calculations also suggest that the hydride migration (**8** → **9**) is the rate-determining step of the catalytic cycle. The relative activation barrier of the hydride-migration step, which leads to the linear product, is 16.7 kcal mol<sup>-1</sup> for the phosphine ligand, while it is 16.0 kcal mol<sup>-1</sup> for the silylene ligand, relative to the previous intermediate. The same relative activation barrier of the hydride-migration step that leads to the branched product is 16.6 kcal mol<sup>-1</sup> for the phosphine ligand, while it is 14.9 kcal mol<sup>-1</sup> for the silylene ligand. These results confirm that the formation of the branched product is definitely more favourable than that of the linear, as the barrier is 1.1 kcal mol<sup>-1</sup> lower for the branched version in the case of the silylene ligand. This is in very good agreement with the experimental results, which suggests a 12:88 ratio in favour of the branched product. The 1.1 kcal mol<sup>-1</sup> barrier difference can be translated into a 4.8 times faster reaction rate in the case of the branched product (see details in the Supporting Information), which means a 17:83 product ratio in favour of the branched product at 80 °C. For the phosphine ligand, the relative activation-barrier difference for the hydride-migration step is only 0.1 kcal mol<sup>-1</sup>, which still suggests minor favouring of the branched product. Using similar reaction-rate considerations, as we just used for the silylene ligand, we can calculate a 46:54 ratio in favour of the branched product. This is also in very good agreement with the experimentally observed 47:53 ratio at 80 °C. We can also compare the relative activation-energy barrier of the phosphine and silylene ligands, which leads to the same product. For the branched product, which is the major product, this activation-energy barrier difference is 1.7 kcal mol<sup>-1</sup>. Using this, the relative reaction rate can be estimated (see details in Supporting Information), which gives a rate 11.2 times faster for the silylene ligand. This is higher than the experimentally observed rate, which had only a four times larger TOF at 80 °C; however, considering the error associated with DFT calculations, this is still a good qualitative agreement, which provides another good explanation for the higher reaction rate.

## Conclusion

The results presented here reveal the suitability of bis-NHSi ligands for the catalytic hydroformylation of alkenes. Probably, due to their enhanced σ-donor/π-acceptor properties, the activity is significantly higher than for the diphosphines DPPF and xantphos, but the *l/b* selectivity ratio is lower, due to the structural difference of the NHSi ligand. In contrast to bidentate silylene ligands, the monodentate ones hamper the hydroformylation of styrene, probably due to the formation of a fully substi-

tuted rhodium complex. We are currently investigating this process further, in particular, using other bis-NHSi ligands and other substrates, and we will report on these endeavours in due course.

## Experimental Section

**General:** All experiments were carried out under dry oxygen-free nitrogen using standard Schlenk techniques. Solvents were dried by standard methods and were freshly distilled and degassed prior to use. NMR spectra were recorded with Bruker spectrometers (AV400 or AV200) referenced to residual solvent signals as internal standards {<sup>1</sup>H NMR: [D<sub>6</sub>]benzene, δ = 7.15 ppm; [D<sub>8</sub>]THF, δ = 3.58 ppm (left signal); <sup>13</sup>C{H} NMR: [D<sub>6</sub>]benzene, δ = 128.0 ppm; [D<sub>8</sub>]THF, δ = 67.6 ppm (left signal)} or with an external standard (SiMe<sub>4</sub> for <sup>29</sup>Si NMR). Concentrated solutions of samples were sealed in a Young-type NMR tube for measurements. The NHSi ligands were prepared according to literature procedures, and, unless otherwise stated, general Schlenk and glove-box techniques were used throughout.<sup>[21,29,31]</sup> The rhodium precursor [HRh(CO)(PPh<sub>3</sub>)<sub>3</sub>] and the bidentate ligands 4,5-bis(diphenylphosphino)-9,9-dimethylxanthene (xantphos; purity 97 %) and 1,1'-bis(diphenylphosphino)ferrocene (dppf; purity 97 %) were obtained from Sigma-Aldrich and used without further purification. The synthesis gas (1:1 mixture by volume of CO/H<sub>2</sub>) was acquired from AIR Liquide. These chemicals are used without further purification. Styrene was purified by passage through activated alumina and was degassed three times by freeze-pump-thaw cycles and stored over molecular sieves for use. Toluene was freshly distilled from sodium and collected prior to use. The analytical standards 2-phenylpropionaldehyde (purity 98 %) and 3-phenylpropionaldehyde (purity 95 %) were obtained from Sigma-Aldrich to calibrate the gas chromatograph.

### NMR Spectroscopic Experiments of [HRh(CO)(PPh<sub>3</sub>)<sub>3</sub>] + Ligand

**1:** In a glove box, [HRh(CO)(PPh<sub>3</sub>)<sub>3</sub>] and ligand **1** were combined in a 1:3 ratio and [D<sub>6</sub>]benzene (0.5 mL) was added, affording a yellow solution. The NMR spectra indicated selective formation of the complex [HRh(CO)(**1**)<sub>3</sub>]. After the NMR spectra had been recorded, an ESI mass spectrum was also recorded, showing selective formation of the trisubstituted product. <sup>1</sup>H NMR (200 MHz, [D<sub>6</sub>]benzene, 298 K): δ = -10.45 (d, <sup>1</sup>J<sub>H,Rh</sub> = 9.2 Hz, 1 H) (no P coupling visible), 1.14 (s, 18 H, 6 *H*-Me), 1.43 (s, 54 H, 6 *H*-*t*Bu-N), 6.94–6.97 (m, 15 H, 3 *H*-Ph), 7.03–7.05 (m, 45 H, *H*-PPh<sub>3</sub>) ppm. <sup>31</sup>P NMR (81 MHz, [D<sub>6</sub>]benzene, 298 K): δ = -5.3 (s, *P*-PPh<sub>3</sub>) (exclusively free PPh<sub>3</sub>, no other resonance signals visible) ppm. <sup>29</sup>Si NMR (79 MHz, [D<sub>6</sub>]benzene, 298 K): δ = 62.8 (d, <sup>1</sup>J<sub>Si,Rh</sub> = 80.4 Hz) (no P coupling visible) ppm. ESI-MS (toluene): calcd. for [M]<sup>+</sup> 1042.5503, found 1042.5480; calcd. for [M - SiNMe<sub>2</sub>]<sup>+</sup> 738.3338, found 738.3333; calcd. for [free ligand + H]<sup>+</sup> 304.2159, found 304.2201. Repeated experiments of [HRh(CO)(PPh<sub>3</sub>)<sub>3</sub>] with ligand **1** in a 1:1 ratio showed the formation of the trisubstituted product [HRh(CO)(**1**)<sub>3</sub>], along with unreacted [HRh(CO)(PPh<sub>3</sub>)<sub>3</sub>] and free PPh<sub>3</sub> in the NMR spectra.

### NMR Spectroscopic Experiments of [HRh(CO)(PPh<sub>3</sub>)<sub>3</sub>] + Ligand

**2:** In a glove box, [HRh(CO)(PPh<sub>3</sub>)<sub>3</sub>] and ligand **2** were combined in a 1:3 ratio, and [D<sub>6</sub>]benzene (0.5 mL) was added, affording a light-orange solution. The NMR spectra indicated selective formation of the trisubstituted complex. <sup>1</sup>H NMR (200 MHz, [D<sub>6</sub>]benzene, 298 K): δ = -9.68 (d, <sup>1</sup>J<sub>H,Rh</sub> = 5.2 Hz, 1 H) (no P coupling visible), 1.58 (s, 54 H, 6 *H*-*t*Bu), 6.57 (s, 12 H, 3 CH<sub>2</sub>=CH<sub>2</sub>), 7.03–7.05 (m, 45 H, *H*-PPh<sub>3</sub>) ppm. <sup>31</sup>P NMR (81 MHz, [D<sub>6</sub>]benzene, 298 K): δ = -5.3 (s, *P*-PPh<sub>3</sub>) (exclusively free PPh<sub>3</sub>, no other resonance signals visible) ppm. <sup>29</sup>Si

NMR (79.5 MHz, C<sub>6</sub>D<sub>6</sub>, 298 K):  $\delta$  = 106.0 (d,  $^1J_{Si,Rh}$  = 72.0 Hz) (no P coupling visible) ppm. Repeated experiments of [HRh(CO)(PPh<sub>3</sub>)<sub>3</sub>] and ligand **2** in a 1:1 ratio showed the formation of the trisubstituted product [HRh(CO)(**2**)<sub>3</sub>], along with unreacted [HRh(CO)(PPh<sub>3</sub>)<sub>3</sub>] and free PPh<sub>3</sub> in the NMR spectra.

#### NMR Spectroscopic Experiment of [HRh(CO)(PPh<sub>3</sub>)<sub>3</sub>] + Ligand **4**:

The rhodium precursor [HRh(CO)(PPh<sub>3</sub>)<sub>3</sub>] and ligand **4** were dissolved in [D<sub>6</sub>]benzene (0.5 mL) in a 1:1 ratio and transferred to an NMR tube. A light-orange colour was noticed immediately. The NMR spectra showed selective formation of the product [HRh(CO)-(PPh<sub>3</sub>)<sub>2</sub>( $\kappa^2$ -**4**)]. <sup>1</sup>H NMR (200 MHz, [D<sub>8</sub>]THF, 298 K):  $\delta$  = -9.43 (pseudo-t,  $^1J_{H,Rh}$  =  $^2J_{H,P}$  = 11.4 Hz, 1 H) (P coupling visible), 0.87 (s, 18 H, 2 *H*-*t*Bu-N), 1.29 (s, 18 H, 2 *H*-*t*Bu-N), 4.15 (m, 8 H, 4 *H*-ferrocene), 7.03–7.70 (m, 55 H, *H*-PPh<sub>3</sub> + m, 10 H, *H*-Ph) ppm. <sup>31</sup>P NMR (81 MHz, [D<sub>8</sub>]THF, 298 K):  $\delta$  = -5.4 (s, *P*-PPh<sub>3</sub>) (free ligand), 44.7 (d,  $^1J_{P,Rh}$  = 98.7 Hz) ppm. Repeated NMR spectroscopic experiments of [HRh(CO)(PPh<sub>3</sub>)<sub>3</sub>] with excess **4** revealed the formation of [HRh(CO)(PPh<sub>3</sub>)<sub>2</sub>( $\kappa^2$ -**4**)] with unreacted **4** and no other products.

#### NMR Spectroscopic Experiment of [HRh(CO)(PPh<sub>3</sub>)<sub>3</sub>] + Ligand **5**:

The rhodium precursor [HRh(CO)(PPh<sub>3</sub>)<sub>3</sub>] and ligand **5** were dissolved in [D<sub>6</sub>]benzene (0.5 mL) in a 1:1 ratio and transferred to an NMR tube. A light-orange colour was noticed immediately. After the NMR spectra were recorded, an ESI mass spectrum of the mixture was recorded. The NMR spectra showed selective formation of the product [HRh(CO)(PPh<sub>3</sub>)<sub>2</sub>( $\kappa^2$ -**5**)]. <sup>1</sup>H NMR (200 MHz, [D<sub>6</sub>]benzene, 298 K):  $\delta$  = -9.91 (pseudo-q,  $^1J_{H,Rh}$  = 10.4,  $^2J_{H,P}$  = 5.0 Hz, 1 H) (P coupling visible), 0.99 (s, 18 H, 2 *H*-*t*Bu-N), 1.38 (s, 18 H, 2 *H*-*t*Bu-N), 4.47 (br. s, 4 H, 4 *H*-ferrocene), 4.66 (br. s, 4 H, 4 *H*-ferrocene), 7.03–7.05 (m, 30 H, *H*-PPh<sub>3</sub>), 7.34–7.42 (m, 10 H, *H*-Ph) ppm. <sup>31</sup>P NMR (81 MHz, [D<sub>6</sub>]benzene, 298 K):  $\delta$  = -5.4 (s, *P*-PPh<sub>3</sub>) (free ligand), 49.7 (d,  $^1J_{P,Rh}$  = 164.2 Hz) ppm. ESI-MS (toluene): calcd. for [M]<sup>+</sup> 1186.2119, found 1186.2065; calcd. for [M - CO + H]<sup>+</sup> 1158.2170, found 1158.2233; calcd. for [M - CO - PPh<sub>3</sub> - H]<sup>+</sup> 898.1249, found 898.1246; calcd. for [free ligand + H]<sup>+</sup> 792.2125; found 792.5467. Repeated NMR spectroscopic experiments of [HRh(CO)(PPh<sub>3</sub>)<sub>3</sub>] with excess **5** revealed the formation of [HRh(CO)(PPh<sub>3</sub>)<sub>2</sub>( $\kappa^2$ -**5**)] with unreacted **5** and no other products.

**Preparation of the Catalyst Reaction Mixture:** The rhodium precursor (0.01 mmol, 9.188 mg, 1 equiv.) and the corresponding ligand were weighed into a 100 mL Schlenk tube in a glovebox. Distilled styrene (0.038 mol, 4.0 g, 3800 equiv.) and distilled toluene (0.434 mol, 40.0 g) were added.

**Experimental Procedure for the Hydroformylation:** A 100 mL stainless-steel autoclave from PREMEX was used to perform the hydroformylation reactions. Before adding the reaction mixture, the autoclave was heated to 110 °C for 1 h, and after that, the reactor was evaporated and flushed with nitrogen three times. Then the autoclave was cooled to reaction temperature, and the reaction mixture was added during a nitrogen counterflow. The mixture was pressurized to 30 bar during stirring at 200 rpm. The consumed gas was readjusted through a mass flow controller to realise isobaric conditions. The reaction was initiated at a stirrer speed of 1200 rpm. Samples were taken, diluted with acetone and analysed by gas chromatography. Gas chromatography analysis was conducted with a Shimadzu GC-2010 gas chromatograph equipped with a flame ionisation detector (FID) and a Supelcowax 10 fused-silica column (30 m × 0.53 mm) × 1 μm film thickness. The temperature programme for the column was: 140 °C (5 min),  $\Delta T$  = 15 °C min<sup>-1</sup> to 200 °C (5 min). The temperature of the injector was 220 °C, that of the detector was 270 °C. The split ratio was 30:1. Nitrogen was used as carrier gas, with a flow rate of 3 mL min<sup>-1</sup>. For further details, see the Supporting Information.

**DFT Calculations:** DFT calculations were performed at the  $\omega$ B97X-D/cc-pVTZ(-PP)(SMD=toluene)//B97-D/6-31G(d)[Rh:cc-pVTZ-PP] level of theory.<sup>[43–48]</sup> Stationary points on the potential energy surface (PES) were characterized by harmonic vibrational frequency calculations. The temperature was set to the experimentally applied 353 K. Calculations were carried out using the Gaussian 09 program. Further details are described in the Supporting Information.

## Acknowledgments

Financial support by the Deutsche Forschungsgemeinschaft (Cluster of Excellence UniCat, ExIn 314-2 and Collaborative Research Center/Transregio 63 “Integrated Chemical Processes in Liquid Multiphase Systems”) is gratefully acknowledged.

**Keywords:** Hydroformylation · Homogeneous catalysis · Silicon · Ferrocene ligands · Germlyenes

- [1] B. Cornils, W. A. Herrmann, M. Rasch, *Angew. Chem. Int. Ed. Engl.* **1994**, *33*, 2144–2163; *Angew. Chem.* **1994**, *106*, 2219.
- [2] R. Franke, D. Selent, A. Börner, *Chem. Rev.* **2012**, *112*, 5675–5732.
- [3] M. Beller, B. Cornils, C. D. Frohning, C. W. Kohlpaintner, *J. Mol. Catal. A* **1995**, *104*, 17–85.
- [4] A. Gual, C. Godard, S. Castellón, C. Claver, *Tetrahedron: Asymmetry* **2010**, *21*, 1135–1146.
- [5] J. T. Carlock, *Tetrahedron* **1984**, *40*, 185–187.
- [6] V. K. Srivastava, R. S. Shukla, H. C. Bajaj, R. V. Jasra, *Appl. Catal. A* **2005**, *282*, 31–38.
- [7] A. M. Trzeciak, J. J. Ziółkowski, *J. Mol. Catal.* **1986**, *34*, 213–219.
- [8] P. W. N. M. van Leeuwen, C. F. Roobeek, *J. Organomet. Chem.* **1983**, *258*, 343–350.
- [9] M. L. Clarke, D. Ellis, K. L. Mason, A. G. Orpen, P. G. Pringle, R. L. Wingard, D. A. Zaher, R. T. Baker, *Dalton Trans.* **2005**, 1294.
- [10] A. Van Rooy, J. N. H. de Bruijn, K. F. Roobeek, P. C. J. Kamer, P. W. N. M. van Leeuwen, *J. Organomet. Chem.* **1996**, *507*, 69–73.
- [11] R. L. Pruet, J. A. Smith, *J. Org. Chem.* **1969**, *34*, 327–330.
- [12] C. A. Tolman, *J. Am. Chem. Soc.* **1969**, *91*, 2953–2956.
- [13] M. Sparta, K. J. Børve, V. R. Jensen, *J. Am. Chem. Soc.* **2007**, *129*, 8487–8499.
- [14] P. C. J. Kamer, P. W. N. M. van Leeuwen, J. N. H. Reek, *Acc. Chem. Res.* **2001**, *34*, 895–904.
- [15] P. W. N. M. van Leeuwen, P. C. J. Kamer, J. N. H. Reek, P. Dierkes, *Chem. Rev.* **2000**, *100*, 2741–2769.
- [16] M. Kranenburg, Y. E. M. van der Burgt, P. C. J. Kamer, P. W. N. M. van Leeuwen, *Organometallics* **1995**, *14*, 3081–3089.
- [17] G. K. Ramollo, M. J. López-Gómez, D. C. Liles, L. C. Matsinha, G. S. Smith, D. I. Bezuidenhout, *Organometallics* **2015**, *34*, 5745–5753.
- [18] W. Gil, A. M. Trzeciak, *Coord. Chem. Rev.* **2011**, *255*, 473–483.
- [19] A. C. Chen, L. Ren, A. Decken, C. M. Crudden, *Organometallics* **2000**, *19*, 3459–3461.
- [20] M. Bortenschlager, J. Schütz, D. von Preysing, O. Nuyken, W. A. Herrmann, R. Weberskirch, *J. Organomet. Chem.* **2005**, *690*, 6233–6237.
- [21] M. Denk, R. Lennon, R. Hayashi, R. West, A. V. Belyakov, H. P. Verne, A. Haaland, M. Wagner, N. Metzler, *J. Am. Chem. Soc.* **1994**, *116*, 2691–2692.
- [22] M. Haaf, T. A. Schmedake, R. West, *Acc. Chem. Res.* **2000**, *33*, 704–714.
- [23] N. J. Hill, R. West, *J. Organomet. Chem.* **2004**, *689*, 4165–4183.
- [24] B. Blom, D. Gallego, M. Driess, *Inorg. Chem. Front.* **2014**, *1*, 134.
- [25] B. Blom, M. Stoelzel, M. Driess, *Chem. Eur. J.* **2013**, *19*, 40–62.
- [26] S. Raoufoghaddam, Y.-P. Zhou, Y. Wang, M. Driess, *J. Organomet. Chem.*, *10.1016/j.jorganchem.2016.07.014*.
- [27] Y.-P. Zhou, S. Raoufoghaddam, T. Szilvási, M. Driess, *Angew. Chem. Int. Ed.* **2016**, *55*, 12868–12872; *Angew. Chem.* **2016**, *128*, 13060.
- [28] T. Schmedake, M. Haaf, B. J. Paradise, A. J. Millevolte, D. R. Powell, R. West, *J. Organomet. Chem.* **2001**, *636*, 17–25.
- [29] C. W. So, H. W. Roesky, P. M. Gurubasavaraj, R. B. Oswald, M. T. Gamer, P. G. Jones, S. Blaurock, *J. Am. Chem. Soc.* **2007**, *129*, 12049–12054.

- [30] Z. Benedek, T. Szilvási, *RSC Adv.* **2015**, *5*, 5077–5086.
- [31] W. Wang, S. Inoue, S. Enthaler, M. Driess, *Angew. Chem. Int. Ed.* **2012**, *51*, 6167–6171; *Angew. Chem.* **2012**, *124*, 6271–6275.
- [32] J. Feng, M. Garland, *Organometallics* **1999**, *18*, 417–427.
- [33] C. Bergounhou, D. Neibecker, R. Mathieu, *J. Mol. Catal. A* **2004**, *220*, 167–182.
- [34] L. Damoense, M. Datt, M. Green, C. Steenkamp, *Coord. Chem. Rev.* **2004**, *248*, 2393–2407.
- [35] A. Brück, D. Gallego, W. Wang, E. Irran, M. Driess, J. F. Hartwig, *Angew. Chem. Int. Ed.* **2012**, *51*, 11478–11482; *Angew. Chem.* **2012**, *124*, 11645.
- [36] B. Blom, S. Enthaler, S. Inoue, E. Irran, M. Driess, *J. Am. Chem. Soc.* **2013**, *135*, 6703–6713.
- [37] E. Boymans, M. Janssen, C. Müller, M. Lutz, D. Vogt, *Dalton Trans.* **2013**, *42*, 137–142.
- [38] R. Lazzaroni, A. Raffaelli, R. Settambolo, S. Bertozzi, G. Vitulli, *J. Mol. Catal.* **1989**, *50*, 1–9.
- [39] I. Jacobs, B. de Bruin, J. N. H. Reek, *ChemCatChem* **2015**, *7*, 1708–1718.
- [40] I. del Río, O. Pàmies, P. W. N. M. van Leeuwen, C. Claver, *J. Organomet. Chem.* **2000**, *608*, 115–121.
- [41] N. C. Breit, T. Szilvási, T. Suzuki, D. Gallego, S. Inoue, *J. Am. Chem. Soc.* **2013**, *135*, 17958–17968.
- [42] T. T. Metsänen, D. Gallego, T. Szilvási, M. Driess, M. Oestreich, *Chem. Sci.* **2015**, *6*, 7143–7149.
- [43] T. H. Dunning Jr., *J. Chem. Phys.* **1989**, *90*, 1007.
- [44] M. J. Frisch, J. A. Pople, J. S. Binkley, *J. Chem. Phys.* **1984**, *80*, 3265.
- [45] A. D. Becke, *J. Chem. Phys.* **1997**, *107*, 8554.
- [46] S. Grimme, *J. Comput. Chem.* **2006**, *27*, 1787–1799.
- [47] J.-D. Chai, M. Head-Gordon, *Chem. Phys.* **2008**, *10*, 6615–6620.
- [48] K. L. Schuchardt, B. T. Didier, T. Elsethagen, L. Sun, V. Gurumoorathi, J. Chase, J. Li, T. L. Windus, *J. Chem. Inf. Model.* **2007**, *47*, 1045–1052.

---

Received: February 14, 2017

# PAPER 7

## **Palladium catalyzed methoxycarbonylation of 1-dodecene in biphasic systems - Optimization of catalyst recycling**

Marcel Schmidt, Tobias Pogrzeba, Lena Hohl, Ariane Weber, André Kielholz, Matthias Kraume, Reinhard Schomäcker

Molecular Catalysis, 2017, 439, 1-8

Online Article:

<https://www.sciencedirect.com/science/article/pii/S2468823117303218>

Reprinted with permission from “Palladium catalyzed methoxycarbonylation of 1-dodecene in biphasic systems - Optimization of catalyst recycling; Marcel Schmidt, Tobias Pogrzeba, Lena Hohl, Ariane Weber, André Kielholz, Matthias Kraume, Reinhard Schomäcker. Molecular Catalysis, 2017, 439, 1-8.” Copyright (2017) Elsevier B.V.





Research paper

# Palladium catalyzed methoxycarbonylation of 1-dodecene in biphasic systems – Optimization of catalyst recycling



Marcel Schmidt<sup>a,\*</sup>, Tobias Pogrzeba<sup>a</sup>, Lena Hohl<sup>b</sup>, Ariane Weber<sup>a</sup>, André Kielholz<sup>a</sup>, Matthias Kraume<sup>b</sup>, Reinhard Schomäcker<sup>a</sup>

<sup>a</sup> Technische Universität Berlin, Department of Chemistry, Straße des 17. Juni 124, 10623 Berlin, Germany

<sup>b</sup> Technische Universität Berlin, Chair of Chemical and Process Engineering, Ackerstraße 76, 13355 Berlin, Germany

## ARTICLE INFO

## Article history:

Received 12 April 2017

Received in revised form 9 June 2017

Accepted 13 June 2017

Available online 21 June 2017

## Keywords:

Palladium

Hydroesterification

Alkoxy-carbonylation

Biphasic system

Recycling

## ABSTRACT

The palladium catalyzed methoxycarbonylation of long-chain olefin 1-dodecene in a liquid/liquid biphasic system composed of methanol as polar phase and the substrate/product as nonpolar phase is reported. The immobilization of the palladium based catalyst in the methanol phase is affected by the use of the watersoluble ligand SulfoXantPhos and methanesulfonic acid as co-catalyst. We investigated these systems with respect to reaction performance and catalyst recycling by variation of the type and amount of co-solvent in both existing phases. By modifying these systems with a co-solvent, catalyst recycling could be improved compared to the benchmark system without co-solvents to a palladium and phosphorous leaching <1 ppm. The applied homogeneously dissolved palladium catalyst could be quantitatively recycled four times via a simple phase separation without any loss in activity and selectivity.

© 2017 Elsevier B.V. All rights reserved.

## 1. Introduction

The carbonylation of olefins with carbon monoxide and a nucleophile, also known as Reppe carbonylation, is an auspicious tool for upgrading low value feedstocks like olefins and alkynes [1]. If the nucleophile is an alcohol, the reaction is also called hydroesterification or alkoxy-carbonylation and offers an atom efficient access to esters [2]. The functionalized products are of great interest as bulk chemicals in industry as well as in fine chemistry and pharmaceutical industry. Particularly the formation of carboxylic acids from styrene derivatives is an emerging field to produce active pharmaceutical ingredients based on 2-arylpropionic acid like ibuprofen and ketoprofen [3,4]. A commercially implemented process of an alkoxy-carbonylation, known as Lucite or rather Alpha process, is the formation of methyl methacrylate (MMA), an important intermediate for the production of a broad range of polymers such as acrylic glass [5,6].

Since several years the development of new catalytic systems got much effort with the goal to improve the activity and regioselectivity of the carbonylation, especially the methoxycarbonylation, as well as the long term stability of the catalyst. In general, phosphine based palladium complexes with an acid co-catalyst are in the

focus of current research, particularly the influence of monodentate and bidentate phosphine ligands on activity and regioselectivity is being investigated [7–10]. Cole-Hamilton et al. reported the use of bis-(di-*tert*-butylphosphinomethyl)benzene as bidentate ligand for the methoxycarbonylation of different terminal and internal alkenes, which showed a high selectivity towards the linear product [11]. Concerning the type and amount of co-catalyst, similar trends were found for different substrates towards reactivity and stability [12,13]. Acids with non-coordinating counterparts such as methanesulfonic acid (MSA) or *para*-toluenesulfonic acid (p-TSA) lead to a higher catalyst activity due to their reduced ability to coordinate to the metal centre. Additionally, high acid to palladium ratios (in range of 2:1–40:1) lead to an increase in activity and avoid the formation of palladium black due to the reactivation of any occurring Pd(0)-species by the acid during reaction. Moreover, to understand and control the activity and selectivity of the palladium catalyst several studies about the mechanism and kinetics of the carbonylation were done [6,14,15].

Besides the development of new catalytic systems and the understanding of the reaction mechanism, the recycling of the homogeneously dissolved catalyst system plays a crucial role for reaction engineering in terms of green chemistry and sustainability. The difficulty of separating the product and the applied catalyst hampers the commercialization of palladium catalyzed carbonylation in large scale processes. Van Koten et al. have reviewed several approaches to overcome recycling difficulties of alkoxy-

\* Corresponding author.

E-mail address: [marcel.schmidt@tu-berlin.de](mailto:marcel.schmidt@tu-berlin.de) (M. Schmidt).

## Nomenclature

### Greek letter

$\varepsilon$	Turbulence dissipation rate [ $\text{m}^2/\text{s}^3$ ]
$\sigma$	Interfacial tension (liquid/liquid) [ $\text{mN/m}$ ]

### Latin letters

b	Baffle width [m]
c	Baffle thickness [m]
D	Tank diameter [m]
$d_{\text{st}}$	Stirrer diameter [m]
H	Fluid level [m]
h	Stirrer bottom clearance [m]
$h_{\text{st}}$	Height of stirrer blade [m]
n	Rotational speed [rpm]
p	Pressure [bar]
T	Temperature [ $^{\circ}\text{C}$ ]
TOF	Turn over frequency [ $\text{h}^{-1}$ ]
V	Volume [L]
X	Conversion [%]
Y	Yield [%]

carbonylation reactions [16]. On the one hand the immobilization of homogenous catalysts on solid supports is a feasible approach. By a modification of the ligand or the catalyst precursor, the catalyst can be linked to a polymeric or silica based support and thus it can be recycled via simple filtration after the reaction [17–20]. Another possibility to immobilize palladium catalysts is the application of carbon-based graphene-oxide nanosheets as support which has been reported recently together with interesting structural information [21,22]. However, additives like non-coordinated ligand and the acidic co-catalyst, which are both dissolved in the liquid phase, cannot be recycled by this technique. Moreover, the implementation of this recycling strategy in a continuously operated industrial process is challenging due to the filtration step. On the other hand liquid/liquid multiphase systems offer another promising approach for the separation of product and catalyst, which has already been applied in industrial scale processes for several years by now. A representative example is the well-known Ruhrchemie/Rhône-Poulenc process, in which propene is converted to butanal in an aqueous biphasic system [23]. The rhodium catalyst is immobilized in the aqueous phase due to water soluble trisulfonated triphenylphosphine (TPPTS) ligand. The product forms a second phase and can be decanted from the reaction mixture. Inspired by the Ruhrchemie/Rhône-Poulenc process the palladium catalyzed carbonylation in aqueous biphasic systems has been investigated by several groups during the last two decades [13,24–26], mainly with focus on the hydroxycarbonylation reaction due to the presence of water that is required for the applied watersoluble catalyst systems. For the methoxycarbonylation reaction only a few examples for the application in liquid/liquid biphasic systems are known, particularly in thermomorphic multicomponent solvents (TMS) [27–30]. The special feature of these multiphase systems is the temperature induced phase transition. Under reaction conditions, a one phase system can be formed in order to overcome mass transfer limitations which can be switched into a two phase system after the reaction for the catalyst recycling. However, the disadvantages of these systems are the elaborate solvent selection and the use of often environmentally hazardous solvents.

In this study we demonstrate a systematic approach for the application of palladium catalyzed methoxycarbonylation of 1-dodecene in liquid/liquid biphasic systems composed of methanol, a co-solvent and 1-dodecene. We applied a watersoluble bidentate

phosphine ligand in order to recycle the catalyst system within the polar (methanol) phase. The effect of non-toxic co-solvents (both in the polar and nonpolar phase) on the reaction performance and recycling results has been investigated. Furthermore, we studied the physico-chemical properties of the resulting systems, e.g. interfacial tension and droplet size.

## 2. Experimental

### 2.1. Chemicals

The substrate 1-dodecene (94%) and the co-solvents decane (94%) and hexadecane (99%) were purchased from Merck. Octane (98%), dodecane (98%) and tetradecane (92%) were received from ABCR, Fluka and Sigma-Aldrich. The catalyst precursor  $\text{Pd}(\text{OAc})_2$  (99.9%) and the cocatalyst methanesulfonic acid (MSA, 99.5%) were obtained from Sigma-Aldrich. The ligand SulfoXantPhos (SX) was donated by Molisa GmbH. Methanol (99.9%) and water (HPLC grade) were purchased from VWR. The carbon monoxide was received from Air Liquide with a purity of 99.9%. All solvents were degassed with nitrogen before use and all chemicals were used as received without further purification.

### 2.2. Preparation of the catalyst

The catalyst precursor  $\text{Pd}(\text{OAc})_2$  (0.16 mmol, 1 eq.) and the ligand SulfoXantPhos (0.64 mmol, 4 eq.) were evacuated and flushed with argon three times in a Schlenk tube. The degassed polar phase (methanol and water) was added and the reaction mixture was stirred over night. A homogenous green solution indicates the formation of the catalyst complex.

### 2.3. Experimental procedure for methoxycarbonylation

In a typical experiment, the nonpolar phase, consisting of 1-dodecene and the co-solvent, and the co-catalyst (6.4 mmol, 40 eq.) were introduced in a 100 mL stainless steel autoclave, equipped with a gas dispersion stirrer and baffle. After evacuation and flushing with nitrogen (three times) the catalyst mixture was added to the reactor under nitrogen counterflow. The reactor was heated to  $80^{\circ}\text{C}$ , pressurized with carbon monoxide (30 bar) and stirred at 1200 rpm. The pressure was kept constant during the reaction and the gas consumption was measured via a mass flow controller. After 20 h reaction time the reactor was depressurized and cooled down to room temperature, then the reaction mixture was transferred into a graduated cylinder under inert conditions. The phase separation usually completed within 20 min and samples from both resulting phases were taken for further analysis. GC analysis was carried out on a Shimadzu GC2010 Plus with a FID (flame ionization detector) packed with Restek RTX5-MS column ( $30\text{ m} \times 0.25\text{ mm} \times 0.25\text{ }\mu\text{m}$ ). The column is coated with a 5% diphenyl/95% dimethyl polysiloxane phase. Yield and linear to branched ratio of the product was determined via an absolute calibration, no internal standard was used.

### 2.4. Experimental procedure for recycling experiment

For the recycling experiment, 1-dodecene (17.8 mmol, 110 eq.), methanesulfonic acid (6.4 mmol, 40 eq.) and octane (9 g) were introduced into the reactor and the prepared catalyst solution (0.16 mmol  $\text{Pd}(\text{OAc})_2$  and 0.64 mmol SulfoXantPhos in 12 g MeOH) was added under nitrogen counterflow. Then the experiment was prepared following the usual procedure. After 2 h reaction time, the reactor was depressurized and cooled to  $40^{\circ}\text{C}$ . The whole reaction mixture was removed by a syringe under nitrogen counterflow. Phase separation of the reaction mixture inside the syringe has

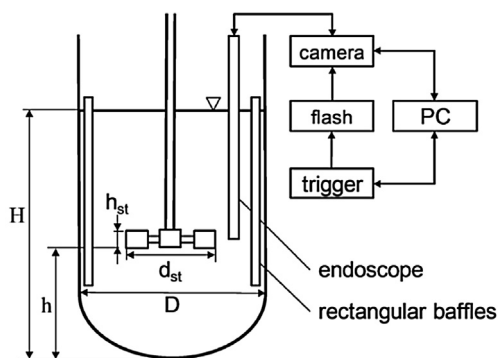


Fig. 1. Stirred tank and endoscope measurement setup.

been awaited for 10 min. Afterwards the polar phase was reinjected into the reactor, the remaining nonpolar phase in the syringe was removed and new 1-dodecene (17.8 mmol) and octane (9 g) was added to the reactor under nitrogen counterflow. The reactor was heated up again to 80 °C and pressurized with carbon monoxide (30 bar) for the second run. This procedure was repeated for the further recycling runs.

### 2.5. Determination of palladium and phosphorous leaching

After completed phase separation, the nonpolar phase was transferred into a round bottom flask and distilled under reduced pressure (3.6 mbar, 180 °C). The residue was digested with 1 mL nitric acid (65 wt%), 3 mL hydrochloric acid (37 wt%) and 2 mL sulfuric acid (96 wt%) and filled up to 20 mL with water (HPLC grade). The solution was analysed via ICP-OES for palladium and phosphorous concentration. The results are stated as amount of palladium and phosphorous in the nonpolar phase denoted in parts per million (ppm).

### 2.6. Determination of the interfacial tension

The interfacial tension  $\sigma$  at the liquid/liquid interface between nonpolar (1-dodecene) and polar (water/methanol) phase was determined via Pendant Drop (Dataphysics OCA15) and Spinning Drop (Dataphysics SVT20) method at  $T = 40$  °C. Spinning Drop measurements were carried out at constant capillary rotation of  $n = 10,000$  rpm.

### 2.7. Determination of the droplet size distribution

Droplet size distribution measurements of the water/methanol/1-dodecene systems were carried out in a stirred tank using an endoscope measurement technique and image analysis (SOPAT GmbH) as depicted in Fig. 1. The double-walled glass tank ( $H = 0.12$  m,  $D = 0.1$  m,  $V = 0.8$  L) was kept at a constant temperature of  $T = 40$  °C using a thermostat. A Rushton turbine ( $d_{st} = 0.05$  m,  $h_{st} = 0.0125$  m,  $h = 0.05$  m) and four rectangular baffles ( $b = 0.007$  m,  $c = 0.001$  m) were used. The endoscope tip was positioned at stirrer height. All drop size measurements

were carried out at a constant stirrer frequency of  $n = 700$  rpm ( $\varepsilon \approx 3.78 \text{ m}^2/\text{s}^3$ ) in steady state. The droplet images were taken using a camera (AVT Prosilica GX2750), stroboscope and trigger box controlled by a computer. Only droplets with nearly spherical shape could be analysed by the automated drop detection software, but the amount of non-spherical droplets that evaded analysis was negligible (less than 1%). Details about the endoscope technique and analysis software and its limitations have been published e.g. by Maaß et al. or Ritter and Kraume [31–33].

## 3. Results and discussion

The methoxycarbonylation of long-chain olefins has been investigated with 1-dodecene as substrate. Both reactants (methanol and 1-dodecene) form an own phase for the liquid/liquid biphasic reaction mixture. As shown in Fig. 2, the methoxycarbonylation generally yields to linear and branched esters. The applied catalyst system consisted of  $\text{Pd}(\text{OAc})_2$  as precursor, methanesulfonic acid (MSA) as co-catalyst and SulfoXantPhos (SX), a watersoluble bidentate ligand introduced by van Leeuwen et al. [34]. Preliminary experiments suggested a molar ratio of  $\text{Pd}:\text{SX}:\text{MSA} = 1:4:40$  to ensure the stability of the catalyst system during the entire reaction time.

If water is available in the reaction mixture it can also act as nucleophile, which leads to the formation of the corresponding linear and branched acid via hydroxycarbonylation reaction. Moreover, the hydrolysis of the ester can lead to the formation of acids as well.

### 3.1. Characteristics of the biphasic system

For a general characterisation of the biphasic liquid/liquid system, the interfacial tension and drop size distributions were determined for different compositions of 1-dodecene, water and methanol. Therefore, equal masses of the polar phase (water/methanol) and nonpolar phase (1-dodecene) were used. The polarity of the polar phase was increased by changing the ratio of water to methanol (0–100 wt% water in the polar phase). The interfacial tension between the liquid phases was determined via Pendant Drop and Spinning Drop method (Fig. 3, left). The higher polarity induced by the increase of water in the polar phase is reflected in the measurement results. The interfacial tension at equilibrium increases from  $\sigma = 1.98$  mN/m at 0 wt% water to  $\sigma = 29.52$  mN/m at 100 wt% water in the polar phase (Pendant Drop). Differences between the results of Pendant Drop and Spinning Drop especially at high interfacial tensions are caused by the optimal operating range of the respective measurement systems. The relative experimental error (three repetitions) was less than 3%.

The corresponding drop size measurements are in agreement with these results. The Sauter mean diameter in steady state is depicted in Fig. 3 (right) as a function of the polar phase composition. The vertical error bars depict the maximum experimental error (8% of Sauter mean diameter). The Sauter mean diameter increases from  $d_{3,2} = 92$   $\mu\text{m}$  at 0 wt% water to  $d_{3,2} = 315$   $\mu\text{m}$  at

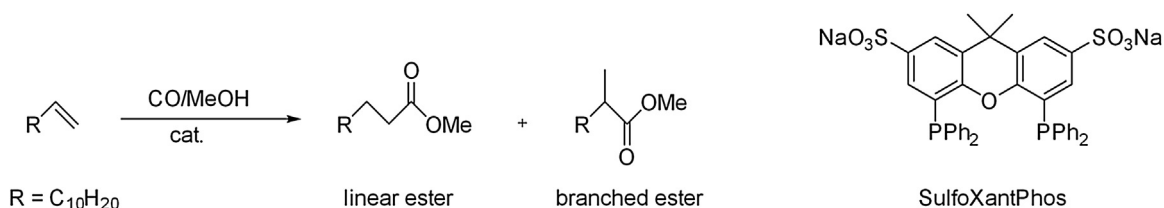
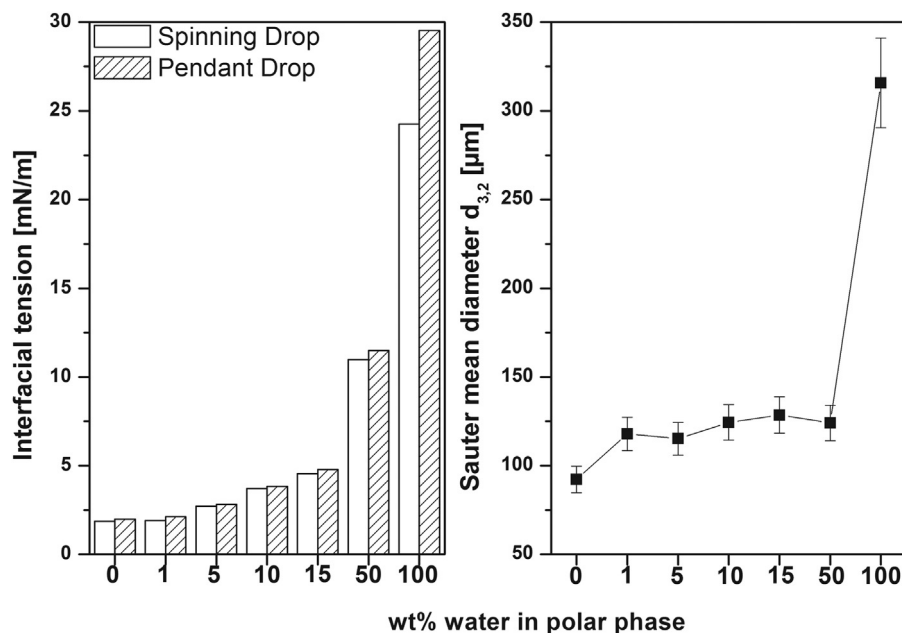


Fig. 2. Methoxycarbonylation of 1-dodecene to the corresponding linear and branched ester, and the structure of the ligand SulfoXantPhos.



**Fig. 3.** Interfacial tension and drop size of the biphasic system composed of methanol, water and 1-dodecene. Experimental conditions:  $T = 40^\circ\text{C}$ , Spinning drop capillary rotational speed  $n = 10,000$  rpm, Laplace-Young method, Stirrer rotational speed  $n = 700$  rpm (for details see experimental section).

100 wt% water in the polar phase at a constant stirring speed of  $n = 700$  rpm. In the range of 0–50 wt% only a small effect on the drop sizes can be observed, since several parameters beside the interfacial tension affect the droplet size distributions. Both polar phase density and viscosity increase with the amount of water in the polar phase. Furthermore, the dispersed volume fraction slightly decreases. However, the change of interfacial tension especially between 50 and 100 wt% of water in the polar phase is the main influencing factor on the drop size distributions. The volume-specific surface area decreases by a factor of nearly 3.5 (comparing 0 wt% and 100 wt%) or 1.35 (comparing 0 wt% and 50 wt% water in the polar phase), thereby diminishing potential mass transfer during reaction. The increasing interfacial tensions and drop sizes also indicate that the phase separation process is promoted by high amounts of water in the polar phase.

### 3.2. Variation of the catalyst concentration

Preliminary tests for the methoxycarbonylation reaction were carried out by variation of the catalyst concentration and without additional co-solvents (see Table 1). The substrates 1-dodecene and methanol form the biphasic reaction system, in which the catalyst is immobilized in the polar (methanol) phase. As expected, the reaction results show that an increasing amount of catalyst leads to a higher yield of ester. In contrast, turn-over frequency (TOF) and linear-to-branched ratio (l:b) do not change significantly by increasing the catalyst concentration and are in range of  $76\text{ h}^{-1}$  to

$80\text{ h}^{-1}$  and 67:33 to 70:30, respectively. The constant TOF indicates a first order dependency according to the catalyst concentration, which is consistent with the literature [35]. This also confirms that a mononuclear palladium complex is involved in the reaction. The nearly constant selectivity of the reaction is attributed to the applied catalyst complex with SulfoXantPhos as ligand and is not affected by the catalyst concentration. It has to be mentioned that an induction period exists at the beginning of the reaction, probably due to the formation of the active palladium hydride complex [14].

Interestingly, significant differences in the phase separation results could be found. A small amount of catalyst ( $<0.04$  mmol Pd, Table 1 entry 1) leads to the formation of a one phase system after the reaction, which inhibits the catalyst recycling. It became apparent that systems with high amount of the produced ester and low catalyst concentration form a one phase system because the ester is more hydrophilic than the substrate 1-dodecene. However, increasing the concentration of catalyst resulted in a biphasic system at separation conditions (entry 2–3) even with a yield of the ester close to 100%. Furthermore, the leaching of palladium and phosphorous is strongly influenced by the catalyst concentration. The experiment with 0.08 mmol Pd (entry 2) resulted in a high palladium and phosphorous leaching into the nonpolar phase of 50 ppm and 203 ppm, respectively. The experiment with 0.16 mmol Pd (entry 3) enabled a better catalyst recycling, indicating that the adjustment of catalyst concentration plays a crucial role in terms of quantitative catalyst recycling. By doubling the catalyst concentra-

**Table 1**  
Methoxycarbonylation of 1-dodecene: Variation of the catalyst concentration.<sup>a</sup>

Entry	n(Pd) [mmol]	Yield (Ester) <sup>b</sup> [%]	TOF <sup>c</sup> [1/h]	l:b <sup>b</sup>	Recycling possible	Pd leaching <sup>d</sup> [ppm]	P leaching <sup>d</sup> [ppm]
1	0.04	79.1	80	70:30	No	–	–
2	0.08	94.9	76	68:32	Yes	50	203
3	0.16	97.6	76	67:33	Yes	4.6	45.7

<sup>a</sup> Experimental conditions: Pd(OAc)<sub>2</sub> as precursor, Pd: SX:MSA (1:4:40), polar phase (methanol) = 12 g, nonpolar phase (1-dodecene) = 12 g, p(CO) = 30 bar,  $T = 80^\circ\text{C}$ ,  $t = 20$  h,  $n = 1200$  rpm, phase separation at room temperature.

<sup>b</sup> Determined by GC.

<sup>c</sup> Determined by gas consumption at a conversion of 50%.

<sup>d</sup> Determined by ICP-OES.

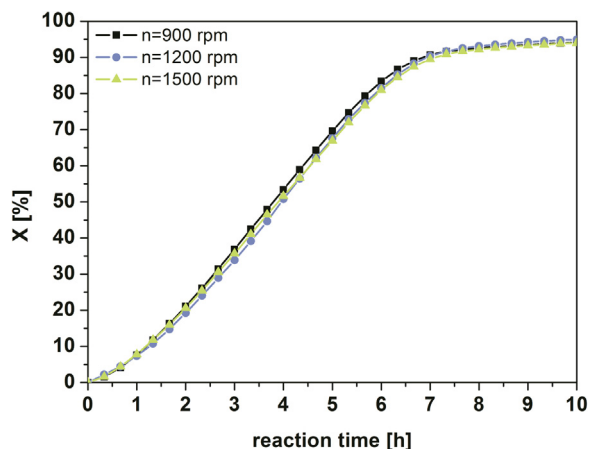


**Fig. 4.** Conversion over time for the methoxycarbonylation of 1-dodecene at different stirring speeds. Experimental conditions: Pd(OAc)<sub>2</sub> (0.16 mmol), Pd: SX:MSA:1-dodecene (1:4:40:445), polar phase (methanol) = 12 g, nonpolar phase (1-dodecene) = 12 g, p(CO) = 30 bar, T = 80 °C.

tion the palladium and phosphorous leaching could be decreased to 4.6 ppm and 45.7 ppm, respectively, which means that 0.5% of the initial palladium precursor and 2.2% of SulfoXantPhos were irreversibly lost. In order to ensure high catalyst retention, we decided to use 0.16 mmol Pd in all further experiments.

### 3.3. Variation of the stirring speed

Mass transfer can be crucial for the rate of a reaction in multiphase systems. In order to determine whether mass transfer is a limiting factor for the investigated reaction, an experiment has been performed in which the stirring speed was varied. Fig. 4 depicts the conversion over time for the three investigated stirring speeds. It was found that the variation of the stirring speed did not change the rate of the reaction. Hence, the results of this experiment negate the possibility of mass transfer limitation and indicate a kinetically controlled reaction.

### 3.4. Modification of the polar phase

Due to the water solubility of the applied catalyst, we tried to increase the polarity of the polar phase by the addition of water in order to reduce catalyst leaching. Since the addition of water to the system should have an influence on the methoxycarbonylation reaction as well, we also investigated the reaction behaviour. The total mass of the polar phase (from now on composed of methanol and water) was kept constant, while the ratio of water and methanol was varied. In general, a sigmoid trend of the time-

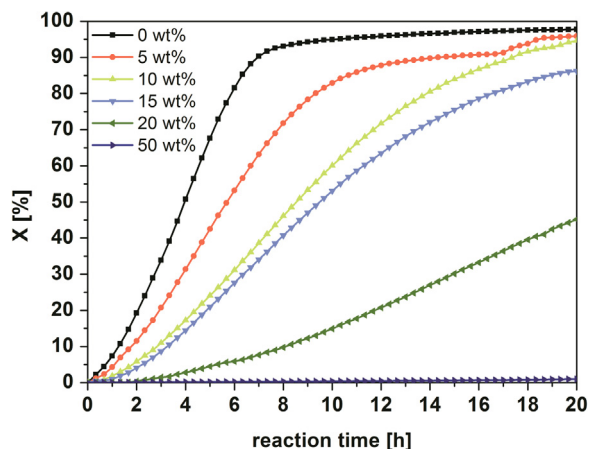


**Fig. 5.** Conversion over time for the methoxycarbonylation of 1-dodecene with different amounts of water (wt%) in the polar phase. Experimental conditions: Pd(OAc)<sub>2</sub> (0.16 mmol), Pd: SX:MSA:1-dodecene (1:4:40:445), polar phase (methanol and water) = 12 g, nonpolar phase (1-dodecene) = 12 g, p(CO) = 30 bar, T = 80 °C, n = 1200 rpm.

dependent conversion is obtained for all reactions as depicted in Fig. 5.

At reaction start, the conversion of 1-dodecene increases only slightly due to the induction period for the formation of the active palladium hydride complex. At the end of the reaction the conversion usually reaches a plateau because 1-dodecene is fully converted. However, there are significant differences in the reaction progress which are induced by the addition of water to the polar phase. Already small amounts of water increase the polarity of the catalyst phase and clearly lead to a decrease of the slope of the conversion over time, which is equivalent to a decrease in activity and reaction rate. Generally, the higher the amount of water in the polar phase the lower is the reaction rate. Since the reaction is kinetically controlled and should mainly take place in the polar catalyst phase, the rate is affected by the concentrations of 1-dodecene, methanol and carbon monoxide in this particular phase. With an increasing amount of water the solubility of 1-dodecene and carbon monoxide in the polar phase is decreasing, which could both lead to a reduction of the reaction rate. The solubility of carbon monoxide can be calculated with an empirical equation found by Chaudhari et al. and is in a range of 0.03 mol/L for pure water to 0.28 mol/L for pure methanol [36]. In an earlier work, Rosales et al. considered the methanolysis step to be the rate determining step of the reaction [14]. An increasing amount of water in the polar phase reduces the concentration of methanol in this phase significantly and with that also the reaction rate decreases.

As shown in Table 2, the TOF decreases from 63 h<sup>-1</sup> with no additional water to 14 h<sup>-1</sup> with 20 wt% water in the polar phase. It

**Table 2**  
Methoxycarbonylation of 1-dodecene: Modification of the polar phase.<sup>a</sup>

	water in polar phase [wt%]	Yield (Ester) <sup>b</sup> [%]	Yield (Acid) <sup>b</sup> [%]	TOF <sup>c</sup> [1/h]	l:b <sup>b</sup> (ester)	Pd leaching <sup>d</sup> [ppm]	P leaching <sup>d</sup> [ppm]	product in nonpolar phase <sup>b</sup> [%]
1	0	97.6	0	63	67:33	4.6	45.7	94.7
2	5	95.1	0.7	47	68:32	1.0	4.4	96.1
3	10	93.6	0.8	31	70:30	0.8	1.7	98.7
4	15	84.6	1.8	29	69:31	0.5	0.9	99.0
5	20	44.5	0.7	14	72:28	0.1	0.3	99.4
6	50	0.9	0.1	–	80:20	0.1	0.9	99.8

<sup>a</sup> Experimental conditions: Pd(OAc)<sub>2</sub> (0.16 mmol), Pd: SX:MSA:1-dodecene (1:4:40:445), polar phase (methanol and water) = 12 g, nonpolar phase (1-dodecene) = 12 g, p(CO) = 30 bar, T = 80 °C, t = 20 h, n = 1200 rpm, phase separation at room temperature.

<sup>b</sup> Determined by GC.

<sup>c</sup> Determined by gas consumption at a conversion of 20%.

<sup>d</sup> Determined by ICP-OES.

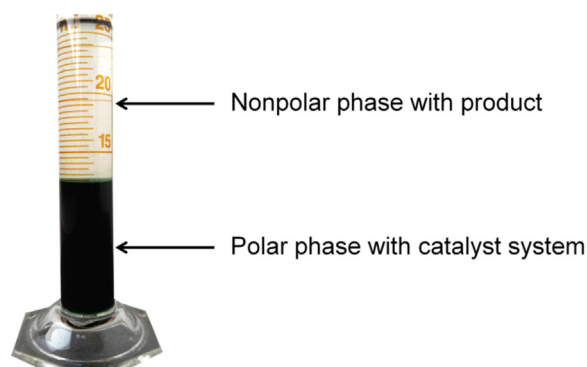


Fig. 6. Reaction mixture after separation at room temperature for entry 3.

has to be mentioned that the TOF was calculated at a conversion of 20% to avoid the induction period of the reaction. A further increase of the water amount in the polar phase to 50 wt% (entry 6) finally obliterates the reaction. At this point the catalyst phase became such polar that the solubility of 1-dodecene in this phase is too low to be measured.

Surprisingly, despite of an increasing amount of water available in the polar phase, only traces of the corresponding linear and branched acid are formed via hydroxycarbonylation reaction or hydrolysis. At 15 wt% water in the polar phase the yield of the acid reaches a maximum of 1.8%, while the yield of the ester decreases continuously from 97.6% with no additional water to 0.9% with 50 wt% water in the polar phase. Presumably, the reaction conditions shift the hydrolysis-equilibrium to the side of the ester. Due to an excess of methanol in the polar phase and also due to the acidic reaction conditions, only traces of the acid are formed. As a result, the applied biphasic systems are chemoselective towards the formation of the ester, despite competing water in the reaction mixture. The regioselectivity for the ester is moderate and lies in a range of 67:33–80:20, mainly controlled by the applied catalyst complex. However, it seems that an increasing amount of water in the polar phase increases the l:b ratio. We assume that the regioselectivity is slightly influenced by the polarity of the catalyst phase. In addition, the promotion of the decomposition of the active Pd-hydride complex by an increasing amount of water, as stated in literature, could not be confirmed [37]. No Pd black formation was observed under the here investigated reaction conditions.

Considering the phase separation of the different reaction mixtures, the water containing systems (entries 2–6) showed a decrease in the required separation time compared to the unmodified system (entry 1). Already within a few minutes, one greenish polar phase with the catalyst system and a colourless nonpolar product phase are formed, exemplarily depicted in Fig. 6 for entry 3. This observation clearly indicates a complete immobilization of the catalyst in the polar phase, which could be also confirmed by induc-

tively coupled plasma (ICP) analysis: the leaching of palladium and phosphorous could be successfully reduced by the addition of water to the polar phase. The addition of 5 wt% water to the polar phase decreases the palladium and phosphorous leaching from 4.6 ppm to 1.0 ppm and from 45.7 ppm to 4.4 ppm, respectively. A further increase of the water amount leads to a further reduction of leaching to a minimum of 0.1 ppm for palladium and 0.3 ppm for phosphorous. The experimental results indicate that the partition coefficient of the catalyst system is strongly affected by the polarity of the polar phase. The addition of water to the polar phase leads to an increase of the polarity of this phase, which promotes an excellent partition coefficient for a quantitative recycling of the catalyst system. However, not only the recycling of the catalyst system is crucial for an economic and sustainable process but also the quantitative separation of the product within the nonpolar phase. The ester content in the nonpolar phase was found to be over 90% in each investigated reaction mixture. The increasing polarity of the polar phase tends to result in a higher amount of product in the nonpolar phase. The partition of the product to the nonpolar phase reaches over 99%, if the polar phase contains at least 15 wt% water.

### 3.5. Modification of the nonpolar phase

The modification of the nonpolar phase by the use of different co-solvents is another promising approach to optimize phase separation and catalyst recycling. Compared to the use of pure 1-dodecene as nonpolar phase, the addition of co-solvents allows for a constant polarity of the nonpolar phase almost independent from the reaction progress. Hence, the separation conditions do not change significantly with the formation of the more hydrophilic methyl tridecanoate during the reaction progress. As seen in Table 3 the reaction and separation results are not affected by the choice of the co-solvent, if the nonpolar phase is composed of 25 wt% 1-dodecene and 75 wt% co-solvent. Several co-solvents with different carbon chain lengths were tested in methoxycarbonylation reaction starting from octane to hexadecane. The yield of ester and the catalyst activity are comparable for all applied co-solvents and reach values above 95% and TOFs between  $19 \text{ h}^{-1}$  and  $21 \text{ h}^{-1}$ , respectively, while the l:b ratio remains constant at 66:34.

Interestingly, with co-solvent in the mixture the separation time and the catalyst leaching are decreased compared to the system without co-solvent (Table 2, entry 1), which justifies the application of co-solvents as mediator for fast phase separation and lower catalyst leaching. The phase separation begins immediately after stirring is stopped and a greenish catalyst phase and a nonpolar phase without any coloration are formed within a few minutes. The leaching could be reduced to 0.1 ppm for palladium and below 1 ppm for phosphorous. The system with octane as co-solvent is an exception with leaching values of 0.5 ppm for palladium and 2.3 ppm for phosphorous, probably due to the higher solubility of

**Table 3**  
Methoxycarbonylation of 1-dodecene: Modification of the nonpolar phase.<sup>a</sup>

Entry	Co-solvent	Yield (Ester) <sup>b</sup> [%]	TOF <sup>c</sup> [1/h]	l:b <sup>b</sup>	Pd leaching <sup>d</sup> [ppm]	P leaching <sup>d</sup> [ppm]	product in nonpolar phase <sup>b</sup> [%]
1	Octane	96.6	20	66:34	0.5	2.3	88
2	Decane	94.9	21	66:34	0.1	0.5	88
3	Dodecane	95.5	19	66:34	0.1	0.3	85
4	Tetradecane	96.1	20	66:34	0.1	0.6	88
5	Hexadecane	96.6	20	66:34	0.1	1.0	90

<sup>a</sup> Experimental conditions: Pd(OAc)<sub>2</sub> (0.16 mmol), Pd: SX:MSA:1-dodecene (1:4:40:110), polar phase (methanol) = 12 g, nonpolar phase (1-dodecene and co-solvent) = 12 g, co-solvent = 9 g, p(CO) = 30 bar, T = 80 °C, t = 20 h, n = 1200 rpm, phase separation at room temperature.

<sup>b</sup> Determined by GC.

<sup>c</sup> Determined by gas consumption at a conversion of 20%.

<sup>d</sup> Determined by ICP-OES.

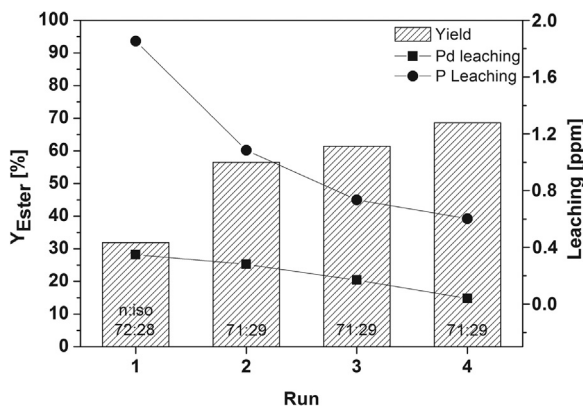


**Fig. 7.** Yield and leaching results for the recycling experiment. Experimental conditions: Pd(OAc)<sub>2</sub> (0.16 mmol), Pd: SX:MSA:1-dodecene (1:4:40:110), polar phase (methanol)= 12 g, nonpolar phase (1-dodecene and octane)= 12 g, octane (9 g), p(CO)= 30 bar, T= 80 °C, t= 2 h, n= 1200 rpm.

the catalyst system in octane. In all experiments at least 85 % of the product could be separated within the nonpolar phase after the reaction. The type of co-solvent does not significantly change the distribution of the product between both phases. Considering these results, the application of co-solvents in the nonpolar phase is beneficial, although the co-solvent has to be removed after the phase separation step for product purification. With this in mind, the boiling point of the co-solvent becomes also an important parameter that has to be considered for the choice of an appropriate co-solvent for a chemical process: The higher the boiling point, the higher the costs for purification of product probably will be. Therefore, octane could be the preferable co-solvent in this particular case since it offers the lowest boiling point of all the investigated alkanes with only minor losses in catalyst leaching.

### 3.6. Catalyst recycling

With the knowledge of all the previous experiments a recycling experiment was performed to evaluate the feasibility of the investigated biphasic reaction system for industrial application. For this purpose, we chose a biphasic system composed of methanol as polar phase and 1-dodecene/octane as nonpolar phase. After each run, the nonpolar phase was removed and new substrate with co-solvent was filled into the reactor without any refreshment of the catalyst components. As a result, the catalyst complex was successfully recycled for four times. Fig. 7 shows the yield of the desired ester as well as the leaching of palladium and phosphorous.

Interestingly, the yield of the ester is significantly lower in the first run (32%) than in the following experiments (>55%). This is mainly due to the induction period for the formation of the active catalyst complex that only occurred during the first run. In addition, the yield also increases slightly from 55% in the second run to almost 70% in the fourth run. We assume that some amounts of the slightly hydrophilic product methyl tridecanoate remained in the catalyst phase after each run. This led to an increasing solubility of the substrate in this phase and thus an increasing yield. In contrast, the l:b ratio remained constant in all runs, which indicates the high stability of the catalyst complex during the recycling procedure. Furthermore, the leaching of both palladium and phosphorous decreased from 0.3 ppm to <0.1 ppm and 1.9 ppm to 0.6 ppm, respectively. However, it has to be mentioned that the volume of the catalyst phase slightly decreased after each recycle from a relative phase height of 45% after the first run to 20% after the fourth run, presumably due to the loss of methanol into the nonpolar phase and consumption by the reaction itself.

## 4. Conclusion

The here presented results reveal the feasibility of the palladium catalyzed methoxycarbonylation of 1-dodecene in liquid/liquid biphasic systems. It was found that the applied catalyst can be immobilized in the polar methanol phase by the use of the water-soluble ligand SulfoXantPhos. With that, the applied methanol acts as reactant and as solvent for the catalyst in the reaction mixture. This finding also allows for an easy catalyst recycling after the reaction, since the catalyst remains within the polar phase while the hydrophobic product is mainly dissolved in the nonpolar phase. In a recycling experiment the catalyst system was quantitatively recovered for four times without any loss in activity and selectivity. The results of this experiment indicate that the continuation of this series would be possible and only limited by catalyst leaching and stability. Moreover, the modification of both the polar and nonpolar phase with co-solvents has a significant impact on the reduction of the catalyst leaching (0.1 ppm for palladium and <1 ppm for phosphorous under optimized conditions) and accelerates the time for phase separation. However, the reaction performance was downgraded by the use of the here investigated co-solvents. Thus the formulation of the reaction mixture has to be done carefully in order to optimize catalyst separation and reaction performance. All things considered the here investigated liquid/liquid biphasic systems offer an easy possibility to perform the palladium catalyzed methoxycarbonylation of 1-dodecene with subsequent catalyst recycling by phase separation.

## Acknowledgements

This work is part of the Collaborative Research Center/Transregio 63 “Integrated Chemical Processes in Liquid Multiphase Systems” (subprojects A2 and B8). Financial support by the Deutsche Forschungsgemeinschaft (DFG, German Research Foundation) is gratefully acknowledged (TRR 63).

## References

- [1] W. Reppe, H. Kröper, *Justus Liebigs Ann. Chem.* 582 (1953) 38–71.
- [2] G. Kiss, *Chem. Rev.* 101 (2001) 3435–3456.
- [3] H. Neumann, A. Brennfürer, M. Beller, *Adv. Synth. Catal.* 350 (2008) 2437–2442.
- [4] E.J. Jang, K.H. Lee, J.S. Lee, Y.G. Kim, *J. Mol. Catal. A Chem.* 138 (1999) 25–36.
- [5] K. Nagai, *Appl. Catal. A. Gen.* 221 (2001) 367–377.
- [6] V. de la Fuente, M. Waugh, G.R. Eastham, J.A. Iggo, S. Castellón, C. Claver, *Chem. – A Eur. J.* 16 (2010) 6919–6932.
- [7] I. del Río, N. Ruiz, C. Claver, L.A. Van Der Veen, P.W.N.M. Van Leeuwen, *J. Mol. Catal. A Chem.* 161 (2000) 39–48.
- [8] C. Zúñiga, S.A. Moya, P. Aguirre, *Catal. Lett.* 130 (2009) 373–379.
- [9] E. Guio, M. Caporali, B. Munoz, C. Müller, M. Lutz, A.L. Spek, C. Claver, P.W.N.M. Van Leeuwen, *Organometallics* 25 (2006) 3102–3104.
- [10] C. Holzapfel, T. Bredenkamp, *ChemCatChem* 7 (2015) 2598–2606.
- [11] C. Jimenez Rodriguez, D.F. Foster, G.R. Eastham, D.J. Cole-Hamilton, *Chem. Commun.* (2004) 1720–1721.
- [12] A. Seayad, A.A. Kelkar, L. Toniolo, R.V. Chaudhari, *J. Mol. Catal. A Chem.* 151 (2000) 47–59.
- [13] G. Verspui, J. Feiken, G. Papadogianakis, R.A. Sheldon, *J. Mol. Catal. A Chem.* 146 (1999) 299–307.
- [14] M. Rosales, I. Pacheco, J. Medina, J. Fernández, Á. González, R. Izquierdo, L.G. Melean, P.J. Baricelli, *Catal. Lett.* 144 (2014) 1717–1727.
- [15] P. Roesle, C.J. Dürr, H.M. Möller, L. Cavallo, L. Caporaso, S. Mecking, *J. Am. Chem. Soc.* 134 (2012) 17696–17703.
- [16] J.J.M. de Pater, B.-J. Deelman, C.J. Elsevier, G. Van Koten, *Adv. Synth. Catal.* 348 (2006) 1447–1458.
- [17] J.P.K. Reynhardt, H. Alper, *J. Org. Chem.* 68 (2003) 8353–8360.
- [18] H. Ooka, T. Inoue, S. Itsuno, M. Tanaka, *Chem. Commun.* (2005) 1173–1175.
- [19] K. Mukhopadhyay, B.R. Sarkar, R.V. Chaudhari, *J. Am. Chem. Soc.* 124 (2002) 9692–9693.
- [20] S. Rostamnia, E. Doustkhah, R. Bulgar, B. Zeynizadeh, *Microporous Mesoporous Mater.* 225 (2016) 272–279.
- [21] S. Rostamnia, E. Doustkhah, Z. Karimi, S. Amini, R. Luque, *ChemCatChem* 7 (2015) 1678–1683.
- [22] S. Rostamnia, E. Doustkhah, H. Golchin-Hosseini, B. Zeynizadeh, H. Xin, R. Luque, *Catal. Sci. Technol.* 6 (2016) 4124–4133.

- [23] C.W. Kohlpaintner, R.W. Fischer, B. Cornils, *Appl. Catal. A Gen.* 221 (2001) 219–225.
- [24] G. Papadogianakis, G. Verspui, L. Maat, R.A. Sheldon, *Catal. Lett.* 47 (1997) 43–46.
- [25] S. Tilloy, F. Bertoux, A. Mortreux, E. Monflier, *Catal. Today* 48 (1999) 245–253.
- [26] M.D. Miquel-Serrano, A. Aghmiz, M. Diéguez, A.M. Masdeu-Bultó, C. Claver, D. Sinou, *Tetrahedron: Asymmetry* 10 (1999) 4463–4467.
- [27] R. Pruvost, J. Boulanger, B. Léger, A. Ponchel, E. Monflier, M. Ibert, A. Mortreux, M. Sauthier, *ChemSusChem* 8 (2015) 2133–2137.
- [28] T. Gaide, A. Behr, M. Terhorst, A. Arns, F. Benski, A.J. Vorholt, *Chemie-Ingenieur-Technik* 88 (2016) 158–167.
- [29] T. Gaide, A. Behr, A. Arns, F. Benski, A.J. Vorholt, *Chem. Eng. Process. Process Intensif.* 99 (2016) 197–204.
- [30] A. Behr, A.J. Vorholt, N. Rentmeister, *Chem. Eng. Sci.* 99 (2013) 38–43.
- [31] J. Ritter, M. Kraume, *Chem. Eng. Technol.* 23 (2000) 579–581.
- [32] S. Maaf, J. Rojahn, R. Hänsch, M. Kraume, *Comput. Chem. Eng.* 45 (2012) 27–37.
- [33] S. Maaf, S. Wollny, A. Voigt, M. Kraume, *Exp. Fluids* 50 (2011) 259–269.
- [34] M. Schreuder Goedheijt, J.N.H. Reek, P.C.J. Kamer, P.W.N.M. van Leeuwen, *Chem. Commun.* (1998) 2431–2432.
- [35] S. Zolezzi, S.A. Moya, G. Valdebenito, G. Abarca, J. Parada, P. Aguirre, *Appl. Organomet. Chem.* 28 (2014) 364–371.
- [36] S.B. Dake, R.V. Chaudhari, *J. Chem. Eng. Data* 30 (1985) 400–403.
- [37] A. Vavasori, L. Toniolo, G. Cavinato, *J. Mol. Catal. A Chem.* 191 (2003) 9–21.

# PAPER 8

## **Understanding the role of nonionic surfactants during the catalysis in microemulsion systems on the example of rhodium-catalyzed hydroformylation**

Tobias Pogrzeba, Marcel Schmidt, Natasa Milojevic, Carolina Urban, Markus Illner, Jens-Uwe Repke, Reinhard Schomäcker

Industrial & Engineering Chemistry Research, 2017, 56, 9934-9941

Online Article:

<https://pubs.acs.org/doi/abs/10.1021/acs.iecr.7b02242>

Reproduced (or 'Reproduced in part') with permission from "Understanding the Role of Nonionic Surfactants during Catalysis in Microemulsion Systems on the Example of Rhodium- Catalyzed Hydroformylation; Tobias Pogrzeba, Marcel Schmidt, Natasa Milojevic, Carolina Urban, Markus Illner, Jens-Uwe Repke, and Reinhard Schomäcker. Industrial & Engineering Chemistry Research, 2017, 56, 9934-9941." Copyright (2017) American Chemical Society.



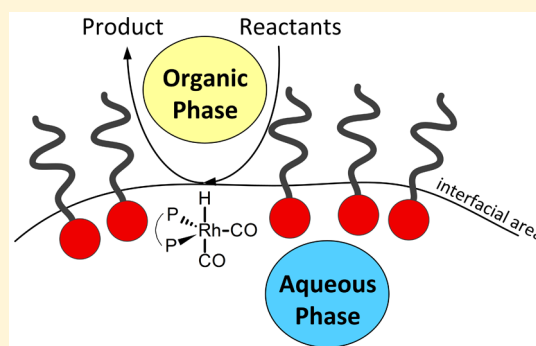
# Understanding the Role of Nonionic Surfactants during Catalysis in Microemulsion Systems on the Example of Rhodium-Catalyzed Hydroformylation

Tobias Pogrzeba,<sup>\*,†</sup> Marcel Schmidt,<sup>†</sup> Nataša Milojevic,<sup>†</sup> Carolina Urban,<sup>†</sup> Markus Illner,<sup>‡</sup> Jens-Uwe Repke,<sup>‡</sup> and Reinhard Schomäcker<sup>†</sup>

<sup>†</sup>Department of Chemistry, Technische Universität Berlin, Straße des 17. Juni 124, Sekr. TC-8, Berlin D-10623, Germany

<sup>‡</sup>Chair of Process Dynamics and Operation, Technische Universität Berlin, Straße des 17. Juni 135, Sekr. KWT-9, Berlin D-10623, Germany

**ABSTRACT:** The application of microemulsion systems as switchable reaction media for the rhodium-catalyzed hydroformylation of 1-dodecene is being reported. The influence of temperature, phase behavior, and the selected nonionic surfactant on the reaction has been investigated. The results revealed that the structure and the hydrophilicity (degree of ethoxylation) of the applied surfactant can have a strong impact on the performance of the catalytic reaction in microemulsion systems, in particular on the reaction rate. The surfactant determines the boundary conditions for catalysis (interfacial area, local concentrations) and can also interact with the catalyst at the oil–water interface and hinder the reaction. In addition to the discussion of the experimental results, we present a proposal for the impact of surfactant-based reaction media on the reaction mechanism of the catalyst reaction.



## 1. INTRODUCTION

The use of water as solvent in transition metal-catalyzed chemistry is today still rather unusual and rarely the first choice of a chemist. To be fair, this is not very surprising because the poor solubility of most organic educts in water makes it difficult to perform reactions in aqueous media and to predict their results. However, if we want to make a switch to a greener chemistry and reduce the environmental implications of our work, we should start to intensify the efforts in research of catalysis in aqueous media. As Lipshutz et al. pointed out recently,<sup>1</sup> the path toward greener chemistry offers exciting opportunities and surprises associated with this new environment for catalysis, which should attract the interest of many scientists worldwide. To enable the transfer of the already established organic transition metal-catalyzed chemistry into the medium water, micellar catalysis can provide the crucial “solution” for substrate and catalyst solubilization and subsequent reaction under mild conditions.<sup>2–6</sup> Often it is sufficient to employ a suitable surfactant or a micelle producing agent to solubilize the reactants and to enable the reaction. However, in case of the application of expensive transition metal catalysts in such media, an old problem occurs again that is already known from homogeneous organic solutions: the recovery of the catalyst. One possible way to tackle this problem in micellar media is the application of filtration techniques, for example, ultrafiltration. A catalyst that is embedded in the micelles can be retained during the ultrafiltration process if a micelle rejecting membrane is

applied. With this so-called micellar enhanced ultrafiltration (MEUF) technique, the active catalyst can be recycled within the retentate and reused for reaction.<sup>7,8</sup> Another approach to combine reaction and catalyst recycling in micellar systems is the utilization of microemulsion systems (MES) as switchable solvents. Microemulsions are ternary mixtures consisting of a nonpolar component, water, and a surfactant (often nonionic surfactants are chosen in this context). Because of the strong surface activity of the surfactant, microemulsions provide a high interfacial area between the polar and nonpolar domains during the reaction. Additionally, their phase separation behavior can be manipulated through temperature changes and thus makes them switchable solvent systems. According to Winsor, microemulsions are thermodynamically stable and can be either a one-phase system (Winsor IV) or part of a multiphase system (Winsor I, II, or III) in which the microemulsion can be of three different types: water-in-oil (w/o), oil-in-water (o/w), or bicontinuous; the phase behavior is described in detail in the literature.<sup>9–11</sup> The switchability of microemulsion systems offers many interesting options for chemical processes with industrial relevance in aqueous media, like Suzuki and Heck coupling reactions<sup>12,13</sup> as substeps in the total synthesis of complex organic molecules (e.g., total synthesis of Boscalid<sup>14</sup>).

**Received:** May 31, 2017

**Revised:** August 2, 2017

**Accepted:** August 18, 2017

**Published:** August 18, 2017

Another application is the rhodium-catalyzed hydroformylation of long-chained alkenes that has already been performed successfully in a continuously operated mini-plant over a 200 h campaign.<sup>15,16</sup>

Regarding the already numerous examples for transition metal catalysis in surfactant-based reaction media, it seems to be only a question of time until the first industrial application in these systems becomes reality. However, these complex multiphase systems require a profound knowledge of the influence of a variety of system parameters regarding reaction and separation. In particular, the applied surfactant seems to have a strong impact on the result of a reaction, which is today still not completely understood and raises the question of how catalysis works in these systems. To gain more knowledge about the role of the surfactant during catalysis, we decided to investigate the rhodium-catalyzed hydroformylation of 1-dodecene in microemulsion systems in a detailed study with regards to phase behavior of the MES, concentration and hydrophilicity of surfactant, and temperature dependency of the reaction. The obtained results are of great importance for understanding these complex reaction systems and contribute to further development and enhancement of chemical processes in surfactant-based reaction media.

## 2. MATERIALS AND METHODS

**2.1. Chemicals.** The reactant 1-dodecene (95%) and water (HPLC grade) were purchased from VWR. The precursor (acetylacetonato)dicarbonylrhodium(I) [Rh(acac)(CO)<sub>2</sub>] was contributed by Umicore, Germany. The water-soluble ligand 2,7-bissulfonate-4,5-bis(diphenylphosphino)-9,9-dimethylxanthene (SulfoXantphos, SX) was purchased from Molisa, where it was synthesized according to a procedure described by Goedheijt et al.<sup>17</sup> The syngas (1:1 mixture of CO and H<sub>2</sub>, purity 2.1 for CO and 2.1 for H<sub>2</sub>) was purchased from Air Liquide. The technical grade nonionic surfactants from the Marlipal 24 series were contributed by Sasol Germany. To adjust the ionic strength, we used sodium sulfate (Na<sub>2</sub>SO<sub>4</sub>, 99%) purchased from Merck. All of the chemicals were used without further purification.

**2.2. Preparation of Catalyst Solution.** For the preparation of the catalyst complex, 12.9 mg (0.05 mmol, 1 equiv) of [Rh(acac)(CO)<sub>2</sub>] and 156.7 mg (0.20 mmol, 4 equiv) of SulfoXantphos were evacuated three times in a Schlenk tube and flushed with argon. The solvent (5 g of degassed water, HPLC grade) was added through a septum. The catalyst solution then was stirred overnight at room temperature to ensure the formation of the catalyst complex.

**2.3. Investigation on Phase Behavior.** Investigations on the phase behavior of the microemulsion systems were performed by using small glass reactors (50 mL volume) with a heating jacket. The lid of such a reactor offers connections for sampling, for vacuum establishment, and argon inertization. We investigated the phase behavior of several microemulsion systems consisting of 1-dodecene/water/nonionic surfactant. The applied nonionic surfactant from the Marlipal 24 series was varied with respect to the degree of ethoxylation (EO), from Marlipal 24/50 (average EO = 5) to Marlipal 24/90 (average EO = 9). In addition, every mixture consisted of 1.0 wt % sodium sulfate, 0.04 mol % [Rh(acac)(CO)<sub>2</sub>], and 0.16 mol % SulfoXantphos. The oil-to-water ratio was kept constant for all experiments at  $\alpha = 0.5$  with an amount of 95 mmol (16 g) of 1-dodecene (rhodium/ligand/alkene ratio = 1/4/2500). The amount of surfactant was varied from 1 to 16 wt % ( $\gamma = 0.01$  to

0.16). For each sample, the different amounts of oil, water, sodium sulfate, and the particular surfactant were weighted into the reactor and evacuated and flushed with argon at least three times. The catalyst solution then was injected with a syringe. We studied the phase behavior from 50 to 90 °C in 2 °C steps. The microemulsions were stirred during the heating periods by a magnetic stirrer. After the desired temperature was reached, the stirrer was stopped and the phase separation was observed.

The important composition parameters to characterize the MES are the weight fractions of oil ( $\alpha$ ) and surfactant ( $\gamma$ ) (eq 1), which are calculated from the mass  $m$  of the corresponding component:

$$\alpha = \frac{m_{\text{oil}}}{m_{\text{oil}} + m_{\text{H}_2\text{O}}} \quad \gamma = \frac{m_{\text{Surf}}}{m_{\text{oil}} + m_{\text{H}_2\text{O}} + m_{\text{Surf}}} \quad (1)$$

**2.4. Hydroformylation Experiments.** The hydroformylation reactions were performed in a 100 mL stainless steel high-pressure vessel from Premex Reactor AG, equipped with a gas dispersion stirrer and mounted in an oil thermostat from Huber (K12-NR). The reactor setup has already been illustrated in previous contributions.<sup>15</sup> The typical reaction conditions for the hydroformylation were 15 bar pressure of syngas, an internal reactor temperature of 65–120 °C, and a stirring speed of 1200 rpm, using a gas dispersion stirrer. The reaction mixture usually consisted of 120 mmol (20 g) of 1-dodecene, water (HPLC grade,  $\alpha = 0.5$ ), 1.0 wt % sodium sulfate, surfactant (Marlipal 24 series), and catalyst solution. The ratio of rhodium/ligand/alkene was 1/4/2500 in every experiment.

The reaction was performed as described in the following. At first the reactor was filled with the desired amounts of alkene, water, sodium sulfate, and surfactant. The catalyst solution then was transferred by a syringe to the reactor. The reactor was closed and evacuated and purged with nitrogen at least three times. The stirrer was started at a rate of 500 rpm, and the reactor was heated to the desired temperature. After reaching the temperature, the stirring was slowed (200–300 rpm), and the reactor was pressurized with syngas. The reaction was started by increasing the stirring speed again to 1200 rpm. For the evaluation of reaction progress, samples were withdrawn at several time intervals via a sampling valve and analyzed by gas chromatography (GC). To ensure homogeneous liquid sampling, the stirring speed was not changed, while the samples were taken from the reactor. No further purification steps were performed to isolate the product from the reaction mixture before the samples were measured via GC. In addition, consumption of syngas during the experiments has been recorded via the mass flow controller.

The important parameters (conversion  $X$ , yield  $Y$ , selectivity  $S$ , and TOF) for the evaluation of experimental data were calculated as shown in eqs 2–5, where  $n$  is the amount of substance, 1-dodecene is the substrate, and 1-tridecanal is the product.

$$X(t) = \frac{n_{t=0,\text{Substrate}} - n_{t,\text{Substrate}}}{n_{t=0,\text{Substrate}}} \quad (2)$$

$$Y(t) = \frac{n_{t,\text{Product}}}{n_{t=0,\text{Substrate}}} \quad (3)$$

$$S(n:\text{iso}) = \frac{n_{\text{Product}}}{n_{\text{iso-Aldehydes}}} \quad (4)$$

$$\text{TOF}_{\text{Ald}} = \frac{n_{t=0, \text{Substrate}} \cdot Y_{\text{Ald}}(t)}{n_{\text{cat}} \cdot t} \quad (5)$$

**2.5. Analysis.** Reaction progress and selectivity of hydroformylation reactions were analyzed by gas chromatography on a Shimadzu model GC-2010, equipped with a Supelcowax 10 capillary column, a flame ionization detection analyzer, and nitrogen as carrier gas.

### 3. RESULTS AND DISCUSSION

#### 3.1. Phase Behavior of the Microemulsion Systems.

The phase behavior of the investigated microemulsion systems consisting of 1-dodecene, water, and varying technical grade surfactants from the Marlipal 24 series (Figure 1) was recorded

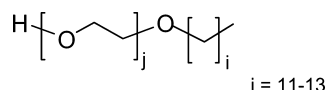


**Figure 1.** Structure of the applied surfactants from the Marlipal 24 series ( $j$  = degree of ethoxylation (EO)). EO increases from Marlipal 24/50 (average  $j = 5$ ) to Marlipal 24/90 (average  $j = 9$ ).

in the form of phase diagrams as illustrated exemplarily in Figure 2a for 1-dodecene/water/Marlipal(24/70). The presence of sodium sulfate and the rhodium catalyst in the mixture led to a shift of the phase boundaries to lower temperatures in comparison to the pure microemulsion system.<sup>18</sup> The applied nonionic surfactants are characterized by their degree of ethoxylation, which is responsible for the hydrophilic character of each surfactant. The hydrophilicity increases with the number of ethoxylate groups in the surfactant chain and affects the phase behavior of the resulting MES. While the shape of the “fish” in the phase diagram (as in Figure 2a) follows a general pattern for each of the investigated surfactants due to their related chemical structure, the phase boundaries are shifted to lower or higher temperatures with changing EO (see Figure 2b). It is also apparent that the three-phase area becomes slightly larger with an increasing EO number. The information about the position of the “fish” in the phase diagram is of great importance for the application of a MES in a chemical process, because it marks the switchable area that is essential for reaction and catalyst recycling in these systems. At the same time, it is also a good indicator for the temperature range at which the application of a particular MES for a reaction is feasible or not. The reason for this is that every surfactant has its own specific working area (temperature range), which is determined by its chemical structure. In this particular area, the surfactant shows the strongest surface activity and therefore the highest ability to function as emulsifier and thus provides the most stable emulsions. In case of the investigated surfactants (Figure 2b), the results indicate that the optimal operation temperature of the corresponding MES increases with increasing EO number (or rather hydrophilicity).

**3.2. Hydroformylation of 1-Dodecene.** The rhodium-catalyzed hydroformylation of 1-dodecene in microemulsion systems (Figure 3) has been investigated by our working group for several years by now.<sup>15,19,20</sup> In previous experiments, we found the aliphatic surfactants from the Marlipal series to provide good results as emulsifier for this reaction. By the application of the surfactant Marlipal 24/70, 31.3% yield of aldehyde (98% linear product) has been obtained after 4 h reaction time under optimized reaction conditions:  $\alpha = 0.5$ ,  $\gamma =$

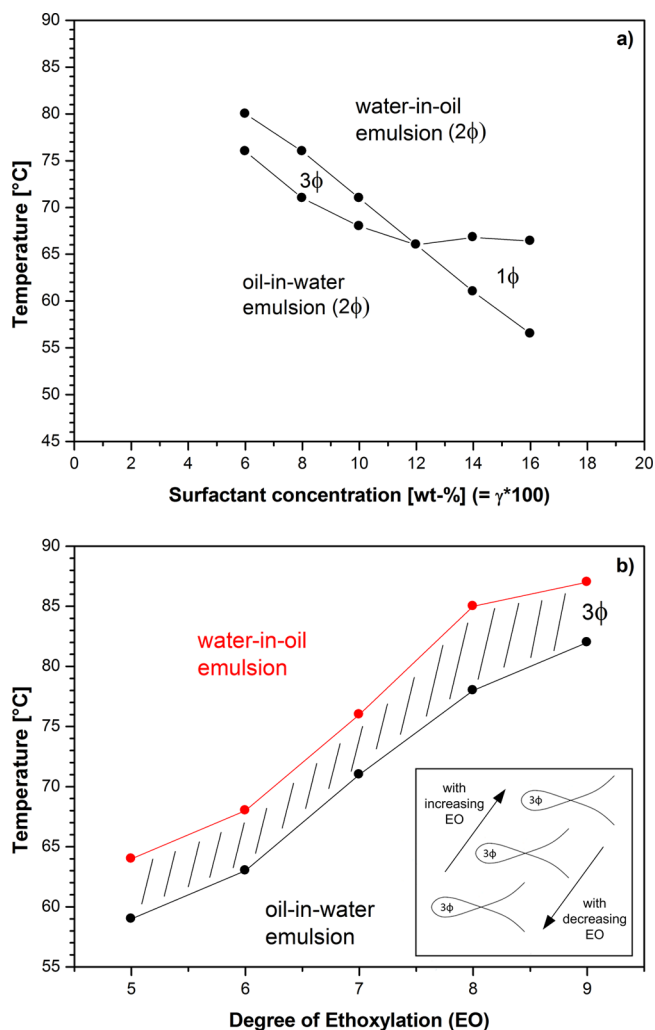


**Figure 2.** (a) Phase diagram of 1-dodecene/water/Marlipal(24/70) for  $\alpha = 0.5$  with 1.0 wt %  $\text{Na}_2\text{SO}_4$ , 0.04 mol %  $[\text{Rh}(\text{acac})(\text{CO})_2]$ , and 0.16 mol % SulfoXantphos. (b) Temperature shift of the three-phase area as a function of degree of ethoxylation with 1-dodecene/water/Marlipal(24/50–90) for  $\alpha = 0.5$  and  $\gamma = 0.08$  with 1.0 wt %  $\text{Na}_2\text{SO}_4$ , 0.04 mol %  $[\text{Rh}(\text{acac})(\text{CO})_2]$ , and 0.16 mol % SulfoXantphos.

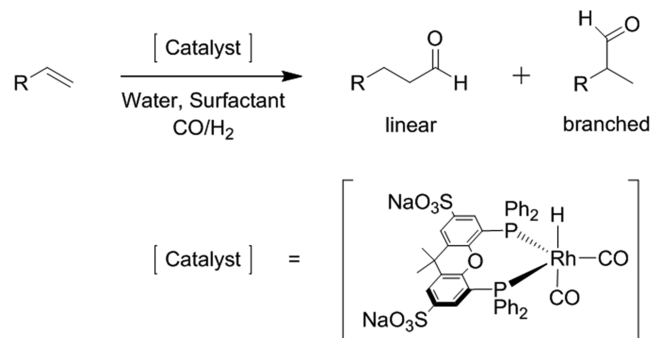


**Figure 3.** Hydroformylation reaction in microemulsion systems and the applied rhodium catalyst.

0.08, 95 °C reaction temperature, 15 bar syngas pressure, 1200 rpm stirring speed, and 1:4 metal-to-ligand ratio. The applied catalyst remains stable during the entire reaction time, and no sign of catalyst degradation can be observed. Recycling of the catalyst within the aqueous phase is easily possible by temperature-induced phase separation with a very low leaching

of Rh (<1 ppm) into the organic phase.<sup>21,22</sup> The successful transition of the reaction system into an integrated process on a mini-plant scale has been reported recently.<sup>16</sup>

**3.3. Effect of Salt Addition.** Preceding the discussion of general effects of surfactants in hydroformylation, we would like to explain the use of Na<sub>2</sub>SO<sub>4</sub> in the reaction mixture. The decision to add a salt to the reaction system originates from observations during the first continuous operation of the process (integrated reaction and separation) on miniplant scale, in which almost no phase separation of the reaction mixture could be achieved. This finding was in strong disagreement to the lab scale results where the separation of the system has always been achievable. In consequence, a systematic analysis of the separation dynamics of the reaction mixture was performed in a temperature and pressure controlled glass reactor with a gas dispersion stirrer to ensure realistic process conditions during the experiments. The experimental setup and procedure has already been reported in ref 23. In Figure 4 is illustrated the

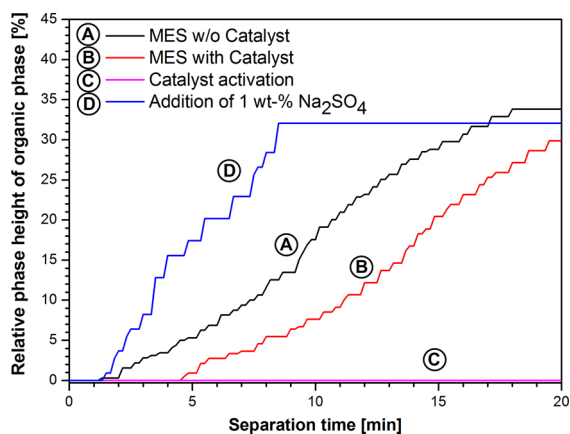


**Figure 4.** Relative height of organic (product) phase over separation time under process conditions. All experiments were performed at 85 °C and 10 bar pressure of argon (for A+B) or 10 bar pressure of syngas (C+D). MES was formulated from 1-dodecene, water, and Marlupal 24/70 ( $\alpha = 0.5$ ,  $\gamma = 0.08$ ). Additionally, 0.04 mol % [Rh(acac)(CO)<sub>2</sub>] and 0.16 mol % SulfoXantphos were added for B, C, and D.

evolution of the organic phase during the phase separation for the four crucial experiments of the screening. It becomes apparent that the activation of the rhodium catalyst with syngas inhibits the separation of the reaction system drastically. The separation time of the system increased from 18 min for the pure MES (Figure 4A) to around 25 min after the addition of catalyst (Figure 4B) and in the end to over several hours after the addition of syngas (Figure 4C). Moreover, it has to be noted that a complete separation of the reaction mixture under these conditions could not be observed. The surface activity of the applied catalyst complex has been observed only recently during parameter studies in lab scale.<sup>15</sup> However, such a strong impact of the catalyst on the phase separation was not to be expected and has not been reported before in the literature for other MES. To overcome this undesirable effect for the continuous operation, the reaction mixture has been modified by the addition of 1.0 wt % Na<sub>2</sub>SO<sub>4</sub>. With this adjustment of the ionic strength in the aqueous part of the reaction mixture, the effect of the catalyst complex as an ionic, surface active substance could be mostly suppressed by electrostatic screening. As a result, the separation dynamic of the system was

significantly improved, and thus the separation time decreased to roughly 8 min (Figure 4D).

Subsequent to these findings, we investigated the effect of the addition of Na<sub>2</sub>SO<sub>4</sub> on the reactivity and stability of the catalyst during hydroformylation reaction. For this purpose, the reaction was performed with varying concentrations of Na<sub>2</sub>SO<sub>4</sub>. The experimental results are shown in Figure 5. In

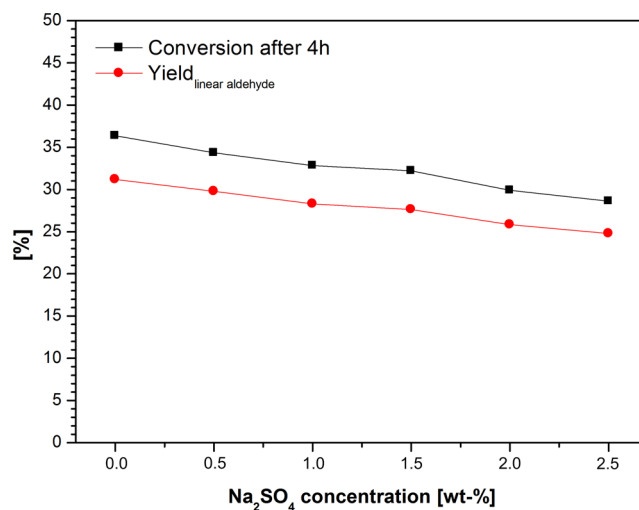


**Figure 5.** Effect of Na<sub>2</sub>SO<sub>4</sub> concentration on hydroformylation reaction. Test conditions: 0.04 mol % Rh(acac)(CO)<sub>2</sub>, 0.16 mol % SulfoXantphos, 120 mmol of 1-dodecene, water ( $\alpha = 0.5$ ),  $\gamma = 0.08$  (Marlupal 24/70),  $V_R = 50$  mL,  $T = 95$  °C,  $p = 15$  bar, stirring speed = 1200 rpm,  $t_R = 4$  h. Statistic deviation of results:  $\pm 3\%$ .

general, the reaction rate decreased with increasing amount of salt. The yield of linear aldehyde was reduced by roughly 1.2% per 0.5 wt % Na<sub>2</sub>SO<sub>4</sub> as compared to the reaction without salt after 4 h reaction time (31.3% yield). For 1.0 wt % Na<sub>2</sub>SO<sub>4</sub> in the system, a yield of 28.9% could be obtained. The most likely explanation for these results is an increasing destabilization of the MES with higher amounts of salt, which leads to larger emulsion droplets and consequently to a smaller interface for the reaction. Apart from the reactivity, the selectivity of the reaction remained unchanged at a high 98:2 ratio of linear to branched aldehydes, which proves the stability of the catalyst in the modified reaction mixture. The catalyst stability has also been tested in long-term experiments over 48 h with no sign of catalyst degradation. Concluding the results for separation and reaction, the application of Na<sub>2</sub>SO<sub>4</sub> is a feasible method to enable the phase separation of the reaction mixture under process conditions with only minor implications on catalysis. Thus, we decided to apply the salt in the reaction mixture for all following experiments, including the experiments presented in Figure 2.

**3.4. Effect of Temperature and Phase Behavior.** The hydroformylation of 1-dodecene was carried out at different temperatures between 68 and 120 °C. In general, the formation of the linear aldehyde could be increased by using higher temperatures (see Figure 6). Until 110 °C the reaction rate increased exponentially with the temperature and indicated a simple Arrhenius behavior. After 1 h reaction time, a TOF of 50 h<sup>-1</sup> was achieved at 68 °C, which could be raised to 380 h<sup>-1</sup> at 110 °C, while the selectivity toward the linear product remained at a very high value of 98%. As was recently reported in ref 24, an activation energy of 59 kJ/mol could be calculated

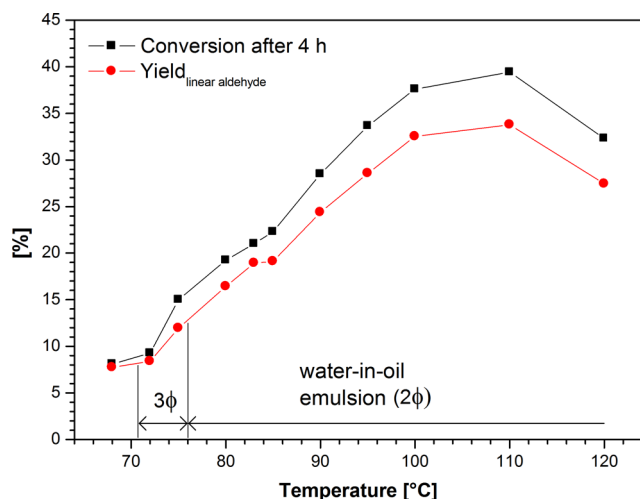


**Figure 6.** Effect of temperature on hydroformylation reaction. Test conditions: 0.04 mol % Rh(acac)(CO)<sub>2</sub>, 0.16 mol % SulfoXantphos, 120 mmol of 1-dodecene, water ( $\alpha = 0.5$ ),  $\gamma = 0.08$  (Marlipal 24/70), 1 wt % Na<sub>2</sub>SO<sub>4</sub>,  $V_R = 50$  mL,  $p = 15$  bar, stirring speed = 1200 rpm,  $t_R = 4$  h. Statistic deviation of results:  $\pm 3\%$ .

for the hydroformylation, which is in good accordance with literature data collected for the applied catalyst in single phase systems.<sup>25</sup> However, a decrease of reaction rate could be observed at temperatures higher than 110 °C, which is related to the applied surfactant. Regarding the phase behavior of the reaction mixture (shown in Figure 2a and also indicated in Figure 6), the optimal working area of Marlipal 24/70 as emulsifier is in the range of 70–80 °C. The application at far higher temperatures leads to a destabilization of the microemulsion system because the ability of the surfactant to work as an emulsifier is constantly decreasing with increasing temperature. In consequence, the droplet size of the emulsion increases, which leads to a smaller interfacial area and thus rising mass transfer limitations of the reaction.

Interestingly, the phase behavior of the microemulsion system has no noticeable influence on the reaction. The MES underwent two phase transitions between 68 and 82 °C that completely changed the type of microemulsion (oil-in-water (2 $\phi$ )  $\rightarrow$  bicontinuous (3 $\phi$ )  $\rightarrow$  water-in-oil (2 $\phi$ )). However, these changes of the emulsion type did not lead to an abrupt alteration of the reaction rate that would indicate a major change of mass transfer conditions. To further investigate this matter, an experiment was performed in which the reaction was carried out in each of the three microemulsion types at a constant temperature of 85 °C and constant values of  $\alpha$  and  $\gamma$ . Therefore, the phase behavior of the MES was adjusted by different amounts of Na<sub>2</sub>SO<sub>4</sub> in the mixtures. The results of this experiment are depicted in Figure 7. The reaction was performed with nearly similar rates for the oil-in-water (o/w) and the bicontinuous emulsion resulting in a conversion of roughly 24% and 25% after 4 h reaction time, respectively. As expected, the hydroformylation in the water-in-oil (w/o) emulsion was slightly slower due to the higher amount of salt in the mixture (compare with Figure 5). The results of this experiment confirm that the phase behavior of MES has no significant influence on the reaction rate of the hydroformylation due to the kinetic control of the reaction. This finding however is in clear contradiction to the conclusions from earlier works of Rost et al.<sup>20</sup> and Hamerla et al.<sup>19</sup> in which the hydroformylation of 1-dodecene in MES was found to

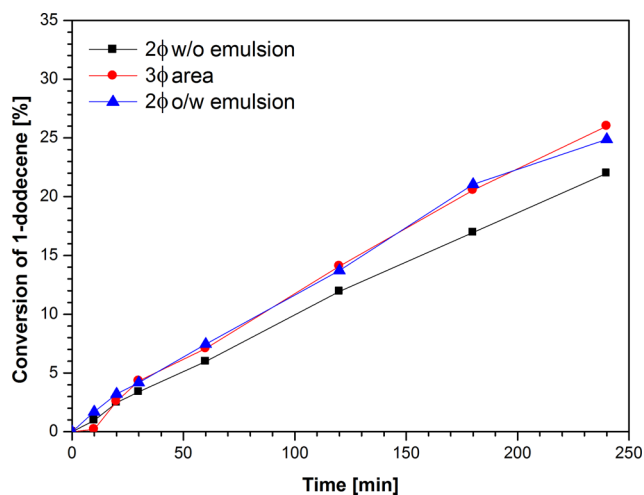


**Figure 7.** Effect of phase behavior on hydroformylation reaction. Test conditions: 0.04 mol % Rh(acac)(CO)<sub>2</sub>, 0.16 mol % SulfoXantphos, 120 mmol of 1-dodecene, water ( $\alpha = 0.5$ ),  $\gamma = 0.08$  (Marlipal 24/90),  $V_R = 50$  mL,  $T = 85$  °C,  $p = 15$  bar, stirring speed = 1200 rpm,  $t_R = 4$  h. Amount of Na<sub>2</sub>SO<sub>4</sub>: 0.1 wt % for 2 $\phi$  o/w emulsion, 1.0 wt % for 3 $\phi$  area, 3.0 wt % for 2 $\phi$  w/o emulsion. Statistic deviation of results:  $\pm 3\%$ .

perform the fastest inside the 3 $\phi$  area. The experiments that led the authors to their conclusion at that time were very similar to that from Figure 7 in this contribution. However, the main and very important difference between the earlier experiments and the one presented here is that they did adjust the phase behavior of their MES by changing the applied type of surfactant. Unfortunately, that was not the appropriate approach to perform this particular experiment. Although all of the received experimental data were correct, the interpretation was mistaken because they did mainly observe the influence of the chemical structure and chain length of the applied surfactants on the reaction rate of the hydroformylation and not the influence of the phase behavior. As we recently reported in ref 26, the constitution of the surfactant can have a relatively strong impact on reactions in MES. For instance, different functional groups of the surfactant can interact with the catalyst during catalysis and inhibit the reaction rate. In addition, the hydrophilicity (chain length, degree of ethoxylation) of the surfactant influences the reaction rate as well. This matter will be further discussed in the following section.

**3.5. Degree of Ethoxylation.** To investigate the influence of the surfactant chain length on the hydroformylation reaction, we varied the degree of ethoxylation (EO) from 5 to 9 (Marlipal 24/50 to 24/90). It was found that the reaction rate and EO number are in linear dependency at a constant reaction temperature; see Figure 8. However, it depends on the applied temperature whether it is a linear decrease or increase of the rate with increasing EO number. As explained in section 3.1, this is mainly due to the specific ability of the applied surfactants to work as emulsifiers for the reaction system, which changes with temperature. During the investigation on phase behavior in Figure 2b, it became evident that a higher EO number equals a higher temperature required for the surfactants to work efficiently. This characteristic is reflected in Figure 8 and gives an explanation why the reaction performs best at 80 °C with the short chained Marlipal 24/50, while at 95 °C the longest chained surfactant Marlipal 24/90 is clearly superior. Also, the higher density of the surfactant film with an increasing EO might enhance the adsorption of reactants at the

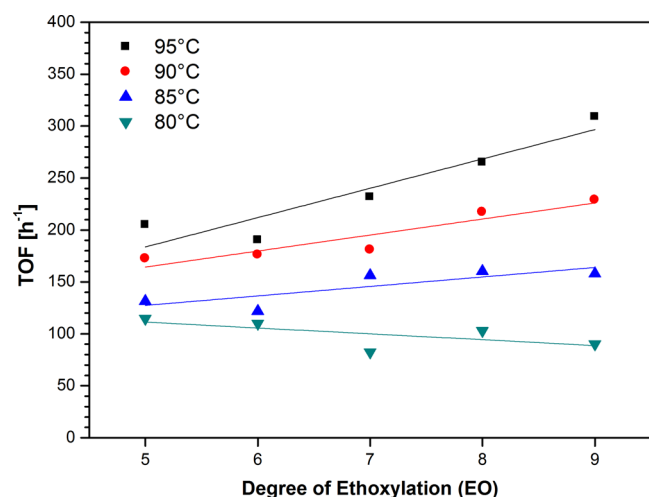


**Figure 8.** Degree of ethoxylation versus TOF for different reaction temperatures. Test conditions: 0.04 mol % Rh(acac)(CO)<sub>2</sub>, 0.16 mol % SulfoXantphos, 120 mmol of 1-dodecene, water ( $\alpha = 0.5$ ),  $\gamma = 0.08$  (Marlipal 24 series), 1 wt % Na<sub>2</sub>SO<sub>4</sub>,  $V_R = 50$  mL,  $p = 15$  bar, stirring speed = 1200 rpm,  $t_R = 1$  h. Statistic deviation of results:  $\pm 3\%$ .

oil–water interface and by that increase the reaction rate. Furthermore, it should be mentioned that the temperature dependency of the reaction for each applied surfactant confirms the findings in Figure 6. For better comparability, we listed the experimental results for a reaction temperature of 95 °C in Table 1. For Marlipal 24/50, an aldehyde yield of 25% was achieved after 4 h reaction time with a very high selectivity of 99% toward the linear product. By changing the EO number of the surfactant to 9 (Marlipal 24/90), the yield could be increased to 38%. To show that this is a general characteristic of these systems, we added the experimental results of a different

**Table 1.** Results for the Hydroformylation of 1-Dodecene with Different Surfactants at Constant Temperature<sup>a</sup>

no.	surfactant	conversion 1-dodecene [%]	yield (linear aldehyde) [%]	<i>n</i> : <i>iso</i> selectivity
1	Marlipal 24/50	28	25	99:1
2	Marlipal 24/60	25	24	98:2
3	Marlipal 24/70	34	29	98:2
4	Marlipal 24/80	38	33	98:2
5	Marlipal 24/90	43	38	98:2
6	Marlophen NPS <sup>b</sup>	4	4	99:1
7	Marlophen NP6 <sup>b</sup>	8	6	99:1
8	Marlophen NP7 <sup>b</sup>	10	9	98:2
9	Marlophen NP9 <sup>b</sup>	15	13	98:2

<sup>a</sup>Reaction conditions [1–5]: 0.04 mol % Rh(acac)(CO)<sub>2</sub>, 0.16 mol % SulfoXantphos, 120 mmol of 1-dodecene, water ( $\alpha = 0.5$ ),  $\gamma = 0.08$ , 1 wt % Na<sub>2</sub>SO<sub>4</sub>,  $V_R = 50$  mL,  $T = 95$  °C,  $p = 15$  bar, stirring speed = 1200 rpm,  $t_R = 4$  h. Statistic deviation of results:  $\pm 3\%$ . Reaction conditions [6–9]: 0.05 mol % Rh(acac)(CO)<sub>2</sub>, 0.25 mol % SulfoXantphos, 180 mmol of 1-dodecene, water ( $\alpha = 0.88$ ),  $\gamma = 0.10$ ,  $V_R = 50$  mL,  $T = 110$  °C,  $p = 40$  bar, stirring speed = 1000 rpm,  $t_R = 4$  h. <sup>b</sup>Data extracted from ref 26.

type of nonionic surfactant to Table 1. The surfactants from the Marlophen NP series contain an aromatic ring in their hydrophobic part instead of a solely aliphatic chain like in the Marlipal series. It is evident that the dependency of reaction rate and EO is similar for both types of surfactants. However, it is an interesting observation that the different structure of the Marlophen surfactants turned out to be not beneficial for the rate of the hydroformylation. We assume that the aromatic ring of the surfactant hinders the catalytic reaction, most probably through electronic interactions with the catalyst at the oil–water interface.<sup>5</sup> This leads to much lower aldehyde yields after 4 h reaction time as compared to Marlipal under mostly comparable reaction conditions.

**3.6. Effect of Surfactant Concentration.** The hydroformylation of 1-dodecene was carried out at different surfactant concentrations at a constant reaction temperature of 95 °C. In general, it was found that a higher concentration of surfactant leads to an increase in aldehyde yield after the same reaction time (see Figure 9). The yield increased from roughly

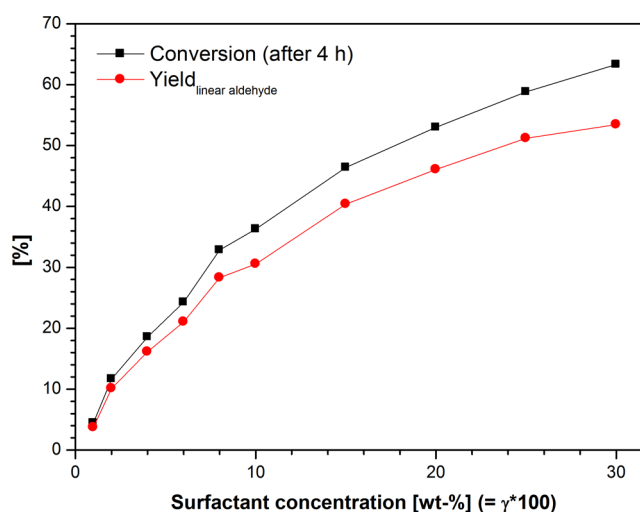


**Figure 9.** Effect of surfactant concentration on hydroformylation reaction. Test conditions: 0.04 mol % Rh(acac)(CO)<sub>2</sub>, 0.16 mol % SulfoXantphos, 120 mmol of 1-dodecene, water ( $\alpha = 0.5$ ), Marlipal 24/70, 1 wt % Na<sub>2</sub>SO<sub>4</sub>,  $V_R = 50$  mL,  $T = 95$  °C,  $p = 15$  bar, stirring speed = 1200 rpm,  $t_R = 4$  h. Statistic deviation of results:  $\pm 3\%$ .

4% with 1 wt % surfactant in the mixture to 53% with 30 wt % surfactant. The selectivity toward the linear product remained unchanged at a value of 98% in all experiments. In the case where no surfactant was applied in the mixture, no reaction progress could be observed during 4 h reaction time, confirming that the surfactant is needed to enable the hydroformylation. It stands out that the rate of the reaction continues to increase with the surfactant concentration (illustrated in Figure 10) even after the MES already became a macroscopic one-phase microemulsion (for  $\gamma > 0.12$ ). Considering the biphasic character of the system at  $\gamma < 0.12$ , more surfactant in the mixture generally means a larger interfacial area for the reaction and thus a higher potential reaction rate. In addition, the reaction rate is not affected by mass transfer limitation, which has been experimentally verified (see Figure 11). However, the significant further increase of the reaction rate at higher surfactant concentration cannot be solely addressed to the larger interfacial area, because all of the reactants are already located in one emulsion phase. Thus, this

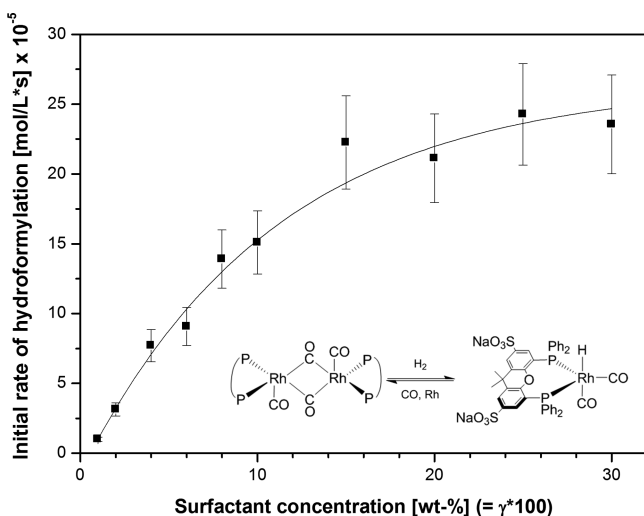


**Figure 10.** Effect of surfactant concentration on the rate of hydroformylation. Test conditions: 0.04 mol % Rh(acac)(CO)<sub>2</sub>, 0.16 mol % SulfoXantphos, 120 mmol of 1-dodecene, water ( $\alpha = 0.5$ ), Marlipal 24/70, 1 wt % Na<sub>2</sub>SO<sub>4</sub>,  $V_R = 50$  mL,  $T = 95$  °C,  $p = 15$  bar, stirring speed = 1200 rpm,  $t_R = 4$  h. Initial rates were calculated from syngas consumption. Statistic deviation of results:  $\pm 15\%$ .

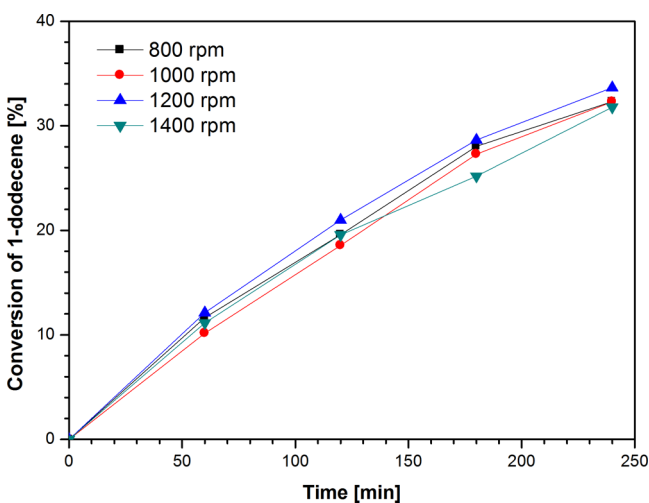


**Figure 11.** Effect of stirring speed on hydroformylation reaction. Test conditions: 0.04 mol % Rh(acac)(CO)<sub>2</sub>, 0.16 mol % SulfoXantphos, 120 mmol of 1-dodecene, water ( $\alpha = 0.5$ ),  $\gamma = 0.08$  Marlipal 24/70, 1 wt % Na<sub>2</sub>SO<sub>4</sub>,  $V_R = 50$  mL,  $T = 95$  °C,  $p = 15$  bar,  $t_R = 4$  h. Statistic deviation of results:  $\pm 3\%$ .

finding could be explained by a change in the local catalyst concentration at the oil–water interface. It has to be clarified first, that while the interfacial area of the reaction system (corresponding to the volume of the emulsion phase) is increasing with the surfactant concentration, the total amount of catalyst in the system remains constant. This means that the catalyst, which is located at the interface within the emulsion phase due to its surface activity, should be more diluted when the volume of this particular phase is increased. In consequence, the local catalyst concentration in the emulsion phase should decrease with increasing surfactant concentration. It is already known that rhodium catalysts with bidentate phosphine ligands, in particular the here applied rhodium sulfoxantphos catalyst, are able to form inactive dimeric catalyst species.<sup>19,27</sup> Because the equilibrium between monomer and

dimer is influenced by the concentration of catalyst (see drawing in Figure 10), a decrease of the local catalyst concentration in the emulsion phase should lead to a higher amount of the monomeric species and thus to a higher reaction rate. This would also give an explanation for the diminishing increase of the reaction rate at higher surfactant concentrations, because the equilibrium should be already strongly shifted to the monomer.

At last, it has to be mentioned that a too high concentration of surfactant in the MES bears a major drawback considering catalyst recycling. To maintain a good and fast switchability of the MES and, by that, enable an easy catalyst recycling, it is necessary to work with surfactant concentrations that do not exceed the 3 $\phi$  area (fish body) in the phase diagram. The 3 $\phi$  area is the most feasible state of the MES for catalyst recycling, because the phase separation performs here the fastest and most of the catalyst is located in the middle phase of the system together with the surfactant.<sup>21</sup> Higher surfactant concentrations would make it necessary to separate the system in one of the 2 $\phi$  systems, which would lead to longer separation times and higher potential losses of surfactant and catalyst into the product phase. Considering these points, the surfactant concentration of the investigated MES in Figure 9 should not exceed 12 wt % ( $\gamma = 0.12$ , compare with Figure 2a) to be applicable in an integrated chemical process.

#### 4. CONCLUSION

The performed experiments demonstrated that catalysis in microemulsion systems can be affected by several parameters, with the applied surfactant in a major role. To summarize this newly gained knowledge, Figure 12 schematically illustrates the

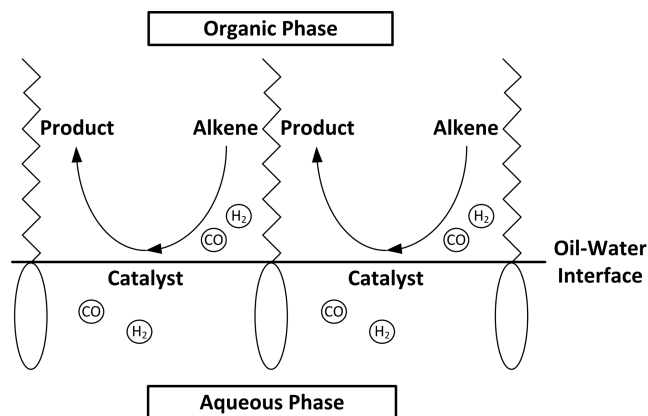


**Figure 12.** Schematic illustration of two-phase catalysis in micro-emulsions systems on the example of the hydroformylation reaction.

impact of the MES on the catalytic reaction. We assume that the catalyst complex is mainly located at the oil–water interface due to its surface activity. Consequently, the reaction should mainly take place at the interface as well. Regarding the temperature dependency of the investigated reaction (Figure 6), it seems likely to assume that the hydroformylation of long-chain alkenes in MES is a kinetically controlled two-phase reaction. With that, the role of the surfactant in these multiphase systems is of utmost importance. In its function as emulsifier, the surfactant determines the stability of the MES and the local concentrations at the oil–water interface, which are both important requirements for catalysis in MES (Figure 8). In addition, the surfactant provides the interfacial area for

the reaction and in consequence can also interact with the catalyst because both are in immediate vicinity to each other at the interface. Thus, it is possible that the catalytic reaction might be hindered by the surfactant due to electronic interactions with the catalyst (Table 1). All aspects considered, these findings point out the good applicability of MES as switchable reaction media in homogeneous catalysis and their high optimization potential for any given application by the choice of a proper surfactant.

## AUTHOR INFORMATION

### Corresponding Author

\*E-mail: tobias.pogrzeba@tu-berlin.de.

### ORCID

Tobias Pogrzeba: 0000-0003-3727-9589

### Notes

The authors declare no competing financial interest.

## ACKNOWLEDGMENTS

This work is part of the Collaborative Research Center/Transregio 63 "Integrated Chemical Processes in Liquid Multiphase Systems" (subprojects A2 and B4). Financial support by the Deutsche Forschungsgemeinschaft (DFG, German Research Foundation) is gratefully acknowledged (TRR 63). Furthermore, we gratefully acknowledge the support of the company Umicore for sponsoring the rhodium catalyst acetylacetonato-dicarbonylrhodium(I) (CAS: 14874-82-9).

## ABBREVIATIONS

2 $\phi$  = two phase

3 $\phi$  = three phase

EO = degree of ethoxylation

MES = microemulsion system

SX = SulfoXantphos, 4,5-bis(diphenylphosphino)-9,9-dimethylxanthene

TOF = turnover frequency

## REFERENCES

- (1) Lipshutz, B. H.; Gallou, F.; Handa, S. Evolution of Solvents in Organic Chemistry. *ACS Sustainable Chem. Eng.* **2016**, *4*, 5838.
- (2) Dwars, T.; Paetzold, E.; Oehme, G. Reactions in Micellar Systems. *Angew. Chem., Int. Ed.* **2005**, *44*, 7174.
- (3) Lipshutz, B. H.; Taft, B. R. Heck Couplings at Room Temperature in Nanometer Aqueous Micelles. *Org. Lett.* **2008**, *10* (7), 1329.
- (4) Lipshutz, B. H.; Ghorai, S.; Abela, A. R.; Moser, R.; Nishikata, T.; Duplais, C.; Krasovskiy, A.; Gaston, R. D.; Gadwood, R. C. TPGS-750-M: A Second-Generation Amphiphile for Metal-Catalyzed Cross-Couplings in Water at Room Temperature. *J. Org. Chem.* **2011**, *76* (11), 4379.
- (5) Schwarze, M.; Milano-Brusco, J. S.; Stempel, V.; Hamerla, T.; Wille, S.; Fischer, C.; Baumann, W.; Arlt, W.; Schomäcker, R. Rhodium Catalyzed Hydrogenation Reactions in Aqueous Micellar Systems as Green Solvents. *RSC Adv.* **2011**, *1* (3), 474.
- (6) La Sorella, G.; Strukul, G.; Scarso, A. Recent Advances in Catalysis in Micellar Media. *Green Chem.* **2015**, *17*, 644.
- (7) Dwars, T.; Haberland, J.; Grassert, I.; Oehme, G.; Kragl, U. Asymmetric Hydrogenation in a Membrane Reactor: Recycling of the Chiral Catalyst by Using a Retainable Micellar System. *J. Mol. Catal. A: Chem.* **2001**, *168* (1–2), 81.
- (8) Schwarze, M.; Schmidt, M.; Nguyen, L. A. T.; Drews, A.; Kraume, M.; Schomäcker, R. Micellar Enhanced Ultrafiltration of a Rhodium Catalyst. *J. Membr. Sci.* **2012**, *421–422*, 165.
- (9) Winsor, P. A. Hydrotrophy, Solubilisation and Related Emulsification Processes. Part I. *Trans. Faraday Soc.* **1948**, *44*, 376.
- (10) Kahlweit, M.; Strey, R.; Busse, G. Microemulsions: A Qualitative Thermodynamic Approach. *J. Phys. Chem.* **1990**, *94*, 3881.
- (11) Schwarze, M.; Pogrzeba, T.; Volovych, I.; Schomäcker, R. Microemulsion Systems for Catalytic Reactions and Processes. *Catal. Sci. Technol.* **2015**, *5*, 24.
- (12) Nowothnick, H.; Blum, J.; Schomäcker, R. Suzuki Coupling Reactions in Three-Phase Microemulsions. *Angew. Chem., Int. Ed.* **2011**, *50*, 1918.
- (13) Volovych, I.; Kasaka, Y.; Schwarze, M.; Nairoukh, Z.; Blum, J.; Fanun, M.; Avnir, D.; Schomäcker, R. Investigation of Sol-gel Supported Palladium Catalysts for Heck Coupling Reactions in O/w-Microemulsions. *J. Mol. Catal. A: Chem.* **2014**, *393*, 210.
- (14) Volovych, I.; Neumann, M.; Schmidt, M.; Buchner, G.; Yang, J.-Y.; Wölk, J.; Sottmann, T.; Strey, R.; Schomäcker, R.; Schwarze, M. A Novel Process Concept for the Three Step Boscalid® Synthesis. *RSC Adv.* **2016**, *6*, 58279.
- (15) Pogrzeba, T.; Müller, D.; Hamerla, T.; Esche, E.; Paul, N.; Wozny, G.; Schomäcker, R. Rhodium-Catalyzed Hydroformylation of Long-Chain Olefins in Aqueous Multiphase Systems in a Continuously Operated Miniplant. *Ind. Eng. Chem. Res.* **2015**, *54*, 11953.
- (16) Illner, M.; Müller, D.; Esche, E.; Pogrzeba, T.; Schmidt, M.; Schomäcker, R.; Wozny, G.; Repke, J.-U. Hydroformylation in Microemulsions: Proof of Concept in a Miniplant. *Ind. Eng. Chem. Res.* **2016**, *55*, 8616.
- (17) Goedheijt, M. S.; Kamer, P. C. J.; Leeuwen, P. W. N. M.; Van, A. Water-Soluble Diphosphine Ligand with a Large "Natural" Bite Angle for Two-Phase Hydroformylation of Alkenes. *J. Mol. Catal. A: Chem.* **1998**, *134*, 243.
- (18) Kasaka, Y.; Bibouche, B.; Volovych, I.; Schwarze, M.; Schomäcker, R. Investigation of Phase Behaviour of Selected Chemical Reaction Mixtures in Microemulsions for Technical Applications. *Colloids Surf., A* **2016**, *494*, 49.
- (19) Hamerla, T.; Rost, A.; Kasaka, Y.; Schomäcker, R. Hydroformylation of 1-Dodecene with Water-Soluble Rhodium Catalysts with Bidentate Ligands in Multiphase Systems. *ChemCatChem* **2013**, *5*, 1854.
- (20) Rost, A.; Müller, M.; Hamerla, T.; Kasaka, Y.; Wozny, G.; Schomäcker, R. Development of a Continuous Process for the Hydroformylation of Long-Chain Olefins in Aqueous Multiphase Systems. *Chem. Eng. Process.* **2013**, *67*, 130.
- (21) Pogrzeba, T.; Müller, D.; Illner, M.; Schmidt, M.; Kasaka, Y.; Weber, A.; Wozny, G.; Schomäcker, R.; Schwarze, M. Superior Catalyst Recycling in Surfactant Based Multiphase Systems – Quo Vadis Catalyst Complex? *Chem. Eng. Process.* **2016**, *99*, 155.
- (22) Nowothnick, H.; Rost, A.; Hamerla, T.; Schomäcker, R.; Müller, C.; Vogt, D. Comparison of Phase Transfer Agents in the Aqueous Biphasic Hydroformylation of Higher Alkenes. *Catal. Sci. Technol.* **2013**, *3* (3), 600.
- (23) Müller, D.; Esche, E.; Pogrzeba, T.; Illner, M.; Leube, F.; Schomäcker, R.; Wozny, G. Systematic Phase Separation Analysis of Surfactant Containing Systems for Multiphase Settler Design. *Ind. Eng. Chem. Res.* **2015**, *54*, 3205.
- (24) Pogrzeba, T.; Illner, M.; Schmidt, M.; Repke, J.-U.; Schomäcker, R. Microemulsion Systems as Switchable Reaction Media for the Catalytic Upgrading of Long-Chain Alkenes. *Chem. Ing. Tech.* **2017**, *89* (4), 459.
- (25) Bhanage, B. M.; Divekar, S. S.; Deshpande, R. M.; Chaudhari, R. V. Kinetics of Hydroformylation of 1-Dodecene Using Homogeneous HRh(CO)(PPh<sub>3</sub>)<sub>3</sub> Catalyst. *J. Mol. Catal. A: Chem.* **1997**, *115*, 247.
- (26) Schwarze, M.; Pogrzeba, T.; Seifert, K.; Hamerla, T.; Schomäcker, R. Recent Developments in Hydrogenation and Hydroformylation in Surfactant Systems. *Catal. Today* **2015**, *247*, 55.
- (27) Deshpande, R. M.; Kelkar, A. A.; Sharma, A.; Julcour-lebigue, C.; Delmas, H. Kinetics of Hydroformylation of 1-Octene in Ionic Liquid-Organic Biphasic Media Using Rhodium Sulfoxantphos Catalyst. *Chem. Eng. Sci.* **2011**, *66*, 1631.

# PAPER 9

## **Alkaline hydrolysis of methyl decanoate in surfactant based systems**

Marcel Schmidt, Johannes Deckwerth, Reinhard Schomäcker, Michael Schwarze

The Journal of Organic Chemistry, 2018, 83, 14, 7398-7406

Online Article:

<https://pubs.acs.org/doi/10.1021/acs.joc.8b00247>

Reproduced (or 'Reproduced in part') with permission from "Alkaline hydrolysis of methyl decanoate in surfactant based systems; Marcel Schmidt, Johannes Deckwerth, Reinhard Schomäcker, Michael Schwarze. The Journal of Organic Chemistry, 2018, 83, 14, 7398-7406." Copyright (2018) American Chemical Society.



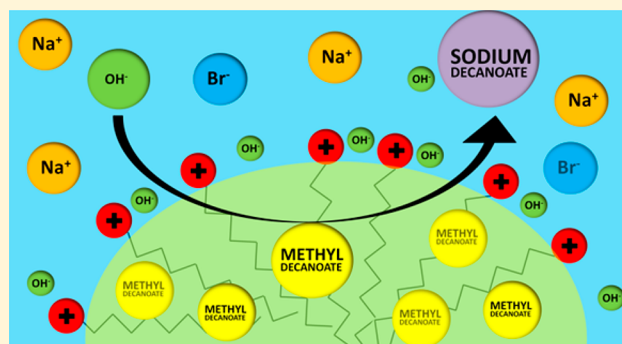
# Alkaline Hydrolysis of Methyl Decanoate in Surfactant-Based Systems

Marcel Schmidt,<sup>\*,†</sup> Johannes Deckwerth,<sup>†</sup> Reinhard Schomäcker,<sup>†</sup> and Michael Schwarze<sup>‡,§</sup>

<sup>†</sup>Department of Chemistry, Technische Universität Berlin, Strasse des 17. Juni 124, Sekretariat TC-8, Berlin D-10623, Germany

<sup>‡</sup>Department of Process Engineering, Technische Universität Berlin, Strasse des 17. Juni 135, Sekretariat TK-01, Berlin D-10623, Germany

**ABSTRACT:** Surfactant-modified reaction systems are one approach to perform organic reactions with water as the solvent involving hydrophobic reactants. Herein, the alkaline hydrolysis of the long-chain methyl decanoate in cationic and nonionic surfactant-modified systems is reported. The physicochemical behavior of the reaction mixture and the performance of the alkaline hydrolysis were systematically investigated. In water as the solvent, the reaction is slow, but at elevated temperatures, the alkaline hydrolysis of methyl decanoate is accelerated because the reaction product sodium decanoate acts as an ionic surfactant, leading to an increased solubility of methyl decanoate in the aqueous phase. The rate can be significantly increased by the addition of surfactants as solubilizers. In nonionic TX-100 solutions, the reaction rate can be increased by a factor of about 100 for a surfactant concentration of 5 wt %. If cationic surfactants are applied, the reaction rate can be further increased due to the electrostatic interaction between the hydroxide ions in solution and the charged head groups of the cationic micelles.



## INTRODUCTION

Surfactant-based reaction media have attracted much attention during recent years as alternatives to conventional organic solvents. Their outstanding properties, such as water as solvent, increased interfacial area, and advanced separation concepts, have classified them as green solvents. Manifold stoichiometric, noble-metal-, as well as biocatalyzed reactions were successfully performed in these media.<sup>1–3</sup> Above the critical micelle concentration (CMC), surfactant monomers spontaneously aggregate into micelles that act as nanosized carriers able to solubilize hydrophobic reactants in water. In many stoichiometric reactions involving surfactants, a significant increase in the reactions rate is observed for which the term *micellar catalysis* was introduced.<sup>4</sup> Mubofu and Engberts studied Diels–Alder reactions, and compared to pure water as the solvent, the rate increased by a factor of about 80 when SDS (10 mM, pH 2) was used as the surfactant.<sup>5</sup> Bahrami et al. synthesized benzimidazoles and obtained almost quantitative yield using SDS, whereby in pure water the yield was only 23%.<sup>6</sup> The main reason for the higher reaction rate is the locally higher concentration of reactants. In both examples, the hydrophobic reactants are solubilized in the core of the micelles, where they accumulate and react. In other examples, especially hydrolysis reactions involving OH<sup>−</sup> ions, one reactant accumulates at the surface of the micelles if cationic surfactants are applied.<sup>7–10</sup> One group of reactants where this phenomenon can be followed visually are triarylmethane dyes, where the solution at full conversion becomes colorless. Several studies for hydrolysis

reactions catalyzed by cationic micelles are shown in the literature.<sup>11–13</sup> The effects that surfactants can have on the rate of chemical reactions have been reviewed by Samiey et al.<sup>14</sup> From the huge number of commercially available surfactants, sodium dodecyl sulfate (SDS), linear alkyl sulfonate (LAS), cetyltrimethylammonium bromide (CTAB), and (*tert*-octylphenoxy) polyethoxyethanol (TX-100) are most frequently used. In addition, new so-called designer surfactants, e.g., PTS, PQS, or TPGS-750, have been synthesized by the Lipshutz group at the University of California, Santa Barbara. These surfactants possess higher solubilization capacity and show good performance in noble-metal-catalyzed coupling<sup>15,16</sup> or metathesis<sup>17,18</sup> reactions. Besides the solubilization of hydrophobic reactants, micellar reaction media allow for the recycling of expensive noble-metal catalyst complexes in their active state, e.g., by micellar enhanced ultrafiltration<sup>19,20</sup> or phase separation.<sup>21,22</sup> Recently it was shown that such an advanced separation concept can be applied on a technically relevant scale in a continuously operated mini plant, e.g., for the hydroformylation of long-chained olefins.<sup>23</sup>

In this contribution, we study the hydrolysis of methyl decanoate in aqueous-micellar solutions of various cationic and nonionic surfactants. The investigations on the alkaline

**Special Issue:** Organic and Biocompatible Transformations in Aqueous Media

**Received:** January 27, 2018

**Published:** May 15, 2018

hydrolysis are part of collaborative research project called InPROMPT “Integrated Chemical Processes in Liquid Multi-phase Systems”. A strong focus of InPROMPT is catalytic reactions in multiphase systems to recycle the homogeneously dissolved catalyst by a simple phase separation under simultaneously discharge of the product.<sup>24–26</sup> The formation of long-chained acids like decanoic acid can be carried out with a one-step sequence (hydroxycarbonylation) or with a two-step sequence (methoxycarbonylation with consecutive hydrolysis) (see Figure 1).

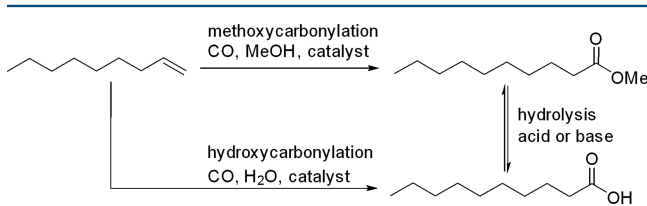


Figure 1. Reaction network for the synthesis of decanoic acid.

To evaluate the advantages and disadvantages of the two reaction pathways, investigations on the alkaline hydrolysis are indispensable. The reaction can be catalyzed by a base, involving only irreversible reaction steps. Generally, water is used as the solvent for the alkaline hydrolysis process to dissolve both the ester and the base. However, methyl decanoate is poorly soluble in water, and the obtained two-phase system provides only a small interfacial area, resulting in low reaction rates. The addition of surfactants as solubilizers will lead to an increased solubility of methyl decanoate in water. For the micellar system, the properties of the surfactant and the reaction rate depend on the composition of the reaction mixture and the temperature; therefore, we determined first the impact of the reaction conditions on the CMC and the phase behavior. Thereafter, we investigated the hydrolysis of methyl decanoate using TX-100 and alkyl trimethylammonium bromide surfactants with variable alkyl chain lengths ( $\text{CH}_3(\text{CH}_2)_n\text{N}(\text{CH}_3)_3\text{Br}$ ,  $n = 9–15$ ). Detailed investigations of the reaction rate as a function of surfactant type and concentration were performed to select the minimum concentration of surfactant for the reaction mixture and to facilitate the subsequent product isolation.

## RESULTS AND DISCUSSION

**Reaction.** The alkaline hydrolysis is an important reaction for the synthesis of carboxylic acids from the corresponding esters. We selected the poorly water-soluble long-chained methyl decanoate as a model substrate that reacts with sodium hydroxide as the base to sodium decanoate (Figure 2).

With aqueous NaOH solutions, methyl decanoate will form a two-phase system where the reaction will slowly take place at the interphase. To increase the reaction rate, we applied different surfactants. The main surfactant characteristics needed to select an appropriate additive to the reaction mixture are the CMC of the surfactant and the phase behavior of the reaction mixture. Both were evaluated prior to the stoichiometric

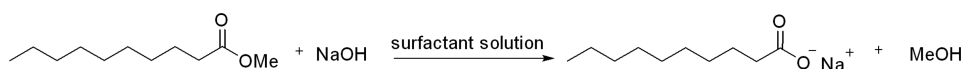


Figure 2. Reaction scheme for the alkaline hydrolysis of methyl decanoate with sodium hydroxide (NaOH) to sodium decanoate.

reaction to relate the observed kinetics to the properties of the reaction system.

### Determination of the Critical Micelle Concentration.

Since TX-100 is frequently investigated as a solubilizer for organic reactions in water, e.g., for coupling reactions,<sup>15,27</sup> and available with high purity, it was chosen as the benchmark surfactant. The CMC of the surfactant is a crucial parameter for organic reactions in water. Hence, the CMC of the applied surfactant TX-100 has been measured with a bubble pressure tensiometer at room temperature. In addition, the CMC of sodium decanoate and mixtures of sodium decanoate and Triton X-100 have been determined, since the alkaline hydrolysis of methyl decanoate forms sodium decanoate. Because of its amphiphilic structure, the sodium decanoate may act as a surfactant, leading to the formation of single micelles or mixed micelles with TX-100. Consequently, the CMC could vary significantly, depending on the conversion of methyl decanoate hydrolysis. For TX-100, the determined CMC in water is  $4.1 \times 10^{-4}$  mol/L, which is in accordance with the literature.<sup>28–30</sup> The pure sodium decanoate, which can be classified as an ionic surfactant, has a CMC of 0.1 mol/L, which is significantly higher compared to TX-100. The CMC of a mixture of sodium decanoate and Triton X-100 with a mole fraction of 0.5 is  $5.8 \times 10^{-4}$  mol/L. With a lower mole fraction of TX-100 ( $x = 0.25$ ), the CMC is further increased to  $6.9 \times 10^{-4}$  mol/L. As expected, the CMC values of the mixtures are between the values of the pure components (see Figure 3).

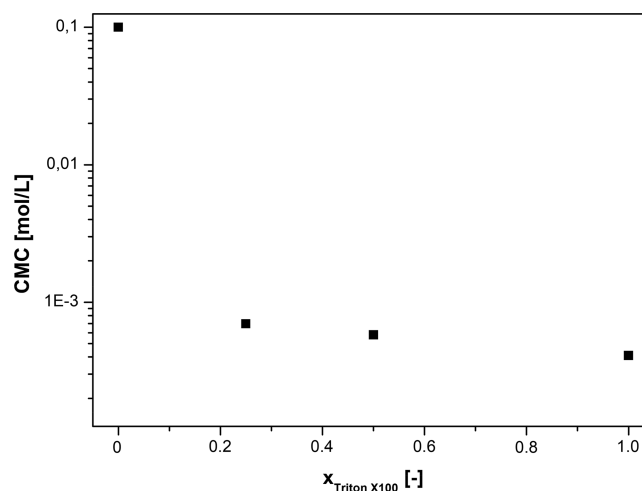
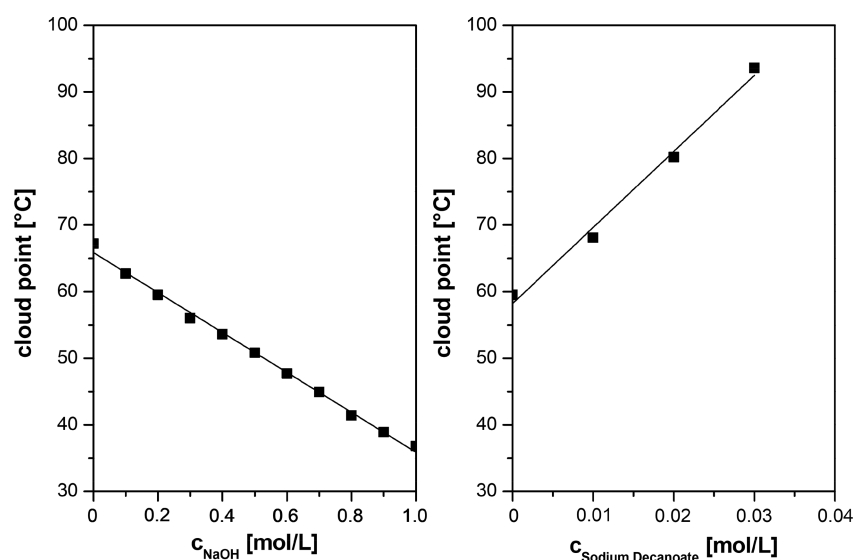


Figure 3. CMC of TX-100, sodium decanoate, and mixtures of TX-100 and sodium decanoate at room temperature, standard deviation 3%.

However, the CMCs of the mixtures resemble predominantly the CMC of the nonionic surfactant TX-100, which is typical for mixed micelles consisting of an ionic and nonionic surfactant.<sup>31,32</sup> The electrostatic repulsion of the anionic head groups of sodium decanoate is drastically reduced with the addition of TX-100, causing micellization and a significant decrease in the CMC value already for low mole fractions of TX-100. The results show that the formed sodium decanoate



**Figure 4.** Effect of sodium hydroxide (left) and sodium decanoate (right) on the cloud point of an aqueous TX-100 solution. Experimental conditions:  $V = 20$  mL,  $c_{\text{TX100}} = 5$  wt %, (right)  $c_{\text{NaOH}} = 0.2$  mol/L.

molecules aggregate with TX-100 molecules in aqueous solutions. In summary, the formation of sodium decanoate leads to an increase of the CMC, especially at low mole fractions of TX-100, which has to be kept in mind for the evaluation of the reaction performance for the alkaline hydrolysis of methyl decanoate.

**Investigation on Phase Behavior.** Besides the impact of aqueous mixtures on the CMC, knowledge about the phase behavior, especially the cloud point, is essential for the investigation of the alkaline hydrolysis in aqueous TX-100 solutions, particularly for the separation of the applied surfactant TX-100. Since the hydrolysis takes place under alkaline conditions, the impact of the sodium hydroxide concentration and, additionally, the impact of the formed sodium decanoate on the cloud point of TX-100 has been investigated. Figure 4 (left) shows the cloud point of aqueous TX-100 solutions (5 wt %) as a function of the concentration of sodium hydroxide in a range of 0 to 1 mol/L. The cloud point of TX-100 (5 wt %) in an aqueous solution without sodium hydroxide was determined to be 67.2 °C and is in good agreement with the literature.<sup>33</sup> With increasing concentration of sodium hydroxide, the cloud point decreases linearly to 36.8 °C at 1 mol/L of sodium hydroxide. As expected, sodium hydroxide acts as an electrolyte and leads to a salting out process, decreasing the cloud point with increasing electrolyte concentration. The sodium hydroxide molecules are cosmotropic ions, binding strongly to water and thus belonging to the “water-structure-making” ions. Hence, the strong interaction of the electrolyte molecules with water molecules leads to a dehydration of the polyethylene glycol chains of the applied surfactant, resulting in a lower cloud point, which is known as salting out effect.<sup>34</sup> On the basis of these findings, the sodium hydroxide concentration for all further experiments was fixed to 0.2 mol/L.

Next, the effect of sodium decanoate on the cloud point was investigated (Figure 4, right). Interestingly, sodium decanoate strongly influences the cloud point of the mixtures. The cloud point increases drastically from 58.1 to 93.6 °C with only 0.03 mol/L of sodium decanoate, showing a linear tendency. The sodium decanoate acts as an anionic cosurfactant forming

mixed micelles with TX-100. The incorporation of the anionic molecules into the micelles, formed by TX-100, leads to a negative surface charge of the micelles. Thus, the incorporation of charged cosurfactants forces a repulsion between the micelles, resulting in an increased water solubility, which makes the micelles more hydrophilic.<sup>35</sup> Consequently, the cloud point of the mixtures is drastically increased. We have to mention that a full conversion of methyl decanoate corresponds to a sodium decanoate concentration of 0.2 mol/L. In Figure 4 (right), the concentration of sodium decanoate was varied between 0 and 0.03 mol/L, which corresponds to a conversion of methyl decanoate in the alkaline hydrolysis between 0 and 15%. As the cloud point is increased to very high temperatures with increasing conversion of methyl decanoate, a one-phase solution is expected after the reaction.

#### Alkaline Hydrolysis of Methyl Decanoate in Water.

Initially, the alkaline hydrolysis of methyl decanoate in an aqueous sodium hydroxide solution has been studied at different temperatures, which is shown in Figure 5. At 40 and 60 °C, the conversion after 20 h reaction time is 3% and 5%, respectively. As expected, the low solubility of methyl decanoate in water causes the low reaction rates, resulting in low conversions. Surprisingly, the conversion obtained after 20 h reaction time at a reaction temperature of 80 °C is 82%, although no further additives were used. Furthermore, the slope of the conversion plot for the reaction temperature of 80 °C increases as the reaction proceeds, which is an atypical trend for a second-order reaction. Apparently, the conversion of methyl decanoate to sodium decanoate accelerates the reaction. The determined CMC of sodium decanoate at room temperature is 0.1 mol/L, which is equal to 50% conversion of methyl decanoate. Hence, the formation of micelles, initiated by the formation of sodium decanoate during the reaction, increases the solubility of methyl decanoate, resulting in an enhancement of the reaction rate with proceeding reaction time. Obviously, the slope of the conversion plot is slightly increasing at a conversion of 40% (see Figure 5), which confirms this assumption, since the CMC of sodium decanoate is reached. We have to keep in mind that the CMC of sodium decanoate is

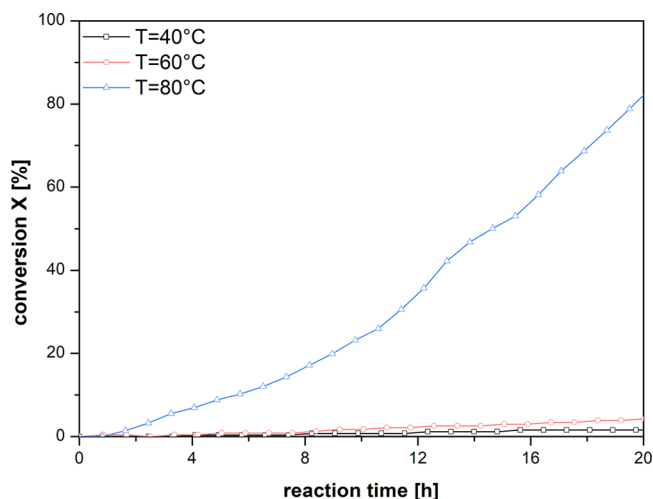


**Figure 5.** Effect of the temperature on the conversion plot of the alkaline hydrolysis of methyl decanoate in water. Experimental conditions:  $V = 20$  mL,  $c_{\text{methyl decanoate}} = 0.2$  mol/L,  $c_{\text{NaOH}} = 0.2$  mol/L.

slightly temperature dependent, which could lead to a small mismatch.

**Alkaline Hydrolysis of Methyl Decanoate in Aqueous TX-100 Solution.** On the basis of the findings of the CMC and the phase behavior, the alkaline hydrolysis of methyl decanoate was performed at three different temperatures. To perform the reaction below and above the cloud point of the reaction mixture, we decided to operate at 40, 60, and 80 °C. The 2-fold amount of the determined CMC for TX-100, which was measured at room temperature, has been used as TX-100 concentration for the temperature variation. As seen in Figure 6, the addition of TX-100 is crucial for the reaction

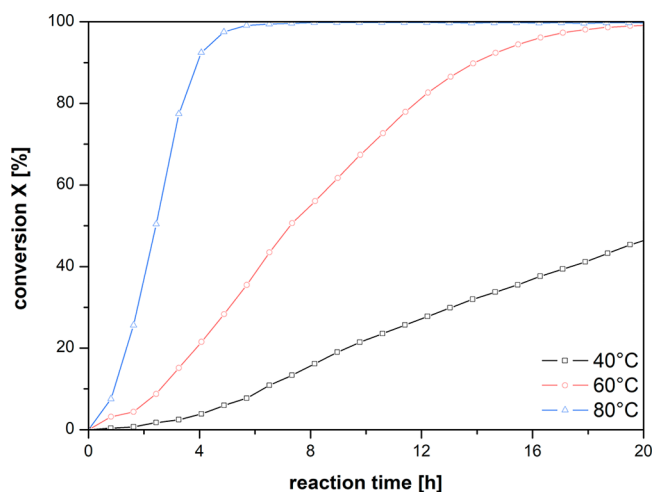


**Figure 6.** Effect of the temperature on the conversion plot of the alkaline hydrolysis of methyl decanoate in aqueous TX-100 solution. Experimental conditions:  $V = 20$  mL,  $c_{\text{methyl decanoate}} = 0.2$  mol/L,  $c_{\text{NaOH}} = 0.2$  mol/L,  $c_{\text{TX-100}} = 2 \times \text{CMC}$ .

performance of the alkaline hydrolysis of methyl decanoate comparing both reaction systems, with and without phase-transfer agent (Figure 5). Already the addition of small amounts of TX-100 leads to a significant increase in the reaction rate. Comparing the reaction at 80 °C with and without added TX-100, the reaction rate, which is proportional to the slope of the conversion plot, is increased by a factor of

30. Moreover, the conversion reaches 100% after 8 h reaction time. If the temperature is lowered to 60 or 40 °C, the reaction is still much faster than in the absence of the surfactant. Even for the reaction performed at 40 °C, noticeable conversions of 40% are obtained after 20 h reaction time. Since the added TX-100 forms micelles above the CMC, methyl decanoate can be solubilized in the aqueous phase, and the reaction rate is significantly enhanced. If hydrolysis reactions are performed under conventional two-phase conditions, the rate is often influenced by film diffusion, resulting in apparent low activation energies. The application of surfactants with concentrations above the CMC will not only increase the solubility of the hydrophobic reactants in the aqueous phase but also provide a high interfacial area for mass transport. In this case, the temperature dependency of the reaction using the Arrhenius law should result in much higher apparent activation energy. The activation energy of the alkaline hydrolysis of methyl decanoate was calculated from Figure 6 to be 56.4 kJ/mol, which indicates a kinetic control of the reaction in aqueous TX-100 solution that results in a stronger acceleration of the reaction at elevated temperature.

Additionally, the impact of the TX-100 concentration has been studied with regard to the reaction performance, especially the initial rate of reaction. As it can be seen in Figure 7 the amount of surfactant plays a crucial role for the

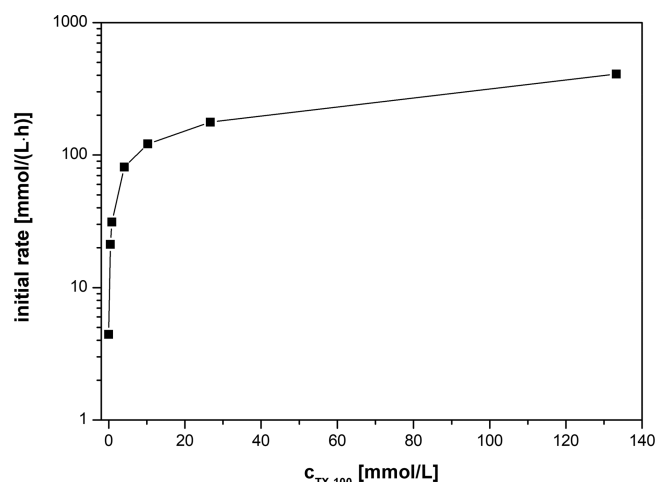


**Figure 7.** Effect of the TX-100 concentration on the initial rate of the alkaline hydrolysis of methyl decanoate. Experimental conditions:  $T = 80$  °C,  $V = 20$  mL,  $c_{\text{methyl decanoate}} = 0.2$  mol/L,  $c_{\text{NaOH}} = 0.2$  mol/L, initial rate determined at a conversion of 10%.

reaction rate of the alkaline hydrolysis of methyl decanoate in aqueous systems. The reaction temperature was kept constant at 80 °C. As expected, the reaction rate increases substantially with increasing concentration of the phase-transfer agent; for instance, an increase of the surfactant concentration from 4.1 mmol/L, which is equal to 10× CMC, to 133.3 mmol/L (5 wt %) leads to an enhancement of the reaction rate by a factor of 5. On the one hand, the higher the concentration of TX-100 the higher the concentration of methyl decanoate in the aqueous phase since more micelles can be formed. As a result, the reaction rate is enhanced. On the other hand, the amount of surfactant increases the interface between water and oil, which could result in higher reaction rates. However, the increase of the reaction rate is not proportional to the increase of the surfactant concentration. Obviously, the reaction rate converges

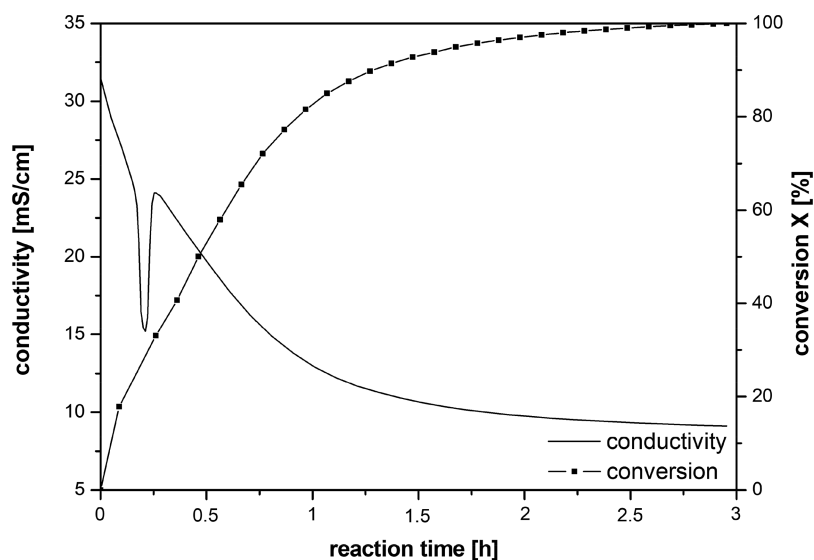


**Figure 8.** Conversion and conductivity plot of the alkaline hydrolysis of methyldecanoate. Experimental conditions:  $T = 80\text{ }^{\circ}\text{C}$ ,  $V = 20\text{ mL}$ ,  $c_{\text{TX}100} = 5\text{ wt \%}$ ,  $c_{\text{NaOH}} = 0.2\text{ mol/L}$ ,  $c_{\text{methyl decanoate}} = 0.2\text{ mol/L}$ .

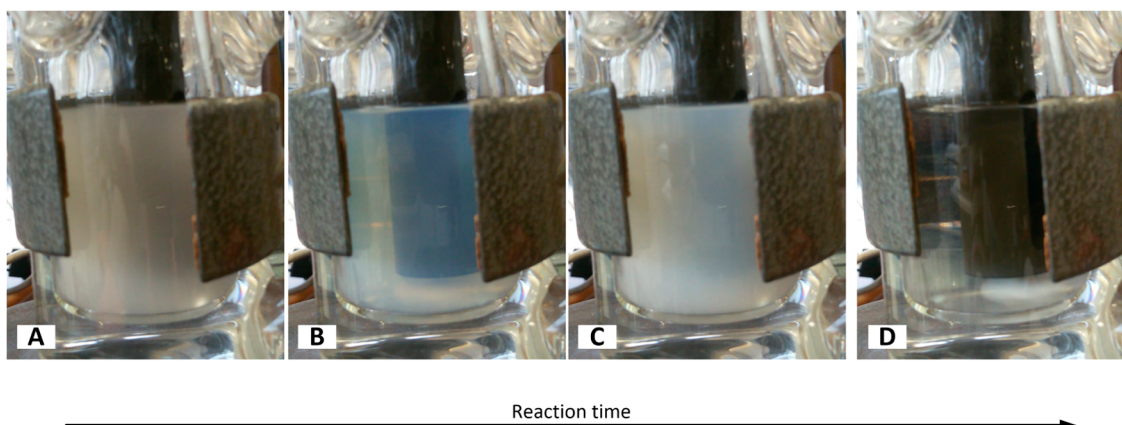


**Figure 9.** Reaction mixture with proceeding reaction time, (A) 0 min, (B) 12 min, (C) 15 min, (D) 180 min.

at a maximum rate with increasing surfactant concentration since the rate is limited by the concentration of methyl decanoate in the aqueous phase. At high TX-100 concentrations, all of the substrate can be solubilized in the micelles. A further increase of the surfactant concentration could lead to a decrease of the reaction rate since the methyl decanoate is diluted with higher amount of surfactant. This trend was also shown by other researchers, e.g., for the fading of dyes.<sup>36,37</sup>

Moreover, no correlation can be found between the reaction rate and the phase behavior of the systems. Starting above the cloud point ( $80\text{ }^{\circ}\text{C}$ ), indicated by a white and turbid reaction mixture after injection of the substrate, the mixture turns into a clear solution at the end of the reaction, indicating a micellar solution below the cloud point. As mentioned, the formed sodium decanoate has a strong impact on the cloud point of the mixture, leading to an increase of the cloud point with increasing conversion of methyl decanoate. However, no change in the conversion plot can be observed, concluding no correlation between reaction performance and phase behavior. This is another indication that no mass-transfer limitation is involved in the reaction kinetics.

Interestingly, the electrical conductivity of the reaction mixture drops drastically using high concentrations of Triton

X-100 (5 wt %), resulting in an unexpected minimum at the beginning of the reaction. Figure 8 shows the conductivity and the calculated conversion over time for a Triton X-100 concentration of 5 wt %. Starting above the cloud point (Figure 9A), the reaction mixture passes through different phase states with increasing conversion, herein expressed by the proceeding reaction time. First, a blue transparent reaction mixture can be observed after 12 min reaction time (Figure 9B), indicating a phase transition to a lamellar phase. Due to the bilayer structure of the lamellar phase, the movement of the ions is restricted, which explains the minimum in the conductivity plot.<sup>38</sup> The distance of the surfactant layers is in the range of the wavelength of visible light, which describes the blue color of the solution. After that, the reaction mixture turns back into a turbid biphasic reaction mixture, leading to an increase of the conductivity (Figure 9C). At the end, with increasing conversion the solutions are transparent, since the cloud point increases strongly due to the formation of sodium decanoate (Figure 9D). Because of these overlapping effects of the concentration of ionic reactants and phase behavior of the system, the conductivity measurement has to be corrected to monitor the progress of the reaction. Hence, the minimum of the electrical conductivity, due to the formation of a lamellar

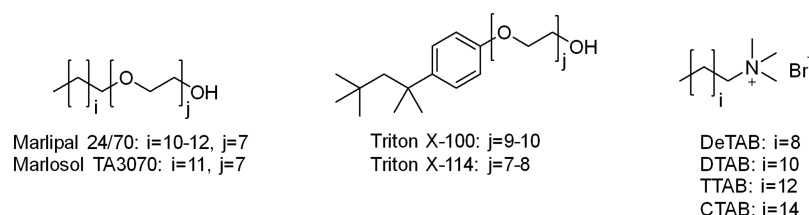


Figure 10. Chemical structures of the applied surfactants.

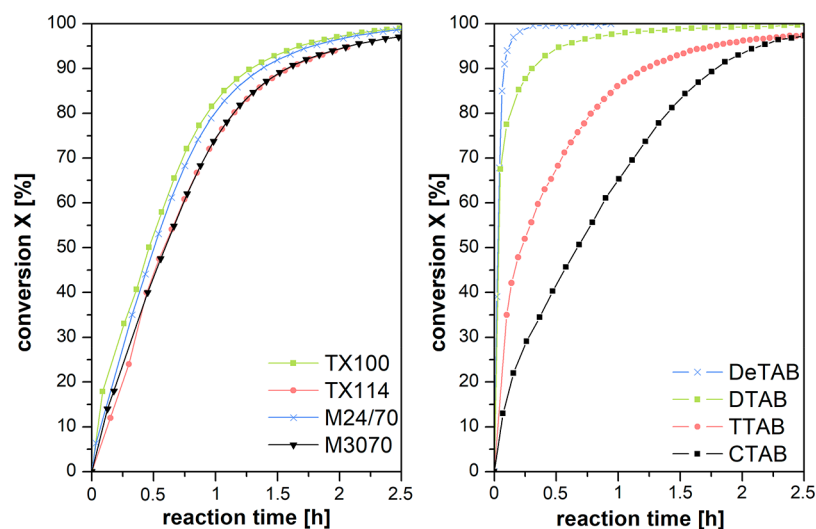


Figure 11. Variation of the type of surfactant. Experimental conditions:  $T = 80\text{ }^{\circ}\text{C}$ ,  $V = 20\text{ mL}$ ,  $c_{\text{NaOH}} = 0.2\text{ mol/L}$ ,  $c_{\text{methyl decanoate}} = 0.2\text{ mol/L}$ , (left) nonionic surfactants (5 wt %), (right) cationic surfactants ( $10 \times \text{CMC}$ ).

Table 1. CMC Values and Initial Reaction Rates for the Cationic Surfactants<sup>a</sup>

surfactant	CMC <sup>b</sup> (mmol/L)	CMC <sup>c</sup> (mmol/L)	initial rate $r_0^d$ (mmol/(L·h)) $10 \times \text{CMC}$	normalized rate	initial rate $r_0^d$ (mmol/(L·h)) $c\text{-CMC} = 10\text{ mM}$	normalized rate
DeTAB	61.1	62.1	3839	11.9	1023	3.5
DTAB	14.4	14.5	2813	8.7	632	2.2
TTAB	5.8	4.6	703	2.2	461	1.6
CTAB	1.4	1.0	322	1	291	1
no surfactant			5	0.015		

<sup>a</sup>CMC was measured at  $25\text{ }^{\circ}\text{C}$ . <sup>b</sup>Determined by bubble pressure tensiometer, standard deviation 3%. <sup>c</sup>Determined by conductivity measurements, standard deviation 3%. <sup>d</sup>Determined at a conversion of 10% from the conversion plot. Experimental conditions:  $T = 80\text{ }^{\circ}\text{C}$ ,  $V = 20\text{ mL}$ ,  $c_{\text{NaOH}} = 0.2\text{ mol/L}$ ,  $c_{\text{methyl decanoate}} = 0.2\text{ mol/L}$ .

phase, was not considered in the calculation of the conversion of methyl decanoate.

**Effect of the Type of Surfactant.** Besides the widely used TX-100, several nonionic and cationic surfactants for the alkaline hydrolysis of methyl decanoate have been tested (see Figure 10). To increase the hydrophobicity of the surfactant, TX-114 has been chosen, which has a lower amount of ethoxy units compared to the polar headgroup but the same hydrophobic alkyl chain as TX-100. Furthermore, the nonionic surfactants Marlipal 24/70 and Marlosol TA3070 have been tested, which have a linear alkyl chain without any aromatic groups as the hydrophobic part. In addition to the nonionic surfactants, alkyltrimethylammonium bromides with an alkyl chain length from 10 to 16 have been investigated as cationic surfactants to evaluate the impact of the hydrophobicity of the surfactant on the reaction performance. The cationic surfactants have been applied as they frequently show the potential to increase the reaction rate of hydrolysis reactions.<sup>39–41</sup>

As seen in Figure 11 (left), the type of nonionic surfactant has only a minor impact on the reaction performance since the conversion plots are nearly identical. Interestingly, the same reaction rate is observed using TX-100 and Marlipal 24/70 as phase-transfer agents, which have the same cloud point around  $60\text{ }^{\circ}\text{C}$  and, thus, almost an identical hydrophobicity. In contrast, the more hydrophobic surfactants TX-114 and Marlosol TA3070, indicated by their lower cloud points around room temperature, show a slightly lower reaction rate compared to TX-100 and Marlipal 24/70. Apparently, the hydrophobicity of the surfactant has a low impact on the reaction performance. Since the more hydrophobic surfactants TX-114 and Marlosol TA3070 exhibit a lower cloud point, the solubility of methyl decanoate is lower, resulting in a lower reaction rate compared to TX-100 and Marlipal 24/70. However, the more or less equal reaction profiles clarify that the surfactants are utilized as phase-transfer agents, and as the substrate is noncharged and nonaromatic further interactions between the substrate and the surfactant are not expected.

Additionally, several cationic surfactants have been investigated (see Figure 11, right). Compared to the nonionic surfactants, much less surfactant is needed to obtain similar reaction rates. Since the head groups of the alkyltrimethylammonium bromides carry a positive charge, an electrostatic attraction of the hydroxide ions is obtained, increasing the local concentration of hydroxide ions at the water–oil interface and enhancing the reaction rate.

Since the CMC of cationic surfactants is much higher compared to the applied nonionic surfactants, the effect of the CMC toward the reaction performance has to be investigated. Therefore, the amount of surfactant was varied in two series of experiments, in which first the 10-fold CMC and second a constant *c*-CMC value of 10 mM was used. The results are given in Table 1 expressed as the initial rates which were calculated from the conversion plots. For a better comparison, also the normalized rates (based on CTAB with the lowest observed reaction rate) are given. Additionally, the CMC values were determined by bubble pressure tensiometer and conductivity measurements. As expected, with increasing chain length of the alkyl chain from 10 to 16, the CMC decreases significantly from 60 to 1 mmol/L (see Table 1), indicating a higher hydrophobicity of the cationic surfactant. Using the 10-fold CMC, the initial rate decreases from 3839 mmol/(L·h) with DeTAB to 322 mmol/(L·h) with CTAB as surfactant. Since the CMC increases from CTAB to DeTAB, the amount of surfactant in the reaction mixture increases drastically using the 10-fold CMC, resulting in higher solubilization of methyl decanoate and, thus, a much higher initial reaction rate. Hence, experiments were carried out using the same concentration of the surfactant but corrected with the determined CMC (*c*-CMC = 10 mM). As a result, the molar concentration for micellization is constant, which allows for a fairer comparison of the used cationic surfactants. Interestingly, the same trend can be observed whereby the initial rate decreases from 1023 mmol/(L·h) for DeTAB to 291 mmol/(L·h) for CTAB. From the normalized reaction rates it is obvious that for the same micellar concentration the rates are closer together, showing that the CMC cannot be neglected in the screening of ionic surfactants. After correction of the surfactant concentration by its CMC, the more hydrophilic cationic surfactant still shows a higher reaction rate. Two more effects have to be considered in order to discuss the observed reactions rates: (a) the solubilization of methyl decanoate and (b) the local concentration of hydroxide ions at the water–oil interface. Considering the aggregation number for the investigated surfactants, which decreases from CTAB to DeTAB by a factor of about two,<sup>42,43</sup> the number of micelles for DeTAB as the phase transfer agent is higher. Hence, the concentration of methyl decanoate is higher in the water phase which explains the higher initial reaction rate. Nevertheless, to understand the role of the surfactant in detail, investigations of the aggregation behavior, solubilization capacity, and phase behavior are essential.

## CONCLUSION

In summary, the presented results show the impact of the surfactant type and concentration on the reaction performance of the alkaline hydrolysis of methyl decanoate in surfactant-modified systems. The surfactant is needed to increase the water–oil interface, resulting in higher reaction rates compared to the system without additive. The physical properties of the mixtures like phase behavior and CMC are essential to

understand the role of the surfactant. Interestingly, the formation of sodium decanoate has a strong influence on the phase behavior and CMC due to its surface active properties. Hence, an autocatalytic effect of the product can be observed.

## EXPERIMENTAL SECTION

**Chemicals.** The substrate methyl decanoate (99%), sodium decanoate (98%) for the calibration to evaluate the reaction progress, and the surfactants [(*tert*-octylphenoxy)polyethoxyethanol degree of ethoxylation (EO) = 9–10 (Triton X-100), (*tert*-octylphenoxy)polyethoxyethanol EO = 7–8 (Triton X-114), dodecyltrimethylammonium bromide (DTAB, 98%), and tetradecyltrimethylammonium bromide (TTAB, 99%)] were purchased from Sigma-Aldrich. Sodium hydroxide (NaOH) as base with a purity of 99% and the cationic surfactant hexadecyltrimethylammonium bromide (CTAB) with a purity of 99% were acquired from Roth. ABCR has delivered the cationic surfactant decyltrimethylammonium bromide (DeTAB, 99%). The technical-grade nonionic surfactants Marlipal 24/70 and Marlosol TA3070 were purchased from Sasol. Deionized water was used in all experiments. All chemicals were used without further purification.

**CMC Determination.** The electrical conductivity method and the bubble pressure tensiometer were used to determine the critical micelle concentration (CMC) of the alkyltrimethylammonium bromides. Aqueous solutions with different concentrations of the corresponding surfactants were prepared and measured with both methods. For the electrical conductivity method, the conductivity was plotted versus the concentration of the surfactant and the CMC was obtained from the intersection of the two resulting linear slopes. In addition, the surface tension of the solution was measured using a bubble pressure tensiometer, depending on the surface age of the produced bubbles. At a surface age of 14000 ms, when the surface tension remains constant, the surface tension value was taken and plotted versus the concentration of the surfactant to determine the CMC. Also, the CMC of Triton X-100, sodium decanoate, and mixtures of Triton X-100 and sodium decanoate was determined with the bubble tensiometer. All reported values were measured at 25 °C and are indicated as moles of surfactant per volume.

**Investigation on the Cloud Point.** The influence of sodium hydroxide and the surface-active product sodium decanoate on the cloud point of the aqueous TX-100 solution was investigated in a temperature range from 25 to 95 °C. The concentration of TX-100 was fixed at 5 wt %, and the concentration of sodium hydroxide was varied in the range from 0.1 to 1.0 mol/L. In addition, the cloud points of the nonionic surfactants Triton X-114, Marlipal 24/70, and Marlosol TA3070 were examined. To determine the impact of sodium decanoate on the cloud point, the concentration of sodium hydroxide and TX-100 was fixed at 0.2 mol/L and 5 wt %, respectively, and the amount of sodium decanoate was varied between 0 and 0.04 mol/L. The mixtures, prepared in graduated cylinders, were added to a water bath, and the temperature was raised in one degree steps, waiting 1 min to reach the equilibrium for each temperature step. The resulting phase behavior was observed, mainly indicated by the turbidity of the solution.

**General Procedure of the Alkaline Hydrolysis.** The main part of the setup for the alkaline hydrolysis is a 40 mL double-wall reactor to adjust the temperature via a thermostat. The substrates can be injected with a two-way valve at reaction temperature whereby the mixture is mechanically stirred. To follow the reaction progress, the conductivity is measured in situ using a conductivity electrode (WTW). The thermostat and the conductivity probe are connected to a computer to monitor the reaction progress. To perform the reaction, a stock solution containing the surfactant and sodium hydroxide (4 mmol, 1 equiv) was filled into the reactor, stirred mechanically, and heated to the desired reaction temperature. Immediately after the reaction temperature was reached, the substrate methyl decanoate (4 mmol, 1 equiv) was injected via a syringe into the reactor. The bulk volume was 20 mL for each experiment. The reaction was stopped when the conductivity remained constant or at the latest after 24 h.

**Evaluation of Reaction Progress.** Since the conversion depends linearly on the conductivity of the mixture, the conductivity was measured to determine the conversion of methyl decanoate to sodium decanoate. For that, sodium hydroxide, which mainly contributes to the conductivity of the mixture, and the product sodium decanoate were mixed and adapted to the concentrations from the previous section, simulating different conversions between 0 and 100%. After 4 min had passed to reach temperature equilibrium, the corresponding conductivity was measured for 40, 60, and 80 °C and plotted versus the associated conversion. A two-point calibration was performed for the cationic surfactants, mixing the 10-fold critical micelle concentration (CMC) of the corresponding surfactant, sodium hydroxide, and sodium decanoate and measuring the conductivity at 80 °C.

## AUTHOR INFORMATION

### Corresponding Author

\*E-mail: [marcel.schmidt@tu-berlin.de](mailto:marcel.schmidt@tu-berlin.de).

### ORCID

Michael Schwarze: 0000-0002-5632-603X

### Author Contributions

The manuscript was written through contributions of all authors.

### Notes

The authors declare no competing financial interest.

## ACKNOWLEDGMENTS

This work is part of the Collaborative Research Center "Integrated Chemical Processes in Liquid Multiphase Systems" (subproject A2) coordinated by the Technische Universität Berlin. Financial support by the German Research Foundation (Deutsche Forschungsgemeinschaft, DFG) is gratefully acknowledged (TRR 63).

## REFERENCES

- (1) Schwarze, M.; Pogrzeba, T.; Volovych, I.; Schomäcker, R. Microemulsion Systems for Catalytic Reactions and Processes. *Catal. Sci. Technol.* **2015**, *5*, 24–33.
- (2) Dwars, T.; Paetzold, E.; Oehme, G. Reactions in Micellar Systems. *Angew. Chem., Int. Ed.* **2005**, *44*, 7174–7199.
- (3) La Sorella, G.; Strukul, G.; Scarso, A. Recent Advances in Catalysis in Micellar Media. *Green Chem.* **2015**, *17*, 644–683.
- (4) Mc Naught, A. D.; Wilkinson, A. Micellar Catalysis. In *IUPAC Compendium of Chemical Terminology*; IUPAC: Research Triangle Park, NC.
- (5) Mubofu, E. B.; Engberts, J. B. F. N. Surfactant-Assisted Specific-Acid Catalysis of Diels–Alder Reactions in Aqueous Media. *J. Phys. Org. Chem.* **2007**, *20*, 764–770.
- (6) Bahrami, K.; Khodaei, M. M.; Nejati, A. Synthesis of 1,2-Disubstituted Benzimidazoles, 2-Substituted Benzimidazoles and 2-Substituted Benzothiazoles in SDS Micelles. *Green Chem.* **2010**, *12*, 1237–1241.
- (7) Xiancheng, Z.; Qilin, L.; Yingke, H.; Qian, W.; Ziming, Q.; Guanzuo, L.; Qizhong, H. The Effect of Mixed Micelles of Surfactants on the Alkaline Hydrolysis of Esters. *J. Dispersion Sci. Technol.* **1996**, *17*, 101–110.
- (8) Correia, V. R.; Cuccovia, I. M.; Chaimovich, H. Effect of Hexadecyltrimethylammonium Bromide Micelles on the Hydrolysis of Substituted Benzoate Esters. *J. Phys. Org. Chem.* **1991**, *4*, 13–18.
- (9) Xiancheng, Z.; Qilin, L.; Qian, W.; Taming, Q.; Ganzuo, L.; Qizhong, H. The Effect of Cationic, Anionic, and Nonionic Surfactant Micelles on the Alkaline Hydrolysis of Esters. *J. Dispersion Sci. Technol.* **1995**, *16*, 531–541.
- (10) Al-Awadi, N.; Williams, A. Effective Charge Development in Ester Hydrolysis Catalyzed by Cationic Micelles. *J. Org. Chem.* **1990**, *55*, 2001–2004.

(11) Raducan, A.; Olteanu, A.; Puiu, M.; Oancea, D. Influence of Surfactants on the Fading of Malachite Green. *Cent. Eur. J. Chem.* **2008**, *6*, 89–92.

(12) Al-Ayed, A. S.; Ali, M. S.; Al-Lohedan, H. A.; Al-Sulaim, A. M.; Issa, Z. A.; Kabir-ud-Din. Micellar Effects on the Alkaline Hydrolysis of Isatin and Its Derivatives. *J. Colloid Interface Sci.* **2011**, *357*, 393–399.

(13) Dasmandal, S.; Mandal, H. K.; Kundu, A.; Mahapatra, A. Kinetic Investigations on Alkaline Fading of Malachite Green in the Presence of Micelles and Reverse Micelles. *J. Mol. Liq.* **2014**, *193*, 123–131.

(14) Samiey, B.; Cheng, C.-H.; Wu, J. Effects of Surfactants on the Rate of Chemical Reactions. *J. Chem.* **2014**, *2014*, 1–14.

(15) Lipshutz, B. H.; Taft, B. R. Heck Couplings at Room Temperature in Nanometer Aqueous Micelles. *Org. Lett.* **2008**, *10*, 1329–1332.

(16) Lu, G.; Cai, C.; Lipshutz, B. H. Stille Couplings in Water at Room Temperature. *Green Chem.* **2013**, *15*, 105–109.

(17) Lipshutz, B. H.; Ghorai, S. PQS: A New Platform for Micellar Catalysis. RCM Reactions in Water, with Catalyst Recycling. *Org. Lett.* **2009**, *11*, 705–708.

(18) Lipshutz, B. H.; Aguinardo, G. T.; Ghorai, S.; Voigtritter, K. Olefin Cross-Metathesis Reactions at Room Temperature Using the Nonionic amphiphile "PTS": Just Add Water. *Org. Lett.* **2008**, *10*, 1325–1328.

(19) Dwars, T.; Haberland, J.; Grassert, I.; Oehme, G.; Kragl, U. Asymmetric Hydrogenation in a Membrane Reactor: Recycling of the Chiral Catalyst by Using a Retainable Micellar System. *J. Mol. Catal. A: Chem.* **2001**, *168*, 81–86.

(20) Schwarze, M.; Schmidt, M.; Nguyen, L. A. T.; Drews, A.; Kraume, M.; Schomäcker, R. Micellar Enhanced Ultrafiltration of a Rhodium Catalyst. *J. Membr. Sci.* **2012**, *421–422*, 165–171.

(21) Volovych, I.; Neumann, M.; Schmidt, M.; Buchner, G.; Yang, J.-Y.; Wöll, J.; Sottmann, T.; Strey, R.; Schomäcker, R.; Schwarze, M. A Novel Process Concept for the Three Step Boscalid® Synthesis. *RSC Adv.* **2016**, *6*, 58279–58287.

(22) Nowothnick, H.; Blum, J.; Schomäcker, R. Suzuki Coupling Reactions in Three-Phase Microemulsions. *Angew. Chem., Int. Ed.* **2011**, *50*, 1918–1921.

(23) Illner, M.; Müller, D.; Esche, E.; Pogrzeba, T.; Schmidt, M.; Schomäcker, R.; Wozny, G.; Repke, J.-U. Hydroformylation in Microemulsions: Proof of Concept in a Miniplant. *Ind. Eng. Chem. Res.* **2016**, *55*, 8616–8626.

(24) Pogrzeba, T.; Schmidt, M.; Hohl, L.; Weber, A.; Buchner, G.; Schulz, J.; Schwarze, M.; Kraume, M.; Schomäcker, R. Catalytic Reactions in Aqueous Surfactant-Free Multiphase Emulsions. *Ind. Eng. Chem. Res.* **2016**, *55*, 12765–12775.

(25) Pogrzeba, T.; Schmidt, M.; Milojevic, N.; Urban, C.; Illner, M.; Repke, J.-U.; Schomäcker, R. Understanding the Role of Nonionic Surfactants during Catalysis in Microemulsion Systems on the Example of Rhodium-Catalyzed Hydroformylation. *Ind. Eng. Chem. Res.* **2017**, *56*, 9934–9941.

(26) Schmidt, M.; Pogrzeba, T.; Hohl, L.; Weber, A.; Kielholz, A.; Kraume, M.; Schomäcker, R. Palladium Catalyzed Methoxycarbonylation of 1-Dodecene in Biphasic Systems – Optimization of Catalyst Recycling. *Mol. Catal.* **2017**, *439*, 1–8.

(27) Lipshutz, B. H.; Petersen, T. B.; Abela, A. R. Room-Temperature Suzuki-Miyaura Couplings in Water Facilitated by Nonionic Amphiphiles. *Org. Lett.* **2008**, *10*, 1333–1336.

(28) Tan, C. H.; Huang, Z. J.; Huang, X. G. Rapid Determination of Surfactant Critical Micelle Concentration in Aqueous Solutions Using Fiber-Optic Refractive Index Sensing. *Anal. Biochem.* **2010**, *401*, 144–147.

(29) Li, N.; Luo, H.; Liu, S. A New Method for the Determination of the Critical Micelle Concentration of Triton X-100 in the Absence and Presence of  $\beta$ -Cyclodextrin by Resonance Rayleigh Scattering Technology. *Spectrochim. Acta, Part A* **2004**, *60*, 1811–1815.

(30) Zhang, X.; Jackson, J. K.; Burt, H. M. Determination of Surfactant Critical Micelle Concentration by a Novel Fluorescence Depolarization Technique. *J. Biochem. Biophys. Methods* **1996**, *31*, 145–150.

(31) Carnero Ruiz, C.; Aguiar, J. Interaction, Stability, and Microenvironmental Properties of Mixed Micelles of Triton X100 and N-Alkyltrimethylammonium Bromides: Influence of Alkyl Chain Length. *Langmuir* **2000**, *16*, 7946–7953.

(32) Wang, X.; Wang, J.; Wang, Y.; Ye, J.; Yan, H.; Thomas, R. K. Properties of Mixed Micelles of Cationic Gemini Surfactants and Nonionic Surfactant Triton X-100: Effects of the Surfactant Composition and the Spacer Length. *J. Colloid Interface Sci.* **2005**, *286*, 739–746.

(33) Dharaiya, N.; Bahadur, P. Phenol Induced Growth in Triton X-100 Micelles: Effect of pH and Phenols' Hydrophobicity. *Colloids Surf, A* **2012**, *410*, 81–90.

(34) Santos-Ebinuma, V. C.; Lopes, A. M.; Converti, A.; Pessoa, A.; Rangel-Yagui, C. de O. Behavior of Triton X-114 Cloud Point in the Presence of Inorganic Electrolytes. *Fluid Phase Equilib.* **2013**, *360*, 435–438.

(35) Nascentes, C. C.; Arruda, M. A. Z. Cloud Point Formation Based on Mixed Micelles in the Presence of Electrolytes for Cobalt Extraction and Preconcentration. *Talanta* **2003**, *61*, 759–768.

(36) Samiey, B.; Toosi, A. R. Kinetics Study of Malachite Green Fading in the Presence of TX-100, DTAB and SDS. *Bull. Korean Chem. Soc.* **2009**, *30*, 2051–2056.

(37) Samiey, B.; Dargahi, M. R. Kinetics of Brilliant Green Fading in the Presence of TX-100, DTAB and SDS. *React. Kinet., Mech. Catal.* **2010**, *101*, 25–39.

(38) Strey, R.; Schomacker, R.; Roux, D.; Nallet, F.; Olsson, U. Dilute Lamellar and L3 Phases in the Binary Water-C<sub>12</sub>E<sub>5</sub> System. *J. Chem. Soc., Faraday Trans.* **1990**, *86*, 2253–2261.

(39) Shrivastava, A.; Ghosh, K. K. Micellar Effects on Hydrolysis of Parathion. *J. Dispersion Sci. Technol.* **2008**, *29*, 1381–1384.

(40) Gangwar, S. K.; Rafiquee, M. Z. A. Kinetics of the Alkaline Hydrolysis of Fenuron in Aqueous and Micellar Media. *Int. J. Chem. Kinet.* **2007**, *39*, 638–644.

(41) Al-Ayed, A. S.; Ali, M. S.; Al-Lohedan, H. A.; Al-Sulaim, A. M.; Issa, Z. A.; Kabir-ud-Din. Micellar Effects on the Alkaline Hydrolysis of Isatin and Its Derivatives. *J. Colloid Interface Sci.* **2011**, *357*, 393–399.

(42) Evans, D. F.; Allen, M.; Ninham, B. W.; Fouda, A. Critical Micelle Concentration for Alkyltrimethylammonium Bromides in Water from 25 to 160 °C. *J. Solution Chem.* **1984**, *13*, 87–101.

(43) Berr, S. S. Solvent Isotope Effects on Alkyltrimethylammonium Bromide Micelles as a Function of Alkyl Chain Length. *J. Phys. Chem.* **1987**, *91*, 4760–4765.



# PAPER 10

## **Palladium-catalyzed methoxycarbonylation of 1-dodecene in a two-phase system: The path toward a continuous process**

Markus Illner and Marcel Schmidt, Tobias Pogrzeba, Carolina Urban, Erik Esche, Reinhard Schomäcker, Jens-Uwe Repke

Industrial & Engineering Chemistry Research, 2018, 57, 8884-8894

Online Article:

<https://pubs.acs.org/doi/10.1021/acs.iecr.8b01537>

Reproduced (or 'Reproduced in part') with permission from "Palladium-catalyzed methoxycarbonylation of 1-dodecene in a two-phase system: The path toward a continuous process; Markus Illner and Marcel Schmidt, Tobias Pogrzeba, Carolina Urban, Erik Esche, Reinhard Schomäcker, Jens-Uwe Repke. Industrial & Engineering Chemistry Research, 2018, 57, 8884-8894." Copyright (2018) American Chemical Society.



# Palladium-Catalyzed Methoxycarbonylation of 1-Dodecene in a Two-Phase System: The Path toward a Continuous Process

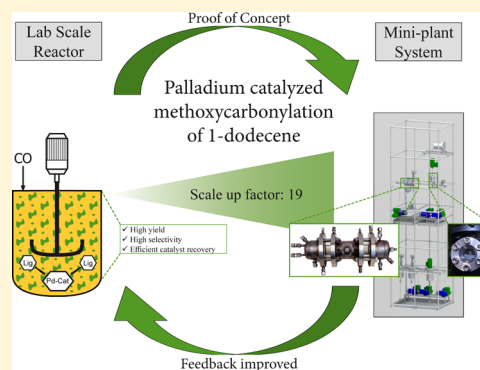
Markus Illner,<sup>\*,§,†,‡</sup> Marcel Schmidt,<sup>\*,§,‡</sup> Tobias Pogrzeba,<sup>‡,§</sup> Carolina Urban,<sup>‡</sup> Erik Esche,<sup>†</sup> Reinhard Schomäcker,<sup>‡,§</sup> and Jens-Uwe Repke<sup>†</sup>

<sup>†</sup>Process Dynamics and Operations Group, Technische Universität Berlin, Str. des 17. Juni 135, Sekr. KWT 9, Berlin D-10623, Germany

<sup>‡</sup>Department of Chemistry, Technische Universität Berlin, Str. des 17. Juni 124, Sekr. TC-8, Berlin D-10623, Germany

## S Supporting Information

**ABSTRACT:** The implementation of homogeneous catalysis in industry is still a challenging task due to the recycling of the mostly expensive catalyst complexes. The application of a liquid two-phase systems provides a viable approach to overcome this issue. Hereof, systematic lab investigations and the transfer to a continuously operated mini-plant for the palladium catalyzed methoxycarbonylation of 1-dodecene are presented (reaction volume scale up factor: 19). Under optimized reaction conditions, a yield of 92% to the corresponding ester was achieved after a reaction time of 20 h in lab-scale experiments. 97% of the product was located in the nonpolar phase and the catalyst was quantitatively immobilized in the polar phase. Subsequently, the proof of concept has been successfully carried out in a mini-plant, which was continuously operated over 100 h. The reaction performance in the mini-plant with a yield of esters of 83.5% and a chemo-selectivity of 91.2% was found to be comparable with the lab experiment. The catalyst leaching was permanently kept below 25 ppb, which validates the previous findings of the lab experiments. The catalyst remains stable and the formation of palladium black was prevented during the entire operation. By comparing lab and mini-plant results, a significant influence of the catalyst preformation process and the mini-plant operation mode on reaction rate and selectivity is identified.



## 1. INTRODUCTION

Since the 12 principles of green chemistry were established by Paul Anastas and co-workers in the beginning of 1990s, efforts toward more green and sustainable chemical processes are steadily increasing.<sup>1,2</sup> The major aspect of these principles is waste prevention rather than treatment or cleaning waste after its formation. This incorporates all kinds of used reagents, solvents, additives, and required fuels or energy produced during the whole process, most often related to the final product output of the process.<sup>3</sup>

To prevent waste, creative solutions were introduced not just in research but also in industry. On the one hand, chemical processes should be designed sustainably in terms of resource and energy efficiency, which means that mass and heat integration should be considered early on instead of standard linear separation trains. On the other hand, catalysis plays a crucial role because new synthesis routes can be unlocked, which reduce necessary steps toward a desired product. As a result, the waste production is reduced. Homogeneous catalysis in particular enables atom efficient reactions, which maximize the conversion of all available reactants into the desired product. Most often, expensive transition metal catalysts such as platinum, palladium, rhodium, and specially designed

ligands are used for homogeneous catalysis, which have to be reused for economic and ecological reasons.

Therefore, this contribution focuses on the homogeneously catalyzed methoxycarbonylation in a biphasic system with efficient catalyst recycling via a simple and robust phase separation and its transfer to a continuous mini-plant operation. Here, the homogeneous catalysis is combined with a green processing concept. Particularly, the catalyst recycling is achieved through the use of two-phase liquid/liquid systems, in which the catalyst is located primarily in one phase and can hence be recycled after the reaction via a simple liquid phase separation, which is energy efficient as well. Moreover, this approach allows for a simple product separation and avoids unnecessary purification steps.

**1.1. State of the Art.** The application of two-phase systems for homogeneous catalysis is a green and sustainable method to reuse catalysts and separate products in an energy efficient way.<sup>4</sup> As an industrial scale example, the Ruhrchemie/Rhone Poulenc (RCH/RP) process developed in the 1980s

**Received:** April 9, 2018

**Revised:** June 15, 2018

**Accepted:** June 15, 2018

**Published:** June 15, 2018

represents a milestone for two-phase catalysis. Propene is hydroformylated with synthesis gas (CO/H<sub>2</sub>) to butanal. Water is used as a (green) solvent, in which the rhodium catalyst is immobilized applying the water-soluble ligand TPPTS (triphenylphosphine-3,3',3''-trisulfonic acid trisodium salt). The catalyst is recycled continuously via a subsequent phase separation, whereas catalyst leaching into the product phase is reportedly lower than 1 ppb.<sup>5</sup> However, this concept is limited to short-chained olefins (<C<sub>5</sub>) due to the reduced solubility of long-chained olefins in water. To cope with this, these systems can be modified with additives (e.g., surfactants) to elevate the interface and consequently increase the rate of reaction.<sup>6–11</sup> Exemplarily, the hydroformylation of the long-chained olefin 1-dodecene in a surfactant modified system has already been carried out successfully in a continuously operated mini-plant.<sup>12,13</sup>

Another important industrial application of two-phase catalysis is the Shell Higher Olefin Process (SHOP), in which alpha-olefins are produced via the oligomerization of ethylene at rather harsh process conditions of 80 to 140 °C and 70 to 140 bar. A polar solvent such as 1,4-butanediol is used to dissolve the homogeneous nickel catalyst. This allows for resource-efficient separation of the hydrophobic products (C<sub>6</sub>–C<sub>20</sub>) and catalyst recycling via phase separation.<sup>14,15</sup>

In Japan in the 1990s, an aqueous biphasic telomerization of butadiene and water was commercialized with a capacity of 5000 tons per year by the Kuraray Corporation. The applied palladium catalyst is immobilized into the aqueous phase by the lithium salt of TPPMS and can be recycled easily via phase separation after the reaction.<sup>4</sup>

Apart from only a few industrially applied processes, several approaches are investigated in research to establish two-phase catalysis for numerous metal-catalyzed reactions.<sup>16–18</sup> Hence, an increasing number of commercial applications can be expected in the near future and especially in the field of green chemistry.

**1.2. Scope and Challenges for the Biphasic Methoxycarbonylation.** However, the major challenge for most multiphase reaction media lies in the quantitative recycling and stability of the expensive catalyst (this work: palladium modified with 4,5-bis(diphenylphosphino)-9,9-dimethyl-2,7-disulfoxanthene disodium) within a viable but low environmental impact multiphase system. Thus, the scope of this contribution focuses on the applicability of two-phase reaction media for an important functionalizing reaction, the methoxycarbonylation. This reaction, also known as hydroesterification, is an atom-efficient reaction discovered in the early 1950s by Walter Reppe in which a homogeneous palladium catalyst is applied.<sup>19,20</sup> The synthesis path enables a direct route from unsaturated substrates to esters. The main focus of the current work is on the transfer of promising lab results into a continuously operated mini-plant to validate the lab results and proof a viable overall process concept. Additionally, occurring challenges from the operation in the technical system with multiple internal recycles are identified immediately and solved through feedback toward the lab-scale. Based on a recent study of our group, the biphasic reaction mixture for the methoxycarbonylation of 1-dodecene is already established.<sup>21</sup> However, suitable reaction conditions have to be determined ensuring catalyst stability, general phase separation behavior and good reaction performance, which is part of current investigations. Based thereon, a modular mini-plant for multiphase reaction media is adapted to the proposed system

and used to determine the technical and economic feasibility and viability.

Of special interest is the applicability of early stage laboratory scale findings on the technical system and a comparison of the reaction and the separation performance in lab (100 mL batch reactor) and mini-plant (1,500 mL reactor, continuous operation with internal recycles). Apart from that, several challenges have to be tackled: The catalyst stability and selectivity under the influence of concentration shifts, pump operation, and varied settler residence times. Additionally, a stable phase separation with adequate product distribution and low catalyst leaching into the oily product phase is desirable for the entire operation time (>100 h). Hereby, experiences from the successful transfer of the hydroformylation of 1-dodecene in microemulsion system from the lab into a continuously operation mini-plant system were helpful.<sup>13,22</sup>

## 2. MATERIALS AND METHODS

**2.1. Chemicals.** The applied substances, their purity and supplier are listed in the [Supporting Information](#). All chemicals were used without further purification.

**2.2. Lab-Scale Experiments.** All experiments in lab-scale were carried out under semibatch conditions at a constant pressure. A typical lab-scale experiment was performed in a 100 mL stainless steel autoclave equipped with a gas dispersion stirrer and a baffle. To avoid palladium black formation at the wall of the reactor, an additional PTFE inlay was used to protect the inner surface. The cosolvent octane (9 g), 1-dodecene (17.8 mmol, 3 g), and MSA (methanesulfonic acid) as cocatalyst (6.4 mmol, 615.1 mg, 36 mol %) were weighed into the PTFE inlay and introduced to the reactor. After evacuation and thrice flushing with nitrogen, the catalyst solution was injected with a syringe under nitrogen counter-current flow to the inlay. The catalyst solution was prepared by weighing Pd(OAc)<sub>2</sub> (0.16 mmol, 35.9 mg, 0.9 mol %) and SulfoXantPhos (0.64 mmol, 501.7 mg, 3.6 mol %) into a Schlenk flask, inerting it with the standard Schlenk technique, adding water (1.2 g) and methanol (10.8 g) through a septum, and stirring the solution for 12 h. The reactor was heated to the desired reaction temperature (60–100 °C), pressurized with carbon monoxide, and stirred at 1,200 rpm. Samples were taken, diluted with acetone and centrifuged to get rid of precipitated ligand. After 20 h reaction time, the reactor was cooled down to room temperature, depressurized, and transferred into a graduated measuring cylinder under inert conditions. Gravity induced phase separation was carried out for 20 min and samples were taken from both existing phases to determine the distribution of the product. GC analyses were performed on a Shimadzu GC2010 Plus with an FID (flame ionization detector) and equipped with a Restek RTX5-MS column (30 m × 0.25 mm × 0.25 μm). Nonane was used as internal standard to calculate the conversion, yields, and linear to branched ratio.

**2.3. Determination of Catalyst Leaching.** The leaching of palladium and phosphorus as their content in the nonpolar product phase was determined for the continuous mini-plant operation. Therefore, the product stream was collected for 8 h, transferred to a flask and distilled under reduced pressure (4 mbar). The residue was solubilized with hydrochloric acid (9 mL), nitric acid (3 mL) and sulfuric acid (6 mL) in the flask and filled up to 50 mL with deionized water. The solution was analyzed with ICP-OES, and results are denoted as parts per billion (ppb).

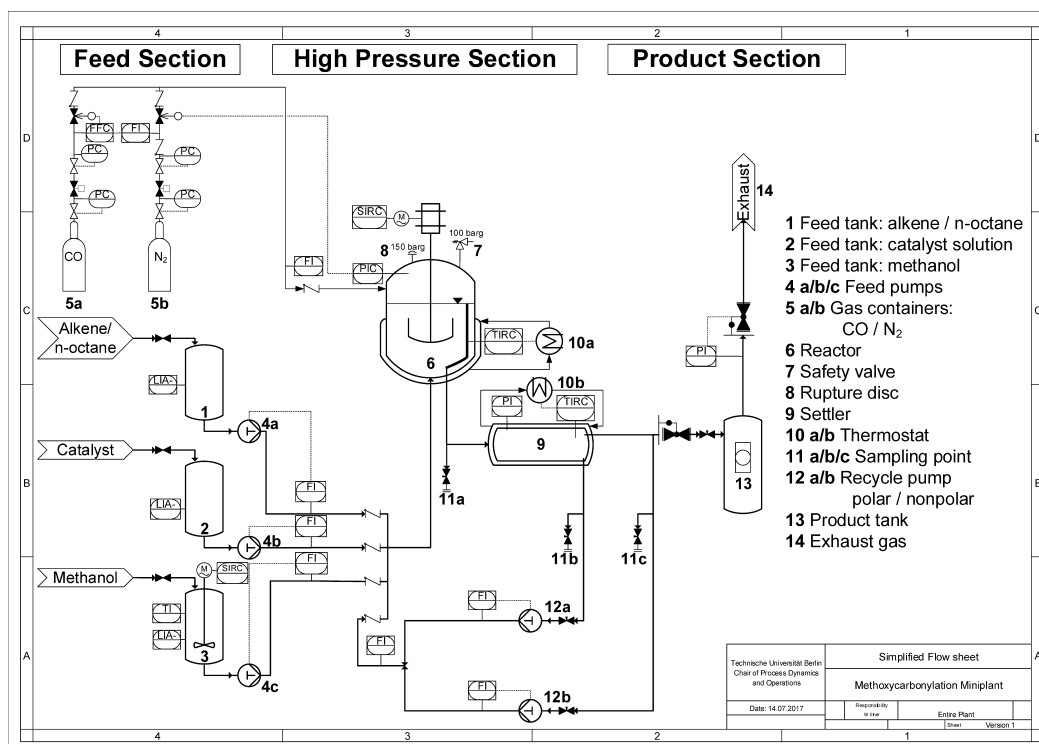


Figure 1. Simplified P&ID of the mini-plant at Technische Universität Berlin.

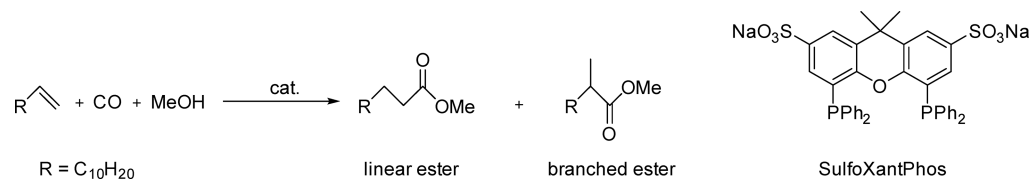


Figure 2. Methoxycarbonylation of 1-dodecene to the linear and branched ester (left); structure of ligand SulfoXantPhos (right).

**2.4. Mini-plant.** **2.4.1. Process Design.** The applicability of the proposed reaction system was tested and investigated, using a continuously operated mini-plant on an intermediate scale. The mini-plant itself was designed to cope with multiphase reaction media, especially microemulsions.<sup>23</sup> A modular design allows for an easy adaption toward a two-phase system. Figure 1 depicts a simplified P&ID of the mini-plant set up at the Process Dynamics and Operations Group at Technische Universität Berlin, which is subdivided into three sections. A feed section provides the feed tanks for the reactants methanol, 1-dodecene dissolved in *n*-octane, and the catalyst solution. Moreover, gas bottles for carbon monoxide and nitrogen for inertization are installed.

Subsequently, the mixer-settler section consists of a 1500 mL pressure reactor equipped with two Rushton turbines affixed to a gassing stirrer and baffles. A liquid drain at approximately 70% reactor height ensures a sufficient liquid level. The phase separation is carried out in a modular settler unit featuring gauge glasses for optical observation of the phase separation and knitted wire meshes as phase separation enhancers. The modular settler design is described in detail in Müller et al., 2015.<sup>24</sup> The settler's volume was set to 350 mL to reduce the residence time regarding an expected short separation time. Two drains are used to recycle the polar and nonpolar phases separately with corresponding pumps (12a,b in Figure 1). A product section is installed for collecting the

product stream in a designated tank (14) for further processing. To finish the continuous operation, the mixture is depressurized and the released carbon monoxide is vented via an exhaust.

**2.4.2. Automation and Analytics.** The process control system SIEMENS PCS 7 is used for full automation of the mini-plant, online-monitoring more than 50 sensors and supervising 20 control loops and 10 actuators (control valves, pumps, pilot valves). Concentration measurements are gathered with an offline gas chromatograph (Agilent HP-5 column with an FID analyzer) from liquid samples.

**2.4.3. Safety Concept.** Due to the use of explosive and hazardous components, the mini-plant is designed to meet "Explosion Zone II" specifications. Based on a HAZOP analysis, multiple layers of protection are applied, as suggested by Seborg et al.<sup>25</sup> (based on the proceedings of the American Institute of Chemical Engineers from 1993<sup>26</sup>), covering technical and organizational counter measures to prevent hazards.

### 3. RESULTS AND DISCUSSIONS

The palladium catalyzed methoxycarbonylation of 1-dodecene was investigated in a two-phase system on the lab and the mini-plant scale. As illustrated in Figure 2, the exemplary olefin 1-dodecene is converted with methanol and carbon monoxide to the corresponding linear and branched ester. Since water is

**Table 1. Methoxycarbonylation of 1-Dodecene: Variation of Pressure<sup>a</sup>**

Entry	Pressure [°C]	Conversion <sup>b</sup> [%]	Yield (ester) <sup>b</sup> [%]	Yield (dodecene isomers) <sup>b</sup> [%]	Selectivity <sup>b</sup> [%]	1:b <sup>b</sup>	Product in nonpolar phase <sup>b</sup> [%]
1	5	94.8	72.6	22.1	76.6	69:31	97.7
2	10	96.4	81.7	14.4	84.8	65:35	97.5
3	15	95.6	82.7	12.7	86.5	67:33	97.8
4	20	91.0	80.6	10.4	88.6	68:32	98.4
5	30	97.8	91.7	5.8	93.8	68:32	97.4

<sup>a</sup>Experimental conditions: Pd(OAc)<sub>2</sub> (0.16 mmol), Pd: SX:MSA (1:4:40), polar phase ( $m_{\text{methanol}} = 10.8$  g,  $m_{\text{water}} = 1.2$  g), nonpolar phase ( $m_{1\text{-dodecene}} = 3$  g,  $m_{\text{octane}} = 9$  g),  $T = 80$  °C,  $t = 20$  h,  $n = 1,200$  rpm, phase separation at room temperature. <sup>b</sup>Determined by GC.

present in the reaction mixture, the corresponding carboxylic acid can be formed as well. Moreover, isomerization of 1-dodecene can lead to internal olefins. In addition, the structure of the applied ligand SulfoXantPhos is shown in Figure 2. The special feature is the water solubility of this ligand due to sulfonate groups at the xanthene backbone, which facilitates the immobilization of the catalyst in the polar phase of the two-phase system.

**3.1. Lab Experiments.** In the following section, the approach and the results for the screening of the reaction conditions (pressure, temperature) for the lab-scale experiments are shown, which enable the continuous process with subsequent phase separation and catalyst recycling in the mini-plant process. Besides the reaction conditions, the composition of the biphasic reaction mixture is crucial for the reaction performance as well as the success of the phase separation. An appropriate two-phase system for the methoxycarbonylation of 1-dodecene is composed of water/methanol as polar phase and octane/1-dodecene as nonpolar phase in order to optimize the catalyst recycling and to ensure a stable phase separation after the reaction.<sup>21</sup> Indeed, small amounts of water in the polar phase (10 wt %) reduce the reaction rate, but significantly decrease the loss of the catalyst compounds toward the nonpolar phase after the reaction. To transfer these findings to a continuously operated mini-plant, suitable reaction conditions, particularly temperature and pressure, have to be found with main focus on the long-term stability of the homogeneous catalyst system.

**3.1.1. Variation of Pressure.** A higher operating pressure influences the reaction rate of gas/liquid reactions by increasing the solubility of the gases in the liquid solution. This effect was investigated for carbon monoxide with a focus on the reaction performance as well as the phase separation. There appears to be no mass transfer limitation to the carbon monoxide. This has been shown in previous work, wherein the methoxycarbonylation of 1-dodecene was found to be a kinetically controlled biphasic reaction.<sup>21</sup> As shown in Table 1, the conversion reaches values above 90% after 20 h for all investigated pressures.

This observation confirms that the operating pressure of carbon monoxide, and the associated higher solubility of carbon monoxide, is not crucial for the reaction rate, most probably because the rate-determining step is the methanolysis step.<sup>27</sup> In such a case, the reaction rate is determined by the concentration of methanol, which is constant for these experiments, multiplied with the equilibrium concentration of the palladium-acyl species. Because carbon monoxide pressure does not influence significantly the reaction rate, the palladium-acyl species seems to be the resting state of the catalytic cycle. Not only the conversion but also the linear to branched ratio (1:b) of the ester does not change significantly by variation of the carbon monoxide pressure and is in a range

of 65:35 to 69:31. Interestingly, a clear trend for the isomerization of 1-dodecene is observed. Higher carbon monoxide pressures reduce the yield of the corresponding dodecene isomers. At a low carbon monoxide pressure of 5 bar, the yield of dodecene isomers reaches 22.1% (entry 1) and decreases to 5.8% at 30 bar carbon monoxide pressure (entry 5). Obviously, a low pressure of carbon monoxide enforces the isomerization of 1-dodecene, whereas high pressure hampers the formation of dodecene isomers. Although the isomerization is boosted at low pressures and internal olefins are formed, the linear to branched ratio of the ester remains unaffected. Probably, internal olefins are converted at a very slow rate to the corresponding ester and hence terminal olefins are mainly converted. This fact explains that only the linear methyltridecanoate and mainly one branched ester is formed during the reaction, i.e., the 2-methyl-methyldodecanoate obtained from the terminal double bond. Moreover, the yield of the ester is increasing from 72.6% to 91.7% with increasing pressure (from 5 to 30 bar), because of the suppression of the isomerization. Hence, the concentration of 1-dodecene is higher, which leads to a slight increase of the palladium-acyl concentration and thus, to higher yields with increasing pressure. Because of the enhanced isomerization at low pressures, the chemoselectivity toward the ester increases from 76.7% at 5 bar to 93.8% at 30 bar carbon monoxide pressure. For characterization the quality of the phase separation, the distribution of the ester between the product and catalyst phase was measured. In all cases, more than 97% of the desired ester is located in the organic phase and can be separated and purified. Obviously, the reaction pressure has no impact on the quality of the phase separation, which is merely controlled by the composition of the two-phase system and less by the reaction conditions. We have to mention that the leaching was not quantified for this series of experiments, but it can be seen in Figure 3 that a clear product phase and a dark greenish catalyst phase is formed after the phase separation. This indicates very low leaching for the homogeneously dissolved palladium complex. Former experiments showed leaching values of less than 0.1 ppm for palladium and less than 1 ppm for phosphorus.<sup>21</sup>

Based on these findings and for safety and economic reasons, a partial pressure of 5 bar for carbon monoxide was chosen to operate the methoxycarbonylation in the mini-plant. The enhancement of the isomerization of the substrate is to be suppressed by an appropriate choice of the operating conditions, especially the residence time in the continuous process.

**3.1.2. Variation of Temperature.** Apart from the reaction pressure, the temperature can be crucial for the activity and stability of the catalyst complex. Consequently, the effect of reaction temperature was investigated concerning the activity and stability of the catalyst as well as the phase separation

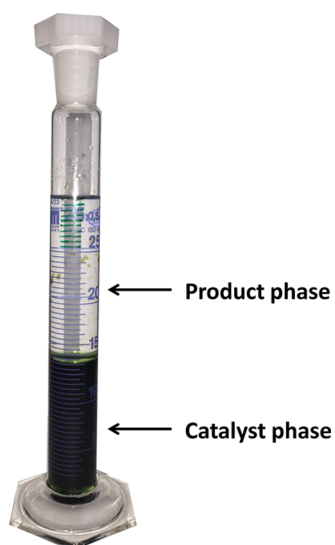


**Figure 3.** Phase separation at room temperature (separation time of 10 min) for the experiment described in Table 1, entry 1.

properties after the reaction. For this purpose, mild reaction temperatures in the range of 60 to 100 °C were chosen. As shown in Table 2, the conversion increases as expected from 13.9% to 94.8% by elevating the temperature from 60 to 80 °C. However, further increase of temperature leads to an unexpected decrease of the conversion to 85.8% and 87.2% at 90 and 100 °C, respectively, while the yield to the esters still increases to 80.2% at 100 °C. There are two reasons explaining this observation. First of all, the isomerization of 1-dodecene is suppressed with increasing temperature, whereas the yield to the corresponding ester is slightly increased. Obviously, the relative rate of methoxycarbonylation and isomerization changes substantially by variation of the temperature, which means that the energetic barriers for both reactions are rather different. Mecking et al.<sup>28</sup> investigated the isomerizing methoxycarbonylation of methyl heptenoate as model substrate, showing a 5-fold higher energetic barrier for the methoxycarbonylation with DFT calculations, which confirms our observations. Second, due to the formation of palladium black at high temperatures (>80 °C) the amount of active catalyst is reduced during the entire reaction time. As a result, the conversion reaches a maximum at 80 °C. Nevertheless, the turnover frequency (TOF), calculated from the slope of the conversion plot at X = 10% (based on the gas consumption), increases constantly from 0.1 to 17.8 h<sup>-1</sup> with increasing temperature, which indicates a catalyst deactivation with proceeding reaction time at high temperatures. Surprisingly, the linear to branched ratio remains constant and is not

affected by the formation of palladium black. Because of the hindered isomerization at higher temperatures, the chemo-selectivity to the ester increases significantly from 12.2% at 60 °C to 92.0% at 100 °C.

The applicability of the phase separation was investigated at room temperature. As shown in Figure 3, the reaction mixture was separated within minutes into a clear product phase and a greenish catalyst phase, which indicates almost no catalyst loss to the product phase. The oil phase of the two-phase system contains more than 95% of the desired product for each reaction temperature, which can be separated and purified. Analogous to the reaction pressure, the reaction temperature has very limited impact on the quality and dynamics of the phase separation in the considered range.

To transfer the lab-scale experiments to the continuously operated mini-plant, it was decided to choose a reaction temperature of 80 °C to ensure the long-term stability of the catalyst and an adequate reaction performance. To allow for a comparison of achieved reaction performances on the lab and the mini-plant scale, the concentration profile for Table 2, entry 8 (80 °C, 5 bar) has been measured in a long-term batch experiment. As it can be seen in Figure 4, 1-dodecene is

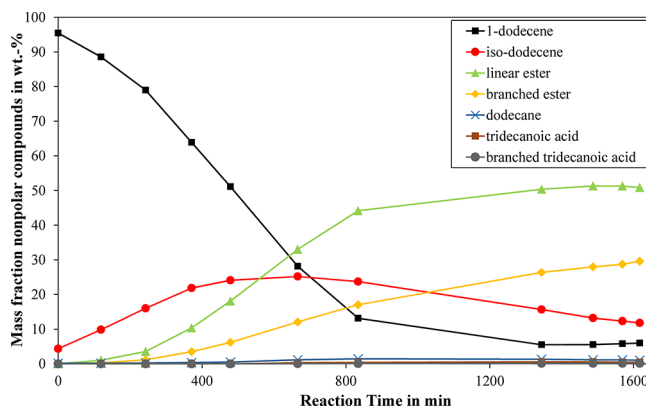


**Figure 4.** Concentration profile for the methoxycarbonylation of 1-dodecene (Table 2, entry 8). Experimental conditions: Pd(OAc)<sub>2</sub> (0.16 mmol), Pd: SX:MSA (1:4:40), polar phase ( $m_{\text{methanol}} = 10.8$  g,  $m_{\text{water}} = 1.2$  g), nonpolar phase ( $m_{1\text{-dodecene}} = 3$  g,  $m_{\text{octane}} = 9$  g),  $p(\text{CO}) = 5$  bar,  $T = 80$  °C,  $n = 1,200$  rpm. Statistic deviation of results: 3%.

consumed while the linear and branched esters are formed in a certain ratio due to the applied catalyst complex. The initial reaction mixture contains already isomerized dodecene with a typical amount of 5 wt %. At the beginning of the reaction, the isomerization takes place predominantly and the 1-dodecene isomers reaches a maximum of 25 wt % at 600 min. After reaching the maximum, the internal olefins isomerize back to

**Table 2. Methoxycarbonylation of 1-Dodecene: Variation of the Temperature<sup>a</sup>**

Entry	Temperature [°C]	Conversion <sup>b</sup> [%]	Yield (ester) <sup>b</sup> [%]	TOF <sup>c</sup> [h <sup>-1</sup> ]	Selectivity <sup>b</sup> [%]	l:b <sup>b</sup>	Product in nonpolar phase <sup>b</sup> [%]
6	60	13.9	1.7	0.1	12.2	73:27	95.2
7	70	38.1	12.5	0.7	32.8	71:29	97.4
8	80	94.8	72.6	6.4	76.6	69:31	97.7
9 <sup>d</sup>	90	85.8	72.4	11.3	84.4	68:32	97.5
10 <sup>d</sup>	100	87.2	80.2	17.8	92.0	69:31	96.7

<sup>a</sup>Experimental conditions: Pd(OAc)<sub>2</sub> (0.16 mmol), Pd: SX:MSA (1:4:40), polar phase ( $m_{\text{methanol}} = 10.8$  g,  $m_{\text{water}} = 1.2$  g), nonpolar phase ( $m_{1\text{-dodecene}} = 3$  g,  $m_{\text{octane}} = 9$  g),  $p(\text{CO}) = 5$  bar,  $t = 20$  h,  $n = 1,200$  rpm, phase separation at room temperature. <sup>b</sup>Determined by GC. <sup>c</sup>Determined by gas consumption at a conversion of 10%. <sup>d</sup>Pd black formation at the end of the reaction.

the terminal 1-dodecene, which is preferably converted via the methoxycarbonylation to the corresponding esters. It is worth mentioning that all dodecene isomers can be identified in the reaction mixture, but mainly the terminal 1-dodecene is converted to the linear methyltridecanoate and the isomer 2-methyl-methyldodecanoate. Only traces of other branched esters are formed because the rate for methoxycarbonylation of internal olefins is significantly lower compared to the rate for terminal 1-dodecene. Interestingly, a logistic increase for the time-dependent formation of the esters is obtained, probably due to the initial formation of the active palladium hydride complex, which is further discussed in section 3.3. Furthermore, only traces of the hydrogenated product dodecane are formed. Despite significant amounts of water in the reaction mixture (10 wt % in the polar phase) the formation of tridecanoic acid and its isomers is prevented.

**3.2. Mini-plant Operation.** After appropriate reaction conditions were derived in lab experiments, the reaction system was transferred into a continuously operated mini-plant to investigate the influence of unknown effects of the internal recycles and concentration shifts in the technical system on reaction performance and catalyst stability. Therefore, this section discusses the experimental mini-plant campaign, lasting for a total of 100 h with different operation modes and transitions, as well as the gathered results on reaction performance and phase separation for the corresponding operation modes.

### 3.2.1. Mini-plant Operation Conditions and Schedule.

**3.2.1.1. Concentrations and Reaction Conditions.** Resulting from section 3.1, a specific applicable two-phase system is identified, which is analogously transferred to the mini-plant operation. The mass fractions for the initial mini-plant feed are approximately 11.93 wt % 1-dodecene, 35.78 wt % *n*-octane, 42.94 wt % methanol, and 4.77 wt % water.

Additionally, 0.14 wt % Pd(OAc)<sub>2</sub>, 2.00 wt % SulfoX-antPhos, and 2.45 wt % methanesulfonic acid were added.

Adhering to section 3.1.1 and 3.1.2, the reactor pressure was set to 5 bar gauge pressure, adjusting the temperature to 80 °C. To ensure a sufficient emulsification of the two-phase system and a sufficient dissolution of carbon monoxide, the stirrer speed was initially set to 1,300 rpm. These conditions, except for the stirrer speed, were kept constant throughout the total operation time.

**3.2.1.2. Operation Schedule.** The mini-plant campaign is partitioned into several operation modes (set points, SP), for which mainly the feed rates and the stirrer speed are varied (see Table 3). Preparations comprise the inertization of the mini-plant with N<sub>2</sub>. Afterward, required masses of substances are fed to fill the plant's high-pressure section according to the above-described concentrations. Then, the plant is operated in a full recycle mode without reaction to establish a stable phase separation in the settler, homogenize the component concentrations in the system, and heat up the reactor. The reaction is started with purging nitrogen from the system and repressurizing the plant with carbon monoxide, which marks operation hours 0 for the following discussions.

Following the operation schedule, set point 1 is used to increase the yield of the main product concentration, applying a full recycle operation, thus only running internal recycles in the plant. Afterward, a continuous operation is established, during which the feed rate is varied to aim for different reaction residence times (SP 2 and 3.1). For set points 1–3.1 (see Table 3), the recycle ratio of nonpolar and polar recycle

**Table 3. Mini-plant Operation Schedule with Applied Process Parameters for Several Operation Set Points (SP 1–3.2)**

	SP 1	SP 2	SP 3.1	SP 3.2
Operation hours (h)	0–20	20–60	60–72	72–101
Operation mode	Full recycle	Continuous	Continuous	
Residence time reactor (h)	0.51	0.49	0.45	
Residence time plant (h)	20.0	20.1	6.1	
Residence time reaction (h)	7.7	7.7	2.4	
Total recycle rate (g h <sup>-1</sup> )	800	800	800	
Recycle ratio (nonpolar:polar)	0.5:0.5	0.5:0.5	0.5:0.5	1:0
Feed rate (g h <sup>-1</sup> )	0	30	100	
Stirrer speed (rpm)	1,300	1,300	1,300	700

stream (see 12a,b in Figure 1) is kept constant to avoid concentration shifts in the reactor. For set point 3.2, the continuous operation mode is continued with a reduced stirrer speed. Thereby, phase separation in the upper reactor part is enforced and predominantly only nonpolar solution leaves the reactor via the upper outlet. Consequently, the polar phase and the dissolved catalyst is contained in the reactor. This way, the influence of the recycle operation on the catalyst performance is tested, as described later. Finally, assuming a rather fast phase separation according to lab results, the settler temperature is set to 25 °C and the total recycle rate is constantly kept at the maximum value for the entire plant operation.

To validate the kinetic information from the laboratory, Table 3 also lists the reaction residence time  $\tau_{\text{Reaction}}$  (eq 1) for the mini-plant's operation modes. Considering that the reaction only takes place in the reactor,  $\tau_{\text{Reaction}}$  is defined as the reactor residence time multiplied with a cycle number  $n_{\text{Cycles}}$ . Simplified, this number of reaction cycles is derived from the ratio of nonpolar phase recycle rate plus feed rate to the sole feed rate (see eq 1). This approach is necessary, because the plant's internal recycle effectuates the feed substrate to pass the reactor several times, before exiting the plant as the product stream within a continuous operation. Therefore,  $n_{\text{Cycles}}$  depends on the resting time of feed in the plant  $\tau_{\text{Plant}}$  and the time needed for one internal recycle  $\tau_{\text{Cycle}}$  (see eq 1).

$$\tau_{\text{Reaction}} = \tau_{\text{Reactor}} \cdot n_{\text{Cycles}}$$

$$n_{\text{Cycles}} = \frac{\tau_{\text{Plant}}}{\tau_{\text{Cycle}}} = \frac{V_{\text{Feed}}^{\text{nonpolar}} + V_{\text{Recycle}}^{\text{nonpolar}}}{V_{\text{Feed}}^{\text{nonpolar}}} \quad (1)$$

**3.2.2. Reaction Performance.** The reaction performance is discussed using conversion, product yield, and the selectivities as main indicators. This is shown for the entire operation time in Figures 5 and 6. Note that the GC samples were solely taken from the reactor (pos. 11a in the P&ID in Figure 1).

**3.2.2.1. Set Point 1.** At operation hour 0, the reaction is immediately initiated with the formation of significant amounts of methyltridecanoate. It can be assumed that the active and selective species of the catalyst, generally known as the palladium hydride species, are already presented in the reaction mixture. Subsequently, the yield of esters reaches 54.9%, together with a total conversion of 82% and a corresponding regioselectivity to the linear ester of 82.2% (see Figure 6). Moreover, the trends for yield and conversion indicate no

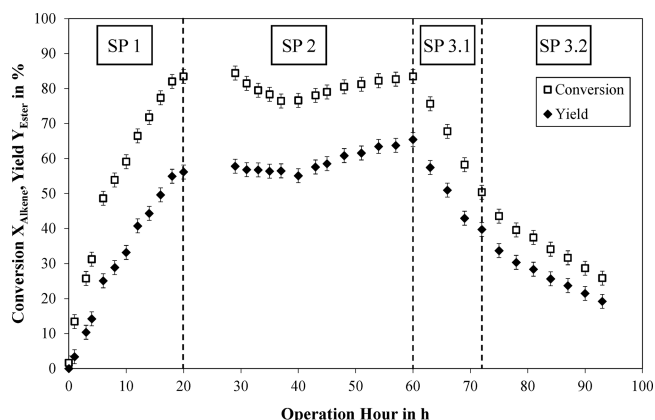


**Figure 5.** Mini-plant operation results for the conversion of 1-dodecene and the total yield of esters over time.

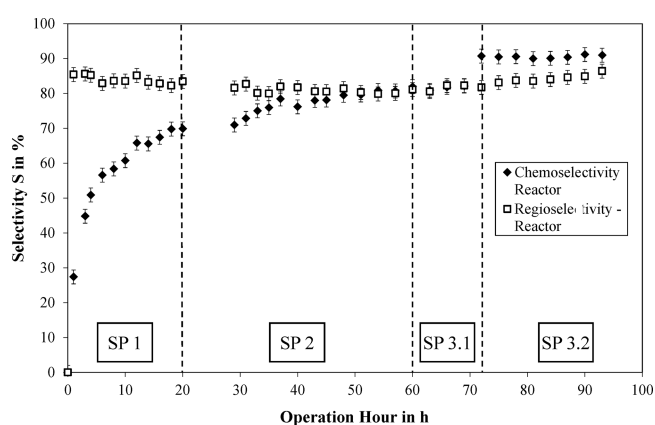


**Figure 6.** Mini-plant operation results for the chemoselectivity in the reactor as well as the regioselectivity as ratio of linear to branched esters over time.

declining reaction rate at higher conversions. However, because of an initial isomerization, the chemoselectivity is typically (see Figure 4) low at the initialization of the reaction but increased to up to 69.7% at the end of operation hour 20.

**3.2.2.2. Set Point 2.** With activating the 1-dodecene/*n*-octane feed-stream and a product withdrawal, the mini-plant is transferred into a continuous operation. The reaction residence time is kept constant, in order to compare the reaction performance of SP 1 and SP 2. Beginning with operation hour 30, a drop of yield and conversion is observed, which is caused by the dilution of the reactor content with fresh substrate. Subsequently, the conversion increases and levels out at 83.5%, when a quasi-steady state is reached, giving a comparable conversion for the full recycle and the continuous operation. The product yield exceeds the findings for SP 1 by 10.6 percentage points and thus the chemoselectivity increases alongside. This is caused by the dilution of the former high isododecene amount and the ongoing reaction at a higher selectivity level. However, the regioselectivity remains stable at a high level of around 82%.

**3.2.2.3. Set Point 3.1 and Set Point 3.2.** Following Figure 4, higher chemo- and regioselectivities are achievable at lower conversion levels. This can be implemented by lower reaction residence times. Therefore, after operation hour 64, the feed rate of 1-dodecene/*n*-octane is increased. As expected, conversion and yield generally drop according to the dilution and reduced reaction residence time. Also, the corresponding chemoselectivity slightly increases as expected. Interestingly though, the stirrer speed reduction in SP 3.2 results in a rather stepwise transition and high increase of the chemoselectivity. The reason for that is assumed to be a transition of catalytic species, which can be caused by temperature changes of the catalyst solution and long resting times outside the reactor. A further discussion is waived here and carried out in Section 3.2.3.

With reaching the end of the operation schedule, the stirrer speed reduction is performed before the concentration profiles reach a steady-state in SP 3.1. Hence, multiple influences are affecting the trajectory shown in Figure 6. However, at the end of the operation, a maximum chemoselectivity of 91.2% is observed alongside a regioselectivity of 86.4%. Additionally, the transient information on the component mass fraction for SP 3.2 indicates an extrapolated conversion at a level of 20% and an ester yield at 15% at steady state.

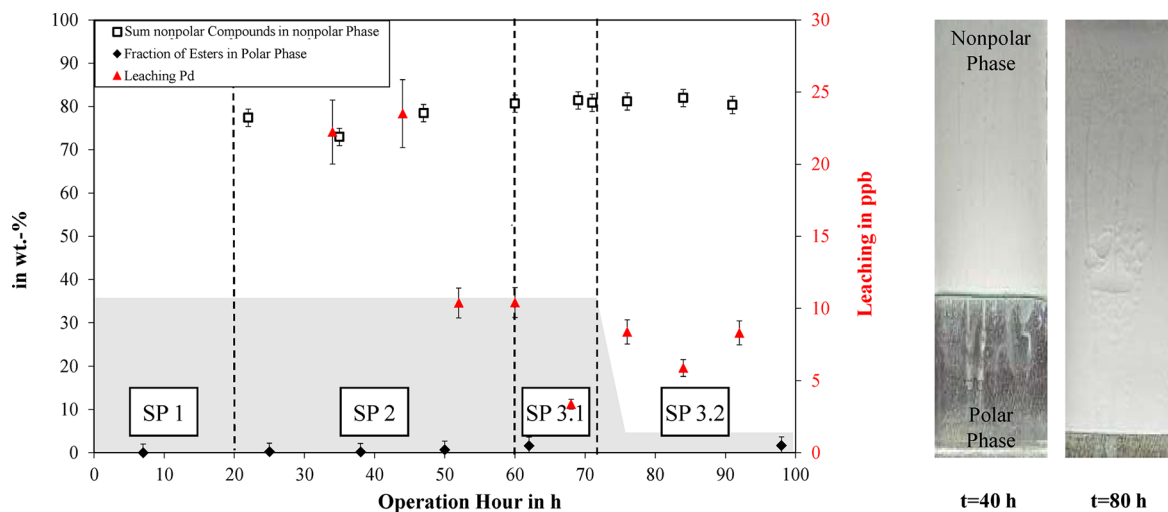


**Figure 7.** Left: Mass fraction of the nonpolar components (reactants) in the nonpolar phase (white) after phase separation in the settler, mass fraction of the esters in the polar phase (gray), and leaching of palladium over operation time. Right: Corresponding state of the phase separation in the settler observed via a gauge glass.

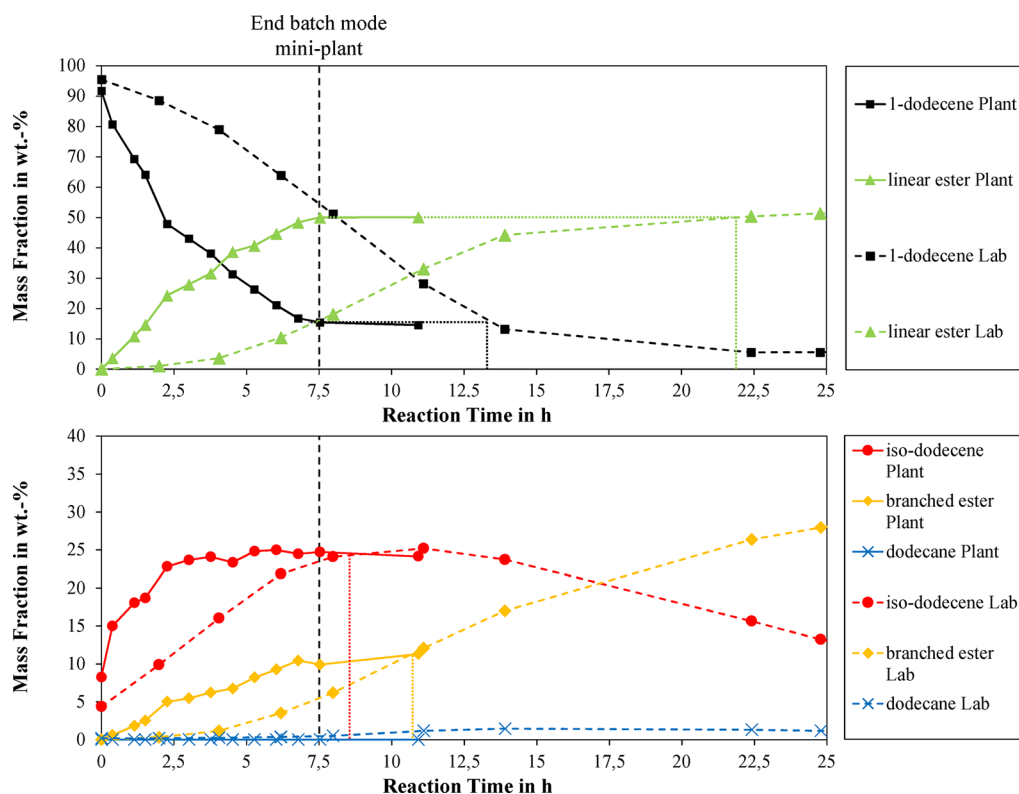


**Figure 8.** Comparison of the concentration profile for the methoxycarbonylation of 1-dodecene for the mini-plant full recycle operation (batch mode) and the lab reference without any catalyst preforming. Mass fractions are related to the total amount of reactants.

Overall, the reaction data indicates a successful proof of concept for the methoxycarbonylation in a continuously operated mini-plant. Furthermore, a good qualitative agreement of the reaction sequence with the lab-scale findings in Figure 4 is shown, as trends for conversion and especially the selectivities are reproduced in the mini-plant campaign. Discussing the long-term catalyst stability, unknown decomposition effects for the mini-plant operation on the catalyst, such as contaminants, side reactions, and an operation with recycle were not observed. Throughout the full operation time, the reaction rates and observed selectivities are comparable to previous findings in the lab experiments. Moreover, no palladium black formation is present at any constructional elements of the mini-plant.

**3.2.3. Separation Results.** Apart from the reaction performance, the quality of the phase separation is of the utmost importance for the overall process concept, which relies on an efficient separation of the nonpolar phase from the reaction medium and an effective catalyst recycling. The separation performance is evaluated using the total amount of nonpolar components in the nonpolar upper phase of the settler and the amount of ester products in the settler's polar phase, both received from GC sampling. Additionally, palladium and phosphorus leaching into this phase is determined. The overall sampling rate is reduced to the feasible minimum (6 h) to avoid catalyst loss and necessary replenishing. This way, the long-term catalyst performance and stability can be evaluated better. The resulting separation performance is depicted in Figure 7.

Here, an average of 77 wt % is achieved for the total amount of nonpolar components in the nonpolar upper phase for SP 2 and SP 3.1. This indicates a successful separation for these operation modes. For SP 3.2, the separation performance

slightly increases, which is mainly caused by the absence of polar phase in the settler. In general, methanol is found to be the main contaminant of the nonpolar phase, which is obvious because of its rather high solubility in octane. Caused by leaching of methanol into the nonpolar phase, methanol needs to be separated from the product phase in further downstreaming steps, which has to be considered for an economic evaluation of the process concept.

The distribution of esters between both settler phases shows an average content of the linear and branched esters in the polar phase of 1 wt %. Thus, 99% of the product is located in the nonpolar phase, which is partially drawn off as the product stream. Herein, the mini-plant shows a slightly better performance compared to prior lab results.

Finally, the leaching of palladium toward the nonpolar phase lies below 25 ppb throughout the full plant operation, which confirms the successful separation operation and is equivalent to prior lab results. Interestingly, no direct correlation between catalyst leaching and product content in the nonpolar phase is observed. However, the lowest leaching is found for rather low product concentrations and the absence of the polar phase in the settler during SP 3.2. The leaching of phosphorus, which corresponds to the ligand loss (SulfoXantPhos), is generally below 250 ppb, which again proves the separation efficiency, especially in relation to the high amount of ligand in the reaction mixture (ligand to metal ratio of 4:1).

**3.3. Comparison of the Lab and the Mini-plant Kinetic.** The methoxycarbonylation has successfully been transferred from the lab into a continuously operated mini-plant showing a promising reaction performance and an overall good separation with efficient catalyst recycling. However, in direct comparison of the reaction trajectories for the mini-plant and the laboratory, deviating selectivities for the progressing

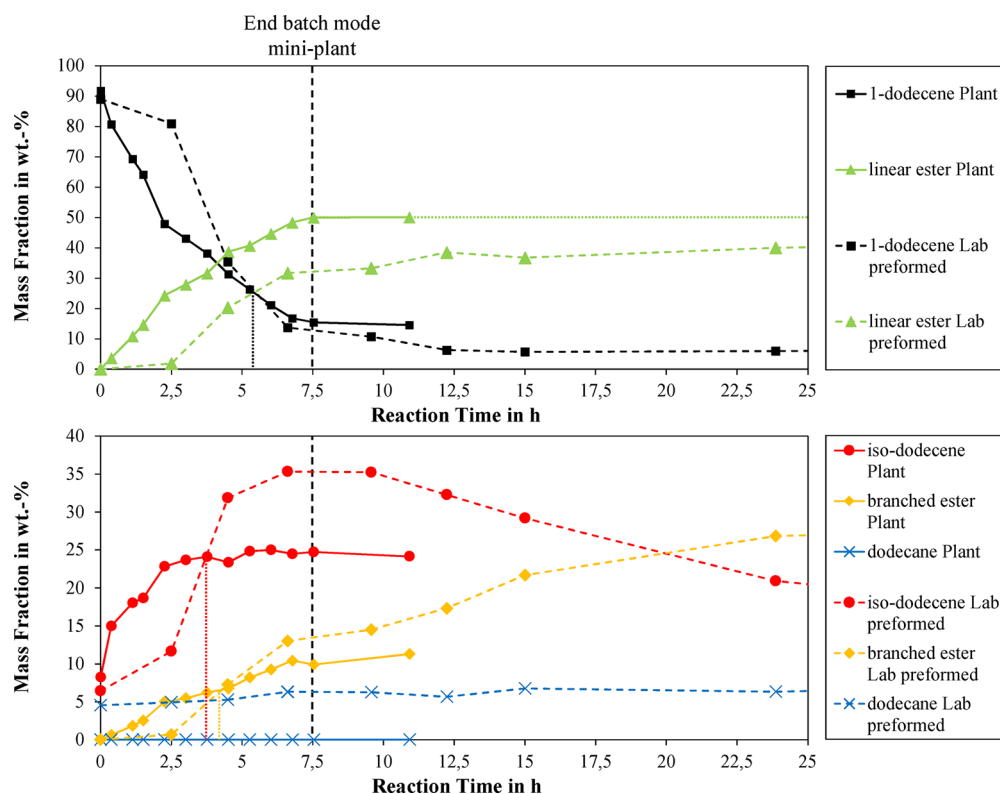


**Figure 9.** Comparison of the concentration profile for the methoxycarbonylation of 1-dodecene for the mini-plant full recycle operation (batch mode) and the lab reference with catalyst preforming. Experimental conditions in lab experiments are similar to the standard lab-scale experiment shown in Figure 4. Mass fractions are related to the total amount of reactants.

reaction are obvious. Thus, Figure 8 is introduced to compare byproduct formation and reaction activity for both. Note that the mini-plant concentration profile is derived from SP 1, an operation mode equivalent to a batch operation (with internal recycles), for which the reaction residence time is calculated using eq 5 with  $\tau_{\text{plant}}$  set to 20 h of batch duration.

It is found that the reaction is much faster in the mini-plant operation. The maximum yield of esters is achieved after 7.5 h in contrast to 22 h for the lab. Thus, the necessary batch time for a desired product content of 50 wt % is reduced by 66%. However, the comparison of the overall conversion of 1-dodecene shows a reduced gap between plant and lab of only 6 h. This stems from a much higher formation rate of the branched ester once the reaction starts, significantly reducing the regioselectivity at equivalent product yields for the lab results. As mentioned, the active catalyst species is a palladium-hydride complex, which has to be formed in situ within the reaction mixture. Claver and co-workers proposed the hydride formation during heating in methanolic solution, whereby the hydride is formed via a  $\beta$ -hydride elimination of coordinated methanol.<sup>29</sup> A water–gas shift reaction could also lead to hydrogen, forming the active palladium-hydride species. With the concentration profiles at hand the active catalyst species is assumed to be present for the mini-plant operation immediately at operation hour 0, whereas it had yet to be formed after starting the reaction in the lab experiment. Additionally, this “in situ” formation of active catalyst obviously passed states of reduced reaction selectivity, during which the formation of byproducts (iso-dodecene and branched ester) is promoted. To identify influence parameters of the catalyst condition and its preforming on the reaction performance, the representative catalyst preparation and

reaction initiation process for mini-plant and the standard lab experiment are compared in Table S2 (see Supporting Information).

Hereof, two main differences for the catalyst preparation and insertion into the reaction vessel are identified. First, a longer contact time of the prepared catalyst solution with methanesulfonic acid is present for the plant operation, because both fluids are stored under nitrogen in a single feed tank. Second, no catalyst preformation is carried out for the lab experiment, whereas after the feeding procedure of the plant, the full reaction mixture is recycled within the plant for 3 h at reaction temperature and nitrogen pressure. Moreover, the reaction initiation is performed rather fast for the mini-plant with stripping nitrogen and repressurizing immediately with carbon monoxide. Thus, a delayed formation of the active catalyst species during lab experiments is possible. Moreover, XantPhos-type ligands promote the formation of inactive dimeric palladium species, as already shown in literature.<sup>30–32</sup> Thus, the applied long complexation time and no additional preforming are prone to have hampered the reaction rates in the lab-scale experiment. However, with the dimer species formation being an equilibrium reaction, elevated temperatures can be applied to regain the active catalyst species.

With the mini-plant start-up procedure of applying a 3 h recycle operation at 80 °C before the reaction starts, it is likely that sufficient active catalyst is formed, which results in the observed high initial reaction rates and reduced byproduct formation. In the same way, the selectivity increase for the transition from operation mode SP 3.1 to SP 3.2 is to be explained:

With the settler being operated at 25 °C, the catalyst-rich polar phase rests a significantly long time

(approximately 3 h) at low temperatures before it is recycled back into the reactor. In this time frame, the dimer formation could take place, forming less selective or inactive catalyst. When the polar phase reenters the heated reactor, the reverse reaction occurs. But with the feed of dimer to the reactor, a significant amount of dimeric species is present in the reactor, which is avoided for SP 3.2. Using the stirrer speed reduction, the polar phase with the catalyst is contained in the reactor at reaction temperature. Thus, remaining dimer species gets converted into active catalyst, which results in the observed improved chemoselectivity.

To verify this assumption, an additional lab experiment is performed, for which the catalyst preparation, preforming, and the reaction initiation procedure is conducted equivalent to the conditions for the mini-plant operation.

Figure 9 compares the results in comparison to the mini-plant experiment. For the conversion 1-dodecene, the profiles for both cases are in good alignment and the absolute values over time are quite similar. The diverging measurement at 3 h of batch time for the lab profile is distorted due to insufficient dead volume purging at the sample valve. The profiles for the linear ester are comparable regarding the initial reaction rate, whereas the ester concentration for the lab experiment constantly remained below the observed mini-plant values. The reason for that lies in an increased formation of isododecene and of the branched ester, which persists throughout the experiment. In contrast, the total byproduct formation for the mini-plant experiment decreased over time, after showing a maximum at the start of the reaction.

Concluding, the catalyst preforming significantly increases the availability of active catalyst at the reaction start for the adapted lab experiment. The key influence parameters on the catalyst state still need to be identified, alongside the design and necessary residence times for preforming or conditioning steps. This then allows for a profound design of the actual process concept and process control strategies, which incorporate an optimal reaction control and economically viable operation.

#### 4. CONCLUSIONS AND OUTLOOK

In this study, the successful transfer of the palladium catalyzed methoxycarbonylation of 1-dodecene in a two-phase system from first lab-scale screening experiments toward the proof of concept in a continuously operated mini-plant is shown, with a resulting reaction volume scale-up factor of 19. Beyond that, the strong interaction between lab and mini-plant enables process concept improvements early on.

The applicability of the system is proven with the catalyst being successfully immobilized in the methanol phase, whereby the formed product is quantitatively located in the nonpolar phase. Suitable reaction conditions for catalyst stability and an overall good reaction performance are found to be 80 °C and 5 bar carbon monoxide pressure. A subsequent mini-plant campaign over 100 h with varied operation modes was performed. For a reaction residence time of 7.5 h, a constant product yield of 65% alongside a chemo- and regioselectivity of approximately 80% were achieved. The leaching of palladium (<25 ppb) and SulfoXantPhos (<250 ppb) indicate successful catalyst recycling. However, a higher conversion at comparable reaction times (200% enhancement) and a selectivity increase (>20%) are revealed for the mini-plant in comparison to the lab. Thus, relevant steps of the catalyst preforming and

recycling conditions were identified and verified with additional experiments.

Nevertheless, a systematic analysis of the influence parameters on the catalyst state in the mentioned system is strived for to identify an optimized process concept and control strategies. Additionally, the long-term operability is to be proven in regard of catalyst stability and robustness of the process toward perturbations in operation and feed composition.

#### ■ ASSOCIATED CONTENT

##### Supporting Information

The Supporting Information is available free of charge on the ACS Publications website at DOI: 10.1021/acs.iecr.8b01537.

Information on the applied chemicals and catalytic details (PDF)

#### ■ AUTHOR INFORMATION

##### Corresponding Authors

\*M. Illner: E-mail: markus.illner@tu-berlin.de.

\*M. Schmidt: E-mail: marcel.schmidt@tu-berlin.de.

##### ORCID

Markus Illner: 0000-0003-1500-9588

Tobias Pogrzeba: 0000-0003-3727-9589

Reinhard Schomäcker: 0000-0003-3106-3904

##### Author Contributions

§Markus Illner and Marcel Schmidt have contributed equally to this article and are both considered primary authors.

##### Funding

German Research Foundation (Deutsche Forschungsgemeinschaft “DFG”)

##### Notes

The authors declare no competing financial interest.

#### ■ ACKNOWLEDGMENTS

This work is part of the Collaborative Research Center “Integrated Chemical Processes in Liquid Multiphase Systems” (subproject A2, B4) coordinated by the Technische Universität Berlin. Financial support by the German Research Foundation (Deutsche Forschungsgemeinschaft, DFG) is gratefully acknowledged (TRR 63). Furthermore, the authors gratefully acknowledge the support of SIEMENS AG for sponsoring the entire process control system SIMATIC PCS7 for the automation of the mini-plant. Finally, the support of Rhodius GmbH for sponsoring the knitted fabrics is gratefully acknowledged.

#### ■ REFERENCES

- (1) Anastas, P.; Eghbali, N. *Green Chemistry: Principles and Practice*. *Chem. Soc. Rev.* **2010**, *39* (1), 301.
- (2) Sheldon, R. A. *Fundamentals of Green Chemistry: Efficiency in Reaction Design*. *Chem. Soc. Rev.* **2012**, *41* (4), 1437.
- (3) Sheldon, R. A. The E Factor: Fifteen Years On. *Green Chem.* **2007**, *9* (12), 1273.
- (4) Cornils, B. *Industrial Aqueous Biphasic Catalysis: Status and Directions*. *Org. Process Res. Dev.* **1998**, *2* (2), 121.
- (5) Kohlpaintner, C. W.; Fischer, R. W.; Cornils, B. *Aqueous Biphasic Catalysis: Ruhrchemie/Rhône-Poulenc Oxo Process*. *Appl. Catal., A* **2001**, *221*, 219.
- (6) Pogrzeba, T.; Schmidt, M.; Milojevic, N.; Urban, C.; Illner, M.; Repke, J.-U.; Schomäcker, R. *Understanding the Role of Nonionic Surfactants during Catalysis in Microemulsion Systems on the*

Example of Rhodium-Catalyzed Hydroformylation. *Ind. Eng. Chem. Res.* **2017**, *56* (36), 9934.

(7) Pogrzeba, T.; Schmidt, M.; Hohl, L.; Weber, A.; Buchner, G.; Schulz, J.; Schwarze, M.; Kraume, M.; Schomäcker, R. Catalytic Reactions in Aqueous Surfactant-Free Multiphase Emulsions. *Ind. Eng. Chem. Res.* **2016**, *55* (50), 12765.

(8) Pogrzeba, T.; Illner, M.; Schmidt, M.; Repke, J.-U.; Schomäcker, R. Microemulsion Systems as Switchable Reaction Media for the Catalytic Upgrading of Long-Chain Alkenes. *Chem. Ing. Tech.* **2017**, *89* (4), 459.

(9) Schwarze, M.; Pogrzeba, T.; Seifert, K.; Hamerla, T.; Schomäcker, R. Recent Developments in Hydrogenation and Hydroformylation in Surfactant Systems. *Catal. Today* **2015**, *247*, 55.

(10) Schwarze, M.; Pogrzeba, T.; Volovych, I.; Schomäcker, R. Microemulsion Systems for Catalytic Reactions and Processes. *Catal. Sci. Technol.* **2015**, *5* (1), 24.

(11) Hamerla, T.; Rost, A.; Kasaka, Y.; Schomäcker, R. Hydroformylation of 1-Dodecene with Water-Soluble Rhodium Catalysts with Bidentate Ligands in Multiphase Systems. *ChemCatChem* **2013**, *5* (7), 1854.

(12) Illner, M.; Müller, D.; Esche, E.; Pogrzeba, T.; Schmidt, M.; Schomäcker, R.; Wozny, G.; Repke, J. U. Hydroformylation in Microemulsions: Proof of Concept in a Miniplant. *Ind. Eng. Chem. Res.* **2016**, *55* (31), 8616.

(13) Pogrzeba, T.; Müller, D.; Hamerla, T.; Esche, E.; Paul, N.; Wozny, G.; Schomäcker, R. Rhodium-Catalyzed Hydroformylation of Long-Chain Olefins in Aqueous Multiphase Systems in a Continuously Operated Miniplant. *Ind. Eng. Chem. Res.* **2015**, *54* (48), 11953.

(14) Lutz, E. F. Shell Higher Olefins Process. *J. Chem. Educ.* **1986**, *63* (3), 202.

(15) Keim, W. Oligomerization of Ethylene to  $\alpha$ -Olefins: Discovery and Development of the Shell Higher Olefin Process (SHOP). *Angew. Chem., Int. Ed.* **2013**, *52* (48), 12492.

(16) Azoui, H.; Baczko, K.; Cassel, S.; Larpent, C. Thermoregulated Aqueous Biphasic Catalysis of Heck Reactions Using an Amphiphilic Dipyridyl-Based Ligand. *Green Chem.* **2008**, *10* (11), 1197.

(17) Yi, W.-B.; Cai, C.; Wang, X. A Palladium/Perfluoroalkylated Pyridine Catalyst for Sonogashira Reaction of Aryl Bromides and Chlorides in a Fluorous Biphasic System. *Eur. J. Org. Chem.* **2007**, *2007* (21), 3445.

(18) Yu, Y.; Lu, B.; Wang, X.; Zhao, J.; Wang, X.; Cai, Q. Highly Selective Oxidation of Benzyl Alcohol to Benzaldehyde with Hydrogen Peroxide by Biphasic Catalysis. *Chem. Eng. J.* **2010**, *162* (2), 738.

(19) Reppe, W.; Kröper, H. Carbonylierung II. Carbonsäuren Und Ihre Derivate Aus Olefinischen Verbindungen Und Kohlenoxyd. *Justus Liebigs Ann. Chem.* **1953**, *582* (1), 38.

(20) Kiss, G. Palladium-Catalyzed Reppe Carbonylation. *Chem. Rev.* **2001**, *101* (11), 3435.

(21) Schmidt, M.; Pogrzeba, T.; Hohl, L.; Weber, A.; Kielholz, A.; Kraume, M.; Schomäcker, R. Palladium Catalyzed Methoxycarbonylation of 1-Dodecene in Biphasic Systems – Optimization of Catalyst Recycling. *Mol. Catal.* **2017**, *439*, 1.

(22) Illner, M.; Müller, D.; Esche, E.; Pogrzeba, T.; Schmidt, M.; Schomäcker, R.; Wozny, G.; Repke, J.-U. Hydroformylation in Microemulsions: Proof of Concept in a Miniplant. *Ind. Eng. Chem. Res.* **2016**, *55* (31), 8616.

(23) Müller, M.; Kasaka, Y.; Müller, D.; Schomäcker, R.; Wozny, G. Process Design for the Separation of Three Liquid Phases for a Continuous Hydroformylation Process in a Miniplant Scale. *Ind. Eng. Chem. Res.* **2013**, *52* (22), 7259.

(24) Müller, D.; Esche, E.; Pogrzeba, T.; Illner, M.; Schomäcker, R.; Wozny, G.; Leube, F. Systematic Phase Separation Analysis of Surfactant Containing Systems for Multiphase Settler Design. *Ind. Eng. Chem. Res.* **2015**, *54* (12), 3205.

(25) Seborg, D. E.; Mellichamp, D. A.; Edgar, T. F.; Doyle, F. J., III. *Process Dynamics and Control*; John Wiley & Sons, 2011.

(26) AIChE Center for Chemical Process Safety. *Guidelines for Safe Automation of Chemical Processes*; AIChE, 1993.

(27) Rosales, M.; Pacheco, I.; Medina, J.; Fernández, J.; González, Á.; Izquierdo, R.; Melean, L. G.; Baricelli, P. J. Kinetics and Mechanisms of Homogeneous Catalytic Reactions. Part 12. Hydroalcoxycarbonylation of 1-Hexene Using Palladium/Triphenylphosphine Systems as Catalyst Precursors. *Catal. Lett.* **2014**, *144* (10), 1717.

(28) Roesle, P.; Caporaso, L.; Schmitte, M.; Goldbach, V.; Cavallo, L.; Mecking, S. A Comprehensive Mechanistic Picture of the Isomerizing Alkoxycarbonylation of Plant Oils. *J. Am. Chem. Soc.* **2014**, *136* (48), 16871.

(29) de la Fuente, V.; Waugh, M.; Eastham, G. R.; Iggo, J. A.; Castellón, S.; Claver, C. Phosphine Ligands in the Palladium-Catalyzed Methoxycarbonylation of Ethene: Insights into the Catalytic Cycle through an HP NMR Spectroscopic Study. *Chem. - Eur. J.* **2010**, *16* (23), 6919.

(30) Baya, M.; Houghton, J.; Konya, D.; Champouret, Y.; Daran, J. C.; Almeida Leñero, K. Q.; Schoon, L.; Mul, W. P.; Van Oort, A. B.; Meijboom, N.; et al. Pd(I) Phosphine Carbonyl and Hydride Complexes Implicated in the Palladium-Catalyzed Oxo Process. *J. Am. Chem. Soc.* **2008**, *130* (32), 10612.

(31) Portnoy, M.; Milstein, D. A Binuclear Palladium(I) Hydride. Formation, Reactions, and Catalysis. *Organometallics* **1994**, *13* (2), 600.

(32) van Leeuwen, P. W. N. M.; Zuideveld, M. A.; Swennenhuis, B. H. G.; Freixa, Z.; Kamer, P. C. J.; Goubitz, K.; Fraanje, J.; Lutz, M.; Spek, A. L. Alcoholysis of Acylpalladium(II) Complexes Relevant to the Alternating Copolymerization of Ethene and Carbon Monoxide and the Alkoxycarbonylation of Alkenes: The Importance of Cis-Coordinating Phosphines. *J. Am. Chem. Soc.* **2003**, *125* (18), 5523.



# PAPER 11

## **Palladium-catalyzed hydroxycarbonylation of 1-dodecene in microemulsion systems: Does reaction performance care about phase behavior?**

Marcel Schmidt, Carolina Urban, Svenja Schmidt, Reinhard Schomäcker

ACS Omega, 2018, 3, 13355-13364

Online Article:

<https://pubs.acs.org/doi/10.1021/acsomega.8b01708>

Reproduced (or 'Reproduced in part') with permission from "Palladium-catalyzed hydroxycarbonylation of 1-dodecene in microemulsion systems: Does reaction performance care about phase behavior?; Marcel Schmidt, Carolina Urban, Svenja Schmidt, Reinhard Schomäcker. ACS Omega, 2018, 3, 13355-13364." Copyright (2018) American Chemical Society.



# Palladium-Catalyzed Hydroxycarbonylation of 1-Dodecene in Microemulsion Systems: Does Reaction Performance Care about Phase Behavior?

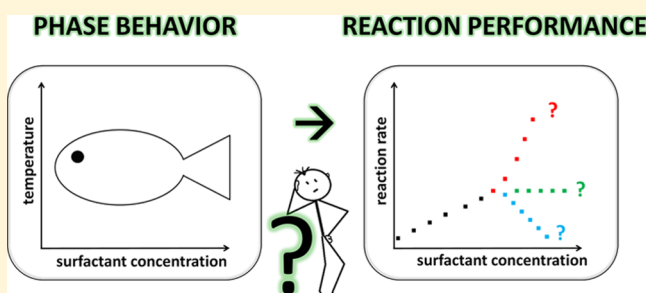
Marcel Schmidt,\*<sup>1</sup> Carolina Urban, Svenja Schmidt, and Reinhard Schomäcker<sup>1</sup>

Department of Chemistry, Technische Universität Berlin, Str. des 17. Juni 124, Sekr. TC-8, D-10623 Berlin, Germany

## Supporting Information

**ABSTRACT:** Catalysis, particularly metal-catalyzed reactions in microemulsion systems, offers a sustainable approach for organic reactions in water. However, it is still a challenging task because of the complex role of the nonionic surfactant in such a system and the interaction of the phase behavior and reaction performance. To get a profound knowledge of this role and interaction, a systematic study of the palladium-catalyzed hydroxycarbonylation of 1-dodecene in a microemulsion system is reported. The influence of the temperature, additives such as cosolvents, the catalyst concentration, and the hydrophilicity of the surfactant and its concentration

has been investigated with regard to both the phase behavior and reaction performance. Interestingly, the investigations reveal that not the phase behavior of the microemulsion system but mainly the dimension of the oil–water interface and the local concentrations of the substrates at this interface, which is provided by the amount and hydrophilicity of the surfactant, control the reaction performance of hydroxycarbonylation in these systems. Moreover, it was found that the local concentration of the active catalyst complex at the interface is essential for the reaction performance. Dependent on the surface active properties of the catalyst complex, its bulk concentration, and the nature and amount of additives, the local concentration of the active catalyst complex at the interface is strongly influenced, which has a huge impact on the reaction performance.



## 1. INTRODUCTION

The application of biphasic catalysis represents a smart approach to perform homogeneously catalyzed reactions in an economical and ecological way. The major advantage is the possibility to separate the product from the reaction mixture and to recycle the expensive catalyst via a simple phase separation step after the reaction. In industry, the Ruhrchemie/Rhône Poulenc process was the first successful example of biphasic catalysis, where in a hydroformylation reaction, propene is converted to butanal using synthesis gas (mixture of CO and H<sub>2</sub>). The applied rhodium catalyst is immobilized into the water phase by the water-soluble ligand TPPTS. Therefore, it can be recycled via a simple phase separation step. The rhodium leaching into the product phase is lower than 1 ppb, which equals to a loss of only 2 kg of rhodium per 2 000 000 tons of butanal.<sup>1</sup> Besides aqueous–organic systems, plenty of innovative biphasic media are considered as smart solvents for homogeneous catalysis, with the goal to overcome the limitations of “ordinary” biphasic systems caused by low solubility of substrates or mass transport in the aqueous phase.<sup>2</sup> An easy approach to solve this problem is the addition of cosolvents to the aqueous or organic phase, which leads to a higher solubility of the substrates in the catalyst phase and thus to a higher overall reaction performance.<sup>3</sup> Moreover, the addition of cyclodextrins, acting as mass transfer promoters, is a promising tool to enhance the catalytic activity in aqueous

biphasic systems.<sup>4,5</sup> In contrast, nonaqueous liquid/liquid biphasic systems including fluorinated biphasic systems,<sup>6,7</sup> thermo-regulated organic liquid/liquid systems,<sup>8,9</sup> and ionic liquids/supercritical fluids biphasic systems<sup>10</sup> are in focus of current research. However, these systems do not meet the requirements of sustainability because of the use of often toxic solvents. Water, on the other hand, fulfills the requirements of a “green” solvent but, as already mentioned, offers only a limited solubility for many organic substrates.

A smart approach to make water applicable as a solvent for a broader range of substrates is the use of surfactants, which is reviewed in the literature for plenty of different organic transformations.<sup>11–13</sup> If large amounts of the organic substrate are added to the micellar solution, microemulsion systems are obtained. Since the first introduction of the term “microemulsion” by J. H. Schulman in the 1950s, numerous publications on the formation, physical properties, and the application of microemulsions sprout up.<sup>14,15</sup> Microemulsions are mixtures of two immiscible liquids, predominantly water and oil, with an amphiphile as an emulsifier. The phase behavior can be easily described by the Gibbs phase prism in which the base of this prism represents the ternary system of

Received: July 19, 2018

Accepted: September 14, 2018

Published: October 17, 2018



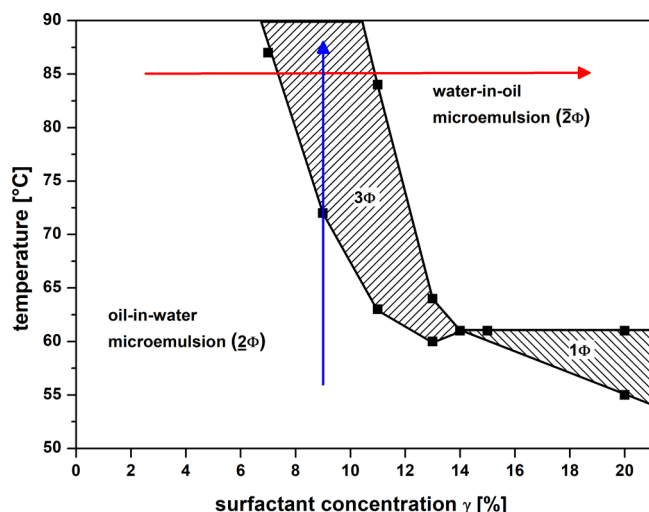


**Figure 3.** Phase diagram of a mixture of 1-dodecene, dodecane, water, and Marlipal (24/50) with  $\alpha = 0.5$ , 1 wt %  $\text{Na}_2\text{SO}_4$ ,  $\text{Pd}_2(\text{allyl})_2\text{Cl}_2$  (0.02 mmol),  $\text{Pd/SX/methanesulfonic acid (MSA)/1-dodecene} = 1:4:40:110$ , and mass ratio 1-dodecene to dodecane = 1:3 (red line: constant temperature, blue line: constant  $\gamma$ ).

to mention that the surfactant is of technical grade with a certain distribution of ethylene oxide units and an apolar alkyl chain distribution. Second, no additional functional groups for example phenyl-groups exist, which could interact with the catalytic system. Third, the phase inversion temperature of the microemulsion system consisting of 1-dodecene, dodecane, water, and Marlipal 24/50 is in the middle of the investigated temperature range. Hence, Marlipal 24/50 is appropriate for our investigations. Dodecane was added as the cosolvent to the oil phase (mass ratio 1-dodecene to dodecane was 1:3) for maintaining a phase separation and for avoiding rigorous shifts of the phase diagram because of the formed product tridecanoic acid during the reaction. Additionally, 1 wt % sodium sulfate was added to microemulsion systems for destabilizing the emulsion, which empirically accelerates the time for phase separation by a factor of 4. We have to mention that the addition of sodium sulfate decreases the initial rate of hydroxycarbonylation, but the selectivity remains constant (see the Supporting Information). The impact of salts on the reaction performance and catalyst stability was investigated in detail for the palladium-catalyzed hydroxycarbonylation of propene in biphasic systems.<sup>24</sup> Nevertheless, 1 wt % sodium sulfate was used because of the enhanced phase separation. All catalyst components were added to the microemulsion system as well to observe the phase behavior for the entire reaction mixture. It has to be mentioned that the investigation on the phase behavior has been performed without carbon monoxide pressure to avoid any reaction progress. Indeed, the pressure has an impact on the phase behavior, but it can be neglected for the mild reaction pressure used in the reactions.<sup>25</sup>

The investigated microemulsion system is characterized by the surfactant concentration  $\tilde{\gamma} = 14\%$  and the phase inversion temperature  $\tilde{T} = 61\text{ }^\circ\text{C}$ . An oil-in-water microemulsion with an excess oil phase ( $2\Phi$ ) is formed at lower temperatures. With increasing temperature, the system shifts to a water-in-oil microemulsion with an excess water phase ( $2\Phi$ ). In between, a macroscopically triphasic system is formed in which the middle phase is the microemulsion phase enclosed by the water-excess and oil-excess phase. Increasing the surfactant concentration

above 14%, oil and water are completely dispersed in a one phase microemulsion. Interestingly, the catalyst system follows the surfactant into the corresponding microemulsion phase because of its surface activity as seen in Figure 4, exemplarily

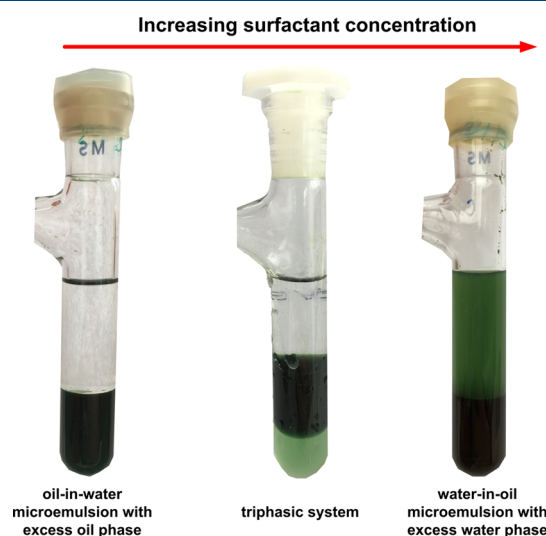


**Figure 4.** Pictures of the investigated microemulsion systems. Test conditions:  $T = 85\text{ }^\circ\text{C}$ ,  $\alpha = 0.5$ , 1 wt %  $\text{Na}_2\text{SO}_4$ ,  $\text{Pd}_2(\text{allyl})_2\text{Cl}_2$  (0.02 mmol),  $\text{Pd/SX/MSA/1-dodecene} = 1:4:40:110$ , mass ratio 1-dodecene to dodecane = 1:3, Marlipal 24/50 as the surfactant,  $\gamma = 4\%$  (left),  $\gamma = 9\%$  (middle),  $\gamma = 14\%$  (right).

recorded for an increasing surfactant concentration at a constant temperature. It is mentionable that the different phases look similar for a constant surfactant concentration with increasing temperature. The surface activity of the catalyst complex results from the surface-active ligand SulfoXantPhos, which was shown in previous publications.<sup>26,27</sup> As a result, the catalyst complex behaves similar to a surfactant and the complex can be incorporated at the water–oil interface. Hence, the catalyst can be solubilized either in the continuous water phase (left picture) and the surfactant-rich phase (middle picture) or even partly in the oil phase (right picture). The change of color is due to the different catalyst complex concentrations in the different phases. Hereby, the dark greenish phases indicate a high concentration of the applied catalyst complex in the corresponding phase.

On the basis of the phase behavior of the applied microemulsion system, the influence of temperature and surfactant concentration has been investigated in terms of reaction performance to correlate it to the phase behavior of the microemulsion system. The effect of the surfactant concentration has been investigated at a constant reaction temperature of  $85\text{ }^\circ\text{C}$  to ensure the shift from an oil-in-water to a water-in-oil microemulsion system (see the red arrow in Figure 3). The conversion of 1-dodecene and the yield to the linear acid are shown in Figure 5. It was found that the higher the surfactant concentration, the higher is the conversion, respectively the yield to the linear acid at a given time. The yield increases from 0.3% with a surfactant concentration of  $\gamma = 0.5$  to 42.6% at a surfactant concentration of  $\gamma = 30\%$  after 20 h reaction time. It has to be mentioned that the addition of surfactant is generally necessary to enable the reaction because no reaction progress is observed without surfactant as the phase transfer agent. Furthermore, a critical surfactant concentration is apparently needed, in this case  $\gamma > 3\%$ , to

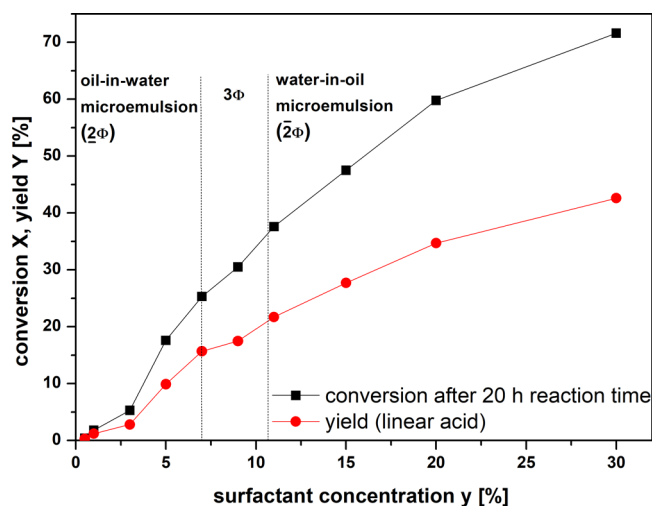


**Figure 5.** Effect of surfactant concentration on the hydroxycarbonylation of 1-dodecene. Experimental conditions:  $\text{Pd}_2(\text{allyl})_2\text{Cl}_2$  (0.08 mmol),  $\text{Pd}/\text{SX}/\text{MSA}/1\text{-dodecene}$  (1:4:40:110),  $\alpha = 0.5$ , dodecane as the cosolvent (9 g), water (12 g), Marlipal 24/50 as the surfactant,  $\text{Na}_2\text{SO}_4$  (1 wt %),  $p(\text{CO}) = 30$  bar,  $T = 85$  °C,  $n = 1200$  rpm,  $t = 20$  h.

accelerate the reaction substantially. Below a concentration of  $\gamma = 3\%$ , only surfactant monomers are dissolved in the oil and the water phase, resulting only in a slow reaction progress. A further increase of the surfactant concentration leads to a strong enlargement of the interfacial area between the aqueous and organic phase. Hence, the local concentrations of the reactants, particularly water, carbon monoxide, and 1-dodecene, at the interface are increased with increasing amount of surfactant in the mixture, which results in higher reaction rates shown by higher yield and conversion.

As stated in the literature, the rate-determining step of hydroxycarbonylation is the hydrolysis step,<sup>28,29</sup> thus particularly the increased amount of water at the interface may lead to the higher reaction rate with increasing surfactant concentration. Furthermore, the local concentration of the active catalyst species plays a crucial role for the reaction performance. The applied catalyst complex is negatively charged because of the ligand SulfoXantPhos. Hence, no electrostatic interaction with the neutral surfactant can be expected. Nevertheless, the catalyst complex accumulates at the water–oil interface because of its surface active properties. Thus, with an increasing interfacial area, the catalyst complex becomes more and more diluted at the interface because the overall amount of catalyst in the system remains constant. As a result, the equilibrium between active and inactive catalyst species might be shifted to a higher concentration of the active catalyst at the interface, and with that to a higher reaction rate. To confirm this assumption, we varied the catalyst concentration at a fixed surfactant concentration that is a constant interfacial area, which is shown in Section 2.3.

Interestingly, the phase behavior of the microemulsion system has no strong impact on the reaction performance of hydroxycarbonylation, which is in good agreement to the findings for hydroformylation of 1-dodecene in the same systems.<sup>21</sup> The initially prepared microemulsion system changes from an oil-in-water microemulsion system at a surfactant concentration of  $\gamma = 7\%$  to a macroscopically three-phase system and finally to a water-in-oil microemulsion system at  $\gamma = 11\%$ . No significant change in the conversion and

yield of the reaction is observed at the shift of the phase states, which would indicate a change in mass transfer conditions. This means that not the phase behavior of the microemulsion system but the interfacial area and the local concentrations of the reactants at the interface have a major influence on the reaction performance of hydroxycarbonylation. Moreover, the surfactant concentration has a minor impact on the 1/b regioselectivity of the formed acid. With increasing surfactant concentration, the 1/b selectivity decreases from 64:36 at a surfactant concentration of  $\gamma = 3\%$  to 61:39 at  $\gamma = 30\%$ . Because of the increased interfacial area the isomerization of 1-dodecene takes place with an increased rate, which leads to the slightly lower 1/b selectivity. It is mentionable that surfactant concentrations above  $\gamma = 20\%$  are not favorable because the one phase region of the microemulsion system makes a subsequent phase separation for recycling of the catalyst system rather difficult in comparison to the other multiphase states.

Furthermore, the surfactant concentration was fixed at  $\gamma = 9\%$  to investigate the effect of the temperature on the reaction (blue arrow in Figure 4). The hydroxycarbonylation of 1-dodecene was carried out at temperatures ranging from 65 to 105 °C (see Figure 6).

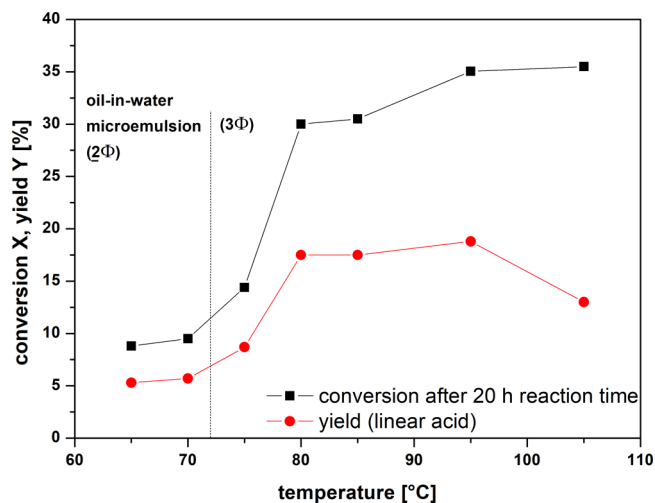


**Figure 6.** Effect of temperature on the hydroxycarbonylation of 1-dodecene. Experimental conditions:  $\text{Pd}_2(\text{allyl})_2\text{Cl}_2$  (0.08 mmol),  $\text{Pd}/\text{SX}/\text{MSA}/1\text{-dodecene}$  (1:4:40:110),  $\alpha = 0.5$ , dodecane as the cosolvent (9 g), water (12 g), Marlipal 24/50 as the surfactant,  $\gamma = 9\%$ ,  $\text{Na}_2\text{SO}_4$  (1 wt %),  $p(\text{CO}) = 30$  bar,  $n = 1200$  rpm,  $t = 20$  h.

Initially, the conversion increases exponentially with increasing reaction temperature from 8% at 65 °C to 30% at 80 °C, which is typical for an Arrhenius type behavior, indicating a kinetically controlled biphasic reaction. After this, the conversion reaches unexpectedly a plateau between 30 and 35% at higher reaction temperatures. The yield of the linear acid shows a nearly similar trend but decreases in the end, resulting in a yield of only 13% at 105 °C. To understand the decreased yield, the initial rate of hydroxycarbonylation was calculated from the gas consumption at a conversion of 5%. As illustrated in Figure 7, the initial rate of hydroxycarbonylation behaves in the same way, there is an exponential increase from 2.5 to 10.5 mmol/(L·h), followed by a inflection point, and a further slightly increase of the initial rate to a critical value of 18 mmol/(L·h). Interestingly, the decline in activity cannot be

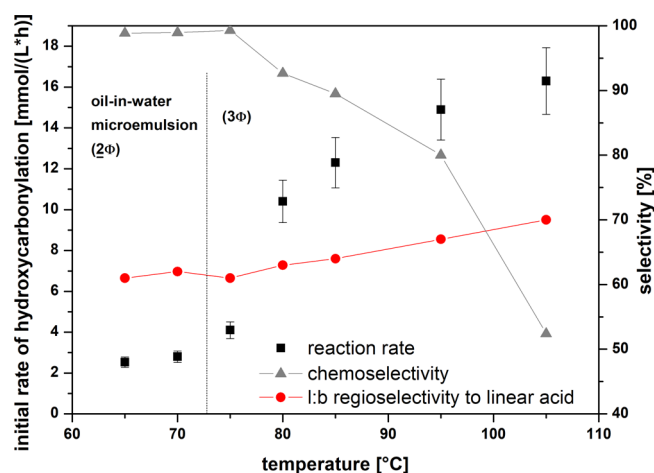


**Figure 7.** Effect of temperature on the initial rate and selectivity of the hydroxycarbonylation of 1-dodecene. Experimental conditions:  $\text{Pd}_2(\text{allyl})_2\text{Cl}_2$  (0.08 mmol), Pd/SX/MSA/1-dodecene (1:4:40:110),  $\alpha = 0.5$ , dodecane as the cosolvent (9 g), water (12 g), Marlipal 24/50 as the surfactant,  $\gamma = 9\%$ ,  $\text{Na}_2\text{SO}_4$  (1 wt %),  $p(\text{CO}) = 30$  bar,  $n = 1200$  rpm,  $t = 20$  h, initial rate calculated from gas consumption at  $X = 5\%$ .

attributed to the change of phase behavior from an oil-in-water microemulsion to a three-phase system because this shift already happens at a temperature of 72 °C (see Figure 3). However, palladium black formation was observed as the precipitate at the reactor wall, particularly at temperatures above 100 °C, which leads to a decrease of the amount of the active catalyst. Thus, the initial rate of hydroxycarbonylation differs from the typical exponential increase and stagnates at higher temperatures. As described in the literature, palladium black formation is a specific drawback for homogeneously catalyzed reactions using palladium.<sup>30</sup> We have to mention that the reaction is not limited by mass transport at high temperatures, which was confirmed by investigations with variation of the stirrer speed, resulting in constant reaction rates.

In addition, the reaction temperature influences slightly the l/b regioselectivity to the linear acid. With increasing temperature from 65 to 105 °C, the regioselectivity of the linear acid increases from 61 to 70%. The hydrolysis step is known as the rate-determining step in the hydroxycarbonylation reaction. Because of the lower activation barrier of the hydrolysis step to the linear acid, compared to the hydrolysis step to the branched acid, hydroxycarbonylation at the terminal double bond proceeds faster.<sup>29</sup> Thus, the formation of the linear acid is enhanced with increasing temperature. Furthermore, chemoselectivity is extremely diminished from nearly 100% at 65 °C to 51% at 105 °C because an increased temperature enhances the isomerization of 1-dodecene.<sup>8</sup> Considering all aspects, the phase behavior, especially the different phase states of the microemulsion system, seems to have no influence on the reaction performance of hydroxycarbonylation. To avoid the isomerization and palladium black formation, the following investigations were carried out at a reaction temperature of 85 °C.

**2.2. Effect of Degree of Ethoxylation (EO).** As described in the Section 2.1, the amount of surfactant is crucial for the performance of hydroxycarbonylation in microemulsion systems. To completely understand the role of the surfactant during the reaction, we investigated the influence of the surfactant chain length toward both the performance of

hydroxycarbonylation and the phase behavior. Therefore, the hydrophobicity of the surfactant was changed by varying the degree of EO from 2 to 9 (Marlipal 24/20 to Marlipal 24/90). As expected, the phase behavior is strongly influenced by the hydrophobicity of the surfactant (Figure 8). The three-phase

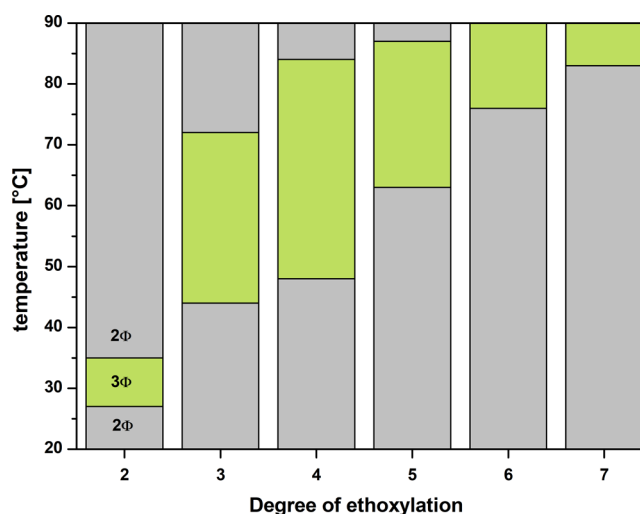


**Figure 8.** Phase behavior of 1-dodecene, dodecane, water, and Marlipal with different degrees of EO. Test conditions:  $\alpha = 0.5$ ,  $\gamma = 9\%$ , 1 wt %  $\text{Na}_2\text{SO}_4$ ,  $\text{Pd}_2(\text{allyl})_2\text{Cl}_2$  (0.02 mmol), Pd/SX/MSA/1-dodecene = 1:4:40:110, mass ratio 1-dodecene to dodecane = 1:3.

region of the resulting microemulsion system is shifted to higher temperatures with the increasing EO number or rather decreasing hydrophobicity of the surfactant. The hydrophilic part of the surfactant, consisting of ethoxy units, undergoes a temperature-dependent conformational transformation, influencing the water solubility of the corresponding surfactant. The higher the EO number, the more temperature is needed to change the conformation of the ethoxy units. As a result of the conformational transformation, the dipole moment is reduced, resulting in a lower water solubility. Hence, the hydrophobicity of the surfactant is increased with higher EO and thus the appearance of the three-phase region is shifted to higher temperatures. The phase boundaries for the systems containing the surfactants Marlipal 24/80 and Marlipal 24/90 could not be determined because of the temperature limitation of the experimental setup.

Besides the shift in the phase behavior, it was found that the number of EO groups of the surfactant has a strong impact on the conversion and yield of hydroxycarbonylation (Figure 9). In general, the higher the EO number, the higher is the conversion or rather the yield of the acid. The yield of the linear acid reaches a maximum of 34% after 20 h reaction time with Marlipal 24/90 as the surfactant. It is notable that the applied surfactants do not differ in their chemical structure. Consequently, the difference in the reaction performance is caused by physical effects, particularly the local concentrations of the substrates at the interface. The density of the surfactant film at the oil–water interface might be the reason. With the increasing number of EO, the thickness of the surfactant film increases, leading to an enhanced adsorption of the reactants to the interface. Hence, the reactants are more accumulated at the oil–water interface with increasing EO number, which enhances the reaction rate. Similar results were obtained for the rhodium-catalyzed hydroformylation of 1-dodecene in

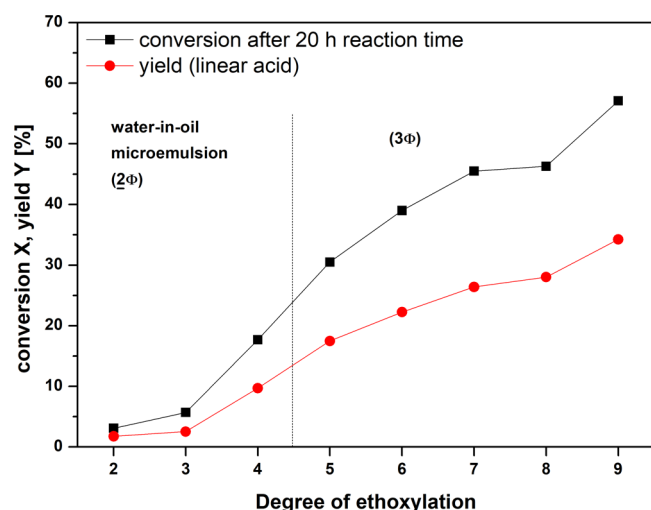


**Figure 9.** Effect of degree of EO on hydroxycarbonylation of 1-dodecene. Experimental conditions:  $\text{Pd}_2(\text{allyl})_2\text{Cl}_2$  (0.08 mmol), Pd/SX/MSA/1-dodecene (1:4:40:110),  $\alpha = 0.5$ , dodecane as the cosolvent (9 g), water (12 g), Marlipal 24/XX as the surfactant,  $\text{Na}_2\text{SO}_4$  (1 wt %),  $p(\text{CO}) = 30$  bar,  $T = 85$  °C,  $n = 1200$  rpm,  $t = 20$  h.

microemulsion systems, which were recently reported by our group.<sup>21</sup> Again, the phase behaviour of the microemulsion system shows no influence on the reaction performance, because no discrete changes of the conversion were observed when changing the phase state by the type of surfactant. We have to mention that the color of the reaction mixture did not change during the reaction, concluding that no palladium nanoparticles were formed.

In summary, the series of experiments confirms the assumption that the local concentrations of the reactants at the oil–water interface are crucial for the reaction performance. These concentrations are mainly determined by hydrophilicity and the amount of surfactant. The EO number of the applied surfactant controls the ability to perform as an emulsifier, which has a strong impact on the local concentrations and thus on the reaction rate for hydroxycarbonylation of 1-dodecene in microemulsion systems.

**2.3. Variation of Catalyst Concentration.** According to Section 2.1, the formation of inactive catalyst species depends on the local concentration of the catalyst complex at the oil–water interface. To confirm the formation of inactive catalyst species at the interface, experiments were carried out with variation of the catalyst concentration whereby the interfacial area was maintained using a constant surfactant concentration. Typically, the reaction rate increases with increasing catalyst concentration, often with a reaction order of 1.<sup>28</sup> In this case, the initial rate of hydroxycarbonylation increases in a concentration range from 0 to 8 mmol/L of palladium as seen in Figure 10 but surprisingly with a fractional reaction order of 1.8. Because the molar ratio of palladium to SulfoXantPhos to MSA remains constant at 1:4:40, we assume that the unexpected reaction order is caused by the increased concentration of MSA in this concentration range. As a result, more acidic reaction conditions are obtained with a higher amount of palladium, leading to a disproportionately high formation of the active palladium hydride species (see Figure 11) and thus to the unexpected reaction order of 1.8. Rodionova et al. investigated methoxycarbonylation of cyclo-

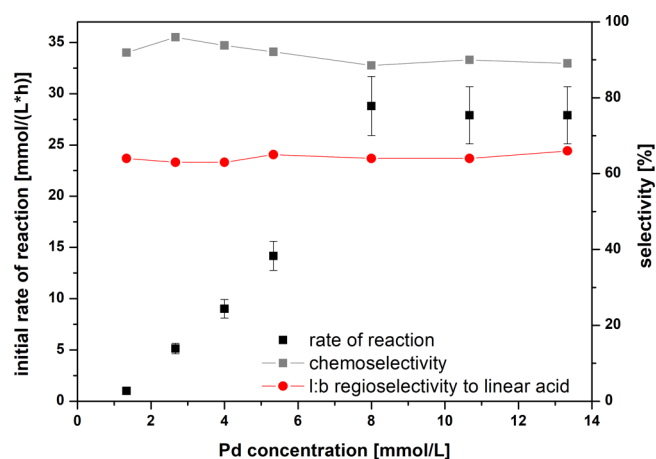


**Figure 10.** Effect of Pd concentration on hydroxycarbonylation of 1-dodecene. Experimental conditions:  $\text{Pd}_2(\text{allyl})_2\text{Cl}_2$  as the precursor, Pd/SX/MSA (1:4:40),  $\alpha = 0.5$ , 1-dodecene (3 g), dodecane as the cosolvent (9 g), water (12 g), Marlipal 24/70 as the surfactant,  $\gamma = 9\%$ ,  $\text{Na}_2\text{SO}_4$  (1 wt %),  $p(\text{CO}) = 30$  bar,  $T = 85$  °C,  $n = 1200$  rpm,  $t = 20$  h,  $V_R = 0.03$  L, initial rate calculated from gas consumption at  $X = 5\%$ .

hexene and found similar results for the reaction order of the used acid as the cocatalyst.<sup>31</sup>

A further increase of the palladium concentration leads to a stagnation of the initial rate of reaction around 28 mmol/(L·h), indicating a catalyst inhibition because of the formation of inactive catalyst species (see Figure 11). We have to mention that variation of the stirrer speed at the highest palladium concentration shows no impact on the initial rate of hydroxycarbonylation, excluding any mass transport limitation. On the one hand, it is well-known that homogeneous palladium catalysts can form dimeric species, which are inactive for the palladium-catalyzed hydroxycarbonylation of 1-dodecene.<sup>32–34</sup> We assume that high palladium and ligand concentrations lead to an enhanced formation of the inactive dimeric species, suppressing a further increase of the initial rate of hydroxycarbonylation. It has to be mentioned that the molar ratio of palladium to SulfoXantPhos to MSA remains constant at 1:4:40 for this experimental series. As a result, not only the palladium concentration is increased at the interface, but also the concentration of the ligand SulfoXantPhos, influencing the formation of the dimeric catalyst species as well. On the other hand, Mecking et al.<sup>35</sup> identified a bimolecular decomposition pathway for the active palladium hydride species forming palladium black, hydrogen, and a fully coordinated (diphosphine)<sub>2</sub>Pd complex under reaction conditions. As a result of both deactivation pathways, the amount of the active catalyst species may stagnate at high concentrations of palladium, which would explain the observed plateau of the initial rate of hydroxycarbonylation.

In addition, the l/b regioselectivity and chemoselectivity of hydroxycarbonylation remains unchanged. Merely, isomerization of 1-dodecene takes place, which decreases chemoselectivity to 90%. As expected, the l/b regioselectivity to the linear acid is at a constant value of 64%, which confirms that an increase of the palladium concentration does not change the structure of the active catalyst species for the hydroxycarbonylation of 1-dodecene.

**2.4. Modification of the Nonpolar Phase.** The effect of cosolvents on the reaction performance and the phase behavior

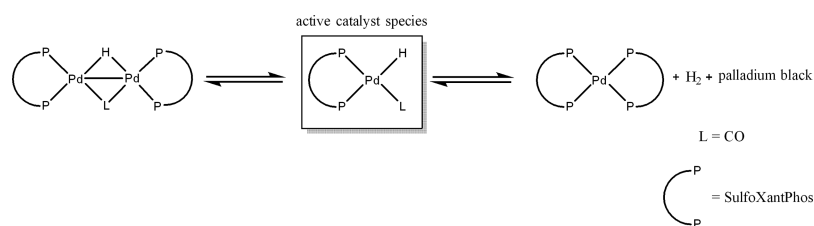


Figure 11. Possible catalyst deactivation pathways.

has also been investigated. The idea behind these experiments is to switch the phase behavior without changing the local concentrations at the oil–water interface, which should lead to similar initial reaction rates, thus verifying the previous results. As seen in Figure 12, the chain length of alkane, which has been applied as the cosolvent, affects the temperature slightly for existence of the three-phase region.

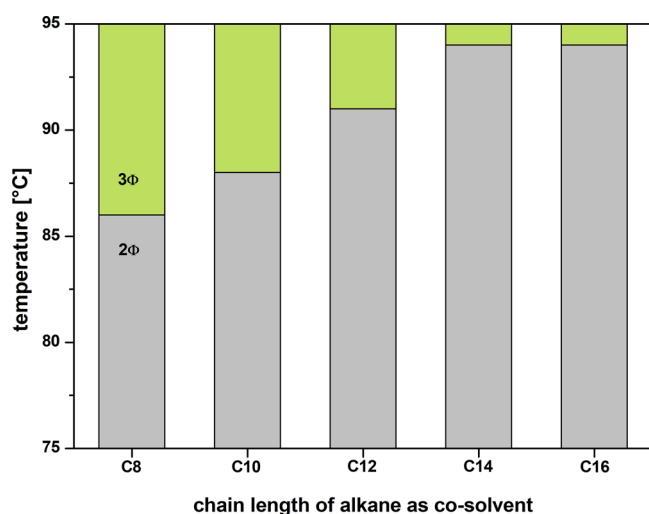


Figure 12. Phase behavior of 1-dodecene, cosolvent, water, and Marlipal 24/70. Test conditions:  $\alpha = 0.5$ ,  $\gamma = 9\%$ ,  $\text{Na}_2\text{SO}_4$  (1 wt %),  $\text{Pd}_2(\text{allyl})_2\text{Cl}_2$  (0.02 mmol),  $\text{Pd}/\text{SX}/\text{MSA}/1\text{-dodecene} = 1:4:40:110$ , and mass ratio 1-dodecene to cosolvent = 1:3.

As expected, with increasing hydrophobicity (chain-length) of the applied cosolvent, the phase boundaries are shifted to higher temperatures. However, the impact of changing the chain length on the phase behavior is rather low. The extension of the chain length by two carbon atoms results in a shift of the three-phase region of about 2 °C to higher temperatures. Furthermore, the slight change of the phase behavior by changing the hydrophobicity of the cosolvent shows no influence on the initial rate of hydroxycarbonylation (Figure 13), indicating no impact of the phase behavior on the reaction performance. Apparently, the local concentrations of the reactants at the oil–water interface do not differ for the applied alkanes as cosolvents despite the slight change of the phase behavior. Both chemoselectivity and l/b regioselectivity remain constant as well. The chemoselectivity is in a range of 90–95% because of isomerization of 1-dodecene. Nevertheless, the adjustment of the three-phase region by the choice of the cosolvent is crucial for a subsequent recycling procedure and product purification.

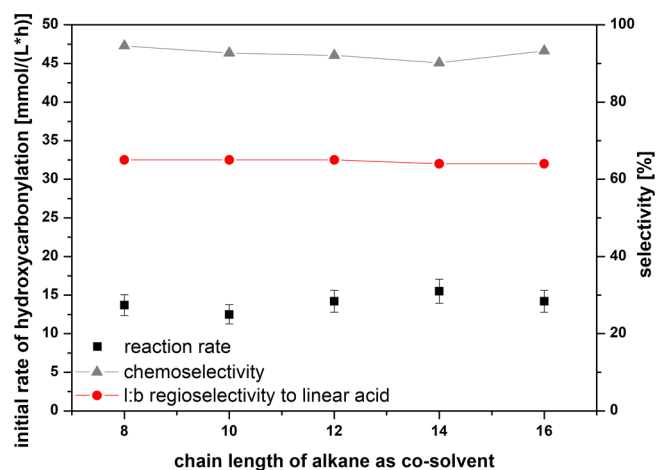


Figure 13. Effect of cosolvent on the hydroxycarbonylation of 1-dodecene. Experimental conditions:  $\text{Pd}_2(\text{allyl})_2\text{Cl}_2$  (0.08 mmol),  $\text{Pd}/\text{SX}/\text{MSA}/1\text{-dodecene}$  (1:4:40:110),  $\alpha = 0.5$ , cosolvent (9 g), water (12 g), Marlipal 24/70 as the surfactant,  $\text{Na}_2\text{SO}_4$  (1 wt %),  $p(\text{CO}) = 30$  bar,  $T = 85$  °C,  $n = 1200$  rpm,  $t = 20$  h,  $V_R = 0.03$  L, initial rate calculated from gas consumption at  $X = 5\%$ .

### 3. CONCLUSIONS

With this contribution, the impact of nonionic surfactants on the palladium-catalyzed hydroxycarbonylation of 1-dodecene in microemulsion systems was demonstrated. Special attention was given to the interaction of the phase behavior of the microemulsion system and the reaction performance. It was found that the phase behavior does not control the reaction performance for catalysis in microemulsion systems. In contrast, the amount and type of the nonionic surfactants are crucial for catalysis in these reaction systems. First, the surfactant provides the interfacial area between oil and water. Because of the surface active properties of the applied catalyst complex, the reaction takes place at the interface. Extending this interfacial area by increasing the amount of surfactant, the reaction performance is substantially improved. Second, the hydrophilicity of the surfactant determines the local concentrations of substrates at the interface influencing the rate of hydroxycarbonylation. The presented results confirm the recently published results where the role of nonionic surfactants in the rhodium-catalyzed hydroformylation of 1-dodecene was investigated. Moreover, the concentration of the active catalyst complex at the interface has a huge impact on the reaction performance of hydroxycarbonylation. Dependent on its bulk concentration, inactive catalyst species are formed reducing the reaction performance. Consequently, the amount and chemical properties of the surfactant and the chemical behavior of the applied catalyst complex are crucial parameters to optimize the reaction performance for catalysis in microemulsion systems.

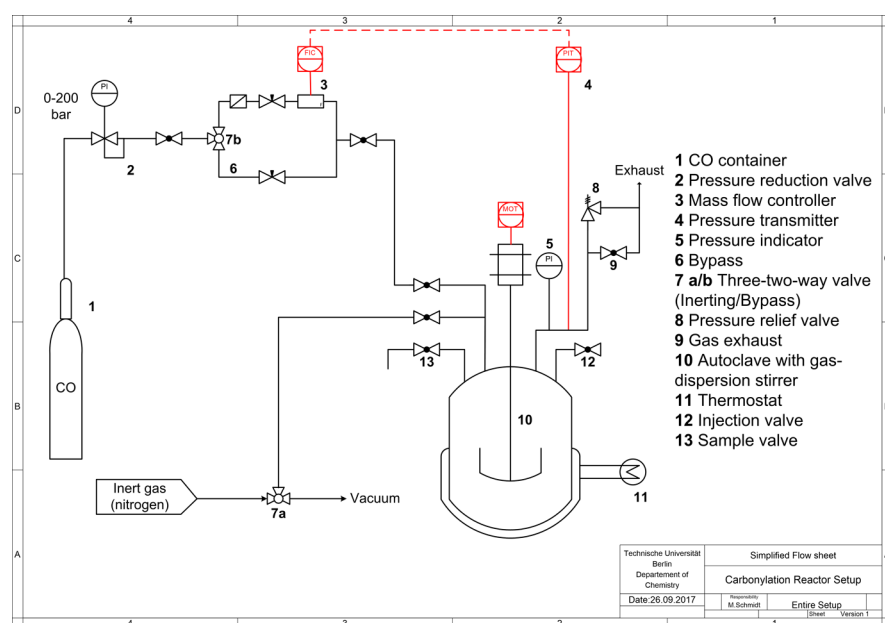


Figure 14. Experimental setup for hydroxycarbonylation.

On the basis of these results, the transfer from the lab scale into a continuously operated miniplant is currently under investigation. Hereby, the phase separation in the decanter unit and the catalyst stability is of special interest because of concentration shifts during the continuously operated reaction. In general, the three-phase region or the oil-in-water microemulsion is desirable to perform the recycling of the catalyst and the separation of the product. However, the time for phase separation is drastically reduced in the three-phase region, facilitating lower residence time in the decanter and thus the three-phase region of the microemulsion system is appropriate for recycling experiments.

#### 4. MATERIALS AND METHODS

**4.1. Chemicals.** The substrates such as 1-dodecene (94%), decane (94%), and hexadecane (99%) were purchased from Merck and the cosolvents such as dodecane (98%) and octane (98%) were received from ABCR. Water was obtained from VWR with the HPLC grade. Sigma-Aldrich has delivered the palladium precursor  $\text{Pd}_2(\text{allyl})_2\text{Cl}_2$  with a purity of 99.9%, the cosolvent tetradecane (92%), and the cocatalyst MSA with a purity of 99.5%. SulfoXantPhos (CAS registry number 215792-51-1) was used as a ligand and was synthesized by MOLISA following a procedure described by Goedheijt et al.<sup>36</sup> It is the water-soluble analogue of the commercially available 4,5-bis(diphenylphosphino)-9,9-dimethylxanthene (XantPhos). Nonane (99%) from Sigma-Aldrich was used as the internal standard. Carbon monoxide was obtained from Air Liquide with a purity of 99.9%. The applied nonionic surfactants of the Marlipal series were provided by Sasol Germany. It is worth to mention that the surfactants are of technical grade with a certain chain length distribution. To control the ionic strength of the reaction media, sodium sulfate ( $\text{Na}_2\text{SO}_4$ ) was used, which was purchased from Merck. All chemicals were used as received without further purification.

**4.2. Determination of the Phase Behavior.** The investigations on the phase behavior were performed in 10 mL Schlenk tubes. The cosolvent (2.25 g), 1-dodecene (0.75 g), the surfactant (Marlipal 24/XX), sodium sulfate ( $\text{Na}_2\text{SO}_4$ ),

and the cocatalyst MSA were weighted into the Schlenk tube and flushed with argon. A stock solution of the precursor  $\text{Pd}_2(\text{allyl})_2\text{Cl}_2$  and the ligand SulfoXantPhos was prepared in water with standard Schlenk technique and stirred overnight. The catalyst solution (3.0 g) was added to the Schlenk tube under an argon counterflow, and the tubes were closed with a septum. Afterward, the Schlenk tubes were placed into a water bath, and the phase behavior of the microemulsion system was investigated in a temperature range between 50 and 90 °C in 1 °C steps. For that, the temperature of the water bath was adjusted as desired, and then the tubes were shaken and the phase separation was observed after 10 min.

#### 4.3. Experimental Setup for Hydroxycarbonylation.

All experiments were carried out in a 100 mL stainless steel autoclave built by Halmosi GmbH. An overview of the reactor setup is given in Figure 14. The autoclave (10) is equipped with a gas dispersion stirrer, a baffle to ensure the dispersion of the reaction mixture, and a PTFE inlay to avoid the formation of palladium black at the inner surface of the reactor wall. To maintain isobaric reaction conditions, a pressure transmitter (4) is connected with a mass flow controller (3) to the reactor. For a fast initial pressurization of the reactor with carbon monoxide, a bypass was installed (6). Additionally, the autoclave has connections for sampling (13), inertization (7a), and the injection of reactants (12) under a nitrogen counterflow. A process control system monitors all process-values and the corresponding set-values such as pressure, temperature, gas flow, and stirring speed and records the data.

**4.4. Experimental Procedure for Hydroxycarbonylation.** In a typical experiment, the cosolvent, 1-dodecene as the substrate, the surfactant, nonane as the internal standard (300 mg), and MSA as the co-catalyst were weighted into the PTFE inlay and introduced to the reactor. After evacuation and flushing the reactor with nitrogen three times, the catalyst solution was injected with a syringe under a nitrogen counterflow. The catalyst solution was prepared overnight, weighting  $\text{Pd}_2(\text{allyl})_2\text{Cl}_2$  (0.08 mmol, 0.5 equiv) and SulfoXantPhos (0.64 mmol, 4 equiv) into a Schlenk flask using standard Schlenk technique and adding water (12 g)

through a septum. The reactor was heated up to the desired reaction temperature, pressurized with carbon monoxide, and stirred at 1200 rpm. Samples were taken at fixed time intervals, diluted with acetone, and centrifuged to precipitate the ligand from the solution. Gas chromatography (GC) analysis was performed on Shimadzu GC2010 Plus with a flame ionization detector (FID) packed with the Restek RTX5-MS column (30 m × 0.25 mm × 0.25 μm). Nonane was used as the internal standard to calculate the conversion of dodecene, yields of acid, chemoselectivity, and linear-to-branched regioselectivity (l/b), expressed as the ratio of linear acid to the sum of linear and branched acids, as shown in eqs 3–6.

$$X(t) = \frac{n_{t=0}(1\text{-dodecene}) - n_t(1\text{-dodecene})}{n_{t=0}(1\text{-dodecene})} \quad (3)$$

$$Y(t) = \frac{n_{t,\text{product}}}{n_{t=0}(1\text{-dodecene})} \quad (4)$$

$$S_{\text{chemo}}(t) = \frac{Y_{\text{acid}}(t)}{X(t)} \quad (5)$$

$$S_{l/b}(t) = \frac{Y_{\text{linear acid}}(t)}{Y_{\text{acids}}(t)} \quad (6)$$

## ■ ASSOCIATED CONTENT

### Supporting Information

The Supporting Information is available free of charge on the ACS Publications website at DOI: 10.1021/acsomega.8b01708.

Information on the chemical structure of the surfactant and variation of ionic strength (PDF)

## ■ AUTHOR INFORMATION

### Corresponding Author

\*E-mail: marcel.schmidt@tu-berlin.de.

### ORCID

Marcel Schmidt: 0000-0002-3988-6342

Reinhard Schomäcker: 0000-0003-3106-3904

### Notes

The authors declare no competing financial interest.

## ■ ACKNOWLEDGMENTS

This work is part of the Collaborative Research Center “Integrated Chemical Processes in Liquid Multiphase Systems” (subproject A2) coordinated by the Technische Universität Berlin. Financial support by the German Research Foundation (Deutsche Forschungsgemeinschaft, DFG) is gratefully acknowledged (TRR 63). We acknowledge support by the German Research Foundation and the Open Access Publication Funds of TU Berlin.

## ■ REFERENCES

- (1) Kohlpaintner, C. W.; Fischer, R. W.; Cornils, B. Aqueous biphasic catalysis: Ruhrchemie/Rhône-Poulenc oxo process. *Appl. Catal., A* **2001**, *221*, 219–225.
- (2) Liu, C.; Li, X.; Jin, Z. Progress in Thermoregulated Liquid/Liquid Biphasic Catalysis. *Catal. Today* **2015**, *247*, 82–89.
- (3) Schmidt, M.; Pogrzeba, T.; Hohl, L.; Weber, A.; Kielholz, A.; Kraume, M.; Schomäcker, R. Palladium catalyzed methoxycarbony-

lation of 1-dodecene in biphasic systems - Optimization of catalyst recycling. *Mol. Catal.* **2017**, *439*, 1–8.

(4) Hapiot, F.; Bricout, H.; Menuel, S.; Tilloy, S.; Monflier, E. Recent Breakthroughs in Aqueous Cyclodextrin-Assisted Supramolecular Catalysis. *Catal. Sci. Technol.* **2014**, *4*, 1899.

(5) Tilloy, S.; Bertoux, F.; Mortreux, A.; Monflier, E. Chemically modified β-cyclodextrins in biphasic catalysis: a fruitful contribution of the host-guest chemistry to the transition-metal catalyzed reactions. *Catal. Today* **1999**, *48*, 245–253.

(6) Horvath, I. T.; Rabai, J. Facile Catalyst Separation without Water: Fluorous Biphasic Hydroformylation of Olefins. *Science* **1994**, *266*, 72–75.

(7) Betzemeier, B.; Lhermitte, F.; Knochel, P. Wacker oxidation of alkenes using a fluorous biphasic system. A mild preparation of polyfunctional ketones. *Tetrahedron Lett.* **1998**, *39*, 6667–6670.

(8) Behr, A.; Vorholt, A. J.; Rentmeister, N. Recyclable Homogeneous Catalyst for the Hydroesterification of Methyl Oleate in Thermomorphic Solvent Systems. *Chem. Eng. Sci.* **2013**, *99*, 38–43.

(9) Gaide, T.; Behr, A.; Arns, A.; Benski, F.; Vorholt, A. J. Hydroesterification of methyl 10-undecenoate in thermomorphic multicomponent solvent systems-Process development for the synthesis of sustainable polymer precursors. *Chem. Eng. Process.* **2016**, *99*, 197–204.

(10) Liu, F.; Abrams, M. B.; Baker, R. T.; Tumas, W. Phase-Separable Catalysis Using Room Temperature Ionic Liquids and Supercritical Carbon Dioxide. *Chem. Commun.* **2001**, 433–434.

(11) Lipshutz, B. H.; Ghorai, S.; Cortes-Clerget, M. The Hydrophobic Effect Applied to Organic Synthesis: Recent Synthetic Chemistry in Water. *Chem.—Eur. J.* **2018**, *24*, 6672–6695.

(12) Dwars, T.; Paetzold, E.; Oehme, G. Reactions in Micellar Systems. *Angew. Chem., Int. Ed.* **2005**, *44*, 7174–7199.

(13) La Sorella, G.; Strukul, G.; Scarso, A. Recent Advances in Catalysis in Micellar Media. *Green Chem.* **2015**, *17*, 644–683.

(14) Mason, T. G.; Wilking, J. N.; Meleson, K.; Chang, C. B.; Graves, S. M. Nanoemulsions: Formation, Structure, and Physical Properties. *J. Phys.: Condens. Matter* **2006**, *18*, R635.

(15) Schwuger, M.-J.; Stickdorn, K.; Schomaecker, R. Microemulsions in Technical Processes. *Chem. Rev.* **1995**, *95*, 849–864.

(16) Schwarze, M.; Pogrzeba, T.; Volovych, I.; Schomäcker, R. Microemulsion Systems for Catalytic Reactions and Processes. *Catal. Sci. Technol.* **2015**, *5*, 24–33.

(17) Handa, S.; Lippincott, D. J.; Aue, D. H.; Lipshutz, B. H. Asymmetric Gold-Catalyzed Lactonizations in Water at Room Temperature. *Angew. Chem., Int. Ed.* **2014**, *53*, 10658–10662.

(18) Haumann, M.; Koch, H.; Schomäcker, R. Hydroformylation in Microemulsions: Conversion of an Internal Long Chain Alkene into a Linear Aldehyde Using a Water Soluble Cobalt Catalyst. *Catal. Today* **2003**, *79–80*, 43–49.

(19) Haumann, M.; Koch, H.; Hugo, P.; Schomäcker, R. Hydroformylation of 1-Dodecene Using Rh-TPPTS in a Microemulsion. *Appl. Catal., A* **2002**, *225*, 239–249.

(20) Gallou, F.; Isley, N. A.; Ganic, A.; Onken, U.; Parmentier, M. Surfactant Technology Applied toward an Active Pharmaceutical Ingredient: More than a Simple Green Chemistry Advance. *Green Chem.* **2016**, *18*, 14–19.

(21) Pogrzeba, T.; Schmidt, M.; Milojevic, N.; Urban, C.; Illner, M.; Repke, J.-U.; Schomäcker, R. Understanding the Role of Nonionic Surfactants during Catalysis in Microemulsion Systems on the Example of Rhodium-Catalyzed Hydroformylation. *Ind. Eng. Chem. Res.* **2017**, *56*, 9934–9941.

(22) Monflier, E.; Tilloy, S.; Bertoux, F.; Castanet, Y.; Mortreux, A. New Prospects for the Palladium-Catalyzed Hydrocarboxylation of Higher Alpha-Olefins in a Two-Phase System: The Use of Chemically Modified Beta-Cyclodextrin. *New J. Chem.* **1997**, *21*, 857.

(23) Tilloy, S.; Monflier, E.; Bertoux, F.; Castanet, Y.; Mortreux, A. A New Fruitful Development in Biphasic Catalysis: The Palladium-Catalyzed Hydrocarboxylation of Alkenes. *New J. Chem.* **1997**, *21*, 529.

(24) Bertoux, F.; Monflier, E.; Castanet, Y.; Mortreux, A. Palladium Catalyzed Hydroxycarbonylation of Olefins in Biphasic System: Beneficial Effect of Alkali Metal Salt and Protective-Colloid Agents on the Stability of the Catalytic System. *J. Mol. Catal. A: Chem.* **1999**, *143*, 23–30.

(25) Kahlweit, M.; Strey, R.; Firman, P.; Haase, D.; Jen, J.; Schomaecker, R. General Patterns of the Phase Behavior of Mixtures of Water, Nonpolar Solvents, Amphiphiles, and Electrolytes. 1. *Langmuir* **1988**, *4*, 499–511.

(26) Schmidt, M.; Pogrzeba, T.; Stehl, D.; Sachse, R.; Schwarze, M.; von Klitzing, R.; Schomäcker, R. Verteilungsgleichgewichte von Liganden in mizellaren Lösungsmittelsystemen. *Chem.-Ing.-Tech.* **2016**, *88*, 119–127.

(27) Pogrzeba, T.; Müller, D.; Illner, M.; Schmidt, M.; Kasaka, Y.; Weber, A.; Wozny, G.; Schomäcker, R.; Schwarze, M. Superior catalyst recycling in surfactant based multiphase systems - Quo vadis catalyst complex? *Chem. Eng. Process.* **2016**, *99*, 155–166.

(28) Rosales, M.; Pacheco, I.; Medina, J.; Fernández, J.; González, A.; Izquierdo, R.; Melean, L. G.; Baricelli, P. J. Kinetics and Mechanisms of Homogeneous Catalytic Reactions. Part 12. Hydroalcoxycarbonylation of 1-Hexene Using Palladium/Triphenylphosphine Systems as Catalyst Precursors. *Catal. Lett.* **2014**, *144*, 1717–1727.

(29) Roesle, P.; Dürr, C. J.; Möller, H. M.; Cavallo, L.; Caporaso, L.; Mecking, S. Mechanistic Features of Isomerizing Alcoxycarbonylation of Methyl Oleate. *J. Am. Chem. Soc.* **2012**, *134*, 17696–17703.

(30) Papadogianakis, G.; Verspui, G.; Maat, L.; Sheldon, R. A. Catalytic Conversions in Water. Part 6. A Novel Biphasic Hydrocarboxylation of Olefins Catalyzed by Palladium TPPTS Complexes (TPPTS=P(C<sub>6</sub>H<sub>4</sub>-m-SO<sub>3</sub>Na)<sub>3</sub>). *Catal. Lett.* **1997**, *47*, 43–46.

(31) Averyanov, V. A.; Sevostyanova, N. T.; Batashev, S. A.; Vorobiev, A. A.; Rodionova, A. S. Kinetics and Mechanism of Cyclohexene Hydrocarbomethoxylation Catalyzed by the Pd(OAc)<sub>2</sub>-PPh<sub>3</sub>-p-Toluenesulfonic Acid System. *Russ. J. Phys. Chem. B* **2014**, *8*, 140–147.

(32) Baya, M.; Houghton, J.; Konya, D.; Champouret, Y.; Daran, J.-C.; Almeida Leñero, K. Q.; Schoon, L.; Mul, W. P.; van Oort, A. B.; Meijboom, N.; et al. Pd(I) Phosphine Carbonyl and Hydride Complexes Implicated in the Palladium-Catalyzed Oxo Process. *J. Am. Chem. Soc.* **2008**, *130*, 10612–10624.

(33) Portnoy, M.; Milstein, D. A Binuclear Palladium(I) Hydride. Formation, Reactions, and Catalysis. *Organometallics* **1994**, *13*, 600–609.

(34) van Leeuwen, P. W. N. M.; Zuideveld, M. A.; Swennenhuis, B. H. G.; Freixa, Z.; Kamer, P. C. J.; Goubitz, K.; Fraanje, J.; Lutz, M.; Spek, A. L. Alcoholysis of Acylpalladium(II) Complexes Relevant to the Alternating Copolymerization of Ethene and Carbon Monoxide and the Alcoxycarbonylation of Alkenes: The Importance of Cis-Coordinating Phosphines. *J. Am. Chem. Soc.* **2003**, *125*, 5523–5539.

(35) Rünzi, T.; Tritschler, U.; Roesle, P.; Göttker-Schnetmann, L.; Möller, H. M.; Caporaso, L.; Poater, A.; Cavallo, L.; Mecking, S. Activation and Deactivation of Neutral Palladium(II) Phosphinesulfonate Polymerization Catalysts. *Organometallics* **2012**, *31*, 8388–8406.

(36) Goedheijt, M.; Kamer, P. C. J.; Van Leeuwen, P. W. N. M. A Water-Soluble Diphosphine Ligand with a Large natural Bite Angle for Two-Phase Hydroformylation of Alkenes. *J. Mol. Catal. A: Chem.* **1998**, *134*, 243.